Indian Journal of Natural Sciences www.tnsroindia.org.in ©IJONS

Vol.9 /Issue 51 / December / 2018 *International Bimonthly* *ISSN: 0976 – 0997*

RESEARCH ARTICLE

Abundance of Sugarcane Internode Borer, *Chilo saccariphagus indicus* (Kapur) (Crambidae: *Lepidoptera*) and Role of Abiotic Factors on Its Incidence

Umashankar H.G[1]* and Patel V.N.[2]

[1]M.Sc Scholar, Department of Agricultural Entomology, University of Agricultural Sciences, Bengaluru, Karnataka, India

[2]Prof., AICRP on Sugarcane, Zonal Agricultural Research Station , VC Farm Mandya-571405, Karnataka, India.

Received: 01 Aug 2018 Revised: 04 Sep 2018 Accepted: 05 Oct 2018

***Address for Correspondence**
Umashankar H.G.
M.Sc Scholar,
Department of Agricultural Entomology,
University of Agricultural Sciences,
Bengaluru, Karnataka, India.
Email : umashankarhg21@gmail.com

ABSTRACT

The results of the present investigation carried out on abundance of sugarcane internode borer, *C. sacchariphagus indicus* (Kapur) (Pyaridae: *Lepidoptera*) in Cauvery command area of Mandya district was carried out at the Zonal Agricultural Research Station, College of Agriculture, V. C. Farm, Mandya, during the period 2014-16. Incidence of internode borer was observed at the time of harvest in all the five commercial varieties. The incidence of INB across the varieties varied from 9.00 to 36.00 per cent, with an intensity ranging from 0.72 to 3.01 per cent and with an infestation index of 0.07 to 0.88. Significantly high incidence of INB was recorded in the commercial variety VCF 0517 with incidence of 36.00 per cent, with an intensity of 3.01 per cent and with an infestation index of 0.88. Significantly lower incidence was recorded in variety Co 8371 with incidence of 9.00, with an intensity of 0.72 per cent and infestation index of 0.07. Correlation studies on pheromone trap catches of INB and meterological variables revealed a negative relationship between morning relative humidity (r= -0.37) and mean relative humidity (r= -0.298) and were found to be significant.

Key words: *Chilo saccariphagus indicus,* internode borer, intensity, percent incidence.

INTRODUCTION

Sugarcane is grown in India since ancient times and it is one of the most important cash crops and industrial crops after textiles. In tropical zone, Karnataka is one of the major sugarcane growing states. It occupies fourth place in the country. The insufficiency in the production and productivity of sugarcane failed to meet out the requirements of ever increasing population due to factors like poor soil fertility, prevalence of pest and diseases and environmental stress. Pests are known to inflict considerable losses on cane yield as well as sugar output.More than 200 species of insect pests were reported on sugarcane during different growth phases of the crop in India (David and Nandagopal, 1986). Based on the feeding habit, the insect pests are broadly classified as borers, sucking pests, subterranean pests, defoliators and non-insect pests. Among these, nine lepidopteran borers are considered as most detrimental in both tropical and sub-tropical sugarcane fields. The larvae of borers may reduce yield upto 80 per cent (Goebel et al., 2011; Kalra and Sidha 1955).

Amongst the borers, *Chilo sacchariphagus indicus* (Kapur) (Lepidoptera: *Pyralidae*), commonly known as internode borer, has remained a major pest in peninsular India (Gupta, 1957). It was first reported from South India as Diatraea venosata (Fletcher, 1914). Later based on its taxonomic status was renamed the as *Chilo saccharipagus indicus* (Kapur) by Hattori in 1971. Internode borer (INB), Chilo sacchariphagus indicus becomes more active when moderately warm and high humid conditions prevail during July-September in subtropical India. The internode borer is distributed in the states of Tamil Nadu, Kerala, Andra Pradesh, Karnataka, Maharashtra, Bihar, Uttar Pradesh and Haryana (Siddiqi and Agarwal, 1957). INB generally attacks the crop from internode formation to harvest, causing estimated crop losses of 10–35 Per cent. When the borer injury extends to three or more internodes per cane, or more than 10% of the total length of the cane, canes suffer significant deterioration in juice quality. The threshold for the internode borer was found to be 13 - 15 per cent bored internodes (Yalawar et al., 2010).

Under this situation, it is quite necessary to understand the seasonal incidence of sugarcane internode borer, reactions of sugarcane varieties with this background the present study on population dynamics of internode borer was undertaken during 2014-16 at Zonal Agricultural Research Station, V. C. Farm, Mandya.

MATERIALS AND METHODS

Five popular sugarcane varieties viz., Co 62175, Co 86032, VCF 0517, CoVC 99463 and Co 8371, were planted in Randomized Complete Block Design with three replications at Zonal Agricultural Research Station V. C. Farm, Mandya in August 2015. The recommended cultural practices are performed equally in all the replications except the plant protection measures. The observation on the incidence of sugarcane internode borer was recorded at the time of harvest in randomly selected 30 canes in each variety in three replications. The observations were also recorded on number of canes, number of canes infested, number of internodes and number of internodes infested.The per cent incidence, per cent intensity and infestation index was calculated by using the formula.

$$\text{Incidence (\%)} = \frac{\text{Total number of affected canes}}{\text{Total canes}} \times 100$$

$$\text{Intensity (\%)} = \frac{\text{Total number of affected internodes}}{\text{Total number of internodes}} \times 100$$

$$\text{Infestation index} = \frac{\text{Total number of affected internodes}}{\text{Total number of internodes}} \times 100$$

Role of abiotic factors on the population fluctuation of sugarcane borer pest

Weather factors influence the activity of insect pest population under field conditions. Activity of sugarcane borers was studied by using pheromone traps. Pheromone trap catches of sugarcane borers were recorded regularly throughout the crop growth. Further, observations on sugarcane borer pests and weather parameters were subjected to Pearson's simple correlation (Pans and Sukhatme, 1967) by fitting different functions using software "SAS Syntax Reference Guide 2010, version 16.0 (SPSS 16), South Wacker Drive, Chicago, IL.

RESULTS AND DISCUSSION

The incidence of INB across the varieties varied from 8.00-29.00 per cent, with an intensity ranging from 0.72 to 3.01 per cent and with an infestation index of 0.07 to 0.88 (Table 1). Significantly higher incidence of INB was recorded in VCF 0517 (36.00 per cent) followed by CoVC 99463 (24.00 per cent) and significantly lower incidence was recorded in Co 8371 (9.00 per cent) which is on par with Co 86032 (10.5 per cent) (Table 4). Significantly higher intensity of INB was recorded in VCF 0517 (3.01%) which was on par with CoVC 99463 (2.71%). Significantly less intensity of INB was recorded in genotype, Co 8371 (0.72%) which was on par with Co 86032 (0.97%). Significantly higher infestation index was recorded in VCF 0517 (0.88) which was on par with Co 99463 (0.64) and lower infestation index was recorded in Co 8371 (0.07) followed by Co 86032 (0.11) (Table 5 and figure 3). This is in confirmity with the findings reported by Anon., (2015).

Studies on relationship of environmental parameters with the trap catch of INB indicated that minimum temperature (r=0.17), maximum temperature (r=0.12) and mean temperature (r=0.17) showed non-significant positive correlation. The morning relative humidity, evening relative humidity and mean relative humidity showed negative correlation. Whereas morning and mean relative humidity were significant with r= -0.37 and r=–0.29, respectively. While rainfall showed negative and non-significant correlation (r= -0.02) with INB trap catches (Table 2). The results are in conformity with the earlier findings by Hapse et al. (1979) and Gajjar et al. (2015) where they reported that the maximum temperature showed significant positive correlation with borer infestation while relative humidity showed a negative relationship. It was thus evident that for borer multiplication, the most important abiotic factor was temperature.

CONCLUSION

The results of the present investigation on abundance of sugarcane internode borer, *C. sacchariphagus indicus* (Kapur) (Pyaridae: *Lepidoptera*) in Cauvery command area of Mandya district was carried out at the Zonal Agricultural Research Station, College of Agriculture, V. C. Farm, Mandya, during the period 2014-16 revealed that Incidence of internode borer was observed at the time of harvest in all the five commercial varieties. Incidence of INB varied from 8.00-29.00 per cent with an intensity of 0.72 to 3.01 per cent and infestation index of 0.07 to 0.88. Highest incidence of INB was recorded on the variety VCF 0517 (36.00 per cent).

ACKNOWLEDGEMENTS

The authors are thankful to the AICRP on sugarcane, at Zonal agricultural research station, V.C farm, Mandya for providing all the facilities during the research.

REFERENCES

1. ANONYMOUS, 2015b, Zonal Research and Extension Programme Workshop. University of Agriculture Sciences, Bengaluru.
2. DAVID, H. AND NANDAGOPAL, V., 1986, Pests of sugarcane – distribution, symptomology of attack and identification. Ind. Sug cane Breed. Inst., Coimbatore. pp. 1–29.
3. FLETCHER, T. B., 1914, Some south Indian insects. Govt. Press, Madras. pp. 422.
4. GAJJAR, S., MAKWANA, K. V. AND MALI, S. C., 2015, Sugarcane borers (Top borer and internode borer) population dynamics in relation to abiotic stress evaluated through pheromone trap. Proc. Sug. Cane Technol., pp. 116-123.
5. GOEBEL, F. R., ACHADIAN, E., KRISTINI, A., SOCHIB, M. AND ADI, H., 2011, Investigation of crop losses due to moth borers in Indonesia. Proc. Aus. Soc. Sugar Cane Technol., 33: 9.
6. GUPTA, B. D., 1957, A note on the scientific and common names of sugarcane pests in India. Indian J. Sug. Cane Res. Dev., 2: 9-13.
7. HAPASE, D. G., PATIL, A. S. AND MOHOLKAR, P. R., 1979, Effect of some climatic factors on the incidence of sugarcane borer. Indian J. Sug. Cane Technol., 2: 1-8.
8. HATTORI, I., 1971, Stem borer of graminaceous crops in south east Asia. Proc. Symp. Rice insects, Kitaku, Tokya, Japan., pp. 145-153.
9. KALRA, A. H. AND A. S. SIDHA., 1955, Studies on biology of sugarcane top borer, Scirpophaga nivella Fabr. Indian Sugar, 15:37-43.
10. PANS, V. G. AND SUKHATME, P. V., 1967, Statistical methods for Agricultural workers, ICAR, Publication, New Delhi, pp. 359.
11. SIDDIQI, Z. A. AND R. A. AGARWAL, 1957, The first record of heavy infestation of Procerus indicus Kapur in Uttar Pradesh. Indian J. Sug. Cane Res. Dev., 2: 36-37.
12. YALAWAR, S., PRADEEP, S., AJITHKUMAR, M. A., HOSAMANI, V. AND RAMPURE, S., 2010, Biology of sugarcane internode borer, Chilo sacchariphagus indicus (Kapur). Karnataka J. Agri. Sci., 23(1): 140–141.

Table 1: Cumulative incidence of borer in five different popular varieties of Sugarcane from January – December 2015.

Varieties	Internode Borer		
	% incidence	% intensity	Infestation index
CoVC 99463	24(29.3)^{d}	2.71(9.4)^{cd}	0.64(4.5)^{cd}
Co 86032	10.5(18.9)^{ab}	0.97(5.6)^{ab}	0.11(1.9)^{b}
Co 8371	9(17.4)^{a}	0.72(4.8)^{a}	0.07(1.5)^{a}
Co 62175	18(25.1)^{c}	2.01(8.1)^{c}	0.38(3.4)^{c}
VCF 0517	36(36.9)^{e}	3.01(10)^{de}	0.88(5.4)^{de}
SEM ±	0.70	0.50	0.40
CD@ P=0.05	2.10	1.60	1.20

*DAP: Days after planting; ESB: Early shoot borer; TSB: Top shoot borer; INB: Inter node borer Values in the column followed by common letters are non-significant at p = 0.05 as per Tuckey's HSD (Tukey, 1965). Figures in the parentheses are arcsine √x transformed values

Table 2: Correlation between Pheromone trap catches of Sugarcane internode borer and weather parameters during 2015

Pest	Temperature (°C)			Relative humidity (%)			Rainfall (mm)
	Max.	Min.	Mean	Mor. RH	Evn. RH	Mean	
INB	0.17	0.12	0.17	-0.37*	-0.19	-0.29*	-0.02

*** Correlation is significant at 0.05 levels**

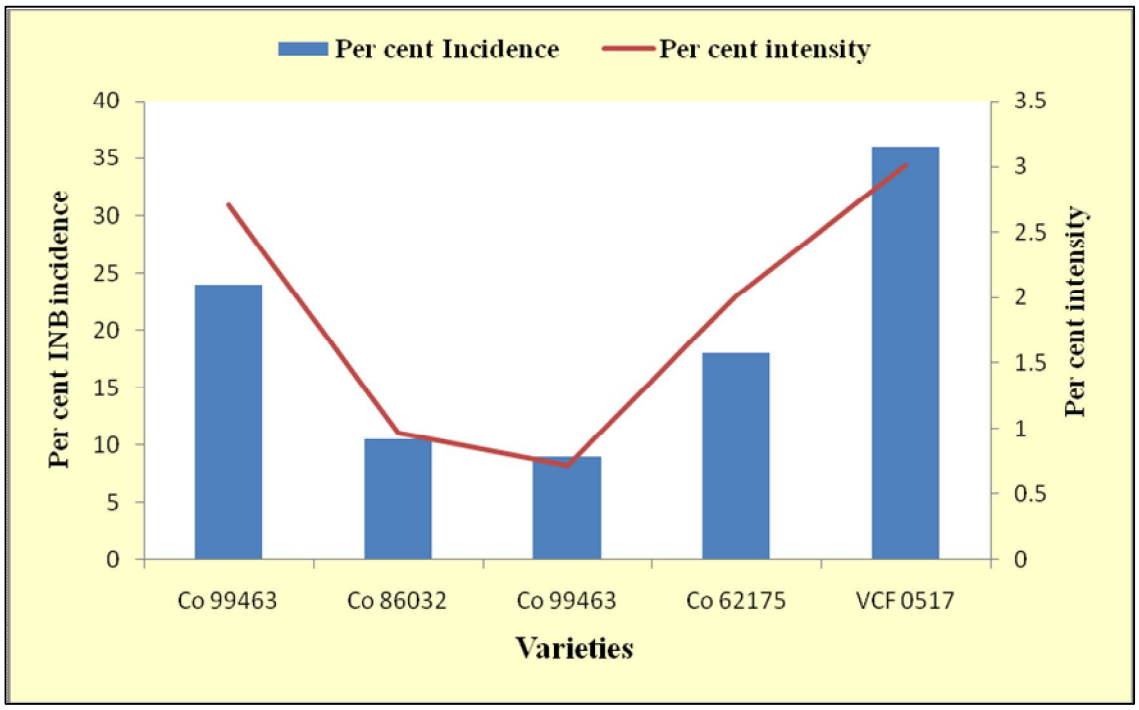

Fig. 1: Per cent incidence and intensity of INB in different varieties

Indian Journal of Natural Sciences www.tnsroindia.org.in ©IJONS

Vol.9 /Issue 51 / December / 2018 *International Bimonthly* *ISSN: 0976 – 0997*

RESEARCH ARTICLE

Correlation between hsCRP with RAAS in Iraqi Chronic Renal Failure Patients

Ali Shalash Sultan[1]* and Dhelal Abdul Khaliq Jumma[2]

[1]Department of Biology, College of Science, University of Al-Mustansiriyah, Iraq.
[2]Al-Imam Khadhum (a.s), University College For Islamic Sciences, Iraq

Received: 25 June 2018 Revised: 28 July 2018 Accepted: 31 Aug 2018

***Address for Correspondence**
Ali Shalash Sultan
Department of Biology,
College of Science,
University of Al-Mustansiriyah,Iraq.

ABSTRACT

The chronic kidney disease (CKD) has become a great problem through the world. It is associated with a higher mortality and morbidity and caused a reduction in the quality of life in patients compared with*renin-angiotensin-aldosterone system* (RAAS). The present study was conducted on106 Iraqi patientswith age range (20-69) yearsto evaluate the correlation between high-sensitivity C-reactive protein(hsCRP)and chronic renal. The patients involved in this study 40 conservative patients (21 Males and 19Females) and 66 hemodialysis patients (44Males and 22 Females). Results revealed a significant positive correlation between hsCRP with active renin and angiotensin II. In conclusion hsCRP correlated positively with active renin and angiotensin II in chronic renal failure.

Keywords*:* High Sensitivity C-Reactive Protein (hsCRP), RAAS, *renin-angiotensin-aldosterone system*.

INTRODUCTION

CKD has become a great problem through the world. It is associated with a higher mortality and morbidity and caused a reduction in the quality of life in patients (1). The RAAS is one of the better significant hormonal systems, manages the functions of kidney, cardiovascular, and adrenal glands through regulating sodium and potassium balance, blood pressure and fluid volume (2). The classical RAAS was discovered more than a century ago, and in 1934 Goldblatt *et al*. (3) showed a renin link between kidney function and blood pressure. Usually, the RAAS is reflected as an endocrine system with angiotensinogen, formed in the liver that is cleaved by renin released from kidney juxtaglomerular cells. Via this way, angiotensin I (ANGI) is produced, which, in turn, is more cleaved by ACE activity of the lungs into the active form of ANGII. Then ANGII links to specific receptors in adrenal cortex, causing in release of aldosterone. In this traditional pathway, the primary function of the RAAS is keeping of blood pressure through ANGII prompted vasoconstriction and aldosterone interceded sodium retention in the collecting duct (4).

CRP concentration is the most common indication ofinflammatory condition. CRP is a nonglycated protein synthesize by human hepatocytes in response to tissue damage, infection and inflammation. It is consist of 5identical noncovalently connected subunits that form asymmetrical pentagonal structure with a molecular weightof 105 kDa (5).CRP is an acute-phase protein formed essentially by the liver in response to cytokine production (TNF, IL-6 and IL-1) through tissue damage, inflammation, infection or malignancy (6). In normal states were found that the CRP concentrations of less than 10 mg/L in the blood, through infectious or inflammatory disease conditions CRP concentrations increase quickly within the first 6 to 8 hours and peak at levels of up to 350–400 mg/L after 48 hours (7).CRP binds to phosphocholine expressed on the surface of injured cells and also binds to polysaccharides and peptosaccharides current on bacteria,fungi and parasites (8).

MATERIALS AND METHODS

The study was designed on 106 Iraqi patientswith age range (20-69) yearswho have chronic renal. The patients involved in this study 40 conservative patients (21Males and 19 Females) and 66 hemodialysis patients (44 Males and 22 Females). hsCRP were estimated in serum of all patients by using an automated quantitative COBAS 400 Integra (from Roche, Germany). Active renin and aldosterone were determined in serum of all patients by using a commercially ELISA Micro wells kit (from LDN, Germany).Angiotensin II was determined in serum of all patients by using a commercially ELISA Micro wells kit (from My Bio Source, USA).

Statistical Analysis

The statistical analysis system-SAS (2012) program is used to estimate the correlation coefficient between difference parameters in this study. $P<0.05$ is considered significant.

RESULTS

Table(1) illustratedthe relationship between the changes in serum hsCRP with active renin and angiotensin II. The mean serum hsCRP wasnon-significantly positive correlated with mean aldosterone in conservative group ($r=0.09$, $p> 0.05$), but non-significantly negative correlated in hemodialysis group ($r=-0.15$, $p>0.05$) and between two groups ($r=-0.05$, $p>0.05$). The mean serum hsCRP was significantly positive correlated with mean active renin in conservative group ($r=0.31$, $p<0.05$) Figure (1), hemodialysis group ($r=0.38$, $p<0.01$) and between two groups ($r=0.27$, $p<0.05$). The mean serum hsCRP was significantlypositive correlated with mean angiotensin II in conservative group ($r=0.36$, $p<0.01$) Figure (2), and non-significantlypositive correlated between two groups ($r=0.13$, $p>0.05$), but non-significantly negative correlated in hemodialysis group ($r=0.006$, $p>0.05$) Table (1).

DISCUSSION

HsCRP showed significant positive correlation with mean active renin in conservative group, hemodialysis group and between two groups. As well as hsCRP showed significant positive correlation with mean ANGII in conservative group. That Inflammation is a component of the major modifiable risk factors in renal disease. Elevated hsCRP levels have been shown to predict all-cause and cardiovascular mortality in patients dependent on dialysis and to predict worsening renal function in patients without overt renal disease. Levels of hsCRP are also predictive of hypertension; a major risk factor for renal disease, across all levels of blood pressure in patients without initial hypertension (9).As hypertension is a major risk factor for progressive renal disease. A role for inflammation in hypertension is indicated by the findings that inflammation correlates with both endothelial dysfunction and increased activity of the renin–angiotensin system, including increased ANGII activity and, as indicated by recent trials, suggesting upregulation of ANGI receptor activity. Elevated hsCRP levels are observed in patients with hypertension, and it has been shown

that increased hsCRP levels are correlated with risk of developing hypertension (9). In conclusion hsCRP correlated positively with active renin and angiotensin II in chronic renal failure

REFERENCES

1. Hallan, S.I.; Coresh, J. and Astor, B.C. (2006). International Comparison of the Relationship of Chronic Kidney Disease Prevalence and ESRD Risk. J Am SocNephrol; 17: 2275–2284.
2. Ferrario, C. M. and Strawn, W. B. (2006). "Role of the renin-angiotensinaldosterone system and proinflammatory mediators in cardiovascular disease," American Journal of Cardiology, vol. 98, no. 1, pp. 121–128.
3. Goldblatt, H.; J. Lynch; R. F. Hanzal and Summerville, W. W. (1934). "Studies on experimental hypertension: I. The production of persistent elevation of systolic blood pressure bymeans of renal ischemia," The Journal of Experimental Medicine, vol. 59, no. 3, pp. 347–379.
4. Christiane, Ru,¨ster and Gunter, Wolf. (2006). Renin-Angiotensin-Aldosterone System and Progression of Renal Disease, J Am SocNephrol 17: 2985–2991. doi: 10.1681/ASN.2006040356.
5. Yu-Jen, Su. ; Shang-Chih, Liao; Ben-Chung, Cheng; Jyh-Chang, Hwangand and Jin-Bor, Chen. (2013). Increasing high-sensitive C-reactive protein level predicts peritonitis risk in chronic peritoneal dialysis patients. BMC Nephrology; 14:185.
6. Bienvenu, J.; Monneret, G.; Fabien, N. and Revillard, J.P. (2000). the clinical usefulness of the measurement of cytokines. ClinChem Lab Med; 38:267-285.
7. Kolb-Bachofen, V. A. (1991). Review on the biological properties of C-reactive protein. Immunobiology; 183:133–45.
8. Ballou, S.P. and Kushner, I. (1992).C-reactive protein and the acute phase response. Adv Intern Med.; 37:313–36.
9. Vidt, D.G. (2006). Inflammation in Renal Disease. Am J Cardiol; 97: 20A-27.

Table 2. Correlation coefficients between hsCRP with Aldosterone, Renin and Angiotensin II

Parameters	Correlation coefficients –r		
	Conservative Group	Hemodialysis Group	Conservative + Hemodialysis
hsCRP& Aldosterone	0.09 NS	-0.14 NS	-0.05 NS
hsCRP& Activerenin	0.31 *	0.38 **	0.27 *
hsCRP& Angiotensin II	0.36 **	-0.006 NS	0.13 NS
* (P<0.05), ** (P<0.01), NS: Non-Significant.			

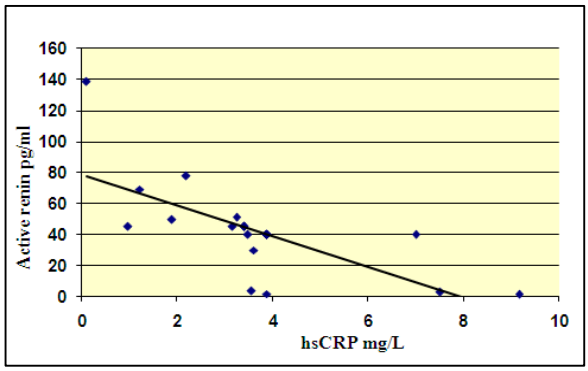

Figure 1.Relationship between hsCRP and Active renin in Conservative

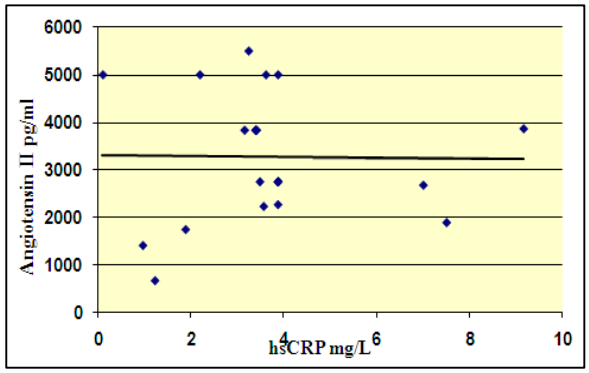

Figure 2. Relationship between hsCRP and Angiotensin II in Conservative

Indian Journal of Natural Sciences www.tnsroindia.org.in ©IJONS

Vol.9 /Issue 51 / December / 2018 *International Bimonthly* *ISSN: 0976 – 0997*

RESEARCH ARTICLE

Prehatching Development of Gizzard in Indigenous Quail (*Coturnixcoturnix japonica*)

Hadaf H. Mohammed*, Dhyaa Ab. Abood and Lamees Ezaldeen M

Department of Anatomy and Histology, College of Veterinary Medicine, University of Baghdad, Baghdad, Iraq.

Received: 10 Aug 2018 Revised: 14 Sep 2018 Accepted: 16 Oct 2018

*Address for Correspondence
Hadaf H. Mohammed
Department of Anatomy and Histology,
College of Veterinary Medicine,
University of Baghdad, Baghdad, Iraq.
Email : sabahali503@yahoo.com

ABSTRACT

The present work wasinvestigated the developmental events of the gizzard in quail.A total 80 fertilized egg samples were allocated into 20 periods involved (65, 69, 72 , 77, 82, 87, 92 and 96 hours) (5, 6, 7, 8, 9, 10, 11, 12, 13, 14, 15, 16,17, 18 days), (four eggs for each).The tissue sections were stained with H&E stain.Theevolution ofgut tube was divided into undifferentiated, differentiated and maturationperiods; the undifferentiated period was started by period of 3 days at which the stomach was appeared as sac like structure of two chamberscomposed of stratified epithelial cells of endoderm and enclosed by mesenchymal tissue of splanchnic mesoderm.During the 4th and 5th day thegizzard primordium showed highly cellular proliferation. At the 6thdays of incubation period the differentiated period has started and the gizzard displaying well distinguished three layers; epithelial layer, prospective muscularis layers which was displaying condensed mesenchymal tissue and the outer most layer of splanchnic mesoderm showed actively mitotic figure. At the 12-16th days, the epithelial cells has extended into lamina propria and showed secretory activities and the muscularis mucosa has composed of dense layer of myoblast, fibroblasts and angiogenesis, with marked differentiation of myoblast which form circular layer and longitudinal layers of tunica muscularis. The maturation period was seen at 18thdaysof incubation at which the gizzard was similar that of post hatching periods.

Key Words : Gizzard, prehatching, development, quail.

INTRODUCTION

In vertebrate the primitive gut is an important organwhich is well adapted for the different types of foods in each animal species [1]. In chicks the primitive gut is begins develop on the first day of incubation period at which the gut appears as undifferentiated simple tube [2][3]. In advanced stages of development the primitive gut gives rise well demarcates primordia; the cranial chamber "proventriculus" and caudal chamber"ventricular stomach" (Gizzard) [4][5]. The evolution of embryonic gut occurs initially along the anterior–posterior axis of embryo,it evoluted from two germ layers; endoderm and mesoderm[6].Because of the birds have no teeth the gizzard has adapted for mechanical crushing of grain by its cuticular layer and prepares food for further digestion process [7][8].The gizzard characterized by presenting a secretion plate on the mucosal surface and a well-developed muscle layer, both characteristics represent an adaptation to grind grains[9]. The current study is aimed to investigate the evolution and the developmental events of the gizzard in indigenous quail.

MATERIALS AND METHODS

A total 80 fertilized egg samples of quailwere brought from Al-Mutasem Company for eggs production in Baghdad governorate. Egg samples were allocated into20 periods involved (72, 77, 82, 87, 92 and 96 hours) (5, 6, 7, 8, 9, 10, 11, 12, 13, 14, 15, 16, 17& 18 days), (four eggs for each).The samples have introduced to the hatchery and eggs were extracted successively according to the required ages.For histological study, in early embryonic stages (72 hours up to 8 days), the whole embryos has dehydrate by passing them for 30 minutes in a series of ascending up grades of ethanol (30%, 40%, 50%, 60%, 70%, 80%, 90% and 100%), then clear in xylen for 15 minutes. After that the embryos have embed in paraffin wax for one hour. Finally blocks have sectioned serially at 5-6 µm thickness. In embryonic stages (9 days and up) the whole embryos has dehydrate by passing them for two hours in a series of ascending up grades of ethanol (50%, 60%, 70%, 80%, 90% and 100%), then clear in xylen for 30-60 minutes[10][11] [12].After that the embryos have embed in paraffin wax for one –two hours. Blocks have sectioned serially at 5-7µm thickness and the sections will be stain with Harris Hematoxylin and Eosin stain[13].

RESULTS

The result showed that, in most samples of quail embryos the gut tube was evoluted at the 3rddays of incubation period which appeared extending with along anterior–posterior axis and composed of esophagus, stomach and the anterior intestinal portal, the stomach was appeared as sac like structure located behind to heart region just cranial to the anterior intestinal portal of the duodenum, the stomach was composed of stratified epithelial cells of endoderm and enclosed by mesenchymal tissue of splanchnic mesoderm (fig.1&2), at this period the stomach was composed of two chambers; the anterior was represented the proventriculus and the posterior was represented the gizzard and both had the same cellular composite. At the 4th and 5th day, the primordium of gizzard located in the left part of coelom, fixed by dorsal mesentery just beside the right lobe of the liver as a sac like organ had thick wall and narrow lumen (fig.3) it showed the cellular composing of showed actively mitotic figures (fig.4). In the 6thday, the gizzard showed well distinguished hree layers (fig.5); epithelial layer, prospective muscularis layers which was displaying condensed mesenchymal tissue (fig. 6) and the outer most layer of

splanchnic mesoderm showed actively mitotic figure (fig.7).In the 8-10thday, the gizzard has enlarged, clearly occupied the left side of coelomic cavity and during these periods the cellular cytoarchitecture has not been showed any differentiation (fig.8).In the 12th day, the epithelial covering of the gizzard showed furthermore enlargement and showed very thick wall (fig.9& 10), the epithelial cells has extended into lamina propria and gave rise secretory activities (fig.10&11), the muscularis mucosa has composed of dense layer of myoblast, fibroblasts and showed marked angiogenesis with newly formed blood vessels (fig.11), the middle of the gizzard wall showed marked differentiation of mesenchymal cells into myoblast which form circular layer of spindle shapedsmooth muscle fibers of prospective tunica muscularis (fig.11). The prospective tunica serosa was still composed of fibroblasts (fig.12).In 14-16 day-old the epithelium showed undulating apical surfacesand the epithelial cells became club-like with elongated nucleus and acidophilic cytoplasm, these changes due to cellular proliferation and the apical surface was covered with a layer of secretion , the muscularis mucosa was thick layer of smooth muscle (fig.13), the tunica muscularis showed mature bundles of smooth muscle fibers (fig.14) .The wall of the gizzard in the 18thday the gizzard was similar that of post hatching periods, thetunicamucosawas occupiedthe lamina propria formedof gizzard pits which were extended into the glandular layer forming thick glandular lamina propria, the epithelium was simple columnar cells lining the simple straight tubular glands (Fig. 15 & 16). The muscularis mucosa resembled a thick band of smooth muscle fibers.

DISCUSSION

The current results revealed that the 3rd days incubation period the primitive gut tube in quail was evoluted and involved both compartments of stomach such result disagree with result of[14] [2] and result of [3] who referred that the digestive tract of Gallus gallus is develop on the first day of incubation, meanwhile at the end third day embryo the stomach differentiate into two distinct chamber [15]. On the other hand the growth pattern of the gut tube was in anterior–posterior axis in quail as it is for the rest of the birds and mammals also the primitive stomach was as the simple chamber [4][6], such behavior wasconsistent with an anterior–posterior patterning role for Hoxc8 inthe gut [16].The structure of primitive gut initially was represented by highly proliferating endodermal cells and splanchnic mesodermal cells which give rise the cellular composite that required for construction the gizzard such results was similar that reported by [14].During the 4th and 5th day, the gizzard has formed its sac like appearancewith thick wall and narrow lumen, and the epithelium was pseudo stratified cells, such sequence of development was recorded by the 5th days by[14][17].During the 6th and 7th day, the gizzard showed well distinguished three layers, such distinguishing has mentioned by[14][15]. During the 8 to 10th day, the cellular cytoarchitecture has not been showed any differentiation[17].In quail the 12th days of incubation period was the time of cellular differentiation at which the pseudo stratified epithelial cells has formeda lamina propria which gave rise secretory activities andthe splanchnic mesoderm have differentiated into of myoblast and blood vessels, such observation similar that of [17], on the other hand such results have recorded during the 7th days of incubation period by [14], differentiation of myoblast was due to the expression of Bmp4 gene in the gut which is regulate mesodermal differentiation into myoblast [18] and acting to accelerator of terminal differentiation of gut muscle, in effect limiting its growth [4].At 14 days incubation the epithelial cells showed highly cellular proliferation and invasion the lamina propria with secretory activity such result disagree with result of [14], such acceleration of epithelial differentiation was due to expression of Bmp4 gene[4] [19] [17] [20]. At 18 days of incubation period the gizzard is located

posteriorly in the stomach and presenting a secretion plate on the apical surface and a well-developed tunica muscularis, both characteristics represent an adaptation to grind grains[9][21] [22].

REFERENCES

1. Coates M, Cohn M J. Fins, limbs, and tails: Outgrowths and axial patterning in vertebrate evolution. Bioessays. 1998; 20.:371–381.
2. Smith DM, Grasty RC, Theodosiou NA, Tabin CJ, Nascone-Yoder NM. Evolutionary relationships between the amphibian, avian, and mammalian stomachs. Evol. Dev. 2000; 2.6:348-59.
3. Shin M, Watanuki K, Yasugi S. Expression of Fgf10 and Fgf receptors during development of the embryonic chicken stomach. Gene Expr. Patterns. 2005; 5.4:511-6.
4. Nielsen C, Murtaugh LC, Chyung JC, Lassar A, Roberts DJ. Gizzard Formation and the Role of Bapx1. Developmental Biology. 2001; 231:164–174.
5. McGeady TA, Quinn PJ, Fitzpatrick ES, Ryan MT. Veterinary Embryology. Blackwell, Oxford. 2006.
6. Gilbert SF."Developmental Biology." Sinauer Associates, Sunderland, MA. 1997.
7. Maya S, Lucy P. Histology of gizzard-duodenal junction in Japanese quail (Coturnixcoturnix japonica). Indian Journal Poultry Science. 2000; 35. 1: 35-36.
8. Enoki Y. Morimoto T. Gizzard myoglobin contents and feeding habits in avian species. Comparative Biochemistry and Physiology Part A; Molecular and Intrgrative Physiology. 2000; 125.1: 33-43.
9. Aksoy A, Cinar K. Distribution and ontogeny of gastrin- and serotonin-immunoreactive cells in the proventriculus of developing chick, Gallus gallus domesticus. J. Vet. Sci. 2009;10 .1:9-13, 2009.
10. Abood DA, Al-Saffar FJ. The post hatching development of the female genital system in Indigenous Mallard Duck (Anas platyrhynchos). The Iraqi Journal of Veterinary Medicine, 2015; 39.2: 17-25.
11. Yassin AA, Abood DA. Peri Hatching Development of the Lens in ISA Brown Chicken (Gallus gallus domesticus). Indian Journal of Natural Sciences. 2018; 8.49:14368-14375.
12. Al-Saffar FJ, Abood DA. 2014. Histomorphological study of the pre hatching development of the female genital system in Indigenous Mallard Duck (Anas platyrhynchos). International Journal of Advanced Research.2014; 2.10: 248-263.
13. Bancroft JD, Marilyn G. Theory and practice of histological techniques. 6th Ed., Elsevier Limited, London. 2008, 168-173.
14. Soliman SA, Ahmed YA, Khalaf MA. Histogenesis of the Stomach of Pre-Hatching Quail: A Light and Electron Microscopic Study. International Scholarly and Scientific Research & Innovation. 2015; 9.2.
15. Fukuda K, Yasugi S. The molecular mechanisms of stomach development in vertebrates. Dev. Growth Differ. 2005; 47.6:375- 82, 2005.
16. Pollock RA. Altering the boundaries of Hox3.1 expression: Evidence for antipodal gene regulation. Cell. 1992;71:911–923.
17. Ventura A, Do Nascimento AA, Dos Santos MJ, Vieira-Lopes DA, Sales A, Pinheiro NL. Histological Description of Morphogenesis of the Gastroesophageal Mucosa of Gallus Gallus Domesticus. Int. J. Morphol., 2013;31.4:1331-1339.
18. Roberts DJ, Smith DM, Goff DJ, Tabin CJ. Epithelial-mesenchymal signaling during the regionalization of the chick gut. Development. 1998;125: 2791–801.
19. Narita T. BMPs are necessary for stomach gland formation in the chicken embryo: A study using virally induced BMP-2 and Noggin expression. Development. 2000;127, 981–988.

20. Pinheiro NL, George LL, Mota DL. Histogenesis and histochemistry of the secretion plate: detection of glycans and neutral glycoproteins synthetized by epithelial components of the gizzard mucosa of Gallus gallus. GegenbaursMorphol. Jahrb., 1989;135.3:385-95.
21. Al-Saffar T, Al-SamawyERM.Microscopic and morphometric study of the proventriculus and ventriculus of the Striated Scope Owl (OtusScorsbrucei). Kufa Journal For Veterinary Medical Sciences. 2014;5.2: 9-23.
22. Gosomji, I.J; Salami, S.O; Nzalak, J.O; Kawu, M.U. Okpe, G. C; Gurumyen, Y. G; Omirinde, J. O; Dung, E.C. and Plang, N. J.(2017). Histogenesis of the Stomach of Helmeted Guinea Fowl (Numidameleagris). Animal Research International (2017) 14(1): 2660-2665.

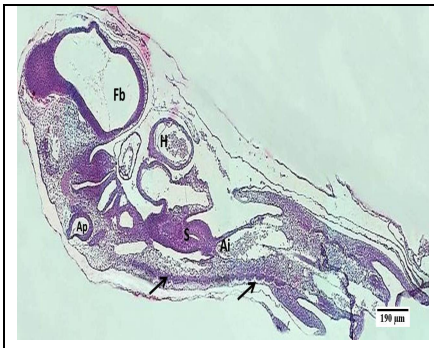

Figure 1: Sagittal section of whole embryo (3 days) shows: fore brain (Fb), Heart (H), auditory pits (Ap), stomach (S), anterior intestinal portal (Ai) & somites (arrows). H&E stain

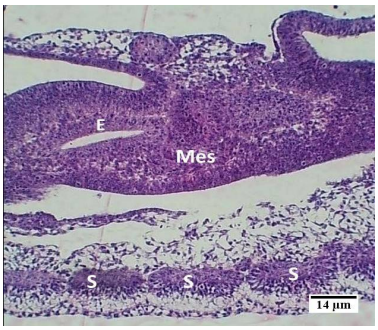

Figure 2: Magnified section of figure (1) shows: epithelium (E), sub epithelial mesenchymal tissue (Mes) & somites (S). H&E stain

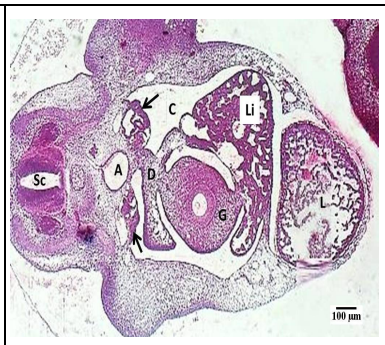

Figure 3: Transvers section of embryo (4 days embryo) shows: spinal cord (Sc), aorta (A), dorsal mesentery (D), Gizzard (G), Liver (Li), lung (L), coelom (C) & mesonephros (Arrows). H&E stain

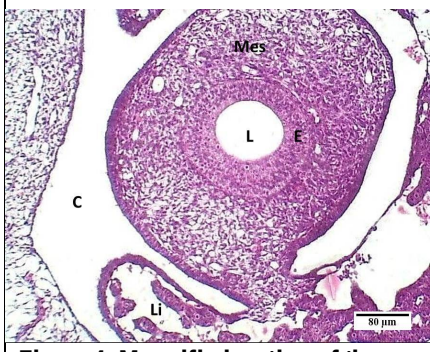

Figure 4: Magnified section of the gizzard in figure 3 shows: lumen of gizzard (L), epithelium (E), mesenchymal tissue (Mes), liver (Li) & coelom (C). H&E stain

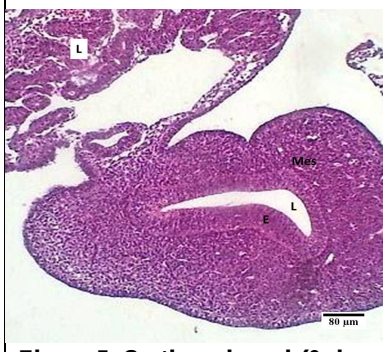

Figure 5: Section gizzard (6 days embryo) showslumen of gizzard (L), epithelium (E), mesenchymal tissue (Mes), liver (Li). H&E stain

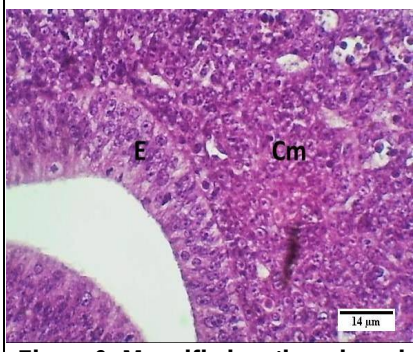

Figure 6: Magnified section gizzard (6 days embryo) shows: condensation of mesenchymal tissue (Cm) & epithelium (E). H&E stain

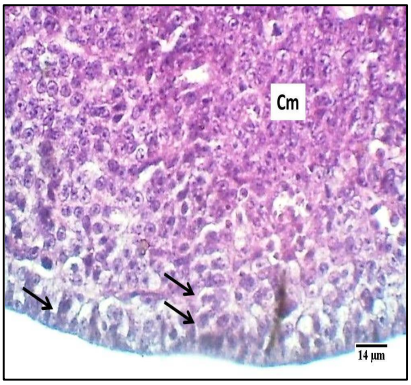

Figure 7: Magnified section of gizzard wall (6 days embryo) show: condensation of mesenchymal tissue (Cm) & marked mitotic figure of splanchnic mesoderm (Arrows). H&E stain

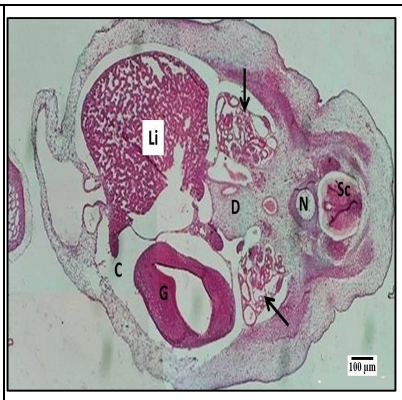

Figure 8: Section of gizzard wall (8 days embryo) shows:spinal cord (Sc), dorsal mesentery (D), Gizzard (G), Liver (Li), notochord (N), coelom (C) & mesonephros (Arrows). H&E stain.

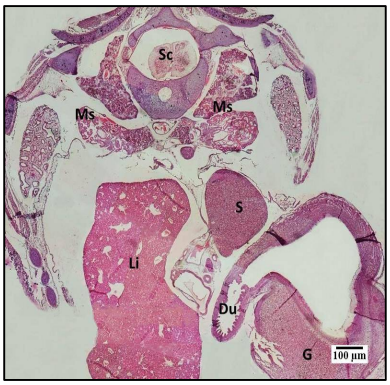

Figure 9: Transverse section throughout abdomen (12 days quail embryo) shows: spinal cord (Sc), Gizzard (G), liver (Li), spleen (S), duodenum (Du) & mesonephros (Ms). H&E stain

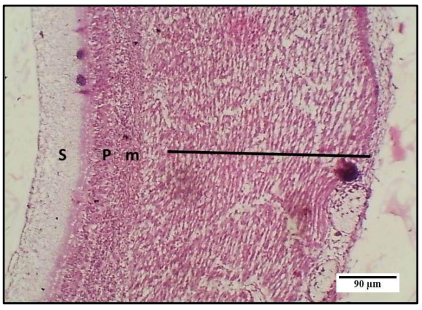

Figure 10: Magnified section of gizzard wall (12 days quail embryo) shows: secretion (S), lamina propria (p), muscularis mucosa (m), tunicamuscularis (black line). H&E stain

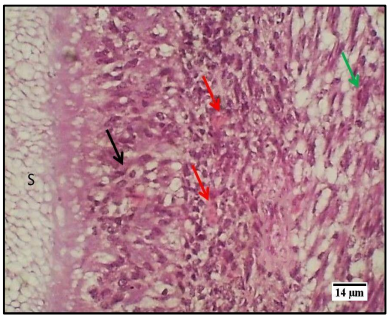

Figure 11: Section of gizzard (12 days quail embryo) shows: secretion (S), lamina propria (Black arrows), prospective muscularis mucosa (Red arrows) & smooth muscle fibers of tunica muscularis (green arrow). H&E stain

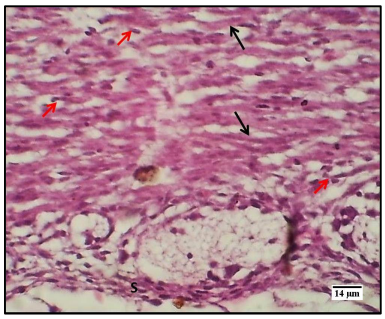

Figure 12: Section of gizzard (12 days quail embryo) shows: smooth muscle fibers (Black arrows), myoblast (Red arrows) & prospective tunica serosa (S). H&E stain

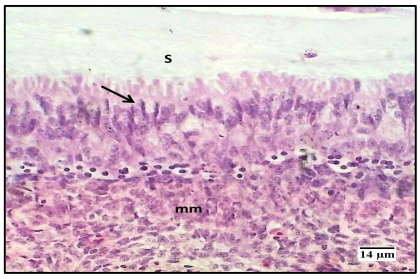

Figure 13: Section of gizzard (16 days quail embryo) shows: secretion (S), proliferating epithelial cells (Arrow), (E), lamina propria (Lp), tunica submucosa (Ts) & tunica muscularis (Tm). H&E stain

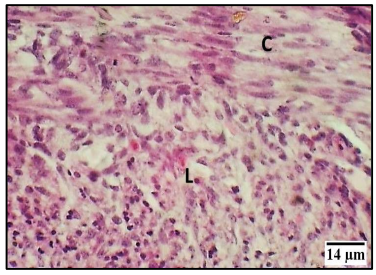

Figure 14: Section of gizzard (16 days quail embryo) shows: circular smooth muscle (C) & longitudinal smooth muscle fibers (L) of tunica muscularis. H&E stain

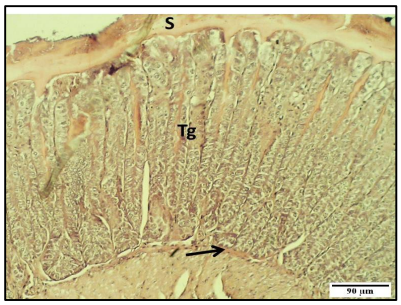

Figure 15: Section of gizzard (18 days quail embryo) shows: secretion (S) & tubular gland (Tg) 7 muscularis mucosa (arrow). H&E stain

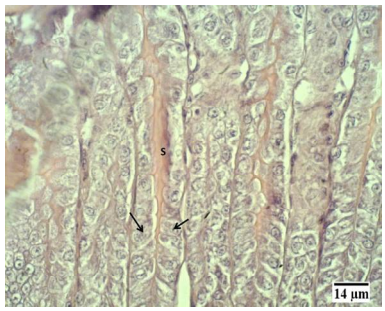

Figure 16: Section of lamina propria (18 days quail embryo) shows: secretion (S) & epithelium of tubular glands (arrow). H&E stain

Indian Journal of Natural Sciences www.tnsroindia.org.in ©IJONS

Vol.9 /Issue 51 / December / 2018 *International Bimonthly* *ISSN: 0976 – 0997*

RESEARCH ARTICLE

Preparation an Iraqi Dye and Compared Its Spectral Properties with Commercial Dye

Akram N. Alhadithi[1]* and Aleya R. Alani[2]

[1]Assistant Professor, Applied Science Department, University of Technology, Baghdad, Iraq.
[2]Physics Department, Science Collage, University of Al-Anbar, Iraq.

Received: 25 Sep 2018 Revised: 27 Oct 2018 Accepted: 01 Nov 2018

***Address for Correspondence**
Akram N. Alhadithi
Assistant Professor,
Applied Science Department,
University of Technology,
Baghdad, Iraq.
Email : akram.noori51@gmail.com

ABSTRACT

In this paper, we presented absorption and fluorescence study of an Iraqi dye (which extracted from castor leaves). Our samples were dissolved in ethanol and methanol (purity 99%) and other same samples of Rhodamine 6G were dissolved in the same solvent and a comparison where taken between them. The obtaining results showed an increment in absorption as concentration of our new dye *Ricinus communis* L. increase until saturated limit, which satisfied Lambert-Beer Law. The absorption diagram where taken from 200 nm – 900 nm. The fluorescence diagrams showed IR shifting as the concentration increased. The sample irradiated separately by two diode lasers (λ_1=402 nm, λ_2= 532nm) each has a power of 200 mw. A blue fluorescence were obtained with $\lambda_1$while a yellow fluorescence where obtained with λ_2. The organic compound of castor leaves was identified by GC-MS test where is pointed to presence of twenty compound eight of them contain conjugated bonds which represent the condition of the laser dye.Thus, we can say that the *Ricinus communis* L. dye can be used as an active laser medium. In addition to its spectral properties, it is a local dye and is widely available.

Keywords: Fluorescence, *Ricinus communis* L., Dye laser, GC-MS..

INTRODUCTION

In this study we focused on dye laser or so-called organic dye laser because its active medium is organic compound can be fluorescent. Our study includes the study of the absorption and the emission spectrum, i.e. the spectral properties of the local plant, which is the powder of the leaves of the castor plant (*Ricinus communis* L.) after drying,

which is abundant in our country in a certain season, by crushing and dissolving the product in ethanol, methanol and water and the effect of these solvents on the spectral absorption and emission of this dye.Generally the dyes are non-local and can only be obtained by importation and are comparatively expensive so, resorted to prepare a dye of plant castor plant (*Ricinus communis* L.) available and abundant in our country has a high fluorescence and works in the range of visible and ultraviolet. The dye lasers have an important feature of being the first laser can be tunable [1]. The broadly tunable is beginning from ultraviolet to the near infrared. In addition to this the other intrinsic of dye laser is ability to generate high average powers and high pulsed energies in the visible spectrum [2].

Organic dyes are described by a strong absorption band in the visible region of the electromagnetic spectrum that only found in organic compounds which contain an extended system of alternating single and double bonds called conjugated bonds [3]. The long wavelength emitted from these dyes is attributed to the transition from the electronic ground state S_0 to the first excited singlet state S1.The reverse operation $S_1 > S_0$ in charge of the stimulated emission and the spontaneous emission known as fluorescence in dye lasers and because of the transition moment for this process is very high. Therefore, the emission rate is also high (the emission lifetime about nanoseconds) and the dye laser gain may exceed the solid state laser gain several times. The dye molecules are excited typically to higher level in the singlet manifold when the dye laser is pumped with an intense light source (laser or flash-lamp) from which they relax within picoseconds to the lowest vibronic level of S_1 [3]. When an electron moves from the higher vibrational level of S_1 to the lower vibrational level, it would be desirable to remain in it for a suitable time period until it is called to descend to S_0 by the stimulated emission, thus increasing the efficiency of the laser. The dyes show undesirable processes, which reduce the efficiency of fluorescence and thus the efficiency of the laser and are depended in a complex way on the molecular structure of the dye and these processes, are (internal conversion and intersystem crossing) [4].The aim of this study is to prepare a local laser dye at low prices for the production and manufacture of dye lasers used in medical, scientific and industrial applications for their broad spectral range, which extends from the ultraviolet to the infrared.

Energy Levels of Dye

The general form of the typical dye energy levels consists of a broad structure caused by the double distribution of the spin electrons. The energy levels are split into two parts: The first is the singlet states energy levels in which the electronic pair's spin has an inverse spin, its total algebraic equals(S=0) [5]. The second is the triplet states energy levels in which the electronic pair's spin has a parallel spin so that the total algebraic equals(S=1) as shown in Fig. 1.When the electrons in the ground states absorb the energy then will excite, and transferred to the high levels of the singlet and the triplet then spontaneous transmissions occurs between the different energy levels and submits those transitions to the electron spinning base. As an example, the absorption of energy by the electrons of the ground state S_0 and its transfer to the upper state S_1 and then emitted the energy as a spontaneous fluorescence at a rate time of fluorescence is equal to 10^{-8} sec. Some of the undesirable processes in the laser work results in a loss of the laser's output, namely the intersystem crossing and the internal conversion.

Types of Laser Dyes

Laser dyes consist of complex molecules containing a number of ring structures, leading to complex absorption and emission spectra. By virtue of their structures that are chemically similar the laser dyes can be classified into different classes. And from popular examples are the coumarins, xanthenes. The composition of the molecule and the structure has an important effect on spectral emission [3].

Experimental Studies

This includes the materials and equipment that used in this research as well as the information for both the dyes and solvents that used. Two dyes were used, one belonging to the Xanthene Dyes (Rhodamine 6G) and known in terms of the visible range of the spectrum and the near-infrared range and characterized by high photochemical stability. Also known as Rhodamine 590, is broadly used as a lasing medium and as a fluorescence tracer [7] and is generally Constitution of Benzoic Acid, 2 - [6 - (ethylamino) – 3 - (ethylimino) – 2,7 – dimethyl – 3H – xanthen -9-yl] - ethylester, monohydrochloride Rhodamine 590.

The Chemical formula is: $C_{28}H_{31}N_2O_3Cl$
The molecular weight is: 479.02 mol /gm.

The other dye is a local dye obtained from a certain plant paper, the castor plant and its scientific name is *Ricinus communis* L..The (*Ricinus communis* L.) castor plant, belonging to the family Euphorbiaceae [8], is also known as Palma(e) Christi or wonder tree [9]where this plant is available in our country in a particular season where the absorption and emission spectra of this dye were studied with two alcoholic solvents and water. The Phytochemical Constituents for the Preliminary study for R. communis showed presence of alkaloids, steroids, flavonoids, saponins, and glycosides. The dried leaves of R. communis showed the presence of alkaloids, ricinine 0.55% and N-demethyl ricinine flavones glycosides kaempferol-3-O kaempferol-3-O-β-D-glucopyranoside, quercetin xylopyranoside, quercetin-3-O-β-D-glucopyranoside, kaempferol O-β-rutinoside and quercetin-3-O-β- monoterpenoids (1, 8-cineole, camphor and α sesquiterpenoid (β-caryophyllene), quercetin,gallic acid, gentisic acid, rutin, epicatechin and ellagic acid are the main phenolic compounds isolated from leaves [10] as shown in Fig.3. Dissolving the product in ethanol the chemical formula is: C_2H_5OH the molecular weight is: 46.07mol /gm, the chemical formula is: CH_3OH, the molecular weight is: 32.04mol /gm. [11] methanol and water The Chemical formula is: H_2O, the molecular weight is: 18.01508 mol /gm.

Samples Preparation

To prepare the dye solution at a certain concentration, an appropriate amount of castor leaves powder was dissolved in a certain volume of solvent (where the sample was weighed in sensitive balance) once in ethanol and again in methanol according to the following relationship: $m= C\times V\times M/1000$ …….. 1
Where: m is the weight of the dye to get the required concentration (gm), C is the required concentration (gm/mol), V is the volume of solvent in cm^3, M is molecular weight of dye.

The samples were weighed in the sensitive balance after that dissolved; it was filtered with nomination papers to remove the remains of the powder. The samples were placed in UV visible (SHIMADZU UV-1800 spectrophotometer Japan source) to determine the absorption peak then we chose (λ_{max}) from absorption peaks at visible region.After that we put the samples in Fluorescence spectrophotometer (type Agilent Technologies Malaysia source) to taste the emission when excited at that peaks wavelength and to get the fluorescence intensity.And finally the organic compound of castor leaves was identified by GC-MS test.

RESULTS AND DISCUSSION

Form the absorption diagram for our dye we observed that the increasing of concentration due to increase of the absorption intensity which are in agreement with Beer-Lambert law as shown in Fig.4, 5. The absorption spectra are relatively insensitive with the change of solvent same in the other dye Rhodamine 6G as shown in Fig.6. We obtained from our new dye that the laser emission was at red region at the wavelength (660-680) nm in ethanol and methanol but two peaks were observed when the material excited at 411 in low concentration in ethanol and methanol as

shown in Fig 7, 8, 9, 10. The laser emission of Rhodamine 6G dye in ethanol and methanol was in the yellow region at wavelength 582.94 nm, 585.97 nm respectively Fig 11this corresponds to a study Schafer [Schafer 1992] andYariv [Yariv 1975] they found that the laser emission region in the yellow region at wavelength (570-610) nm [12]. Our results are an agreement with Beuttner et al. that the wavelength of Rhodamine 6G at concentration 10^{-4}mol/L in ethanol was at 586 nm and what we obtained was at wavelength 582.94 nm. The shift toward the long wavelength by increasing the concentration due to increase the collisions between the atoms and this result in loss of energy and decrease the self-absorption process [13]. From Fig.11 the spectral range of fluorescence of Rhodamine 6G in methanol was at 585 nm in the visible region while the fluorescence spectra range of our dye was at 411 and 677 which mean the spectral included the violet region and the red region i.e. we can get a greater tunning range of this dye see Fig. 7, 9. The shorter wavelength mean higher energy, and that's what we get when we tested the *Ricinus communis* L. dye by pumping it by diode laser using 200 mw, λ_1=402 nm, λ_2=532 we get a good results in both but a bigger fluorescence at 402 nm as shown in Fig. 12.

GC-MS analysis of the ethanol extract of *Ricinus communis* L. showed the appearance of twenty main peaks and the components corresponding to the peaks were determined as follows. The first peak was determined to be Thieno [2, 3-d] pyrimidine-6-carbonitrile, 2, 5-diamino -4-methylsulfanyl. The second peak was determined to be Benzoic acid, 4-methyl-2-trimethylsilyoxy-, trimethylsilyl ester. The next peaks determined to be 5H-Naphtho[2,3-b]carbazole, Ethanol, Bicyclo[3.1.1]heptane, 2,6,6- trimethyl-,[1R-(1α,2α,5α)], Hexadecanoic acid, methyl ester, 11-Octadecenoic acid, methyl ester, 9, 17-Octadecadienal, (Z)-, Methyl stearate, Nonadecanoic acid, 11-methyl-, methyl ester, Octadecanoic acid, 5,9,13,17-tetramethyl-, methyl ester, [5R-(5R9,*R13,*R1,2 ,-[(*-Benzisothiazole-3-acetic acid, methyl ester, 2-Butenenitrile, 2-chloro-3- (4-methoxyphenyl) -, Tricyclo [7.4.0.0(3,8)] tridec-12-en-2-one, 5,6 - epoxy-4-methyl-1- (2-propynyl)-, 1,4-Naphthalenedione, 2 - (3, 7, 11, 15, 19, 23, 27 - heptamethy l-2,6,10,14,18,22,26-octacosaheptaenyle) -3-methyl, Octasiloxane,1 ,1 ,3 ,3 ,5 ,5 ,7 ,7 ,9 ,9 ,11 ,11 ,13 ,13 ,15 ,15 - hexadecamethyl-, Methyl9,12-heptadecadienoate,Octasiloxane ,1 ,1 ,3 ,3 ,5 ,5 ,7 ,7 ,9 ,9 ,11 ,11 ,13 ,13 ,15 ,15 - hexadecamethyl-, Pyrido[2,3-d]pyrimidine, 4-phenyl, and Vitamine E. Form the results above of GC-MS test we get it we observed there are about eight compound have three double bond or more. The condition of the laser material exist a two double bond or more which called conjugated and this condition agree with our results. These double bonds have a profound effect on the spectral properties of the compound [14]. So, *Ricinus communis* L. material can be used as a dye laser material.

CONCLUSIONS

- We get here a new laser dye cheap, high intensity and wide tuning range.
- Another important discovery is it wide ranges in UV-region which may open a wide range of applications in our life, also the ability by pumping of this dye by pulsed Nitrogen or Ximer lasers which will open a door for another too important application in medicine and technology parts.
- The *Ricinus communis* L. dye tested in the fluorescence spectrophotometer according to absorption peaks it will obtain fluorescence spectra for each exited wavelength between 400 nm to 675 nm.
- Shifted the fluorescence spectra of *Ricinus communis* L. dye in ethanol and methanol toward the long wavelength (red region).
- Fluorescence of *Ricinus communis* L. dye has been experimented using diode laser p=200 mw, λ_1=402 nm (blue laser), λ_2=532 nm (green laser). Violet fluorescence has been observed of blue laser radiation over distance 1 cm in quartz cell. Yellowfluorescence showed of green laser radiation.
- The organic compound of *Ricinus communis* L. leaves was identified by GC-MS test where is showed to presence of twenty compound eight of them contain conjugated bonds which represent the condition of laser material.
- It has been shown that the photochemical stability is very high because it did not cause any damage to the sample during use with stay the fluorescence.

REFERENCES

1. Liao PF, Kelley P. Dye Laser Principles: With Applications. Elsevier; 2012 Dec 2.
2. Duarte FJ. Tunable laser applications.CRC press; 2016 Feb 22.
3. Schäfer FP, editor. Dye lasers. Springer Science & Business Media; 2013 Apr 17.
4. Sorokin PP, Lankard JR. This week's Citation Classic. reason. 1981 Sep 4..
5. NEWG. Dye lasers(Organic dye lasers use as continuously tunable sources of coherent light, discussing molecular energy level systems and transitions). (International School of Quantum Electronics, Course on Physical and Technical Measurements with Lasers, Erice, Italy) 1971 May 8-21 Alta Frequenza (English Edition),41:706-710.
6. Nanakar H. Characterization and optimization of a homemade ring dye laser. Optics & Laser Technology. 2018 Feb 1;99:133-7.
7. Zehentbauer FM, Moretto C, Stephen R, Thevar T, Gilchrist JR, Pokrajac D, Richard KL, Kiefer J. Fluorescence spectroscopy of Rhodamine 6G: concentration and solvent effects. SpectrochimicaActa Part A: Molecular and Biomolecular Spectroscopy. 2014 Mar 5;121:147-51.
8. Hussein, A. O., Hameed, I. H., Jasim, H., & Kareem, M. A. (2015). Determination of alkaloid compounds of *Ricinus communis* by using gas chromatography-mass spectroscopy (GC-MS). Journal of Medicinal Plants Research, 9(10), 349-359.
9. Misra, B., Saha, A., &Mahata, P. P. (2016). RICINUS COMMUNIS: A REVIEW. Journal of Pharma technology, ISSN: 2454-5546.
10. Fallström, S. (2014). *Ricinus communis* L. varietes: Taxonomical description.
11. Al-HadithiAN, Affect the solvent and Paramagnetic atoms in the spectral properties of laser dyes. (A thesis of M.Sc), Applied Science Department, University Technology/Baghdad 1987 Oct22.
12. Al-Ammar K,KazemYH, & Abdulrahman, NH. Study of some optical properties of Rhodamine 6G dye in dye laser. Journal of the University of Babylon 2011 Jul 5; 2(20):614-625.
13. Albrecht C. Joseph R. Lakowicz: Principles of fluorescence spectroscopy. Analytical and Bioanalytical chemistry. 2008 Mar 1;390(5):1223-4.
14. Dawood YZ, Jaber MM. Effect concentration on spectral properties of Rhodamin 6G dye. Journal of College of Education. 2016(5):455-62.

Table 1 stock shift between Absorption and Fluorescence spectral.

Dye	C (mol/L)	Abs. λ_{max}(nm)	Flu. λ_{max}(nm)	Stock Shift
R.Communis L.	High con. (ethanol)	411	677	266
R.Communis L.	Low con.	411	411 ,673	0,262
R.Communis L.	High con.	665	665	0
R.Communis L.	Low con.	665	665	0
R.Communis L.	High con.(methanol)	411	677	266
R.Communis L.	Low con.	411	411,673	0,262
R.Communis L.	High con.	665	665	0
R.Communis L.	Low con.	665	670	5
Rhodamine 6G	10^{-4} (ethanol)	561	598	37
Rhodamine 6G	10^{-5}	561	557	-4
Rhodamine 6G	10^{-4} (methanol)	533	585	52
Rhodamine 6G	10^{-5}	533	551	18

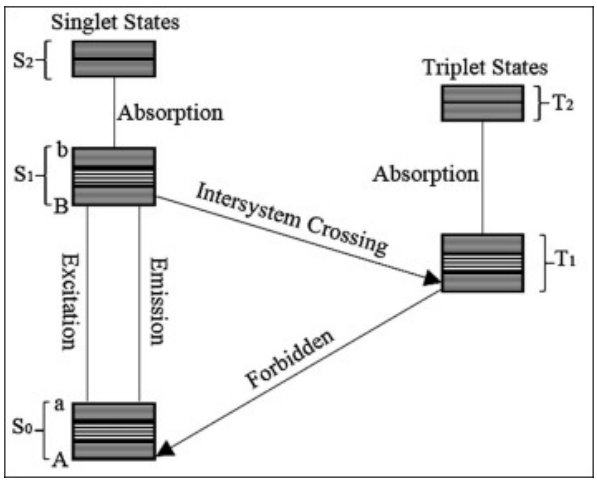

Fig. 1 Energy level diagram for a photoluminescence system [6]

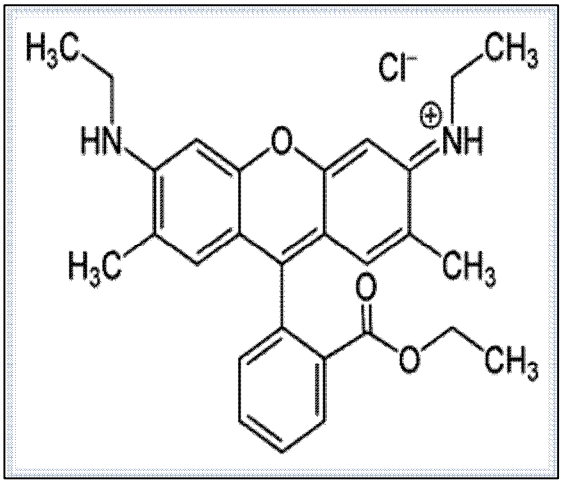

Fig. 2 Chemical structure of Rhodamine 6G

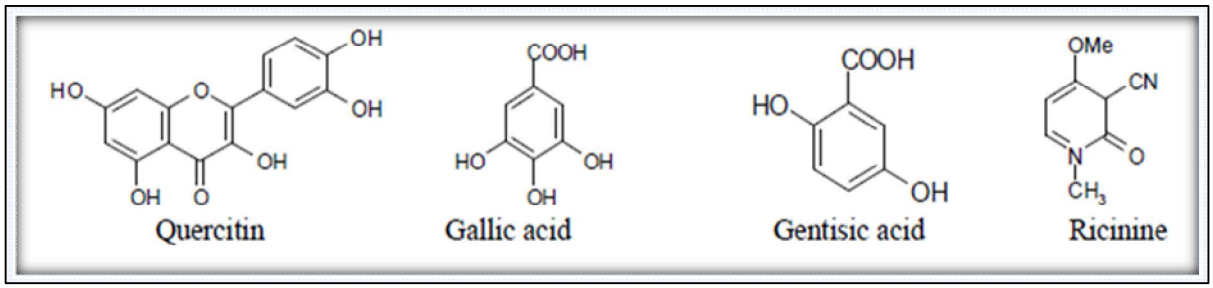

Fig. 3 Some of chemical compound of dried leaves of *R.communis* L.

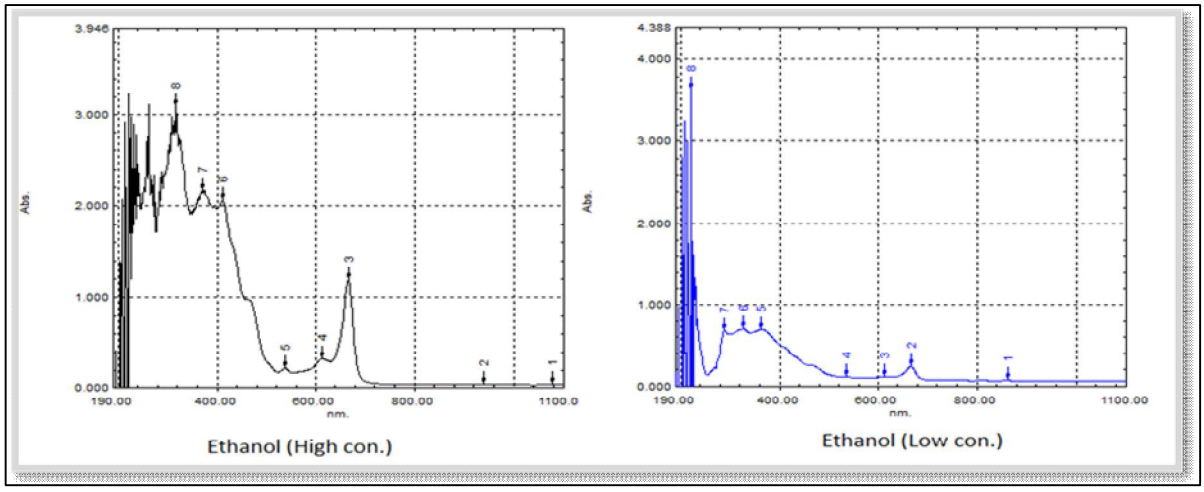

Fig. 4 Absorption diagram of *Ricinus communis* L. in ethanol.

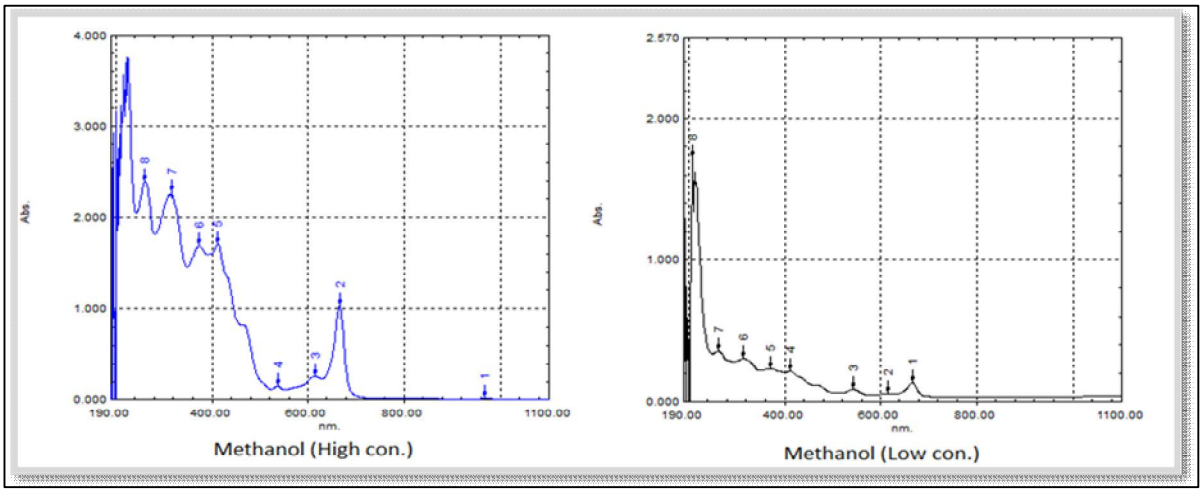

Fig. 5 Absorption diagram of *Ricinus communis* L. in methanol.

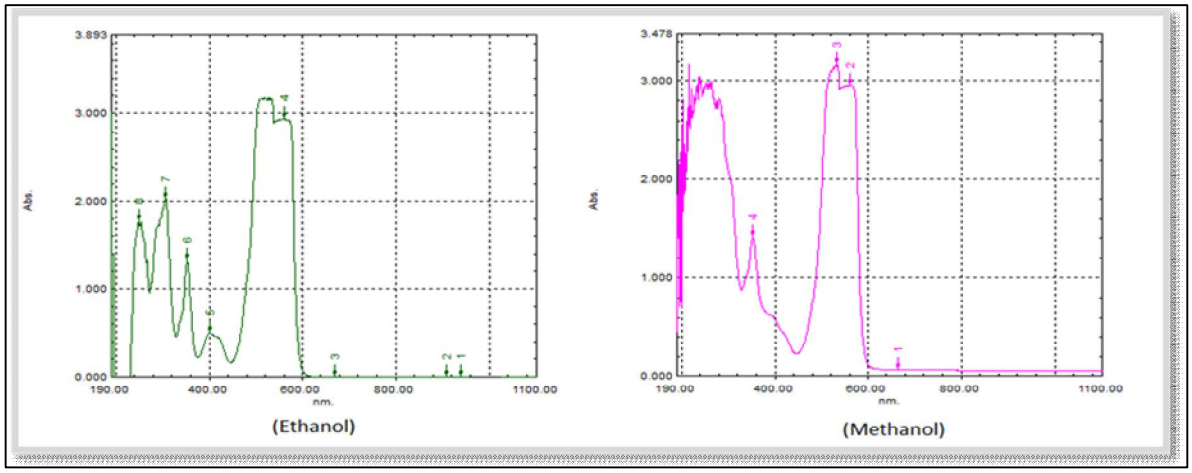

Fig. 6 Absorption diagram of Rhodamine 6G at 10^{-4}mol/L.

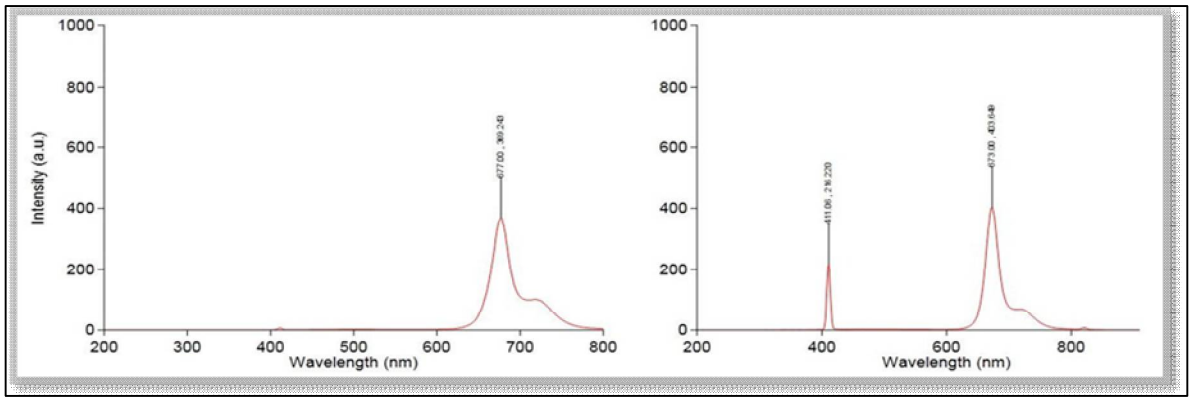

Fig. 7Fluorescence spectra of *Ricinus communis* L. when the material exicted at 411 nm in ethanol (High & Low con.).

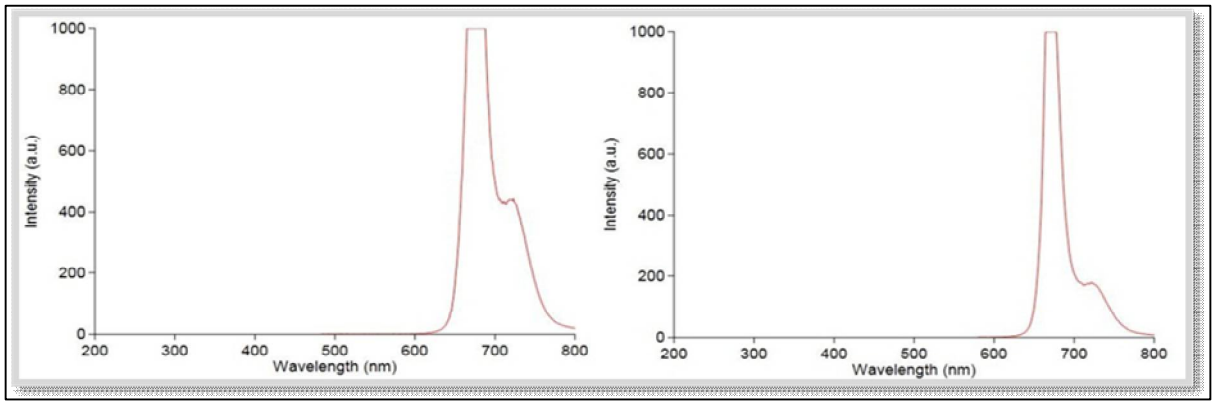

Fig. 8 Fluorescence spectra of *Ricinus communis* L. when the material exicted at 665 nm in ethanol (High & Low con.).

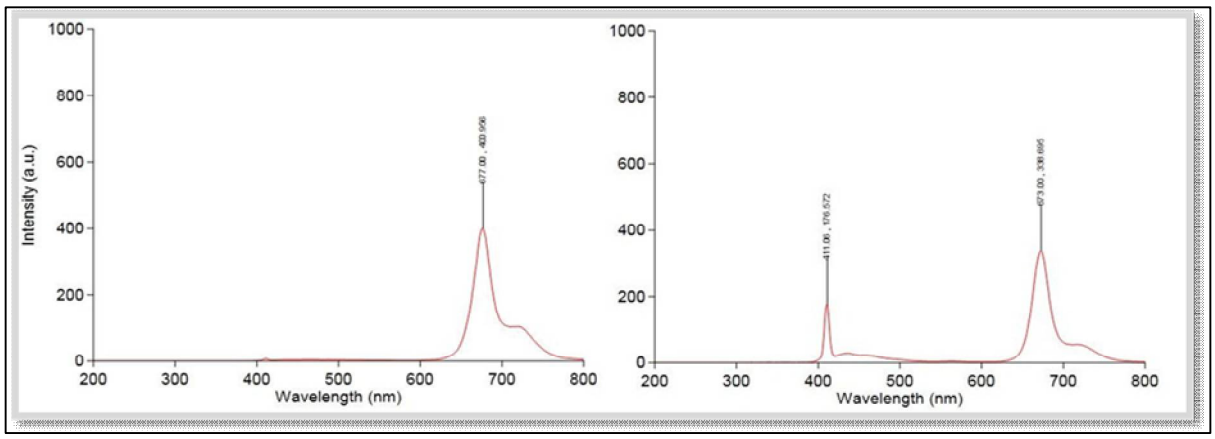

Fig. 9 Fluorescence spectra of *Ricinus communis* L. when the material exicted at 411 nm in methanol (High & Low con.).

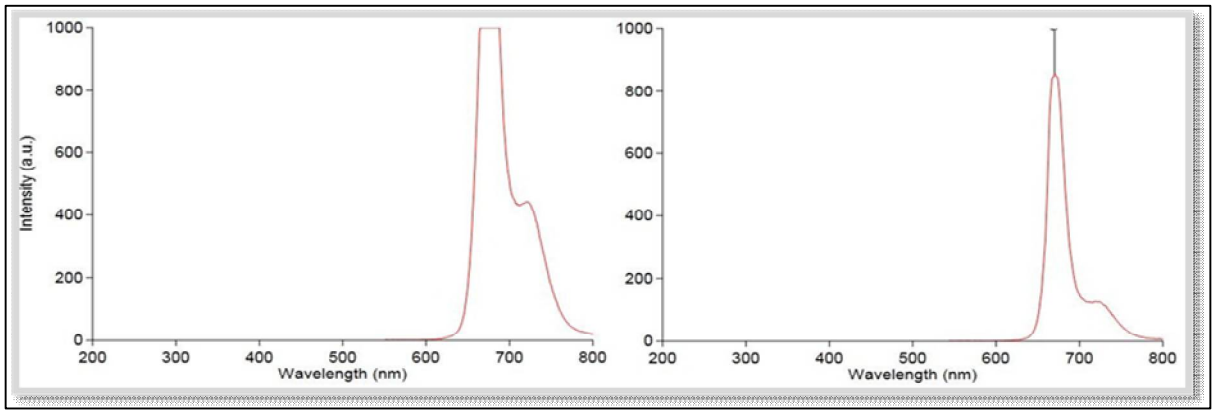

Fig. 10 Fluorescence spectra of *Ricinus communis* L. when the material exicted at 665 nm in methanol (High & Low con.).

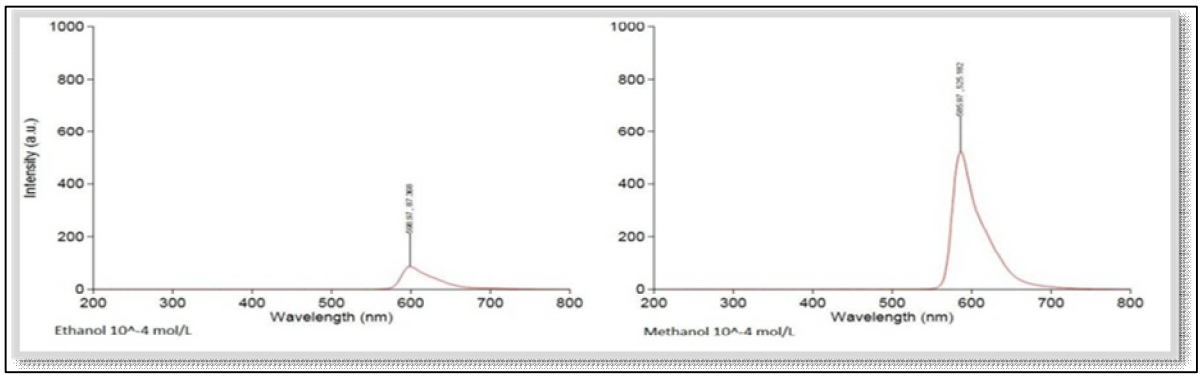

Fig. 11 Fluorescence spectra of Rhodamine 6G at 10^{-4}mol/L

Fig. 12 The experimental fluorescence of new dye with pumping source 200 mw, 402 nm & 532 nm.

Indian Journal of Natural Sciences www.tnsroindia.org.in ©IJONS

Vol.9 /Issue 51 / December / 2018 *International Bimonthly* *ISSN: 0976 – 0997*

RESEARCH ARTICLE

Determination of Some Liver Enzymes Activities in Iraqi Sound Cats

Ahmed NOAMAN AL-ANI[1]*, Kefah ODA AL-JEBURII[2] and Harith ABDUL-HADI AL- HADITHY[3]

[1]Lecturer, Department of Veterinary Internal and Preventive Medicine, College of Veterinary Medicine, University of Baghdad, Baghdad, Iraq.
[2]Professor, Department of Veterinary Internal and Preventive Medicine, College of Veterinary Medicine, University of Baghdad, Baghdad, Iraq.
[3]Ass. Professor Department of Veterinary Internal and Preventive Medicine, College of Veterinary Medicine, University of Baghdad, Baghdad, Iraq.

Received: 20 July 2018 Revised: 25 Aug 2018 Accepted: 27 Sep 2018

***Address for Correspondence**
Ahmed NOAMAN AL-ANI
Lecturer,
Department of Veterinary Internal and Preventive Medicine,
College of Veterinary Medicine,
University of Baghdad,
Baghdad, Iraq.
Email : ahmedana1977@covm.uobaghdad.edu.iq

ABSTRACT

The present study was aimed to evaluate some liver enzymes activities: Alanine amino transferase (ALT), Aspartate amino transferase (AST), Alkaline Phosphatase (ALP) and Gamma glutamyl transferase (GGT) in 60 (30 males and 30 females) Clinically Healthy Iraqi domestic Short Hair Cats (CHIDSHC) in several districts of Baghdad governorate(ALAadamia, ALAmmeria, ALKadraa, ALGazalia, ALYermuk, ALShaab, Abu-Ghraib, Elsaydiea, Hay Tunis, Hay Aljehaad, Hay Elhamraa, Hay Summer, Karrada), at period August 2015 to July 2016. Both sexes grope was aged 1-15 years. Collected blood samples turn in plain tubes toisolated sera that used for the measurement of studied parameters. The ranges and means ± SE of these enzymes were as follows: ALT 4.1 - 80.6 U/L and 12.35 ± 1.09 U/L, AST 6.65 - 68.9 U/L and 25.85 ± U/L, ALP 14.8 – 157 U/L and 60.82 ± 3.99 U/L, and GGT 0.87 – 6.55 U/L and 3.13 ± 0.29 U/L. There weren't any significant differences between males and females in all subgroups, nor between age groups except in ALP. The data can represent the range and mean values for clinically normal cats in Iraq.

Key Words: Serum, ALT, AST, ALP, GGT, Iraqi cats.l,

INTRODUCTION

This study was designed to establish normal liver enzymes levels in serum of Clinically Healthy Iraqi Domestic Short Hair Cats (CHIDSHC) by using the most available methods in Baghdad veterinary laboratories. Cats marked fifty-five breeds, for this clinical pathology each specific Reference interval should be determined [1]. In addition, there are no clearly defined breed barriers available in cats [2]. However, geographical area and feed may alter laboratory results [3,4]. The laboratory methods for determining liver enzymes activity differ from each other, and therefore each Laboratory has to study biochemical ranges and find its normal values [5]. Feline diseases of hepatic and bile tissue can be difficult to diagnose [6].

Detecting of some liver disease In the Cats and dogs showed increase serum (ALT) activity more than (AST) but less sensitive[7]. This related to concentrations of (ALT) in hepatocytes is high, and 25% activity in liver than 5% in muscle [8]. But in other animals (ALT) high due to muscles are larger [9]. In other hand cats, Serum (AST) has only 77 minutes half- life[8], comparable with 3.5 hours in (ALT) [10]. (AST) and (ALT) called leakage enzymes and it develops quickly in serum within hours [7], while induced enzymes need days of Stimulation to production induced enzyme, and leakage enzyme occurs in just alteration of the cell membrane or cell injury that release into serum [9]. Also, may membrane blebs cracks later causing increased leakage enzyme activity [11]. Induced enzymes (ALP) and (GGT) are cholestasis detecting enzymes [9]. In spite of liver (ALP) found in bone, intestine, kidney [5]. hepatic (ALP) in feline had 6 hours half-life [7]. but only 2 minutes intestinal (ALP) [12]. Only liver origin (GGT) present in Feline serum however it found in many organs [5]. (GGT) is attached to the cell membrane so rapid release during Acute liver injury [11]. There are many researches determined these enzymes as reference intervals and showed differentiations among these references due to differentiation of laboratories, laboratories, materials, and methods availability , and breeds were studied. ALT was studied by[1, 13, 14, 15, 16, 17, 18, 19, 20, 21, 22, 23, 24]. Also, AST studied by [13,14, 15, 18, 20, 21, 23, 24, 25,26,27] . Although, ALP was studied by [1, 13,14,15,17,19, 20, 21, 22,24, 26, 28]. While few researchers studied GGT [16, 21,24, 25].

MATERIALS AND METHODS

Animals

Cats were obtained from many areas of Baghdad (ALAedamia, ALAmmeria, ALKadraa, ALGazalia, ALYermuk, ALShaab, Abu-Ghraib, Elsaydiea, Hay Tunis, Hay Aljehaad, Hay Elhamraa, Hay Summer, Karrada), during one year period from August 2015 to July 2016. Sixty clinically healthy domestic shorthair cats (*Feliscatus*), 30 home adapted and 30 stray cats were collected by using safe mash box traps. They were divided into 30 males and 30 females, according to age groups 27 cats aged 1-5 year and 33 cats aged 6-15 year. All cats are under same environment exposures, then examined clinically to choose healthy sound cats and checking mucous membrane for singes of ictric or paleness also palpated liver to find any pain or enlargement.The pregnant cats were excluded [18, 24], as well as home adapted cats with a 1-month history of medical treatment due to oxidative stress which may be motivated liver damage [29].

Sample Collection

Blood samples were collected into plain tubes (without anticoagulant) from the jugular vein of sixty clinically normal cats using 22G needle under sedation by ANESTANE® (Halothan 100% Bb stabilized by 0.01% thymol) to decrease excitement and stress [30]. Blood samples were then centrifuged (3000rpm for 10 minutes) for serum separation and serum was stored at -20 C^0 until use [5]. All serum samples were incubated in 37^{0}c for 30 minutes, Serum ALP, ALT, and AST were assayed by using REFLATRON ®the instrument (Roch trademarks) measured the enzyme's activity kinetically at 567nm as quantitative determination method according to [31]. (GGT) enzyme activity was determined

from serum by using Spectrophotometer at 405nm with colorimetric method [32]. Unit per Liter (U/L) recommended as enzyme activities, it defined as 1µmol of the substrate that catalyzed by an amount of enzyme per minute [33].

Statistical analysis

Collecting and calculating results to get range, mean, and standard error for each group examined by using a computer. Was performed using t-test and significant means were compared at level ($p< 0.05$) according to [34].

RESULTS

The ranges and mean values ± SE of studied liver enzymes activities within serum in total cats,males and females werepresent in Table (1)as follows:ALT 4.1 - 80.6 U/L and 12.35 ± 1.09 U/L. It was 13.88 ± 2.38 U/L in males and 10.82 ± 2.53 U/L in females, AST 6.65 – 68.9 U/L and 25.85 ± 2.143 U/L. 23.548 ± 2.708 U/L and 28.15 ± 3.315 U/L in males and females respectively, ALP 14.9 – 157 U/L and 60.915 ± 3.991 U/L. 65.207 ± 6.132 U/L in males and 56.624 ± 5.094 U/L in females, GGT 0.87 – 6.55 U/L and 3.128 ± 0.285 U/L. 3.323 ± 0.44 U/L and 2.958 ± 0.376 U/L in males and females respectively. There wasn't any significant difference between males and females values.(Table1). The mean values of serum liver enzymes activities in home and stray cats were as follows: ALT10.535 ± 1.24 U/L and 14.161 ± 3.234 U/Lrespectively, AST 23.367 ± 2.47 U/L and 28.331 ± 3.488 U/L, ALP 64.867 ± 6.29 U/L and 56.963 ± 4.917 U/L,and GGT 2.653 ± 0.315 U/L and 3.989 ± 0.509 U/Lrespectively. Furthermore, the liver enzymes activities in normal cats aged 1-5 and 6-15 years were as follows: ALT 11.49 ± 1.63 U/L and 13.05 ± 2.87 U/L respectively,AST 25.74 ± 2.849 U/L and 25.939 ± 3.163 U/L respectively, ALP 72.56 ± 7.2 U/L and 51.391 ± 3.674 U/L and,GGT 3.105 ± 0.462 U/L and 3.1497 ± 0.352 U/L respectively (Table2).There was a significant difference ($p< 0.05$) between the two age groups in serum ALP activity(Table 2).

DISCUSSION

The values were obtained from (CHIDSHC) to provide the lower and upper range limits and means to compare with the relevant studies. Several textbooks recorded liver enzymes within serum [21, 35, 36, 37, 38]. (Table 3). The serum ALT of the present study revealed a lowest lower limit range and a lower upper limit [21, 38], closed to [35, 37], and a higher than [36]. On the other hand, AST enzyme of this work showed the lowest low range limit and higher upper range limit in comparison with [21, 36, 37, 38]. While serum ALP range was higher than ranges that reported by [21, 35, 36, 37, 38]. Lastly, serum GGT activity was higher than [21], While the ranges registered by [37, 38] were within the range of this study. Also, higher range limits reported by [36]compared to this study.Many unremarkable interpretations that might affect the results of liver enzyme activity investigations as the first stage of developing liver problems like hypoxic injury, trauma, and inflammatory diseases [39], and due to liver had fast regeneration that needs to make short time examination tests [40]. Of course, injury to an organ other than liver may release some concentration of these enzymes to the serum.In contrast some time there is an injury to the liver but find normal (ALT, AST, and GGT) activity as in case of cirrhosis[41].

Moreover Kaneko et al. (2008)[37] reported non-significantly higher ALT and AST, and anon significantly lower ALP. So the slight elevation or drop off studied enzymes must not be taken as problem, but liver problem must reach far away from higher limit of known normal range . for example : mild obstruction in bile duct need increase 2-3 fold normal level (ALP) [5], and elevation up to 16 times (GGT) in occlusion bile duct [42].AlsoNorris et al. (2005)[43] determined elevated (ALT) 85-147U/L and elevated (AST) 64-302 U/L as an abnormal range. WhileCorneliys(1970)[40] account moderate necrosis when(ALT) 50-400U/ L, and 400 units for sever.However many researchers appear reported higher mean values for ALT activities [1, 13, 14, 16, 17, 19, 20, 21, 22, 23, 24, 27, 44], also Borku et al.(2007)[15]; and Fresno et al.(2012)[18] whom they reported close range while Arion et al.,(2013); Buckely et al. (2017); Butterwick R. & Markwell P.(1996); Reynolds et al.(2008); and Reynolds et al.(2010) [1, 13, 14, 22, 45] they registered higher ranges in upper and lower

limits both compared to the finding of this study. This fluctuating (ALT) results may back to muscle injury and its incomplete liver-specific [46]. Many factors like some studies Shoorjeh et al. (2012)[23], andMosallanejad et al. (2012)[20]applying treatment, and vaccinated cats as control group This may lead to differing our result. On the other hand, O'Brien et al. (1998)[21] reported more or less similar mean value. moreover Arion et al. (2013); Lawler et al., (2006); Mosallanjad et al. (2012); and Shoorijeh et al., (2012)[13, 20, 23, 26]reported higher mean values. A slightly higher [24, 27] and lower [14] compared to this work levels. However AL-Ani (2013) ; Arion et al., (2013); Butterwick R. & Markwell P. (1996) ; Fresno et al. (2012) ; Krofic et al. (2014) ; and Simsek et al. (2015)[13,14,18,19,24,28]they reported AST activity ranges within our range. Inadequate information of cats exclusion and inclusion criteria may explain cause of these divergences of the references [22].Moreover ,diagnostic methods [4].

Arion et al. (2013); O'Brien et al. (1998) ; and Reynolds et al. (2008)[13, 21, 22] Showed no significant difference ALP activities value while Butterwick R. & Markwell P.(1996); Krofic et al. (2014); Lawler et al. (2006); Mosallanjad et al. (2012); and Simsek et al. (2015)[14,19, 20,24, 26] they documented lower ALP activities in comparison with this findings. That's disagreement may be related to blood sample collecting methods neither from cephalic vein nor jugular vein showed significant difference under level ($p \leq 0.001$) between two sites of vein puncture on (ALP) results [21]. Moreover Reynolds et al. (2008)[22] studied ALP activities indoors and outdoors cats and the mean values non-significantly higher and more or less close to this findings respectively.

ALP activities documented by [1, 22] were higher than the range of this research, this elevation may due to breed differences, because [1] have similar elevation in studied four breeds cats, but[14,19] lower, and [26] within the range of this research.There was a significant ($p < 0.05$) difference found between the two age groups in serum ALP activity (Table 2). That is compatible with Allison (2012), and Levy et al. (2006)[9, 47] who display that adult animals commonly have decreased level serum (ALP) activates than young ones. However Da Silva et al. (2011); and Simsek et al. (2015)[16,24] reported non-significantly higher GGT activities, O'Brien et al. (1998)[21] reported lower GGT activity compared to mean values of this study. On the other hand lower GGT activity range reported by [25] compared to the range of this work, a compatible range with this study was showed by [45] as reference interval, though.However, the observed differences in the values of present investigation compared with the results of other researchers may be attributed to one or more of the following factors; absence of balanced feeding programs, hot weather, stress, and genetic factors. Altunok et al.(2007)[4] Revealed Geographical area ,and diet .as addition individual variation among species as diseases ,stress , fatness [48].

CONCLUSION

In conclusion, our results of (ALP, ALT, AST, and GGT) ranges were as follows: ALP 14.8 – 157 U/L, ALT 4.1 - 80.6 U/L, AST 6.65 - 68.9 U/L, and GGT 0.87 – 6.55 U/L. There weren't any significant differences found between males and females in all subgroups, nor between age groups except in ALP. Most international references claim on the necessity of establishment normal range particular to each region or even laboratory if possible. There were few previous studies found about liver enzymes of Iraqi breed cats. This study simulates the reality of some liver biochemical ranges in Baghdad area according to stress factor that may naturally affect some blood parameters like high weather temperature in a summer season, hormone effect by the duration of day and night, available some material in drinking water. So our results should be represented the clinically healthy Iraqi domestic short hair cats in Baghdad areas, and it must be adopted as a comparative range to future studies for diagnosis liver infection in cats at these areas. Further biochemical study on healthy Iraqi domestic short hair cats is required to monitor the remaining biochemical value.

ACKNOWLEDGMENTS

We are grateful to the Department of Veterinary Internal and Preventive Medicine Laboratory, in College of Veterinary Medicine, University of Baghdad, where the sampling test are made.

REFERENCES

1. Reynolds BS, Concordet RD, Germain CA, Daste T, Boudet K, Lefebvre HB. Breed dependency of reference intervals for plasma biochemical values in cats. J. Vet. Intern. Med. 2010;24:809-818.
2. Menotti-Raymond M, David VA, Pflueger SM. Patterns Of Molecular Genetic Variation Among Cats Breeds. Genomics 2008;91:1-11.
3. AL-Ani AN. Some hematological and biochemical values as relate to anima in local cats. MSc Thesis, University of Baghdad college of veterinary medicine, Baghdad. 2012,53-99.
4. Altunok V, Yazar E, Yuksek N. Selected blood serum elements in van (turkey)cats. Acta. Vet. Brno. 2007;76:171-177.
5. Coles EH. Liver Function. In: Clinical biochemistry of domestic animals, 4th Ed., Vol.7, W.B. Saunders co., 1986, 129-151.
6. Byfield VL, Callahan Clark GE, Turek BJ, Bradley CJ, Rondeau MP. Percutaneous cholecystocentesis in cats with suspected hepatobiliary disease. Journal of feline medicine and surgery, 2017;19(12):1254-1260.
7. Center S. A interpretation of liver enzymes. Vet. Clin. North am small animpract. 2007; 35:225-229.
8. Boyd JW. The Mechanism Relating To Increases In Plasma Enzymes And Isoenzymes In Diseases Of Animals. Vet. Clin. Pathol . 1983;12:9-24.
9. Allison RW. Laboratory evaluation of the liver. In: Anna MT, Weiser G, Allison RW, Campbell T, Veterinary hematology and clinical chemistry, 2nd Ed., Vol. 26, Wjohn wilier and sons.(Eds.), 2012; 401-424.
10. Pappas NJ. Source Of Increased Serum Aspartate And AlaninAminotranferase : Cycloheximide Effect On Carbon Tetrachloride Hepatotoxicity. ClinChimActa .1986;154:181-189.
11. Gores GJ, Herman B, Lemasters JJ. Plasma membrane bleb formation and rupture : a common feature of hepatocelluar injury . Hepatology 1990;11:690-698 .
12. Fernandez NJ, Kidney BA. Alkaline Phosphatase : Beyond The Liver. Vet. Clin. Pathol. 2007;36:223-233.
13. Arion A, Benedek B, Imre M, Stefanut C, Barabasi I, Vlasia A et al. Investigations of metabolic profile in a group of cats during bioequivalence test. Bulletin UASVM, Veterinary medicine. 2013;70(1):1-6.
14. Butterwick R, Markwell P. Changes in the body composition of cats during weight reduction by controlled dietary energy restriction. The veterinary record. 1996;138:354-357.
15. Borku MK, Aydin Y, Ozkanlav Y, Beaz L. Clinical case : Primary hemangiosarcoma in a cat. Revue. Med. Vet. 2007;158(12):603-606.
16. Da silva As, Castro V, Tonin A, Brebdler S, Costa M, jaques J et al. Secnidazole for the treatment of giadiasis in naturally infected cats. Parasitology international. 2011;1: 1-4.
17. Donald JC, Duncan JK. Clinical chemical values for some common laboratory animals. Clinical chemistry . 1980; 26(13):1877-1879.
18. Fresno L, Rodrigues-Gil JE, Rigau T, Pastor J, Riveradelalamo MM. Modulation of the biochemical composition of amniotic and allantoic fluids as control mechanism of feline foetal development. Placenta . 2012; 33:522-527.
19. Krofic M, Tozon N, Nemec A. Plasma and erythrocyte glutathione peroxidase activity , serum selenium concentration , and plasma total antioxidant capacity in cats with iris stage i-iv chronic kidney disease. J. Vet. Intern. Med. 2014; 28:130-136.
20. Mosallanjad B, Avizeh R, Najafzadehverzi V, Pourmahdi M. evaluation of prophylactic and therapeutic effect of silymarine on acute toxicity due to tetracycline sever over dose in cats : A preliminary study. Indian journal of veterinary research , Shiraz University. 2012;13(1):38:16-22.

21. O'Brien M, Murphy G, Lowe AJ. Hematology and clinical chemistry parameters in the cat (felisdomesticus). American society for nutritional sciences. J. Nutr. 1998;128: 2678S–2679S.
22. Reynolds BS, Boudet KG, Germain CA, Braun JD, Lefebvre HP. Determination of reference intervals for plasma biochemical values in clinically normal adult domestic shorthair cats by use of a dry-slide biochemical analyzer. Am. J. Vet. Res. 2008;69:471–477.
23. Shoorijeh SJ, Tamalon A, Vahedi M, Behzadi MA. Hematology and biochemistry alternations due to over dosage of Enroloxacin in cats. Pak. Vet. J. 2012; 32(1):73–76.
24. Simsek O, Arikan S, Cinar M. Reference value for selected hematological and biochemical blood parameters from pregnancy to advanced gestation in angora cats . Turkish of veterinary and animal sciences. 2015;39:29-33.
25. Center S, Crawford M, Guida L, Erb H, King J. A Retrospective study severe hepatic of 77 cats with lipidosis: 1975-1990. Journal of veterinary internal medicine. 1993;7(6):350-359.
26. Lawler FD, chase K, Teckenbrock R, Lark KG. Heritable components of feline hematology, clinical chemistry and acid base profile. Journal of heredity advance access. 2006;10:1093.
27. Xia Z, Man J, Chey Y, He Y, Yu J. Experimental oriental hybrid lilies (Lilium hybrids) poisoning in cats. J. Clinic toxicol. 2013;3:152.
28. AL-Ani AN. Evaluation of some circulating cardiac enzymes concentration in clinically healthy Iraqi cats. Applied science reports. 2013;(4)3:225-228.
29. Öztürk AS, Altuğ N, Köse SI, Öztürk OH. The effects of l-Carnitine in budd-chiari syndrome in a domestic cat . Macedonian veterinary review. 2016;39(1):123-127.
30. Rajan H, Nazifi S, Nayeri K, Sofa F. Effect of 2h anesthesia with halothane on blood cell count and serum biochemical values in sheep and calves. Comparative clinical pathology. 2008;17(1):13-16.
31. Haenseler E. Anew assay for the Reflotron system; Alkalinee Phosphatase activity. In: Poster presented at the medib 97,12th IFCC European congress of clinical chemistry (1997), Basel, Switzerland. 1997.
32. Persijn JP, Vandersilk W. Anew method fore to determination of γ-glutamyltransferase in serum. J. Clin. Chem. Clin. Biochem. 1976;14:421-427.
33. Moss DW, Henderson AR. Principle Of Clinical Enzymology . In: Tietz Fundamentals Of Clinical Chemistry. edited by Burtis C.A. &Ashwood, E.R., 5th ed., W.B. Saunders ,Philadelphia .2001;Pp.157-176..
34. Johnson RA, Wichern DW. Applied multivariate statistical analysis. 6th Ed. Pearson education international. 2007.
35. Jacobs RM, Lumsden JH, Taylor JA. Canine and feline reference values . In: Bonagurajd. et al.(Eds), Kirk's current veterinary therapy XIII: small animal practice. Philadelphia: W.B. Saunders . 2000;1207–1227.
36. Kahn CM, Scott L, susan AE. Serum biochemical reference guides. In :The Merck veterinary manual. 9th Ed. Merck & Co., Inc. &Meral limited, a Merck and Aventis com.usa. 2005.
37. Kaneko JJ, Harvy JW, Bruss ML. Veterinary clinical biochemistry of domestic animals 6th Ed. Elsevier inc. 2008;889-896.
38. Willard MD, Tvedten H. Small animal clinical diagnoses by laboratory methods. 4th Ed. Elsevier. 2004;417-418.
39. Weingarten MA, Sande AA. Acute Liver Failure In Dogs And Cats. J. Of Vet. Emergency And Critical Care . 2015;25(4): 455-473.
40. Corneliys CE. Liver Function In : Clinical Biochemistry Of Domestic Animals , 2nd Ed. Edited By Kaneko JJ, Corneliys CE. Academic Press , New York . 1970;7:161.
41. Elhiblu MA, Dua K, Mohindroo J, Mahajan SK, Sood NK, Dhaliwal PS. Clinic-Hemato-Biochemical Profile Of Dogs With Liver Cirrhosis. Veterinary World . 2015;8(4):487-491.
42. Spano JS, Augast JR, Henderson RA, Dumas MB, Groth AH. Serum Gamma – GlutamyleTranspeptidase Activity In Healthy Cats And Cats With Induced Hepatic Disease . Am. J. Vet. Res. 1983;44:2049-2053.
43. Norris JM, Bosward KL, White JD, Baral RM, Malik R. Clinicopathological Findings Associated With Feline Infectious Peritonitis In Sydney , Australia : 42 Cases (1990-2002). Australian Veterinary Journal . 2005;83(11): 666-673.
44. Schoeman T, Lobetti RG, Jacobson LS, Penzhorn BL. Feline Babesiosis: Signalment, clinical pathology and concurrent infections. Journal of the south african veterinary association. 2001;72(1):4-11.

45. Buckely FI, Mahony O, Webster CR. Adrenal function in cats with cholestatic liver disease. Journal of veterinary diagnostic investigation. 2017;29(1):14–19.
46. Swenson CL, Graves TK. Absence Of Liver Specificity For Canine Alanine Amino Transferase (ALT). Vet. Clin. Pathol. 1997;26:26-28.
47. Levy JK, Crawford PC, Werner LL. Effect of age on reference intervals of serum biochemical values in kittens. J. Am. Vet. Med. Assoc. 2006;288:1033-1037.
48. Kaneko JJ . Clinical Biochemistry Of Domestic Animals. 3rd ed. Academic press , New York. 1980.

Table 1: Liver enzymes activities within the serum of CHIDSHC according to sex (Ranges; Means ± SE).

Liver Enzymes					
		ALT (U/L)	**AST** (U/L)	**ALP** (U/L)	**GGT** (U/L)
Total Cats		4.1 – 80.6 12.348 a ± 1.087 **(n=** 60)	6.65 – 68.9 25.85 a ± 2.143 **(n=** 60)	14.9 – 157 60.915 a ± 3.991 **(n=** 60)	0.87 – 6.55 3.128 a ± 0.285 **(n=** 45)
Gender	**Males**	4.2 – 65.8 13.879 a ± 2.377 (n= 30)	6.92 – 68.8 23.548 a ± 2.708 (n= 30)	15.1 – 157 65.207 a ± 6.132 (n= 30)	0.923 – 6.55 3.323 a ± 0.44 (n= 21)
	Females	4.1 – 80.6 10.817 a ± 2.532 (n= 30)	6.65 – 68.9 28.15 a ± 3.315 (n= 30)	14.9 – 125 56.624 a ± 5.094 (n= 30)	0.87 – 6.54 2.958 a ± 0.376 (n= 24)

No significant differences between different groups at level ($p < 0.05$)
SE= standard error ; SD= standard deviation ; CHIDSHC = clinically healthy Iraqi Domestic short hair cats; U/L= Unit per liter ;ALP= Alkaline phosphatase ; ALT= Alanine amino transferase ; AST= Aspartate amino transferase ; GGT = Gamma glutamyl transferase

Table 2: Liver enzymes activities within the serum of CHIDSHC according to Housing and Age(Ranges; Means ± SE).

Liver Enzymes					
		ALT (U/L)	**AST** (U/L)	**ALP** (U/L)	**GGT** (U/L)
Housing	**Indoor (Home)**	4.1 - 34.2 10.535 a ± 1.24 (n= 30)	6.65 - 68.9 23.367 a ± 2.47 (n= 30)	23.5 – 157 64.867 a ± 6.29 (n= 30)	0.87 - 6.55 2.653 a ± 0.315 (n= 29)
	Outdoor (stray)	4.1 - 80.6 14.161 a ± 3.234 (n= 30)	6.92 - 68.9 28.331a ± 3.488 (n= 30)	14.9 – 125 56.963 a ±4.917 (n= 30)	0.9 - 6.55 3.989a ± 0.509 (n= 16)
Age	**1-5 Year**	4.1 - 34.2 11.485 a ± 1.633 (n= 27)	6.65 - 68.6 25.74 a ± 2.849 (n= 27)	23.5 – 157 72.56 a ± 7.2 (n= 27)	0.87 - 6.54 3.105 a ± 0.462 (n= 22)
	6-15 Year	4.2 - 80.6 13.054 a ± 2.874 (n= 33)	6.92 - 68.9 25.939 a ±3.163 (n= 33)	14.9 – 112 51.391 b ±3.674 (n= 33)	0.9 - 6.55 3.1497a ± 0.352 (n= 23)

Different small letters (a, b) refers to significant differences al level ($p < 0.05$)
SE= standard error ; SD= standard deviation ; CHIDSHC = clinically healthy Iraqi Domestic short hair cats; U/L= Unit per liter ;ALP= Alkaline phosphatase ; ALT= Alanine amino transferase ; AST= Aspartate amino transferase ; GGT = Gamma glutamyl transferase

Table 3: Range Values Of Some Liver Enzymes Activity In Some International Textbook

Liver enzymes	O'Brien et al. 1998	*Jacobs et al. 2000*	Willard & Tvedten 2004	Kahn et al. 2005	*Kaneko* et al. 2008
Serum ALP (U/L)	13.9 - 80.9	13 - 116	4 - 81	12 – 65	25 - 93
Serum ALT (U/L)	47.4 - 97.3	20 - 85	23 - 109	8.3 – 53	6 – 83
Serum AST (U/L)	17.8 - 35.7		14 - 41	9.2 – 40	23 - 43
Serum GGT (U/L)	0.25 - 1.92		1 - 3	1.8 - 12	1.3 – 5.1

Indian Journal of Natural Sciences www.tnsroindia.org.in ©IJONS

Vol.9 /Issue 51 / December / 2018 *International Bimonthly* *ISSN: 0976 – 0997*

RESEARCH ARTICLE

Biochemical and Histological Investigateons of Harderian Gland of Wild Adult Female Rabbits *(Oryctolagus cuniculus f. domestica)* in AL-Qadisiyah Province in Winter Season

Hassaneen Ali Al-Sharoot*, Miran A Alrammahi and Nabeel Abd Murad AL-Mamoori

Department of Anatomy & Histology, College of Veterinary Medicine, University of Al- Qadisiyah, Iraq.

Received: 01 Aug 2018 Revised: 03 Sep 2018 Accepted: 06 Oct 2018

***Address for Correspondence**
Hassaneen Ali Al-Sharoot
Department of Anatomy & Histology,
College of Veterinary Medicine,
University of Al- Qadisiyah, Iraq.
Email : hassaneen.alsharoot@qu.edu.iq

ABSTRACT

The samples used in the study (24) harderian glands (HG) obtained from a total number of (12) adult female rabbit was collected in winter season from a local commercial market of animals in qadisiyah.The histological studies of the gland revealed of parenchyma tissue of Harderian gland was surrounded by acapsule of collagenous connective tissue which divided the gland into lobules. It was made up blood vessels, elastic and reticularfibers, adipose tissue, nerve bundles, collagenous, and parasympathetic ganglia. The result of this study showed the parenchyma of gland consist of tubule alveolar secretory units which characterized by wide and irregular lumen, which were consistent from round nuclei and tall conical cells, these alveoli surrounded by basalcells myoepithelial. The histochemical analysis of the (HG) shows it is a mixed gland. The staining by PAS demonstrated reaction is observed in the basement membrane and the surrounding connective tissue gave positive reaction also the stratified cuboidal epithelial cell layerlinedthe interlobular duct with its apical part showed strong PAS positivegranules.

Key Words: histological, harderian gland, female rabbit

INTRODUCTION

The Harderiangland is external secretion glandin mammals, amphibians, reptiles, rodents, birds.It locatesin orbit ventral and posteromedial to the eyeball extend rostral from the region of the optic nerve,and its anterior extremity emerges its duct, which passes inferior to the origins of the superior and inferior oblique muscles. It is loosely attached to the periorbital fascia so that when the eye is removed, it usually remains in the cavity of the orbit (1).This gland is developed in rodents (guinea pig, golden hamster, mouse, rat, and Mongolian gerbil), lagomorphs (pika and rabbit) (2) some mammals like ahorse, and cows loss this gland (3).

In many mammals, this gland is big in size and consist of porphyrins and lipid that secreted by the duct that opens directlyinto the nictitating membrane (4). The functions of theglandaresurface of the eyeball lubrication and nictitating membrane, secretion of growth hormone, pheromones, photoprotection, osmoregulation and ermoregulation (5) and in some the species, it was work associated with functions of salivary, vomeronasal, nasal (6-12).The rabbit is common animal species that used for economic and laboratory purposes; it is a common model using in many of scientific experiments and teaching section (13). The anatomical location of HG, size, colour and histological stricture varied among different species (14).

In our investigation, histochemical and histological of the harderian gland in female rabbitduring the winter season to establish astandard against which be compared with the different seasons of the year also histochemical characterization of the harderian gland is very important to study the relationships between functions and histological of this glands and provide information about the comparative anatomy of harderian gland in domestic species.

MATERIALS AND METHODS

The Experimental Animals

Twenty-fours amples used in this our study the study. harderian glands (HG) obtained from a total number of (12) adult female rabbit was collected in winter season from a local commercial market of animals in qadisiyah city weight between (2000 -2500) gramat (5-6) month's age. Use Inhalation route for anaesthetised the animals.

Histologic study

Specimens for histology were collected immediately after slaughtered. The specimens were fixed in 10% formalin for about 24 hours. The samples keep at ethyl alcohol (70%) for dehydrated in thegraded series concentration of alcohol, then use xylene for cleared thenput in paraffin wax. Sections of (4– 6) μ as thickness were put on clean glass slides and stained byeosin and haematoxylin to verify general histological structure details by use light and fluorescent microscope. For ademonstration of the glycoprotein used (PAS) stain. Methods were adopted according to **(**16**)**.

RESULTS

Gross inspection of the HG of the female rabbit was bilobedformed of thesmall white lobe and large pink one. The histology and histochemistry of the white and pink lobes of (HG) was an exocrine gland formed of stroma and parenchyma. The stroma formed thin connective tissue capsule surrounding the gland Fig (1).Capsules of connective tissue consisting of blood vessels, adipose tissue, nerve bundles, and parasympathetic ganglia. And there are septa (connective tissue) divided the gland into the lobesand lobulessmall and big Fig (2).The septa were formed of both collagen, reticular fibers and sometimes adipose tissue. The reticular fibers were thick in the septa and formed a thin network between and around the acini. No elastic fiberswere detected in the connective tissue stroma.

Histological examination shows the parenchyma of the harderian glandhad numerous blood vessels and appeared lighter in the staining affinity than the white one inthe winter season Fig (3and4).The parenchyma formed of compound tubuloalveolar secretory units. These secretory units varied in both size and shape. The white lobe was lined with columnar epithelial cells while the parenchyma of the pink lobe was lined with cuboidal epithelial cells with spherical basally situated nuclei Figs. (5 and 6).The duct system of the pink and white lobe consists of the intralobular duct which was lined with simple cuboidal epithelium Fig. (7).These interlobular ducts united to form large duct at the end of both the white and the pink lobes. These ducts drained into the main excretory duct.The latter the main excretory duct opened in the inner surface of the third eyelid. Histochemical studies of the harderian gland

of female rabbits, with PAS stain, revealed faint reaction in the epithelial cells cytoplasm, the basement membrane and the surrounding connective tissue gave strong positive reaction Fig. (8).

DISCUSSION

Gross inspection of the harderian glands of the female rabbit was bilobed organ formed of two lobes that can be distinguished grossly; this finding was in agreement with that of (17).The histological studies of the glandrevealed of parenchyma tissue wassurrounded with a collagenous connective tissue capsule which dividing the gland into lobules,this result confirmed the studies of (17) in rabbit,(18 and 19) in domestic geese, (20)in osprey and (12) in the local chickens**.** It consistedof blood vessels, elastic and reticular fibers, adipose tissue,nerve bundles, parasympathetic ganglia and collagenous (12) in localchickens. Inour report, the septa penetrate the connective tissue of the gland and dividing it for many of lobes and lobules withdifferent sizes thatagreement with (19 and 20). Our result showsthe gland parenchyma composed of units of tubuloalveolar secretory and wide and irregular lumen. Also, itcomposed of round nuclei and tall conical cells, and the alveoli surrounded by basal myoepithelial cells, thisresult similar to (17)in therabbit.

The histochemical analysis of the (HG) revealed is a mixed gland. The PAS staining demonstrated reaction is observed in the basement membrane and the surrounding connective tissue gave positive reaction alsothe interlobular duct was lined with stratified cuboidal epithelial cell layer with its apical part showed strong PAS-positive granules, similar observations are found (21).

REFERENCES

1. Dyce KM, Sack WO, Wensing CJG. Textbook of Veterinary Anatomy. 3rded. Saunders-Elsevier Science, Philadelphia2002; 840 pp.
2. Yousuke Seyama and YasunobuUchijima. Novel function of lipids as a pheromone from the Harderian gland of thegolden hamster. Proc. Jpn. Acad., Ser.2007; B 83
3. Payne, A. P. The Harderian gland: a trecentennial review. J. Anat.1994; 185, 1-49.
4. Sabry I, Al-GhaithL.TheHarderian gland of the Dhub lizard Uromastyxmicrolepis of the Kuwaiti desert: an ultrastructural approach. Tissue and Cell. 2000; 32,71–78.
5. Sabry I, Al Azemi M and Al Ghaith L. The Harderian gland of the heesman's gerbil (Gerbilluscheesmani) of the Kuwaiti desert. Eur.J.Morphol. Apr; 2000; 38(2):97-108.
6. Pradidarcheep W, Asavapongpatana S, Mingsakul T, Poonkhum R, Nilbu-Nga S, Somana R. Microscopic anatomy of the orbital Harderian gland in the Common Tree Shrew (Tupaiaglis). J. Morphol., 2003;255: 328-36.
7. Altunay H, Kozlu T .The fine structure of the Harderian gland in the ostrich (StruthioCamelus). Anat. Histol. Embryol. 2004; 33: 141-45.
8. Marcos HJA, Affanni JM. Anatomy, histology, histochemistry and fine structure of the Harderian gland in the South American armadillo Chaetophractusvillosus (Xenarthra, Mammalia). Anat. Embryol.2005;209: 409-24.
9. Munkeby BH, Smith HJ, Larssen EHW, Bjornerud A, Bjerkas I. Magnetic resonance imaging of the Harderian gland in piglets. J. Anat 2006; 209: 699-705.
10. Khan MZI, Jahan MR, Islam MN, Haque Z, Islam MR, Kon Y. Immunoglobulin (Ig)-containing plasma cells in the Harderian gland in broiler and native chickens of Bangladesh. Tiss. Cell.2007; 39: 141-49.
11. Ortiz GG, Feria-Velasco A, Tarpley RL, Bitzer-Quintero OK, Rosales-Corral SA, Velazquez-Brizuela IE, Lopez-Navarro OG, Reiter RJ. The orbital Harderian gland of the male Atlantic Bottlenose Dolphin (Tursiops truncates): A morphological study. Anat. Histol. Embryol.2007; 36: 209-14.
12. Mobini B. Histological and histochemical studies on the Harderian gland in native chickens. Vet. Med-Czech.2012; 57: 404-409.

13. Hristovl H, Kostoll D, and Vladova D. Topographical anatomy of some abdominal organs in rabbits. *Trakia J. of Sci.* 2006. 4 (3) pp: 7-10.
14. EL-Leithy E.; El-Sakhawy M.A.; Al-SabaaA.;El-Habak H. and Shaheen Y. Seasonal Immunohistochemical Expression of Androgen Receptor (AR) in The Harderian Gland (HG) of Male Rabbit. International Journal of Advanced Research Volume 2015;3, Issue 8, 479-489 .
15. Luna, L. G.Manul of histological staining methods of armed forces institute of pathology.threeedition .New York, U.S.A. 1968; 39-110
16. Drury, R. A. B. and Wallington, E.A. Histological technique. 4th Ed. New York, Toronto Oxford University Press.MMM1980.
17. Sohair A. M. Eltony. A Comparative Study of the Harderian Gland in the Female Rat and Female Rabbit (A Histological, Histochemical, Scanning Electron Microscopic and Morphometric study) Egypt. J. Histol. 2009;Vol. 32, No. 1, June, 46 – 65.
18. Murat Boydak, Mehmet F. Aydin.Histology of the Harderian Gland of Domestic Geese(*Anseranserdomesticus*) ACTA VET. BRNO2009; 78: 199–204.
19. Boydak M, Aydin MF: Histology of the Harderian gland of domestic geese (Anserdomesticus). Acta. Vet. Brno.2009; 78: 199-204.
20. Kozlu T, Bozkurt YA, Altunay H, Sari EK. Histological and Histochemical Studies on the Harderian Gland of the Osprey (Pandion haliaetus). J. Anim. Vet. Adv. 2010;9: 1875-79.
21. Pinard CL, Welss ML, Brighttman AH, Fenwick BW, Davidson HJ. Normal anatomical and histochemical characteristics of the lacrimal glands in the American bison and cattle. Anatomia Histologia Embryologia 2003 b;32(5): 257-262. doi: 10.1046/j.1439-0264.2003.00460.

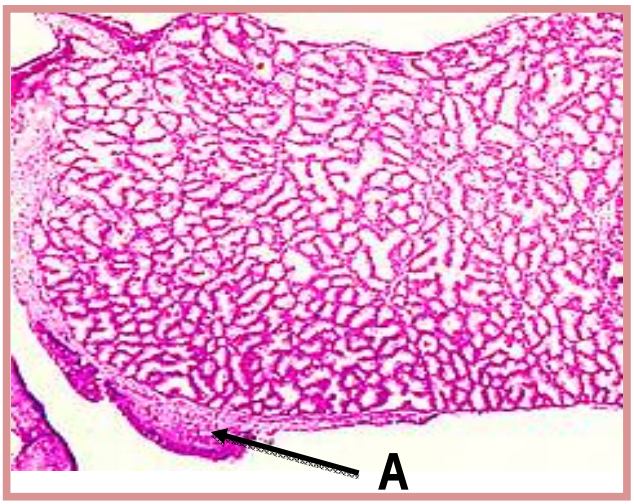

Figure (1): A photomicrograph of harderiangland section in the winter season showing the connective tissue capsule (A) H&E 100x

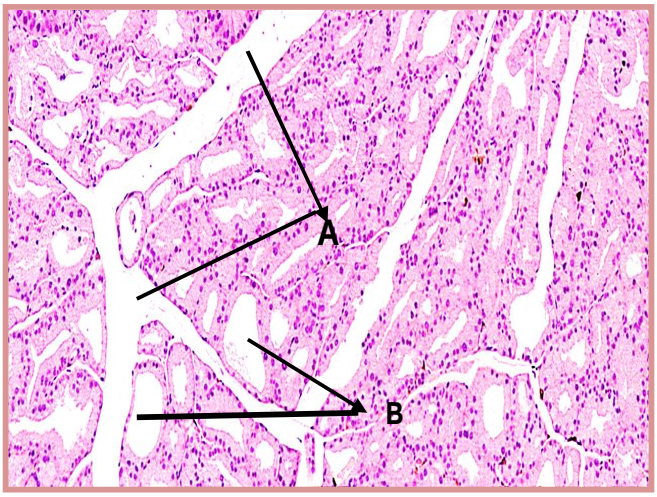

Figure (2): A photomicrograph of harderian gland (HG) section in the winter season showing the connective tissue septa (A) and the lobulation (B) of the gland. H & Estain. 100x

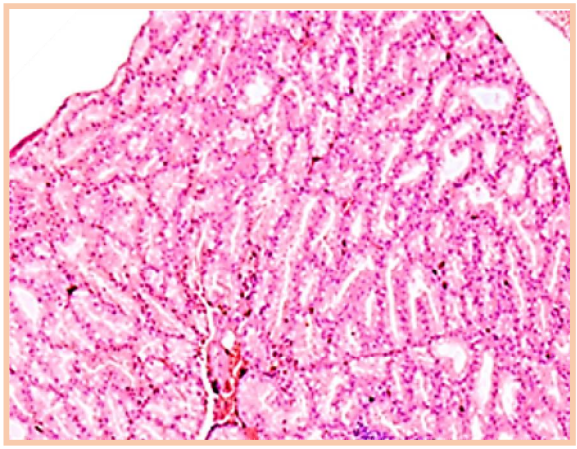

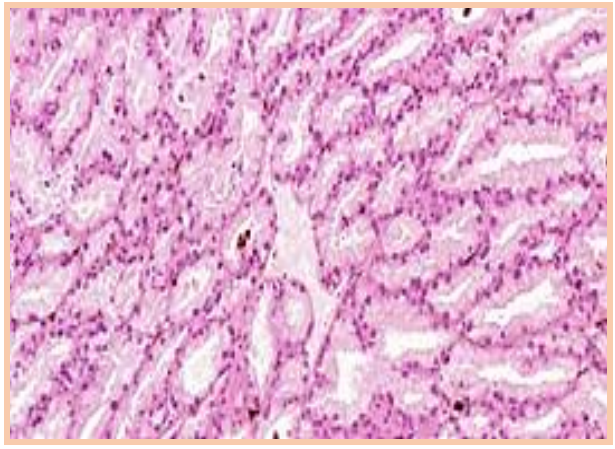

Fig. (3) (pink lobe) 100xFig. (4) (white lobe) 400x

Figure. (3,4): A photomicrograph of harderian gland (HG) in the winter season showing the large pink lobe (PL) and small white lobe (WL). H&E

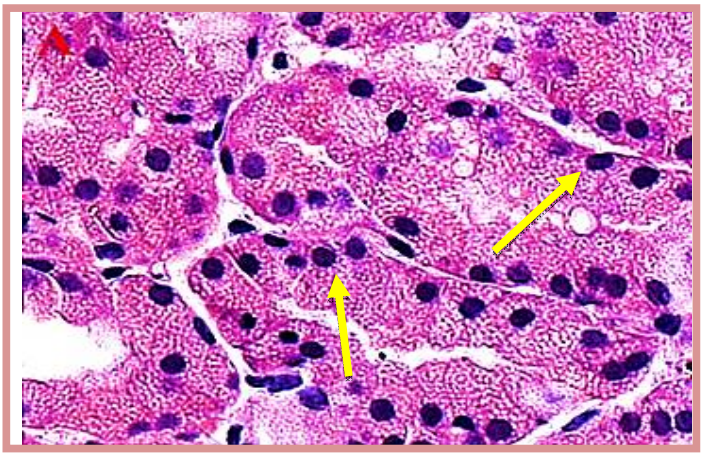

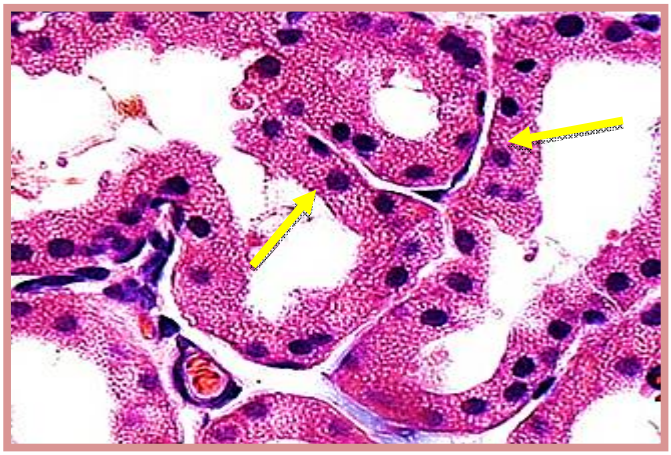

Figure. (5): A photomicrograph of the pink lobe of harderian gland (HG) in the winter season showing the secretory unites lined with a single layer of epithelium variation in both size and shape and presence of buddings (arrow) H&E stain, X 400

Figure (6): A photomicrograph of the white lobe of an adult male rabbitharderian gland (HG) in the winter season showing the secretory unites lined with a singlelayer of epithelium variation in both size and shape and presence of buddings(arrow).H&E stain,400x X 400

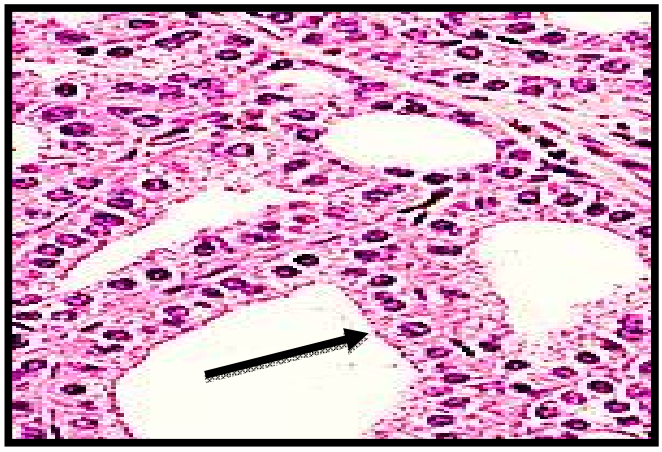

Figure (7): A photomicrograph of the white lobe of an adult female rabbitharderian gland (HG) in the autumn season showing interlobular duct lined withsimple cuboidal epithelium (arrow).H&E stain, X 400

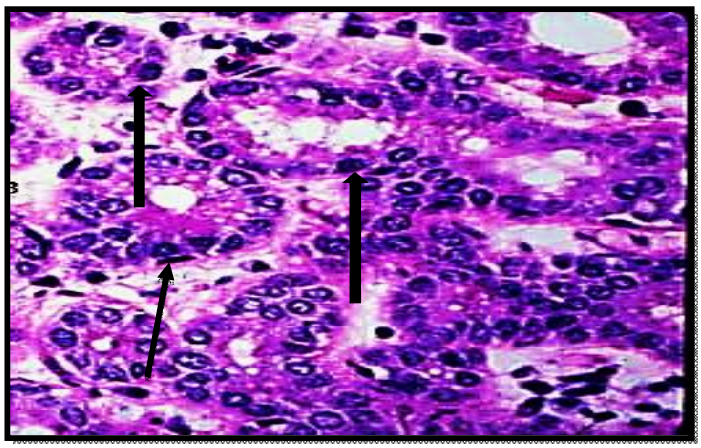

Figure (8): A photomicrograph of the white lobe harderian gland (HG) in the winter season showing strong PAS positive reaction in the basement membrane PAS stain, X 400

Indian Journal of Natural Sciences www.tnsroindia.org.in ©IJONS

Vol.9 /Issue 51 / December / 2018 *International Bimonthly* *ISSN: 0976 – 0997*

RESEARCH ARTICLE

Detail Survey of Water Bodies and Study of pH and Conductivity of Water at Vidavalur Mandalam, Nellore District, Andhra Pradesh, India.

L.Ramu*[1], Supraja Dharini[2] and Narendra.K[3]

[1]Department of Physics, MES College of arts Commerce and Science, Karnataka, India.
[2]Chairperson,TREE foundation,Chennai,Tamil nadu,India
[3]Department of Biology, MES College of arts Commerce and Science, Karnataka, India

Received: 08 Sep 2018 Revised: 10 Oct 2018 Accepted: 12 Nov 2018

***Address for Correspondence**
L.Ramu
Department of Physics,
MES College of arts Commerce and Science,
Karnataka, India.
Email: sarasaramu@gmail.com.

ABSTRACT

Water and its nutrients are supplements for growth of plants. Research was conducted to know the water sources and pH and conductivity is studied 6 diffrent Gunta/Cheruvu for the suitability of growth of plant.

Key words: Nellore District, Chittoor District, pH, GPS, conductivity, toxins, micro and macro nutrient.

INTRODUCTION

Soil and water are nature's gift to nurture the plants, which intern nourishes the biotic community thus ecosystem. Now a day's this soil and water as become pool for various, toxins, syntactic non degradable chemicals, heavy metals etc. Soil has been polluted in all possible means; polluted water being reservoirs of chemicals heavy metals let this chemical percolate into the soil. Polluted air caring all the toxin dust depositing on the soil, Human population explosion, rapid industrialization, increased deforestation, unplanned urbanization, scientific and technological advancement etc. have further hyped all kinds of pollution Narendra Kuppan.(2012).

Water and soil becomes essential for growth of flora and fauna in any habitat as plants becomes the primary source for energy and fundamental of an ecosystem, all living organism are dependent on them no organism can live in opulence if the flora of the habitat is not taken care.Growth of flora depends on water and soil these are the natural resources should be preserved, richness should be documented to know the suitability of plants to be grown in this habitat. There is no documented record for most of these valuable resources in many developing countries. At several instances undefined, unnoticed destruction and human habitation have occurred in the places of this natural habitat of ponds, pools, lakes.These water bodies over human civilization has vanished.Nellore district is called rice bowl of

Andhra Pradesh .Nellore district is known for rice cultivation agriculture is pre dominant because of fertile soil and water resources.This paper details the water body present at Vidavalur Mandalam at Nellore district .

Study Area

Nellore District, the Southernmost Coastal District of Andhra Pradesh lies between 13-30' and 15-6' of the Northern latitude and 70-5' and 80-15' of the Eastern Longitude and extending over an area of 13076 Sq.Kms, accounting for 4.75% of the total area of the state. It is bounded on the north by Prakasam District on the East by Bay of Bengal on the South by Chittoor District and Chengalpattu District of Tamilanadu and on the West by Veligonda Hills which separate it from Kadapa District.Revenue Administratively the District is divided into 46 Mandals, covering Five Revenue Divisions with Head Quarters at Nellore, Gudur, Kavali, Atmakkur and Naidupeta. There are Five Municipalities namely Gudur, Kavali Venkatagiri, Atmakur and Sullurpet and one Municipal Corporation i.e. Nellore.The district broadly 2 natural divisions from North to South. The eastern Half of the District adjoins coastal belt is fairly fertile and the western half of the district has low elevation towards west with large track of low shrub jungles diversified with rocky will stony plains. The Pennar and Swarnamukhi are the principal rivers, besides the streams like Kandaleru and Boggeru.

Climate and Rain fall

The climate of Nellore town is generally dry and salubrious. April and May are the hottest months and the hot winds generally last till the end of the June. As the Bay of Bengal is at s distance of 15 miles from the city, the sea breeze renders the climate of the city moderate both in winter and in summer. The hottest day falls in May with some shift to June during some years. The coolest day falls between the months of December and February. The southwest Monsoon is not very important for this town. Winds are from west and North – West during this season. This town and region depends mainly on the North – East monsoon. The North – East monsoon occurs along the East Coast of India during the month of October and continues till December. This period gives about 60% annual rainfall. The Normal Rainfall of the District is 1080 mm. During the year 2010-11 the actual Rainfall received was 1080 mm.

LAND USE

The total Geographical area of the District is 13.08 lakh Hectares. Of this 20.09% is forest area. The rest is distributed among Barren and Uncultivable Land (10.56%) and Land put into Non Agricultural uses (18.68%). The net area sown forms 25.96% while cultivable waste and fallow (current and old) lands Constitute 17.75%.

MATERIALS AND METHODS

A survey was conducted at Vidavalur Mandalam at Nellore district the survey number hectors of water body was obtained and water sample was collected in non reactive Thermo Scientific Nalgene Certified Wide-Mouth Amber HDPE bottle with Closure and brought to the lab and pH was measured using digital pH meter and conductivity was measured using Elico CM180 conductivity meter.

RESULTS AND DISCUSSION

S.No	Name of Water body	Water Body type	Village / Mandalam	Survey No	Extent in acre	GPS		pH	Conductivity/ µS/cm
						Latitude	Longitude		
1	Water Body 1	Gunta/ Cheruvu	Vidavalur	11/1	1.6	N:14.56.983	E:080.09.702	6.8	1200
2	Water Body 2	Gunta/ Cheruvu	Vidavalur	234	0.67	N:14.38.508	E:080.08.443	6.7	1150
3	Water Body 3	Gunta/ Cheruvu	Vidavalur	787	5.4	N:14.38.760	E:080.08.388	6.1	1115
4	Water Body 4	Gunta/ Cheruvu	Vidavalur	798	0.6	N:14.39.591	E:080.08.327	6.0	1025
5	Water Body 5	Gunta/ Cheruvu	Vidavalur	996/A	0.14	N:14.39.986	E:080.08.389	6.9	1015
6	Water Body 6	Gunta/ Cheruvu	Vidavalur	996/B	4.29	N:14.39.008	E:080.08.391	6.8	1011

Six different Gunta/Cheruvu are identified and GPS was recorded and pH and conductivity was noted. The "p" in the word pH stands for potential and the "H" stands for Hydrogen. A measure of acidity or alkalinity of water soluble substances (pH stands for 'potential of Hydrogen'). A pH value is a number from 1 to 14, with 7 as the middle (neutral) point. Values below 7 indicate acidity above seven alkanity and 7 is neutral. All the water samples examined are neutral. Conductivity of water is the water's ability to conduct electricity. Common ions in water that conduct electrical current include sodium, chloride, calcium, and magnesium. Because dissolved salts and other inorganic chemicals conduct electrical current, conductivity increases as salinity increases.

REFERENCES

1. Raajasubramanian Devarajan , Krishna Ram Hanumappa and NarendraKuppan 2015. The study of change in physico-chemical properties of soil due to cement dust pollution-an hazardous terrorization to ecosystem; Canadian Journal of Pure and Applied Sciences Vol. 9, No. 1.
2. D.Raajasubramanian*etal.*Cement dust pollution on growth and yield attributes of groundnut (Arachishypogaea L.).International Multidisciplinary Research Journal 2011, 1/1:31-36.
3. Rajasubramanian Devarajan*...,et al.*: Study of Morphological and Germination Parameters of Legume Crops *Vigna* L. Treated with Cement Dust, ALEXANDRIA SCIENCE EXCHANGE JOURNAL, VOL. 39, No.3. JULY-SEPTEMBER 2018.
4. Rajasubramanian *et al.*: Cement Establishments and Process at Ariyalur, the Cement City of India, IJEP 38 (9) : 779-786 (2018).
5. Rajasubramanian *et al.*: Study Of Bio-Diversity In Ariyalur, Cement City Of India And Impact Of Cement Dust Pollution On Some Important Agricultural Crops, International Journal on Biological Sciences 9 (1) : 45-53, April Special Issue 2018

Indian Journal of Natural Sciences www.tnsroindia.org.in ©IJONS

Vol.9 /Issue 51 / December / 2018 *International Bimonthly* *ISSN: 0976 – 0997*

RESEARCH ARTICLE

Effect of Betaine and or Acrylamide on Serum Lipids Profile and Antioxidant Status of Female Rats

Sadiq J.Ramadhan* and Khalisa K. Khudair

Department of Physiology, Biochemistry and Pharmacology, College of Veterinary Medicine, University of Baghdad, Iraq

Received: 02 Aug 2018 Revised: 04 Sep 2018 Accepted: 06 Oct 2018

***Address for Correspondence**
Sadiq J.Ramadhan
Department of Physiology,
Biochemistry and Pharmacology,
College of Veterinary Medicine,
University of Baghdad, Iraq.
E- mail: khalisakhadim0@gmail.com

ABSTRACT

This study was designed to evaluate the ameliorative role of betaine on dyslipidemia and oxidative stress induced by acrylamide in female rats. Thirty two (32) adult female rats were randomly and equally divided into four groups (G1, G2, G3 and G4) and were treated for (65) days as following: Group G1 (Control group), G2: rats were intubated 250mg/kg B.W of betaine; animals in group G3 were intubated 1mg/kg B.W of acrylamide; In addition to acrylamide, 250mg/kg B.W of betaine were administered orally to rats in groups G4. Fasting (8-12 hrs.) blood samples were collected by cardio puncture technique at the end of experiments and serum were collected for measuring the following parameters: serum lipid profile including: total cholesterol (TC), triacylglycerol (TAG), cholesterol in High density Lipoprotein (HDL-c), Low density lipoprotein (LDL-c) and very low density lipoprotein (VLDL-c) concentrations; antioxidant status including Serum reduced glutathione (GSH) and malondialdehyde (MDA) concentration. The protective (hypolipidemic) role of betaine was clarified in groups (G2) manifested by hypocholesterolemia, significant decrease ($P<0.05$) in serum, TAG, LDL-c, and VLDL-c concentration with significant elevation ($P<0.05$) in serum HDL-c concentration and its antioxidative effect manifested by significant decrease ($P<0.05$) in serum MDA and elevation in GSH concentration. On conclusion the results of herein study illustrated the deleterious (dyslipidemia and oxidative stress) effect of acrylamide and documented hypolipidemic and antioxidant effect of betaine.

Key words: Betaine, Acrylamide, Malondialdehyde, Lipid profile, Female rats.

INTRODUCTION

Lipotropic agents are factors are substances that provide an effective nutritional strategy to decrease the evidence metabolic high energy diet (1). These agents hosted the removal of fats from liver and decrease fats deposition in liver in ports, due to stimulating the liberation of lipid from liver (2) Betaine, Oxibetaine, choline, inositol, lecithin, methionine, folic acid and B12 are major lipotropic agent (3).Betaine that serves as an effective methyl donor is commonly used in animals and human beings for the purpose of sparing dietary methionine, and helping to treat homocysteinaemia (4,5).Betaine is a powerful osmostress protectant (6)it plays a vital role in the integrity of cell membranes, methylation reactions and memory development (7).Betaine might have potential to improve adipose tissue function (8, 9),In addition to its antiproliferative effects(10).Betaine supplementation with ascorbic acid, decrease mortality and increase productivity of broiler chicken (11). It may also exert free-radical- scavenging ability against lipid peroxidation(12), it could activate AMP-activated protein kinase to reduce lipid synthesis and fat accumulation in the liver and to improve nonalcoholic fatty liver disease (13,3).Since the oxidative stress is a major factor in liver injury initiation (14), previous studies have suggested the hepatoprotective activity of Betaine may be related to its antioxidant capacity to protect hepatocyte from free radicals (12). Betaine decreases lipid peroxidation in the breast muscles of broiler chickens, and, hence, the quality of broiler meat (12) and against chemicals-induced liver fibrosis (15).

Acrylamide (AA) (CH_2=CHCONH_2) is a widely used industrial chemical. It is a white, odorless, crystalline solid at room temperature,used worldwide for the synthesis of polyacrylamide and other polymers, is also manufactured for a number of commercial and industrial uses (16).The main source of acrylamide in human diet are fried potatoes products (17), cereal products, black olive , roasted almonds, cocoa powder and chocolate. Tobacco smoke may be another significant source of exposure to acrylamide (18,19,20).In 2002, there was an alarming report from Swedish National Food Administration revealed the occurrence of ACR toxicity at the levels up to 3 mg/kg in heated starchy plant-derived foods as a result of a reaction between asparagine and reducing sugars via Mallard reaction(21, 22). The average daily intake of ACR for adults is approximately 0.3-0.8 μg/kg body weight (23,24, 25).Acrylamide appears to be metabolized into glycidamide via P450 2E1 (26). AA and glycidamide can form covalent adducts with hemoglobin leading to dysfunction of O2 transport causing hypoxia that lead to vascular disturbance (27). They also can form adduct with DNA and different functional groups of proteins like SH, inducing gene mutation and chromosomalaberration (28, 29).

Clinical manifestations due exposure to AA depend on the dose, duration, and frequency of contact. Acrylamide is classified as an extremely hazardous substance in the United States as defined in Section 302 of the U.S., AAis oftencontain traces of toxic monomers (30), therefore it has been linked to exhibit carcinogenicity (31, 32),neurotoxicity(33, 34), genotoxicity (35) and hasadverse effects on male reproduction (36, 37), furthermore, it is able to increase lipid peroxidation (LPO) and thereby, induced oxidative stress (38, 39, 40). The lifelong exposure of people to AA at low intake levels through food smoking and environments has raised concerns regarding its potential health effects. In the present study, an attempt was made to assess the beneficial effects of Betaine on AA with respect to changes in lipid profile and antioxidant status in AA treated female rats.

MATERIALS AND METHODS

Albino Wister rats (aged 8-9 weeks and weighted 200±10g). Were used in this investigation,animals in all stages of the experiment were housed in plastic cages in conditioned room (22-25˚C) for the period from January 2018 to march 2018 providing daily light of twelve hours (7.00 to 19.00) and twelve hours night cycle. They were left for ten days for adaptation with the experimental conditions. Animals had free access to water and standard pellet diet along the experiment.Thirty two adultfemale rats were randomly and equally divided into four following groups (8 rat/group) and treated daily for (65) days as below:Group G1: Animal in this group were received ordinary distal water served

as control group,G2: rats were intubated 250mg/kg B.W of betaine; animals in group G3 were intubated 1mg/kg B.W of acrylamide; In addition to acrylamide, 250mg/kg B.W of betaine were administered orally to rats in groups G4. Fasting (8-12 hrs.) blood samples were collected at the end of the experiment by cardiac puncture technique from rats anesthetized by intra muscular injection of Ketamine-HCL 90mg/Kg B.W. and Xylazine 40mg/kg B.W.,blood sample were kept in tube not more than 4 hours followed by centrifugation for 15 minutes at 3000 rpm. Serum were isolated and frozen at -20°C until analysis for measuring the following parameters.Determination of (a) total cholesterol (TC) concentration was using total cholesterol kit(Linear chemicals S.L, Spain), (b) serum triacylglycerol (TAG) concentration using triacylglycerol kit(Linear chemicals S.L, Spain), (c) serum high density lipoprotein (HDL-c) concentration using HDL – cholesterol kit (Linear chemicals S.L, Spain). Respectively (d) Serum very low density lipoprotein (VLDL-c) concentration and (e) serum low density lipoprotein (LDL-c) concentration according to (41). Serum GSH and MDA concentration were measured according to (42) and (43) respectively Statistical analysis of data was performed on the basis of one-Way Analysis of Variance (ANOVA) using a significant level of ($P<0.05$). Specific group differences were determined using least significant differences (LSD) as described by (44).

RESULTS

Effect of Betaine administration on serum lipid profile in Acrylamide treated rats

Figures (1 → 5), Illustrates the mean values of serum lipid profile concentration in control & treated groups after (65) day of treatment. While there were non-significant ($P>0.05$) difference in serum TC concentration in all groups at the end of the experiment, significant decrease ($P<0.05$) in serum TAG concentration was observed after combined intubation of both Betaine and Acrylamide, (75.30 ± 5.42) comparing to the value in AA treated group (137.90 ± 9.52). Besides serum VLDL-C concentration showed same changes that observed in TAG with mean value of (19.20 ± 1.63) (13.70 ± 0.88) (27.50 ± 2.75) & (15.00 ± 0.48) for groups G1, G2, G3, & G4 respectively. The same table also showed that oral intubation of Betaine showed significant decrease ($P<0.05$) in serum LDL-C concentration in group G2 (4.90 ± 0.26) compared to the values in other treated groups & control. Besides, combination of Betaine & Acrylamide (group G4) caused significant decrease ($P<0.05$) in serum LDL-C concentration compared to the value in control (24.70 ± 2.48), and G3 (34.40 ± 2.71) group, while the values of serum HDL-C concentration showed significant elevation ($P<0.05$) in G2 (103.40 ± 7.21) and G4 (92.80 ± 9.02) compared to the value in G3 (68.50 ± 7.46) and G1 (84.30 ± 4.39).

Effect of Betaine administration on serum glutathione (GSH) and malondialdehyde (MDA) concentration in Acrylamide treated rats

The result in figure (6 and 7), explained the mean values of serum GSH, MDA concentration control & treated groups along the experimental period. Significant decrease ($P<0.05$) in serum GSH concentration were observed after Acrylamide administration (13.9 ± 0.18) compared to the value in G2 (25.2 ± 0.90) & G4 (21.6 ± 0.86) which showed significant elevation. Significant ($P<0.05$) elevation in serum MDA concentration were observed in G3 (AA) group with mean value of (12.75 ± 0.37), compared to the value in Betaine (G2), Betaine & Acrylamide (G4) & control group with mean value of (8.63 ± 0.26), (8.89 ± 0.52) and (9.19 ± 0.33) respectively.

DISCUSSION

Effect of betaine, Acrylamide and combination of both in rat on serum lipid profile

Betaine and lipid profile

Betaine intubation in here in study has been found to be inversely correlated to a case of dyslipidemia, and positively correlated to HDL cholesterol concentration. Betaine increased plasma HDL which may reflect the favorable effects of Betaine on liver function-related metabolic metabolism in Asian population (45).The positive effects of Betaine on lipid metabolism have been attributed to the fact that it is an important methyl donor, resulting in a considerable increase in hepatic SAM concentrations (46, 47, 48). The increased SAM availability is thought to regulate phosphatidylcholine (PC) synthesis by PEMT and this normalizes VLDL production rates (49). Further investigations found that Betaine supplementation could decrease hepatic triglyceride accumulation(50). Betaine may also reduce uptake of triglycerides from circulating lipoproteins by decreasing the mRNA expression of lipoprotein lipase (51, 52).Furthermore, betaine treatment significantly suppressed hepatic DGAT1 and DGAT2 which is a rate-limiting enzyme in TG synthesis (53) and thus provides hepatic protection against TG accumulation via reduction of TG synthesis in the alcohol-fed rats (54). Besides, it can be inferred that Betaine affected fatty acid oxidation in muscle via activating AMPK and up-regulated PPARα (a nuclear receptor, activated by fatty acids), and carnitine palmitoyl transferase- 1 (CPT1) gene expression (55, 56, 57), and thus preventing fat accumulation in liver (50).

Acrylamide and lipid profile

The data obtained from this study regarding the effect of AA on serum lipid profile (significant increase in serum TC and TAG with significant depression in serum HDL-C concentration) is compatibly inconsistent to those obtained by (58, 59, 60, 61, 62)on their study on rats using different concentration and different periods.On the contrary, the finding of the current study is in agreement with (63, 61).Consequently, the results can be explained by the AA involvement in lipid peroxidation (58, 64). High plasma oxidative stress markers positively correlated with elevated plasma triglycerides and inversely correlated with low HDL (65). The present studies document this suggestion.The expected IR induced after AA exposure (66), may lead to an atherogenic dyslipidemia through suppression of lipolysisthrough inhibition of lipoprotein lipase anddecline in VLDL clearance in adipocyte attributed to impairment in insulin signaling (67). It also elevated levels of free fatty acids (FFA) in the liver that serves as a substrate for the synthesis of TAG leading to hyper triacyglycerieldemia. The FFA also stabilizes Apo B (the major apoprotein of VLDL particle) production leading to fatty liver and atherogenic dyslipidemia (68).Significant increase in serum cholesterol, LDL-C and depression in HDL- C concentration was recorded following supplementation with AA in (79).

Effect of betaine, Acrylamide and combination of both in rat on Antioxidant status

Betaine and antioxidants

The current study indicated the antioxidant activity of betaine manifested by significant elevation in serum glutathione and reduction in MDA concentration. Earlier reports (70, 71) indicated its antioxidants effectBetaine exerts its antioxidant properties through its ability to scavenge free radicals (12), or by increasing the activity of antioxidases mainly SOD (72, 12, 73). Other studies showed no change in the activity of antioxidases was observed after treatment with BET (74, 75). In conclusion, the antioxidant mechanism of BET was found to enhance nonenzymatic antioxidant defenses via the methionine–homocysteine cycle and form a protective membrane around cells (76). BET is a precursor of S-adenosylmethionine (SAM), which contributes to an increase in the supply of substrate needed for the synthesis of GSH (77, 48). Besides, Experimental evidence suggests that SAM has direct antioxidant activity via ROS scavenging and chelation of iron ions used to inhibit hydroxyl radical generation (48). Furthermore, SAM is more effective than GSH in directly scavenging the hydroxyl radical (78). It might play a role as an antioxidant under conditions of persistent oxidative stress (79).

Acrylamide and antioxidant status

The current data showed a significant increase of MDA and decrease in GSH concentrations as a result of oxidative stress and an excess production of ROS probably generated by AA, which is inconsistent with the previous reports (80, 81,82,83,84,). An overload of ROS is known to modify proteins and to generate LPO products and markers of oxidative injury. Acrylamide treatment induced a rise of protein carbonyls and hydrogen peroxide levels suggesting the dysfunction of the mitochondrial respiratory chain. According to (85), AA caused changes in oxidative status and mitochondrial function including the excessive ROS generation, function of electron transport chain (ETC) and membrane permeability (86).Acrylamide is oxidized to glycidamide and then conjugate with GSH, such conjugation could explain the observed redaction in GSH (87, 88). Also, it has been shown that AA can create apoptosis as a result of oxidative stress (89).

REFERENCES

1. Leeson, S. and Summers, J.D. (2005). Commercial Poultry Nutrition, third ed. Nottingham Univ. Press, Nottinghan, UK.
2. Wen, C.; Chen, X.; Chen, G.Y.; Wu, P.; Chen, Y.P.; Zhou, Y.M. and Wang, T. (2014). Methionine improves breast muscle growth and alters myogenic gene expression in broilers. J. Anim. Sci. 94:1068-1073.
3. Rajdl, D.; Racek J.; Trefil, L.; Stehlik, P.; Dobra J. and Babuska V. (2016). Effect of Folic Acid, Betaine, Vitamin B6, and Vitamin B12 on Homocysteine and Dimethylglycine Levels in Middle-Aged Men Drinking White Wine. US National Library of Medicine National Institutes of Health v.8(1).
4. Bidulescu, A.; Chambless, L. E.; Siega-Riz, A. M.; Zeisel, S. H. and Heiss, G. (2007). "Usual choline and betaine dietary intake and incident coronary heart disease: the Atherosclerosis Risk in Communities (ARIC) Study," BMC Cardiovascular Disorders, vol. 7(20).
5. Cholewa, JM, Guimara˜es-Ferreira L&Zanchi NE (2014). Effects of betaine on performance and body composition: a review of recent findings and potential mechanisms. Amino Acids 46, 1785 – 1793.
6. Bremer, E. (2014).Liberate and grab it, ingest and digest it: the gbdrregulon of the pathogen pseudomonas aeruginosa. J. Bacteriol. 196(1):3–6.
7. Hogeveen, M,;Heijer M, ;Semmekrot BA,; Sporken JM; Ueland PM and Blom HJ. (2013).Umbilical choline and related methylamines betaine and dimethylglycine in relation to birth weight. Pediatr Res., 73:783–787.
8. Wang, Z, Yao T, Pini M. (2010). Betaine improved adipose tissue function in mice fed a high-fat diet: a mechanism for hepatoprotective effect of betaine in nonalcoholic fatty liver disease. Am J PhysiolGastrointest Liver Physiol 298, G634 – G642.
9. Deminice, R, Da Silva, RP, Lamarre, SG, Kelly, KB, Jacobs, RL, Brosnan, ME, (2015). Betaine supplementation prevents fatty liver induced by a high-fat diet: effects on one-carbon metabolism. Amino Acids, 47(4):839–846.
10. Lee, I. (2015). Betaine is a positive regulator of mitochondrial respiration. Biochemical and Biophysical Research Communications. ;456(2):621–625.
11. Ayo, J. O.; Egbuniwe, I.; Kawu, M. U. and Sinkalu V. O. (2014). Ameliorative effects of betaine and ascorbic acid administration to broiler chickens during the hot-dry season in Zaria: A review. African Journal of Biotechnology.Vol. 13(23), pp. 2295-2306.
12. Alirezaei, M.; Gheisari, H. R.; Ranjbar, V. R. and Hajibemani, A. (2012). Betaine: a promising antioxidant agent for enhancement of broiler meat quality Br. Poult. Sci., 53, 699– 707.
13. Kathirvel, E., Morgan, K., Nandgiri, G.,Sandoval, B.C.,Cau- dill, M.A., Bottiglieri, T., French, S.W. and Morgan, T.R. (2010). Betaine improves nonalcoholic fatty liver and associ- ated hepatic insulin resistance: a potential mechanism for hepatoprotectionby betaine. Am. J. Physiol. Gastrointest. Liver Physiol., 299,G1068-G1077.
14. Lozovoy, M. A.; Simão, A. N. and Panis. C. (2011). "Oxidative stress is associated with liver damage, inflammatory status, and corticosteroid therapy in patients with systemic lupus erythematosus," Lupus, vol. 20, no. 12, pp. 1250–1259.

15. Kim, S. K.; Seo,J. M.; Chae,Y. R.; Jung,Y. S.; Park,J. H. and Y. C. Kim, (2009). "Alleviation of dimethylnitrosamine-induced liver injury and fibrosis by betaine supplementation in rats," Chemico-Biological Interactions, vol. 177, no. 3, pp. 204–211.
16. Prabu, C. S. and Thatheyus, A. J. (2007). Biodegradation of acrylamide employing free and im- mobilized cells of Pseudomonas aeruginosa. International Biodeterioration and Biode- gradation. , 60-69.
17. Fang, J, Liang, CL, Jia XD, Li, N. (2014). Immunotoxicity of Acrylamide in Female BALB/c Mice. Biomed Environ Sci;27:401-9.
18. Amrein, T.; Lukac, H.; Anders, L. and Amado, R. (2005). Acrylamide in Roasted Almonds and Hazelnuts. J Agric Food Chem., 53(20): 7819-7825.
19. Moiska, H.; Gielecinska, I. and Cendrowski, A. (2016). Acrylamide content in cigarette mainstream smoke and estimation of exposure to acrylamide from tobacco smoke in Poland. Ann Agric Environ Med., 23(30: 456-461.
20. Raters, M. (2018). Acrylamide in cocoa: a servey of acrylamide levels in cocoa and cocoa products sourced from the German market. Eur Food Res Technol., 244 (8): 1381-1388.
21. Mottram, D. S, Wedzicha, B. L. and Dodson, A. T.(2002). Acrylamide is formed in the Mail- lard reaction. Nature., 419-448.
22. International Food Safety Authorities Network (INFOSAN). (2005). Acrylamide in food is a potential health hazard. INFOSAN information note No. 2/2005.
23. WHO. (2002). Health implications of acrylamide in food. Geneva, Switzerland: FAO/WHO.
24. Sansano, M,;Heredia A,; Peinado I, and Andrés A. (2017). Dietary acrylamide: what happens during digestion. Food Chem. 2017;237:58–64.
25. European Food Safety Agency (EFSA). (2018). Scientific Opinion on acrylamide in food .
26. Sumner, S. C., Fennell, T. R., Moore, T. A., Chanas, B., Gonzalez, F., and Ghanayem, B. I. (1999). Role of cytochrome P450 2E1 in the metabolism of acrylamide and acrylonitrile in mice. Chem. Res. Toxicol.12,1110–1116.
27. Schettgen, T, Kutting B, Hornig M, Bechmann M, Weiss T, Drexler H, Angerer H. (2004). Trans-placental exposure of neonates of acrylamide a pilot study. Int. Arch. Occup. Environ. Health. 77(3):213–216.
28. Tsuda, H.; Shimizu, C.S.; Taketomi, M.K.; Hasegawa, M.M.; Hamada, A.; Kawata, K.M. and Inui, N. (1993). Acrylamide; induction of DNA damage, chromosomal aberrations and cell transformation without gene mutations. Mutagenesis. 8 (l):23-29, 1993.
29. Sakr, S.A, Badawy G.M, El-Sayyad H.I, and Afify H.S. (2011). Adverse effects of acrylamide on the developing retina of albino rats. J. Basic. Appl. Sci. Res. 1(7):706–712
30. Lipworth, L; Sonderman J.S; Tarone R.E and Mclaughlin J.K. (2012). Review of epidemiologic studies of dietary acrylamide intake and the risk of cancer. Eur J Cancer Prev., 21:375.
31. Maronpot, M.M; Thoolen, R.J.M.M. and Hansen, B. (2015). Two-year carcinogenicity study of acrylamide in Wistar Han rats with in utero exposure. ExperToxicolPathol., 67(2): 189-195.
32. National Cancer Institute (NCI). (2017). Acrylamide and Cancer Risk. (U.S. Department of Health and Human Services).
33. Lai,S.; Gu, Z.; Zhao,M.; Li,X.; Ma,Y.; Luo,L. and Jing, J. (2017). Toxic effect of acrylamide on the development of hippocampal neurons of weaning rats. Neural Regen Res. ., 12(10): 1648–1654.
34. Zamani, E.; Shokrzadeh, M.; Fallah, M. and Shaki, F.(2017). A review of acrylamide toxicity and its mechanism . Pharm Biomed Res., 3(1): 1-7
35. Pfeifer, G.P. and Besaratinia, A. (2004). Genotoxicity of acrylamide andeglycidamid. JNCI., 96(13) : 1023e-1029.
36. Pourentezari, M.; Talebi, A.; Abbasi, A.; Khalili, M.A.;Mangoli, E. and Anvari, M. (2014) . Effects of acrylamide on sperm parameters, chromatin quality, and the level of blood testosterone in mice. Iran J Reprod Med. 12(5): 335–342.
37. Sen, E, Tunali Y, Erkan M.(2015). Testicular development of male mice offsprings exposed to acrylamide and alcohol during the gestation and lactation period. Hum Exp Toxicol.,34:401–414.
38. Taha, N.; Korshom, M.;Mandour, A. and Sadek,K. (2013). Effects Of Garlic And Acrylamide On Some Antioxidant Enzymes. Global Journal of Medicinal Plant Research, 1(2): 190-194.

39. Hossam, S.; El-Beltagi, H.S. and Ahmed, M.M.(2016). Assessment the Protective Role of Quercetin on Acrylamide-Induced Oxidative Stress in Rats. Journal of Food and Biochemisrty., 40(6):705-771.
40. Huang, M.; Jiao, J.; Wang, J.; Xia, Z. and Zhang, Y. (2018). Exposure to acrylamide induces cardiac developmental toxicity in zebrafish during cardiogenesis. Environ Pollut., 234:656-666.
41. Friedewald, W.T.; Levy, R.I. and Fredrickson, D.S. (1972). Estimation of the concentration of low-density lipoprotein cholesterol in plasma, without use of the preparative ultracentrifuge. ClinChem. ;18:499–502.
42. Burtis, C. and Ashwood, E. (1999). Textbook of clinical chemistry. 3d Ed. London. Vol.2 Chapter (33): 1145-1150.
43. Guidet, B. and Shah S.V. (1989). Am. J. Physiol. 257(26): 440.
44. Snedecor, G.W. and Cochran W.G. (1973). Statistical Methods. 6P thPed.the Iowa state University press., Pp:238-248.
45. Tiihonen, K.; Saarinen, M. T; Alhoniemi, E.; Mitsuya, N. and Yamaki, G. (2016). Effect of Dietary Betaine on Metabolic Syndrome Risk Factors in Asian Males with Mild Fatty Liver. J. of Diabetes & Metab. 7:7.
46. Kharbanda, K.K. (2013). Methionine metabolic pathway in alcoholic liver injury. Curr. Opin. Clin. NutrMetab. Care., 16:89–95.
47. Kawakami, S.; Han, KH. and Nakamura, Y. (2012). Effects of dietary supplementation with betaine on a nonalcoholic steatohepatitis (NASH) mouse model. J. Nut. Sci. Vitaminol., 58:371–375.
48. Jung, Y. S.; Kim, S. J.; Ahn, C. W.; Kim, Y. S.; Choi, D. W and Kim, Y. C. (2013). Alleviation of alcoholic liver injury by betaine involves an enhancement of antioxidant defense via regulation of sulfur amino acid metabolism Food Chem. Toxicol., 62: 292– 298 .
49. Kharbanda, K.K.; Todero, S.L and Ward, B.W. (2009). Betaine administration corrects ethanol-induced defective VLDL secretion. Mol. Cell Biochem., 327:75–78.
50. Xu, L.; Huang D, ;Hu Q, ;Wu J, ;Wang Y, ;Feng J. (2015). Betaine alleviates hepatic lipid accumulation via enhancing hepatic lipid export and fatty acid oxidation in rats fed with a high-fat diet. Br. J. Nutr. 113(12):1835–43.
51. Yi, X.J; Kang L.; Hu, Y.; QinYing, X.; NingBo, Z. and YunLiang, J. (2009). Effect of dietary betaine supplementation on mRNA expression and promoter CPG methylation of lipoprotein lipasegene in laying hens. J. Poult. Sci. 46:224-228.
52. Xing, J, Kang L, Jiang Y. (2011). Effect of dietary Betaine supplementation on lipogenesis gene expression and CpG methylation of lipoprotein lipase gene in broilers. Mol. Biol. Rep.; 38:1975–1981.
53. Monetti, M, Levin MC, Watt MJ, Sajan MP, Marmor S, Hubbard BK, Stevens RD, Bain JR, Newgard CB, Farese RV, Sr, (2007). Dissociation of hepatic steatosis and insulin resistance in mice overexpressing DGAT in the liver. Cell Metab.;6:69–78.
54. Yang, W.; Huang L.; Gao J.; Wen S.; Tai Y.; Chen M.; Huang Z.; Liu R.; Tang C.; and Li J. (2017). Betaine attenuates chronic alcohol-induced fatty liver by broadly regulating hepatic lipid metabolism. Mol. Med. Rep., 16(4): 5225–5234.
55. Wang, L, Chen L, Tan Y, et al. (2013). Betaine supplement alleviates hepatic triglyceride accumulation of apolipoprotein E deficient mice via reducing methylation of peroxisomalproliferator-activated receptor alpha promoter. Lipids Health Dis 12, 34.
56. Albuquerque, A, Neves JA, Redondeiro, M, Laranjo M, Felix, MR, Freitas, A, (2017). Long term betaine supplementation regulates genes involved in lipid and cholesterol metabolism of two muscles from an obese pig breed. Meat Sci. 124:25–33.
57. Li, S.; Wang, H.; Wang, X.; Wang, Y. and Feng, J. (2017). Betaine affects muscle lipid metabolism via regulating the fatty acid uptake and oxidation in finishing pig.Journal of Animal Science and Biotechnology. 8:72.
58. Teodor, V.; Cuciureanu ,M.; Slencu ,B .J.; Zamosteanu ,N.; Cuciureanu ,R.(2011).potential protective role of selenium in acrylamide intoxication. a biochemical study. studiauniversitatis "vasilegoldiş", seriaştiinţelevieţiivol. 21(2);2011, 263-268.
59. Eid, M .M.; Ahmed ,A .A.; Saleh ,N.T. and Sheir ,M.A.(2012). Effect of some phytochemicals on reduction of acrylamide in fried potato chips and their biological effect on blood lipid profile. Minia J. of Agric. Res. J Develop.,32(6):939-963.

60. Rawi, S.R.; Marie ,M.A.S.; Fahmy ,S.R. and El-Abied ,S.A. (2012). Hazardous effects of acrylamide on immature male and female rats. Afr. J. Pharm. Pharamacol., 6(18): 1367-1386.
61. El –Shafey, A. A. and Nour El –Din, M.S.; El -Ezab,y M. M.; Ezaat, S. M. and Abd El –Maksoud, M. A.(2013). Protective effects of garlic "allium satIvum" and karkada "hibiscus sabdarrifa" on acryl amide treated male albino rats. Egypt. J. Exp. Biol. (Zool.)., 9(1): 101 – 107.
62. Osman, M.A,;Romeilah R.M,; Elgammal M.H,; Eman S. Ramis, and Hasan R.S. (2016). Subchronic toxicity of acrylamide in fried rice and preventive effect of grape leaves. Asian J Biochem.,11:68-81.
63. Allam, A.; El-Ghareeb ,A.W.; Abdul-Hamid ,M.; Bakery ,A.E.; Gad ,M. and Sabri ,M. (2010). Effect of prenatal and perinatal acrylamide on the biochemical and morphological changes in liver of developing albino rat. Arch. Toxicol., 84(2):129–41.
64. AL-Agele, F. A.L. and Khudiar, K.K. (2016). Effect of acrylamide and feructose on some parameters related to metabolic syndrome in adults male rats. The Ira. j. of veterna. Med., 40(1): 125-135.
65. Marques, de Mattos A, Marino LV, Ovidio PP, Jordão AA, Almeida CC, Chiarello PG (2012). Protein oxidative stress and dyslipidemia in dialysis patients. TherApher Dial,16:68-74.
66. Lin, C.Y.; Lin ,Y.C.; KuoHK;Hwang ,J.J.; Lin ,J.L.; Chen ,P.C. and Lin ,L.Y. (2009). Association among acrylamide, blood insulin, and insulin resistance in adults. Diabetes Care, 32(12): 2206-2211.
67. Totani, N.; Yawata ,M.; Ojiri ,Y. and Fujioka ,Y.(2007). Effects of trace acrylamide intake inWistar rats. J Oleo Sci;56:501–506.
68. Eckete, R.H.; Grundy S.M. and Zimmet, P.Z. (2005). the metabolic syndrome. Lancet, 365:1415–28.
69. Mahmood, S,A,F ; Amin,K, ; Rahman, H,S and Othman,H,H. (2016). The Pathophysiological Effects of Acrylamide in Albino Wister Rats. Int. J Med. Res. & Health Sci., 5 (7):42-48.
70. Pourahmad, J.; Rabiei M.; Jokar, F. and O'brien, P.J. (2005). A comparison of hepatocyte cytotoxic mechanisms for chromate and arsenite. Toxicol., 206:449–460.
71. Kanbak, G.; Arslan, OC.; Dokumacioglu, A.; Kartkaya, K.; Inal, ME. (2008). Effects of chronic ethanol consumption on brain synaptosomes and protective role of betaine. Neurochem. Res.;33:539–544.
72. Erman, F.; Balkan, J.; Cevikbaş, U.; Kocak-Toker, N.; Uysal, M. (2004). Betaine or taurine administration prevents fibrosis and lipid peroxidation induced by rat liver by ethanol plus carbon tetrachloride intoxication Amino Acids , 27, 199– 205.
73. Alirezaei, M.; Khoshdel, Z.; Dezfoulian, O.; Rashidipour, M.; Taghadosi, V. (2015). Beneficial antioxidant properties of betaine against oxidative stress mediated by levodopa/benserazide in the brain of rats J. Physiol. Sci., 65, 243– 252.
74. Alirezaei, M. (2014). Betaine as a methyl donor and an antioxidant agent in levodopa-induced hyperhomocysteinemia and oxidative stress in rat's kidney Iran. J. Vet. Med., 8, 91– 99.
75. Balkan, J., Oztezcan, S., Kucuk, M., Cevikbas, U., Kocak-Toker,N.andUysal,M.(2004).Theeffectof betaine treatment on triglyceride levels and oxida- tivestressintheliverofethanol-treatedguineapigs, Exp. Toxicol. Pathol.,55,505–509.
76. Zhang, M.; Wu, X.; Lai, F.; Zhang, X.; Wu, H. and Min, T. (2016). Betaine inhibits hepatitis B virus with an advantage of decreasing resistance to lamivudine and interferon α. J. Agric. Food Chem.,64(42):7921-7930.
77. Kim, S. J.; Jung, Y. S.; Kwon, D. Y. and Kim, Y. C. (2008). Alleviation of acute ethanol-induced liver injury and impaired metabolomics of S-containing substances by betaine supplementation Biochem. Biophys. Res. Commun., 368, 893– 898.
78. Pastor, A.; Collado, P. S.; Almar, M.; González-Gallego, J. (1996). Microsomal function in biliary obstructed rats: effects of S-adenosylmethionine J. Hepatol. , 24, 353– 359.
79. Kwon, d.o; Jung Y.; Kim Y.S., , Park S.J.; Park, H.K., ; J.H.and Kim, Y.C. (2009). Impaired sulfur-amino acid metabolism and oxidative stress in nonalcoholic fatty liver are alleviated by betainesupplementationinrats.J.Nutr., 139,63-68.
80. Tarskikh, MM. (2006). Damage to erythrocyte membranes as the mechanism for acrylate toxicity. Bull. Exp. Biol. Med. 142:690-2.

81. Mogda, ,K.; Ibrahim ,E .M.; Maha ,M El-Kholy and Sahar, A. El-Madawy. (2008): "Antioxidant andhistopathological effect ofcatechin and neem leaves extractin acrylamide toxicity ofrats." Egypt. J. Comp. andClinic. Pathol., 21(1): 290-313.
82. El-Sheikh, N.M.; Kolief ,T.E; Hassanin ,E-A. andHassan,R.M.(2008). The ability of albumin and cycteine to mitigate toxic effect of acrylamide in rats. Egyption J. Natural Toxins., 5(192): 20-35.
83. Allam, A.A.; Abdul-Hamid, M.; Bakry,A.; El-Ghareeb,A.; Ajarem,J.S. and Sabri, M. (2013). Effect of Acryl amide on Cerebral Neurons Development in Albino. Rat. Life Sci. J., 10 (3):1760-1771.
84. Swamy, M.V.; Subbaiah ,K.V.; Suman ,B.; Kamala ,K.; Rao ,K.J. (2013). Toxic Effect of Acrylamide on Body Weight, the Study ofAntioxidants and Histoarchitecture of Heart in the Developing Chick Embryo. Indian Journal of applied research. Volume: 3 (7) Issue: 7.
85. Zhao, M, Wang P, Zhu Y, Liu X, Hu X, Chen F. (2015). The chemoprotection of a blueberry anthocyanin extract against the acrylamide-induced oxidative stress in mitochondria: unequivocal evidence in mice liver. Food Funct. 6:3006-12.
86. Ghorbel, I.; Chaabane, M.; Elwej, A.; Kallel, C.; Kamoun, N. G. and Zeghal, N. (2017). Extra Virgin olive oil mitigates hematotoxicity induced by acrylamide and oxidative damage in adult rats.Pharm. Biomed. Res., 3(1): 34-40.
87. Yousef, M, El-Demerdash F. (2006). Acrylamide-induced oxidative stress and biochemical perturbations in rats. Toxicol 219:133-41.
88. Chen, Y.T.; Tsai,T.H.; Yang,C.C.; Sun,C.K.;Chang,L.T.; Chen,H.H.andChang,C.L. etal. (2014). Exendin-4 and sitagliptin protect kidney from ischemia-reperfusion injury through suppressing oxidative stress and inflammatory reaction . j. Translat. Medicine. 11:270 .
89. Liu, S, Jiang L, Zhong T, Kong S, Zheng R, Kong F. (2015). Effect of Acrylamide on Oocyte Nuclear Maturation and Cumulus Cells Apoptosis in Mouse In Vitro. PLoS One;10:e0135818.

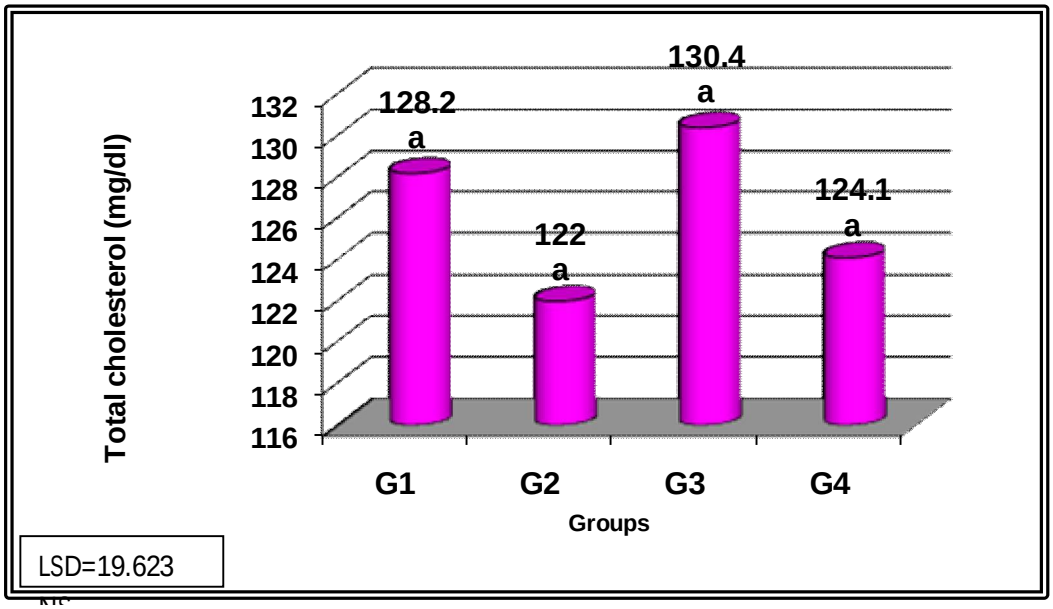

Figure 1: Effect of Betaine administration on Total cholesterol in acrylamide treated female rats.
Values are expresses as mean ± SE. n= 8 / each groups.
G1: Control Group, G2: Rats Received 250mg/kg B.W Betaine for 65 day.
G3: Rats Received 1mg/kg B.W of Acrylamide for 65 day. G4: Rats Received 1mg/kg B.W of Acrylamide and 250mg/kg B.W of Betaine for 65 day

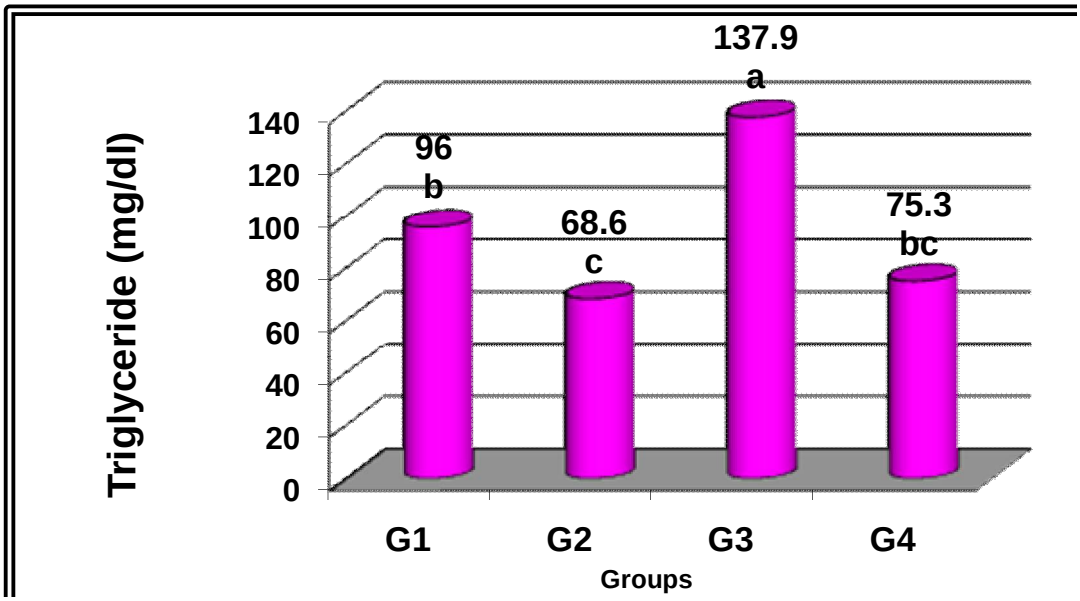

Figure (2): Effect of Betaine administration on Triglyceride in acrylamide treated female rats.
Values are expresses as mean ± SE. n= 8 / each groups.
G1: Control Group, G2: Rats Received 250mg/kg B.W Betaine for 65 day.
G3: Rats Received 1mg/kg B.W of Acrylamide for 65 day. G4: Rats Received 1mg/kg B.W of Acrylamide and 250mg/kg B.W of Betaine for 65 day

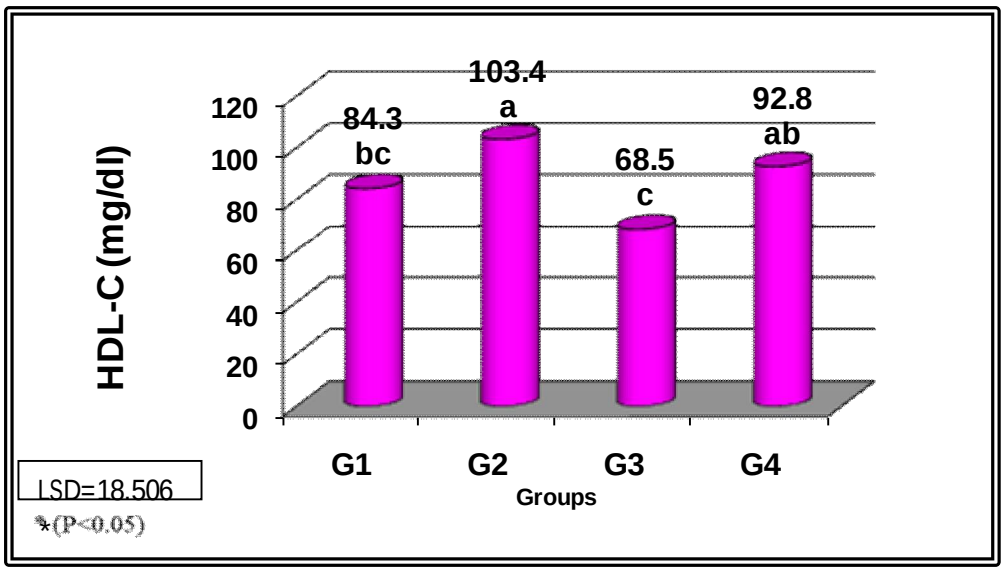

Figure 3: Effect of Betaine administration on HDL-C in acrylamide treated female rats.
Values are expresses as mean ± SE. n= 8 / each groups.
G1: Control Group, G2: Rats Received 250mg/kg B.W Betaine for 65 day.
G3: Rats Received 1mg/kg B.W of Acrylamide for 65 day. G4: Rats Received 1mg/kg B.W of Acrylamide and 250mg/kg B.W of Betaine for 65 day

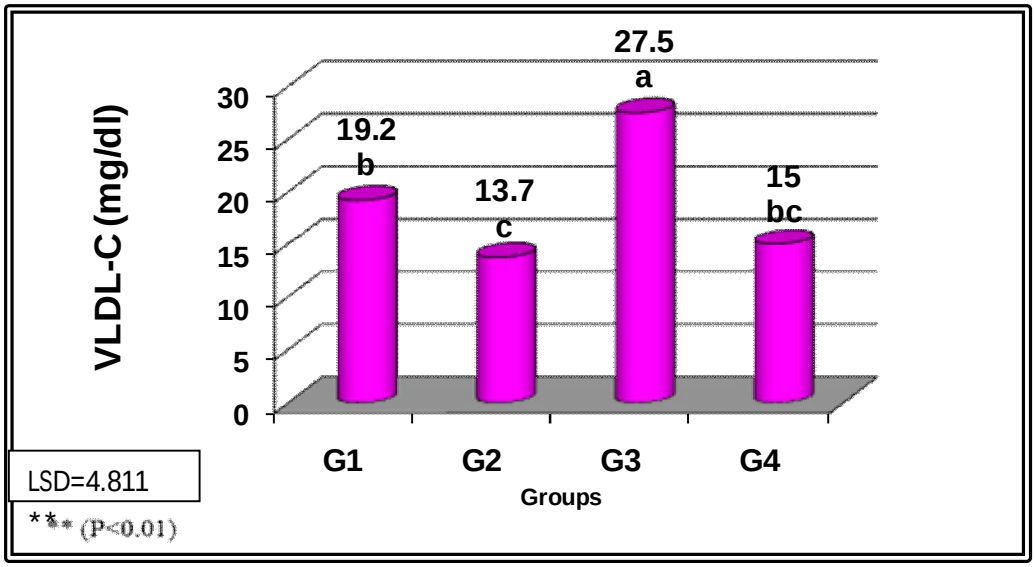

Figure 4: Effect of Betaine administration on VLDL-C in acrylamide treated female rats.
Values are expresses as mean ± SE. n= 8 / each groups.
G1: Control Group, G2: Rats Received 250mg/kg B.W Betaine for 65 day.
G3: Rats Received 1mg/kg B.W of Acrylamide for 65 day. G4: Rats Received
1mg/kg B.W of Acrylamide and 250mg/kg B.W of Betaine for 65 day

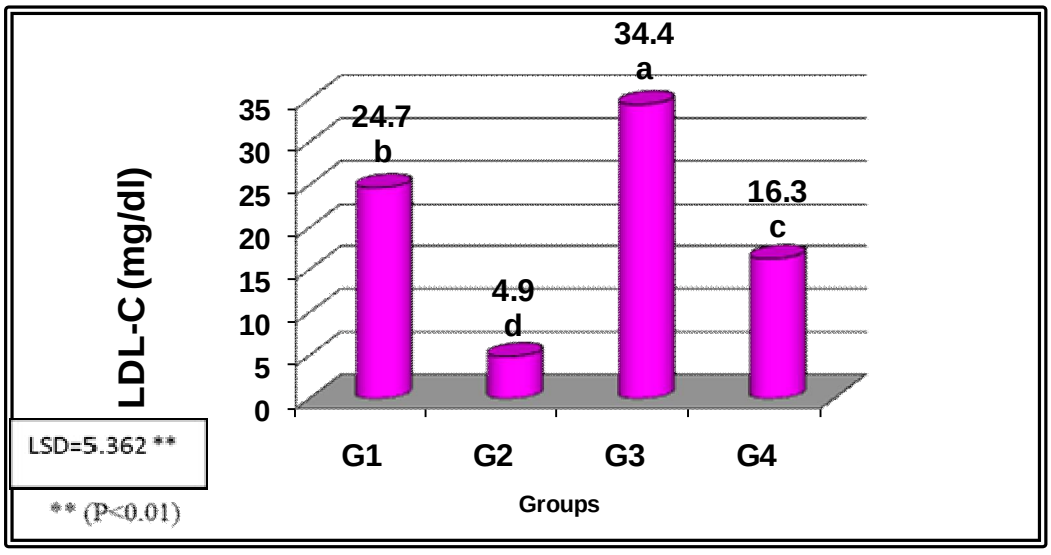

Figure 5: Effect of Betaine administration on LDL-C in acrylamide treated female rats.
Values are expresses as mean ± SE. n= 8 / each groups.
G1: Control Group, G2: Rats Received 250mg/kg B.W Betaine for 65 day.
G3: Rats Received 1mg/kg B.W of Acrylamide for 65 day. G4: Rats Received
1mg/kg B.W of Acrylamide and 250mg/kg B.W of Betaine for 65 day

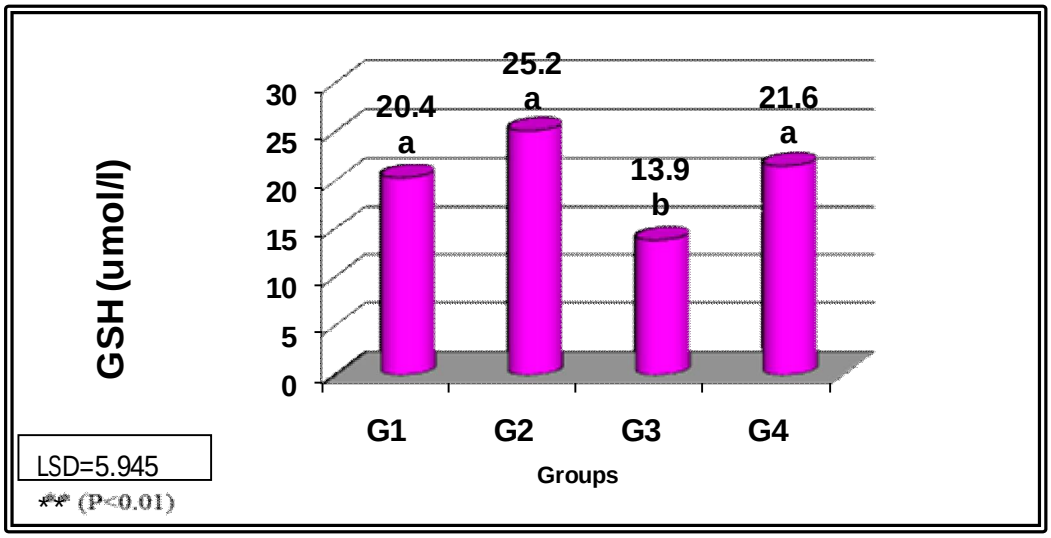

Figure 6: Effect of Betaine administration on serum glutathione (GSH) concentration in acrylamide treated female rats.
Values are expresses as mean ± SE. n= 8 / each groups.
G1: Control Group, G2: Rats Received 250mg/kg B.W Betaine for 65 day.
G3: Rats Received 1mg/kg B.W of Acrylamide for 65 day. G4: Rats Received
1mg/kg B.W of Acrylamide and 250mg/kg B.W of Betaine for 65 day

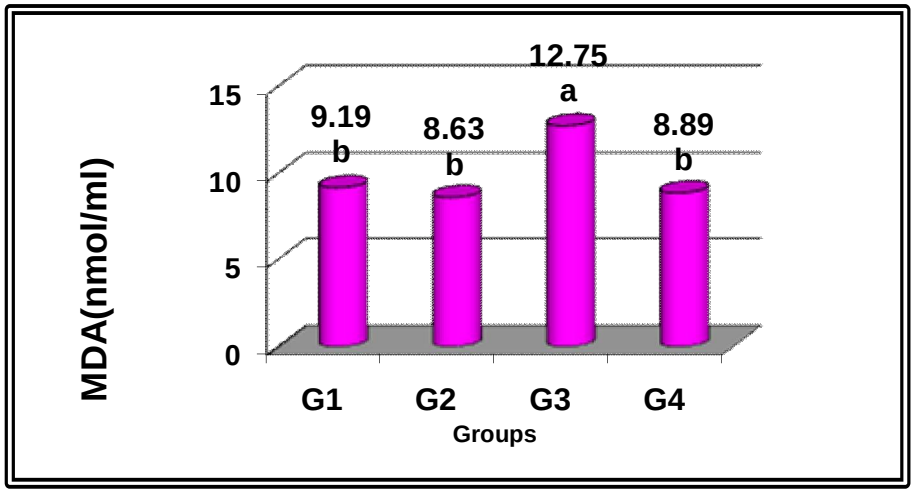

Figure 7: Effect of Betaine administration malondialdehyde (MDA) concentration in acrylamide treated female rats.
Values are expresses as mean ± SE. n= 8 / each groups.
G1: Control Group, G2: Rats Received 250mg/kg B.W Betaine for 65 day.
G3: Rats Received 1mg/kg B.W of Acrylamide for 65 day. G4: Rats Received

Indian Journal of Natural Sciences www.tnsroindia.org.in ©IJONS

Vol.9 /Issue 51 / December / 2018 *International Bimonthly* *ISSN: 0976 – 0997*

RESEARCH ARTICLE

Structural and Electrical Investigations of Cobalt Ferrite Nanoparticle Prepared by Metallurgy Method

Zena Mohammed Ali Abbas

Department of Physics, College of Science, University of Diyala, Iraq

Received: 31 July 2018 Revised: 01 Sep 2018 Accepted: 02 Oct 2018

***Address for Correspondence**
Zena Mohammed Ali Abbas
Department of Physics,
College of Science,
University of Diyala, Iraq.
Email : zenaalbana@yahoo.com

ABSTRACT

Cobalt ferrite was prepared by standard metallurgymethod and characterized by XRD, SEM techniques. The X-ray analysis confirms the formation of single phase cubic spinel structure. The lattice constant decreases slightly and porosity increases with increase in sintering temperature... Theaverage crystallite size obtained by Scherrer's formula is of the order of 34.75 nm.The lattice constant determined from XRD data is in the reported range (8.3 nm). The porosity estimated from X- ray density and bulk density shows large value of the order of 33.7 %, and it's observed that the values of losstangent decrease with increasing in frequency.

Keywords: Cobalt Ferrite, X-ray diffraction, ceramic method.

INTRODUCTION

Nanosized ferrite materials have attracted great attention in recent years. "They exhibit unusual physical and chemical properties significantly" different from those of the bulk materials due to their extremely small size and large specific surface area [1,2]. The properties of nanoferrites are influenced by the composition and microstructure, which are sensitive to the preparation methodology used in the synthesis and to the sintering conditions. Ferrite nanoparticles are usually prepared by various physical and chemical "methods like high energy milling", plasma deposition, inert gas condensation, citrate precursor technique, reverse micelle technique, microemulsion, hydrothermal reaction, polymer pyrolysis, sol-gel technique, chemical coprecipitationetc [3,4]. Nano crystalline ferrites are technologically important materials because of their unique electric, dielectric, magnetic and optical properties, which makes them suitable for many technological applications like microwave devices, transformers, electric generators, storage devices etc. [5].These ferrites have provided series of "compounds with general formula MFe2O4 where M is a mixture of divalent diamagnetic elements [6].Nanosized spinel" ferrite particles, a kind of soft magnetic materials with structural formula of MFe_2O_4 (M =divalent metal ion, e.g. Mn, Mg, Zn, Ni, Co, Cu, etc.), are

one of the most attracting class of materials due totheir interesting and important properties such as low melting point, high specific heating, large expansioncoefficient, low saturation magnetic moment and low magnetic transition temperature, etc.[7,8].Ferrites are ferrimagnetic oxides consisting of ferric oxideand metal oxides. On the basis of crystal structure ferrites aregrouped into three classes "namely hexagonal ferrite, garnetand spinel ferrite. The spinel ferrites are widely studiedbecause of their numerous applications in several fields.In the last ten years research on nano-size spinel ferrite hasbeen considerably increased due to their superior propertiesand applications in new fields "like magnetic drug delivery,catalyst, sensors etc [9]. Extensive work on structural andmagnetic characterization of spinel ferrite in the form of nano-size has been done by many workers [10, 11]. In this diverse group, Co-ferrite is an attractive material due to the large anisotropy, moderate "magnetization, chemical stability and high Currie temperature [12,13]. However, not only chemical composition is determinative for the properties of final material. It is well known that magnetic" properties are depended also on the size, morphology and purity of ferrite particles [14,15].The most remarkable sizedependent properties of magnetic material is an increase inelectrical resistivity, saturation magnetization, coercivity etc.as compared to bulk material as the particle size reduces tonanoscale [16].Cobalt ferrite nanoparticleswereproposed as a promising solution in biomedical applications, suchas magnetic thermo-drug delivery and hyperthermia, biosensorsand magnetic resonance imaging [17–18].Many techniques have already been employed in thedevelopment of cobalt" ferrite nanoparticles including a novelsolvothermal approach [19], microemulsions [20], a new nonaqueousroute [21],The aim of the present work is to synthesize "cobalt ferrite nanoparticles by powder metallurgy method and to investigate the "structural and electrical properties.

EXPERIMENTAL DETAILS

Materials used

Analytical grade cobalt oxide, CoO and Fe_2O_3were supplied from a commercial supplier and were "used without any further purification".

Preparation of cobalt ferrite nanoparticles

Mixing

The weights of oxides powder needed to prepare$\mathbf{(CoO)_x (Fe_2O_3)_{1-x}}$with (x=0.4)are mixed to obtain a uniform distribution of the components using avariable speed electric mixer for two hours for the purpose of obtaining a homogeneous mixture and the nonagglomeratedmixtures are "then dried in an oven at 80°C for 2 hours".

Pellet formation

"A mold is designed for the manufacture" of samples in the form of pellet in diameter of (2cm) and thickness of (3mm) and the weight of the sample is (3 g). Hydraulic press with a pressure of (500 700 psi) was used, and" the diameter of the mold used (2cm)" with a height of (5cm).

Sintering

The "green Pellets are loaded on refractory" plates (pure alumina container) and sintered at temperature of (1000 °C)" for four hours, and then cooled in the furnace to room temperature".

Structural characterization of cobalt ferrite

X-ray diffraction pattern were recorded using" XRD-6000 with CuKα (λ=1.5406A°) "that have an accelerating voltage of" (220/50) HZ which is produced by SHIMADZU company. The morphology and image of samples were done by scanning electron microscope "(SEM) type VEGA//EasyProbe which is a favorable combination of a scanning electron microscope" and a fully integrated energy dispersive X- ray microanalyser produced by "TESCAN, s.r.o., Libušinatrída 21".

RESULTS AND DISCUSSION

XRD pattern of $(CoO)_{0.4}$ $(Fe_2O_3)_{0.6}$nano ferrite.

Fig. 1 shows X-Ray diffraction (XRD) has been performed for the identification of the crystal structure and growth orientation of the nanostructures. All diffraction data are in good agreement with JCPDS files No.22-1086.
Figure 1. shows the X-ray diffraction pattern (XRD) ofcobalt ferrite nano-particles. A careful examination of XRDpattern reveals the appearance of slightly broader peakssignifying the low crystallite size of the prepared samples. Allthe peak belongs to cubic spinel structure and the analysis ofXRD pattern prove the formation of single phase samples.The average crystallite size was calculated using theScherrer's formula [22,23] from the broadening of XRD peakcorresponding to most intense (311) peak of the XRD pattern.The detailed analysis of the XRD and the assignments of various reflectionspeaks are given in Table 1.

Particle Size Calculation from X-ray diffraction

Average particle size has been estimated by using"Scherrer formula".
$D = 0.9\lambda / \beta \cos\theta$
D =34.75 nm

The lattice constant 'a' was calculated using the relation

$$a = d_{hkl}\sqrt{h^2 + k^2 + l^2}$$
$$a = 8.30\ nm$$

where h, k, l are the Miller indices of the crystal planes and d_{hkl} is the inter planer spacing. The lattice constant obtained from XRD data is in reported range.

The X-ray density (dx) was calculated using the relation

$$d_x = \frac{8M}{Na^3}$$
$$d_x = 5.42\ g/cm^3$$

where, M is molecular weight," N is Avogadro's number" and ais the lattice constant. The X-ray density is found to be of theorder of 5.42gm/cm3.The bulk density of cobalt ferritenano particles was measured from the Archimedes principle.The value of bulk density is of the order of 3gm/cm3.The apparent density calculated by Archimedes method (Actual density (D)) and the calculation of porosity using the formula [24]: Porosity = [1-(D/DX)]* 100%
Porosity %=44.6 %

Scanning electron micrograph of $(CoO)_{0.4}(Fe_2O_3)_{0.6}$

"SEM measurements are carried out in order to understand the "morphology and the shape" of the synthesized nanomaterrials", this image has been used to estimate of nanoparticle size distribution."the asymmetric shape of histogram" may indicate that some agglomeration had taken place ,with the formation of particles with larger sizesaround (35)nm.The study of SEM micrographs reveals less number of pores with smaller lump size.SEM micrograph of $(CoO)_{0.4}(Fe_2O_3)_{0.6}$ pellet show the grain boundary of the sample being sintering at 1000°C.

Electrical measurements (Dispersion Factor (Tangent Loss))

The Tangent Loss was measured by LCR meter which connected tocomputer the sample puts between the poles and make sure that the poles touch sample surface. Dispersion factor data have recorded on computer's screen via mathematic formulas that studied previously. The values of loss tangent of dielectric constant (tan δ) it has ranged between(0.1-0.33) at frequencies within the range (50Hz – 20MHz) respectively, Suddenly decreasing after this level to low values with increasing frequency.The values of magnetic loss tangent represents the ratio between thedissipated energy to stored energy, figure (2) show that the values of losstangent is high at low frequency (50Hz-1KHz), then begin to decline at thefrequency (1KHz-1MHz) .This values are varies from one compound to another depending on the typeof ferrite mixture, and so it's less of prepared ferrite at high degrees of sintering,the high values of the magnetic loss tangent at sintering temperature 1000 ℃ itresult of the presence of pores and small grain size, and possibly micro cracksthat works to stop the movement of the wall of the magnetic field so leads thesethings combined to decreasing the magnetic permeability.

CONCLUSION

Cobalt ferrite nanoparticles**$(CoO)_{0.4}(Fe_2O_3)_{0.6}$**were prepped by powder metallurgy simple method.When preparing ferrite and studying its synthetic properties, it was found Ferrite samples under investigation show single phase cubic spinel structureby XRD pattern . Average particle size has been estimated by using" Scherrer formula" (34.75 nm) .The X-ray density (dx) was calculated($5.42\frac{g}{cm^3}$).the porosity (44.6 %).A SEM measurements shows the homogeneity of the internal structure.

REFERENCES

1. A. Animesh, C. Upadhyay and H.C. Verma, Physics Letters A, 311(2003)410.
2. D-H. Chen and Y-Y. Chen, Journal of Colloid and Interface Science, 235(2001)9.
3. A. Chattergee, D. Das, S.K. Pradhan, D. Chackravorty, J. Magn. Magn. Mater. 127 (1993) 214.
4. S. Mishra, N. Karak, T.K. Kundu, D. Das, N. Maity, D. Chakravorty, Material Letters 60 (2006) 1111.
5. D. Niznansky, M. Drillon and J. L. Renspinger, "Preparation of Magnetic Nanoparticles (γ-Fe2O3) in the Silica Matrix," IEEE Transaction on Magnetics, Vol. 30, No. 2, 1994, pp. 821-823.
6. S. Gubbala, H. Nathani, K. Koziol and R. D. K. Misra, "Magnetic Properties of Nanocrystalline Ni-Zn, Zn-Mn, and Ni-Mn Ferrites Synthesized by Reverse Micelle Technique," Physica B: Condensed Matter, Vol. 348, No. 1-4, 2004, pp. 317-328.
7. Xu Q, Wei Y, Liu Y, Ji X, Yang L, Gu M: Preparation of Mg/Fe spinel ferrite nanoparticles from Mg/Fe-LDH microcrystallites under mild conditions.Solid State Sci 2009, 11(2):472-478.
8. Tian MB: Magnetic Material Beijing: Tsinghua University Press; 2001.
9. SasmitaMohapatra , Smruti R. Rout , SwatilekhaMaiti , Tapas K.Maiti and Asit B. Panda, "Monodispersemesoporous cobalt ferrite nanoparticles: synthesis and application intargeted delivery of antitumor drugs" J. Mater. Chem., 21 (2011)9185.

10. K. Maaz, S.Karim, A.Mumtaz, S.K.Hasanain, J.Liu, J.L.Duan,"Synthesis and magnetic characterization of nickel ferritenanoparticles prepared by co-precipitation route" J Magn. Magn.Mater. 321 (2009) 1838.
11. Y. Ichiyanagi, M. Kubota, S. Moritake, Y. Kanazawa, T. Yamada andT. Uehashi, "Magnetic properties of Mg-ferrite nanoparticles" J.Magn. Magn. Mater. 310 (2007) 2378.
12. X. A. Fan, J. G. Guan, X. F. Cao, W. Wang, and F. Z. Mou, "Low-Temperature Synthesis, Magnetic and Microwave Electiomagnetic Properties of Substoichiometric Spinel Cobalt Ferrite Octahedra," European Journal of Inorganic Chemistry, pp. 419-426, Jan 2010.
13. H. M. El-Sayed, "Effect of induced magnetic anisotropy on the hysteresis parameters of Co-ferrite prepared from nano-sized particles," Journal of Alloys and Compounds, vol. 474, pp. 561-564, Apr 2009
14. J. Wang, T. Deng, and Y. J. Dai, "Comparative study on the preparation procedures of cobalt ferrites by aqueous processing at ambient temperatures," Journal of Alloys and Compounds, vol. 419, pp. 155-161, Aug 2006.
15. M. Sajjia, M. Oubaha, T. Prescott, and A. G. Olabi, "Development of cobalt ferrite powder preparation employing the sol-gel technique and its structural characterization," Journal of Alloys and Compounds, vol. 506, pp. 400-406, Sep 2010.
16. Mukta V. Limaye, Shashi B. Singh, Sadgopal K. Date,Deepti Kothari, V. Raghavendra Reddy, Ajay Gupta,VasantSathe, RamJane Choudhary, and Sulabha K. Kulkarni. "High coercivity of oleic acid CoFe2O4 nanoparticles at room temperature" J. Phys. Chem. B113, (2009), 9070-9076.
17. N.B. Ekreem, A.G. Olabi, T. Prescott, A. Rafferty, M.S.J. Hashmi, An overview of magnetostriction, its use and methods to measure theseproperties, Journal of Materials Processing Technology 191 (2007) 96–101.
18. M. Pita, J.M. Abad, C. Vaz-Dominguez, C. Briones, E. Mateo-Martí, J. A. Martín-Gago, M.P. Morales, V.M. Fernández, Synthesis of cobaltferrite core/metallic shell nanoparticles for the development of a specific PNA/DNA biosensor, Journal of Colloid and Interface Science 321(2008) 484–492.
19. J. Ma, J. Zhao, W. Li, S. Zhang, Z. Tian, S. Basov, Preparation of cobalt ferrite nanoparticles via a novel solvothermal approach using divalentiron salt as precursors, Materials Research Bulletin 48 (2013) 214–217.
20. S. Li, L. Liu, V.T. John, C.J. O'Connor, V.G. Harris, Cobalt–ferrite nanoparticles: correlations between synthesis procedures, structural characteristics and magnetic properties, IEEE Transactions on Magnetics 37 (2001) 2350–2352.
21. L. Ajroudi, S. Villain, V. Madigou, N. Mliki, C. Leroux, Synthesis and microstructure of cobalt ferrite nanoparticles, Journal of Crystal Growth312 (2010) 2465–2471.
22. S.Nath S., D.Chakdar, and G.Gope;" Synthesis of CdS and ZnS quantum dots and theiapplications in electronics,Nanotrends- A journal of nanotechnology and its application", 02(03), (2007).
23. B. D. Hall, D. Zanchet and D. Ugarte ; "Estimating nanoparticle size from diffraction measurements , Journal ofApplied Crystallography", Volume 33, Part 6 (2000(.
24. MAAhmed, NOkasha and S I El-Dek1" Preparation and characterization of nanometricMn ferrite via different methods" Nanotechnology 19,(2008).

Table 1. Strongest three peaks of fig.1

No.	Peak No.	2 Theta (deg.)	d (A°)	FWHM (deg)
1	6	35.8394	2.50354	0.21050
2	16	62.9197	1.47595	0.20520
3	14	57.3369	1.60566	0.19090

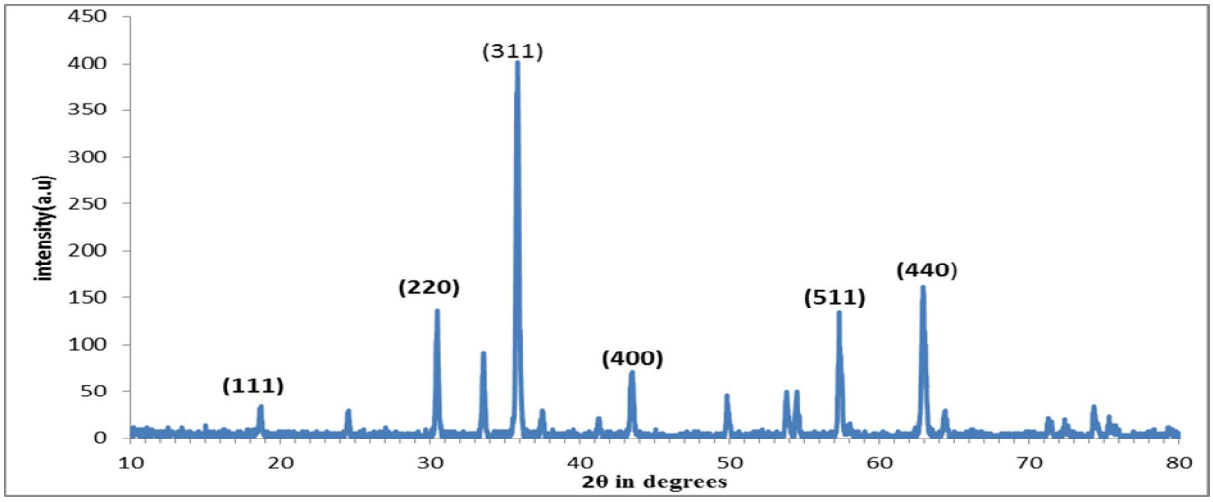

Figure 1. XRD pattern of $(CoO)_{0.4}(Fe_2O_3)_{0.6}$nano ferritesintered at 1000 °C

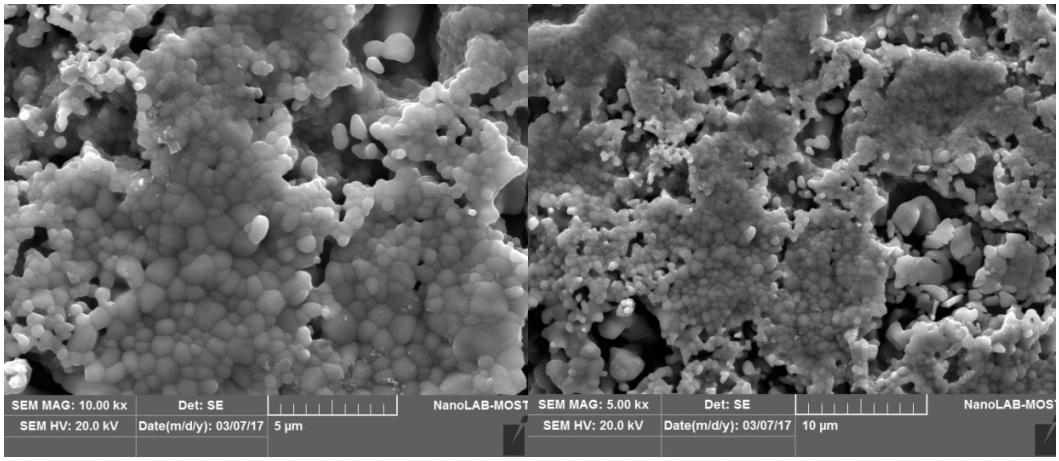

Figure 2. Scanning electron micrograph of $(CoO)_{0.4}(Fe_2O_3)_{0.6}$

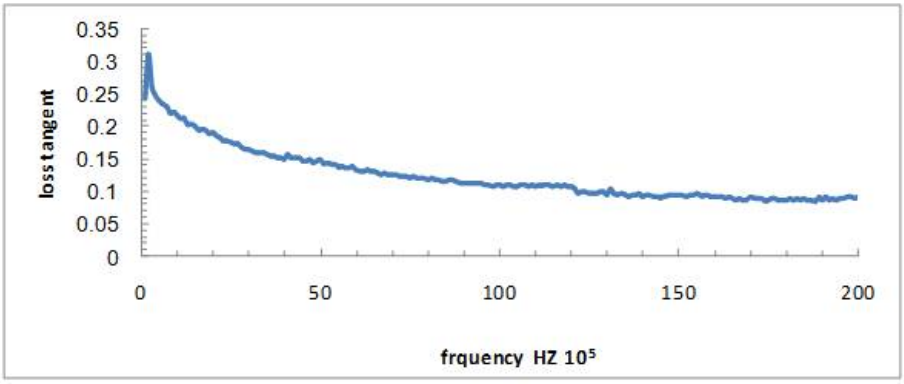

Figure 3. The variation of loss tangent with frequency of$(CoO)_{0.4}(Fe2O3)_{0.6}$ferrite sintering at 1000°C

Indian Journal of Natural Sciences www.tnsroindia.org.in ©IJONS

Vol.9 /Issue 51 / December / 2018 *International Bimonthly* *ISSN: 0976 – 0997*

RESEARCH ARTICLE

Evaluate of *Trichophyton tonsurans* Sensitivity to *Tagetes erecta* Extract and *Trichoderma harzianum* Filtrate

Sara Asaed Ali[1]* Mohammed Jubair Hanawi[1] and Firas Ahmed Abed Iesa[2]

[1]College of Science, University of Wasit, Iraq
[2]Alzahra Teaching Hospital, Wasit Province, Iraq

Received: 02 Aug 2018 Revised: 05 Sep 2018 Accepted: 07 Oct 2018

***Address for Correspondence**
Sara Asaed Ali
College of Science,
University of Wasit, Iraq

ABSTRACT

Biological control represents an important approach for controlling many pathogenic fungi. *Trichoderma* spp. and medicinal plant are the most promising and effective bioagents against many pathogenic fungi. In this paper *Trichoderma harzianum* and *Tagetes erecta* were screened for their efficacy against *Trichophyton tonsurans.* The results had been revealed that the culture filtrate of the fungus *Trichoderma harzianum*was affected the radial growth of the dermatophyte fungus *Trichophyton tonsurans.*Water and alcohol extract of *T. erecta* at all test concentrations had inhibitory effect on the radial growth of *T. tonsurans.* The results also showed that the types of interaction between the clotrimazole and the plant extract or fungal filtrate refer to synergistic pattern.

Key words: Biocontrol, *Trichophyton tonsurance, Tageteserecta, Trichoderma harzianum*.

INTRODUCTION

Fungal infections of human like dermatophytes pose serious medical issues. Till now, more than a hundred thousand fungal species are considered as natural contaminants (Kacaniova, 2003). More than three hundreds are now recognized as true pathogens responsible for mycosis in human. All mycosis , opportunistic fungal infections and the disseminated endemic fungal infections occurred with high frequency and severity in recent decades because of the introduction of immunosuppressive therapy , antimycrobials, emergency of acquired immune deficiency syndrome (AIDS), human immune deficiency virus (HIV) infected patients and the use of chemotherapeutic agents (Merz and Hay, 2005). Taxonomically, dermatophytes comprise three genera: *Epidermophyton*, *Microsporum* and *Trichophyton*. The Genera specially *Trichophyton* the most frequently agent of dermatophytosis worldwide (Ohst, *et al.* 2004). Antifungal agents used worldwide against the fungal infection but the majority have various draw backs in terms of toxicity, efficacy , cost and their frequent use has led to emergence of resistant strains. Hence there is a great needed for new antifungal drugs belonging to a wide range of structural classes, selectively acting on new targets with least side effects (Sati and Joshi, 2010). Pure compounds in natural products, either or standardized plant

extracts, provide unlimited opportunities for new antifungal drug against mycosis because of their broad spectrum of activity , harmless, economical and the low levels of toxicity (Lee *et al.*, 2003). *Tageteserecta*, popularly known as marigold and *Tagetespatula* shown a complex chemical compounds, antibacterial and antifungal activity against different pathogenic microorganisms (Politi, *et al.* 2016 ; Faizi, *et al*. 2008). Omero , *et al*. (2004) have been found that the *Trichodermavirens* being the effective biocontrol agent against the dermatophyte fungus *Trichophyton rubrum.* This study has been conducted to evaluate the antifungal activity of *Trichoderma harzianum* and *Tagetes erecta* extract against the pathogenic fungus *Trichophyton tonsurans*.

MATERIALS AND METHODS

Source of *Trichophyton tonsurans* isolates

Specimens were collected from patients in Alzahraa Hospital and cultured on SDA medium and identified morphologically with the corporation of central health laboratory- Baghdad.

Source of *Trichoderma* isolates

Trichoderma harzianum isolate was obtained from the Ministry of science and Technology - Directorate of Agriculture Research - Department of Biotechnology.

Source of antifungal drug

The antifungal drug (Clotrimazole) obtain as a standard solution from AL-Haitham pharmacy in wasit province .

Source of *Tagetes erecta* Plants

Tagetes erecta Plants were obtained from the College of Agriculture – University of Wasit. The parts of the whole plants were washed by tap water to remove debris and then dried at room temperature in the shade and then ground into powder by blender and transferred to the laboratory.

Preparation of aqueous plant extracts

The powdered air-dried plant materials (100 g) were mixed with water by using flask contains 400ml of distilled water. The mixture was kept at room temperature for 24hours.The extracts were separating from the residues by filtering through Whatman No.1 filter paper. The filtrate was centrifuged at (3000r/m) for 10 minutes. Then the supernatant pass through Millipore filter 0.2µm into clean conical flasks and subjected to water bath evaporation, where the aqueous solvents were evaporated. The standard extracts thus obtained were then stored in a refrigerator (4°C) until further use (Akueshi*et al*., 2002).

Preparation of alcohol plant extracts

The powdered air-dried sample (100g) was mixed with 400 ml of ethanol (76%) for 24 hours at room temperature. The mixtures thus obtained were filtered through Whatman No. 1 filter papers. The extracted liquids were subjected to rotary evaporation in order to remove the ethanol. The semisolid extracts that produced were then dried and then the extracts were stored in the refrigerator (4°C) until further use. (Chessbrough, 2000).

Effect of fungal Filtrate on growth of *Trichophyton tonsurans*

To determine the effects of the *Trichoderma* filtrate on mycelia growth of the *Trichophyton*, three discs of mycelial agar plugs (5 mm diameter) were removed with a cork borer from the edge of the young culture of *Trichoderma* and inoculated in 100 ml sterilized potato dextrose broth (PDB) in 300 ml conical flasks and incubated at 28 ± 2°C.The culture was filtered through Millipore filter for removing mycelial mats and then sterilized through 0.2 μm pore biological membrane filter. Different volumes of fungal filtrates were added to the molten SDA medium to obtain final concentrations of 50 , 25 and 10% (v/v). The control set was made by pouring 20 ml of SDA medium only in sterilized Petri-plate. The medium was placed (10ml) in Petri-plate and inoculated with 5 mm diameter mycelial disc of 7 days-old culture of *Trichophyton* in the center of the plates and incubated at 28 ± 2°C until the colony reached the plate edge (Rashmi, et al. 2016). There were 3 replicates for each treatment. Radial growths of the *Trichophyton* were recorded. Inhibition percent (%) of mycelial growth was calculated as follows:

$$L = [(C - T)/C] \times 100$$

Where L is inhibition (%) of radial mycelial growth; C is radial growth measurement of the *Trichophyton* in control; T is radial growth of the *Trichophyton* in the presence of *Trichoderma* Filtrate (Edington et al.,1971).

Effect of plant extract on growth of *Trichophyton tonsurans*

The effect of the water and alcohol plant extract on mycelia growth of the *Trichophyton* was evaluated by using the food poisoning technique (Kumar et al., 2008). Stock solution from each one prepared by dissolve 1gm of dried extract in 100ml distilled water. Different volumes from stock solution were mixed with SDA medium to obtain different concentration (8000ppm, 6000ppm, 4000ppm, 2000ppm) of alcoholic and aqueous extract. The medium poured in petri- plate (9cm). Each petri-plate was inoculated with 5mm discs from 7 days old culture of *Trichophyton*. Control petri-plates without extract were inoculated also. After 7 days of inoculation colony diameter were recorded and percent of inhibition was calculated according to Edington *et al.,* 1971.

Effect of Clotrimazole in culture media

Clotrimazole was obtained as standard solution in a concentration 10 μg/ml from AL-Haitham pharmacy and consider as a stock solutions (S). Different volumes of stock solution were mixed with melted SDA medium to obtain the concentrations 50, 25 and 10%. 10ml of each concentration were poured in petri-plate (9cm). Each petri-plate was inoculated with 5mm discs from 7 days old culture of *Trichophyton*. Control petri-plates without Clotrimazole were inoculated also. After 7 days of inoculation colony diameter were recorded and percent of inhibition was calculated according to Edington *etal*.,1971.Integral effect of Clotrimazole with the fungal filtrate and plant extract on growth of *Trichophyton tonsurans.*To evaluate the combined activity of Clotrimazole with plant extract and fungal filtrate on growth of *Trichophytontonsurans*5ml of Clotrimazole in a concentration 5 μg/ml (S/2) were mixed with 5ml of plant extract in a concentration 4000ppm(S/2) and 5ml of fungal filtrate (concentration 50%) separately. Each 10ml of the above combination were mixed with 100ml of melted SDA medium. 10ml of Clotrimazole alone were mixed with 100ml of melted SDA medium as a ppositive control, 10ml of distilled water were mixed with 100ml of melted SDA medium as a negative control. All media were poured in petri-plate (9cm). Each petri-plate was inoculated with 5mm discs from 7 days old culture of *Trichophyton*. After 7 days of inoculation colony diameter were recorded and percent of inhibition was calculated according to Edington *et al*.,1971.. The effect of combination may be additive, indifferent or antagonistic effect (Hu, *et al*. 2002).

RESULTS

Effect of fungal Filtrate on growth of *Trichophyton tonsurans*

The results of the study of the effect of *Trichoderma harzianum* filtrate in growth of *Trichophyton tonsurans* had been revealed that the culture filtrate of the fungus *Trichoderma harzianum*was affected the radial growth of the dermatophyte fungus *Trichophyton tonsurans*and the effect was increased with the increasing of the concentration of culture filtrate and the radial growth ranged between 2.16 cm to 4.26cm as compared with the control 8.06cm after 7 days of treatment (figure 1). Lowest effect was recorded in the case of the concentration S/4. All tested concentrations had a marked significant inhibitory effect on the growth of the test fungus *Trichophyton tonsurans* compared with the control and the percentage of inhibition in the case of stock(s) solution was 73.20% followed by the concentration S/2 which was 65.70% while in the case of the concentration S/4was 47.14%. Significant differences were recorded between the all concentrations and the control and between the test concentrations.

Effect of plant extract on growth of *Trichophyton tonsurans*

Results of antifungal activity of *Tagetes erecta* extract in radial growth of *T. tonsurans* are shown in Table (1). The water and alcohol extract of *T. erecta*at all test concentrations had inhibitory effect on the radial growth of *T. tonsurans* and reduced the growth significantly as compared with the control. The inhibition of *Trichophyton*growth was always directly proportional to the tested concentration. The rate of radial growth ranged from 2.90cm to 5.50cm in the case of water extract and from 2.33cm to 5.26cm in the case of alcohol extract as compared with the control 8.46cm. The alcohol extract exhibited higher antifungal activity than the water extract. The lowest radial growth was recorded in the case of alcohol extract which was 2.33cm at the concentration 8000ppm Figure (), but without significant difference with the same concentration of water extract.The percentages of growth inhibition of *T. tonsurans* range between 34.98 - 65.72% in the case of water extract and between 37.82 - 72.45% in the case of alcohol extract of *Tagetes erecta*.The highest percentage of growth inhibition of *T. tonsurans* was recorded at the concentration 8000ppm of alcohol extract which was 72.45% and the lowest percentage of growth inhibition of *T. tonsurans* was recorded at the concentration 2000ppm of water extract which was34.98%.

Effect of Clotrimazole in radial growth of *T. tonsurans* in culture media

Antifungal activity of Clotrimazoleon growth of *T.tonsurans* in culture media was shown in the figure (2). The antifungal Clotrimazole exhibited significant effect against the test fungus as compared with the control, and the activity increased significantly with the increasing of the concentration of drug .The Radialmycelial growth of *T.tonsurans* after 7 days of inoculation was 2.06cm at the concentration 10 µg/ml and 2.66, 3.30cm at the concentrations 5 , 2.5 µg/ml respectively as compared with the control 8.16cm. The result also showed that the percentage of growth inhibition of *T.tonsurans* was 74.75% at the concentration 10 µg/ml and 67.40, 59.55% at the concentrations 5 , 2.5 µg/ml respectively.

Integral effect of Clotrimazole with the fungal filtrate and plant extract on growth of *Trichophyton tonsurans*

The result of this study had been revealed that the antifungal drug Clotrimazole alone or in combination with the fungal filtrate or extract of T. *erecta* affected the growth of T. *tonsurance* significantly as compared with control and the radial growth of *T. tonsuranc e*ranged between 2.2cm to 2.5cm compared with control 8.3cm (Table 2).The lowest radial growth of *T. tonsurance* were recorded in the case of the combination between the clotrimazole and the extract of T. *erecta* which 2.2cm after 7 days of inoculation while the radial growth of the dermatophyte fungus was 2.5cm in the case of clotrimazole alone after the same period.The percentage of inhibition of growth of *T. tonsurance* in the case

of the combination between the clotrimazole and the extract of T. *erecta* was 73.49% and between the clotrimazole and the filtrate of T. *harzianum* was 71.08% as compared with the case of clotrimazole alone which was 69.87%.The types of interactionbetween the clotrimazole and the plant extract or fungal filtrate refer to synergistic pattern and there is no reduction in the activity of clotrimazole when it combined with them.

DISCUSSION

Antagonist potential of *Trichoderma* species against different pathogenic fungi has been reported by several researchers (Patil*, et al*., 2017 ; Omero*, et al*. 2004). The effects of the inhibitory actions on *Tricophyton tonsurans* by the filtrate of *Trichoderma harzianum* appear to be associated with toxic volatile compounds produced by *Trichoderma harzianum*. *Trichoderma* spp. especially *Trichoderma harzianum* and *Trichoderm aviride* are known to produce a range of metabolites hydrolytic enzymes like chitinases , glucanases and antibiotics that may affects the growth of *T. tonsurans* (Kubicek*, et al*., 2011).In fungal species from the genus *Trichoderma*, over 180 secondary metabolites have been characterised up to date, representing different classes of chemical compounds. These compounds may be divided into volatile antibiotics, water soluble compounds and peptaibols. *T. viride*, *T. harzianum*, and *T. koningii*are able to produce 6PAP (6-pentyl-α-pyrone) that belongs to the group of volatile antibiotics playing a role in biocontrol (Reino*et al*. 2008 ; Degenkolb*et al*. 2003).The result of this study showed that both extract (water and alcohol) of *Tageteserecta* exhibited antifungal activity against *T. tonsurance* and this may be due the presence of antifungal compounds like , limonene, caryophyllene , patulitrin , ocimene and flavonoidswhich restricted the growth of this fungus. Several studies were recorded the antifungal activities of these compounds against pathogenic fungi (Behidj-Benyounes, *et al*. 2014 ; Tripathi, *et al.* 2012 ; Rhama and Madhavan, 2010).

Carlos*, et al*. (2006) found the dimethoxy compounds which extracted from *Tageteslucida* showed a strong activity against the dermatophytefumgus T. *mentagrophytes.*Similar study had been revealed that the flower extract of *Tagetespatula*showed very strong activity against *Trichophyton mentagrophytes* (Faizi, *et al*. 2008). Aguiar*, et al* (2018) used Gas Chromatography/Mass Spectrometry technique to identify *the chemical composition of the essential oil of the leaves of T. erecta* and they found that the *essential oil contain 31 compounds and the* monoterpenes , caryophyllene are the main constituents and the antifungal activity against dermatophyte was due to the presence of them. They refer also to the synergistic manner and their mutual interaction which may be plays an important role in the overall activity**.** From the results it appear that the antifungal clotrimazole was highly active against*T. tonsurans* and this results were agree with the results of Fernández-Torres*, et al*. (2000). Khadka*, et al*. (2017) investigate the susceptibility of *Trichophyton tonsurans*and other dermatophytes to Clotrimazole.Nenaah and Ahmed (2011) found that there is a synergistic effect between the methanolic extract of the leaves, flowers of *Calotropisprocera* and the antifungal drug clotrimazole. Another studies were recorded the antifungal effect of medicinal plants against *Trichophyton tonsurans* , *Trichophyton mentagrophytes* and *Trichophy tonrubrum* and its synergism with antifungal drugs like clotrimazole and ketoconazole (Zhou, *et al*. 2012 ; Cornejo-Garrido, *et al.* 2015).

CONCLUSIONS

This study demonstrated the efficacy of *Trichoderma harzianum*and medicinal plant *Tageteserecta* in controlling *Trichophyton tonsurance* andrevealed that there is an synergistic effect between the culture filtrate of *T. harzianum*, extract of the *T. erecta*and the antifungal drug clotrimazole against the growth of *Trichophyton tonsurans*.

REFERENCES

1. Aguiar, G.P. ; Lima, K.A.;Severiano, M.E.;Groppo, M.;Ambrósio, S.R.*et al*. (2018) Antifungal Activity of the essential oils of *Plectranthusneochilus* (Lamiaceae) and *Tageteserecta* (Asteraceae) cultivated in Brazil. Internationa Journal of Complementary & Alternative Medicine 11(1):1 - 5.

2. Akueshi, C. O. ; Kadiri, C. O. ; Akueshi, E.U. ; Agina, S. E. andNgurukwem, B. (2002): Antimicrobial potentials of *Hyptissauvedens*Poit (Lamiaccae), Nigeria. J Bot 15: 37–41.
3. Behidj-Benyounes, N. ; Bennaamane, S. ; ZohraBissaad,F. ; Chebouti, N. ; Mohandkaci, H. ; Abdalaziz, N. and Iddou, S. (2014). Antimicrobial potentials of flavonoids isolated from *Tageteserecta*. International Journal of Bioengineering and Life Sciences 8 (11) : 2265 – 2268.
4. Carlos, L. C. ; Guillermo A. ; Andreä, S. M. ; Blanca, S. ; Joseä, C. C. M. and Rafael, S. G. (2006). Antifungal and Antibacterial Activities of Mexican Tarragon (*Tageteslucida*). J. Agric. Food Chem. 2006, 54, 3521-3527.
5. Chessbrough M (2000). Medical Laboratory Manual for Tropical Countries. Linacre House, Jordan Hill, Oxford, p. 260.
6. Cornejo-Garrido, J. ; Salinas-Sandoval, M. ; Díaz-López, A. ; Jácquez-Ríos, P. ; Arriaga-Alba, M. and Ordaz-Pichardo, C. (2015). In vitro and in vivo antifungal activity, liver profile test, and mutagenic activity of five plants used in traditional Mexican medicine. RevistaBrasileira de Farmacognosia 25 : 22–28.
7. Degenkolb, T. ; Berg, A. ; Gams, W. ; Schlegel, B. and Grafe, U.(2003) The occurrence of peptaibols and structurally related peptaibiotics in fungi and their mass spectrometric identification via diagnostic fragment ions. J PeptSci 9:666–678.
8. Edington L.V. ; Khew, K.L. and Barron, G. I. (1971).Fungitoxic spectrum of benzimidazole compounds. Phytopathology, 61:42-44.
9. Faizi, S. Siddiqi, H. ; Bano, S. ; Naz, A. ; Mazhar, K. ; Nasim, S. ; Riaz, T. ; Kamal, S. ; Ahmad, A. and Khan, A. S. (2008). Antibacterial and Antifungal Activities of Different Parts of *Tagetespatula*: Preparation of Patuletin Derivatives. Pharmaceutical Biology, 46 (5) : 309–320.
10. Fernández-Torres, B. ;Vázquez-Veiga, H. ;Llovo , X. ;Pereiro, J. M. and Guarro, J. (2000).In vitro Susceptibility to Itraconazole, Clotrimazole, Ketoconazole and Terbinafine of 100 Isolates of *Trichophyton rubrum.* Chemotherapy;46:390–394.
11. Hu, Z.Q. ;Zhao, W.H. ;Yoda, Y. ;Asano, N. ;Hara, Y. and Shimamura, T. (2002). Additive, indifferent and antagonistic effects in combinations of epigallocatechingallate with 12 non-beta-lactam antibiotics against methicillin-resistant *Staphylococcusaureus*.J AntimicrobChemother. 50(6):1051-4.
12. Kacaniova, M. (2003). Feeding soybean colonization by microscopic fungi. Trakya University. Journal of Science, 4: 165-168.
13. Khadka, S. ; Sherchand, J.B. ; Pokhrel, B.M. ; Dhital, S. ; Manjhi, R. and Rijal, B. (2017). Antifungal susceptibility testing of dermatophytes by agar based disk diffusion assay in tertiary care hospital, Nepal. Microbiology Research Journal International 19(2): 1-5.
14. Kubicek, C.P. ; Herrera-Estrella A. ;Seidl-Seiboth, V. and Martinez, D.A.(2011) Comparative genome sequence analysis underscores mycoparasitism as the ancestral life style of *Trichoderma*. Genome Biol 12:R40.
15. Kumar, A. ; Shukla, R. ; Singh, P. ; Prasad, C.S. and Dubey, N.K. (2008). Assessment of *Thymus vulgaris* L. essential oil as a safe botanical preservative against post harvest fungi infestation of food commodities. Innovat. Food Sci. Emerg. Technol. 9:575–580.
16. Lee, Y. L. ;Cesario T. ; Wang Y. ;Shanbrom E. and Thrupp L. (2003). Antibacterial activity of vegatables and juices. Nutrition,19:994 -996.
17. Merz, W. G. and Hay, R. J. (2005) . Medical mycology. 10th Edition. ASM Press.
18. Nenaah, E. G. and Ahmed, M. E.(2011). Antimicrobial activity of extracts and latex of *calotropisprocera*(ait.) and synergistic effect with reference antimicrobials. Research Journal of Medicinal Plants , 5 (6): 706-716.
19. Ohst,T. ; de Hoog, S. ; Presber, W. ; Stavrakieva, V. and Graser, Y. (2004). Origins of Microsatellite Diversity in the *Trichophytonrubrum* -T. *violaceum* Clade (Dermatophytes). Journal of Clinical Microbiology, 42 (10): 4444–4448.
20. Omero, C. ; Dror, Y. and Freeman, A. (2004). *Trichoderma* spp. antagonism to the dermatophyte *Trichophytonrubrum*: implications in treatment of onychomycosis. Mycopathologia.;158 (2) : 173-80.
21. Patil, R.K.A. and Prajapati, B.K.(2017). Effect of *Trichoderma* Spp. and its culture filtrate antagonists on growth and management of *Rhizopus* rot of tomato fruit *in vitro* and *in vivo* .Journal of Pharmacognosy and Phytochemistry; 6(4): 394-398.

22. Politi, F.A.S. ; Queiroz-Fernandes, G. M. ; Rodrigues , E. R. ; Freitas, J. A. and Pietro , R.C.L.R. (2016) . Antifungal, antiradical and cytotoxic activities of extractives obtained from *Tagetespatula* L. (Asteraceae), a potential acaricide plant species.Microbial Pathogenesis; 95:15-20.
23. Reino J.L., Guerrero R.F., Hernandez-Galan R. and Collado I.G. (2008). Secondary metabolites from species of the biocontrol agent *Trichoderma.* Phytochem. Rev., 7 (1): 89–123.
24. Rhama, S. and Madhavan, S.(2010). Antibacterial activity of the flavonoid, patulitrin isolated from the flowers of *Tageteserecta*L." International Journal of Pharm Tech Research., 3 (3) 1407-1409.
25. Rashmi, S. ; Sudarshan, M. and Ram, S. U. (2016).The improvement of competitive saprophytic capabilities of *Trichoderma* species through the use of chemical mutagens. Brazilian Journal of Microbiology, 47 : 10–17.
26. Sati S. C. and Joshi S. (2010). Antibacterial potential of leaf extracts of *Juniperuscommunis*L. from Kumaun Himalaya. *African Journal of Microbiology*, Res., 4:1291-1294.
27. Tripathi, B. ; Bhatia, R. ; Walia, S. and Kumar, B.(2012). Chemical composition and evaluation of *Tageteserecta*(Var. PusaNarangiGenda) essential oil for its antioxidant and antimicrobial activity. Biopestic. Int.8(2): 1-9 .
28. Zhou, Y., He, P., Liu, A., Zhang, L., Liu, Y. and Dai, R., (2012). Drug-drug interactions betweenketoconazole and berberine in rats: pharmacokinetic effects benefit pharmaco-dynamic synergism. Phytother. Res. 26, 772–777.

Table 1. Effect of *Tagetes erecta* extract in radial growth of *T. tonsurans*

Treatments	Concentrations (ppm)	Radial growth (cm)	Growth inhibition %)
Water extract	8000	2.90 ab	65.72
	6000	3.73bc	55.91
	4000	4.73def	44.08
	2000	5.50 f	34.98
Alcohol extract	8000	2.33 a	72.45
	6000	3.56bc	57.91
	4000	3.90bcd	53.90
	2000	5.26ef	37.82
Control	-	8.46 g	-
LSD (0.05)	0.8481		

*** Each value is a mean of 3 replicates.**
***Similar letter means no significant difference**

Table 2. Effect of Clotrimazole with fungal filtrate and plant extract in radial growth of *T. tonsurans*

Treatment	Radialgrowth(cm) after 7 day	Inhibition (%)	Type of Interaction
Clotrimazole alone (Cl)	2.5 a	69.87	-
T. *harzianum*+ Cl	2.4 a	71.08	Additive
T. *erecta* + Cl	2.2 a	73.49	Additive
Control	8.3 b	-	-
LSD(0.05)	0.911		

***Each value is a mean of 3 replicates**
***Similar letter means no significant difference**

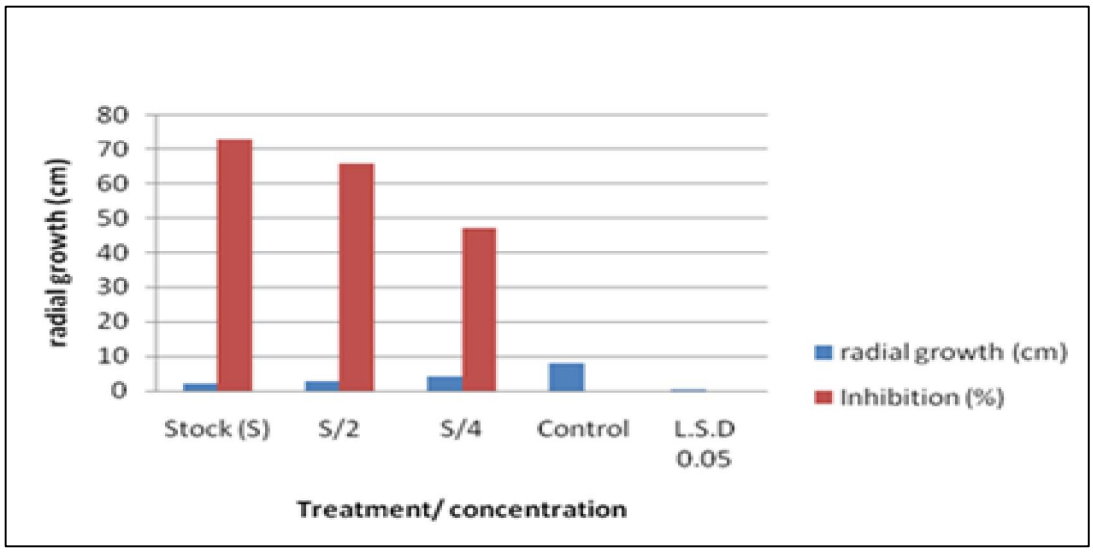

Figure 1.Fungal Filtrate on growth of *Trichophyton tonsurans* after 7 days of treatment

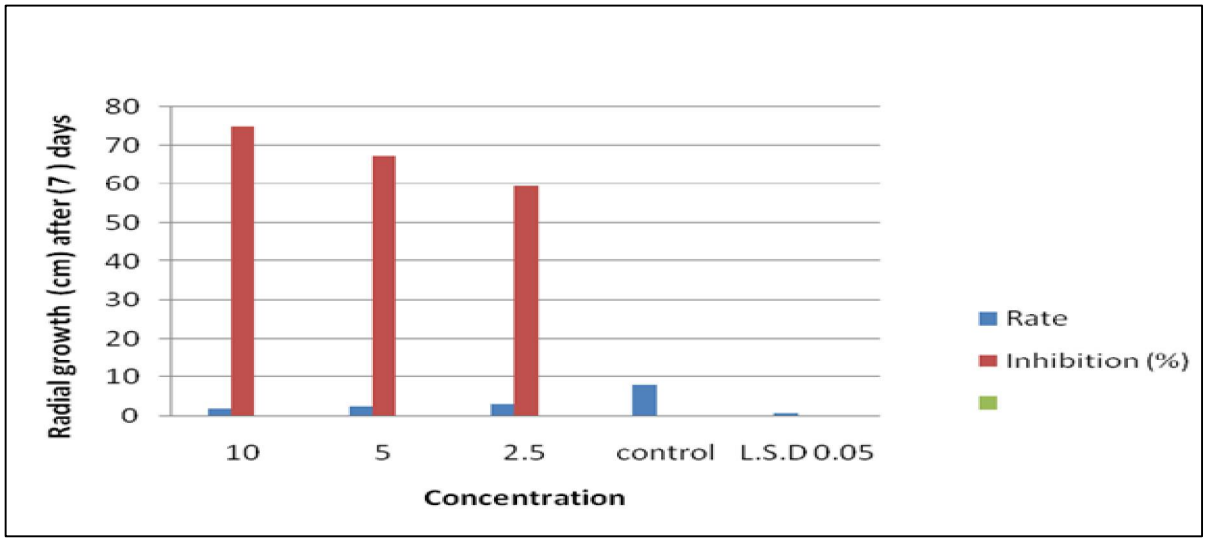

Figure 2. Clotrimazole in radial growth of *T. tonsurans* in culture media

Indian Journal of Natural Sciences www.tnsroindia.org.in ©IJONS

Vol.9 /Issue 51 / December / 2018 *International Bimonthly* *ISSN: 0976 – 0997*

RESEARCH ARTICLE

Histological and Histochemical Study of the Mandibular Salivary Gland in Adult Male Gazelle (*Gazellasubgutturosa*)

M.S.H. Simawy* and Mahd. A. Atya

Department of Anatomy, College of Veterinary Medicine, University of Baghdad, Iraq.

Received: 01 Aug 2018 Revised: 02 Sep 2018 Accepted: 07 Oct 2018

***Address for Correspondence**
M.S.H. Simawy
Department of Anatomy,
College of Veterinary Medicine,
University of Baghdad, Iraq.

ABSTRACT

Two head (four specimen of each gland), were used in histological and histochemical study , slide were stain with (Harris hematoxylin& eosin , Masson's Trichrome , van giessen , PAS , AB-PAS , AF-AB and Toldine blue). The mandibular salivary gland of gazelle was of mixed type consist of more muocus acini with and without demilons and few seros acini , the duct system inside the gland was started by intercalated ,striated ,intralobar , interlober ducts , the main mandibular duct accompanying with sublingual duct in their cores to open in the sublingual caruncle . The PAS stained mandibular salivary gland in gazelle show deep positive reaction with serous acini ,demilion , goblet cell and basement membrane , moderate positive reaction show in the muocus acini . By the AB-PAS stain the serous acini and demilions show positive reaction for PAS , the muocus acini show positive reaction to AB , goblet cell positive to both AB-PAS. In AF-AB stain serous acini , demilions and duct show positive for AF, while the muocus acini and goblet cell appear positive reaction for AB. Mandibular gland when stain by toldine blue show the serous acini and the demilion week positivereaction , the muocus acini show strong positive .

Key words: Mandibular salivary gland , Histological , Histochemical, Gazella.

INTRODUCTION

The salivary gland is organ of many important function excretory, digestive, protective and endocrine functions [1]. In ruminant the salivary gland secretions regulates the digestion in fore stomach [2]. The oral cavity mucosa are always moistened by the saliva secreted by the associated major and minor salivary gland [3].Salivary glands develop in different location , they has different structure and produce more than one type of saliva [4].This is highly important for the animal , because they need to relocate phosphorous and nitrogenous structure , glands are important factors for microbial growth in the fore stomach [5].The gland usually consist of two part secretory and transport ducts [6]. In

ruminant the saliva is mostly serous, containing enzymes that initiate carbohydrate digestion, water to moisten the food, mucopolysaccharides (complex carbohydrates) and lubricating glycoprotein that facilitate deglutition , saliva contains anti-microbial factors such as lysozyme and lactoferrin also it contain proteins such as salivary amylase, lysozyme, lactoferrin[7],[8]. Gazelle subgutturosa has saved in several nature reserves located in many provinces including the district of AL Madaen in the outskirts of the capital Baghdad , an area of 157 acres, where ksiab-reservoir to save the species and varieties from the risk of extinction , include Gazella subgutturosa which involved in this study [9].

MATERIALS AND METHODS

Our study was done on specimen isolated from tow heads (four from each gland) of adult male gazelle (2-3) years, were used in histological and histochemical study. Immediately after slaughter several histological sample 0.5 × 0.8 cm from different parts of gland, execratory duct, parotid opining and sublingual carncle were taken. for histologiacal study the specimen was fixed in 10% neutral buffered formalin. While in Histochemical studythe Specimens were taken are fixed in Bouin's solution. After 24 hour both sample of histological and histochemical study were dehydrated in ascending series of ethyl alcohol(70%, 80%, 90% and 100%), cleared in xylene and embedded in paraffin wax . section of Six micrometer were prepare to stain : (Harris hematoxylin& eosin stains for general morphological features , masson's Trichrome and van giessen methods for the demonstration of the connective tissue fibers, PAS stain for the basement membrane and glycoprotein , AB-PAS for acidic& neutral mucins , AF-AB for differentiate sulfated from non-sulfated mucins , Toldine blue for glycosaminoglycan) .The colored slide were examination and photed by using light microscope (Olympus BH-2 microscope) and digital camera .

RESULTS

Histological results

The mandibular salivary gland of gazelle was covered entirely by capsule of dense connective tissue formed from collagen, little elastic and reticular fiber, which sent many trabiculi from capsule divided the gland parenchyma into multi different size and shape lobes and lobules (fig.1). The gland was of mixed type consist of more mucous acini with and without demilons and few serous acini distributed in between the mucous acini which made the parenchyma of gland. The serous acini was lined with pyramidal cells of rounded centrally located nuclei, the mucous acini lined with cuboidal cell of basically located nuclei, elongated nucleus of basket cell present between the acini and basal lamina of the mucous cell (fig.2). The demilons weregroups of serous cells aggregated in crescent shape capped the mucous cells (fig.2). Small, intermediate and large acini can be distinguished depending on their diameter, the small acini of (10.02±1.02) in diameter lined with 3-4 cells , the intermediate acini were (19.30 ±0.90) diameter lined with 5-6 cells , while the large acini were (28.12±1.23) in diameter lined with 9-10 cells (fig. 3). The duct system of the gland was started by the intercalated, striated, intralobar and interlober ducts. The intercalated duct was lined with low cuboidal cells; the striated duct was lined with cuboidal cells. Myoepithelial cells were presented around both intercalated and striated ducts (fig.2). The intralobar duct was large and present in the intralobar connective tissue and lined with simple columnar cells (fig 3).Finally the interalobar duct lined with cuboidal to double cuboidal cells (fig.4).The main mandibular duct accompanying with sublingual duct in theircores to open in the sublingual carncle (fig.5). The main duct was lined with double cuboidal cell change gradually to become stratified squamous cell with few goblet cellnear the orifice (fig 6). The external orifice of mandibular duct open in the sublingual carncle by common orifice with sublingual duct (fig 7).

Histochemical results

The mandibular salivary glandshowed intense positive reaction PAS of serous acini and the demilion of mucous aciniand moderate positive reaction in the mucous acini, the goblet cells showintense positive reaction with PAS stain, while the intraglandular duct system show weak positive reaction (fig.8). With the combined AB-PAS stain, the serous acini and demilions were positive reaction for PAS and negative to AB stain, the intraglandular duct showed weak positive reaction for PAS stain, while the mucous acini were positive reaction for AB and negative for PAS, the goblet cell positive for both stain (fig.9). The serous acini as well as the demilions of mucous acini and the epithelia of lining cells of the intraglandular duct were positive for AF and negative for AB stain, while the mucous acini appear the positive reaction for AB and negative for AF (fig.10).The serous acini and the demilion were week positive (deep purple) reaction with toldine blue, the mucus acini showed intense positive (pale purple) reaction in compare to moderate positive reaction of the duct system, while the goblet cells werenegative (fig.11).

DISCUSSION

Mandibular salivary gland was lobulated surrounded by of dense connective tissue capsule that supported the parenchyma bytrabeculi, such result similar to all mandibular salivary gland in the animals, in Camel , ox [10], in Sheep [11], in Goat [12] and in rabbit [13]. The gland was mixed mostly mucous with or without demilons and few serous acini was similar to that in buffalo [14], in bovine [15] , in Ox [10] , in goat [16], also our result was similar in Sheep [11] , in Goat [12] and barking deer [17] but they don't remember that the animal has demiloin in their gland. The intraglandular duct system consist of intercalated duct, striated duct , intralobar duct and inter lobar duct, this was also agreement with findings of in Camel[10] and disagreement with that of in bovine [15], in barking deer[17] and in rabbit [13] who remember that has two duct (intercalated and striated duct) and also different with in Ox [10], in Sheep [11], in buffalo[14] and in Goat [12] who describe the intraglandular duct was consist of (intercalated , striated and interlobar duct). The main execratory duct was stratified cuboidal cells change to stratified squamous epithelia and had few goblet, this result was similar to buffalo [14]. The type of epithelia line here is similar to that of in barking deer [17] but does not remember the goblet cells.The serous acini and demilion as well as the goblet cell of execratory mandibular showeddeep positive reaction for PAS, while the mucus acini was moderate positive and the intraglandular duct system was week positive, the positive PAS reaction indicator present of glycoprotein ,there are complete similarity between our result and findings of camel , ox [18] and rabbit [13].With combined AB-PAS stain, the serous acini, demilion were positive for PAS, this reactionwas due to present of neutral carbohydrate, goblet cell show positive to both AB-PAS stains this indicated to present acidic (AB) and neutral (PAS) carbohydrate, the mucous acini positive reaction to AB indicated to present acidic mucin , the intraglandular duct positive for PAS (neutral), our findings in acini is similar with result of camel [18] and bovine [19] , otherwise the result of ox [18] and barking deer [17] was differ from that result in gazelle. Staining with AF-AB show the serous acini, demilion and intraglandular duct were positive for AF, this was give indicator that they has sulfated carbohydrate, while the mucus acini show positive AB reaction which indicator present of non-sulfated mucin, our result is same as in rabbit[13] and it is disagreement with Cat [20] which found the mucus acini has sulfated mucin. When stain by toldine blue the gland was week positive in serous acini and demilions, the mucous acini show strong positive and the intraglandular duct system was moderate positive,the positive reaction to toldine blue indicator present of glucosaminoglucans , the goblet cell was negative , our result is differ from [21] recorded the mucous and intraglandular duct was negative in Cat

REFERENCES

1. Miletich I. Introduction to salivary glands: structure, function and embryonic development. Front Oral Biology,2010; 14: 1-20.
2. Kay RB, and MaloiyGMO.Digestive secretions in camels.Options mediterreaneseries seminaries-n.1989 2.

3. 3.Nanci A. Salivary glands. In: Nanci A, editor. Ten Cate's oral histology: development, structure, and function, Elsevier Inc. St. Louis, Missouri;2013:253-277.
4. Jaskoll T, Zhou YM, Chai Y, Makarenkova HP, Collinson JM, West JD, Carvalho AD. Embryonic submandibular gland morphogenes is: stage –specific protein localization of FGFs,BMPs,Pax6 and Pax 9 in normal mice and abnormal phenotypes in FgfR2-IIl c(t/Delta),BMP(-/-)and Pax(-/-)mice cells tissue organs.2002; 170: 83-90.
5. Breves G, Rosenhagen C, Hooeller H. Saliva secretion of in organic phosphorous in phosphorous -depleted sheeep .J.V.Med,.1987; 43:42-47.
6. Vissink A, Mitchell JB, Baum BJ, Limesand KH, Jensen SB, Fox PC, Elting LS, Langendijk JA, Coppes RP, Reyland ME. Clinical management of salivary gland hypofunction and xerostomia in headand- neck cancer patients: successes and barriers. Int J RadiatOncolBiol Phys2010; 78: 983–991.
7. Marchetti L, Gabrielli MG, Materazzi G, Menghi G. Cellular compartmentation of lysozime and alpha amylase in the mouse salivary glands. Immunogold approaches at light and electron microscopy level. Histol.Histopathol.2000; 15: 337–346.
8. Akers RM, Denbow DM. Anatomy and Physiology of Domestic Animals. USA: Blackwell Publishing.2008.
9. Abood DA, Hussein ZM. Histological features of vomer nasal organ in indigenous Gazella (Gazella subgutturosa). J Entomol. Zool. Studies, 2017; 5:598-604.
10. Mursal NJ, Hassan AA, Zarroug HI. Comparative Anatomical and Histological Studies of the Mandibular gland of Camel, Ox, Sheep and Goat. Sudan Journal of Science and Technology,2016; 17.2: 1-11.
11. Muthukrishnan S. Microanatomical Studies On The Parotid And Mandibular Salivary Glands In Sheep (Ovisaries) (Doctoral dissertation, Tamil Nadu Veterinary and Animal Sciences University)2011.
12. Rauf SMA, Islam MR, Anam MK. Macroscopic and microscopic study of the mandibular salivary gland of Black Bengal goats. Bangladesh Journal of Veterinary Medicine,2004;2: 137-142.
13. AL-Saffar FJ, Simawy MSH. Histomorphological and histochemical study of the major salivary glands of adult local rabbits. Int. J.Adv, research. 2014;2 .11:378-402.
14. AL-Saadi AIJ.Anatomical , histological and ultra-structural study of the major salivary gland in indigenous buffalo . MSC.thesis in anatomy and histology . Bagdad university .veterinary medicine collage.2002.
15. Adnyane IKM, Novelina S, Wresdiyati W, Winarto A, Agungpriyono S.Lysozime producing cells are detected in the bovine salivary glands by immunohistochemical method. JuVet. UNUD,2007;8: 10–15.
16. Singh AD, Jain RK, Kumar P. Histomorphological and histochemical studies on the dorsal buccal gland of sheep (Ovisaries). Indian Journal of Veterinary Anatomy,2012; 24: 26-28.
17. Adnyane IKM, Zuki AB, Noordin MM, Agungpriyono S. Histological study of the parotid and mandibular glands of Barking Deer (Muntiacusmuntjak) with special reference to the distribution of carbohydrate content. Anat. Histol. Emryol.2010;39: 516-520.
18. Mursal NJ, Hassan AA, Zarroug, HI. Comparative Morphological, Histometric and Histochemical studies of Parotid and Mandibular Salivary Glands of Camel, Ox, Sheep and Goat,2016:03-13.
19. Suzuki S, Nishinakagawa H,Otsuka J. Fine Structure of the Bovine Mandibular Gland. Mem.Fbc, Agr, KhgoshimaUhiv, 1981; 17, 147-155.
20. Sozmen M, Brown PJ, Cripps PJ. Quantitation of histochemical staining of salivary gland mucin using image analysis in cats and dogs. Veterinary Research, BioMed Central,1999; 30.1:.99-108.
21. EL-Kordy EA, Alanazi AD, Ali SS, Makhlouf MM. Rabah SO. Histological, Histochemical and UItrastructural Changes in the Submandibular Gland of Starved Young Male Cats .CytolHistol.,2014; 5:4.

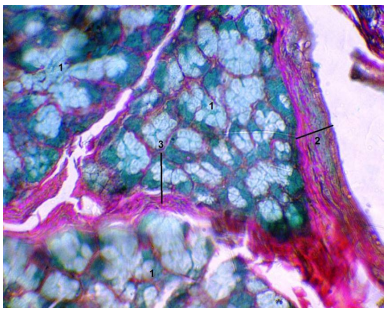

Figure 1:Tissue section of mandibular gland in gazelle. Show: lobes of gland (1), capsule (2), & trabiculae (3). Masson Trichrom, X20

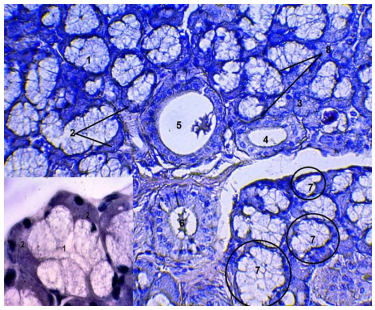

Figure 2:Tissue section of mandibular gland in gazelle. Shows: mucus acini (1), demilions (2), serous acini (3), Intercalated duct (4), striated duct (5), intra lobar duct (6) , different shape and size of acini (7) & myoepithelial cells (9). H&E, X20 (the main figure) and H&E, X100 (the rectangle figure).

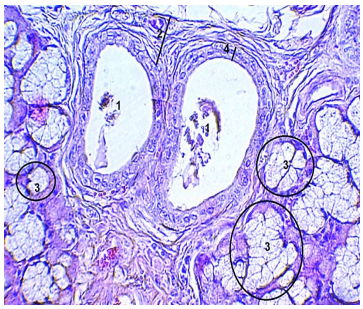

Figure 3: Tissue section of mandibular gland in gazelle. Shows: Lumen of intralobar duct (1), Intralobar connective tissue (2), different shape and size of acini (3) . H&E, X20

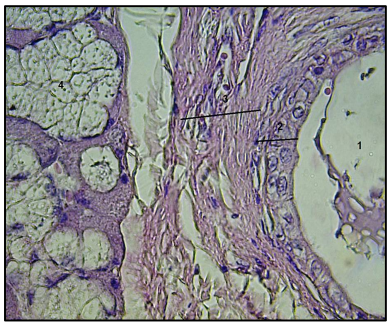

Figure 4: Tissue section of mandibular gland in gazelle. Shows: Lumen of interlobar duct (1),cuboidal cells (2) & Interlobar connective tissue (3). H&E , X40.

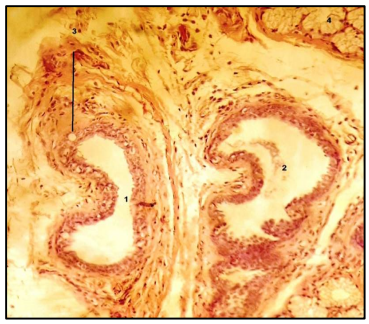

Figure 5: Tissue section of mandibular gland in gazelle. Show: Mandibular duct (1), sublingual duct (2), goblet cell (3) &sublingual gland (4) . H&E , X4.

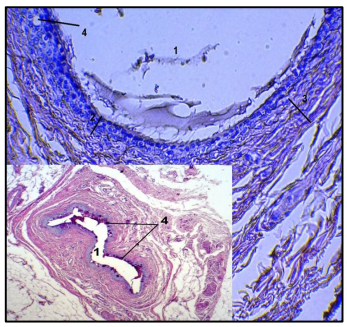

Figure 6:Tissue section of mandibular gland in gazelle shows : Lumen of execratory duct (1), stratified squamous epithelia (2), connective tissue(3) & goblet cells (4) . H&E , X20 (the main figure) and PAS , X4 (the rectangle figure).

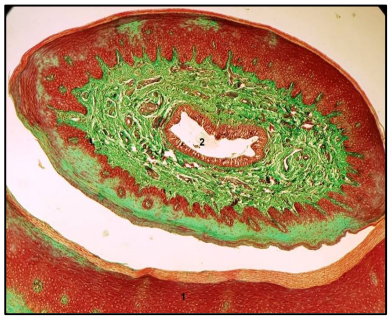

Figure 7: Tissue section of mandibular gland in gazelle shows: Floor of mouth cavity (1), common orifice of both sublingual and mandibular gland (2). Masson Trichrome , X10 .

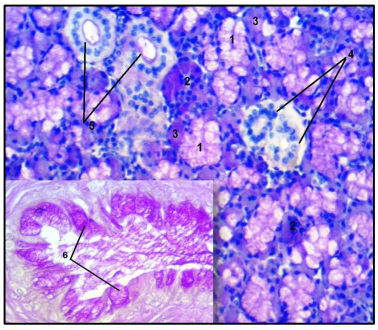

Figure 8 : Section of mandibular gland in gazelle. Shows: Mucus acini (1), serous acinus (2), demilions (3), intercalated duct (4), striated duct (5) & goblet cell (6).PAS , X20 (the main figure) and X40, (the rectangle figure).

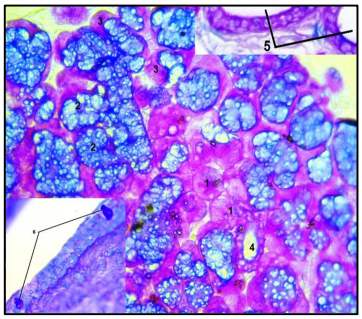

Figure 9 : section of mandibular gland in gazelle .shows: Serous acini (1),.mucus acini (2), demilions (3), intercalated duct (4),striated duct (5) & goblet cell (6). AB-PAS, X20 (the main figure) and X40 , (the rectangle figure).

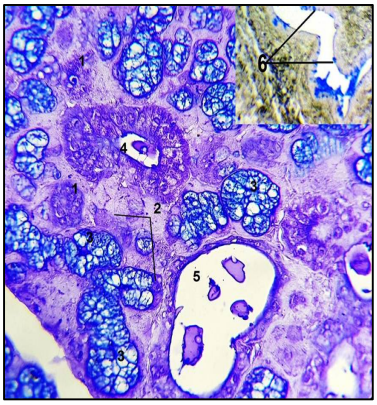

Figure 10 : Section of mandibular gland in gazelle shows: Serous acini(1),demilions (2), mucus acini (3), striated duct (4), intralobar duct (5) & goblet cells (6). AF-AB , X20 (the main figure) and X20 , (the rectangle figure).

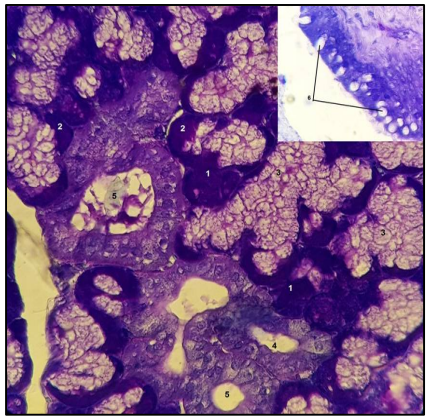

Figure 11:Toldine blue stain section of mandibular gland in gazelle .shows: Serous acini (1), demilions (2), muocus acini (3),intercalated duct (4), striated duct (5) & goblet cells(6).ToldineBlue , X40 (the main figure) and X40 , (the rectangle figure).

Indian Journal of Natural Sciences www.tnsroindia.org.in ©IJONS

Vol.9 /Issue 51 / December / 2018 *International Bimonthly* *ISSN: 0976 – 0997*

RESEARCH ARTICLE

Synthesis of Cr Doped TiO_2 Using Sol-Gel Technique and Calculation of its Photocatalytic Activity

Ansam Hadi Hasan* and Falah H. Ali

Department of Physics, College of Science, University of Baghdad, Baghdad, Iraq.

Received: 12 Aug 2018 Revised: 15 Sep 2018 Accepted: 19 Oct 2018

***Address for Correspondence**
Ansam Hadi Hasan
Department of Physics,
College of Science,
University of Baghdad,
Baghdad, Iraq.

ABSTRACT

The present study exposure undoped TiO_2 and chromium doped $TiO_2$with many concentrations (2%,4%,6% and 8%) has been synthesized by simple sol-gel technique using dip-coating method. The resulting samples were characterized by X-ray diffraction, scanning electron microscopy, UV-VIS absorption. The results showed a clear shift in the light absorption from UV region (387.5 nm) to visible region (496 nm).XRD results explained anatase phase of TiO_2.SEM results showed the morphology was changed after doping process compared with the pure anatase TiO_2. Experimental results revealed that the dopants had no effect, at these concentrations: from 2% to 8%,on the phase of products. the photocatalytic activities of samples were evaluated using MB as a model organic dye compound under UV and visual irradiation. The results illustrated that the 4% Cr-doped TiO_2calcined at 450 ºC for three hours exposure the best photocatalytic activity under visible light irradiation. The results from this work showed that doping with transition metal ions could turn the inert TiO_2 to become photocatalytically active. Considering the simplicity in preparation and low cost, this should be an attractive choice to self-cleaning surface.

Keywords: Photocatalytic activity, Cr-doped TiO_2, sol-gel method, Methylene Blue.

INTRODUCTION

Nanomaterials reveal new functions which are derived both from the geometric size of nanostructures and from their material specific properties. In the investigation of material properties, compounds that are employed as photocatalysts include oxides such as TiO_2 , ZnO, Nb_2O_5 ,WO_3 , SnO_2 andZrO_2 , as well as sulfides such as CdS and ZnS. Among these, titanium dioxide (TiO_2) is one of the most commonly used.TiO_2 nanoparticles have characteristics such as strong reduction and oxidation capability, high chemical stability, and low costs and they are harmless to the

environment, thus making them a promising new type of photocatalyst [1].The most thermodynamically steadfast crystalline TiO_2 has two polymorph forms which are rutile and anatase, where rutile is the more thermodynamically stable form, with band gap energy of 3.02 eV and 3.20 eV for anatase. However, TiO_2 is not an efficient photocatalyst because of its large band gap energy that only allows operation within ultraviolet range and high electron-hole recombination rate which retains a limited amount of hydroxyl species on its surface. Besides that, its low surface area (~50 m^2/g) has been a major disadvantage[2].In order to solve these problems, modifications of TiO_2 such as coupling with noble metals as co-catalyst, transition metal oxides and non-metal doping have been carried out[3].Recently, as ways to improve the photocatalytic activity of titania, chromium doping has proven as a likely strategy [4]. Metal doping in TiO_2 for photocatalytic application has gained lot of attention since enhancing the visible light response by lowering the charge carrier recombination. It is well known that metal ions doping in TiO_2 can influence the intrinsic properties of the semiconductor photocatalyst by extending its photoresponse into the visible. Importantly, metal-doped TiO_2 facilitates electron-hole separation and promotes the interfacial electron transfer processes.

The optical absorption edge of the different transition metal ion doped TiO_2 is found to shift from UV to visible region of electromagnetic spectrum of light. This red shift in metal-doped TiO_2 was attributed to the charge-transfer transition between the electrons of the dopant and the conduction band (CB) ofTiO_2 [5]. The report came in 2010, Choi et al. [6] studied the effect of 13 different single metal ion dopants Ag^+, Rb^+, Ni^{2+}, Co^{2+}, Cu^{2+}, V^{3+}, Ru^{3+}, Fe^{3+}, Os^{3+},Y^{3+}, La^{3+}, Pt^{4+}, Pt^{2+}, Cr^{3+}, and Cr^{6+}on visible light reactivity of TiO_2. Among the various transition metal ions, Cr has been mostly used as a dopant since Cr doping extends the photoresponse to visible-light range by narrowing the band gap [7,8].Doping TiO_2 with Cr has found to promote photoelectrochemical water decomposition and photo-degradation of organic compounds using solar energy [9].Zhang et al. [10] investigated the photocatalytic activities of Cr/TiO_2 nano tubes prepared by the combination of sol–gel process with hydrothermal treatment. Buddee et al. [11]reported the improvement in the photocatalytic property of amorphous TiO_2 by doping it with Cr(III) and Fe(III) ions for methylene blue degradation. Choudhury et al. [12]investigated the effect of Cr-doping on the structural, optical and magnetic properties of TiO_2 nanoparticles. The photocatalytic behavior of chromium-doped titania and chromium supported on the surface of titania were studied by Ould-Chikh et al. [13]. in this work Cr-doped TiO_2 nanoparticles have been prepared with various doping concentration by modified sol–gel method. The structural, optical and photocatalytic properties of the doped nanoparticles were also investigated. X-ray diffraction (XRD) is used to calculate crystallite size. Scanning electron micrograph (SEM) images are shown to clearly see the particle size and grain size respectively.

MATERIALS AND METHODS

These chemical materials were adopted in this work: Chromium nitrate $Cr(NO_3)_3$, Nitric acid(HNO_3),and methylene blue (MB), all supplied from Merck Co. Titanium tetraisopropoxide (TTIP), $Ti[OCH(CH_3)_2]_4$, purity 97%, from Sigma-Aldrich ,deionized water and methylene blue (MB) .

(TiO_2) Sol preparation

(TiO_2)sol was prepared using the following procedure: Deionized water was mixed with (TTIP) in terms of a molar ratio of Ti: H_2O=1:4. Nitric acid was used to adjust the pH at (1.5) for restrain the hydrolysis process of the solution. The solution was put on a magnetic stirrer for (24 hours). The resultant sol was aged for six hours at (55ºC) yielding a transparent sol.

Cr- doped TiO_2sol preparation

The Cr-doped TiO_2 nanoparticles were synthesized with the slightly modified sol–gel method, In the preparation, Nitric acid was mixed with deionized water to adjust PH value at (1.5),this mixture is denoted as mixture (A).Meanwhile, taking about (5ml) from (A) and mix with several concentrations of(2, 4, 6 and 8 %) of $Cr(NO_3)_3$,This mixture was denoted as mixture B. Slightly, TTIP was added to the first mixture (A). Separately mixture B was added to mixture (A)drop by drop, this process was done at room temperature. The resultant sol was stirred for (24hours),and then aged for six hours at (55ºC), yielding light green transparent sol related to Cr, doped sample. The different samples such as pure TiO_2,2 % Cr-doped TiO_2, 4% Cr-doped TiO_2, 6% Cr-doped TiO_2 and 8% Cr-doped TiO_2 are denoted asT,TC1, TC2,TC3 and TC4, respectively.

Photocatalytic activity test

The photocatalytic activity of the prepared samples was evaluated with the degradation of MB under UV and visible light irradiations. an amount of (30ml) aqueous solution of Methylene Blue (MB) dye with concentration (10^{-5})[M] was placed in a petri dish. Different prepared samples were placed in this solution. The distance between the applied lamps and the surface of MB solution was 15 cm. Then, the samples were placed in a UV light exposure cabinet in which they were illuminated with (18W), UV-Source of range (200nm-400nm) and (18W) VIS-Source .Representative samples of (MB) solution were taken at each equal time intervals and measure the absorbance by spectrophotometer, CTECTOR, SV200, Korea. Fixed at the wavelength of (665 nm), which represents the absorption peak value of the (MB) dye.

Characterizations

The prepared samples have been characterized by various techniques such as XRD, UV–Vis spectroscopy, SEM.

Structural characterizations

The X-ray Diffraction patterns for the prepared samples were achieved. XRD patterns of the nanoparticles were recorded at room temperature using Cu Ka (k =1.5418 A$^\circ$) radiation to identify the crystal phase. The positions of the diffraction peaks in the films were compared with those given in ASTM data card (# 96-900-9087) for anatase [14]. X-ray pattern for all samples are shown in the Figure (1). This figure shows that, the films were polycrystalline having totally anatase phase. It is observed that all films exhibited characteristic peaks of anatase crystal plane (010), (004), (200), (105) and (211). Scanning electron microscopy images (Figure 2) are present the surface profile and particle size for the prepared samples thin films.

Optical characterizations

Optical characterizations were achieved by means of the absorption spectra, where the band gap energies were calculated for the prepared samples. The Absorbance of pure and Cr-doped TiO_2 samples were recorded with a UV–visible spectrophotometer (CTECTOR, SV200, Korea) in the spectral range of (200-800 nm) is shown in the Figure (3). From this figure, it is clear that the absorption edge are red shifted with respect to the bare sample in the direction of Cr-doped TiO_2.

RESULTS AND DISCUSSION

X-ray diffraction analysis

XRD patterns of TiO_2 and Cr-doped TiO_2 nanoparticles are shown in the Fig. 1. XRD was used to investigate phase structures and crystallite size of the prepared nanoparticles. All Cr-doped TiO_2 nanoparticles consist of anatase as a unique phase. The crystallite size calculated by using Scherer's equation. The diffraction pattern does not show any peak of secondary phase or other impurities such as chromium oxides. The peak position and intensity were not significantly affected by doping of Cr into the TiO_2 host lattice.

Scanning electron microscopy (SEM)

Surface profile and particle size of pure TiO_2 and Cr-doped TiO_2thin films prepared were observed by scanning electron microscopy. Figure(2)The magnification of this image is (350 kx) and scale is (100 nm).

UV–Vis absorption spectroscopy

UV–Vis absorption spectra of TiO_2 and Cr-dopedTiO_2 nanoparticles are presented in Fig. 3.The sol–gel synthesized pure TiO_2 (T) and Cr-doped TiO_2 nanoparticles show absorption edge at 387.5,400, 496,416 and 413 nm for TC1, TC2,TC3 and TC4 samples, respectively. The band gap energy values were determined by linear fitting the absorption edge. The band gap energy values were calculated to be3.2, 3.1, 2.5,2.98 and 3 eV for pure TiO_2(T), TC1,TC2,TC3,TC4 samples, respectively. The increase of Cr ions contents in TiO_2 host lattice leads to linear increase in the optical absorption to the visible light region. The extended absorption in the visible region is due to the excitation of the electrons from the Cr to the conduction band of TiO_2[6].The absorption spectra of the Cr–TiO_2 samples show more absorption than TiO_2 in the visible region, which indicates the existence of surface states. The oxygen vacancies should have been created to maintain charge neutrality due to metal doping, inducing bath chromic shift in the band gap transitions [15, 16].

Photocatalytic activity

MB is a distinguished histological dye that has extensive applications in dying cottons, wools, temporary hair colorant, coloring papers and coating for paper stock [17, 18].Although MB is not strongly dangerous, it can cause some harmful effects such as heart rate, shock, Heinz body formation, cyanosis, jaundice, vomiting, quadriplegia, and tissue necrosis in humans [19].In this study, Methylene blue (MB) dye was chosen as pollutant model for photocatalytic activity test. The photodegradation efficiency of this dye was examined asa function of UV and visible irradiation time for pure and doped samples respectively. The absorbance decays of (MB) dye versus UV and VIS irradiation time are illustrated in the Figure (5,6).

CONCLUSIONS

Cr doped anatase TiO_2 nanoparticles with visible light activity were successfully synthesized by modified sol–gel method using dip coating at room temperature. XRD analysis of Cr–TiO_2 nanoparticles show characteristic features of nano crystalline TiO_2 in tetragonal anatase phase. In conclusion from SEM images; Chromium doping in TiO_2 via sol-gel technique, in sol phase, reducing the final product particle size,. Calcination temperature should not exceed 450 ºC to keep anatase phase. The effect of low concentration chromium doping on the photocatalytic activity of TiO_2 was investigated by performing the photodegradation of MB. The presence of chromium dopant plays a vital role in altering physiochemical and photocatalytic properties of TiO_2. The optical band gap energy of Cr-doped TiO_2 nanoparticles shifted in the visible light region.Cr–TiO_2 nanoparticles showed higher photoactivity than undoped

samples. The photocatalytic degradation of MB is enhanced with increasing chromium concentration in TiO_2 host lattice. Cr-doped TiO_2 photocatalyst are found to be plausibly applicable for environmental remediation applications.

REFERENCES

1. M. Koelsch, S. Cassaignon, J. F. Guillemoles and J. P. Joivet: Thin Solid Films, 403–404 (2002) 312–319.
2. M. Zhang, L. Shi, S. Yuan, J. Fang. 2009. "Synthesis and Photocatalytic Properties of Highly Stable and Neutral TiO_2/SiO_2 Hydrosol". J. Colloid Interf. Sci. 330: 113–118 .
3. T.Al. Ouafa,T.N. Quang, R. Touria. 2009. "Preparation and Characterization of a New TiO_2/SiO_2 Composite Catalyst for Photocatalytic Degradation of Indigo Carmin". Environ. Chem. Lett. 7: 175–181.
4. S. Quorzal, N. Barka, M. Tamimi, A. Assabbane, A. Nounah, A. Ihlal, Y. Ait-Ichou. 2009. "Sol-gel Synthesis of TiO_2-SiO_2Photocatalyst for β-Naphthol Photodegradation". Mater. Sci. Eng. C. 29: 1616–1620.
5. J.C.S. Wu, C.H. Chen, "A visible-light response vanadium-doped titania nanocatalyst by sol–gel method". J. Photochem. Photobiol. A Chem. 163, 509–515 (2004).
6. J. Choi, H. Park, M.R. Hoffmann, "Effects of single metal-ion doping on the visible-light photoreactivity of TiO_2". J. Phys. Chem. C 114, 783–792 (2010) .
7. J. Zhu, Z. Deng, F. Chen, J. Zhang, H. Chen, M. Anpo et al., "Hydrothermal doping method for preparation of Cr^{3+}–TiO_2photocatalysts with concentration gradient distribution of Cr^{3+}".Appl. Catal. B Environ. 62, 329–335 (2006) .
8. X. Li, Z. Guo, T. He, "The doping mechanism of Cr into TiO_2 and its influence on the photocatalytic performance". Phys. Chem. Chem. Phys. 15, 20037–20045 (2013) .
9. C.C. Tsai, H. Teng, "Chromium-doped titanium dioxide thin-film photoanodes in visible-light-induced water cleavage". Appl. Surf. Sci. 254, 4912–4918 (2008) .
10. S. Zhang, Y. Chen, Y. Yu, H. Wu, S. Wang, B. Zhu et al., "Synthesis, characterization of Cr-doped TiO_2 nanotubes with high photocatalytic activity". J. Nanoparticle Res. 10, 871–875 (2007) .
11. S. Buddee, S. Wongnawa, U. Sirimahachai, W. Puetpaibool, "Recyclable UV and visible light photocatalytically active amorphous TiO_2 doped with M(III) ions (M = Cr and Fe)". Mater. Chem. Phys. 126, 167–177 (2011) .
12. B. Choudhury, A. Choudhury, "Structural, optical and ferromagnetic properties of Cr doped TiO_2 nanoparticles". Mater. Sci. Eng., B 178, 794–800 (2013) .
13. S. Ould-Chikh, O. Proux, P. Afanasiev, L. Khrouz, M.N. Hedhili, D.H. Anjum et al., "Photocatalysis with chromium-doped TiO_2: bulk and surface doping". Chem Sus Chem 7, 1361–1371 (2014) .
14. T. Ihara, M. Miyoshi, Y. Iriyama, O. Matsumoto, S. Sugihara; Environmentally benign photocatalysts: "Applications of Titanium Oxide-based", Appl. Catal., B, 42, 403 (2003) .
15. A.T. Vu, Q.T. Nguyen, T.H.L. Bui, M.C. Tran, T.P. Dang, T.K.H. Tran, "Synthesis and characterization of TiO_2photocatalyst doped by transition metal ions (Fe^{3+},Cr^{3+} and V^{5+})". Adv. Nat. Sci. Nanosci. ,Nanotechnol. 1, 015009 (2010).
16. H.M. Yadav, S.V. Otari, R.A. Bohara, S.S. Mali, S.H. Pawar, S.D. Delekar, "Synthesis and visible light photocatalytic antibacterial activity of nickel-dopedTiO$_2$ nanoparticles against Gram-positive and Gram-negative bacteria". J. Photochem. Photobiol. A Chem. 294, 130–136 (2014) .
17. J.P. Tardivo, A. Del Giglio, C.S. de Oliveira, D.S. Gabrielli, H.C. Junqueira, D.B. Tada et al.," Methylene blue in photodynamictherapy: from basic mechanisms to clinical applications". Photo-diagn. Photodyn. Ther. 2, 175–191 (2005) .
18. B.H. Hameed, A.A. Ahmad, "Batch adsorption of methylene blue from aqueous solution by garlic peel, an agricultural waste bio-mass". J. Hazard. Mater. 164, 870–875 (2009).
19. Y. Bulut, H. Aydın, "A kinetics and thermodynamics study of methylene blue adsorption on wheat shells". Desalination 194,259–267 (2006).

Table1experimental X-ray peaks for (Cr- doped TiO_2) samples

W%	2θ (degree)	FWHM(degree)	Crystalline size (nm)	hkl	Phase
2%	25.36	0.47	32.6	(101)	Anatase
4%	25.19	0.74	20.8	(101)	Anatase
6%	25.27	0.44	34.8	(101)	Anatase
8%	25.5	0.41	37.5	(101)	Anatase

Table 2.$TiO_2$and Cr-doped TiO_2 particle size of samples extracted from SEM images

Samples	Particle size (nm)
T	11.84
TC1	13.91
TC2	10.90
TC3	13.81
TC4	12.82

Table 3 Band gap energy and its corresponding wavelength for the prepared Samples

M-TiO_2	Samples	wt%	Energy gap(eV)	Wavelength(nm)
TiO_2	T	0	3.2	387.5
Cr-doped TiO_2	TC1	2	3.1	400
	TC2	4	2.5	496
	TC3	6	2.98	416
	TC4	8	3	413

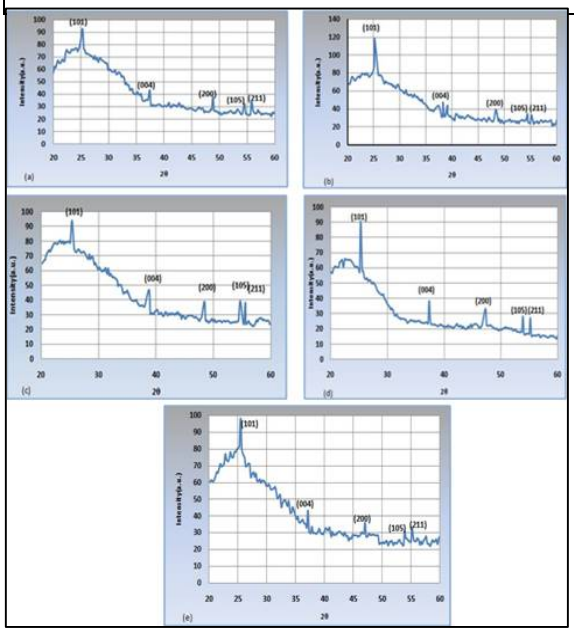

Fig.1: XRD for pure and Cr-doped TiO_2

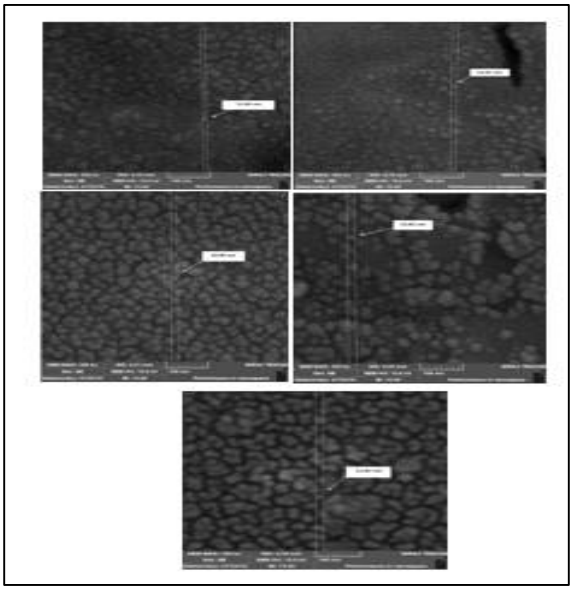

Fig (2): SEM images of T,TC1,TC2,TC3,TC4 samples

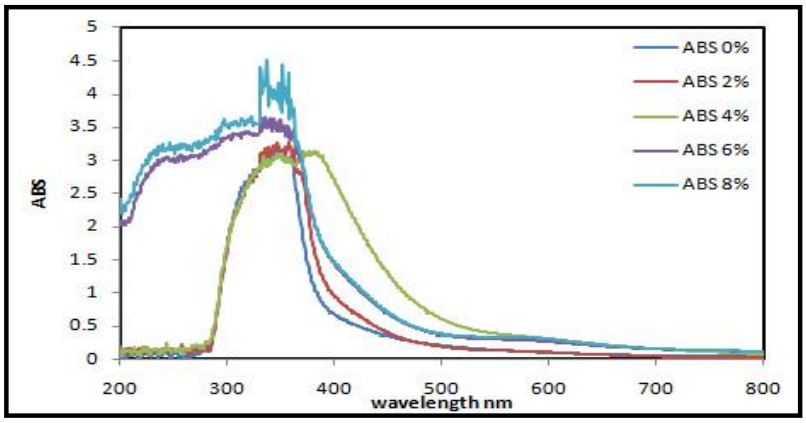

Fig (3): The Absorption spectrum of pure and Cr-doped TiO_2 samples .

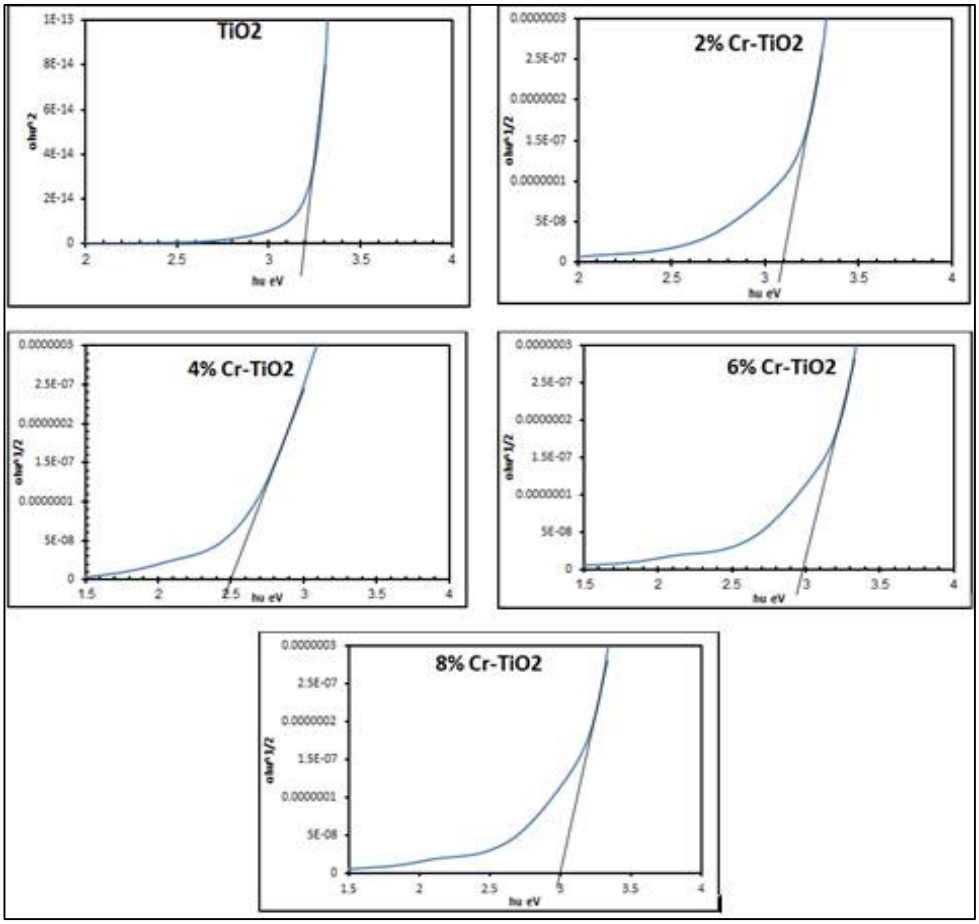

Fig.4: Band energy gap for all samples

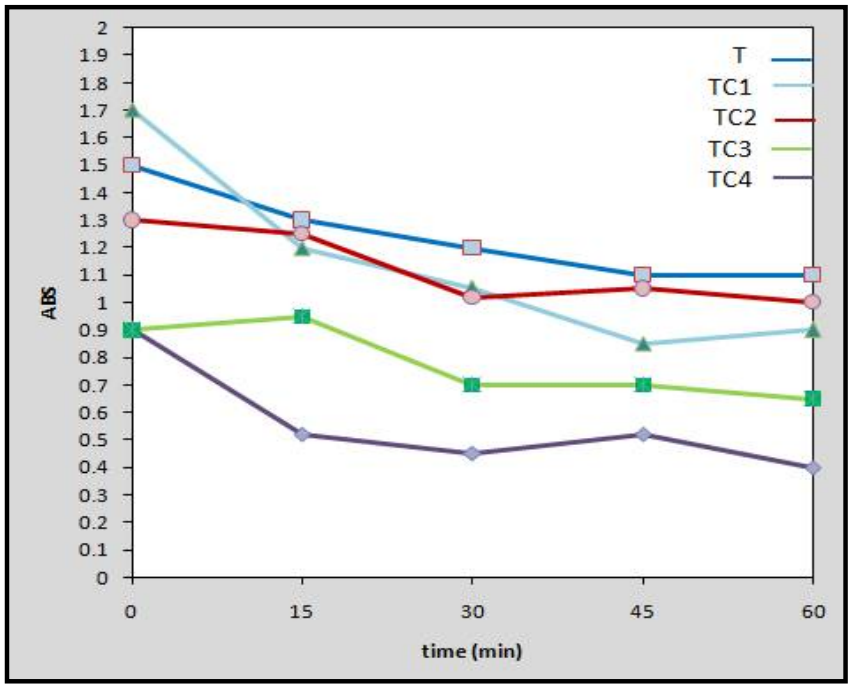

Fig 5 : Absorbance decay of methylene blue dye versus irradiation time in minutes for all samples under UV irradiation

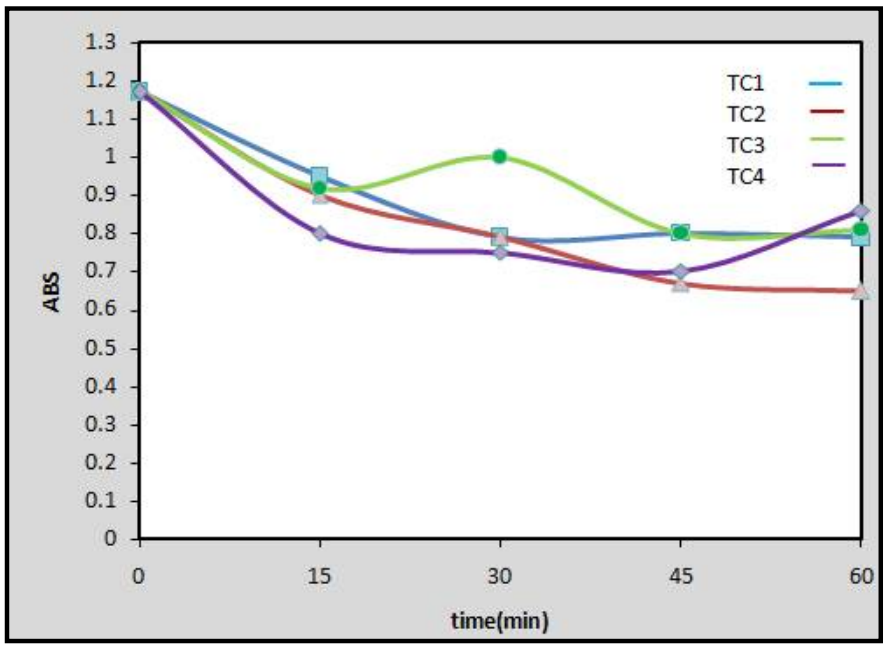

Fig 6 : Absorbance decay of methylene blue dye versus irradiation time in minutes for all samples under VIS irradiation

Indian Journal of Natural Sciences www.tnsroindia.org.in ©IJONS

Vol.9 /Issue 51 / December / 2018 *International Bimonthly* *ISSN: 0976 – 0997*

RESEARCH ARTICLE

Binary System Enhanced Sensing Properties of SnO_2Thin films Gas Sensors

Bushra A.Hasan[1]* and Leena F.Hamza

Department of Physics, College of Science, University of Baghdad, Baghdad, Iraq

Received: 10 Aug 2018 Revised: 12 Sep 2018 Accepted: 14 Oct 2018

***Address for Correspondence**
Bushra A.Hasan
Department of Physics,
College of Science,
University of Baghdad,
Baghdad, Iraq,
E-Mail:Bushra_abhasan@yahoo.com

ABSTRACT

This work devoted with the sensitivity enhancement of SnO_2 through out making binary system with various metal oxides like (TiO_2, Fe_2O_3, Cr_3O_4, Co_3O_4,WO_3 and MoO_3. Thin film from single and binary system were prepared on glass and c-Si substrates using pulsed laser deposition PLD method .The surface morphology structure of the single and binary thin films systems were studied using atomic force microscope. The absorbance and transmittance provided from UV- Visible spectrophotometer were used to estimate the optical energy gap and the optical constants. The sensitivity of the prepared thin film gas sensors were obtained by measuring the resistance as function to time in the air and in an NO_2 gas ambient.

Keywords: binary, metal, structure, sensitivity, gas

INTRODUCTION

Tin oxide SnO_2 is a petition-band gap n-type semiconductor and the frequently used as a sensitive material for the gas sensors. They belong to a class of transparent conductive oxides due to a number of unique functional properties, of which the most important are the electrical conductivity, the visibility in a wide spectral range and the high reactivity of the surface [1-3].Metal oxides gas sensors are used alot due to their high sensitivity to harmful for human health or hazardous gases (such as CO, NO, NO_2, H_2, etc.) in conjunction with easy fabrication methods and low manufacturing costs. Tin (IV) oxide is avery good sensor material among a many set of semiconducting metal oxides [4-7]. There are several approaches for sensitivity enhancement of gas sensor such as choosing appropriate operating temperature, using additives and using sensor arrays [8]. Using additives can provide new active centers on the material's surface or change electronic structure of material. In the first case, we are talking about modification

of sensitive material; second variant belongs to the doping process. There are a lot of papers devoted to study additives effect on selectivity of gas sensor devices [9-17]. However, there is a lack of attention on the difference between modification properties through out mixing binary system in equal ratio 1:1 and doping processes. The present work concern with sensitivity enhancement of SnO_2 gas sensor using binary system withTiO_2, Fe_2O_3, Cr_3O_4, Co_2O_3 , $WO_3$and MoO_3.

MATERIALS AND METHODS

In order to prepared SnO_2- TiO_2, SnO_2-Fe_2O_3, SnO_2-Cr_3O_4, SnO_2- Co_2O_3, SnO_2- WO_3,and SnO_2-MoO_3 binary systems , appropriate amount the of high purity (99.99) Indium oxide powder and TiO_2, Fe_2O_3, Cr_3O_4, Co_2O_3 , $WO_3$and MoO_3 with 50%50 are weighed using an electronic balance with the least count of (10^{-4}gm) and put in a quartz ampoule (length ~ 25 cm and internal diameter ~ 8 mm) are centered at 1273K and let at this temperature for 5 hours. After the calcinations, the fine powder was formed and pressed in bulk pellet form (1cmx1cm) as laser targets for thin film preparation. I wafer cut in small pieces(1x1)cm^2.Cleaning glass slides and Si wafer substrates were used which were subjected to several steps to remove any contamination such as dust ,oily material ,grease and some oxides using soap solution , then the glass sildes and Si were placed in a clean beaker containing distilled water and with ethanol solution then the glass slides and Si were dried by blowing air. Thin films were deposited using pulsed lased deposition technique under vacuum of (10^{-3} Torr). Thin films were obtained by focusing Nd:YAG (Huafei Tongda Technology–Diamond-288 pattern EPLS) Q-switching laser beam which coming from a window is incident on the target surface making an angle of 45° with it. The characteristics of the laser tool were (1)Laser model: Q-switched Nd: YAG Laser Second Harmonic Generatio (SHG).Laser wavelength: (1064 /532) nm.(2)Pulse energy: (100-1000) mJ.(3)Pulse width: 10ns.(4)Repetition frequency: (1, 2, 3,4,5,6) Hz .(5)Cooling method: inner circulation water cooling and (6)Applied voltage: 220V.The substrate is placed in front of the target with its surface parallel to that of the target. The structure of the prepared alloys and thin films was examined using X-ray diffraction (XRD) . The present work x-ray diffractrometer type (Miniflex II), with Cu-K_α x-ray tube (λ = 1.54056 Å) was used . The thicknesses of the prepared thin films were estimated from optical interference fringes.Fizeau fringes of equal thickness are obtained ,the film thickness(t) is given by: $t = \frac{\lambda}{2}.\frac{\Delta x}{x}$ (1) Where ΔX is the shift between the interference fringes, X is the distance between the interference fringes and λ is the He:Ne wavelength (6320 Å).The optical transmission spectra of the as-deposited and annealed films were recorded using a Perkin-Elmer Lambda 35 UV-VIS double-beam spectrophotometer in the wavelength range 300-1100 nm.

RESULTS AND DISCUSSION

Atomic Force microscopy (AFM)

The surface morphology of pure SnO_2 and SnO_2- TiO_2, SnO_2-Fe_2O_3, SnO_2- Cr_2O_3, SnO_2- Co_3O_4, SnO_2- WO_3, and SnO_2-MoO_3 binary systems were investigated by AFM as shown in Fig(1-to7). The single and binary systems thin films were prepared by pulsed laser deposition technique and deposited on a glass substrate. AFM parameters such as average diameter, average roughness for these samples are shown in Table (1) .This table illustrates an increment in the average diameter for the binary compound,SnO_2-$Fe_2O_3$and SnO_2-Co_2O_3 SnO_2-WO_3 as compared with SnO_2while a reduction in the average diameter was observed for the residual binary compound .Maximum roughness (8.21 nm)was observed for SnO_2- Cr_2O_3.

Optical Properties

The transmittance spectrum of single and binary system SnO_2 thin films prepared by PLD are presented in figure 8. It it clear that transmittance of binary thin films SnO_2/Co_3O_4, SnO_2/TiO_2 and SnO_2/MoO_3 are lower than that of single

system SnO_2 i.e. the prepared thin films become more opaque or less transparent to the incident light and this will reflect of the hole properties as seen later, while the transmittance of binary thin films SnO_2/Fe_2O_3, SnO_2/WO_3,and SnO_2/Cr_2O_3 exceeded that of SnO_2 i.e. the prepared thin films become less opaque or more transparent to the incident light .The optical enegy gap of the prepared thin films were estimated from Tauc relationFrom the transmittance spectra, the optical band gap energy of the thin films values can be estimated using Tauc's relation [18]:

$$(\alpha h\nu)^{1/r} = A(h\nu - Eg) \quad (2)$$

hυ is incident photon energy, α is the absorption coefficient, A is a constant and Eg is the band gap of the material and the exponent r depends on the type of the transition. For direct and allowed transition r=1/2, indirect transition r=2 and for direct forbidden r=3/2 , for indirect forbidden r=3 [19, 20]. For calculating the direct band gap value $(\alpha h\upsilon)^{1/r}$ versus hυ is plotted and it is shown in the inset of Figure. 9 by extrapolating the straight portion of the graph on hυ axis at α=0, so the band gap value is calculated. The intercept values on the energy axis have been found to be 3.1 eV which is higher than that founded by Selvi1 etal. [21]where the energy gap was 2.6 of Tin oxide (SnO_2) nanoparticles synthesized via solvothermal method using the microwave oven technique at various calcination temperatures. On the other side [22] pointed out that optical energy gap of tin oxide for SnO_2 prepared by spray pyrolysis technique was 3.94 eV decreases to3.64 eV . The optical energy gap get of SnO_2 e.V get to decrease (as expected) for the more opaque samples SnO_2/Co_3O_4, SnO_2/TiO_2 and SnO_2/MoO_3 or the sample experience red shift as a result of introduction of Co_3O_4, TiO_2 ,and MoO_3 while the optical energy gap get of SnO_2 e.V get to increase for the less opaque samples SnO_2/Fe_2O_3, SnO_2/Fe_2O_3,and SnO_2/Cr_2O_3. The refractive index value can be calculated from the formula [19]:

$$n = \left(\frac{4R}{(R-1)^2} - k^2 \right)^{\frac{1}{2}} - \frac{(R+1)}{(R-1)} \quad \text{.....(3)}$$

Where R is the reflectance, and can be expressed by the relation [20]:

$$R = \frac{(n-1)^2 + k^2}{(n+1)^2 + k^2} \quad \text{.....(4)}$$

The wavelength dependence of refractive for single and binary system of SnO_2 thin films are shown in figure 10. The refractive index (n) of SnO_2 was 2.4 at λ= 550 nm , this result is similar to the finding of Baco et al. [24]. They measured refractive index were in the range of 2.33 – 2.80 at λ =550 nm and the absorption coefficients were in the range of 10^4 – 10^5cm- The refractive index increases to2.588 for SnO_2/TiO_2 and to 2.626 for SnO_2/Co_2O_3 .On the other side the refractive index decreases to 2.417 for SnO_2/WO_3 and to 2.222 for SnO_2/Cr_2O_3 and reach minimum value 2.108 for SnO_2/Fe_2O_3 .The increase of n attributed to the reduction of transmittance giving rise to high opaque material which leads to more dense (increasing the packing density)which in turn decreases propagation velocity of light through them which resulting in increasing of n values since n represent the ratio of light velocity through vacuum to velocity through any medium.while the reduction of n is related to the inverse i.e . Increment of transmittance giving rise to less opaque material which leads to less dense (reducing the packing density) which in turn increases propagation velocity of light through them which resulting in reducing of n values . The extinction coefficient, which is related to the exponential decay of the wave as it passes through the medium, is defined as [19]:

$$k = \frac{\alpha\lambda}{4\pi} \quad \text{.....(5)}$$

Where λ is the wavelength of the incident radiation and (α) is given by [19]:

$$\alpha = 2.303\frac{A}{t} \quad \text{.....(6)}$$

Where A is the absorbance and t is the sample thickness. The behavior of the extinction coefficient of single and binary system of SnO_2 thin films prepared by PLD are presented in figure 11. One can observe from the figure and Table .1 that the extinction coefficient gets to change in similar trend to that of n. The extinction coefficient of It is clear that for SnO_2 was 0.112 decreases for the most transparent (low absorption coefficient)samples which are SnO_2/Fe_2O_3 SnO_2/WO_3 and reach minimum value for SnO_2/Cr_2O_3 , while k increases for the most opaque samples(high absorption coefficient) which are SnO_2/Co_2O_3, SnO_2/TiO_2 and attain maximum value for SnO_2/MoO_3 .The wavelength dependence in the range (200–1100)nm of the real (ε_r) and imaginary (ε_i) parts of single and binary system of SnO_2 thin films prepared by PLD are presented in figure 12 and 13. The behavior of ε_r is similar to that of the refractive index because of the smaller value of k^2 compared with n^2 according to equation 9 , while ε_i is mainly depends on the k values. It is found that ε_r increases for the most opaque. While ε_r decrease for the most transparent ones. Moreover ε_r found to increase from 6.015 to 6.87 for SnO_2 and for SnO_2/Co_2O_3 respectively while ε_r found to reduce from 6.015 to 4.439for SnO_2 and for SnO_2/Fe_2O_3as shown in Table.1.The real and imaginary part of dielectric constant can be calculated by using the following equations [23]:

$$(n - ik)^2 = \varepsilon_r - i\varepsilon_i \quad \text{.....(7)}$$

Where

$$\varepsilon_r = n^2 - k^2 \quad \text{.....(8)}$$

and $$\varepsilon_i = 2nk \quad \text{.....(9)}$$

The imaginary part of dielectric constant ε_i reveals the same behavior of ε_r .It is clear from Table.2 that ε_i decreases from 0.553 to 0.272 for $SnO_2$and SnO_2/Fe_2O_3films.The same explanation of n and k can be given to ε_r and ε_i .

Sensing Measurements

Figures 14 to 19 display the variation of resistance with time for single and binary SnO_2 thin films to NO_2 oxidizing gas at different operating temperature prepared at silicon with positive conductance .there are many parameters influenced the sensitivity of any gas sensor such as operating temperature addition of any other oxides to enhanced the performance .The project of this research was enhancement of Tin oxides through out addition of different oxides .It is clear that most of the binary sensors as well as single system sensor were n type since there is increase of the resistance followed the exposure to oxidizing gas which get to decrease when gas off. , except SnO_2/Cr_2O_3 which exhibit to change in inverse manner at high operating temperatures i.e. the resistance get to decrease by expositing to oxidizing gas indicating to p – type semiconductor and return to increase in absent of NO_2 gas. . that the all the prepared gas sensor show n-type behavior to the gas inlet i.e. the resistance increases with gas on and return to increase when gas off , converted to p-type at high operating temperatures i.e. the resistance decreased with gas on and return to decreased when gas off. The high values of sensitivity 59% , 56% and 46%were obtained from gas sensors SnO_2/Co_2O_3 ,SnO_2/WO_3 and SnO_2/Cr_2O_3 at 293 K and 473 K respectively. The high sensitivity was attributes to high roughness value which giving rise to high degree of porosity which consequently permit to complete the adsorption and adsorption of the oxidizing gas completely. On the other side it is obvious that sensitivity of all binary system expect SnO_2/Cr_2O_3 showed reduction by the increasing of operation temperatures. This come by the

effect of heat which may eliminate the defects states and reducing the surface roughness, or may be attributed to good compatibility between the sensor layer (p –type semiconductor at high operating temperature and p-type silicon substrates which giving rise to do the sensing operation perfectly.

REFERENCES

1. Batzill M (2006) Surface science studies of gas sensing materials:SnO2. Sensors 6: 1345-1366.
2. Wang C, Yin L, Zhang L, Xiang D, Gao R (2010) Metal oxide gas sensors: Sensitivity and influencing factors. Sensors 10: 2088-2106.
3. Nagirnyak S, Lutz V, Dontsova T, Astrelin I (2016) The effect of thesynthesis conditions on morphology of tin (IV) oxide obtained byvapor transport method. Springer Proc Phys 183: 331-341.
4. Pan J, Shen H, Mathur S (2012) One dimensional SnO2 nanosructures:Synthesis and application.1-12.
5. Köck A, Tischner A, Maier T, Kast M, Edtmaier C, et al. (2009) Atmospheric pressure fabrication of SnO2-nanowires for highly sensitive CO and CH4 detection. Sensors and Actuators B: 160-167.
6. Park JH, Lee JH (2009) Gas sensing characteristics of polycrastallineSnO2 nanowires prepared by polyol method. Sensors and Actuators B: 151-157.
7. Qin L, Xu J, Dong X, Pan Q, Cheng Z, et. al. (2008) The template-free synthesis of square-shaped SnO2 nanowires: The temperature effect and acetone gas sensors. Nanotechnology 19: 1-8.
8. Nagirnyak SV, Dontsova TA (2015) Ways for improvement selectivity of semiconductor gas sensors. Young scientist 10: 15-17.
9. Ramgir NS, Hwang YK, Jhung SH, Mulla IS, Chang JS (2006) Effect of Pt concentration on the physicochemical properties and CO sensing activity of mesostructured SnO2. Sensors and Actuators B 114: 275-282.
10. Yuasa M, Masaki T, Kida T, Shimanoe K, Yamazoe N (2009) Nano-sized PdO loaded SnO2 nanoparticles be reverse micelle method for highly sensitive CO gas sensor. Sensors and Actuators 136: 99-104.
11. Wang S, Zhao Y, Huang J, Wang Y, Kong F, et al. (2006) Preparation and CO gas-sensing behavior of Au-doped SnO2 sensors. Vacuum 81: 397-397.
12. Kaur J, Kumar R, Bhatnagar MC (2007) Effect of indium-doped SnO2 nanoparticles on NO2 gas sensing properties. Sensors and Actuators B 126: 478-484.
13. Aguilar LJ, Maldonado A, Olvera M (2006) Gas-sensing characteristics of ruthenium-doped SnO2 thin films in a propane atmosphere. Sensors and Actuators B Chemical: 1-4.
14. Liu L, Zhang T, Wang L, Li S (2009) Improved ethanol sensing properties of Cu-doped SnO2 nanofibers. Materials Letters 63: 2041-2043.
15. Yang H, Jin W, Wang L (2003) Synthesis and characterization of V2O5- doped SnO2 nanocrystallites for oxygen-sensing properties. Materials Letters 57: 3686-3689.
16. Nakatani Y, Matsuoka M (1982) Effects of sulfate ion on gas sensitive properties of α-Fe2O3 ceramics. Jpn J Appl Phys 21: L758
17. Epifani M, Arbiol J, Pellicer E, Comini E, Siciliano P, et. al. (2008) Synthesis and gas-sensing properties of Pd-doped SnO2 nanocrystals. A case study of a general methodology for doping metal oxide nanocrystals. Cryst Growth Des 8: 1774-1778.
18. Tauc, J., 1974. Amorphous and Liquid Semiconductors.
19. J. Pankove, Optical properties in semiconductors, (Dove Publication Inc., New York, 1971).
20. E. Thamarai Selvi1, S. MeenakshiSundar ,IOSR Journal of Applied Physics (IOSR-JAP) e-ISSN: 2278-4861, PP 69-72 www.iosrjournals.org National Conference on Current Advancements in Physics 3rd&4th February 2017 69 | Page Department of Physics, St. John's College, Palayamkottai-627 002, Tamilnadu, India. DOI 10.9790/4861-17002036972 .
21. J. Themlin, R. Sporken, J. Darville, R. Caudano, J. Gilles, R. Johnson, Resonant-photoemission study of SnO2: cationic origin of the defect band-gap states, Physical Review B 42 (1990) 11914.
22. Turgut G and Erdal S 2014 Superlattices and Microstructures 69 175

23. ALENSO, M., J. VENN, 1971. Physics, 2nd ed.Bruce, P., 1995. Solid State Electrochemistry,Cambridge Univ. Press, Cambridge.
24. Saturi Baco,, Abdullah Chik, Fouziah Md. Yassin, Journal of Science and Technology, 61-72

Table (1): AFM parameters for SnO_2 and the Binary systems .

Sample	Average rashness (nm)	Average diameter (nm)
Pure SnO_2	0.32	62.30
SnO_2/Co_3O_4	0.914	73.17
SnO_2/WO_3	0.887	47.34
SnO_2/Cr_2O_3	8.210	51.03
SnO_2/MoO_3	0.688	54.15
SnO_2/TiO_2	0.373	39.84

Table. 2 Parameters of the optical properties for single and binary SnO_2 Thin Films. λ=550nm

Sample	T%	α (cm^{-1})	k	n	ε_r	ε_i	Eg (eV)
Pure SnO_2	59.91	25621	0.112	2.462	6.051	0.553	3.10
SnO_2/Fe_2O_3	74.52	14710	0.064	2.108	4.439	0.272	3.30
SnO_2/Co_2O_3	48.17	36531	0.160	2.626	6.870	0.840	3.00
SnO_2/WO_3	62.16	23778	0.104	2.417	5.829	0.503	3.95
SnO_2/Cr_2O_3	70.35	17589	0.077	2.222	4.929	0.342	3.40
SnO_2/MoO_3	26.62	66182	0.290	2.327	5.329	1.349	2.75
SnO_2/TiO_2	35.81	51357	0.225	2.588	6.648	1.164	2.90

Table.3 : Illustrates the sensitivity , response , recovery time at various operating temperatures for single and binary SnO_2 gas sensors.

Sample	Operating Temperature(K)	Sensitivity %
Pure SnO_2	298	0.32
	373	1.10
	473	3.52
	573	11.65
SnO_2/Co_3O_4	298	59.47
	373	30.71
	473	2.214
	573	4.77
SnO_2/WO_3	298	56.10
	373	39.13
	473	35.41
	573	29.26
SnO_2/Cr_2O_3	298	-
	373	4.57
	473	46.74
	573	36.18
SnO_2/MoO_3	298	12.03
	373	8.42
	473	1.83
	573	-

SnO_2/TiO_2	298	23.55
	373	9.89
	473	12.01
	573	2.91

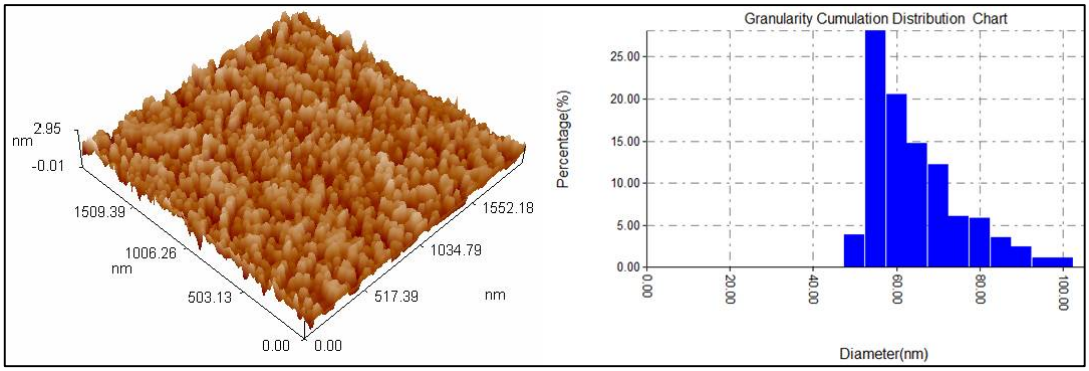

Figure 1. 3D AFM images for of pure SnO_2 thin film .

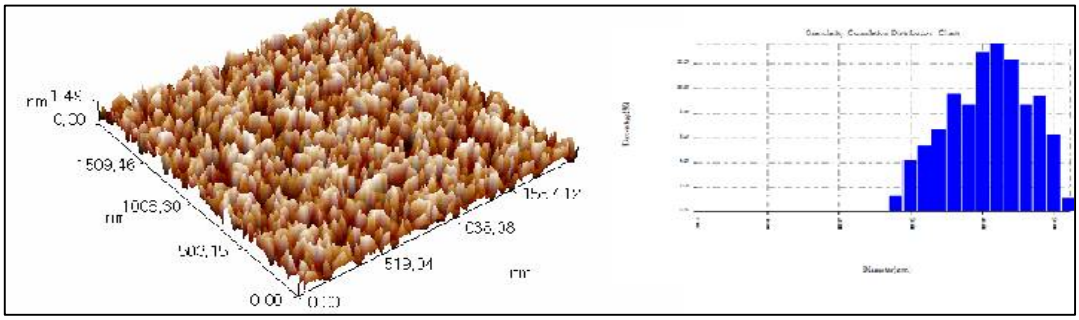

Figure 2. :3D AFM images for of Binary system SnO_2-TiO_2.

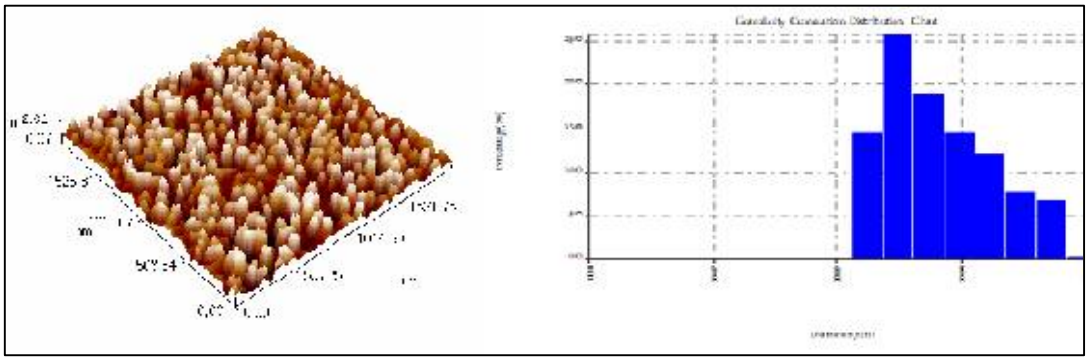

Figure3. :3D AFM images for of Binary system SnO_2-MoO_3.

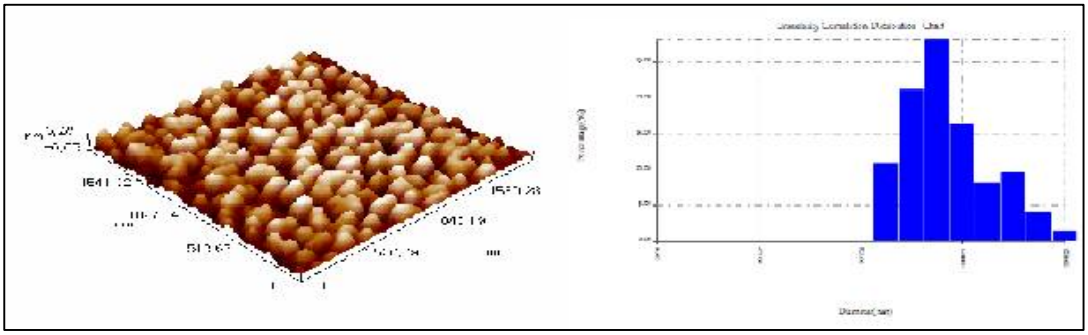

Figure 4. :3D AFM images for of Binary system SnO_2-Fe_2O_3.

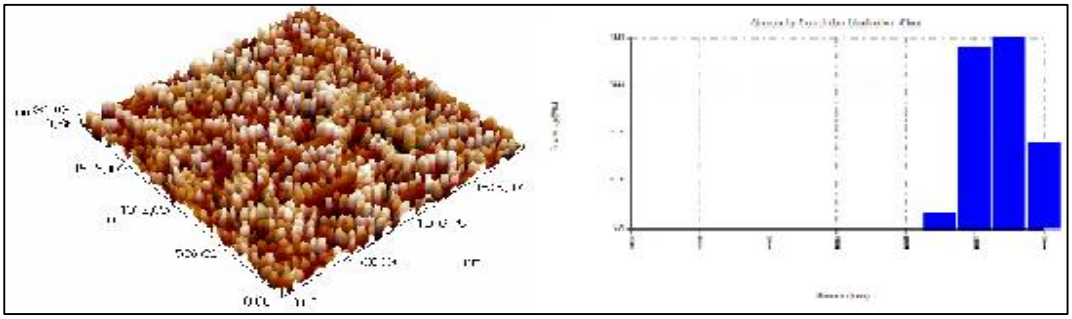

Figure 5.:3D AFM images for of Binary system SnO_2-Cr_2O_3.

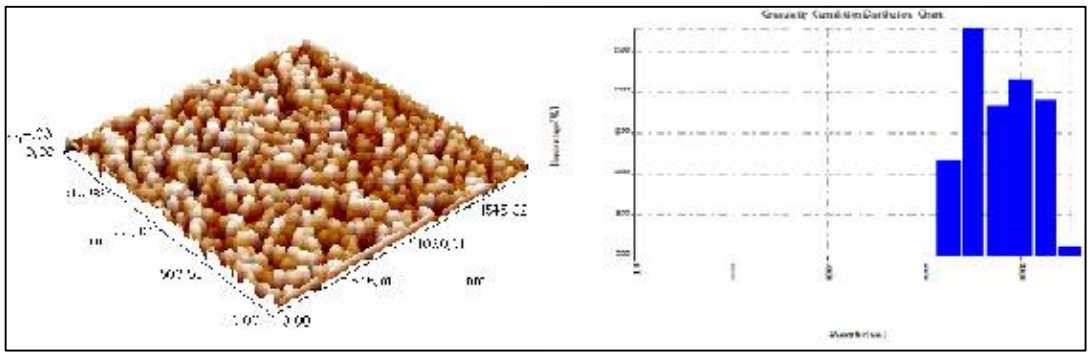

Figure (6) :3D AFM images for of Binary system SnO_2-CO_3O_4.

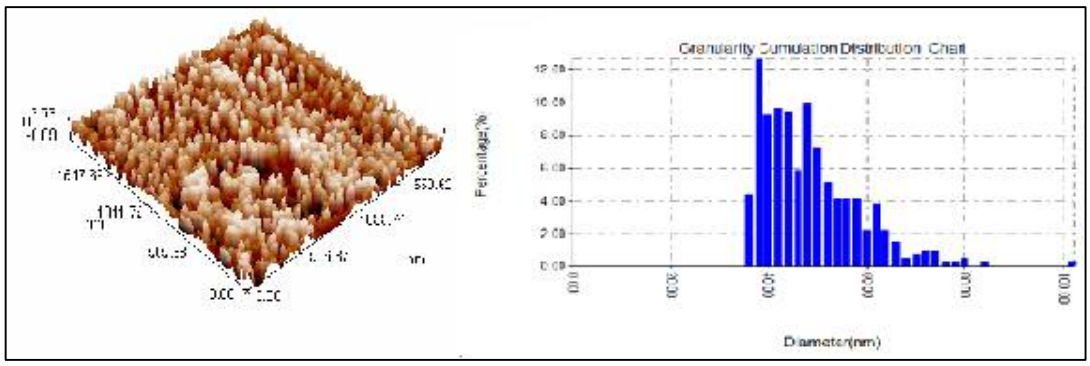

Figure 7. :3D AFM images for of Binary system SnO_2-WO_3.

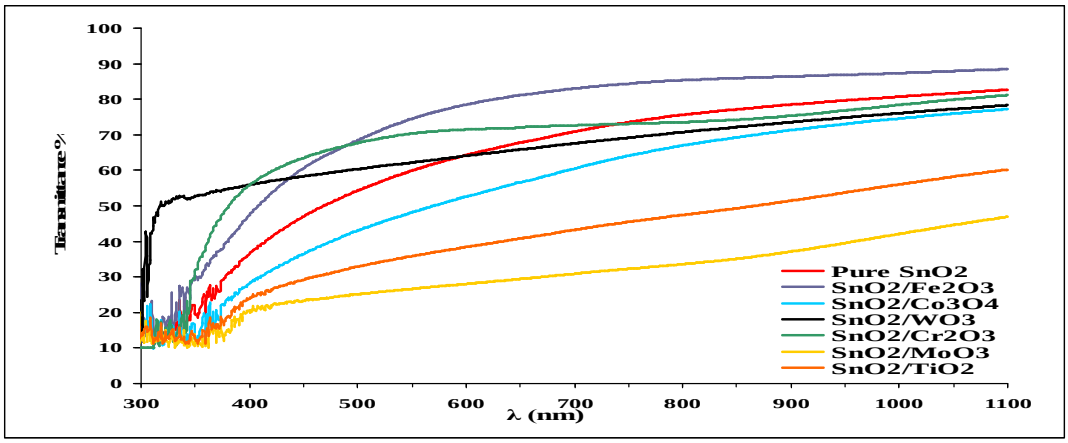

Figure.8 Transmittance spectrum with λ for single and binary SnO_2 **Thin Films.**

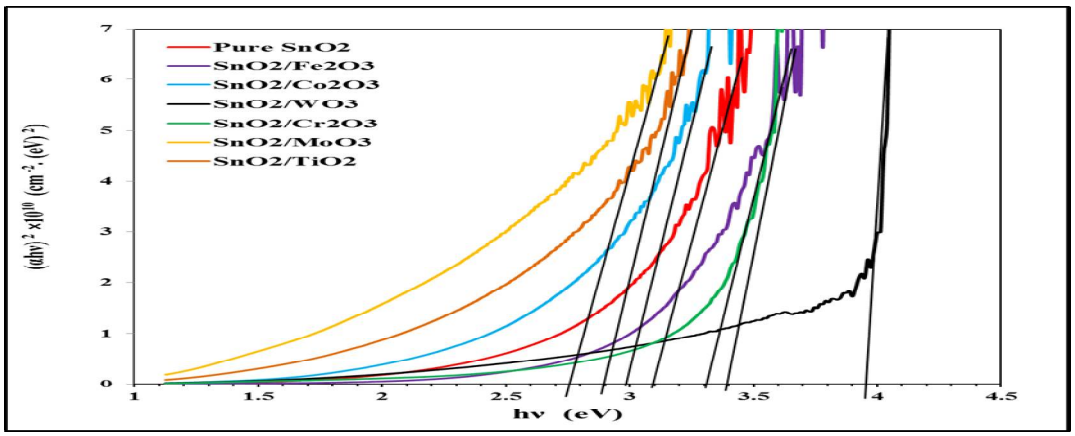

Figure.9 Variation of $(\alpha h\upsilon)^2$with $(h\upsilon)$ for single and binary SnO_2 **Thin Films.**

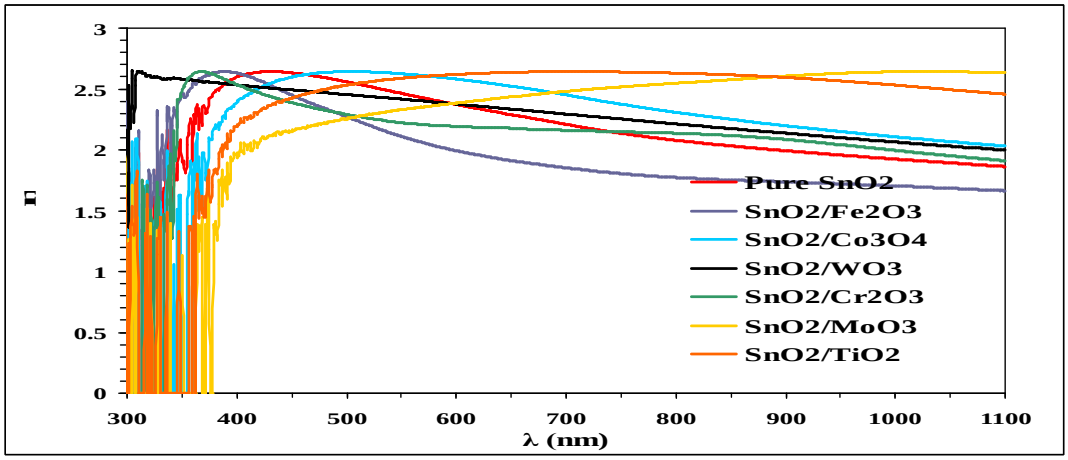

Figure.10 Variation of n with λ for single and binary SnO_2 **Thin Films.**

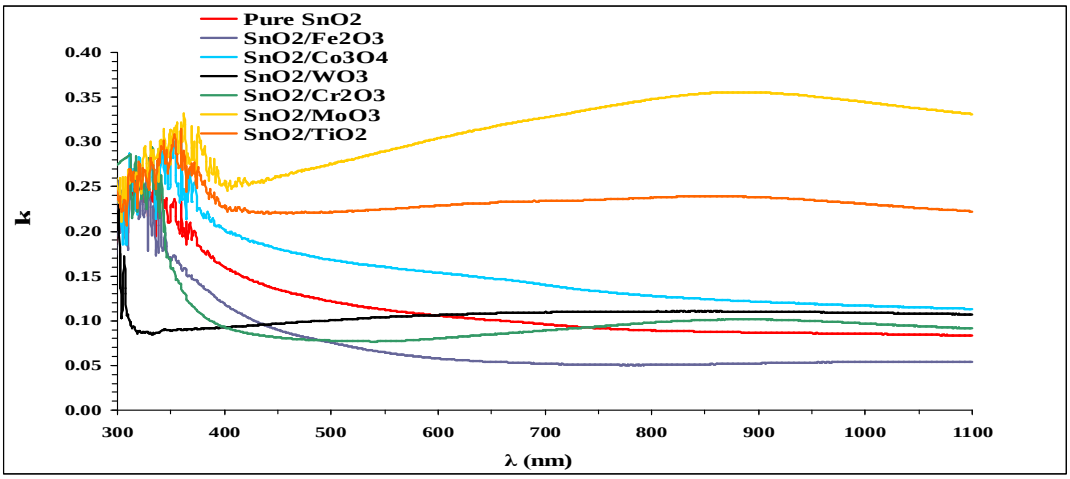

Figure.11 Variation of k with λ for single and binary SnO_2 Thin Films.

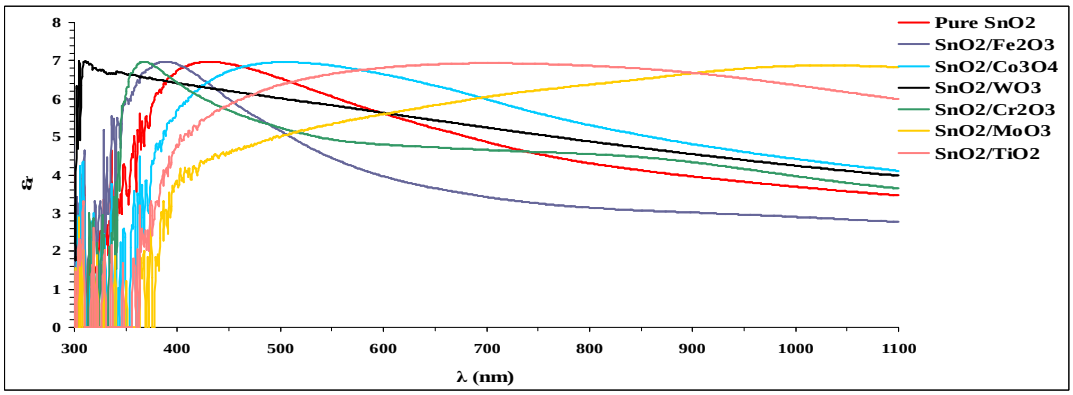

Figure.12 Variation of ε_r with λ for single and binary SnO_2 Thin Films.

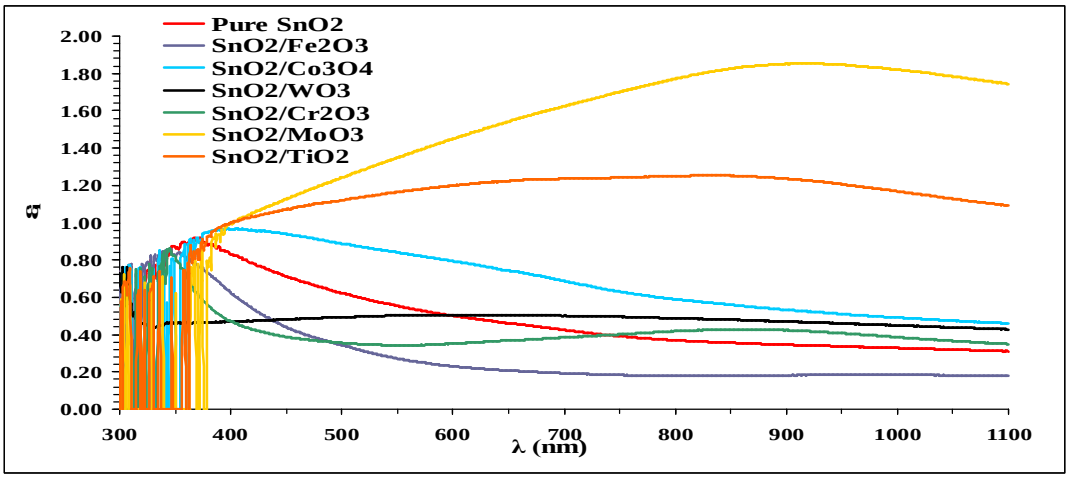

Figure.13 Variation of ε_i with λ for single and binary of SnO_2 Thin Films.

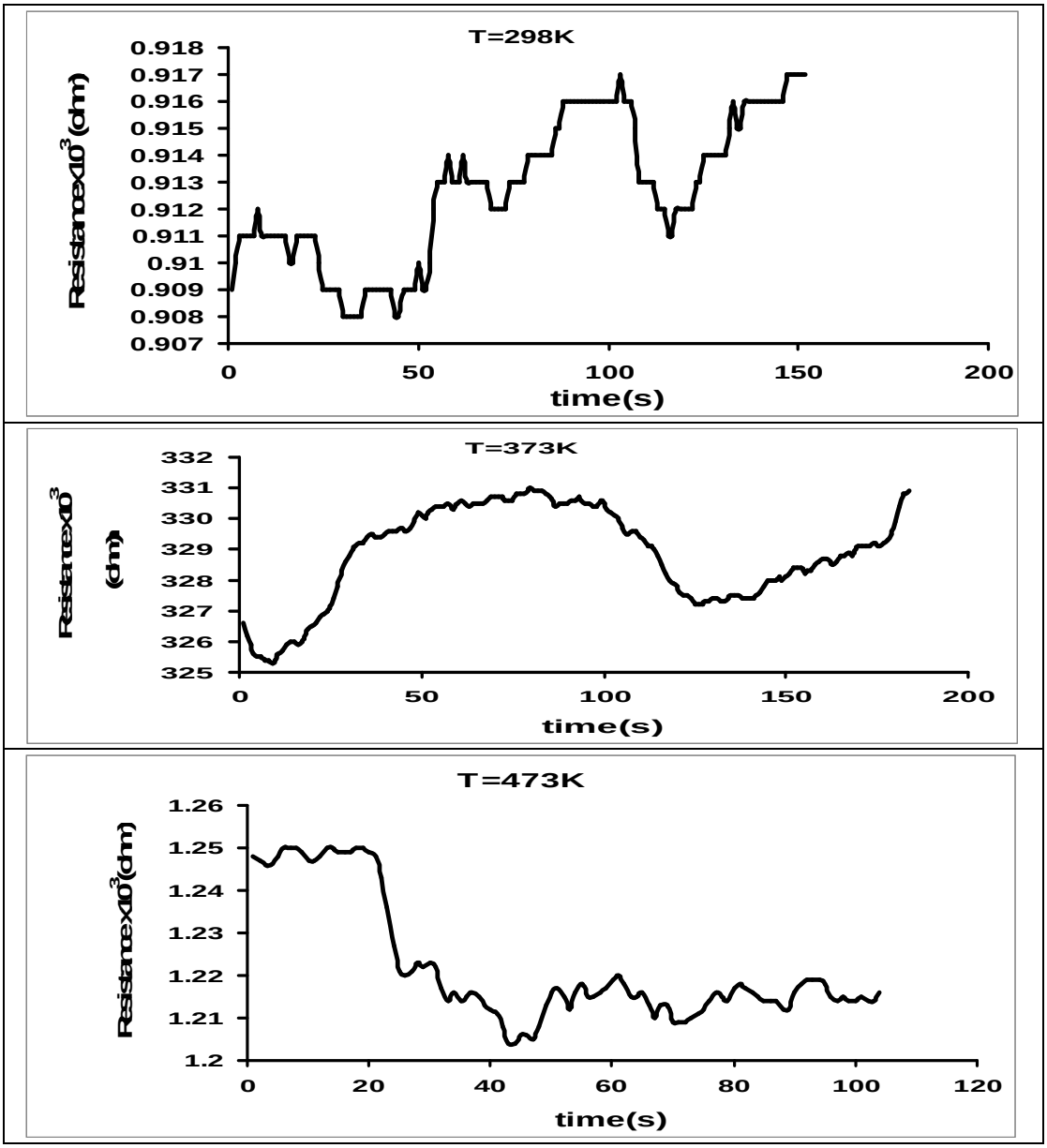
T=298K
Resistance×10^3(ohm)
0.918
0.917
0.916
0.915
0.914
0.913
0.912
0.911
0.91
0.909
0.908
0.907
0
50
100
150
200
time(s)
T=373K
Resistance×10^3 (ohm)
332
331
330
329
328
327
326
325
0
50
100
150
200
time(s)
T=473K
Resistance×10^3(ohm)
1.26
1.25
1.24
1.23
1.22
1.21
1.2
0
20
40
60
80
100
120
time(s)

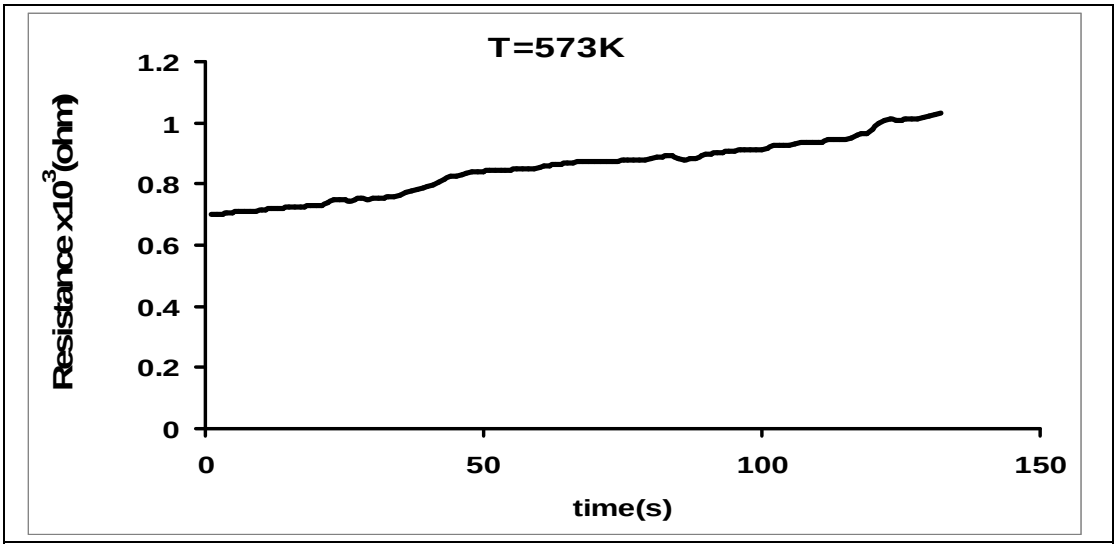

Figure 14 : Variation of resistance with time for SnO_2/c-Si gas sensor

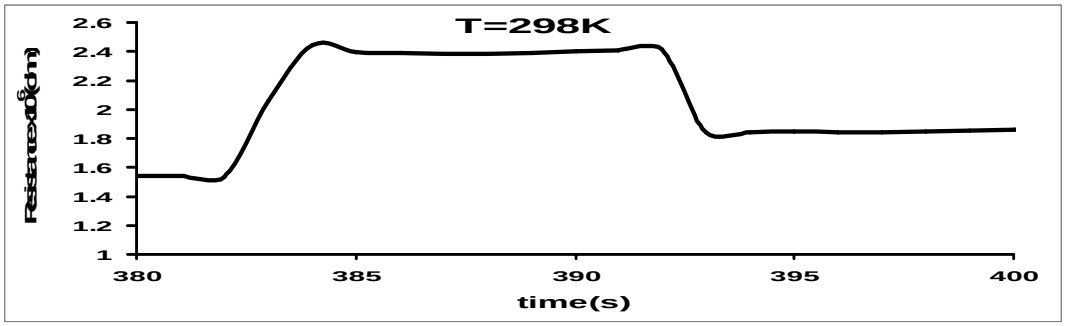

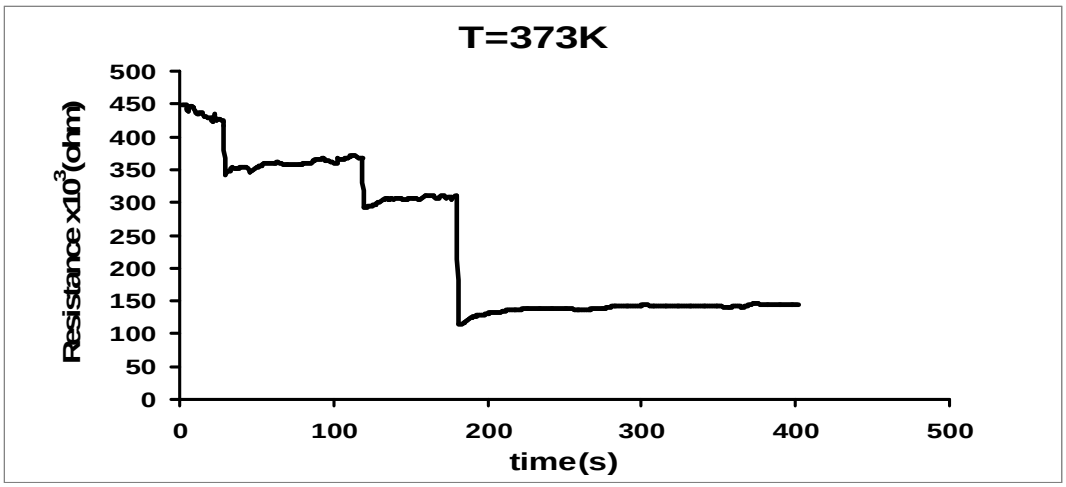

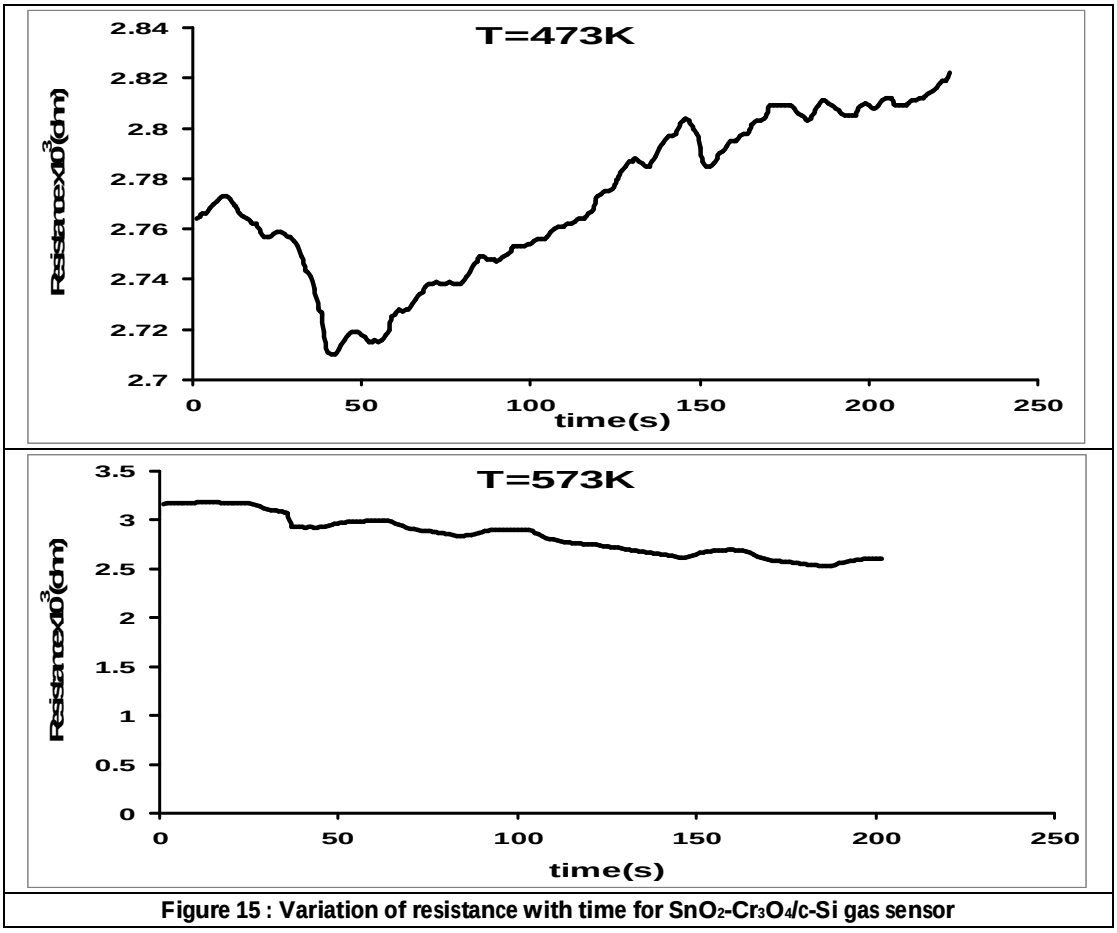

Figure 15 : Variation of resistance with time for SnO_2-Cr_3O_4/c-Si gas sensor

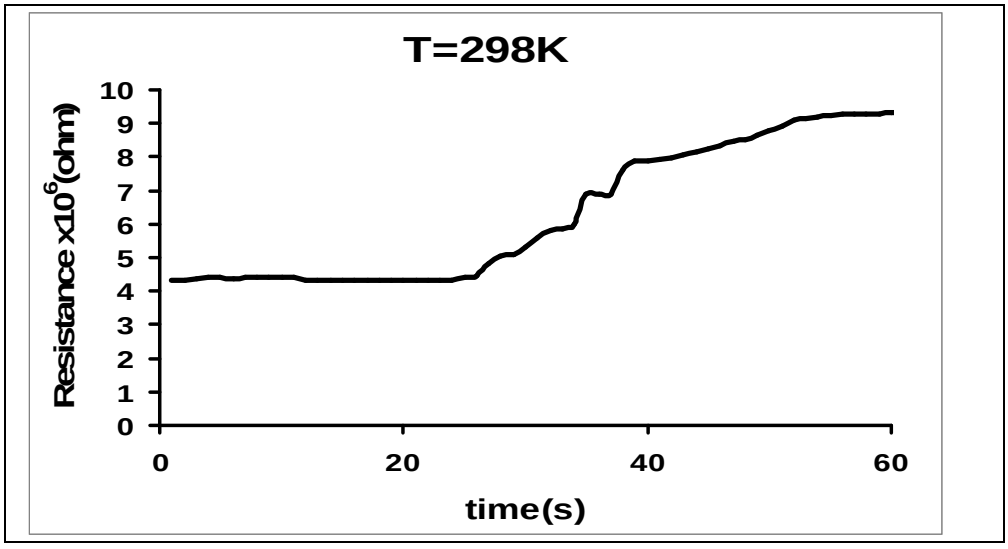

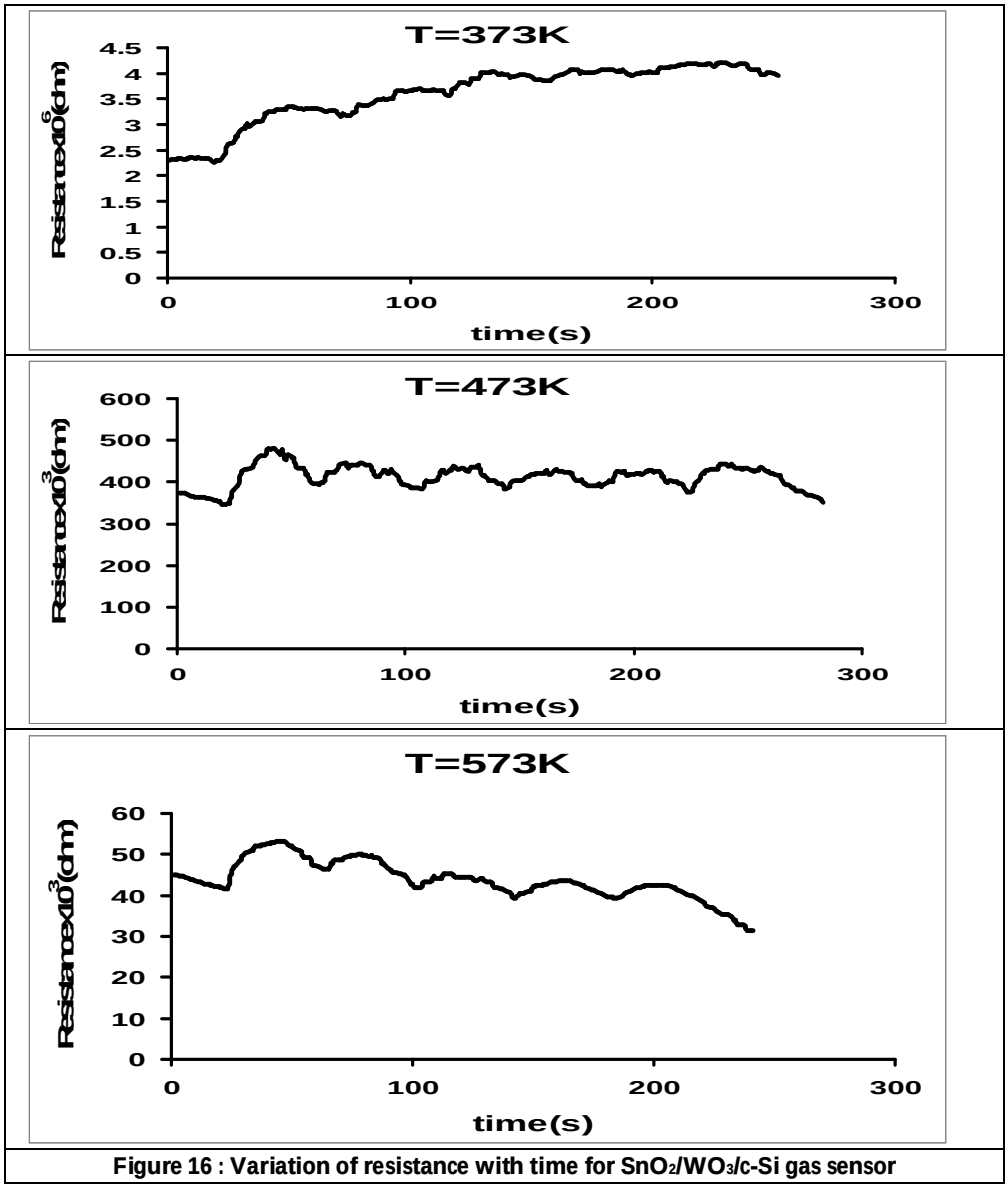

Figure 16 : Variation of resistance with time for SnO_2/WO_3/c-Si gas sensor

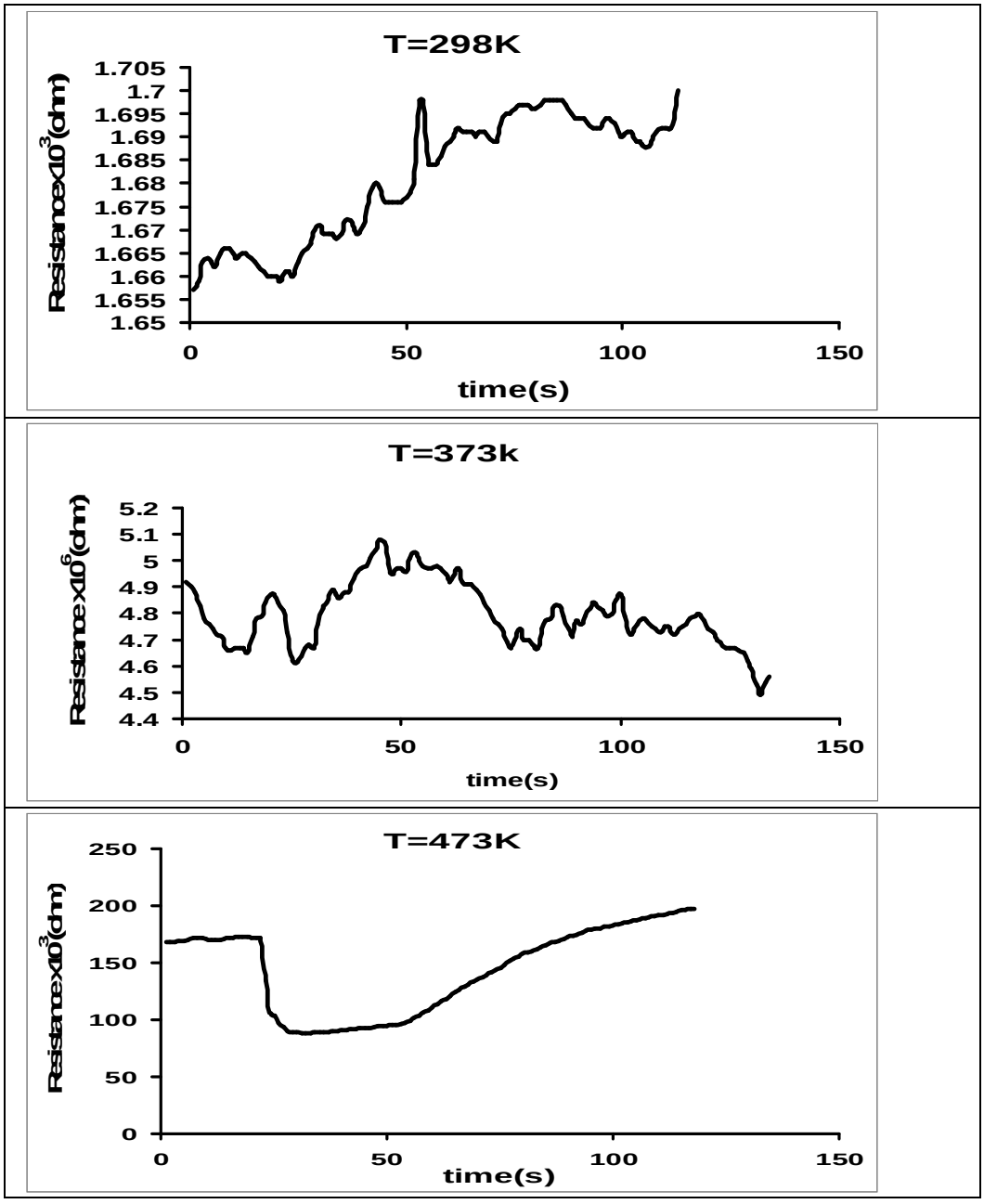
T=298K
Resistance x10^3 (dm)
1.705
1.7
1.695
1.69
1.685
1.68
1.675
1.67
1.665
1.66
1.655
1.65
0
50
100
150
time(s)
T=373k
Resistance x10^6 (dm)
5.2
5.1
5
4.9
4.8
4.7
4.6
4.5
4.4
0
50
100
150
time(s)
T=473K
Resistance x10^3 (dm)
250
200
150
100
50
0
0
50
100
150
time(s)

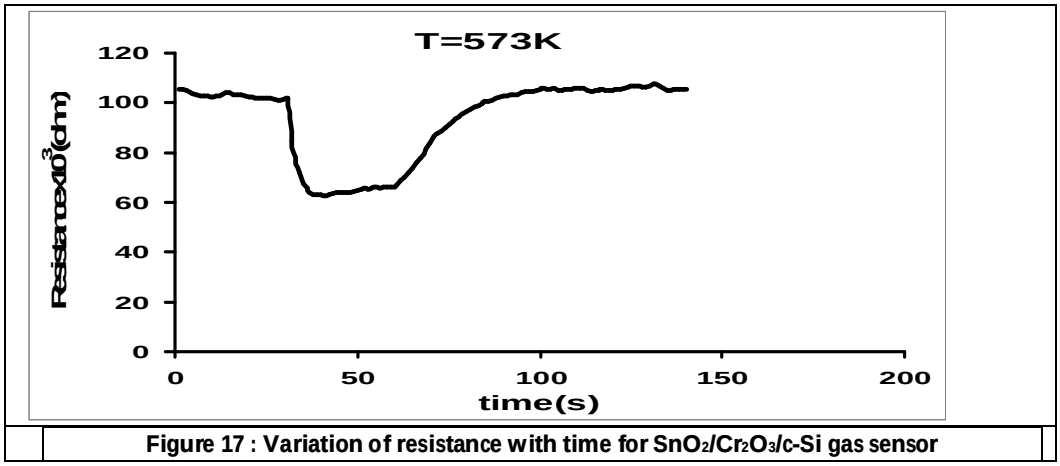

Figure 17 : Variation of resistance with time for SnO_2/Cr_2O_3/c-Si gas sensor

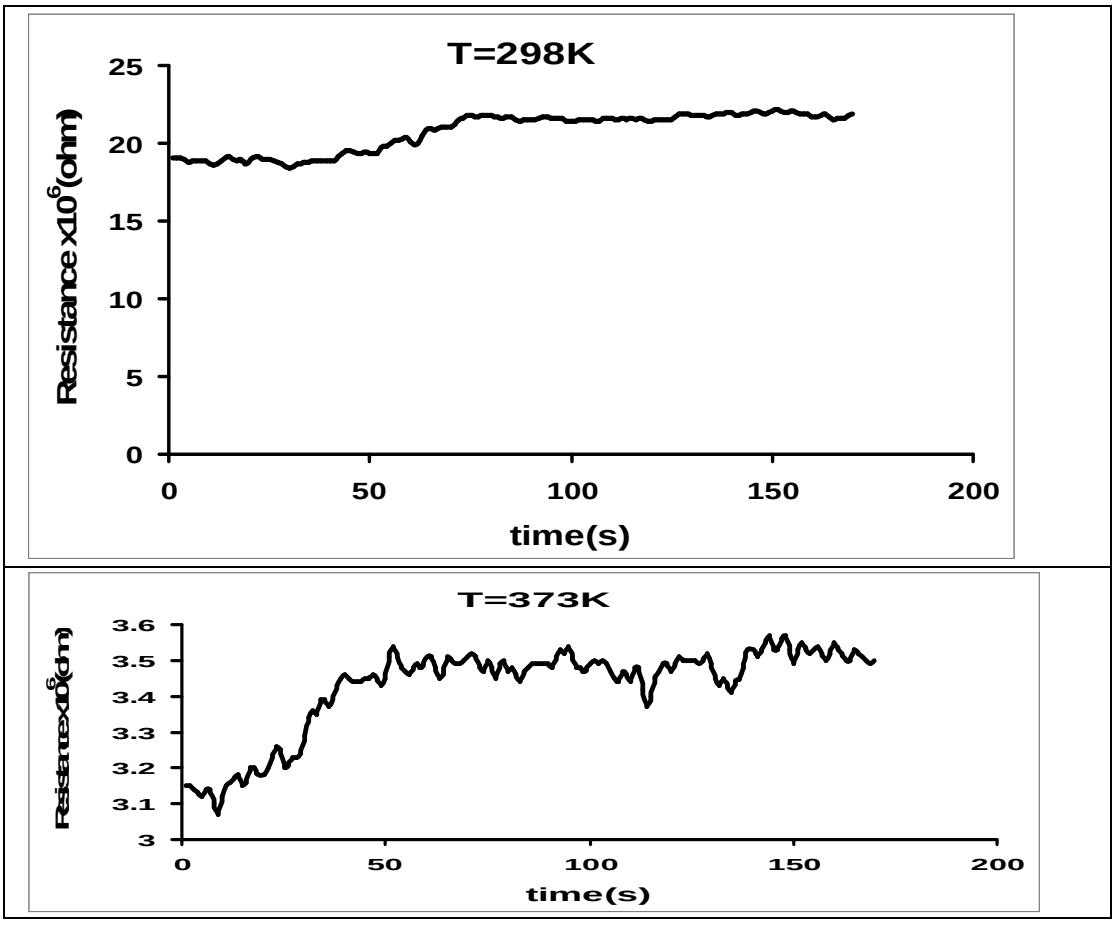

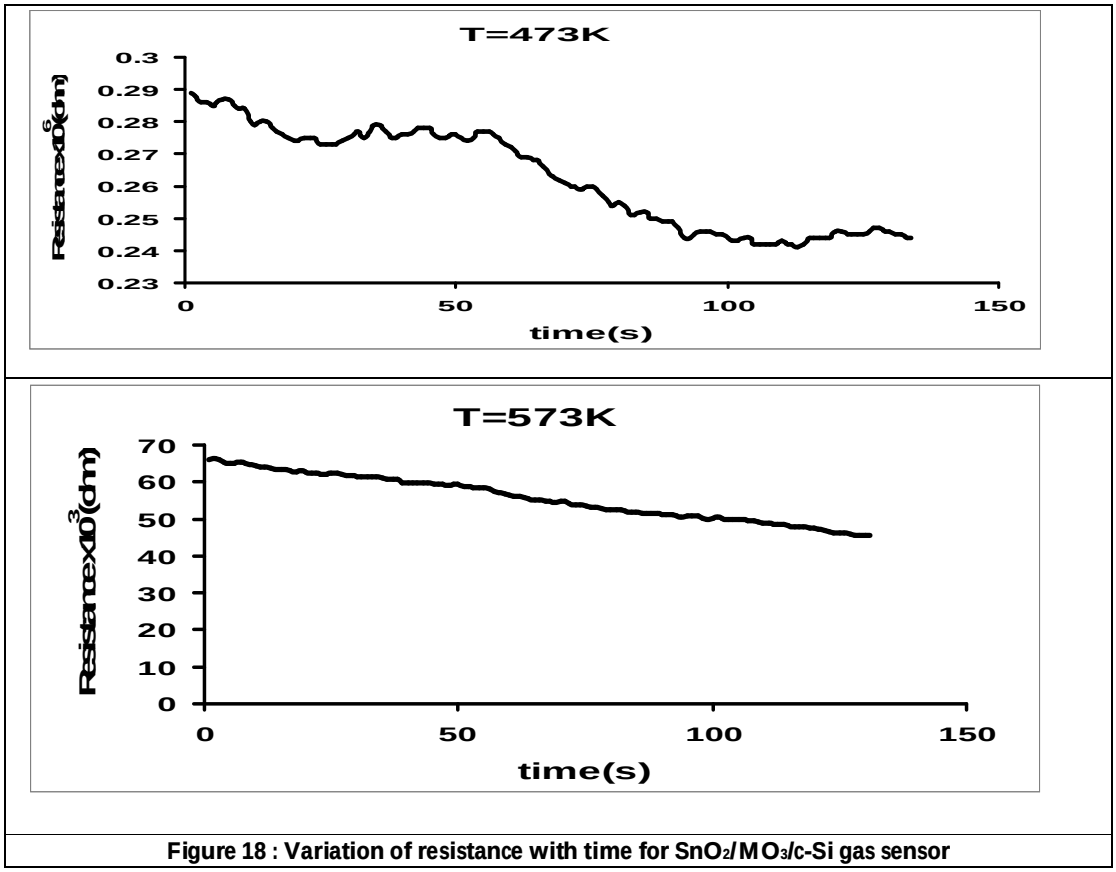

Figure 18 : Variation of resistance with time for SnO_2/MO_3/c-Si gas sensor

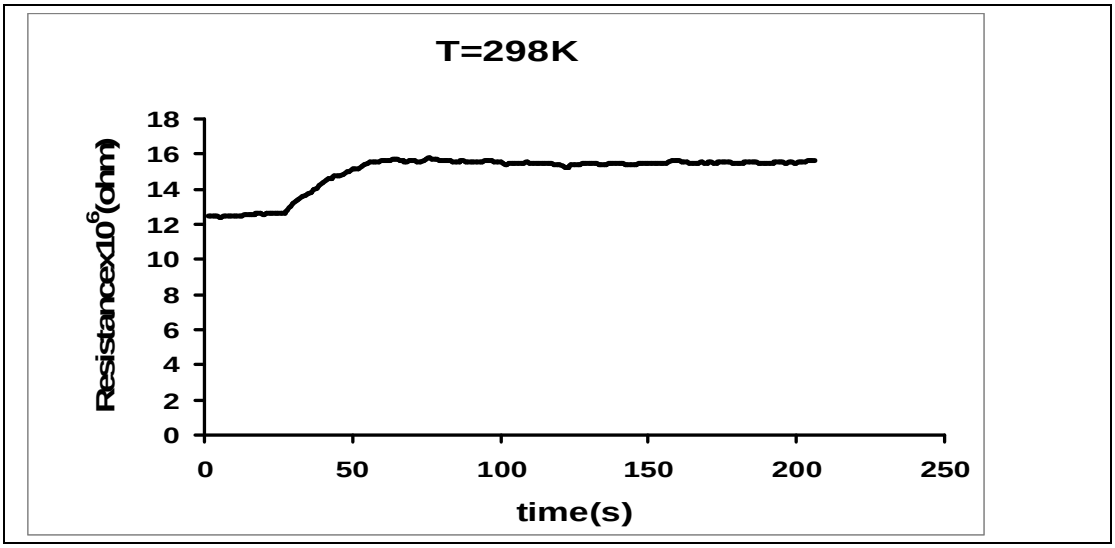

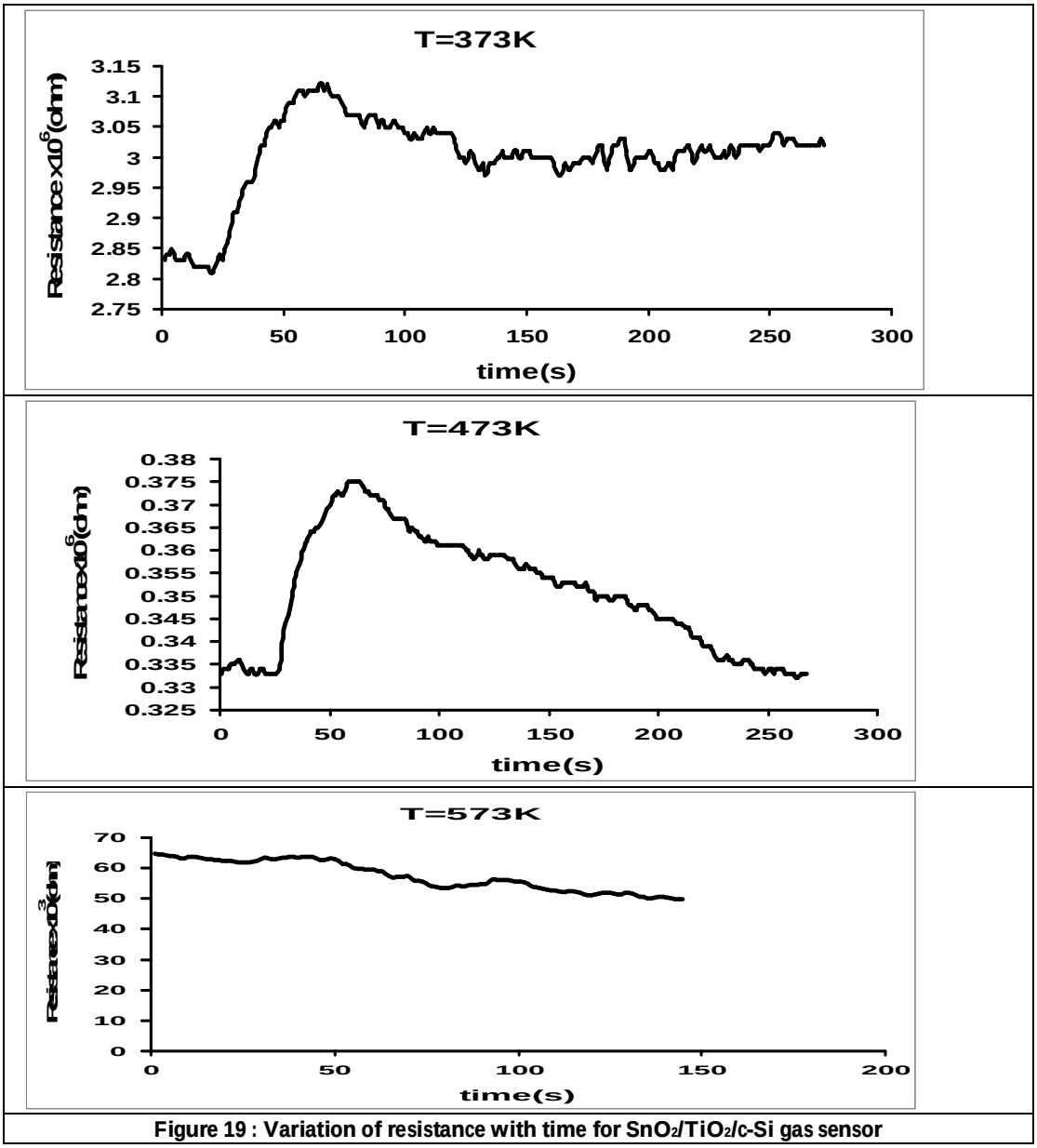

Figure 19 : Variation of resistance with time for SnO_2/TiO_2/c-Si gas sensor

Indian Journal of Natural Sciences www.tnsroindia.org.in ©IJONS

Vol.9 /Issue 51 / December / 2018 *International Bimonthly* *ISSN: 0976 – 0997*

RESEARCH ARTICLE

Role of Zinc Sulfate in Acute and Subchronic Cadmium Chloride Toxicosis in Mice

Ahmed D. Kdair* and Duraid A. Abbas

Collage of Veteraniry Medicine, University of Baghdad, Baghdad, Iraq.

Received: 11 Aug 2018 Revised: 14 Sep 2018 Accepted: 17 Oct 2018

***Address for Correspondence**
Ahmed D. Kdair
Collage of Veteraniry Medicine,
University of Baghdad,
Baghdad, Iraq.

ABSTRACT

A toxicological study was preformed to explain sort of intraction between zinc and cadmium after acute and subchronic administration. Median lethal dose were determined in mice by up and down method after acute administration and subchronic administration of selected doses given orally daily for 45 day in 81 albino mice divided to 21 mice for acute study in three group divided equally and 60 mice for subchronic divided in to four dosed group as following (toxic dose of cadmium chloride 5mg/kg B.W (T1) Zinc sulfate 10mg/kg B.W (T2) their combined dosing (T3) and control group.)Sub chronic index and isobolographic analysis were estimated in order to determine possibility of accumulation and the sort of interaction. The result of the subchronic index for cadmium chloride and zinc sulfate were (1.1 and 1.08) while their result for their combined dosing were (0.67 and 0.78) respectively , which indicate there were decline in the level of cadmium and zinc in the body . The levels of both metals in liver decrease significantly after acute and sub chronic combined administration than of alone one.Isobolographic analysis result showed that the sort of interaction of the two metals were additive after acute exposure and antagonism after subchronic exposure .also there were significant increase in mice weight of combined dose group nearly that of control one , while cadmium alone dosed group showed highly significant decline of mice weight throughout the experimental period . Some signs of toxicity appear in cadmium chloride dosed group as emaciation, general weakness, increase sensitivity and lethargy , the combind group showed little severity signs than cadmium group at last 20 days,while the zinc and control group showed no obvious signs The level of element (zinc and cadmium) in liver were increased in all treated groups but the combined group showed less level than alone.As a result of co-administration of zinc sulfatewith cadmium chloride, it might protect and alleviate cadmium toxicosis

Key words : LD50 , subcronic index , isobolographic analysis , cadmium , zinc, liver.

INTRODUCTION

Cadmium (Cd) is one of the most dangerous heavy metals, known to produce severe and multi-organ toxicity in humans (1,2). It is released into the environment by mining, smelting operations, fuel combustion and other industrial process (3) Humans can be exposed to Cd and it can stimulate free radical production, resulting in oxidative deterioration of lipids, proteins, and DNA, manifesting as gross pathology of the liver, brain, and other organs in humans and animals (4). The extremely long biological half life of cadmium essentially makes it a cumulative toxin, so long past exposures could still result in direct toxic effects of the residual metal (5) The body has limited capacity to respond to cadmium exposure, as the metal cannot undergo metabolic degradation to less toxic species and is only poorly excreted, making long-term storage a viable option for dealing with this toxic element. The long residence time of cadmium is in part attributable to metallothionein (MT), a metal-binding protein that is induced by cadmium and tightly binds the metal . Cadmium accumulates primarily in the liver and kidney where it is bound to MT, and it is felt that cadmium bound to MT is essentially detoxicated, at least temporarily, through this high affinity sequestration (6,7).

major detoxification mechanisms protecting the cell from Cd-induced damage is the direct binding of Cd2+ to metal chelators like Metallothionein (MT) is a ubiquitous low molecular weight (usually <10 kDa) protein with high cysteine content and has strong affinity for heavy metals (8). The other way to induction (MT) is giving zinc which is an essential trace element play roles in structure and function of proteins, metabolism of RNA and DNA, signal transduction, gene expression, and regulation of apoptosis (9) . It is required for the action of more than 200 metalloenzymes and more than 2000 Zn dependent transcription factors have been recognized.(10) . Zinc has antioxidant properties and plays an important role in scavenging reactive oxygen species, and they also hypothesized that in the absence of zinc, the possibility of increased oxidative damage exists. (11) . Several research showed that treatment with Zn during Cd exposure prevented or decreased the harmful effects of Cd(12,13). Zn might reduce uptake of Cd by competition for a common transporter (14). Moreover, zinc induced the synthesis of metallothionein in the liver, which caused Cd accumulation in the liver and delayed its transfer to the kidney. The zinc is a well-established antioxidants and it can protect against Cd-induced oxidative stress (15, 16)

MATERIALS AND METHODS

Animals

The study was conducted in albino mice (30–32 g) in the animal house of Veterinary Medicine -Baghdad University,Iraq. The animals were bred and maintained under standard conditions: temperature 25+2_C and a 14 -h light cycle. Commercial pellet diet and water were given ad libitum. This study was performed under the rule of ethics for management laboratory animals submitted by university of Baghdad - college of veterinary medicine

Experimental design

Twenty one animals for acute Study while sixty were used in subchronic study .Twenty one mice were divided into three groups: each group (7 mice). First group used to study acute toxicity of cadmium chloride which administered at oral toxic to lethal doses ranged between (175-250 mg/kg/ b.w) the second group were used to study acute toxicity of zinc sulfate which administered at oral toxic to lethal doses ranged between(350 -650 mg\kg\b w) while ,the third group were administered toxic to lethal doses of cadmium chloride and zinc sulfate in combination and their LD50 calculated according to up & down method. For subchronic study we used sixty adult mice were divided into four group of 15 for each group . they were administered the dosage daily orally at morning with overnight fasting by using gavages needle lasted for 45 day. The first group of mice was (T1) administered cadmium chloride once at day at (5mg /kg B.W). The second group (T2) administered dose at NOAEL range of zinc sulfate (10 mg/kg B.W) orally. .

The third group(T3) administered combination of both zinc sulfate (10 mg/kg B.W) and after four hours administered cadmium chloride(5mg /kg B.W) (1,17) The forth group act as control (C) and administered distilled water orally. At the end of sub chronic study all groups of animal scarified surgically under anesthesia and their liver submitted to digestion process for determine cadmium and zinc level (18).

Clinical examination

Mice were examined clinically during the period of experiment; the clinical signs were recorded daily , while the body weight calculated for all groups every 15 day

Isobolographic analysis study and subchronicity index

This analysis usually used to determine the sort of interaction of two metals, in which a line draw to join the LD50 of each of the two metals studied in isobolograph and an intersection point determined by lines drew vertically from the LD50 values of each combined metals . The conclusion of metals interaction was determined accordingly to the position of this intersection point to the two metals joined LD50 line. If the point is to the right, it mean there is an antagonistic effect (>I), to the left, mean potentiation or synergistic effect (<I), while on the line (=I), it mean there is an additive effect between the two metals. The sort of interaction was estimated according to the following equation (19).

$$\frac{\boldsymbol{acute\ or\ subchronic\ combined\ metal\ (a)}}{\boldsymbol{acute\ or\ subchronic\ alone\ dosing\ metal\ (A)}} + \frac{\boldsymbol{acute\ or\ subchronic\ combined\ dosing\ metal\ (b)}}{\boldsymbol{acute\ or\ subchronic\ alone\ dosing\ metal\ (B)}}$$

Subchronicity index

It is a modulation of chronicity index equation of klassen (20). It was a measure of the possibility of a drug accumulation after its sub chronic administration based on comparison the ratio of LD50 Value in acute and chronic exposure to the drugs according to aduptive equation:

$$\textbf{Subchronicity index} = \frac{\boldsymbol{LD50\ of\ acute\ dose\ alone\ or\ in\ combination}}{\boldsymbol{LD50\ after\ 45\ days\ with\ sub\ lethal\ dose\ alone\ or\ in\ combination}}$$

If the result exceed 1 , there is possibility of accumulation (20). Estimation Of Cadmium And Zinc At Liver : The cadmium and zinc in liver tissue samples were measured by flame atomic absorption spectrophotometer method (18)

RESULTS

Clinical observation

Toxicity signs for acute study

The toxicity symptoms were noticed after cadmium dosing in mice which were , increase breath rate, that decreased after 1 hr , diminish in water intake and appetite , decrease movement eye congestion and loss attention incoordination and fallen then death occur . The toxicity signs of zinc sulfate were not obvious well. there was a lethargy , the animal take a corner with rapid death occur in 3 from 5 animals (died after 4 hr from dosing) The toxicity symptoms for their combined dosing were similar to cadmium group with with less sever lethargy , weakness and mortality.

Toxicity signs for sub chronic study

Cadmium group

The toxicity signs that were noticed in sub chronic toxicity study of cadmium chloride appear at second week of dosing. it was firstly characterize by decrease in food intake and lethargy . The animals gathered around in one corner. after that the signs get more sever, continue loss in body weight ,loss of attention , turn off the eye color from bright red to black red . Black diarrhea in some time. After four week from dosing the nervous sings appear. Increase in sensitivity when dosing done , the animal tend to bite and jumping above the cage . At the last two week the loss of body weight increased and animal appear weakly and decrease of sensitivity , however ,some animal still tend to bite, sever emaciation and dehydration but no death occur at the period of 45 day of dosing.

Zinc group

There was no toxicity symptoms at 10mg/kg dosing of zinc sulfate for 45 days. but some of decrease in body weight due to decrease food intake appear at the second week of dosing then return to normal

Zinc and Cadmium combination group

The signs of toxicity appear at the second week but less in severity from cadmium group , there was a decrease in food intake and some lethargy . At last two week some of increase in sensitivity and nervous behavior appear like tend to bite and jump that is appeared in 6 from 15 mice

Body weight change

Table (1) showed that all dosed mice group have a significant (P>0.01) decline in body weight at the second week ,while at the 4th week the decline in body weight was more obvious in cadmium dosed group than the other dosed group of zinc sulfate and combined dosed group , however , still they are significantly less than control group. Same pattern were noticed at the 6th week of dosing as in 4th week in which the weight of mice in zinc sulfate group and that given in combination with cadmium chloride showed nearly weight of control group but still significantly less (p >0.01).

Estimation of LD50 at acute and sub chronic administration

Acute toxicity study

Acute toxicity Studies showed that LD50 for cadmium chloride and zinc sulfate according to up and down method (Dixon)(21) was (243 and 636.9 mg / kg BW) respectively that reduced after their combination interaction to (106.6 and 363 mg/kg.B.W) for cadmium and zinc respectively (table 2):

Lsobolographic analysis

Figure (1.1) showed that the intersected lines of LD50 levels of cadmium chloride and zinc sulfate after their combined administration together was on the line that joined LD50 values of both metals alone estimated according to Miranda (19) equation.

$$\frac{106.5}{243.43} + \frac{363}{637} = 1.007$$

The result showed that there was a additive toxic effect after the combination of zinc sulfate and cadmium chloride at acute administration

Sub chronic toxicity study for determination of LD50

Sub chronic toxicity study showed that LD50 for cadmium chloride and zinc sulfate after the end of sub chronic administration for (45 days) by up and down method (Dixon)(21) were 218 mg/kg for CdCl2 and 587 mg/kg for Znso4 that reduced after their combined administration to (157 mg/kg) for cadmium chloride and (463 mg/kg) for zinc sulfate (table 3)

Lsobolographic analysis

The intersected lines of LD50 levels of cadmium chloride and zinc sulfate after sub chronic dosage and their combined administration together was after the line that joined LD50 values of both metals alone estimated according to Miranda (19) equation

$$\frac{\mathbf{157}}{\mathbf{218}} + \frac{\mathbf{463}}{\mathbf{587}} = \mathbf{1.5}$$

The result of sub chronic isobolographic interaction between the cadmium chloride and zinc sulfate were antagonistic effect (figure 4.2).

Subchronicity index

Subchronicity index was adapted of chronicity index that approved by Klaassen (20) It was measured according to LD50 after acute and sub chronic administration of different treatment by using the adaptive equation

$$\text{cadmium chloride alone} = \frac{243}{218} = 1.1$$

$$\text{cadmium chloride combination} = \frac{106.5}{157} = \mathbf{0.67}$$

$$\text{zinc sulfate alone} = \frac{637}{587} = \mathbf{1.08}$$

$$\text{zinc sulfate in combination} \frac{363}{463} = \mathbf{0.78}$$

Cadmium level in liver for acute study

The result showed these were significant increase (p >0.01) in cadmium level in both cadmium and combined dosed groups while the zinc group showed no significant difference from control group. The cadmium level increase up to 59 in cadmium chloride dosed group above the control group level while the combined elevated to 37 times above control group. As in table (4)

Cadmium level in liver for sub chronic study

The result showed that was a significant increase (p >0.01) in cadmium level in both cadmium and combined dosed groups but the zinc group showed no significant difference from control one. The cadmium group had an elevation in cadmium level up to 49 time above the control group while the combined group elevated to 35 times than control group mice as in table (5).

Zinc level in liver for acute study

The result show that was a significant (p >0.01) increase of zinc level in lever of mice in all treated group The zinc group showed the highest increase level by 1.9 times from control group while the cadmium group the less increase by increased to 1.14 times above control group . The combined dosed group showed increase to 1.3 times above control group as in table (6).

Zinc level in liver for subchronic study

The result showed a significant increase (p >0.01) of zinc level in liver of mice in all treated group . The zinc group showed the highest increase by 1.7 times above control group and the cadmium group the less increase by 1.19 elevation above control group The combination group showed elevation by 1.4 times above control group as in table (7)

DISCUSSION

Cadmium (Cd) is transitional metal with chemical behavior similar to Zn. It is well-known that Cd interacts with bioelements at different sites of their kinetic (absorption, distribution inbody organism, elimination) and with their biological functions , so the interaction with zinc was studied in different research (12,22,23). In our study the results of interactions of Cd and Zn showed obvious role of zinc in decreasing of cadmium toxicity by different means such as competition of zinc with cadmium on absorption site in GIT and distribution in blood by albumin or deposition in tissue by metallothionien. The clinical signs that were noted during LD50 experiment in animals dosed with zinc sulfate and cadmium chloride at acute doses in alone and in combined form were increased in respiratory rate, the cause behind the increase might be due to the lesions occurred in the lungs (24), beside that an increase demand of the tissues for oxygen because of histotoxic hypoxia or damage of lungs tissues might resulting due to cadmium toxicity leading to shallow and labored respiration (25).

The decrease in food intake may be due to acute hepatotoxicity. Much of the Cd absorbed in the intestines is delivered first to the liver via portal circulation and intestinal (duodenum) damage (26). The in coordination happened may be due to acute central and peripheral neurotoxicity of cadmium(27) then death occur . The zinc group showed rapid death due to the ingestion of zinc or zinc-containing compounds has resulted in a variety of systemic effects in the gastrointestinal and hematological systems and alterations in the blood lipid profile in humans and animals. In addition, lesions have been observed in the liver, pancreas, and kidneys of animals and that may caused the rapid death(17) The combined group showed rapid death relatively with other group might be due to additive effect of both lethal dose of cadmium and zinc and the short period of dosing to allowed zinc to protect the body. In sub chronic dosing there were a decrease in food intake in all treated groups that reflected on body weight . Toxicity signs that developed throughout sub chronic administration of cadmium was indicative of accumulation since, there were many toxicity signs were developed throughout the experiment .While no clear clinical symptoms appeared in zinc group. After combined subchronic administration there were a dcrease in toxic effect than cadmium alone group .

The bloody diarrhea that appeared at the 4th week of cadmium dosing might be due to sloughing of intestinal mucosa (26). While the eye congestion attributed to ROS and oxidative stress that might cause aseptic fever due to damage of the blood vessels and cells. (28) At the last two week the mice tend to be vicious might be due to central and peripheral neurotoxicity (27). The combined at last period also showed some of vicious behavioral that might be due to incre ase the cadmium level in body that saturated all site of synthesized MTII that lead to a portion of free cadmium in body that made some of toxic signs but less than cadmium group .

The results of body weight change were supported by the symptoms and clinical observation that recorded through the period of experiment in chronic administration for both cadmium and zinc alone and in combination. The body weight during the 2nd week of experiment showed significant slightly decline in all dosed group , while at the 4th week the results showed continuous decline in the body weight of cadmium group but increase in both zinc and combined group which still significant different when compared with control the reason behind the first decline at zinc and combined groups might be side effect for decreasing appetite, food intake that possibly due to disturbance physiology of body . The cadmium group body weight continued decline till the end of experiment decrease to 17% while the combined group increased by 13% .The decrease in body weight in cadmium group, this might due to decreasing appetite, food intake, gastrointestinal disorder in addition to hypatoctic toxicity and oxidative stress (22).

The result of Isobolographic analysis showed additive effect after acute lethal administration of both metals possibly due to low period for MTs synthesis while after sub chronic administration, the combined administration showed antagonistic possibly due to enough period for increase synthesis of MTs that protect from cadmium oxidative stress toxicosis as well as zinc might act as antioxidant that help to antagonist cadmium toxicosis and that with agreement with Klaassen and Diwan and Brzóska (8,29). The result of subcronic index indicate that cadmium accumulation not effected after alone administration with toxic doses but the result of combined administration was indicative of nearly 32% loss in their toxic level in the body of dosed group mice . the same pattern was for zinc that showed no change in its level in the body after its alone dosed in acute and subchronic but after its combined administration with $CdCl_2$ its level in the mice body decline nearly 22% of toxic level . These decline in zinc and cadmium levels after their combined administration could be attributed to both metal induced MTs specially for cadmium which was given at toxic dose but zinc at NOAEL dose they caused more MTs induction in liver and possibly in kidney (6, 30,31).The binding site for zinc and cadmium were more available the matter that kept both element in the bound form with MT that made both element especially cadmium in non toxic form that give the body opportunity to overcome its toxicity . also the competition between zinc and cadmium for absorption in the intestinal tract and the transport in blood by binding to albumin and in tissue especially liver to MTs by competing to bind site in the induced MTs protein this made both element available for excretion in both urine and feces that lead to lower sub chronic index to lower than1. (22,23,32)

The level of cadmium in acute study in cadmium group liver showed significant increase up to 59 times above control group may be occurred due to cadmium alone administration, which ultimately transported and accumulated in the liver, kidney and other tissue while minimum amount of cadmium remain in the serum connected with albumin after giving single toxic to lethal dose of cadmium chloride ,while the combined dosed group also showed significant increase up to 37 times above control group, but this result was less than the value of cadmium alone group by 38% but still high value when compared with control , the cause behind that may be the combination were for both lethal large dose after acute administration and the time were too short to overcome the toxicity case. After sub chronic dosing, the cadmium level showed significant increase up to 49 times above control group The higher cadmium level in the liver may be due to the cadmium accumulated in the liver and kidneys which considered the main target for cadmium accumulation and that agreed with Jarup et al and Rikaby (30). Ridha (34) referred to accumulation of cadmium in tissue depend on rout of administration and exposure time for this element. the oral administration of cadmium lead to equally accumulation in both liver and kidney. Liver and kidney considered the main source for metallothionine which has important role against cadmium toxicity because of its high affinity to bind with cadmium as chelating protein. In addition to that it is transport cadmium leading to accumulation of cadmium in liver and kidneys The combined group showed also high level of Cd, 35 times above control. Even this increase was high but the combination decline the cadmium level by 28% of alone adminstration this mean excessive intake of Zn might decreased Cd level in liver and other organs as mention by (12,22,23) The zinc level at acute and subchronic dose showed significant increase in all treated group. The alone zinc group showed the highest increase in both acute and subchronic dosed group by 1.9 and 1.7 respectively also the combined group in both acute and sub chronic dosing showed increase by 1.3 and 1.4 respectively the zinc level may be increased in these treated groups due to repeated zinc administration with cadmium these lead to induce MT synthesis which

lead to competition between the two metals on the binding site in MTs as well known the MT molecule contain 7 molecule of zinc or cadmium. The hepatic level of Zn tended to be increased by both a small oral dose of Cd and a large oral dose. The increase in the hepatic concentration of Zn might be due to the induction of MTs by Cd which is normally have Zn in its structure (6).

CONCLUSION

so zinc sulfate at low dose act as antidote in case of cadmium toxicosis this was supported by the result of clinical physiological as well as the level of zinc and cadmium in liver.

REFERENCES

1. ATSDR (Agency for Toxic Substances and Disease Registry) (2012) Toxicological profile for Cadmium. Atlanta: ATSDR/US department of Health and Human Services.
2. Singh P, Chaudhary S, Patni A, et al. (2007) Effect of cadmium chloride induced genotoxicity in bone marrow chromosomes of swiss albino mice and subsequent protective effects of Emblica officinalis and vitamin C. Journal of Herbal Medicine and Toxicology 1(2): 67–71.
3. Chen Z, Wang K, Ai YW, et al. (2014). The effects of railway transportation on the enrichment of heavy metals in the artificial soil on railway cut slopes. Environmental Monitoring and Assessment 86(2): 1039–1049.
4. Manca D, Ricard AC, Trottier B, et al. (1991) Studies on lipid peroxidation in rat tissues following administration of low and moderate doses of cadmium chloride. Toxicology 67(3): 303–323.
5. Goering P.L., Waalkes M.P., Klaassen C.D. (1994). Toxicology of Cadmium, in: R.A. Goyer, M.G. Cherian (Eds.), Handbook of Experimental Pharmacology: Toxicology of Metals, Biochemical Effects, vol. 115, Springer-Verlag, New York, pp. 189–214
6. Klaassen C.D., J. Liu, S. Choudhuri(1999). Metallothionein: an intracellular protein to protect against cadmium toxicity, Annu. Rev. Pharmacol. Toxicol. 39 267–294.
7. Waalkes M.P. (2000). Cadmium Carcinogenesis in review, J. Inorg. Biochem. 79 241–244.
8. Klaassen C. D., and Diwan, B. A. (2009). Metallothionein protection of cadmium toxicity. Toxicology and Applied Pharmacology, 238, 215–220.
9. Michael K. Hambidge and Nancy F. Krebs(2007). Zinc Deficiency: A Special Challenge . The Journal of Nutrition.
10. Cai L, Li XK, Song Y, Cherian MG(2005). Essentiality, toxicology and chelation therapy of zinc and copper. Curr Med Chem; 12 (23): 2753–2763
11. Colagar AH, Marzony ET and ChaichiMJ (2009) Zinc levels in seminal plasma are associated with spermquality in fertile and infertile men. Nutrition Research 29(2): 82–88.
12. Vesna Matovic, Aleksandra Buha, Zorica Bult, and Danijela Đukic-Ćosic(2011). cadmium toxicity revisited: focous on oxidative stress induction and intraction with zinc and magnesium . Arh Hig Rada Toksikol ;62:65-76
13. Kamil Pabis, Claudia Gundacker, Robertina Giacconi, Andrea Basso, Laura Costarelli , Francesco Piacenza , Sergio Strizzi , Mauro Provinciali , Marco Malavolta (2018). zinc supplementation can reduce accumulation of cadmium in aged metallothionein transgenic mice. Chemosphere, 211, 855- 860
14. El Heni Jihen a, Messaoudi Imed b, Hamouda Fatima a, Kerkeni Abdelhamid(2008). Protective effects of selenium (Se) and zinc (Zn) on cadmium (Cd) toxicity in the liver and kidney of the rat: Histology and Cd accumulation. Food and Chemical Toxicology, 46 , 3522–3527
15. Brzóska MM, Rogalska J, Galażyn-Sidorczuk M, Jurczuk M, Roszczenko A, Kulikowska- Karpińska E, et al.(2007).

Table (1) Effect of body weight change of mice groups dosed sub chronically with cadmium chloride and zinc sulfate and their combination:

Week / Group	Zero week	2nd week	4th week	6th week
(T1)Cadmium Cloride 5mg/kg	30.75 ± 0.34 a	29.00 ± 0.30 b	27.86 ± 0.40 c	25.43 ± 0.36 c
(T2)Zinc Sulfate 10mg/kg	30.61 ± 0.46 a	29.43 ± 0.37 b	33.00 ± 0.31 a	34.28 ± 0.28 b
(T3)Cadmium and Zinc 5mg/kg+10mg/kg	30.96 ± 0.32 a	29.71 ± 0.28 b	31.28 ± 0.28 b	34.00 ± 0.31 b
(C)Control Distilled water	30.86 ± 0.23 a	31.85 ± 0.26 a	33.57 ± 0.29 a	35.57 ± 0.29 a
LSD value	0.691 NS	0.901 **	0.955 **	0.924 **

Means having different letters in same column differed significantly . ** (P<0.01).

Table (2) : Estimation acute oral LD50 value for Cadmium Chloride and Zinc Sulfate and their combination in Acute mice according to Dixon method

Treatment / Group	Initial dose mg/kg	Final dose mg /kg	Difference between dose mg/kg	Result after 24 hrs	LD50 mg /kg
Cadmium Chloride	175	225	25	OOOXOXO	243.43
Zinc Sulfate	500	600	50	OOOXOXO	637
Cadmium Chloride + Zinc Sulfate	175 + 500	125+ 400	25 + 50	XXXOXOX	106.5+ 363

Table (3) : Estimation of oral LD50 value for Cadmium Chloride and Zinc Sulfate and their combination in sub chronic toxicity Study in mice

Treatment / Group n =15	Initial dose mg/kg	Final dose mg /kg	Difference between dose mg/kg	Result after 24 hrs	LD50 mg /kg
Cadmium Chloride	**150**	**200**	**25**	**OOOXOXO**	218
Zinc Sulfate	**450**	**550**	**50**	**OOOXOXO**	587
Cadmium Chloride + Zinc Sulfate	**225 + 600**	**175+ 500**	**25 + 50**	**XXXOXOX**	157+ 463

Table (4) Cadmium level (Mg/g) in liver of mice groups dosed acutly with cadmium chloride and zinc sulfate and their combination

Group **n: 7**	Cd In liver Mean ± SE
(T1)Cadmium 175-250mg/kg	27.05 ± 0.17 a
(T2)Zinc 500-650mg/kg	0.315 ± 0.01 c
(T3)Cadmium Chloride (125-175) mg/kg and Zinc Sulfate(400-500) mg/kg	16.74 ± 0.18 b
(C)Control Distilled water	0.456 ± 0.01 c
LSD value	0.389 **
Means having different letters in same column differed significantly . ** (P<0.01).	

Table(5): Cadmium level (Mg/g) in liver of mice groups dosed subchronically for 45 day with cadmium chloride , zinc sulfate and their combination :

Group **n=15**	Cd In liver Mean ± SE
(T1)Cadmium Cloride 5mg/kg	22.99 ± 0.20 a
(T2)Zinc Sulfate 10mg/kg	0.322 ± 0.01 c
(T3)Cadmium and Zinc 5mg/kg+10mg/kg	16.36 ± 0.08 b
(C)Control Distilled water	0.471 ± 0.01 c
LSD value	0.338 **
Means having different letters in same column differed significantly . ** (P<0.01).	

Table (6) Zinc level (Mg/g) in liver of mice groups dosed acutely with cadmium chloride and zinc sulfate and their combination orally

Group **n=7**	Zn In liver Mean ± SE
(T1)Cadmium 175-250mg/kg	31.18 ± 0.09 c
(T2)Zinc 500-650mg/kg	50.37 ± 0.20 a
(T3)Cadmium Chloride (125-175) mg/kg and Zinc Sulfate(400-500) mg/kg	35.64 ± 0.20 b
(C)Control Distilled water	27.82 ± 0.29 d
LSD value	0.651 **
Means having different letters in same column differed significantly . ** (P<0.01).	

Table (7) Zinc level (Mg/g) in liver of mice groups dosed subchronically with cadmium chloride and zinc sulfate and their combination orally

Group **n=15**	Zn In liver Mean ± SE
(T1)Cadmium Cloride 5mg/kg	33.19 ± 0.11 c
(T2)Zinc Sulfate 10mg/kg	48.07 ± 0.22 a
(T3)Cadmium and Zinc 5mg/kg+10mg/kg	37.96 ± 0.25 b
(C)Control Distilled water	27.80 ± 0.12 d
LSD value	0.558 **
Means having with the different letters in same column differed significantly . ** (P<0.01).	

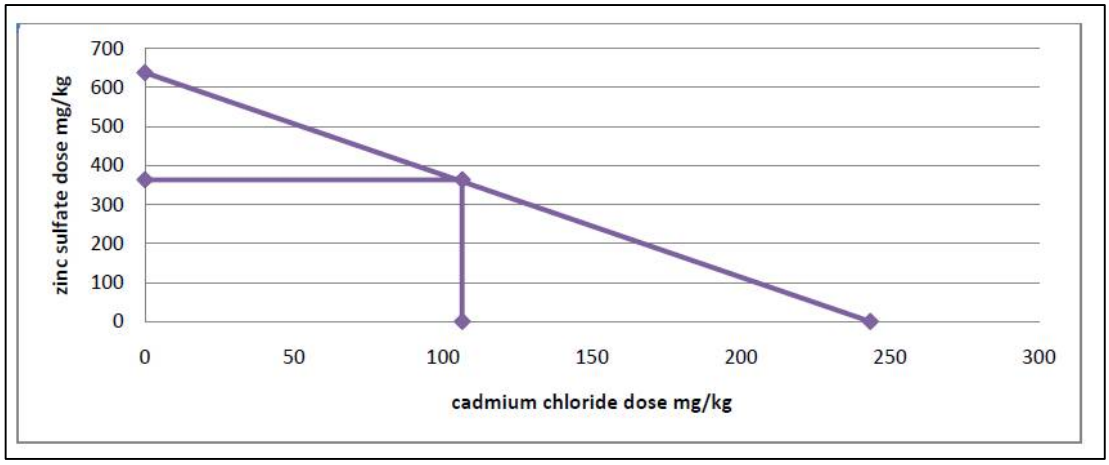

Figure (1): Isobolographic analysis for Acute Toxicity interaction between Zinc sulfate and cadmium chloride

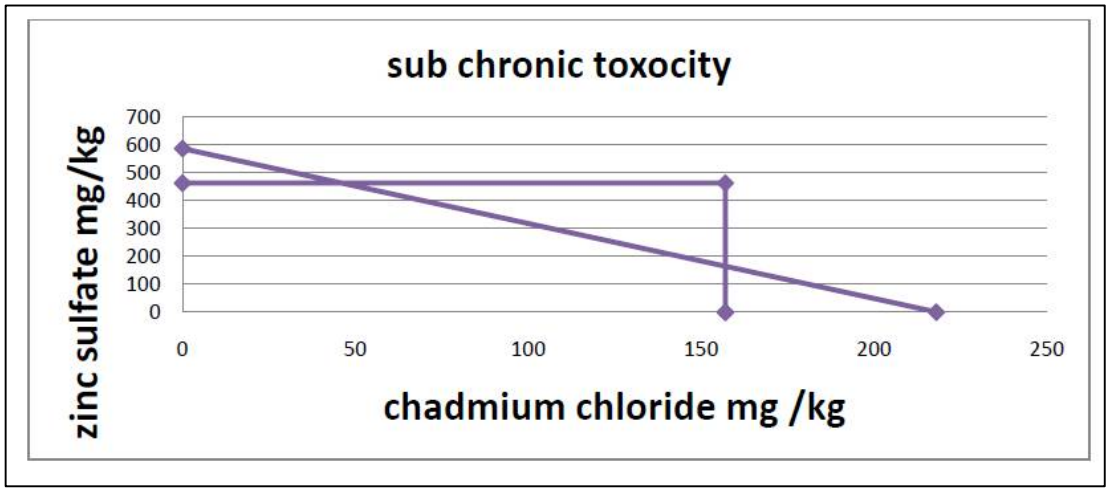

Figure (2): Isobolographic analysis for Acute Toxicity interaction between Zinc sulfate and cadmium chloride

Indian Journal of Natural Sciences www.tnsroindia.org.in ©IJONS

Vol.9 /Issue 51 / December / 2018 *International Bimonthly* *ISSN: 0976 – 0997*

RESEARCH ARTICLE

Study of Some Physiological Parameters of Hemophilia A and Von Willebrand Patients Infected with Hepatitis B and C

Shahad Q. Al-Hamadiny[1*],Kadhum J. Gattia[1] and Safaa A. Faraj[2]

[1]Department of Biology, College of Science, University of Waist, Iraq.
[2]College of Medicine, University of Waist, Iraq.

Received: 20 Aug 2018 Revised: 22 Sep 2018 Accepted: 25 Oct 2018

***Address for Correspondence**
Shahad Q. Al-Hamadiny
Department of Biology,
College of Science,
University of Waist, Iraq.

ABSTRACT

Hemophilia A and Von Willebrand are genetic diseases caused by the deficiency or malfunction of one of the coagulation factors. Hemophilia is caused by the absence of Factor VIII (F.VIII). Von Willebrand is caused by a deficiency or disorder of von Willebrand factor (VWF).This study included 50 patients of both diseases,35 Hemophilia type A from males and 15 Von Willebrand patients from both sexes. The results show significant decrease($P \leq 0.05$) in the value of(Hb, PCV,MCH,MCHC) to each of Hemophilia A and Von Willebrand compared with control, and increase in the level of platelet to each of Hemophilia and Von Willebrand with control. The results showed a significant increase ($P \leq 0.05$) in the Mean values of (AST,ALP, ALT TSB)for Hemophilia and Von Willebrand patients compared to healthy patients. The percentage of patients with hepatitis in general was(45.71)% and (60) % for both Hemophilia and Von Willebrand respectively.

Key Words: Hemophilia , Von Willebrand, Liver enzyme, CBC, Hepatitis B-C.

INTRODUCTION

Hemophilia A and Von Willebrand (VW) are two genetic diseases caused by a deficiency or defect in one of the coagulation factors. Hemophilia A is a genetic disease that carries on the X-linked sex chromosome (1).It occurs as a result of the lack of factor VIII (F.VIII) necessary for blood clotting, hemophilia Type A affects males only, while females are carriers (2) .There are three types of hemophilia A, B and C, the first type occurs as a result of the lack of factor VIII of blood clotting (F.VIII), and the second type is due to the lack of Factor IX (F.IX), and the third is due to the lack of factor Eleventh (XI), The type of hemophilia A is the most common, where the infection rate by about 85% of the total of almost hemophilia patients around the world, and Hemophilia type B is approximately 15%, and Hemophilia type C is less than 1% (3). The most common symptom of hemophilia bleeding in any part of the body.

When the injury that lead to bleeding and this bleeding damage to some of those parts such as joints and cause severe pain and difficulty in movement with swelling of the knee, and may develop the situation of disability and deformity (4). and occur also brain hemorrhage in some hemophilia patients as well as in some important vital organs leading to death (5). Compensatory therapy for hemophilia patients was produced in the mid-1960s, and plasma derived concentration and Cryoprecipitate were collected by plasma from thousands of healthy donors and given to patients intravenously without being subjected to the required tests to ensure that they were free from disease before given to patients From then until the end of 1988, most patients with hemophilia were at risk of serious transient viral infections such as viral hepatitis such as viral hepatitis B (HBV) and C (HCV) and Human Immune Deficiency Virus (HIV) (6). Currently, the treatment of hemophilia patients with intravenous injection of the eighth factor and called the concentration factor on a regular basis to prevent recurrent bleeding episodes also known as the name of preventive treatment, the most effective way to reduce the risk of joint damage, and reduce the deficit.(7) Von Willebrand is a hereditary disorder caused by a deficiency or malfunction of the Von Willebrand factor (VWF), Von Willebrand has an important role in the process of hemostasis. It mediates the process of platelet adhesion in primary hemostasis. In addition, it also carries with it the eighth anticoagulant factor (F.VIII) in the circulatory system, protects it from the rapid decomposition of the protein and gives it to secondary hemostasis sites. Therefore, the deficiency of the Von Willebrand factor causes bleeding by disabling platelet adhesion , Or by reducing the concentration of Factor VIII(8).The von Willebrand factor is produced by endothelial cells in different tissues(9).

MATERIALS AND METHODS

Blood samples

Blood sample were collected from hospitals in Waist province during the period from November 2016 to April 2017. This study included (50) patients. The study included (50) patients from both diseases divided into 35 hemophilia A patients and their male sex group, aged between (1-28) year. And 15 von Willebrand patients from both sexes, compared with a control group which included 25 people (13) male and (12) female, 5 ml of venous blood were withdrawn from both patient and control, divided into 2 groups: the first group (1) ml of blood placed in the EDTA K3 tube, Hematological test.the second group placed(4) ml of blood in a normal tube containing Gel Gel Clot Activator Tubes for the conduct of biochemical tests, and then placed in the centrifuge at 3000 cycles for a minimum of 15 minutes to separate the serum from the rest of the cellular components of blood and then the serum was transferred to test tubes Eppendorf tubes by Micropipette micro pipette and kept at -20°C until the required analyzes are performed**.**

Hepatitis B surface antigen

Test principle

Sandwich principle. Total duration of assay: 18 minutes.

- 1st incubation: 50 µ L of sample, two biotinylated monoclonal anti-HBs Ag antibodies, and a mixture monoclonal anti-HBs Ag antibody and polyclonal anti-HBs Ag antibodies labeled with a ruthenium complex) form a sandwich complex.
- 2nd incubation After addition of streptavidin-coated micro particles, the complex becomes bound to the solid phase via interaction of biotin and streptavidin.
- The reaction mixture is aspirated into the measuring cell where the micro particles are magnetically captured onto the surface of the electrode. Unbound substances are then removed with Porcello /Porcello M. Application of a voltage to the electrode then induces chemiluminescent emission which is measured by a photomultiplier

- Results are determined automatically by the software by comparing the electro-chemiluminescence signal obtained from the reaction product of the sample with the signal of the cutoff value previously obtained by calibration.(10).

Antibody to hepatitis C virus (anti-HCV)

Test principle

Sandwich principle. Total duration of assay:33 minutes.

- 1St incubation: 40 µL of sample, 60 ul of a reagent containing biotinylated HCV antigens and 60 µL of a reagent containing HCV antigens labeled with a ruthenium complex a) react to form a sandwich complex.
- 2 Nd incubation: After addition of streptavidin-coated micro particles, the complex becomes bound to the solid phase via interaction of biotin and streptavidin.
- The reaction mixture is aspirated into the measuring cell where the micro particles are magnetically captured onto the surface of the electrode. Unbound substances are then removed with Porcello /Porcello M. Application of a voltage to the electrode then induces chemiluminescent emissionwhich is measured by a photomultiplier
- Results are determined automatically by the software by comparing the electrochemiluminescence, signal obtained from the reaction product of the sample with the signal of the cutoff value previously obtained by calibration.(11)

Statistical analysis

The results were statistically analyzed by using the statistical program for social science 13 (SPSS 13) by finding (mean $\pm$ SD) and using the LSD (least significant difference) test. Two way ANOVA method was used to compare between results to identifying significant differences between patient and healthy people, and the results are significant if the value of P-value is less than 0.05 ($P \leq 0.05$) (12).

RESULTS

The Results of blood parameters in Table (1) revealed a significant decrease of ($P \leq 0.05$) for both Hemophilia And Von Willebrand compared with control (Mean+SD) HB (12.943$\pm$2.725)(10.987$\pm$1.810)for Hemophilia And Von Willebrand, Respectively, compared to control(14.244$\pm$1.271),PCV(39.700$\pm$7.301) (34.272$\pm$3.805) compared with control VonWillebrand for HB and PCV only. As for MCV, MCH and MCHC, there was no (41.897$\pm$3.445), and MCV (74.46$\pm$ 8.96) (73.33$\pm$7.53) compared to control (87.64 $\pm$3.96) and the MCH (25.069$\pm$5.180) (24.891$\pm$4.056) compared to control (29.816$\pm$1.576).and MCHC (30.780$\pm$6.374) (30.853 $\pm$4.630) compared to control (34.022 $\pm$0.766).The number of Red Blood cells (RBCs) was lower in von Will brand's disease compared to the control, while there was no significant difference between Hemophilia A compared with control patients. Morale elevation ($P \leq 0.05$) included the average platelet for patients with Hemophilia And Von Willebrand Patients . On the same table, significant differences were observed significant difference between hemophilia and Von Willebrand.

The results in Table (2) showed a significant increase ($P<0.05$) in the level of liver enzymes including :Aspartate Transaminase (AST), Alkaline Phosphatase (ALP) and Total Serum Bilirubin (TSB) for both Hemophilia A and Von Willebrand patients compared to control subjects. The results (mean$\pm$ SD) of the transporter enzyme AST (17.469$\pm$2,876) (19.169$\pm$2.581) for Hemophilia And Von Willebrand respectively compared to healthy (12.356$\pm$2.749), and ALP (147.78$\pm$14.23) (156.12$\pm$15.88) for Hemophilia and Von Willebrand, respectively, compared with control (68.78$\pm$8.88),and TSB (1.432$\pm$0.292) (1.341$\pm$0.288) for Hemophilia A and Von Willebrand respectively compared to control (0.606$\pm$0.293). ALT was significantly higher in von Willebrand patients (8.334$\pm$1.239) than in the control

(4.681±0.946). The comparison between the two patients found significant difference (P<0.05) In the ALT standard only, while no significant differences were observed between the two diseases in the other biochemical parameters ALP, AST, TSB.The results in tables (3) (4) (5) showed the percentage of Hemophilia patients and Von Willebrand patients with hepatitis B and C. The number of Hemophilia patients employed in the study was 35 patients, all of whom were male only,(1-28 years) showed that the percentage of patients with hepatitis in the first age group was (45.5%) and the second age group (46.15%).The number of Von Willebrand patients using the study was (15) patients of both sexes with (6) males and (9) females between the ages of (1-14) years. The same table shows that the percentage of patients with Von Willebrand amount to infected with hepatitis (60%) for males and (60%) for females.The percentage of people with hepatitis in the general hemophilia population was 45.71%, while those with hepatitis in both types of von Willebrand patients were generally (60%)

DISCUSSION

The Results in Table (1) show a significant decrease (P<0.05) in the blood parameters of patients with Hemophilia and Von Willebrand Compared to control: Hb, PCV,MCV, MCHC this is due to the frequent bleeding of patients (13).The results showed a significant increase (P≤0.05) in patients with hemophilia and Von Willebrand when compared to control patients due to continuous hemorrhagic disease, which increases the proportion of Platelets to form strokes that help to stop bleeding (14). In comparison with the results of the above table, when comparing Hemophilia And Von Willebrand Patients, there was a significant increase for Hb, PCV and RBCs for patients with Hemophilia compared with Von Willebrand patients, Hemophilia of the Male Sex and Von Willebrand patients Most of them of the sex of females, and that the proportion of hemoglobin in males is higher than that of females about 12% (15).The table showed that was no significant difference at for all the above criteria.There was no significant difference between Hemophilia and Von Willebrand in the standard of blood platelet,because the Hemophilia And Von Willebrand Disease is a defect in the secondary hemostasis which is caused by deficiency of clotting factors (FVIII and FIX), while platelets deficiency cause defect in the primary hemostasis(16).The results in Table

show a significant increase (P≤0.05) in the average value of both the transporter enzyme AST and the ALP enzyme in patients with hemophilia compared to control patients due to liver dysfunction and deterioration of function.To the serum and lead to high levels, or the reason for internal or external hepatic correlations caused by hepatitis (17).It can also be caused by hepatitis C (HCV) and B (HBV),which leads to cirrhosis of the liver as well as cancer, because about 80 % of liver cancer is linked to chronic viral infection(18) Our current study with (19). The results in the same table showed normal levels of ALT for patients with hemophilia A compared to control patients.The cause of the disease is called chronic carriers. In this case,the virus ineffective and does not affect hepatocellular carcinoma, The blood is filtered after a period of normal infection, although no treatment is used. This period of time is estimated to be one to two years for Hemophilia patients and about four weeks for non-infected patients.in this case, The enzyme level is normal (20).From the above table, a significant increase was found in the total serum bilirubin concentration of patients with hemophilia A when compared with healthy patients due to hepatic cell degeneration due to hepatitis C virus infection, gallbladder dysfunction, gallbladder obstruction Gravel, cancerous diseases (21). In the same table, when comparing Von Willebrand patients with control patients, there was also a significant increase in the mean value of AST, ALT,and ALP for patients due to chronic hepatitis In quality due to continuous blood transfusions for treatment, especially after long periods of use of blood products(22) From the same table it was found that the significant increase in the concentration of total bilirubin in the serum of Von Willebrand patients compared with the healthy is due to the damage of liver cells and may also result in increased red blood cell decomposition in patients (23).In the follow-up to the results of the above table, when comparing hemophilia and von Willebrand patients, no significant differences were observed between the two diseases in the biochemical parameters and the enzyme alkaline phosphatase (ALP), the total serum bilirubin level in the serum TSB. This is because the Hemophilia And Von Willebrand

patients The same effect on liver enzymes or the therapeutic dose that patients receive the same therapeutic doses during the disease, and because of the convergence of the ages of patients in the two diseases studied, leading to the convergence or similar levels of enzymes in plasma blood, which led to the absence of any difference (24).Our results showed a significant increase in the level of ALT for Von Willebrand patients when compared with patients with hemophilia. The elevation of ALT in patients is a reliable marker of hepatocellular disease. It is used to determine the amount of liver injury and also the extent of its function. Is the enzyme of cellular cytotoxic, which is found in the liver cells, which causes a more specific indicator of the liver injury. It is also found in other cases such as hepatitis viruses, non-alcoholic fatty liver diseases, hepatitis, liver tumors, alcohol or drugs, It's possible that due to reasons not related to the liver, such as muscle injury which causes a slight increase in the enzyme carrier Osprey AST and digestive disorders as well as possible that are associated with abnormal levels of liver enzymes (25). As for the The results of the tables (3,4,5) showed a high percentage of hemophilia and von Willebrand patients with hepatitis B,C and about 80 percent of the world's hemophilia population in a country with limited or limited medical resources They may have been infected because these patients are always in need of frozen blood or plasma products or Cryo untested for treatment to stop hemorrhage (26). The results of the statistical analysis showed a percentage difference between Hemophilia patients compared with Von Willebrand (45.71%) compared to von Willebrand patients (60%). The reason for von Willebrand patients' increased susceptibility to hemophilia patients was that von We Willebrand IL brand's patients were more susceptible to hepatitis C because of their treatment, Cryo products, and the large number of their use of blood and its derivatives, which has the main role of transmission of the virus (C), which is missing the comprehensive examination, including virus testing, and for patients with Hemophilia,they use coagulation factors (factor VIII and factor IX) Our results came in line with both (6) (27).

CONCLUSIONS

Hemophilia and Von Willebrand patients are affected by liver enzyme parameters, where hepatotoxicity is indicated, which is strongly related to the effect of liver function in these diseases. Hemophilia and von Willebrand patients have a significantly higher risk of HBV (B) and HCV(C) infection, with a sudden incidence of 45.71% in hemophilia and 60% in von Willebrand patients. This is the result of treatment Compensatory agents for coagulation factors, whether Cryo Crystals or plasma derivatives contaminated with these viruses.

REFERENCES

1. Nazeef, M. and Sheehan, J.P. (2016). New developments in the management of moderate-to-severe hemophilia B. Blood Med.,1(7):27-38.
2. Peyvandi, F.; Garagiola, I. and Young, G. (2016).The past and future of hemophilia :diagnosis, treatments, and its complications, Lancet., 388(10040): 187-197.
3. Allen, K.N. and Kachalsky, E.(2010). Aging with hemophilia: mplications for social work practice. Soc Work Health Care, 49(4):327-344.
4. Paroskie, A.; Gailani, D.; De Braun, M.R. and Sidonio ,R.F. Jr. (2015).cross-sectional study of bleeding phenotype in hemophilia A carriers. Br. J. Haematol., 170 (2): 223-228.
5. World Federation of Hemophilia. (2013, May 2012). Hemophilia. Retrieved November 30, 2013.
6. Saleh, R.H. and Hadi, B,H.(2016).Correlation between the Prevalence of Hepatitis B and C Viruses against Tumor Necrosis Factor-α among Patients in Babylon Province. British Micro. Research J., 12(3):1-0.
7. Aznar, J.A. and Marco, A. (2012). Querol F. 5th Congress Association for Haemophilia and allied disorders EAHAD. Secondary prophylaxis in adult severe haemophilic patients: a prospective study in a single center. Haemophilia, 18(1): 22.
8. Starke, R.D.; Ferraro, F.; Paschalaki, K.E.; Dryden, N.H.; McKinnon, T.A.; Sutton, R.E. and et al. (2011).Endothelial Von Willebrand factor regulates angiogenesis Blood. J., 117(3):1071-80.

9. Luo, G.P.; Ni, B.; Yang, X. and Wu, Y.Z. (2012). Von Willebrand factor: more than a regulator of hemostasis and thrombosis. Acta Haemato., 128(3):158-169.
10. Hollinger, F.B.; Hepatitis B virus. In Fields, B.N.; Knipe, D.M. (eds).(1990). Virology ed. 2 New York Raven Press, 2:2171-2236.
11. Choo, Q.L.; Kuo, G.; Weiner, A.J.; Overby, L.R.; Bradley, D.W. and Houghton , M. (1989). Isolation of a cDNA clone derived from a blood-borne non-A, non-B viral hepatitis genome. Science, 244(4902):359-362.
12. Steel, R.G. and Torrie, J. H. (1980). Principles and procedure of statistics. Second ed. New York: McGraw-Hill., P: 481.
13. Soucie, J.M.; Christy, C.; Robert, L.J.; Roshni, K.; Julie, H.; Bruce, E.; Angela, F.;et al. (2004). Joint range of motion limitation among young males with haemophilia: prevalence and risk factors. Blood, 103(7):2467-2473.
14. Frossard, M., Fuchs, I., Leitner, J.M., et al. (2004). Platelet function predicts myocardial damage in patients with acute myocardial infarction. Circulation, 110(2): 1392-1397.
15. Ganji, V. and Kafai, M.R. (2009). Hemoglobin and hematocrit values are higher and prevalence of anemia is lower in the post-folic acid fortification period than in the pre-folic acid fortification period in US adults. Am .J. Clin. Nutr., 89(1):363-371.
16. Kessler, C. (2007). Hemorrhagic disorders: Coagulation factor deficiencies. In: Goldman L,Ausiello D, eds. Cecil Medicine. 23rd ed. Philadelphia, Pa: Saunders Elsevier :chap 180.P.p1210-1212
17. Bruix, J. and Sherman, M. (2011). American Association for the Study of LiverD Management of hepatocellular carcinoma: an update. Hepatology, 53(3):1020-1022.
18. El-Serag, H.B. (2011). Hepatocellular carcinoma. N. Engl. J. Med., 365: 1118-1127.
19. Shetty, S.; Sharma, N.; Ghosh, K. (2015).Epidemiology of hepatocellular carcinoma (HCC) in hemophilia. Crit .Rev .Oncol. Hematol., P.P: 5.
20. Telfer, P.; Sabin, C.; Devereux, H.; Scott, F.; Dusheiko, G.; Lee, C.A. (1994). The progression of HCV-associated liver disease in cohort of hemophilic patients Br. J. Haematol., 87:555-561.
21. Strader, D.B.; Wright, T.; Thomas, D.L. and Seeff, L.B. (2004). Diagnosis, management, and treatment of hepatitis C. Hepatology, 39(4):1147-1171.
22. Maieron, A.; Salzl, P.; Peck-Radosavljevic, M.; Trauner, M.; Hametner, S.; Schofl, R.; Ferenci, P. and Ferlitsch, M. (2014). Von Willebrand factor as a new marker for non-invasive assessment of liver fibrosis and cirrhosis in patients with chronic hepatitis C. Aliment Pharmacol, 39(3): 331-338.
23. Yilmaz, V.T.; Dincer, D.; Avci, A.B. and Cetinkaya, R. (2015). Significant Association between Serum Levels of Von Willebrand Factor (vWF) Antigen with Stages of Cirrhosis. Eur. J. Med., 47(1): 21–25.
24. Franchini, M.; Rossetti, G.;Tagliaferri , A.; Capra, F.; Maria, E.D .; Pattacini , C.; Lippi, G.; et al. (2001).The natural history of chronic hepatitis C in a cohort of HIV- negative Italian patients with hereditary bleeding disorders .J.of the hemophilia population Thromb. blood, (98). 6.Research, 127: 10-13.
25. Arag, G. and Younossi, Z. M. (2010). When and how to evaluate mildly elevated liver enzymes in apparently healthy patients. Cleve and clinic. J., 77(3): 195 - 204v
26. Junaid, M.; Siddique, Abu Nasar.; Khan, M.T.M.; Alam, I.; Waqas, M.; Hameed, S.S. and Muhammad,W. (2017). Detection and prevalence of hepatitis B, C and HIV viral infections among hemophilia patients in Peshawar, Pakistan , J. of Ento. and Zoo. Stu., 5(2): 180-184.
27. Konkle, B.K. (2011). Clinical challenges with in the aging hemophilia population , Thromb. Research, 127: 10-13

Table (1): Changes In Some Blood Parameters For Patients With Hemophilia A And Von Willebrand Patients Compared Control

Patients / Parameter	Hemophilia	Von Willebrand	Control	LSD	P-Value
HB G / DL	A 12.943 ±2.725	B 10.987 ±1.810	C 14.244 ±1.271	1.14	0.00012
PCV %	A 39.700 ±7.301	B 34.272 ±3.805	C 41.897 ±3.445	2.14	0.006
RBC $Mm/^{3}10^{6}$	A 4.5272 ±0.7919	AB 4.1103 ±0.3291	AC 4.7888 ±0.4689	0.434	0.003
PIT $Mm/^{3}10^{6}$	A 288.79 ± 31.90	A 307.91 ± 46.11	B 263.03 ±48.59	21.79	0.0192
MCV Micro Miter	A 74.46 ±8.96	A 73.33 ±7.53	B 87.64 ±3.96	5.44	0.013
MCH Pico grams	A 25.069 ±5.180	A 24.891 ±4.056	B 29.816 ±1.576	2.34	0.026
MCHC G / DL	A 30.780 ±6.374	A 30.853 ±4.630	B 34.022 ±0.766	2.19	0.007

***** Different capital letters show significant difference (P≤0.05) between patients and control.

* LSD: Least significant difference , * HB Hemoglobin, * PCV: Packed Cell Volume

* RBCs: Red Blood Cell, * PLT : Platelets, * MCV: Mean Corpuscular Volume, * MCH: Mean Corpuscular Hemoglobin, * MCHC: Mean Corpuscular Hemoglobin Concentration

Table (2): Changes In Some Biochemical Parameters For Hemophilia And Von Willebrand Patients Compared With Control

Patients / Parameter	Hemophilia	Von Willebrand	Control	LSD	P-Value
ALT Liter	A 5.325 ±0.559	B 8.334± 1.239	A 4.681 ±0.946	1.94	0.027
AST Liter	A 17.469 ± 2.876	A 19.169 ±2.581	B 12.356 ± 2.749	3.4	0.035
ALP Liter	A 147.78 ±14.23	A 156.12 ±15.88	B 68.78 ±8.88	12.33	0.0021
TSB Micromole / L	A 1.432 ±0.292	A 1.341 ±0.288	B 0.606 ±0.293	0.371	0.062

*Different capital letters show significant difference (P≤0.05) between patients and control.

* LSD: Least significant difference, * ALT Alanine Transaminase, *ALP Alkaline Phosphatase .

* TSB Total Serum Bilirubin, *AST Aspartate Transaminase.

Table (3): Percentage of Hemophilia A Patients with Hepatitis B and C by Age Group

Age / Result	1-14 (Hemophilia)	15-28 (Hemophilia)
Positive	%45.5	%46.15
Negative	%54.5	%53.85

Table (4): Percentage of Von Willebrand Patients with Type B and C Hepatitis B by Sex

Sex / Result	Male	Female
Positive	%60	%60
Negative	%40	%40

Table (5): Percentage of Patients with Hemophilia Compared To Von Willebrand Patients with Hepatitis B And C

Patients / Result	Hemophilia	Von Willebrand
Positive	%45.71	%60
Negative	%54.28	%40

Indian Journal of Natural Sciences www.tnsroindia.org.in ©IJONS

Vol.9 /Issue 51 / December / 2018 *International Bimonthly* *ISSN: 0976 – 0997*

RESEARCH ARTICLE

Rock Properties Distribution Modeling of Khasib Formation in Ahdeb Oil Field, Central Iraq

Buraq A. Al-Baldawi* and Madhat E. Nasser

Department of Geology, College of Science, University of Baghdad, Baghdad, Iraq.

Received: 02 Aug 2018 Revised: 06 Sep 2018 Accepted: 08 Oct 2018

***Address for Correspondence**
Buraq A. Al-Baldawi
Department of Geology,
College of Science,
University of Baghdad,
Baghdad, Iraq.
E-mail: buraqadnan81@gmail.com

ABSTRACT

Petrophysical rock property modeling is the process of determining petrophysical property values (porosity and water saturation) to each cell of the 3D grid model. The properties of this grid assign the quantity of fluids present, their relative distribution, and the ease with which they can flow towards production wells.Petrophysicalmodel was builtby geostatistical methods. Thegeostatistical algorithm (Statistical sequential Gaussian simulationalgorithm) is a statistical method, which appropriates with the available data of porosity and water saturation that calculated using well logs data. 3D petrophysical distribution model was built for twelve wells from KhasibFormation in the Ahdeb oil field using Petrel Software. Structural contour maps of Khasib units (Kh-1,Kh-2,Kh-3 and Kh-4) and layering have been made to create 3D porosity and water saturation distribution model.The porosity distribution was closed to homogeneous trend for the entire field and maximum porosity is 0.27 inunit Kh-2 whileminimum water saturation is 20 % in unit Kh-2. The petrophysical properties for unit Kh-2 is regards as good properties because this unit is aprincipleoil production unit in Khasib formation in Ahdeb oil field.

Key Words: Petrophysical, determining, porosity, Structural, water, regards.

INTRODUCTION

The Ahdeb oil field is located in the central section of Mesopotamia plain in Iraq, between Nomania and Kut towns, about 18km NW of Kut city and 180 km south east of Baghdad. Ahdeb oil field is an anticlinal structure elongated in NWW-SEE. It has three domes AD-1, AD-2, and AD-4 .AD-1 is little higher than the other domes. The two sides of the anticline are not steep, the dip angle of the south side is 0.7˚-0.9˚, the dip angle of the north side is 2˚, and the north limb is stepper than the south limb (Figure. 1) (1). Khasib formation represents the base of megasequence AP9.

There are two sequence in AP9 the first is deposited at the base of this megasequence and is late Turonian- Early Campanian sequence while the other sequence deposited at the top of AP9 megasequence is late Campanian-Mastrichtian sequence (2).According to Bellen*et al*,.(1959) (3) the lower contact of the formation is disconformable with Mishrif Formation while upper contact with the Tanuma Formation is gradational. The lower part of formation is predominantly a white limestone interbeded with chalky sediments. Upward, it becomes a brown porous limestone containing fossils, calcite and pyrite, with varying degrees of oil staining. Formation thickness is 100 to 115m.

The goal in reservoir characterization for heterogeneous formations is to establish a reservoir model based upon explicit modeling of known geological heterogeneities. Rock properties such as porosity and related fluid properties, generally are expected to vary among and within reservoir zones. In a good model, the 3D grid zones and layering are designed to include important aspects of the field geology at the scale of the 3D grid cells (porosity and water saturation contrast among and within zones and model layers). It is important to honor these contrasts that control or influence fluid flow and hydrocarbon storage capacity within a reservoir in order to estimate probable hydrocarbon volumes, and ideally to obtain a geologically realistic and usable reservoir simulation history match. This match ultimately can be used to evaluate field development scenarios and related reservoir performance with confidence. Khasib Formation is one of the important reservoirs in Ahdeb oil field, and it will be the main subject in the recent study, in order to provide information of vertical and horizontal variations of petrophysical properties. The purpose of this research is to build a 3D petrophysical model for the Khasib Formation in the Ahdeb field using Petrel software. This model consists mainly of structure, stratigraphy and reservoir characteristics (porosity and water saturation) in three directions(X, Y and Z).

After Evaluating the petrophysical properties (porosity and water saturation) of Khasib formation using available logs data,A 3D petrophysical model has been built and distributes the petrophysical properties through spatial maps (top view) to illustrate the variation of these properties in Khasib formation and to predict the information that leads to developing the field and provide awareness of the hydrocarbons distribution in the reservoir to reach a complete evaluation.

MATERIALS AND METHODS

1. Gathering the available data for all studied wells (AD-A, AD-B, AD-C, AD-E, AD-F, AD-G, AD-H, AD-I, AD-J, AD-K and AD-L) in the Khasib Formation.
2. Well logs such as gamma ray, density, neutron, sonic and resistivity logs were digitized one per 0.25 meter depth using Didger software.
3. Interpretation of the well logs data, and calculating effective porosity using equation of Schlumberger (1998) (4) after total porosity (Øt) corrected from shale volume: **Øe = Øt * (1-Vsh)…… 1**
   And water saturation using Archie (1942)(5) equation: **$Sw = \{(a * Rw) / (Rt * \_m)\}^{1/n}$……..2**
   Where:
   Øe: effective porosity (PHIE), Øt: total porosity, Vsh: shale volume, Sw: water saturation
   Rw: resistivity of formation water, Rt: true resistivity, a,m,n: Archie parameters
4. Using petrel software for building 3D petrophysicalmodels, structured maps were constructed and the petrophysical properties (porosity and water saturation) were distributed throughout well correlation in Khasib formation.

Reservoir Zonation and Properties

Figure (2) shows the computer processes interpretation (CPI) of KhasibFormation in well AD-Awhichisdeduced using Techlog software. This figure shows the full reservoir properties and fluids analysis of Khasib Formation which has been deduced by interpretation of well logs. Khasib Formation in Ahdeb oil fieldis divided into reservoir units or zones. Based on porosity measured data and from log analysis of the Khasib Formation, the formation is classified into four units or zones (Kh-1,Kh-2,Kh-3 and Kh-4) from top to bottom.

Well Correlation

In this study, well correlation has been madewhich represents an easy method to illustrate the changes in the thickness within Khasib units and the variations of the petrophysical properties (Porosity and water saturation).The geological cross-sections NW-SE of Khasib Formation has been made in Ahdeb field as shown in figure (3)in contour map. The cross-section of Khasib Formation is explained the stretch formations from NW to SE and wells location.This section includes wells (AD-A,AD-J,AD-B,AD-H and AD-L) which located in the crest of three domes of Ahdeb field.The figure (4) of wells in correlation section illustrates the variation in reservoir properties (porosity, and water saturation) along reservoir units in Ahdeb field. These figures show nearly similarity in reservoir properties (porosity and water saturation) along reservoir units in Khasib Formation with improvement of the properties toward the southern dome. The zone (Kh-2) is the reservoir zone because it is characterized by high effective porosity and low water saturation when compare with other zones of Khasib formation in Ahdeb oil field.

Structural modeling

Khasib formation geometry is modeled as accurately as possible. Structural maps were built depending on the well tops for Ahdeb wells as well as the available structural map for top of Khasib Formation from 2D seismic. Model horizons are built from seidmic depth grids.The main input grids are tied to horizon depth makers at well locations.The Kh-1 depth surface is the principle input. Contour maps have been built to each zone of the formations under study. Four structural contour maps have been induced for Khasib Formation using petrel software, which represent the units top of Khasib (Kh-1), (Kh-2),(Kh-3) and (Kh-4) as shown in figure (5). These contour maps illustrate that the KhasibFormation in Ahdeb oil field is characterized by three narrow NW-SE trending low amplitude anticlines with three structural crests along its length which are referred to as AD-1, AD-2 and AD-4 separated by broad synclines.

Make Zones

Model zone is the next step in structural modeling that is built from input the structural horizons into the pillar grid. It is a step for building the vertical layering of the 3D grid in petrel.Figure (6) represents the zones of the main units of Khasib Formation.

Layering

Layers of cells are created within each model zone, initially in order to retain vertical geological heterogeneity observed at wells, and later as placeholder locations for geostatistical distributions of model cell properties. Each reservoir unit in Khasib Formation has been divided into many layers depending on petrophysical properties as shown in figure (7).Kh-1 unit is divided into 4 layers, Kh-2 unit has been divided into 20 layers, and Kh-3 unit has been divided into 10 layers, while Kh-4 is divided into 15 layers.

Scale up Well Log

The scale up well logs makes averages the values to the cells in the 3D grid that are penetrated by the wells. Each cell has one value per up scaled log. These cells are used as a beginning point for petrophysical modeling (Schlumberger, 2010) (6). In this model effective porosity (PHIE) and water saturation (Sw) has been scaled up using arithmetic average method.Figure (8) represents the scale up of PHIE and SW for KhasibFormation in well AD-C.

RESULTS AND DISCUSSION

Petrophysical modeling is the process of populating the active cells of the 3D grid with rock and fluid property values. Porosity and water saturation are modeled. Porosity is modeled stochastically using the Sequential Gaussian Simulation method to predict porosity in areas between wells and in areas outside of well control. The simulation method assumes that the data to be modeled would have a Gaussian distribution with an expected value of 0 and a standard deviation of 1. The input well data for the model are the well log curve values scaled up to average values for each cell that is penetrated by a well. These cell values are examined and transformed to remove any trends in the data and force it to fit a normal distribution. Water saturation for each reservoir zone is distributed throughout the model volume using the Sequential Gaussian Simulation method.From 3D property model for KhasibFormation in Ahdeb oil field whichincludes: porosity model and water saturation model, it can be describe the petrophysical properties distribution in each unit of Khasib Formation:

Kh-1 Unit

This unit represents the upper most units in the formation and the smallest unit in thickness, its range (6.4-8.3) m. the porosity in the top of unit is recorded low values then increased gradually towards bottom of unit which indicated that the unit represents cap rock for Khasib Formation. Effective porosity model as shown in figure (11) ranges (1-17%) with mean (10%) while water saturation model (fig.12) ranges (28.3-100%) with mean (56.5%).

Kh-2 Unit

The Kh-2 unit represents the highest thickness unit in Khasib Formation which ranging (38- 46.1) m. It is the most important reservoir unit in the formation because it is characterized by high porosity and low water saturation which is indicated that Kh-2 unit is the best oil production unit in Khasib Formation. This unit has effective porosity ranges (17-27%) with mean 22% as shown in figure (13) and water saturation model in figure (14). The areal variation of the petrophysical properties of this unit indicates that the porosity is relatively high near the southern dome (AD-1) proportion to other domes while oil saturation increases at crests of three Ahdeb anticlines which proportion with the decreasing in water saturation at same areas of field.

Kh-3 Unit

The thickness of unit is about (19.1-24.4) m.This unit is almost similar to the second unit (Kh-2) in porosity values it has high water saturation about (55.3-100 %) which indicates that unit is free of hydrocarbon. Porosity and water saturation models are illustrated by figures (15) and (16) respectively. Although porosity records high values and closed to homogeneous trend along this unit but the high water saturation that appears along three blocks of Ahdeb anticlines indicates that the unit is not oil production in Khasib Formation .

Kh-4 Unit

The thickness of unit ranges (34-41) m. The porosity in this unit is variable which ranges (0-22%) with poor mean (9%). while water saturation is also variable which ranging about (27-100 %) with mean (67.6%).Porosity and water saturation models of this unit are illustrated by figures (17) and (18) respectively.

CONCLUSIONS

A 3D petrophysical model for the Khasib formation in Ahdeb field has been built using Petrel Software; structural contour maps of the four units were created (Kh-1, Kh-2, Kh-3, Kh-4). Unit Kh-1 was divided into 4 layers, unit Kh-2 was divided into 20 layers because it represents the main reservoir in Khasib formation of Ahdeb oil field, unit Kh-3 was divided into 10 layers and unit Kh-4 was divided into 15 layers.Porosity distribution model was built for each unit in Khasib Formation: kh-1, kh-2, kh-3 and kh4. This model shows that unit kh-2 is the best unit then kh-3 but kh1 and kh4 are the bad units. Water saturation distribution model was built for each unit in khasib Formation. This model shows that Kh-2 unit is the best oil production unit in Khasib Formation.

REFERENCES

1. Al Waha Petroleum Company Limited, 2013.The Field Development Plan of Ahdeb Oil Field in Iraq.208p.
2. Jassim S. Z., and Goff J. C., 2006. Geology of Iraq .Dolin, Prague and Moravian Museum, Brno. 341p.
3. 3.VanBellen, R.C., Dunnington, H. V., Wetzel, R., and Norton, D.M., 1959. LexiqueStratigraphique International, Asie, vol.3, Fasc.10a, Iraq.Paris, 333pp.
4. 4.Schlumberger,1998. Cased Hole Log Interpretation Principles/Applications, Houston, Schlumberger Wireline and Testing,198p.
5. Archie G.E., 1942. The Electrical Resistivity Log as an Aid in Determining Some Reservoir Characteristics: AIME, Vol.146, p.54.
6. Schlumberger, 2010. Petrel introduction course.Schlumberger, 13-493p.

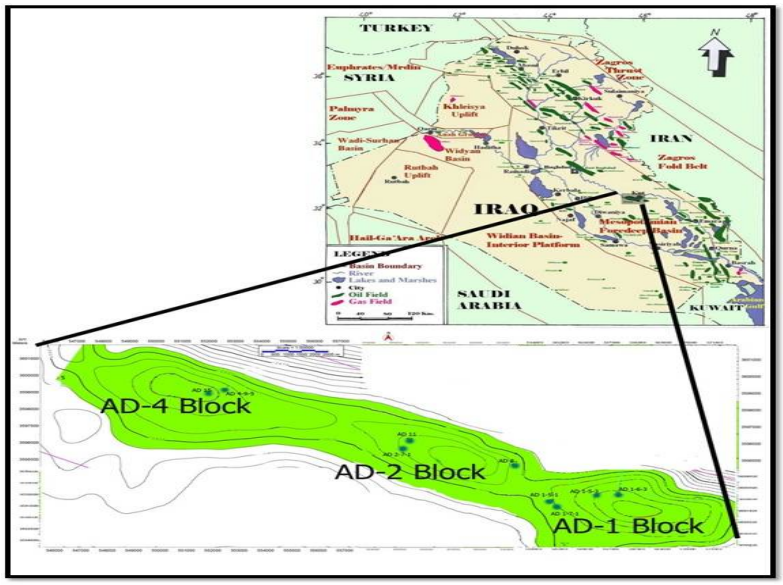

Figure 1.Location map of Ahdeb oil field.

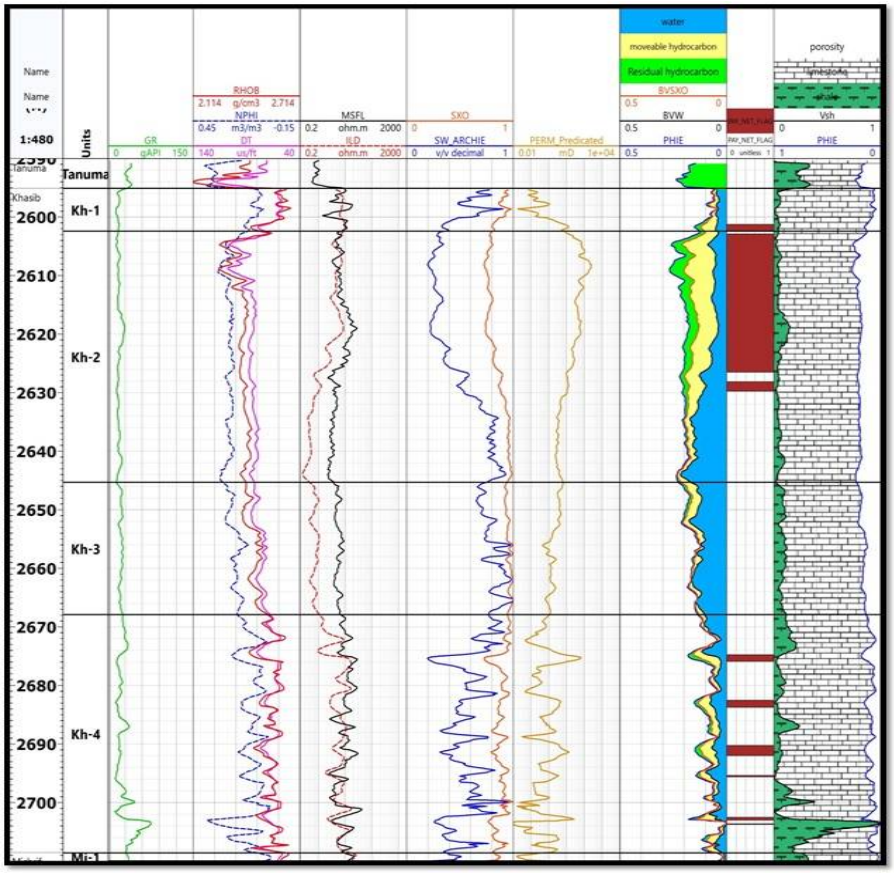

Figure2.Computer processes interpretation (CPI) of well AD-A

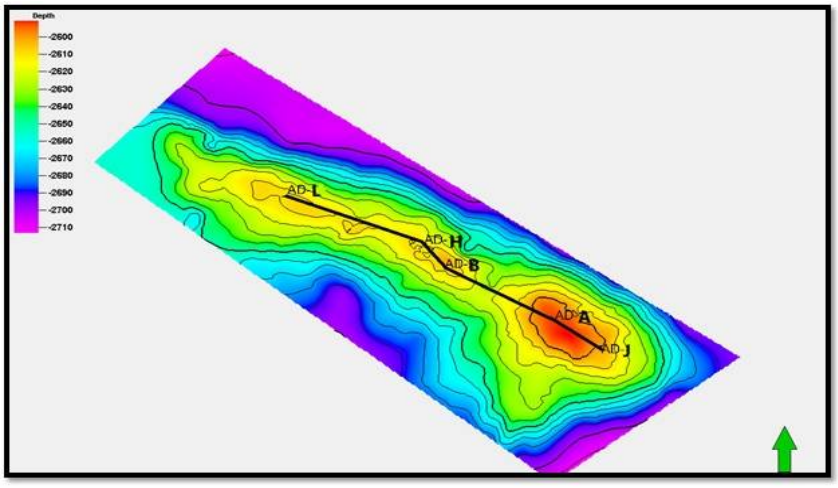

Figure 3.Distribution of correlation section for Ahdeb wells.

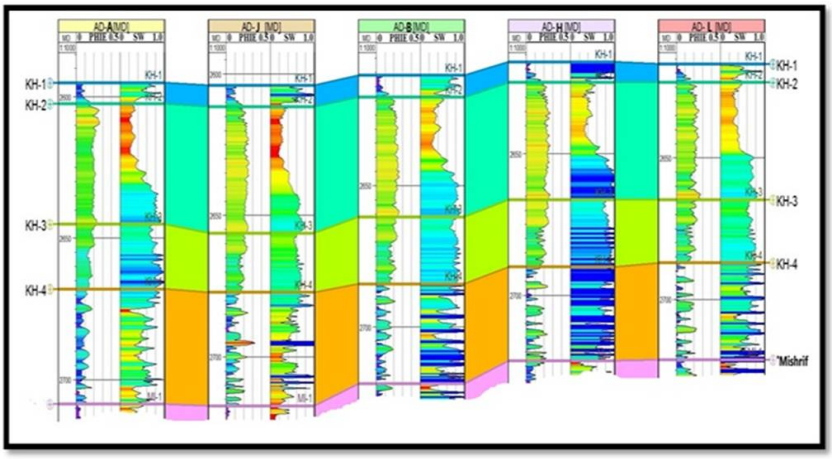

Figure 4.The correlation section of Khasib Formation in Ahdeb field.

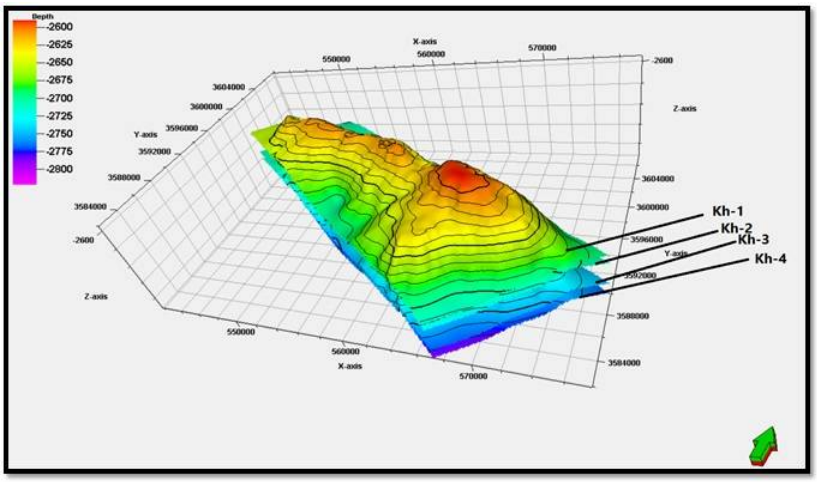

Figure 5.Structural model of Khasib Formation in Ahdeb oil field.

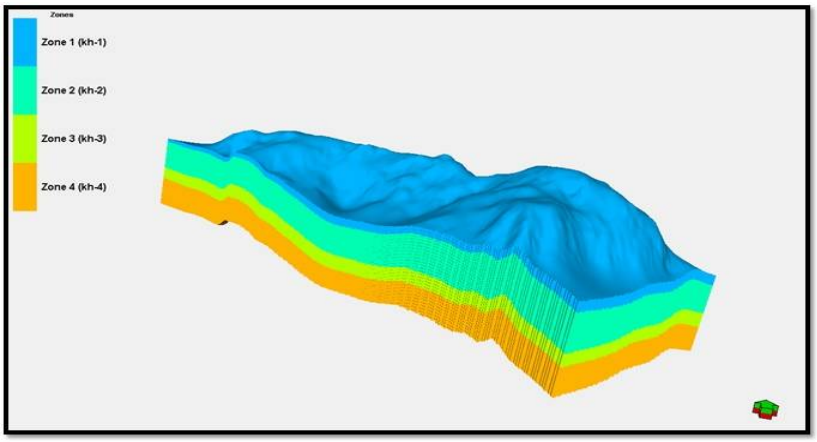

Figure 6.Zones of Khasib Formation in Ahdeb oil field.

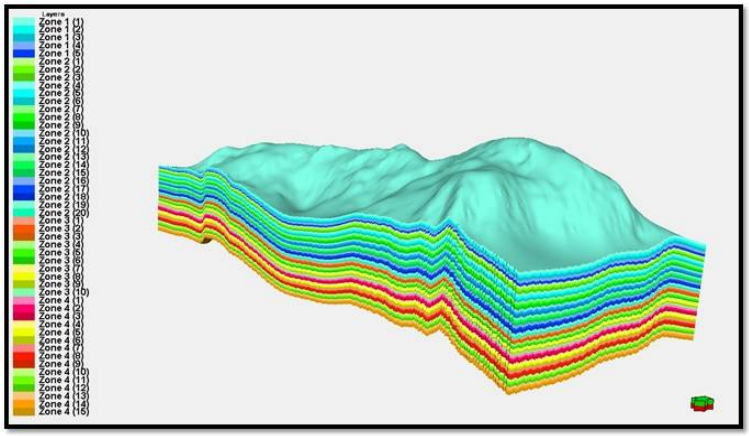

Figure 7.Layers of Khasib Formation in Ahdeb oil field.

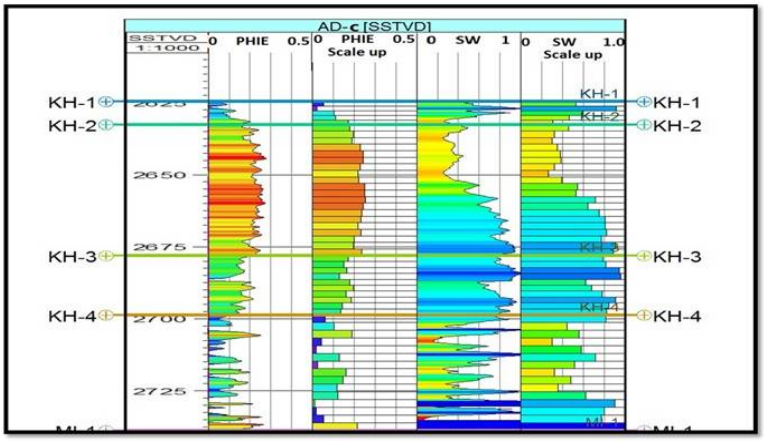

Figure 8.scale up of petrophysical properties of Khasib.

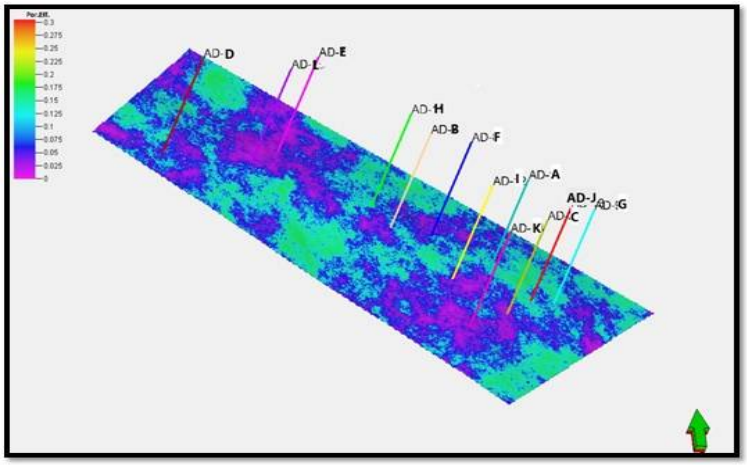

Figure 9.The porosity model of Kh-1 in Khasib formation.

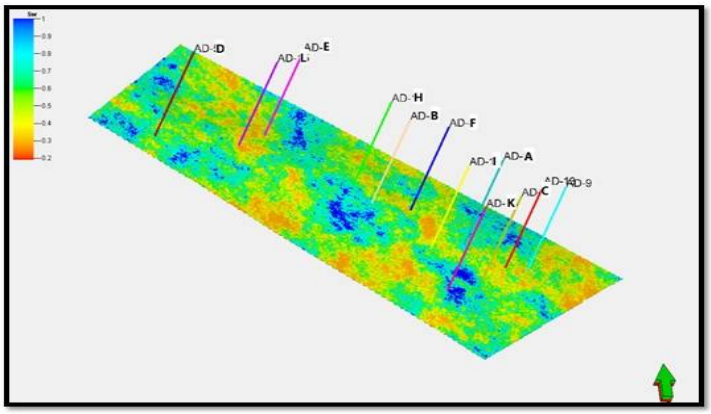

Figure 10.The water saturation model of Kh-1 in Khasib formation.

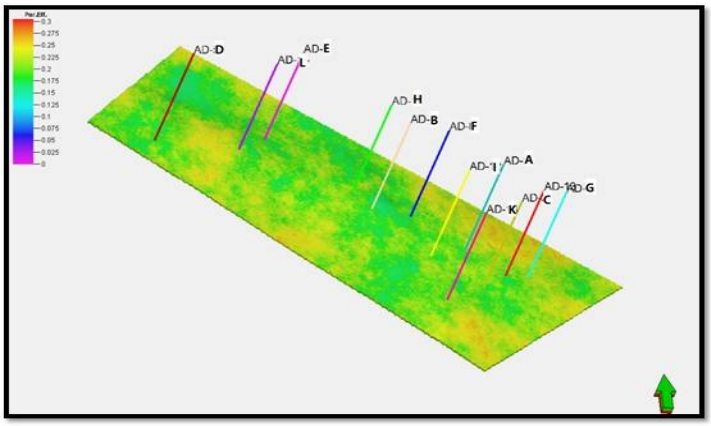

Figure 11.The porosity model of Kh-2 in Khasib formation.

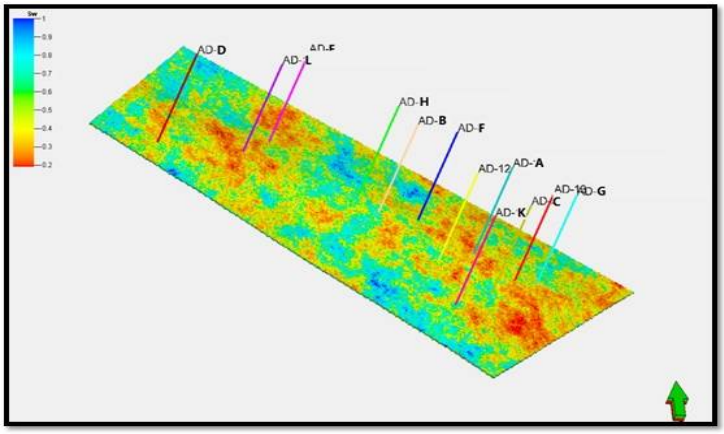

Figure 12.The water saturation model of Kh-2 in Khasib formation.

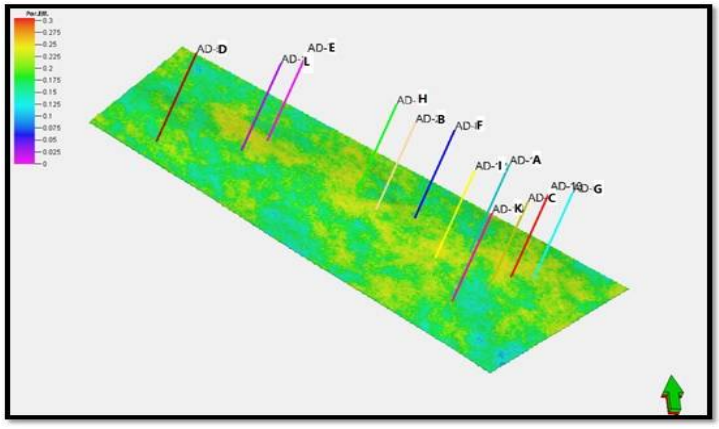

Figure 13.The porosity model of Kh-3 in Khasib formation.

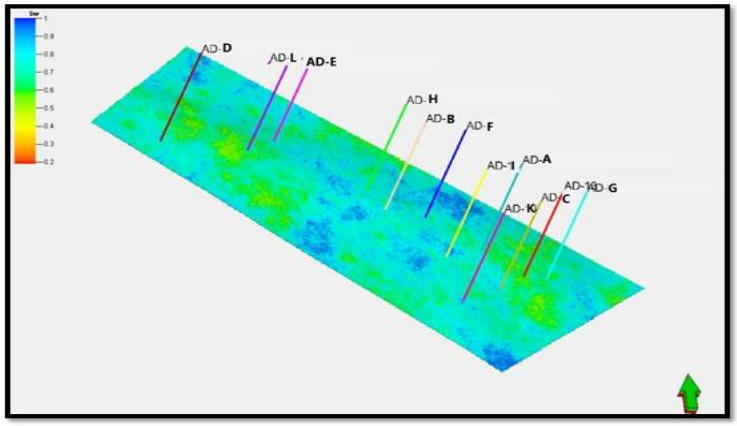

Figure 14.The water saturation model of Kh-3 in Khasib formation.

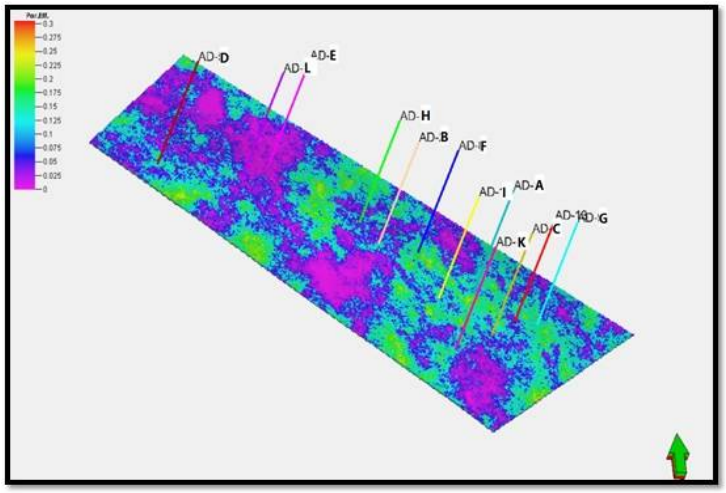

Figure 15.The porosity model of Kh-4 in Khasib formation.

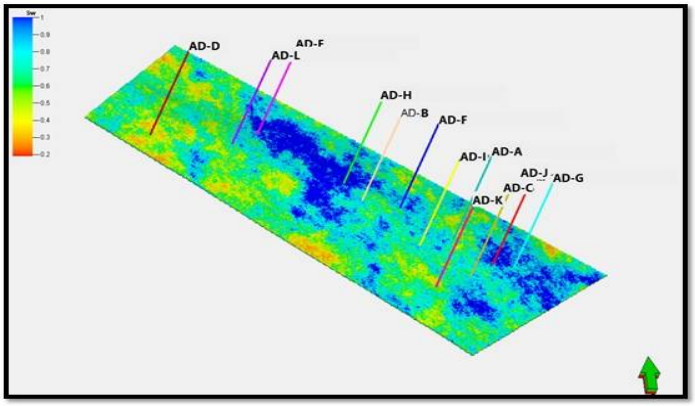

Figure 16.The water saturation model of Kh-4 in Khasib formation.

Indian Journal of Natural Sciences www.tnsroindia.org.in ©IJONS

Vol.9 /Issue 51 / December / 2018 *International Bimonthly* *ISSN: 0976 – 0997*

RESEARCH ARTICLE

Effect of Grain Size and Sintering Temperature on Dielectric Properties of Perovskite $Ba_{0.5}Sr_{0.5}TiO_3$

Hamed Alwan Gatea*and Iqbal S. Naji

Department of Physics, College of Science, University of Baghdad, Baghdad, Iraq.

Received: 08 Aug 2018 Revised: 12 Sep 2018 Accepted: 15 Oct 2018

***Address for Correspondence**
Hamed Alwan Gatea
Department of Physics,
College of Science,
University of Baghdad,
Baghdad, Iraq.
E-mail: hamedalwan14@gmail.com

ABSTRACT

Perovskite Barium Strontium Titanate ($Ba_{0.5}Sr_{0.5}TiO_3$) nanopowders were prepared by sol-gel method. The sol-gel method was employed to obtain fine powders of $Ba_{0.5}Sr_{0.5}TiO_3$ from raw materials Ba, $Sr(CH_3CHOO)_2$,Acetic Acid and Titanate (IV)isopropoxide. The sintering treatment was performed at diverse temperature for 3 hours. EDX, SEM, XRD methods were used for sample characterization. Particles size estimated by Scanning of morphology of sample (20 -100 nm) depend on sintering rise from (900, 1000,1100 ^{0}C). XRD shows peaks belong to cubic structure phase of $Ba_{0.5}Sr_{0.5}TiO_3$ and observed increasing density with a rise temperature due to completed crystalline of nanopowders . Free sintering temperature was used to get high densification of pellets which turn on influence on dielectric properties of BST. Dielectric constant (ε') and dielectric loss (ε") were measured in the temperature range (R.T to 250 ^{0}C) in the frequency range (1 KHz to 200 KHz). Dielectric constant decrease with increase frequency and Temperature.

Keywords : Ferroelectric materials, BST, sol-gel , Perovskite structure.

INTRODUCTION

Ferroelectric materials have shown great promise for different application as tunable device[1].In recent years, considerable interest has been evidenced in ferroelectric materials for different application such as non-volatile random access memories(NVFRAM), dynamic random access memories(DRAM), sensing , actuation , phase shifter, varactors and communication device[2]. From a crystallographic point of view the piezoelectric materials exhibit perovskite crystalline structure type of $ABO_X(ABO_3)$. Many piezoelectric (including ferroelectric) such BaTiO3, PbTiO3, PZT , PMN , KNBO3 and $K_xNa_{1-x}Bo_3$[3] ferroelectric materials is one of the most important issue to develop

next-generation dielectric devices and has become important in recent years with the utilization of nanostructured ferroelectric materials in various dielectric devices[4][5]. Barium Strontium Titanate (BST) ferroelectric continuous to attract broad research attention due to their potential for novel device applications[6].Barium Strontium Titanate (BST) continuous a new materials with attention due to tunable device applications[4]. BST, Ferroelectric materials can display paraelectric phase by controlling Ba/Sr ratio and perform a high transparency as an insulating layer of electroluminescent device[7] . Influence of particles size on the properties of nanostructured materials which turn on due to differing from that bulks attribute to large surface-to-volume ratios[8][9]. Crystal structure and dielectric properties of ferroelectric materials depend on the particles size at nanomaterials. . The final properties of a ferroelectric materials system is closely depend on the crystal structure of the system , therefore depend on the sintering condition(temperature , time) , grain size , porosity , polarization of the crystal cell[10].

Barium Strontium TItanate (BST) has been considered to be a leading candidate materials for new dielectric device by virtue of strong dielectric nonlinearity under bias electric field and linearly variable Curie temperature with the content of strontium[11]. Barium strontium titanate oxide is a perovskite type materials which is known for its various properties such as high dielectric [12]. BST sold solution nanocrystalline ($Ba_{0.5}Sr_{0.5}TiO_3$) with fine average particles have been synthesized and characterization through a simple sol-gel process[13]. Sol-Gel processing is rapidly evolving into versatile technique for preparation of powders. Barium Strontium Titanate (BST) is ceramic compound with the stoichiometric formula ($Ba_{1-x}Sr_xTiO_3$). It is a continuous solid solution containing $BaTiO_3$ and $SrTiO_3$ over the entire composition range[14]. BST is a material with a high degree of crystallinity ,high charge storage capacity, and low leakage current at Curie temperature .It has been widely intensively investigated ferroelectrics and has been widely studied not only because of its variety of out standing physical properties, but also for its practical application[15][16]. BST compounds prepared by sol gel method to obtain fine powder with control in particles size. The sol-gel technology has dramitically grown in last two decades. Concerning the microstructure , the sol gel method applies to nanomaterilas with potential use on practical applications[17]. The electrical properties of BST materials are closely linked to their microstructutral fratutre and fabrication process[18]. Shape of grians shape,particle size , domain size and atomic structure of grian boundaries play an important role and influence in crystal structure, which in turn affects the process of manufacturing technology[19][20].

MATERIALS AND METHODS

$Ba_{0.5}Sr_{0.5}TiO_3$ were prepared by sol gel method route using barium acetate $Ba(CH_3CHOO)_2$ (99.5% , BDH chemical-England) ,Srontium acetate $Sr(CH_3CHOO)_2$ (99% AIdrich) and Titanium isopropoxide $Ti[OCH(CH_3)_2]_4$ (purity 97% , AIrdich) as precursors. Barium and strontium acetates were codissolved in acetic acid. The soulation mixed and stirrreing at 60 ^{0}C 30 min the refluxed at 110 ^{0}C (2 hrs) . Titnate(IV) isopropxide with stabilizer 2-methoxy ethanole mixed at room temperture. Tow solution mixed and refluxed again 2 hours at 110 ^{0}C till get thich white gel . The gel dryimg at 200 ^{0}C and grind then calcinide at 700 ^{0}C to obtain fine powders (20-30 nm). Crystal structure of $Ba_{0.5}Sr_{0.5}TiO_3$ powders were determined by X-ray diffraction (XRD) using a CuK_α radiation (λ=1.54095 Å, 30 Kv, 30 m A) medel (Bruker, Germany) in a wide range of 2Θ=0-80^0) at scanning rate 1 min^{-1}. Microstructure of powders and ceramics was characterized using a field emission scanning electron microscope (SEM) (Hatachi 4700) . For dielectric measurements, the powders were compressed into discs of about (12mm) as diameter and sintering at 1000 ^{0}C for 3 hours . The dielectric properties were measured by LCR meter, in the temperature and frequency [R.T to 250 ^{0}C, 1 KHz to 200 KHz), respectively.

RESULTS

Energy Dispersive X-Ray Analysis (EDX), referred to as EDS or EDAX, is an x-ray technique used to identify the elemental composition of materials. EDX systems are attachments to Electron Microscopy instruments (Scanning Electron Microscopy (SEM) instruments where the imaging capability of the microscope identifies the specimen of

interest. The data generated by EDX analysis consist of spectra showing peaks corresponding to the elements making up the true composition of the sample being analyzed. Elemental mapping of a sample and image analysis are also possible. Figure (1) shows the EDX spectra of $Ba_{0.5}Sr_{0.5}TiO_3$ which sintered at (900, 1000, 1100 ^{0}C) for 3 h . It is clear that the elements Ba, Sr, Ti and O was detected in all spectra, and there is no other elemets which means that the pure BST phase was dominant phase, and no impurties were existed . The composition ratios (Ba/Sr) of the as-prepared powders were confirmed using the microarea EDS analysis. Stoichiometric ratios of the main metallic compounds of BST are shown in table (1) as mass or atomic percentage. It is clear the degree of sintering temperature (1000 ^{0}C) best of all ratios.

Fig. 3. Shows the surface morphologies of the BST powders sintered at (900,1000, 1100 ^{o}C) for 3h The particles are a mixture of spherical and nearly cubic in nature for a& b and less agglomerated specially for c &d . It shows SEM micrograph of the surface morphologies of the $Ba_{0.5}Sr_{0.5}TiO_3$ powders calcined at 700 ^{0}C and sintered at (900, 1000, 1100 ^{o}C) for 3 hrs . It is seen that sintering temperature has obvious effect on the grain size, which indicates that the grain size increases with the rise of sintering temperature. The synthesis parameters such as initial concentration and reaction time (stirrer and reflux time) have a great influence on the size of nanostructure of $Ba_{0.5}Sr_{0.5}TiO_3$. By controlling on these parameters the particles size change to be (22, 43.23, 65.80, 97.42 nm) corresponding to temperatures rise (700 ^{0}C,900 C,1000 ^{0}C , 1100 ^{0}C), respectively. It is clear that the particles size of BST increasing with increased sintering temperature due to change densification and reduced porosity . This result agree with the results of S. Hu *et al* (1) , and Yanling et.al (2).

XRD is the most useful technique to determine the crystal structure, orientation, inter-planar distance, and the crystalline size. The structure of $Ba_{0.5}Sr_{0.5}TiO_3$ powders with different x values which had been produced by sol-gel method are shown in fig. 3. This figure reveled that all samples are polycrystalline in nature. The XRD pattern of $Ba_{0.5}Sr_{0.5}TiO_3$ shows the presence of a number of peaks along the (100), (110), (111), (200), (210), (211), (220) and (221). These peaks are in good agreement with the cubic BST phase (PDF card no.01-039-1395) with cubic phase, space group SPGR Pm-3m (221) and lattice parameter 3.947 Å. Also, there are two weak diffraction peaks as a secondary phase besides the peaks of BST phase, which appeared at (2θ=24.21,26.8^0) and (28.8^0) belong to intermediate oxycarbonates such as $Ba_2Ti_2O_5CO_3$, and (Ba, Sr)$Ti_2O_5CO_3$, respectively [2,3,22,23]. The most probable crystalline impurity are Sr_2TiO_4, $SrTiO_{10}$, $Sr_3Ti_2O_7$ almost appear at 44.6^o [2,24], It is clear that the Intensity of peaks has been increased with increasing sintering temperature that is explained effect of sintering temperature on crystalline completed which turn on disappeared intermediate phases. It is found that the diffraction peaks of $Ba_{0.5}Sr_{0.5}TiO_3$ shift to higher angle with the rise of sintering temperature. This shifted indicates the interatomic space of the BST decrease with the increase of sintering temperature which affected by increased particles size.

Fig.4 shows the graph between dielectric via log frequency constant and dielectric loss .The dielectric constant and dielectric loss factor of BST depended on the physical properties and the fabrication process of BST compounds. The effect of degree crystallization on dielectric properties , there was an increase in dielectric constant with increasing sintering temperature due to better crystallinity and increase in grain size with a rise sintering temperature.The variation in the value of the dielectric constant has been carried out at diverse temperature (1000. 1100 ^{0}C) attributed to the grain size, crystallinity, and porosity of BST compound. At lower sintering temperature poor crystallinity and smaller grain size of the samples induced the dielectric constant (ε) reduction.The frequency dependence of dielectric properties in $Ba_{0.5}Sr_{0.5}TiO_3$ sintering at various sintering temperature , illustrated that the dielectric constant of $Ba_{0.5}Sr_{0.5}TiO3$ sintering at (1000, 1100 ^{0}C) decrease as frequency increase attributed to different types of polarization mechanisms. Space charge polarization and dipole polarization gradually cannot catch up with change of electric field as frequency increases, which make dielectric constant decrease.

As frequency increase , the dissipation factor of $Ba_{0.5}Sr_{0.5}TiO_3$ sintering at (1000,1100 ^{0}C) decreases continuously , and dissipation factor of samples sintering at 1100 ^{0}C greater than samples sintering at 1000 ^{0}C which means hat behavior belong to increase sintering temperature increases the vibration of crystal atoms around its equilibrium position , since resistive loss component of dissipation factor is directly proportional to leakage current so the energy is dissipated such as heat. Fig. 5 illustrated the dielectric properties were studied as function of temperature and different frequency (1 KHz, 20 KHz , 100 KHz) , the real part of the permittivity ε) and dissipation loss factor (tanδ) for $Ba_{0.5}Sr_{0.5}TiO_3$. The dielectric constant decreasing with increased temperature and dissipation factor increase. Some parameters lead to this phenomenon, the increase of the sintering temperature leads to a higher order structure crystalline. $Ba_{0.5}Sr_{0.5}TiO3$ is cubic structure then Curie Temperature may be zero or less than . Above transition temperature, the decrease in the dielectric constant is due to increase of thermal oscillation of the molecules &increase of degree of disorder of dipoles[25].

CONCLUSION

The $Ba_{0.5}Sr_{0.5}TiO_3$ sample has been successfully synthesized by sol-gel method. BST powders synthesized from barium acetate, strontium acetate and Titanate isopropoxide with a solvent such as acetic acid and 2-methoxy Ethanol. EDX spectra of as-prepare $Ba_{0.5}Sr_{0.5}TiO_3$ nanoparticles contains Ba, Sr, Ti and O species. . FESEM investigation showed that the nanoparticles obtained at (700,900, 1000, 1100 ^{0}C) were (22,43,65,97 nm), respectively depend on the sintering temperature. XRD result exhibited all samples belong to cubic perovskite structure with space group (Pm3m). Inter-planer space decreased with increased sintering temperature with attribute to increasing grain size. Dielectric constant and dielectric loss increased with increased sintering temperature.

ACKNOWLEDGEMENTS

Conflict of interest: The authors declare no competing financial interest.

REFERENCES

1. B. Su, J. E. Holmes, C. Meggs, and T. W. Button, “Dielectric and microwave properties of barium strontium titanate (BST) thick films on alumina substrates,” *J. Eur. Ceram. Soc.*, vol. 23, no. 14, pp. 2699–2703, 2003.
2. J. A. V. F.M. Pontesa, E. LONGO . E.R. Leite, “Study of the dielectric and ferroelectric properties of chemically processed Ba x Sr1xTiO3 thin films.pdf,” *Thin Solid Film. 386*, vol. 386, pp. 91–98, 2000.
3. J. N. M.-M. Chilibon, Irinela, “Ferroelectric cermics by sol-gel methods and application : a reviw,” *J. Sol-Gel Sci Technol*, vol. 64, pp. 571–611, 2012.
4. T. Hoshina, “Size effect of barium titanate: fine particles and ceramics,” *J. Ceram. Soc. Japan*, vol. 121, no. 2, 2013.
5. H. T. Martirena and J. C. Burfoot, “Grain-size effects on properties of some ferroelectric ceramics,” *J. Phys. C Solid State Phys.*, vol. 7, no. 17, pp. 3182–3192, 1974.
6. J. Xu, J. Zhai, and X. Yao, “Electrical and Infrared Optical Properties of $Ba_{0.70}Sr_{0.30}TiO_3$ Thin Films Prepared by a Sol-Gel Process,” *Ferroelectrics*, vol. 357, no. 1, pp. 148–153, 2007.
7. T. Zhang, H. Gu, and J. Liu, “Structural and optical properties of BST thin films prepared by the sol-gel process,” *Microelectron. Eng.*, vol. 66, no. 1–4, pp. 860–864, 2003.
8. J. Q. Qi, Y. Wang, W. Ping Chen, L. Tu Li, and H. Lai Wah Chan, “Direct large-scale synthesis of perovskite barium strontium titanate nano-particles from solutions,” *J. Solid State Chem.*, vol. 178, no. 1, pp. 279–284, 2005.
9. Z. Lazarevi, N. Rom?evi, and B. D. Stojanovi, “Synthesis and characterization of barium strontium titanate powder,” *J. Optoelectron. Adv. Mater.*, vol. 10, no. 10, pp. 385–388, 2008.
10. J. M. Siqueiros, J. Portelles, S. GarcÃ-a, M. Xiao, and S. Aguilera, “Study by hysteresis measurements of the influence of grain size on the dielectric properties of ceramics of the $Sr_{0.4}Ba_{0.60}TiO_3$ type prepared under different sintering conditions,” *Solid State Commun.*, vol. 112, no. 4, pp. 189–194, 1999.

11. V. Somani and S. J. Kalita, "Synthesis and characterization of nanocrystalline Barium Strontium Titanate powder via sol-gel processing," *j. Electroceram*, pp. 57–65, 2007.
12. J. D. La Fuente, J. Santiago, A. Román, C. Dumitrache, and D. Casasanto, *Handbook of dielectric, piezoelectric and ferroelectric materials Synthesis, properties and applications*, vol. 25, no. 9. 2014.
13. C. Shen, Q. F. Liu, and Q. Liu, "Sol-gel synthesis and spark plasma sintering of Ba0.5Sr 0.5TiO3," *Mater. Lett.*, vol. 58, no. 17–18, pp. 2302–2305, 2004.
14. M. E. Azim Araghi, N. Shaban, and M. Bahar, "Synthesis and characterization of nanocrystalline barium strontium titanate powder by a modified sol-gel processing," *Mater. Sci.*, vol. 34, no. 1, pp. 63–68, 2016.
15. A. Selmi, O. Khaldi, M. Mascot, F. Jomni, and J. C. Carru, "Dielectric relaxations in Ba0.85Sr0.15TiO3 thin films deposited on Pt/Ti/SiO2/Si substrates by sol–gel method," *J. Mater. Sci. Mater. Electron.*, vol. 27, no. 11, pp. 11299–11307, 2016.
16. J. Zhao, X. Wang, R. Chen, and L. Li, "Synthesis of thin films of barium titanate and barium strontium titanate nanotubes on titanium substrates," *Mater. Lett.*, vol. 59, no. 18, pp. 2329–2332, 2005.
17. I. Chilibon and J. Marat-Mendes, "Ferroelectric ceramics by sol–gel methods and applications: a review," *Journal of Sol-Gel Science and Technology*, vol. 64, no. 3. pp. 571–611, 2012.
18. J. . J.Moon, J. A. Kerchner, H. Krarp, "Particleshape control and formation mechanisms of hydrothemal derived lead titnate," *J. Mater. Res.*, vol. 14, pp. 866–875, 1999.
19. Mazon, T. M.A. Zaghate, J.A Verela, E. Longo, "Barium strontium titante nanocrystalline thin films perpared by soft chemical method," *Int. J. Nano Dimens.*, vol. 2, pp. 85–103, 2011.
20. T. Naoto Koshizaki, Aiko Narazki, "preparation of nanocrystalline titante films by pulse laser depostion at room temperture," *Appl. Surf . Sci.*, vol. 197, pp. 624–627, 2002.
21. S. Hu *et al.*, "Effect of sintered temperature on structural and piezoelectric properties of barium titanate ceramic prepared by nano-scale precursors," *J. Mater. Sci. Mater. Electron.*, vol. 28, no. 13, pp. 9322–9327, 2017.
22. U. Gleissner *et al.*, "Lowering the sintering temperature of barium strontium titanate bulk ceramics by bariumstrontium titanate-gel and BaCu(B2O5)," *Ceram. - Silikaty*, vol. 60, no. 1, pp. 1–11, 2016.
23. M. C. Gust, L. A. Momoda, N. D. Evans, and M. L. Mecartney, "Crystallization of Sol–Gel-Derived Barium Strontium Titanate Thin Films," *J. Am. Ceram. Soc.*, vol. 84, no. 5, pp. 1087–1092, 2001.
24. U. Adem, "Preparation of BaxSr1-xTiO3 Thin Films by Chemical Solution Deposition and Their Electrical Characterization," *Prep. BST thin Film*, no. December, p. 96, 2003.
25. T. L. L. H. A.El ghandouri , S. Sayouri, "Effect of strontium on the structural and piezoelectric properties of the sol gel processed barium titnate," *j.Mater. Env. .Sci*, vol. 8, no. s, pp. 4945–4962, 2017.

Table 1. The Calculated and experimental values of the element content in $Ba_{0.5}Sr_{0.5}TiO_3$ compounds.

x	Elements	Line	Theo.values W%	Exp.values W%	Theo.Values A%	Exp. Values A%
X= 0.5 900 ^{0}C	O	K_a	23.04	28.53	60.00	68.68
	Ti	K_a	22.98	18.05	20.00	14.52
	Sr	L_a	21.03	11.41	10.00	5.02
	Ba	L_a	32.96	42.01	10.00	11.78
X= 0.5 1000 ^{0}C	O	K_a	23.04	26.56	60.00	64.56
	Ti	K_a	22.98	21.60	20.00	17.56
	Sr	L_a	21.03	19.19	10.00	8.53
	Ba	L_a	32.96	32.64	10.00	9.26
X= 0.5 1100 ^{0}C	O	K_a	23.04	26.05	60.00	63.65
	Ti	K_a	22.98	30.16	20.00	21.61
	Sr	L_a	21.03	13.16	10.00	6.90
	Ba	L_a	32.96	30.64	10.00	9.26

Table 2. Structural parameters viz. 2θ values, inter-planar spacing, miller indices,and phase of $Ba_{0.5}Sr_{0.5}TiO_3$ powders.

2 Theta 700 ⁰C	2 Theta 900 0C	2 Theta 1000 0C	2 Theta 1100 0C	d-theo. Theortical	d-Exp. 700 ⁰C	d-Exp 900 ⁰C	d-Exp 1000 ⁰C	d-Exp 1100 ⁰C	hkl
22.4267	22.8516	23.1551	23.3011	3.9660	3.961167	3.888465	3.83818	3.881677	(100)
32.017	32.4419	32.7049	32.8835	2.8060	2.793169	2.75755	2.735973	2.72152	(110)
39.2401	39.7661	39.9482	40.191	2.2900	2.294053	2.264913	2,255007	2.241943	(111)
45.3966	46.3822	46.6654	46.7261	1.9823	1.996223	1.956073	1.94486	1.942475	(200)
51.6427	52.1687	52.3913	52.5931	1.773500	1.613725	1.768501	1.74498	1.588471	(210)
57.024	57.5101	57.7327	58.016	1.61950	1.393786	1.393786	1.59559	1.377327	(211)
67.1006	67.54	67.9097	68.0109	1.4023	1.316798	1.313116	1.23618	1.313759	(220)

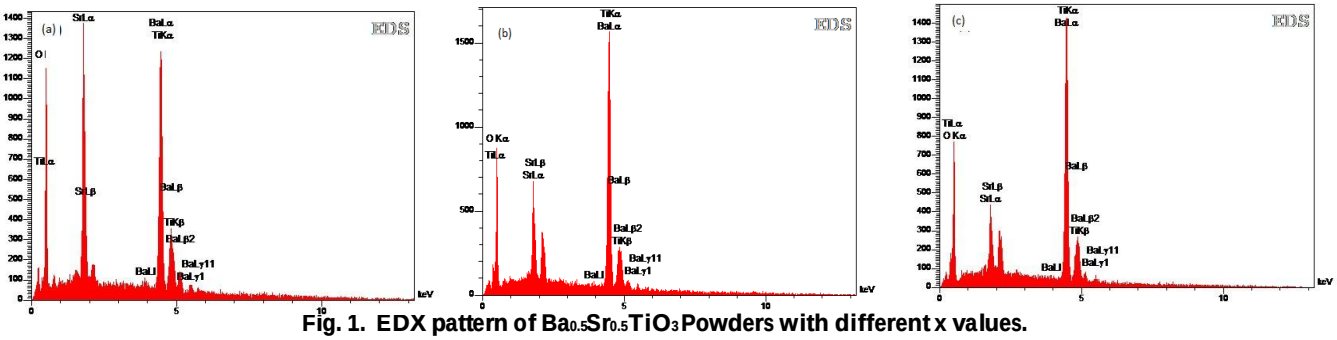

Fig. 1. EDX pattern of $Ba_{0.5}Sr_{0.5}TiO_3$ Powders with different x values.
(a) x=0.5(900 ⁰C) (b)= x=0.5 (1000 ⁰C) (c)= x=0.5(1100)

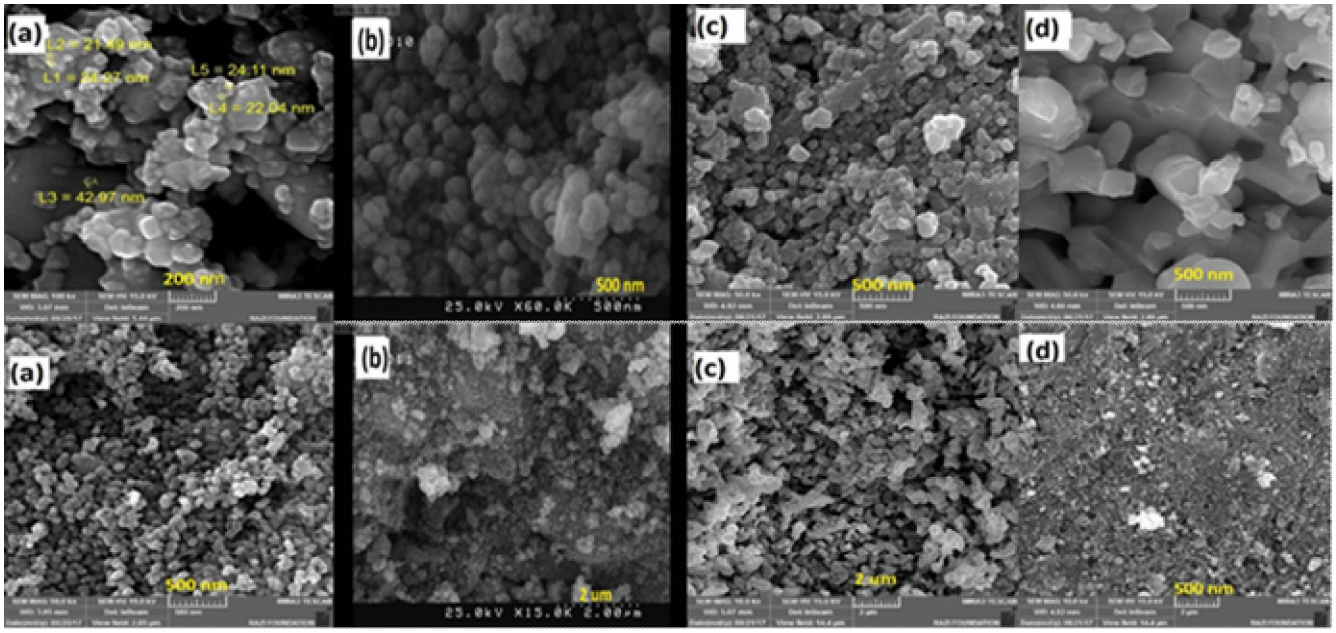

Fig. 2. Field emission scanning electron microscopy (FESEM) images for $Ba_{0.5}Sr_{0.5}TiO_3$
(a) 700 ⁰C (b) 900 ⁰C (c) 1000 ⁰C (d) 1100 ⁰C

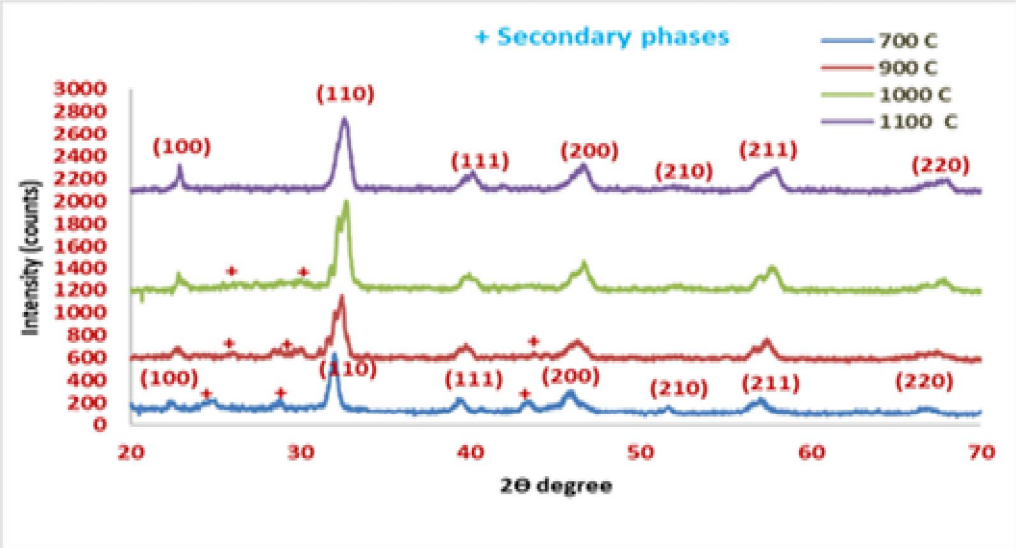

Fig. 3. XRD patterns of $Ba_{0.5}Sr_{0.5}TiO_3$ powders with various Sintering Temperature

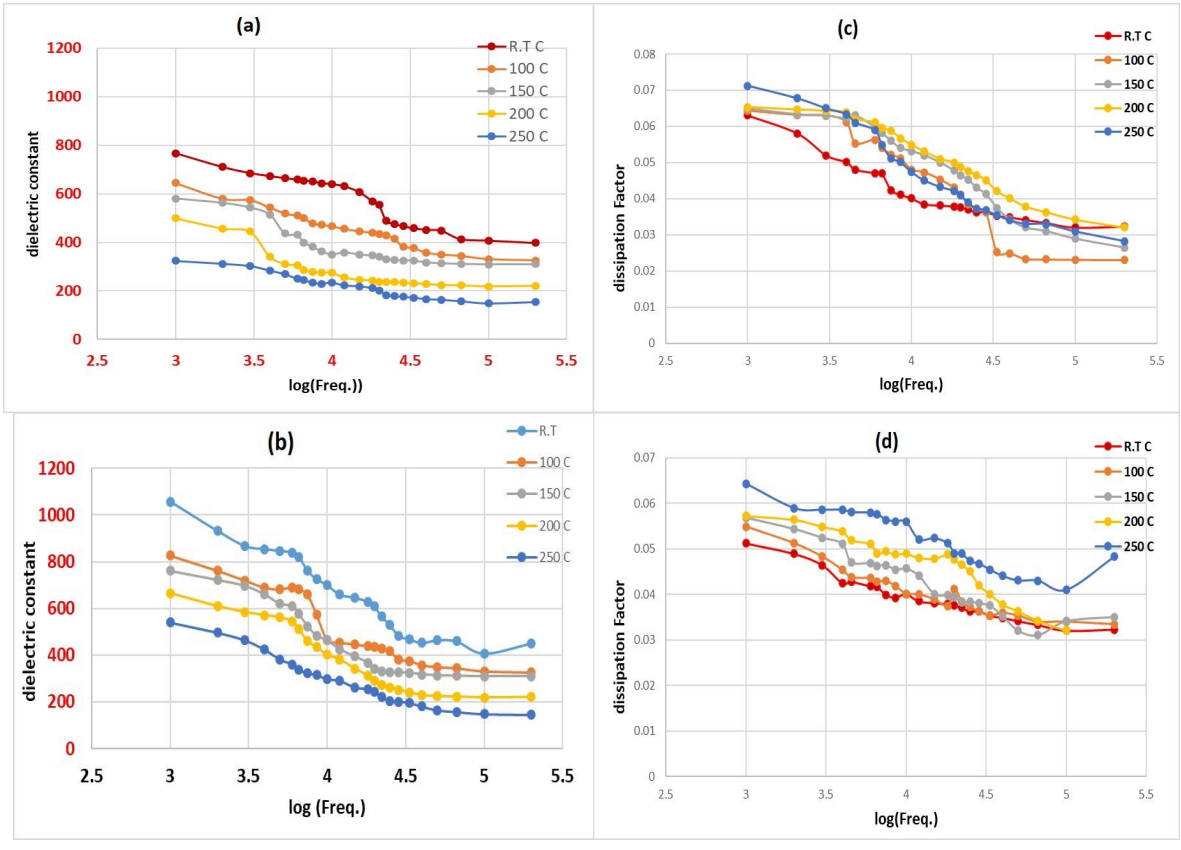

Fig. 4 Frequency dependence of dielectric properties[dielectric constant(a&b), (c,d) dissipation loss factor) for $Ba_{0.5}Sr_{0.5}TiO_3$ at different sintering temperature.

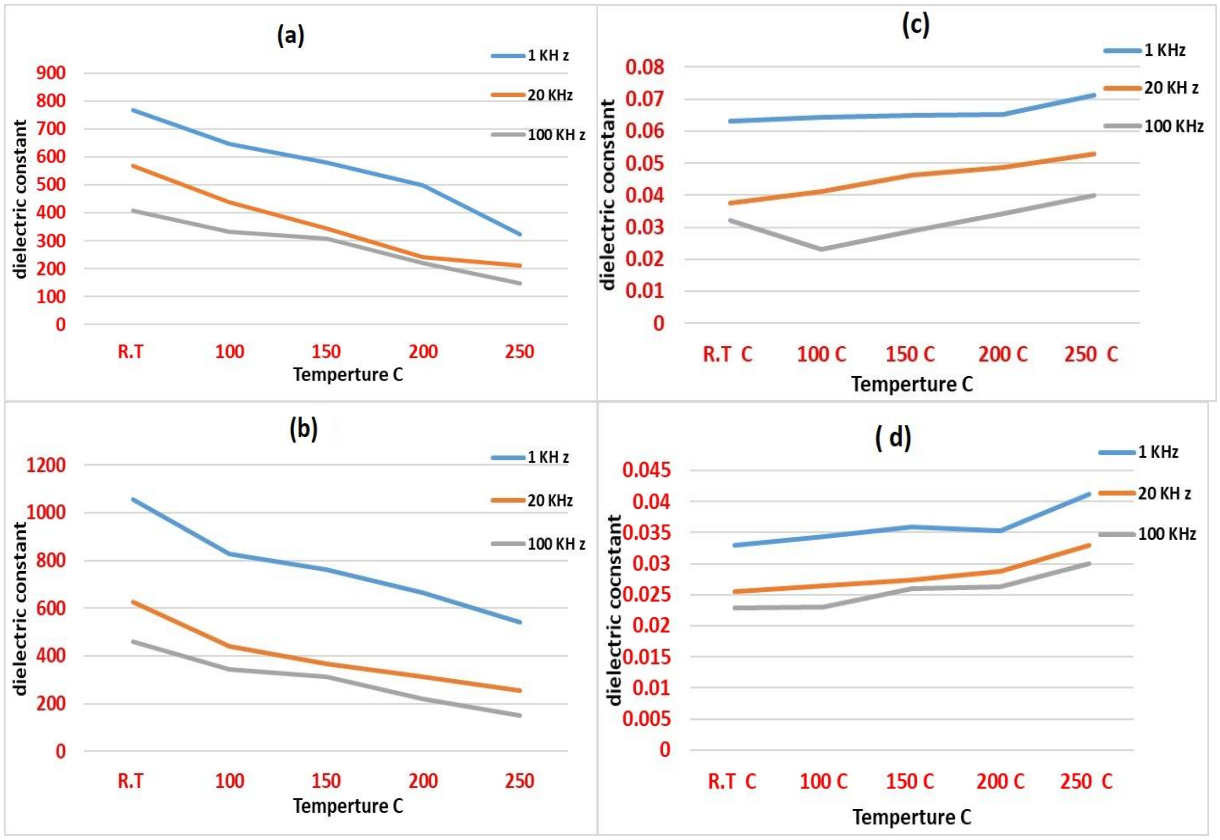

Figure 5. Temperature dependence of the dielectric constant (a&b) and dielectric loss(c&d) for $Ba_{0.5}Sr_{0.5}TiO_3$ with sintering at 1000 , 11000 ^{0}C.

Indian Journal of Natural Sciences www.tnsroindia.org.in ©IJONS

Vol.9 /Issue 51 / December / 2018 *International Bimonthly* *ISSN: 0976 – 0997*

RESEARCH ARTICLE

Phytochemical Screening, Chemical Composition and Antibacterial Activity of Lemongrass (*Cymbopogon citratus*) Leaves Extracts

Amer H.H. Alzobaay* and Baidaa H. Kadhim

Department of Food Sciences, College of Agricultural Engineering Sciences, University of Baghdad, Iraq.

Received: 07 Aug 2018 Revised: 10 Sep 2018 Accepted: 14 Oct 2018

***Address for Correspondence**
Amer H.H. Alzobaay
Department of Food Sciences,
College of Agricultural Engineering Sciences,
University of Baghdad,
Baghdad, Iraq.
Email: ameralzobaay@yahoo.com

ABSTRACT

Lemongrass (*Cymbopogon citrates*) plant leaves contained appreciable amounts of phytochemicals (alkaloids, glucosides, phenols, saponins, flavonoids, tannins, terpenoids and resins), absence of steroids. Chemicals contents of Lemongrass leaves (Moisture, ash, fat, fiber, protein and carbohydrate) were (71.3, 2.41, 0.76, 11.89, 7.21and 6.43) % respectively. Lemongrass leaves were extracted by water, ethanol and hexane extraction. Antibacterial activity of Lemongrass leaves extracts were tested by agar well diffusion against gram positive bacteria (*Bacillus cereus, Staphylococcus aureus and Micrococcus spp.*) and gram negative bacteria (*Pseudomonas spp. ,Escherichia coli and Salmonella typhimurium*). Aqueous extracts exhibited the best activity against tested microorganisms then ethanolic and hexane extracts.The highest inhibition zone of aqueous extract against *Satphylococcus aureus* was (28 mm), while the lowest against *Pseudomonas spp.* was (19mm). Ethanolic extract of *C.citratus* registered (20mm) of inhibition zone against *Satphylococcus aureus* while the lowest was (15mm) against *Salmonella typhimurium*. Where *Micrococcus sp.* and *Satphylococcus aureus* scored (22mm) were more sensitive while *Salmonella typhimurium* rigesered (14mm) was highly resistant to hexane extract .The minimum inhibitory concentration (MIC) of extracts were ranged from (<10 to >80) mg/ml, while the minimum bactericidal concentration (MBC) ranged from (<30 to <100) mg/ml.

Key words: lemongrass, phytochemicals, Antibacterial, leaves extracts, MIC, MBC.

INTRODUCTION

Medicinal plants had a great importance to the individuals health, the medicinal value of plants lies in their containment some chemical substances, the most important of these bioactive constituents of plants include are

alkaloids, tannins, flavonoids and phenolic compounds among other [1], there were about 250,000 species of plants on earth, a relatively small percentage (1 to 10%) of these were used as foods by both human and other animal species [2].

Lemongrass (*Cymbopogon citratus*) an aromatic herb, known in the North and West tropical Africa, in Arabian Peninsula and in Egypt, it was a native of (Southwest Asia) South India but present, in many part of the world were growing in dense clumps In the folk medicine of Brazil and Mexico [3].*C. citrates* staff were popularly known as citronella grass or lemongrass, this species belongs to the *Gramineae* family, which comprises approximately 500 genus and 8,000 herb species, the leaf-blade is linear, tapered at both ends and can grow to a length of 50 cm and width of 1.5 cm [4]. The plant also contained flavonoids which were phenolic compounds that serve as flavoring ingredients of plant leaves, higher contents of tannins, flavonoids and phenolics were observed than alkaloids, saponins and glycosides in lemongrass (*C.citratus*), Isoorientin, Caffeic acid, Quercetin and Chlorogenic acid [5]. lemongrass was found in folk remedy for coughs, consumption, elephantiasis, malaria, ophthalmia, pneumonia and vascular disorders, researchers have found that lemongrass holds antidepressant, antioxidant, antiseptic, astringent, bactericidal, fungicidal, nervine and sedative properties[6]. *C. citrates* had antibacterial, antifungal, antitumoral, and anticancer and insecticide activities, the antimicrobial activity of lemongrass against a series of microorganisms was due to the abundance of citral and essential oil components Geranial, Myrcene, this led to suggestion that *C. citratus* may have antimicrobial activities against *Bacillus cereus, Escherichia coli O157:H7, Klebsiella pneumonia, Staphylococcu aureus and Candida albicans* [7]. The aim of study to examine the phytochemical screening, chemical composition of *C.citratus* leaves and extraction of *C.citratus* (water, ethanol and hexane), antibacterial activities of extracts tested bacteria and studding Minimum Inhibitory Concentration (MIC) and Minimum Bactericidal Concentration (MBC) of extracts.

MATERIALS AND METHODS

Collection and Preparation of Plant Materials

Fresh leaves of C.*citrates* were collected from Agricultural Research office\Department of plant protection and confirmed the diagnosis in the national herb\seed Inspection and certification Department\ministry of Agriculture\ Iraq, leaves were washed under running tap water to remove the surface pollutants, plant leaves were dried in shade at room temperature for 5-7 days, the samples were grinded in an electric mill, the powdered samples obtained was kept in an airtight container before use [8].

Phytochemical screening of *C. citratus* leaves

Qualitative phytochemical analysis of *C.citratus* leaves was carried out according to method was mentioned Shihata (1951) in [11], for PH, detection Soponins, tannins, flavaniods, glycosids and Resins.

pH

Mix 10 g of *C.citratus* leaves powdered with 50 ml distilled water, let in a magnetic mixer for 10 minutes, the mixture was filtered and the pH was measured using a device pH-meter.

Saponins

Add 2ml of the aqueous extract of *C.citratus* and shaken vigorously with 2 ml distilled water in a test tube, the emergence of bubbles of the solution indicated the presence of saponins.

Tannins

5g of *C.citratus* leaves powder was boiled in 50 ml of water and filtered, the infusion was divided into 2 test tubes A and B.Test tube A: (a few drops of 0.1% ferric chloride was added and observed blue green coloration),Test tube B: (5 g of *C.citratus* leaves powder was taken and 0.5 ml of 1% lead acetate solution was added and the formation of precipitate indicates bleaching white the presence of tannins.

Flavaniods

Solution A: dissolve 10 g of *C.citratus* leaves powder with 5ml of 95% ethanol.

Solution B: mix equal sizes of 50% ethanol and 50% Potassium hydroxide. Mix Slo. A with Sol. B, appearance of yellow color precipitate indicates the presence of flavonoids.

Glycosides

Attended the detector according to the method mentioned in[10],Fehling's A:(Copper sulfate solution, dissolve 34.66 g of $CuSO_4 \cdot 5H_2O$ in 500 ml distilled water), Fehling's B: (Alkaline tartrate solution, dissolve 173 g of potassium sodium tartrate (Rochelle salt, $KNaC_4H_4O_6 \cdot 4H_2O$) and 52g of NaOH in 500 ml distilled water) . Two equal parts of A and B Fehling reagent were combined with the water extract of the lemongrass leaves and left in a boiling water for 10 minutes, positive test was indicated with the appearance of a red deposit.

Resins

5 g of lemongrass leaves powder was added to 50 ml of 95% ethanol and left for 2 minutes in 100 ml boiling water, serve the solution and add 100 ml distilled water with 4% hydrochloric acid, the presence resin was evidenced by emergence of turbidity.

Phenols

Followed the method mentioned [12] which mixing 3 ml of lemongrass leaves with 2 ml of 1% ferric chloride, appearance of bluish green color indicated the presence of phenols.

Alkaloids

Boiled 10 g of *C.citratus* leaves powder with 50 ml of 4% hydrochloric acid, applied the solution after cooling, mix 0.5 ml of solute with Wagner's test: (Attend the detector according to the way he mentioned [9] dissolved 2 g of potassium iodide in 5 m of distilled water and add 1.27g iodine and complete the size to 1000 ml), The appearance of a brown deposit indicated the presence of alkaloids [13].

Terpenoids and Steroids

Steroids and terpenoids were tested according the method in [14]: 1ml of *C.citratus* leaves aqueous extract with (1 ml of chloroform, 2–3 ml of acetic anhydride and 1 to 2 drops of concentrated sulfuric acid), dark brown coloration of the solution indicated the presence of terpenoids, and dark blue color indicated the presence of steroids.

Chemical components of *C.citratus* leaves powder

According to the standard methods mentioned in [15], moisture, protein fat/oil, ash and fiber).And total carbohydrates content was calculated by difference
% carbohydrate = 100_ (% moisture + % fibre + % ash+ % fat + % protein).

Extraction of Lemongrass Leaves

Aqueous Extraction

Aqueous extraction was done according the method by [16] with slight modifications, as followed: added 100 g of *C.citratus* leaves powder to 1000 ml of distilled water and shaking for 8 h at 40° C , filtered with paper filter Whatman No.1, collected the extract and poured in Petri dishes in electric oven at 40° C until dried , obtained and stored in refrigerator until use.

Ethanolic and Oily Extraction

C.citratus leaves powder was extracted by ethanol, hexane followed by method of [17]: 10 g of *C.citratus* leaves powder was placed in continuous Soxhlet , added 350 ml of 99% ethanol, 350 ml of 98% hexane at 40 ° C for Ethanolic , Oily Extracts respectively, the extraction process continued for 8 hours, solvent evaporated using rotary evaporator under vacuum at 40 °C and kept in sealed containers and away from light until use.

Bacterial preparation

Gram positive bacteria *(Staphylocuccus aureus, Bacillus cereus* and *Micrococcus spp.),* and gram negative bacteria (*Escherichia coli, Salmonella typhimurium* and *Pseudomonas spp.)* were obtained from Faculty of Agricultural Engineering \ University of Basra \ Iraq. Bacterial isolated have been activated by Nutrient Broth (NB) at 37° C for 24 h, and compared with 0.5 McFarland solutions to yield 10^7 colony foring unit (cfu)/ml [7].Determination of Antibactericidal efficacy of *C.citratus* leaves extraction (aqueous, ethanolic and oily), and Minimum Inhibitory Concentration (MIC) & Minimum Bactericidal Concentration (MBC). Antibacterial activity of *C.citratus* leaves powder extracts (aqueous, ethanolic and oily), MIC and MBC were tested with Mueller Hinton Agar (MH-A) according the method by [18].

RESULTS AND DISCUSSION

Phytochemical constituents of *C.citratus* leaves

Photochemical results of *C.citratus* leaves powder showed presence of saponins , phenols , resins, alkaloids, tannins, flavonoids, glycosides, terpenes and lack of steroids as presented in Table 1.[19] pointed to contain *C.citratus* leaves powder in phenols, flavaniods, saponins, alkaloids, glycosides and terpenoids. [20] confirmed to presence saponans, flavonoids and phenols in aqueous extract . Lemongrass leaves did not contain steroids this is a result agreed with [21], pPlants and their natural constituents were subject to variations due to differences in their locations and climatic condition of where they thrive [2]. pH was 5.4.

Chemical Compounds of *C.citratus*

Figure1 showed the proximate analysis of *C. citratus* leaves powder revealed which moisture, protein, fats, ash, fibre and carbohydrates , (71.3, 7.21,0.76, 2.41,11.89 and 6.43%) respectively, moisture, protein, ash and fibre were similar

to those reported for [19], the results do not agree with what [22] and fat content observed for *C citratus* leaves was similar to those mentioned for [23] and less than scored in [5] , [24] Carbohydrates (6.43%) obtained approach to what found in [25].Differences between proportions of components may be due to differences in plant varies according to the geographical origin, genetic differences, age/stage of maturity, season of harvest, part of the plant used and method of extraction [26].

Antimicrobial Activity of *C.citratus*

Figures 2, 3, 4 showed the antibacterial activity of lemongrass (*C.citratus*) leaves extracts against tested bacteria by agar well-diffusion method, aqueous leaves extract recorded better antibacterial activity when compared with ethanolic and oily leaves extracts, the highest zone of inhibition against *Satphylococcus aureus* was (28 mm) of aqueous extract while the lowest against *Pseudomonas spp.* was (19 mm), [27] pointed aqueous extract performed better than the metabolic extracts against microorganisms.Aqueous leaves extract was found effective against gram positive as compared to gram negative bacteria, differences in sensitivity between Gram-positive and Gram-negative bacteria of the extracts could probably attributed to structural and compositional differences in membranes between the two groups, gram negative bacteria had an outer membrane that serves as an impermeable barrier for many small molecules similar results were obtained by [16].Antibacterial activity of lemongrass ethanolic extract the highest inhibition zone of *Satphylococcus aureus* was (20 mm), while lowest *Pseudomonas spp., Salmonella typhimurium* were (15mm) Similar results were obtained by [28] who stated ethanolic extract of *C.citratus* showed significantly stronger antimicrobial properties against *Satphylococcus aureus* and *Bacillus cereus* while [29] recorded antimicrobial activity of *Enicostemmahyssop folium* ethanolic extract against *Escherichia coli, Staphylococci, Pseudomonas aeruginosa, Enterococcus* and *Candida albicans*. While *Micrococcus spp.* and *Satphylococcus aureus* were more sensitive to hexane extract, *Salmonella typhimurium* was highly resistant oily extract. Also [30] reported lemongrass hexane extract had antimicrobial activity against both bacteria and fungi using the disc diffusion method. [31] Pointed plants essential oils and aqueous or ethanolic extracts were more effective against microorganisms.

Minimum Inhibitory Concentration (MIC) and Minimum Bactericidal Concentration (MBC) of *C.citratus* aqueous, ethologic and hexane extracts. MIC defined as the minimum concentration of the antimicrobial needed to inhibit at least 99% of visible growth of the microorganisms, whereas MBC was minimum of the antimicrobials needed to kill at least 99% of growth [7]. Determination of MIC was important to confirm the resistance of the microorganisms to antimicrobial agents. Figures 5, 6, 7 showed the MIC, MBC values of *C.citratus* leaves extracts against tested bacteria. Aqueous extract of *C.citratus* showed least MIC value registered 20 mg/ml against *Satphylococcus aureu*s, MBC was 30 mg\ml, while the highest MIC value was 50 mg\ml against *E.coli*, and MBC was 60 mg\ml. similar results had been p reported by [6] lemongrass oil was effective against gram positive as compared gram negative bacteria. MIC of the ethanolic extract of *C.citratus* leaves ranged from 50- 90 mg/mL while MBC 60-100 mg\ml. MIC values of ethanolic reached (50 and 100) mg/ml for *Staphylococcus aureus* and *Salmonella typhi* respectively [8]. [32] Referred to *Musa sapientum, Cymbopogon citratus* and *Curcuma longa* aqueous and ethanolic extracts against *Stapyhlococcus aureus Salmonella paratyphi, Shigella flexnerii, Escherichia coli , Klebsiella pneumoniae, Bacillus subtilis and Pseudomonas aeruginosa* which MIC ranged from 4 – 512 mg/ml MBC ranged from 32 – 512 mg/ml depending on isolates and extracting solvent. [33] Noted the activity of lemongrass oil against the fungi had MIC values ranging from 15 to 118 mg/ml , While The MIC of the hexane extract of *C.citratus* ranged from 60-90 mg/ml while the MBC of the hexane extract ranged from 70- 100 mg\ml. [34] Pointed MIC, MBC values of lemongrass methanolic extract against *Escherichia coli* (ATCC:25922) ranging from 100-200 mg\ml. Differences in MIC, MBC of plants extracts demonstrated in several investigations may be due to considerable variation in their method of extraction, constituents as well as bacterial strains used [35].

CONCLUSION

Lemongrass (*Cymbopogon citratus*) leaves possess phytochemical constituents which play role in multi healthy benefits, in other way could extraction in watery, ethanol and hexane. All extracts possess antibacterial activities against undesirable bacteria.

ACKNOWLEDGEMENTS

I am very grateful to my food microbiology team for their help in patients and accuracy , thanks for all technical's and emotional support.

REFERENCES

1. Uraku , A .J ., Okaka ,A .N.C ., Ogbanshi ,M.E and Onuoha ,S.C. Nutritive and anti - nutritive potentials of *Cymbopogon citratus* leaves, American Journal of Food and Nutrition,(2016); 6(1):14-22.
2. Ojo, O. O., & Anibijuwon, I. I. Studies on extracts of three medicinal plants of south-western Nigeria: *Hoslundiaopposita, Lantana camara* and *Cymbopogon citratus*. Advances in Natural and Applied Sciences. (2010); 4(1), 93-99.
3. Uraku, A.J. Determination of Chemical Compositions of *Cymbopogon citratus* leaves by Gas Chromatography-Mass Spectrometry (GC-MS) Method, Research Journal of Phytochemistry ,(2015) ;9 (4): 175-187.
4. Manvitha, K. & Bidya, .B. Review on pharmacological activity of *Cymbopogon citratus,* International Journal of Herbal Medicine,(2014) ;1(6): 5-7.
5. Uraku, A. J., Onuoh, S.C., Edwin, N., Ezeani, N., Ogbanshi, M.E., Ezeali, C., Nwali , B.U & Ominyi, M.C. Nutritional and Anti-Nutritional Quantification Assessment of *Cymbopogon citratus* Leaf . Pharmacology & Pharmacy (2015); 6: 401- 410.
6. Naik, M. I., Fomda, B. A., Jaykumar, E & Bhat, J.A. Antibacterial activity of lemongrass (*Cymbopogon citratus*) oil against some selected pathogenic bacteria. Asian Pacific Journal of Tropical Medicine,(2010); 535-538.
7. Zulfa, Z., Chia, C.T. & Rukayadi, Y.In vitro antimicrobial activity of *Cymbopogon citratus* (lemongrass) extracts against selected foodborne pathogens. International Food Research Journal (2016), 23(3): 1262-1267.
8. Umar, M., Mohammed, I. B., Oko, .J.O., Tafinta, .I. Y., Aliko, A. A. & Jobbi, .D.Y. Photochemical Analysis and Antimicrobial Effect of Lemongrass (*Cymbopogon citratus)* Obtained from Zaria, Kaduna State, Nigeria. Journal of Complementary and Alternative Medical Research (2016);1(2): 1-8.
9. Smolensk, S.J., Silnis, I. I., & Farnsworth, N.R. Alkaloid screening, Part I. Lioydia, (1972); 35(1): 31-34.
10. Fehling, H. Die quantitative Bestimmung von Zucker and Stakmehl mittelst Kufervitriol . Annalen der Chemie and Pharmacie, (1949) ;72(1):106-113.
11. Abdalla, A. E. M., Darwish, S. M. ,Ayade, E. & EL-Hamahmy, R. M. Egy- Ption mango by-product 2: Antioxidant and antimicrobial activites of extract and oil from Mango Seed Kernel, Food Chemistry,(2007); 103: 1141-1152.
12. Harborne, J. B. Photochemical Methods, A Guide to Modern Techniques of Plant Analysis , Chapman and Hall , London , New York(1973) .
13. Fahmy, I. R. Constituents of Plant Crude Drugs , 1 Barby, Cairo (1993).
14. AL-Bid, M. R. Zurrzusamme Mseturumgder Absehle β membrane in *phoenix dactylifera* ,Wuzzburg university , Wazzburg F.R of Germany(1985).
15. A.O.A.C .Association of Official Analytical Chemists. Official Methods of Analysis 16th ed. Association of Official Analytical Chemists International Arligton, Virginia, U.S.A (2008).
16. Balakrishnan, B., Paramasivam, S. & Arulkumar, A. Evaluation of the lemongrass plant *(Cymbopogon citratus)* extracted in different solvents for antioxidant and antibacterial activity against human pathogens. Asian Pac J . (2014); (4):134-139.

17. Al-obaidy, S. M. R. & Radam, .O. N. The effect of Water and alcohol extract of *Cymbopogon citratus* on blood Glucose level and Some Biochemical parameters in normal and experimental Diabetic Male Rat .(2004).
18. Ewansiha, J .U. ,Garba, S. A. ., Mawak, J. D . & Oyewole, O. A. Antimicrobial Activity of *Cymhopogon citratus*(Lemongrass) and It's Phytochemical Propertie, Frontiers in Science,(2012); 2(6): 214-220.
19. Thorat, P. P., Sawate, A. R., Patil, B. M. & Kshirsagar, R. B. Proximate and phytonutrient content of *Cymbopogon citratus*(Lemongrass) leaf extract and preparation of herbal cookies, International Journal of Chemical Studies, (2017):5(6): 758-762.
20. Arekemase, M.O., Gambari-Ambali, R.O., Lawal, A.K., Ahmed, T., Orogu, J.O. & Aliyu, M. B. Studies on the Antibacterial Effects of Leaf Exracts of Lemongrass (*Cymbopogon citratus*) on Some Selected Microorganisms obtained from the University of Ilorin Teaching Hospital (UITH).International Journal of Phytofuels and Allied Sciences. (2015); 4(1): 92 91-110.
21. Soares, M.O., Alves, R.C., Pires, P.C., Oliveira, M.B.P.P & Vinha, A.F. Angolan *Cymbopogon citratus* used for therapeutic benefits: Nutritional composition and influence of solvents in phytochemicals content and antioxidant activity of leaf extracts. Food and Chemical Toxicology (2013); (60): 413–418.
22. Mohamed, Y. N. F., Hakimah, O., Hendrik, S. C. M. & Abdul Rahman, R.. Preparation and Characterization of Active Sio2 from *Cymbopogon citratus* Ash Calcined at Different Temperature. Bio Resources,(2016); 11(1): 2839-2849.
23. Akande, I. S., Samuel, T. A., Agbazue, U. & Olowolagba, B. L. Comparative proximate analysis of Ethanolic and Water extracts of *Cymbopogon citratus* (lemongrass) and four tea brands. Journal of Plant Sciences Reaserch.(2011),3(4): 29-35.
24. Assous, M. T. M., El-Waseif, K. H. M. & Gado, G. B. A. "Production and evaluation of non-traditional products from lemon grass." Egyptian Journal Agricultural Research. 2013; 91(1): 271-283.
25. Asaolu, M. F., Oyeymi, O.A. & Olanlokun, J. O. Chemical compositions, Phytochemical Constitiuents and in vitio Biological Activity of Various Extracts of *Cymbopogon citratus*. Pakistan Journal of Nutrition. (2009); 8(12): 1920 – 1922.
26. Ekpenyong, C. E., Akpan, E. E., & Daniel, N. E. Phytochemical Constituents, Therapeutic Applications and Toxicological Profile of *Cymbopogon citrates* Stapf (DC) Leaf Extract. Journal of Pharmacognosy and Phytochemistry, (2014); 3(1): 133-141.
27. Emmanuel F., D., David ,O. M., Emmanuel,A. I., & Oyedele, O. Chemical composition and antibacterial activities of some selected traditional medicinal plants used in the treatment of gastrointestinal infections in Nigeria. International Journal of Pharmaceutical Sciences Review and Research,(2010); 5(3):192-197.
28. Danlami, U., Rebecca, A., Machan, D.B & Asuquo,T.S . Comparative study on the Antimicrobial activities of the Ethanolic extracts of Lemon grass and Polyalthia Longifolia . Journal of Applied Pharmaceutical Science (2011); 1(09):174-176.
29. Mathur, R. Phytochemical and antimicrobial evaluation of plant extracts of Enicostemmahyssopifolium. Journal of Pharmacognosy and Phytochemistry, (2013); 2(4):30-36.
30. Hamza, I,S., Ahmed, S. H & Aoda, H. Study the antimicrobial activity f Lemongrass leaf extracts. iraq journal of market research and consumer protection,(2009);1(2):198-212.
31. Mourad, M.H., Salih, S.A., Elaasser, M. M., Safwat, N.A. & Ibrahim, M.Y. Antibacterial activity of certain medicinal plant and Their Essential oils on the Isolated Bacteria from Uti patients. International Journal of Advanced Research, (2016);4(12): 1510-1530.
32. Fagbemi, J. F., Ugoji, E., Adenipekun, T., & Adelowotan, O. Evaluation of the antimicrobial properties of unripe banana (*Musa sapientum* L.), lemongrass (*Cymbopogon citratus* S.) and turmeric (*Curcuma longa* L.) on pathogens. African Journal of Biotechnology (2009); 8 (7): 1176-1182.
33. Matasyoh, J. C., Wagara, I. N., & Nakavuma, J. L. Chemical composition of Cymbopogon citratus essential oil and its effect on mycotoxigenic *Aspergillus* species. African Journal of Food Science, (2011); 5(3), 138-142.
34. Jafari, B., Ebadi, A., Aghdam, B. M., & Hassanzade, Z. Antibacterial activities of lemongrass methanol extract and essence on pathogenic bacteria. American-Eurasian Journal Agric Environ Sciences,(2012);12 (8):1042-1046.

35. Mostafa, A. A., Al-Askar, A. A., Almaary, K. S., Dawoud, T. M., Sholkamy, E. N., & Bakri, M. M. Antimicrobial activity of some plant extracts against bacterial strains causing food poisoning diseases. Saudi Journal of Biological Sciences,(2018) 25(2), 361-366.

Table-1:- Phytochemical constituents of *C.citratus* leaves

Phytochemicals	*C.citratus* leaves
Saponins	+
Tannins	+
Flavonoids	+
Glycosides	+
Resins	+
Phenols	+
Alkaloids	+
Terpenes	+
steroids	-
pH	5.4

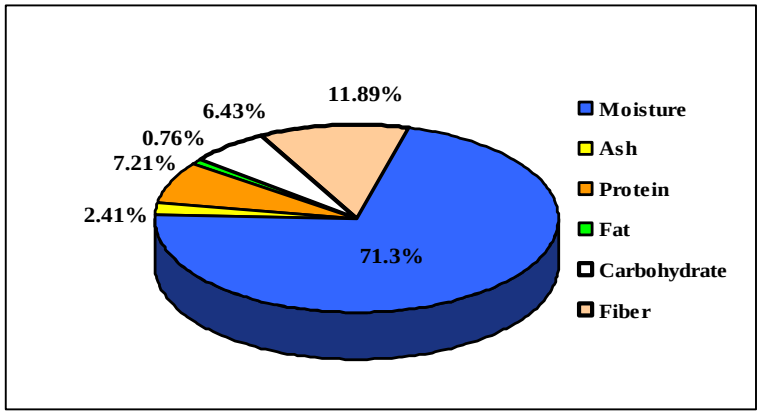

Figure- 1: - Proximate composition of *C.citratus* leaves

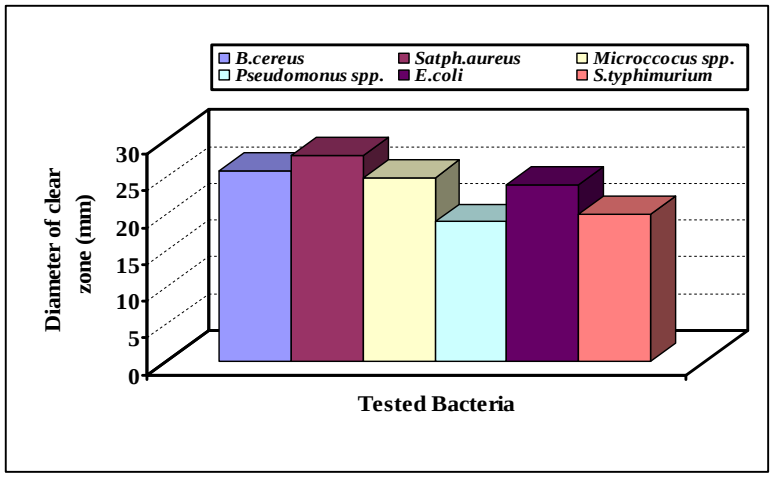

Figure- 2: - Antibacterial activity of *C.citratus* leaves aqueous extract against tested bacteria (mm)

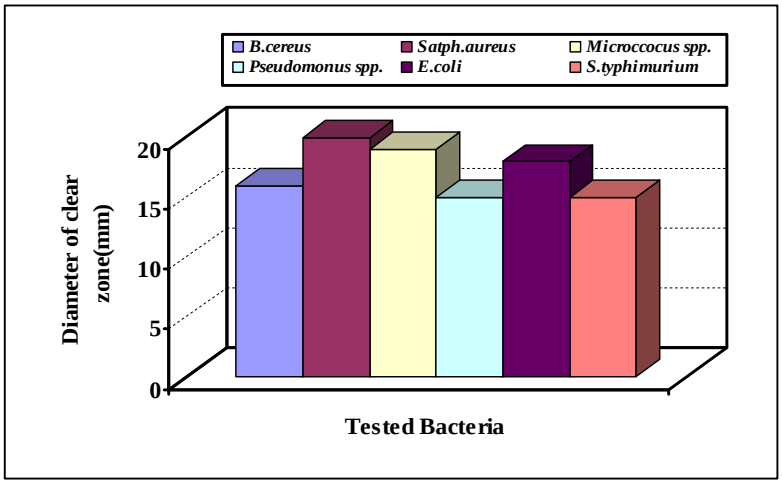

Figure- 3: - Antibacterial activity of *C.citratus* leaves ethanolic extract against tested bacteria (mm)

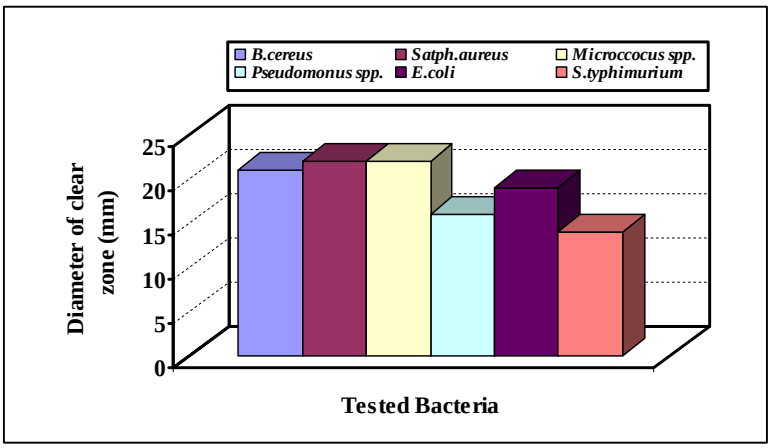

Figure- 4: - Antibacterial activity of *C.citratus* leaves oily extract against tested bacteria (mm)

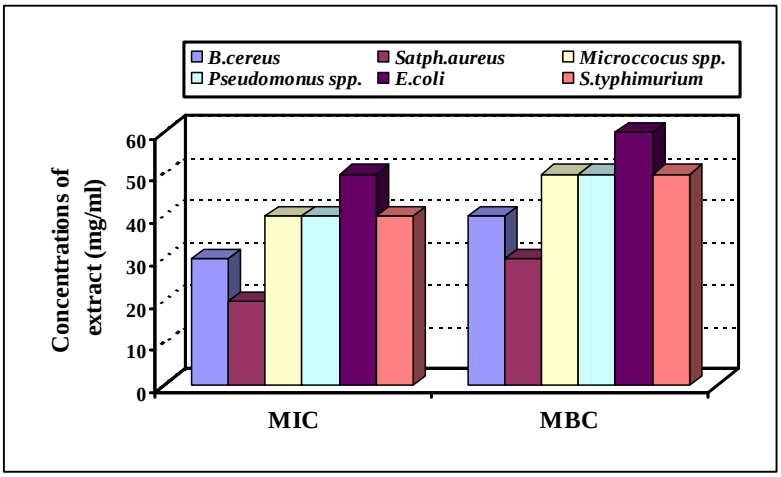

Figure- 5: -MIC and MBC (mg/ml) of *C. citratus* leaves aqueous extract against tested bacteria

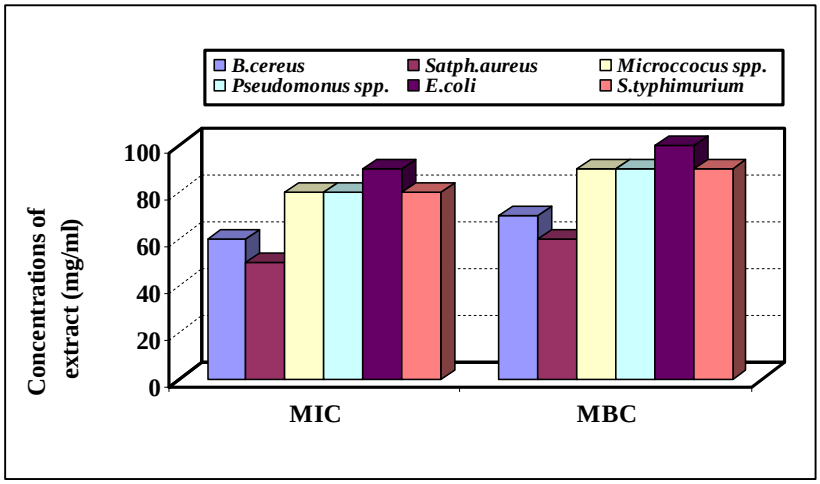

Figure- 6: -MIC and MBC (mg/ml) of *C. citratus* leaves ethanolic extract against tested bacteria

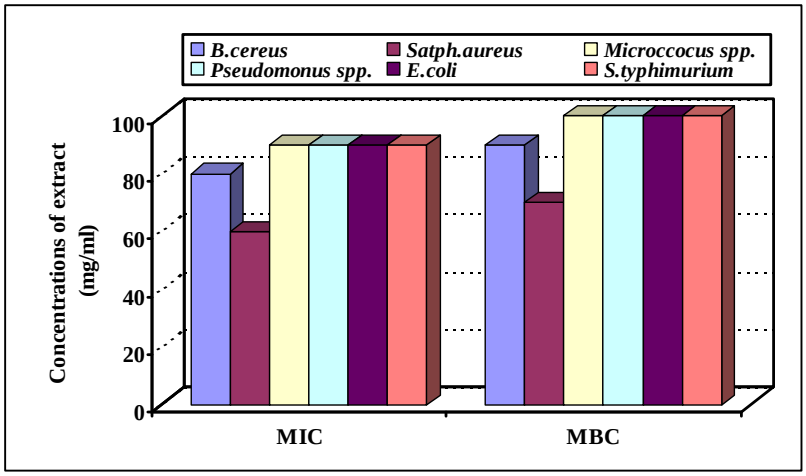

Figure- 7: - MIC and MBC (mg/ml) of *C. citratus* leaves oily extract against tested bacteria

Indian Journal of Natural Sciences www.tnsroindia.org.in ©IJONS

Vol.9 /Issue 51 / December / 2018 *International Bimonthly* *ISSN: 0976 – 0997*

RESEARCH ARTICLE

Investigate the Effect of Global Carbon Dioxide on the Total Column Ozone and Temperature in the Stratosphere above Baghdad

Mawg S. R. and Najat M. R. Al-Ubaidi*

Department of Astronomy and Space, College of Science, University of Baghdad, Baghdad, Iraq.

Received: 10 Aug 2018 Revised: 14 Sep 2018 Accepted: 16 Oct 2018

***Address for Correspondence**
Najat M. R. Al-Ubaidi
Department of Astronomy and Space,
College of Science,
University of Baghdad,
Baghdad, Iraq.

ABSTRACT

The stratospheric ozone layer is the most important protective layer in the atmosphere that absorbs the harmful Ultraviolet rays from the Sun. The aim of this research is to study the effect of the variation of the carbon dioxide (CO_2) in the atmosphere on the total column ozone (TCO) in the stratosphere. To find the relation between them by studying the monthly average variation of carbon dioxide with the monthly average variation of the total column ozone for the period (1997-2011) above Capital Baghdad (latitude 33°N; longitude 44°E) in Iraq. Also to find the effect of this relation on the temperature (T) change at height (20km) in the stratosphere by studying the monthly changes rate of carbon dioxide with the monthly changes rate of the temperatures at the same period and location. The data for the (TCO) and the (T) are taken from The European Centre for Medium-Range Weather Forecasts and ERA satellite for two times hour (00:00) and (12:00) in the Universal Time (UT), while the data for carbon dioxide was taken from Earth System Research Laboratory (ESRL). The results show that, there is inversely proportional for carbon dioxide with the total column ozone and with the temperatures in the stratosphere.

Keywords: Carbon dioxide; Total Column Ozone; Temperature.

INTRODUCTION

Climate changes are one of the big challenges facing humanity over their long history that have a direct effect of the Earth's climate, which in turn affects humans and other organisms. The activities of human for burning of fossil fuels since the mid-nineteenth century led to high concentrations of greenhouse gases (GHGs) specially the carbon dioxide (CO_2) in the atmosphere and rising of the average temperature of the Earth's surface [1]. The bad effects of the climate changes include many fields directly related to human health [2], such as extreme weather, ozone depletion [3, 4], increased the danger of wild land fires, loss of biodiversity, stresses to food producing systems [5]. Climate is

generally defined as the average state of the weather for a given time scale (monthly, seasonally, yearly, decade and so forth) and generally for a specified geographical region [6]. Climate system is a set of processes and interactions consisting of five major components: the atmosphere, hydrosphere, land surface (lithosphere), biosphere, and cryosphere, forced or influenced by various external forcing mechanisms, the most important of which is the Sun. Also, the direct effect of human activities on the climate system is considered an external forcing [7].

The CO_2 content in the atmosphere is currently not in balance, the current atmospheric concentration of CO_2 is about (400 ppm). For many decades, the rate of CO_2 input to the atmosphere has exceeded the rate of removal, leading to a global increase in concentration [8]. Although the inputs and outputs from respiration and photosynthesis are equal, humans increase the input of CO_2 by burning plants for agricultural purposes and by burning fossil fuels, which are made from ancient plants that the Earth's processes have transformed into oil, gas, or coal that use by human, Since the 1958, the concentration of CO_2 has increased at a rate of about (0.11 ppm/year) [9]. Human interaction with the global cycle is most evident in the movement of the element carbon. The burning of biomass, coal, oil, and natural gas to generate heat and electricity has released carbon to the atmosphere and oceans in the forms of CO_2 and carbonate. Because of the relatively slow reactions and removal rates of CO_2, its concentration has been increasing steadily since the beginning of the industrial revolution [10].

Previous Studies

There are many studied about Ozone and its relationship with Carbon dioxide; (Sagar and Ronald, 1993), they studied the greenhouse effect and the impacts of carbon dioxide (CO_2), uitraviolet-B (UV-B) radiation and ozone (O_3) on vegetation [11]. (Loya et al., 2003) showed that, in northern forests in the presence of elevated [CO_2], exposure to elevated [O_3] results a lower rates of accumulation acid-in soil compared with the rates at ambient [O_3] because of lower production rates [12]. (Lingliliu et al., 2005) the elevation of [CO_2] significantly increased litter production, whereas elevated [O_3] decreased it. The results indicate that the small changes in litter chemistry caused by elevated [CO_2] or elevated [O_3], combined with changes in litter production rates, will significantly alter stand level chemical inputs to soil [13].(Basim, 2009) he measured the concentration of pollutants Pb, CO_2, SO_2 and H_2S in Baghdad city. Twenty measuring stations distributed in different regions, which have been classified to industrial, commercial and residential stations. The results of concentrations measuring of air pollutants in Baghdad city showed that the CO_2, CO and NO_2 concentrations exceeded the local and global standard limitations for all measuring stations [14]. (Nicolas Richet et al., 2012) in this research the opposite effects of elevated CO_2 and ozone as single factors on plant growth and biomass have often been investigated, whereas their combined effects are less [15].

(Alexander and Alexey, 2015) they study the Relationship between Atmospheric Carbon Dioxide and Global Temperature indicates that in spite of the steadily growing trend in CO2 there has been no trend in the global temperature during the last 17 years [16]. (Xiaona Wang et al., 2016) they found that the increases of atmospheric carbon dioxide and tropospheric ozone concentration has affected forest ecosystem both above and below ground [17]. (Mohammed and Najat, 2017) they study the relationship between temperature and ozone thickness above three Iraqi cities and they found that the total column ozone in day time is greater than night and its values in the North are greater than the values in the Middle and South. Also there is an inverse relation between total column ozone and temperature along the period of their study in Baghdad and Dahuk, but in Basrah the relationship fluctuated between increase and decrease [18]. **(**Najat and Zahraa, 2018) they study the effect of the geomagnetic storms on the variation of the ozone layer thickness above Iraq; it seems that the total column ozone and temperature increases during the stormy days [19]. In this research the relation between carbon dioxide and total column ozone and their effect on the temperature change above Baghdad in the stratosphere are studied.

Greenhouse Effect and Climate Change

The greenhouse effect is a natural phenomenon that has been operated for a millions of years. Without the greenhouse effect, in the atmosphere the GHGs keep the Earth's mean surface temperature at an average of (-18°C). With the greenhouse effect, the mean surface temperature would be (15°C) [20]. The atmospheric greenhouse effect occurs because H_2O, CO_2, and other trace gases are selective absorbers, they allow most of the solar radiation to reach the surface, but they absorb a good portion of the Earth's outgoing Infrared (IR) radiation, forbidding the radiation from escaping into space [21]. It is the atmospheric greenhouse effect that keeps the temperature of our planet at a level where life can survive. The greenhouse effect is good and essential to life on the Earth. Increasing the tropospheric concentrations of (GHGs) that absorbs (IR) emitted radiation, will increase the difference between the amount of long-wavelength radiation absorbed and that emitted to space, leading to a net increase in the energy deposited in, and hence temperature of the troposphere [16]. In the stratosphere, increased (GHGs) concentrations lead to a net cooling as they emit more (IR) radiation into the upper atmosphere than they absorb [22]. Reduced O_3 will cause the stratosphere to absorb less solar radiation, which further cools the stratosphere [23] and heats the troposphere, further contributing to climate change [24].

Location and Climatic Characteristics of Iraq

The republic of Iraqi region located in the south-west of Asia to the north-east of the Arab homeland bounded on the north by Turkey, on the east by Iran, on the west by Syria, Jordan and Saudi Arabia on the south by Arab Gulf, Kuwait and Saudi Arabia. Iraq lies between (latitudes 29˚ 5′- 37˚ 22′ N; longitudes 38˚ 45′- 48˚ 45′E). The area of Iraq covers 435052 km^2.Climate of Iraq lies within the moderate northern region, system similar to that of Mediterranean where there is no rainfall in summer, but occurs almost in winter, autumn, and spring [25]. Iraq is one of the most Arab countries affected by climate changes, because it faces significant environmental problems such as, the water scarcity, desertification, drought, rising temperatures and heat waves, less precipitation, sea level rise and frequency of dust storms which are represent the results of climate changes in Iraq in recent years. There are other factors contributed in the decadence of the environmental situation in Iraq, such as population growth, war fare, air pollution, lack of suitable planning and absence clear government policies to adapt and mitigate the consequences of climate changes. Maintaining a clean environment must be at the forefront of the priorities of decision makers. Therefore, Iraq joined to number of international conventions that dealing with environmental issues, especially the United Nations Framework Convention on Climate Changes (UNFCCC) for the purpose of participation of the international community to install greenhouse gases (GHGs) in the atmosphere at a level that would avoid dangerous interference of human in the climate change [8]. Although Iraq is one of the biggest oil producing countries in the world, but GHGs emission are considered low compared with other countries [26]. Its climate is continental and subtropical; the climate can be categorized into three kinds: Mediterranean climate, steppes climate, and hot desert climate [27].

The Study Area

Baghdad is the Capital of Iraq which is located in its center, the border of the municipality of Baghdad encompasses fourteen administrative units, eight in Rusafa and six in Karkh. It lies on (latitude 33ºN; longitude 44ºE). Baghdad is situated in a plain area of elevation between (31-39) m above sea level. The climate of Baghdad region is defined as subtropical and continental, dry, hot, long summer, cool winter and short autumn and spring. The maximum recorded temperature was 51ºC in summer, while the minimum was (-10ºC). The area of Baghdad region covers 4555 km^2 [28].

Data Selection

In this research the data selected for the total column ozone (TCO) in Dobson Unit (DU) and temperature (T) at a height 20km in Kelvin above Capital Baghdad (longitude 44°E; latitude 33° N) were taken from the European Centre for Medium-Range Weather Forecasts (ECMWF), from the website (http://apps.ecmwf.int) and from the satellite (ERA). The selected data for monthly average to the period (1997-2011) for total column ozone and temperature and for the two day times (00:00) in the night and (12:00) in noon. The global monthly selected data of carbon dioxide (CO_2) in (ppm) for the period (1997-2011) were taken from Earth System Research Laboratory (ESRL), from the site (https://www.esrl.noaa.gov/gmd/ccgg/trends/data.html).

RESULTS AND DISCUSSION

The data for the period (1997-2011) of the monthly average variation global carbon dioxide (ppm) are represented in Figures (1), while Figures (2 and 3) reveal the total column ozone (DU), and the temperature (K) at 20km height above Baghdad for hours (a) for 00:00 and (b) for 12:00 respectively. In Figure (4) the variation of the temperature between day and night for each year selected in this research are drawn. Figures (5 and 6) show the monthly average variation of global carbon dioxide and the monthly average total column ozone for all years and the hour selected respectively. Figures (7 and 8) represent the monthly average variation of carbon dioxide and the temperature monthly average for hours 00:00 and 12:00 respectively. In general, it seen that the global maximum values of carbon dioxide shown in April, May and June (Spring and Summer) because plant growth is slow, photosynthesis occurs very little, according to that the values of CO_2 became high, while the minimum values in September and October (in Autumn). The maximum values of temperatures at height 20km (in stratosphere) above Baghdad appeared in May, June, July, August and September, while in other months there are a fluctuation in their values. The difference in temperatures in the stratosphere between day and night for every month is about 2K or less. Concerning the total column ozone reveals the maximum values in winter and spring but the minimum values in summer and autumn. The difference in total column ozone between day and night for every month is about 3DU or less.

From figures (5 and 6) it seen that there are non-linear relation between the two parameters (CO_2 and TCO) for each month, and each year, to find the relation between them the ratio ($\Delta TCO/\Delta CO_2$) are taken and drawn for each month along the 15 years, which are shown in Figures (9 and 10) for the two hours (00:00) and (12:00) respectively. It seen from the slops of the linear curve fitting equations (represented in table 1) that there are a reversible relation between the two parameters along the period selected. Also from figures (7 and 8) there are non-linear relation between the (CO_2 and T) for each month, and each year, to find the relation between them, the same way was done by taking the ratio ($\Delta T/\Delta CO_2$) and drawn for each month from the year, which are shown in Figures (11 and 12) for the two hours (00:00) and (12:00) respectively. (Table 2) represents the slops of the linear curve fitting equations, in which the inversely proportional are appears between carbon dioxide and temperatures for all years and times selected except for years (1998, 2000, 2003, 2005 and 2009 at time 12:00) there are a direct relation between them.

From results above we can see that in the stratosphere as the carbon dioxide increases, which is represents one of the greenhouse gases, causes cooling in the stratosphere and causes warming in the top of troposphere, while the decreasing in its concentration causes the opposite behavior. Appearing the anomalies in some cases may be related to effect of other greenhouse gases (i.e. CH_4, H_2O and NO_x, which are not in our research field) are present in the stratosphere and have a significant effect on temperature and the total column ozone. Also the absorption of ultraviolet radiation from the Sun effect on the amount of ozone in the stratosphere, as UV absorption increases the amount of the ozone increases too, which leads to heating in the stratosphere. When the ozone is reducing due to decreasing in UV absorption, this causes a polar pull in the stratosphere resulting a cooling that effects on the temperature in the stratosphere.

CONCLUSIONS

From the results we can conclude that the maximum values of global carbon dioxide appeared in (April, May and June), while the minimum values in September and October. The maximum values of total column ozone appeared in winter and spring while the minimum values in summer and autumn. The maximum values of the temperatures in the stratosphere (20km height) in May, June, July, August and September, but the minimum values are fluctuated in the other months of the years selected. The monthly difference in temperatures between day and night in the stratosphere for each month from the years selected (1997-2011) is 2K and less, while the monthly difference in total column ozone between day and night for each month is 3DU and less. The results show that, there are inverse relation between carbon dioxide and total column ozone also the relation between carbon dioxide and temperature are inversely related, while there is direct proportional between total column ozone and temperatures in the stratosphere. The variation of the temperature, total column ozone, global carbon dioxide reveal that there are increasing in the concentration of carbon dioxide while there are decreasing in the temperature and total column ozone.

ACKNOWLEDGMENTS

This work relates to University of Baghdad/ College of Science/ Department of Astronomy and Space. The data are provided from the European Centre for Medium-Range Weather Forecasts (ECMWF) and European Space Agency (ESA) and Earth System Research Laboratory (ESRL), for whom I would like to introduce my utmost appreciation and thanks.

REFERENCES

1. Shindell D. T., D. Rind, P. Lonergan, (1998), "Increased polar stratospheric ozone losses and delayed eventual recovery owing to increasing greenhouse-gas concentrations", Nature, 392, pp. 589–592.
2. Webb A., (2012), "Health hazards of ozone depletion", Weather, vol. 44, no. 5, pp. 215-220.
3. Varotsos C. Tzanis, S. Tsitomeneas, M. N. Assimakopoulos, A. Mammis, (2008), "Surface solar ultraviolet irradiance and total ozone during summer time", Int. J. Remote Sens., vol. 29, May, pp. 2667-2673.
4. Lacis A. A., D. J. Wuebbles, J. A. A. Logan, (1990), "Radiative forcing of climate by changes in the vertical distributions of ozone", J. Geophys. Res., 95, pp. 9971-9981.
5. Pachauri R. K., Reisinger A., (2008), "Climate Change 2007", Synthesis Report, 4th Assessment Report, Intergovernmental Panel on Climate Change (IPCC), Geneva, Switzerland, pp.104.
6. Houghton D., (2002), "Introduction to Climate Change", WMO Publication, No. 926, pp.143, Geneva, Switzerland. http://dx.doi.org/10.4236/ajcc.2015.43014
7. Lutgens F. K., Tarbuck E. J., (2013),"The Atmosphere: An Introduction to Meteorology", 12th edition, Pearson Education, Inc, USA, pp.533.
8. Mohammed Ali Yousif, (2014), "Measurement and Study some of Air Pollutants in Baghdad Zone", M Sc thesis, University of Baghdad, College of Science, Bepartment of Astronomy and Space.
9. Desonie D., (2007), "Atmosphere: Air Pollution and Its Effects", Chelsea House Publisher, New York, USA, 208 pp.
10. Sons, Wells N. C., (2012), "The Atmosphere and Ocean: A Physical Introduction", John Wiley, Ltd, Oxford, UK, pp. 442.
11. Sagar V. Krupa, Ronald N. Kickert, (1993), "The greenhouse effect: the impacts of carbon dioxide (CO_2), ultraviolet-B (UV-B) radiation and ozone (O_3) on vegetation (crops)", Vegetation 104/105, pp. 223-238.
12. Loya W. M., K. S. Pregitzer, N. J. Karberg, J. S. King, C. P. Giardina, (2003), "Reduction of soil carbon formation by tropospheric ozone under increased carbon dioxide levels", Nature, 425, pp. 705–707.

13. Lingliliu John S. King, Christian P. Giardina, (2005), "Effects of elevated concentrations of atmospheric CO_2 and tropospheric O_3 on leaf litter production and chemistry in trembling aspen and paper birch communities", Tree Physiology, 25, PP. 1511–1522.
14. Bassim M. H., (2009), "Measurements and study the concentration of some air pollutants in the city of Baghdad", M.Sc. Thesis, University of Al-Mustansiriyah, College of Science, Department of the air Science.
15. Nicolas Richet, Dany Afif, Koffi Tozo, Brigitte Pollet, Pascale Maillard, Francoise Huber, Pierrick Priault, Jacques Banvoy, Patrick Gross, Pierre Dizengremel, Catherine Lapierre, Patrick Perre, Mireille Cabane, (2012), "Elevated CO_2 and/or ozone modify lignification in the wood of poplars (populous tremula x alba)", Journal of Experimental Botany, vol. 63, no. 2, pp. 695–709.
16. Alexander and Alexey, (2015), "On the Relationship between Atmospheric Carbon Dioxide and Global Temperature", American Journal of Climate Change, 4, 181-186. Published Online June 2015 in SciRes. http://www.scirp.org/journal/ajcc
17. Xiaona Wang, Eugenios Agathokleous, Laiye QU, Makoto Watanabe, Takayoshi Koike, (2016), "Effect of CO_2 and O_3 on the interaction between root of woody plants and ectomycorrhizae", Journal of Agricultural Meteorology 72(2), pp. 95-105.
18. Mohammed A. A. Alwan, Najat M. R. Al-Ubaidi, (2017), " Study the Variation of Ozone and Temperature above Iraq for a Long Period from Years 2002-2016", International Journal of Science and Research (IJSR), Volume 6 Issue 12, pp. 1287-1301. DOI: 10.21275/ART20179007.
19. Najat M. R. Al-Ubaidi, Zahraa T. I., (2018), "Investigate the Ozone Thickness and Temperature above Iraq during Severe and Strong Geomagnetic Storms", Journal of Geoscience and Environment Protection, 6, pp. 50-61. http://www.scirp.org/journal/gep
20. Saha K., (2008), "The Earth's Atmosphere Its Physics and Dynamics", Springer, USA, pp. 374.
21. Bassim M. H., (2016),"Evaluation the Effects of Industrial CO_2 Emission on Climate Changes in Iraq", PhD Thesis, University of Al-Mustansiriyah, College of Science, Department of the air Science.
22. Brasseur G., H. M. Hitchman, (1988), "Stratospheric Response to Trace Gas Perturbations: Changes in Ozone and Temperature Distributions", Science, 240, pp. 634 637.
23. Sivasakthivel. T, K. K. Siva Kumar Reddy, (2011), "Ozone Layer Depletion and Its Effects: A Review," International Journal of Environmental Science and Development vol. 2, no. 1, pp. 30-37, ISSN: 2010-0264.
24. Muller R., (2012), "Stratospheric Ozone Depletion and Climate Change", Royal Society of Chemistry, Cambridge, UK, pp. 346.
25. Bushra A. J., (2010), "Direction and Deviation from the Rate-General of the elements of the Climte of Iraq", Journal of the Faculty of Arts, University of Al-Mustansiriyah, no. 97, pp.
26. Tolba M. K., and Saab N. W., (2009), "Arab Environment: Climate Change: Impact of Climate Change on Arab Countries". Arab Forum for Environment and Development, Beirut, Lebanon, pp. 181.
27. Sarkoun L. S., Ali A. A., Hikmet G. C., Adel F. A., Abd A. H., Mouna R., Mohammed S. A., Asma A., Dina Y. B., Samia A. H., (2013), " Forecast the state of the environment in Iraq", Republic of Iraq, Ministry of Environment, pp. 9-10.
28. Bassim M. H., Mathim S., (2010), "Using remote sensing data and GIS to evaluate air pollution and their relationship with land cover and land use in Baghdad City", Iranian Journal of Earth Sciences ,vol. 2, pp. 20-24.

Table (1): Trend linear line equations slops for the ($\Delta TCO/\Delta CO_2$) along years (1997-2011) at time 00:00 and 12:00 in UT.

Year	Time 00:00UT	Time 12:00UT
	slope	slope
1997	0.00763-	0.00724-
1998	0.02158-	0.02161-
1999	0.00157-	0.00143-
2000	0.00909-	0.00931-
2001	0.01152-	0.01116-
2002	-0.00388	0.00388-
2003	0.01039-	0.01058-
2004	0.00560-	0.00516-
2005	0.01084-	0.01047-
2006	0.00164-	-0.00149
2007	0.01183-	0.01207-
2008	0.00226-	0.00282-
2009	0.00764-	0.00724-
2010	0.01271-	0.01239-
2011	0.00817-	0.00824-

Table (2): Trend linear line equations slops for the ($\Delta CO_2/\Delta T$) along years (1997-2011) at time 00:00UT and 12:00UT.

Year	Time 00:00UT	Time 12:00UT
	slope	slope
1997	-0.00371	0.00357-
1998	0.00196	0.00229
1999	0.00554-	0.00493-
2000	0.00045-	0.00030
2001	0.00108-	0.00062-
2002	0.00482-	0.00401-
2003	0.00068-	0.00016
2004	0.00460-	0.00401-
2005	0.00134	0.00170
2006	0.00508-	-0.00496
2007	-0.00090	8.19598E-005-
2008	0.00514-	0.00478-
2009	0.00104-	2.63089E-005
2010	0.00118-	0.00101-
2011	0.00118-	0.00062-

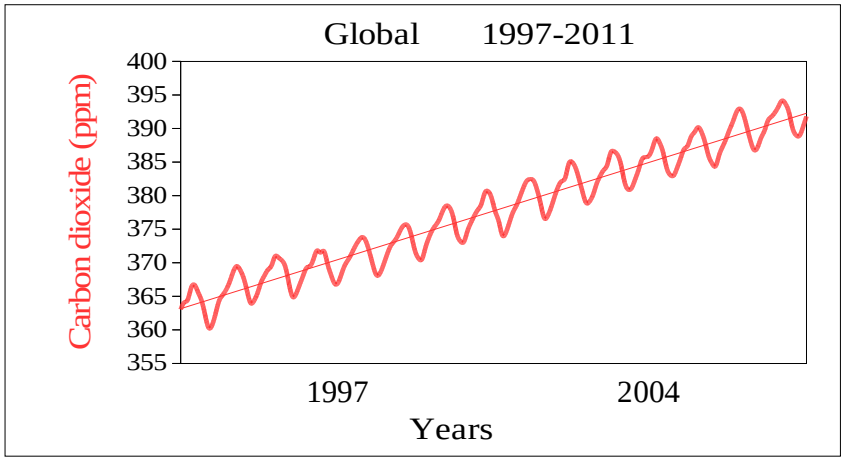

Figure 1: Represent the variation of global carbon dioxide for 15 years from (1997-2011).

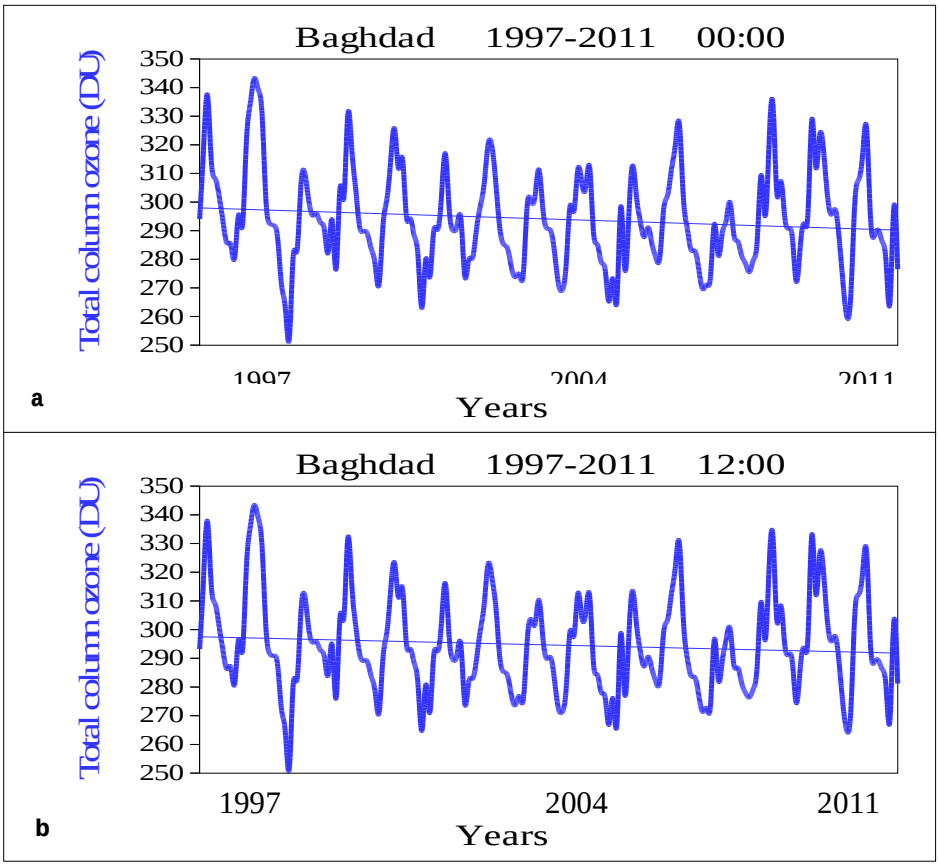

Figure 2: Total Column Ozone above Baghdad for hours a) 00:00 and b) 12:00 from years (1997-2011).

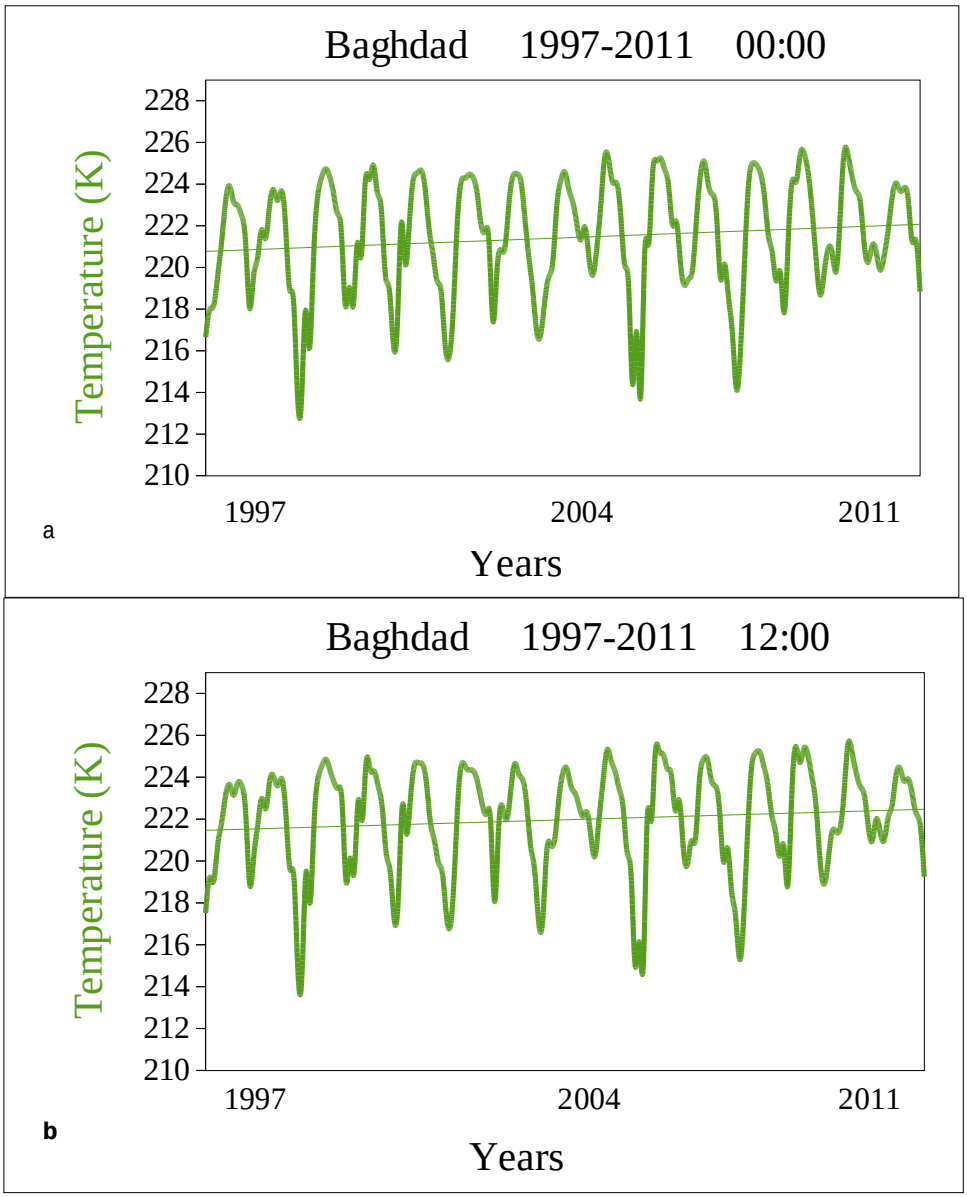

Figure 3: Temperature at 20km height above Baghdad for hours a) 00:00 and b) 12:00 from years (1997-2011).

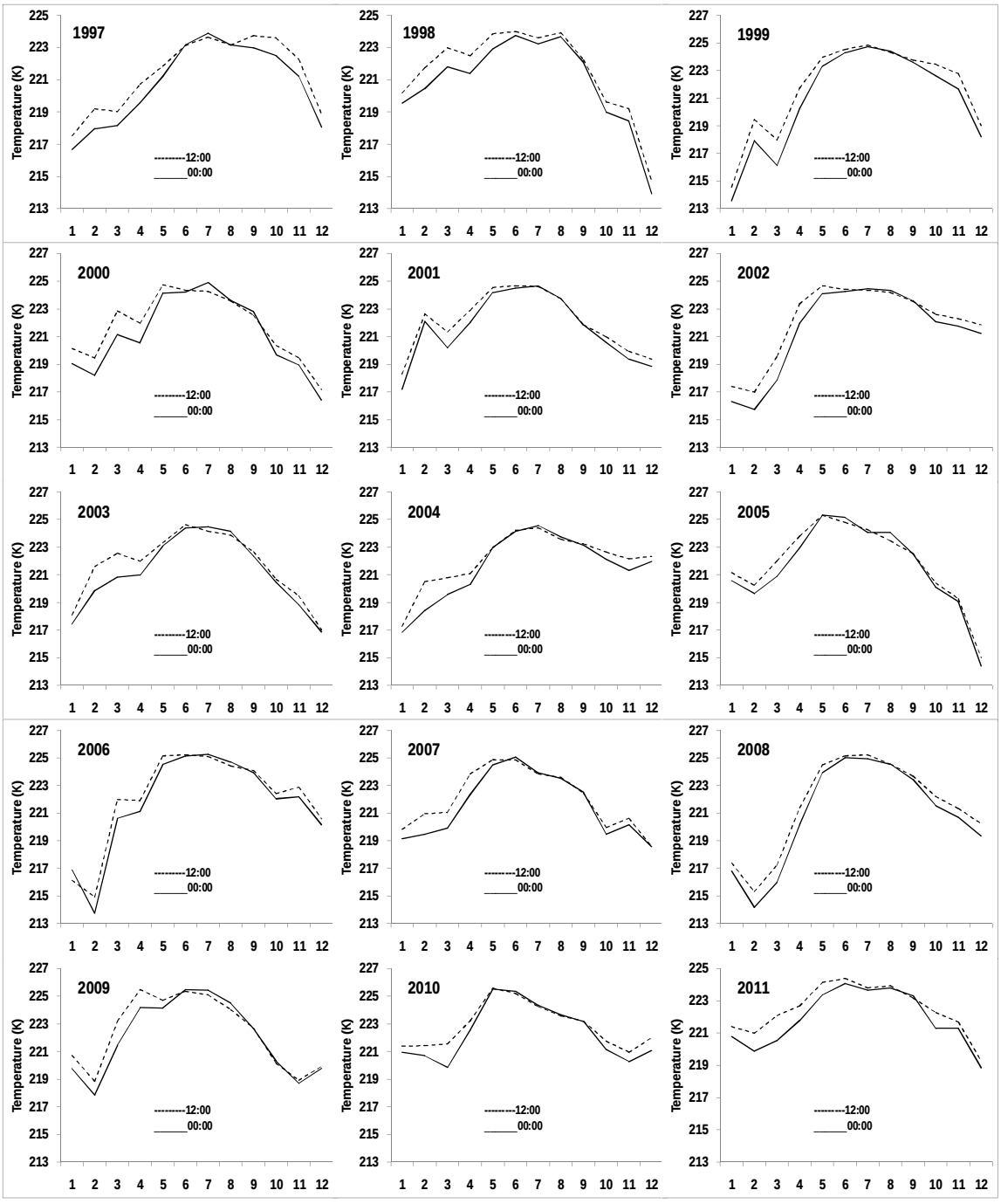

Figure 4: Monthly average temperature at 20km height above Baghdad for hours 00:00 and 12:00 from years (1997-2011).

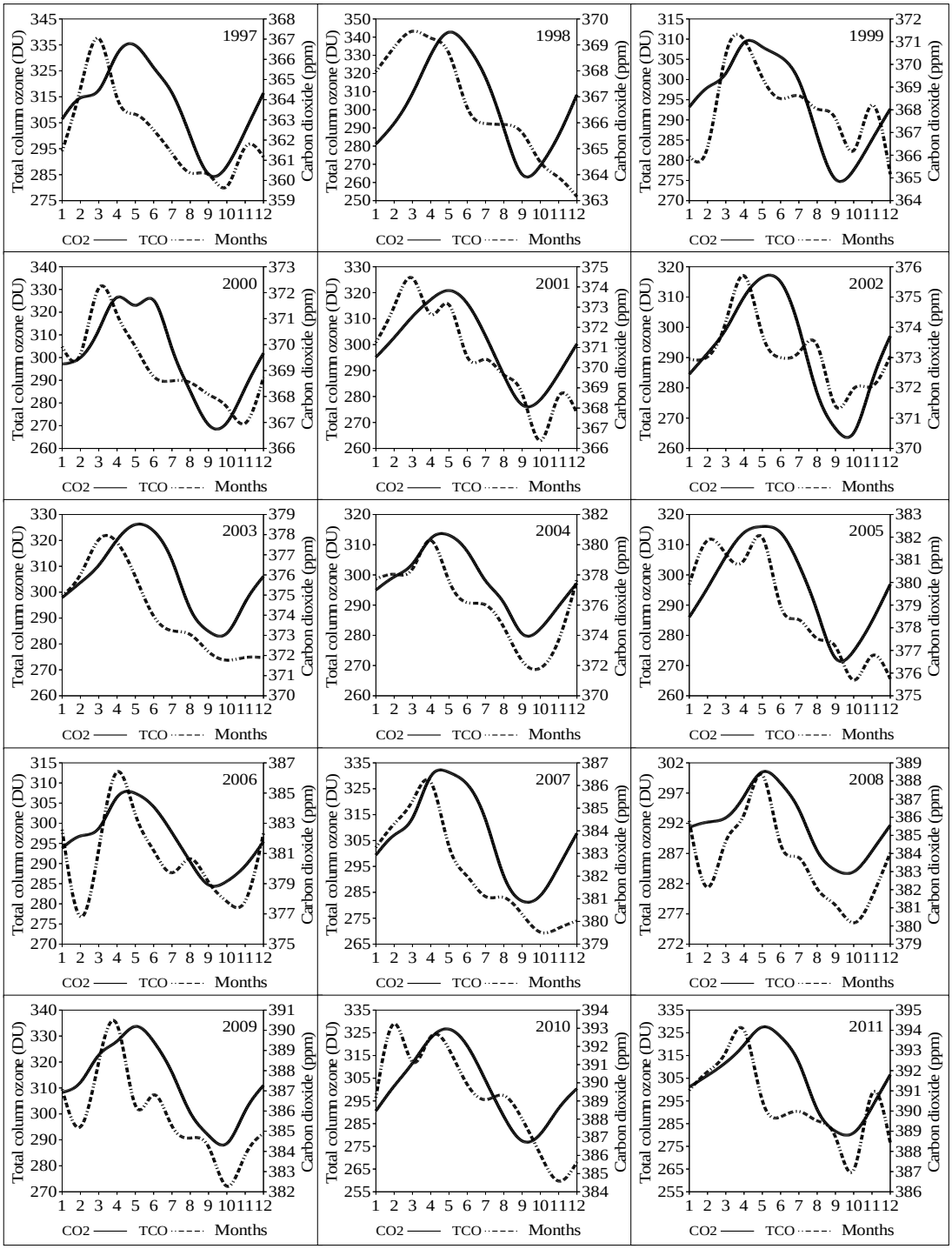

Figure 5: Represent monthly average variation of total column ozone (DU) and carbon dioxide (ppm) for years (1997-2011) at hour 00:00.

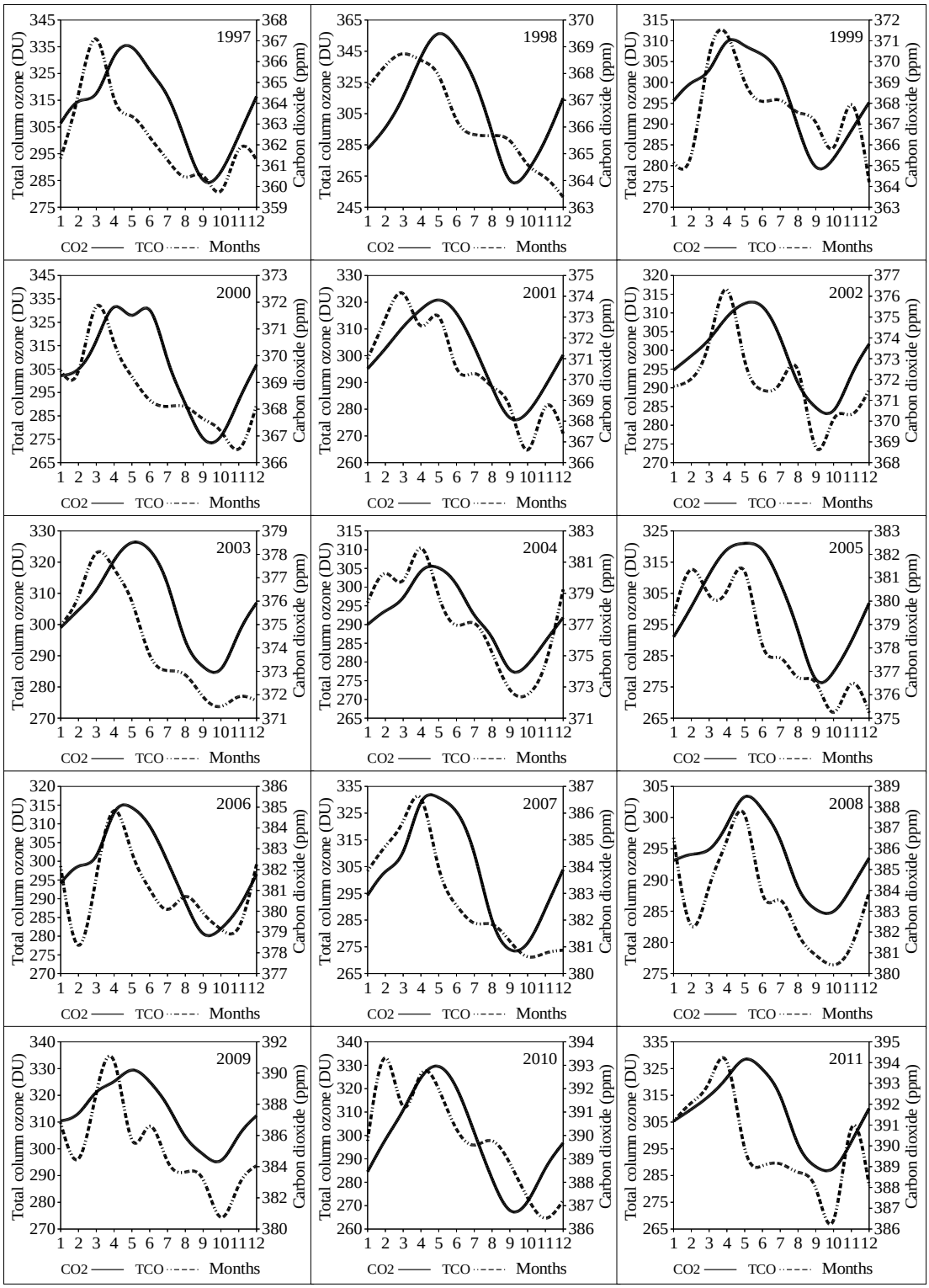

Figure 6: Represent monthly average variation of total column ozone (DU) and carbon dioxide (ppm) for years (1997-2011) at hour 12:00.

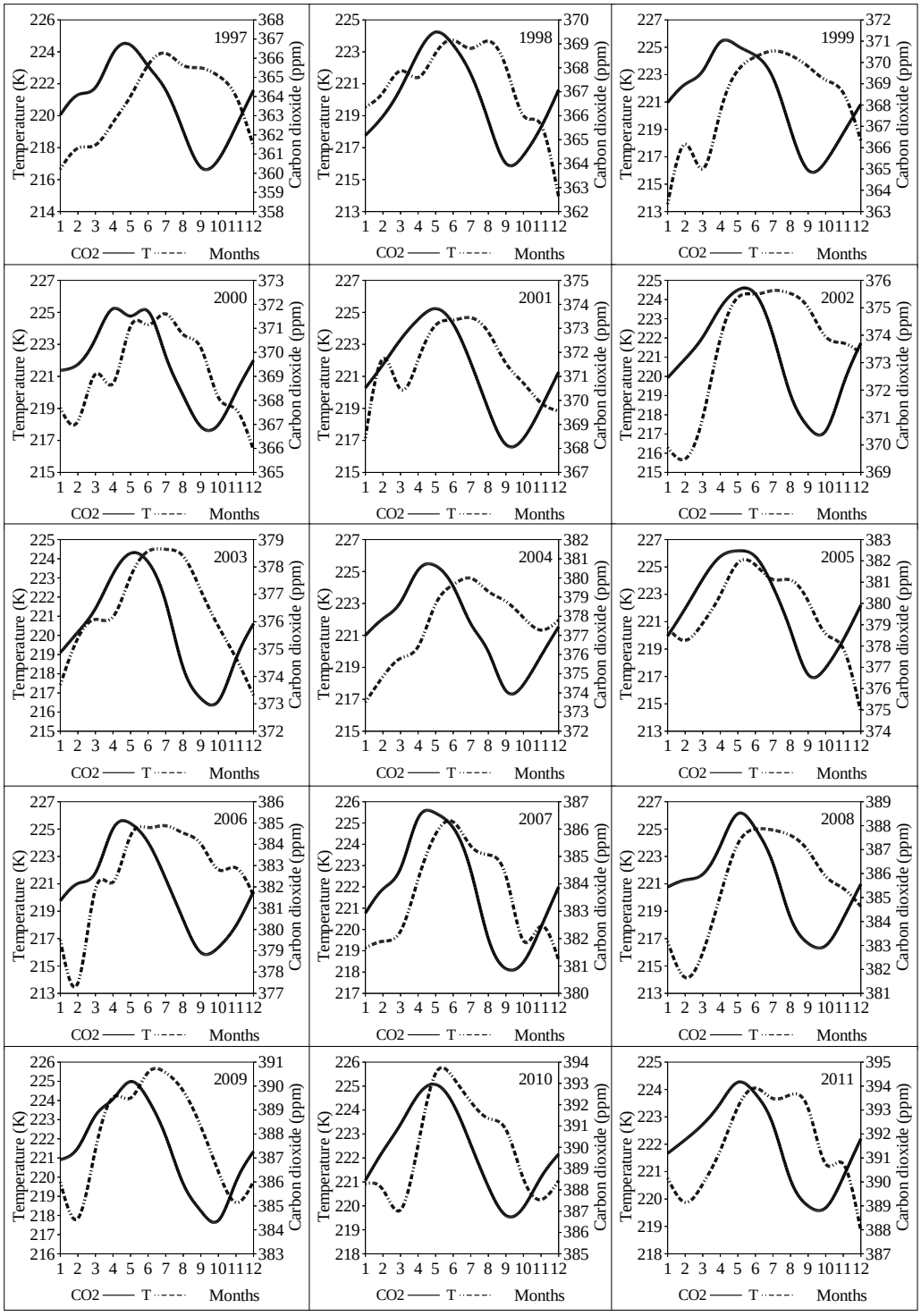

Figure 7: Represent monthly average variation of carbon dioxide (ppm) and temperature (K) for years (1997-2011) at hour 00:00.

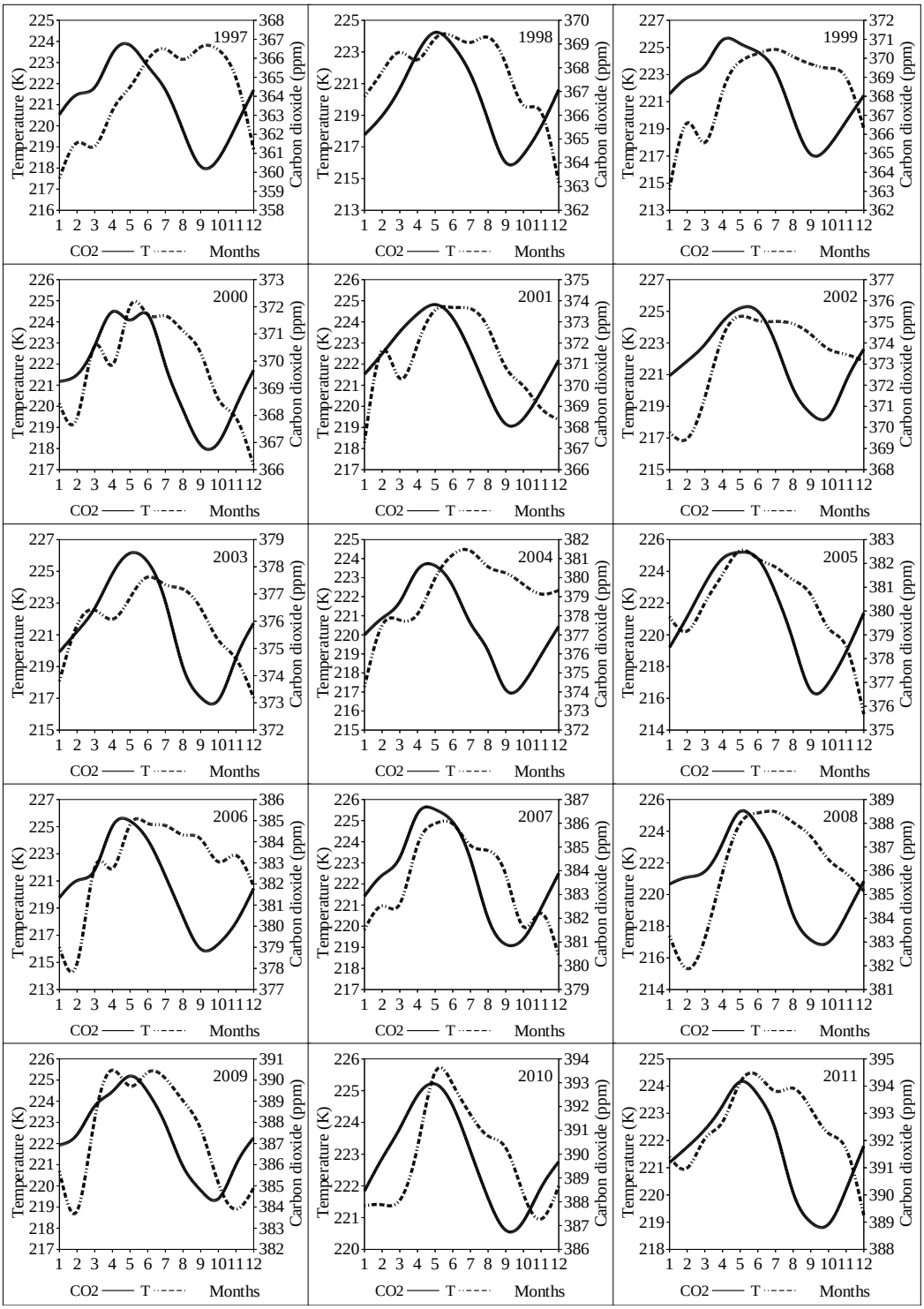

Figure 8: Represent monthly average variation of carbon dioxide (ppm) and temperature (K) for years (1997-2011) at hour 12:00.

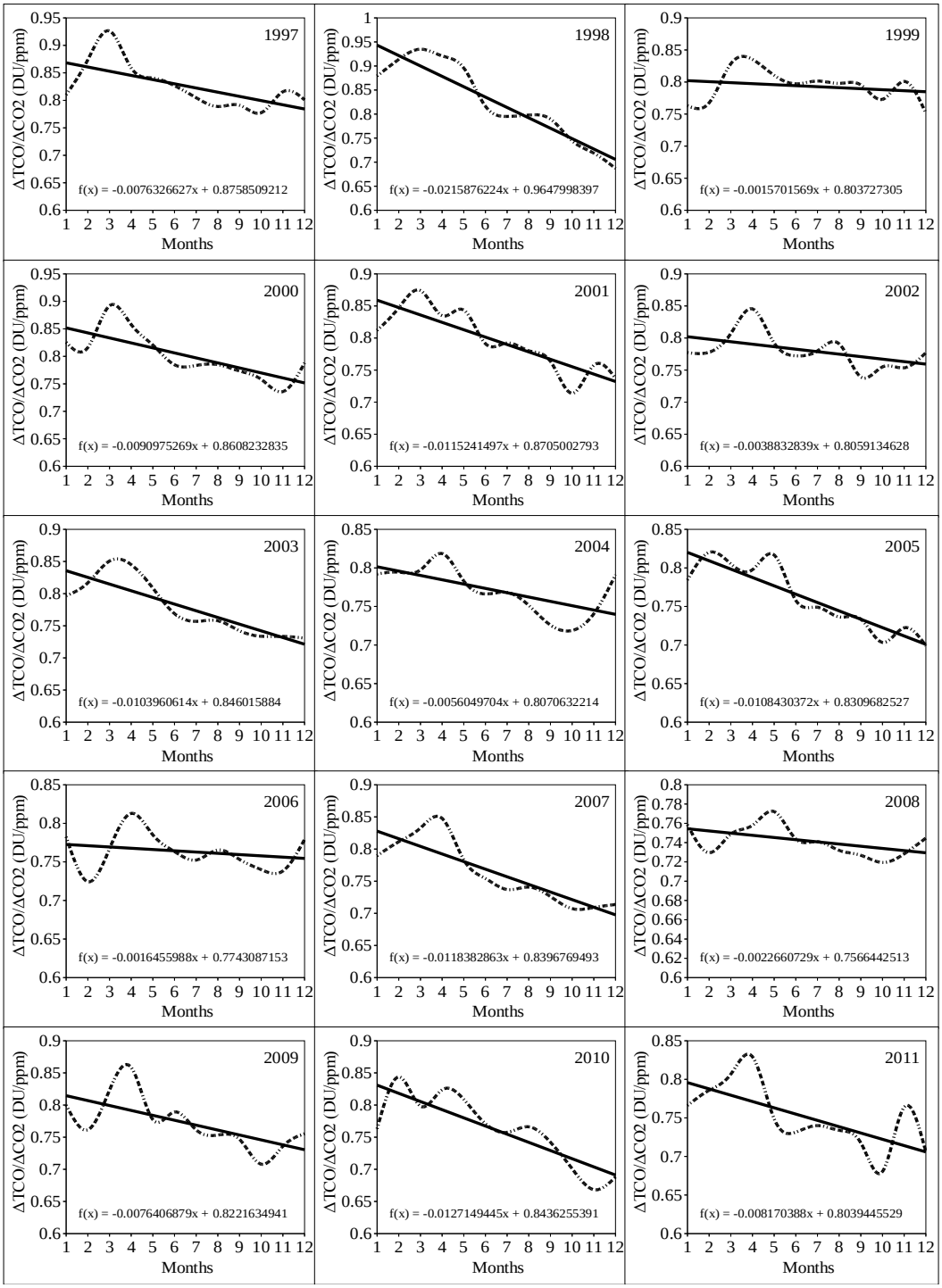

Figure 9: Represent trend line of monthly average variation of total column ozone (DU) to carbon dioxide (ppm) for years (1997-2011) at hour 00:00.

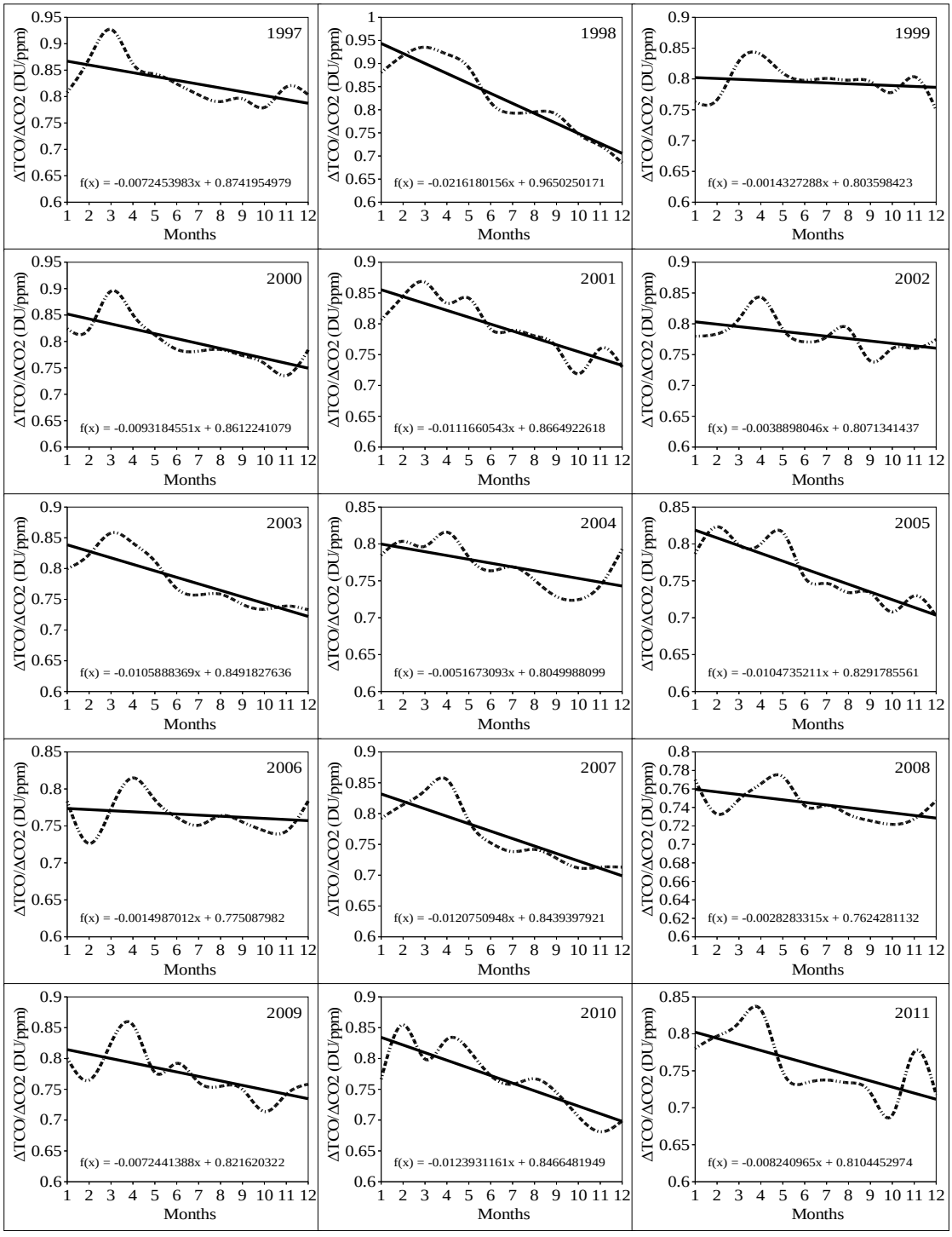

Figure 10: Represent trend line of monthly average variation of total column ozone (DU) to carbon dioxide (ppm) for years (1997-2011) at hour 12:00.

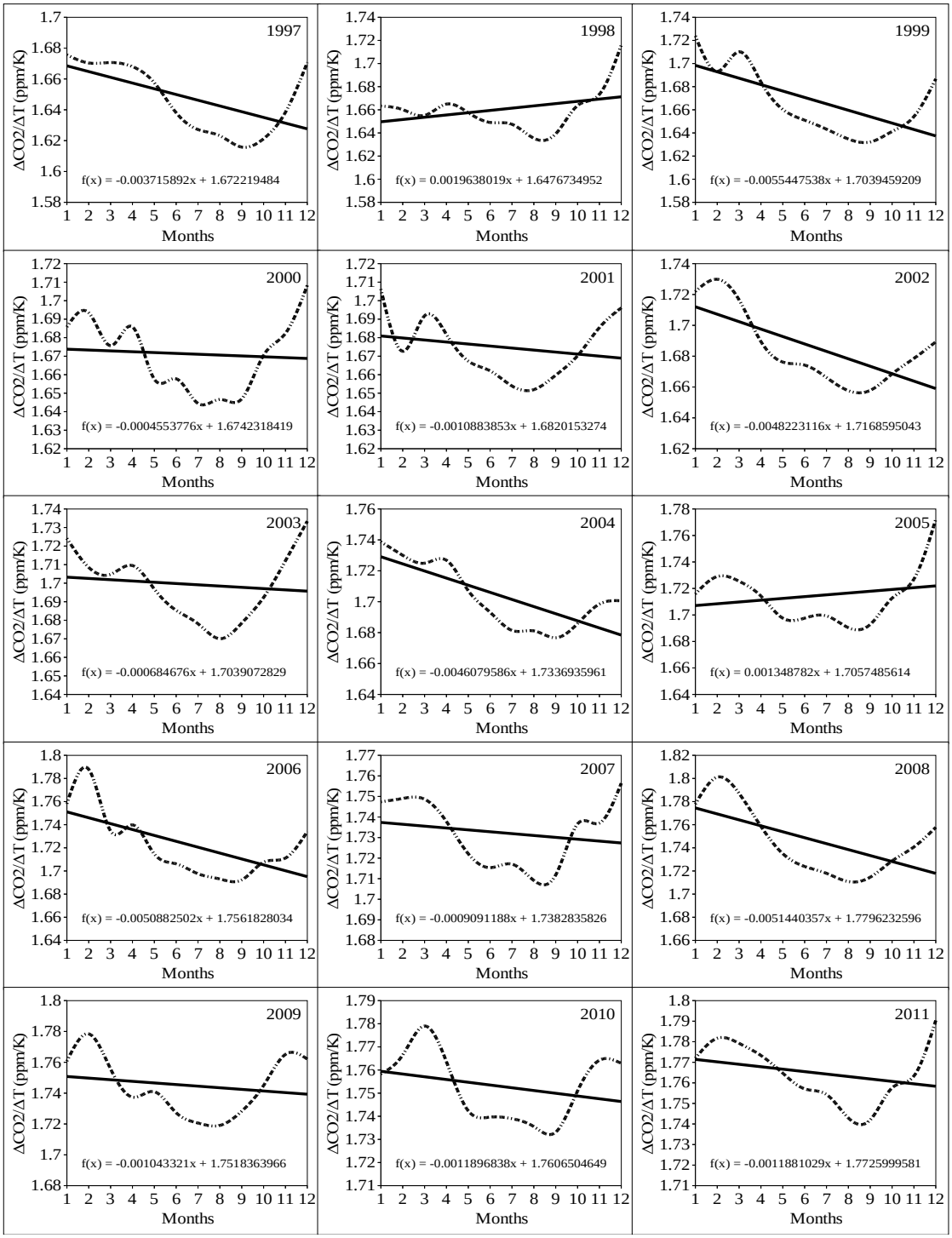

Figure 11: Represent trend line of monthly average variation of carbon dioxide (ppm) to temperature (K) for years (1997-2011) at hour 00:00.

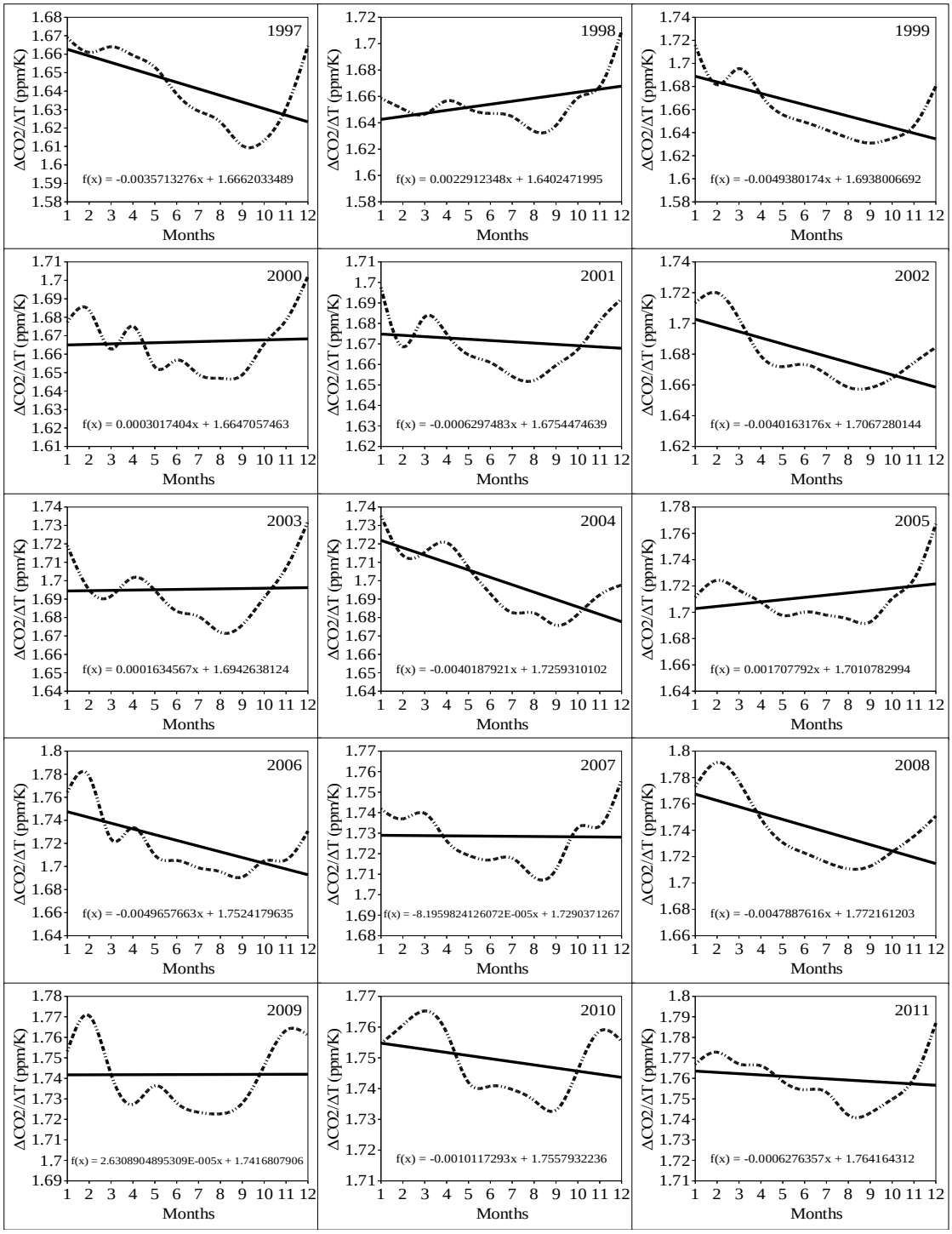

Figure 12: Represent trend line of monthly average variation of carbon dioxide (ppm) to temperature (K) for years (1997-2011) at hour 12:00.

Indian Journal of Natural Sciences www.tnsroindia.org.in ©IJONS

Vol.9 /Issue 51 / December / 2018 *International Bimonthly* *ISSN: 0976 – 0997*

RESEARCH ARTICLE

Comparative Study between Polypropylene Mesh and Polypropylene Kessler Suture for Repair Rupture of Tendon

Saddam Khalid Humadi*

Department of Veterinary Surgery, College of Veterinary Medicine, University of Tikrit,Iraq.

Received: 07 Aug 2018 Revised: 11 Sep 2018 Accepted: 16 Oct 2018

***Address for Correspondence**
Saddam Khalid Humadi
Department of Veterinary Surgery,
College of Veterinary Medicine,
University of Tikrit, Iraq.

ABSTRACT

Inducing tendonrapturewas used to investigate the efficiency of polypropylene mesh comparing with four loop Kessler suture to support the tendon and promote healing.Common calcaneal tendon of 12New Zealand White male rabbits weresevered of all animalsand dividedinto twogroups each group contains six animals. In group I the ruptured tendon repaired with polypropylene mesh either ruptured tendons of group II animals was repaired by four loop Kessler method using polypropylene suture, casting all injured legs using bandage and adhesive tape.The treated tendons were evaluated clinically, grossly and histopathologicallyfor fourmonthsafter treatment.The mesh showed early supporting of animals gait, accelerate the repair of raptured tendon, more collagen fibers maturation and organizationaccording to histopathological, macroscopical and clinical examination data compared withKesslergroup.

Keywords: Polypropylene Mesh, Kessler Suture,Tendon's Rupture.

INTRODUCTION

Flexor tendon injuries are often common, as the tendons lies close to the skin.Injures of the common calcaneal tendon need to be diagnose and treat. The knowledge of the tendon anatomy is necessary in order to understand its biomechanics and pathology (Szaro, 2011). This tendon is the concourse of threeseveralmusculotendinous units at the calcaneus: the gastrocnemius tendon, the superficial digital flexor tendon, and the common tendons of the biceps femoris, gracilis, and semitendinosus muscles (Harasen, 2006).Histologically the tendon composed of dense connective tissue encased in dense connective tissue sheaths.Tendons are composed of parallel arrays of collagen fibers closely packed together; the main sold material of tendon is collagen is composed of about 86%(Narayan, 2009). Tendons Function have been considered to be a mechanism by which muscles connect to bone, to transmit forces (Voleti*et al.,* 2012) also acts as an energy storage device (Silver *et al.,*2006).

Tendon injury can occur via external trauma, depending on the trauma, the severity of the lesion may vary considerably, leading to stretching, small or partial lacerations or a complete rupture (Montgomery and Fitch, 2003).Plantigrade position is the main sign associated with the complete rupture ofthe Common calcaneal tendon(Dal-Bó et al., 2016). Healing of the tendon can be largely divided into three phases, inflammatory repairing and remodeling phases; these overlapping phases are controlled by a variety of growth factors(Hopeand Saxby, 2007). The oxygen consumption of tendons is 7.5 times lower than that of skeletal muscles. That will lead to a low metabolic rate and results in slow healing after injury (Sharma and Maffulli, 2005).

Treatment of tendon injury medically with external support and other choice is surgically attaching healthy ends of the tendons back together with suture and other type of grafts (Truntzer *et al.,* 2017).Repairs of the tendon need to be protected after surgery to prevent excessive weight bearing by healing tendonfor an average of (6-12) week (Stavrou, 2013).The aim of this study is to determine the most affecting surgical treatment of complete rapture tendon according to new surgical perspectives, and presenting the efficacy of polypropylene mesh to supporting the muscle tension during healing.

MATERIALS AND METHODS

Experimental Animals

Twelve New Zealand white male rabbits were usedin the present study. The animals were housed at room temperature (22 ± 3C°). During the experiment, all animals were acclimatized to their environment for a week and given same diet.

Inducing tendon rapture

The posterior aspect of hind limb skin of the rabbits was prepared surgically. Animals were anesthetized with a mixture of 35 mg/kg Ketamin and 5mg Xylazineadministered intramuscularly. A sharp skin incision made above the Common calcaneal tendonfor exposure the tendon and inducing complete catting (fig.1). (Goshima*et al*., 2012; Burgisser *et al*., 2016).

Experimental Design

The animals weredividedinto two experimental groupsrandomly (mesh and Kessler group) 6 animals for each group, the catting tendons in first group wererestorated by applying roll of polypropylene mesh around the ends of severed tendon after apposition of them and the mesh fixed by interrupted suture from each side (fig. 2). The severed tendon in second group was treated with Kessler technique by using 0.2 polypropylene sutures (fig. 3), each group was evaluation after tendon repairclinically for several days for observation the local leg change and animal's gait and the tendon was studied macroscopically and microscopically after 120 days.

Pathological Study

Macroscopic and microscopic Studies of the tendons injury were applied on all animals at 120 days after treatment. After surgical preparation the site of ancient operations, the experimental animals were anesthetized, anda sharp skin incision made above the tendonfor exposure the tendon to examined by naked eye andharvested transverse sectionof tendon Specimens containing the mesh or suture materials. The specimen was fixed in 10% buffered formalin for 48 hours, then washed, dehydrated in a serial graduated alcohol, cleared in xylol, embedded in paraffin wax, sectioned at 5-6 microns thickness and stained with Hematoxylin-Eosin stain, and the slides examined under light microscope (Carriel*et al*., 2017).

RESULTS

Clinical Observations

Animalsof each group showed lameness after surgery with local swelling due to trauma and inflammation, after that the signs of lameness disappear in mesh groupat 10 – 15 days but continuo more than 30 days in animals' of Kessler group. There were two case ofKessler sutures Failure may be due in tolerance totension or sever tendon inflammation, and one case of skin wound dehiscence in mesh group.

Macroscopic Evaluation

At thirdand fourthdayrespectively after surgery there were two case ofthe Kessler suture failure to support approximation of tendon's ends (fig. 4)Due to the rupture of one of the ends resulting from the tension strength of tendon. Skin wound dehiscence that lead to adhesion part of mesh to the skin wound (fig. 5).The macroscopic difference was clear between mesh and Kessler group in term of new tissue transparency, where the mesh group showed greater opacity than the Kessler Group (fig. 6), but lesser hypertrophy (fig. 7).

Microscopic Evaluation

One hundred twenty days period of Kessler group, the longitudinal and transvers sections showed immaturity of tendon at line of rapture according to the collagen deposition and ratio of its organization with dissemination of large number of inflammatory cells particularly around the thread passage areas (fig. 8).Tissue was clearly appeared with high number oflarge nuclei fibroblasts, inflammatory cells and blood capillaries (fig. 9, 10). But Histological finding of Mesh group atsame period showed at the longitudinal sections a complete reattachment of severed linewithdense organized connective tissue(fig. 11), reduction of inflammatory cells and fibroblast number and disappearing of blood capillaries without blood vessels congestion (fig. 12),

DISCUSSION

A number of surgical techniques have been described for the repair of tendon ruptures. Vary technique of suturing; autogenously grafts or free fascia may be used when the gaps are manageable. Synthetics meshes or grafts are useful when autogenous grafts cannot be used. According to these studies we will discuss our study. Study by Yildirim *et al*., (2010), estimated the multilocking loop peripheral suture technique represents a biomechanically stronger than Kessler technique for tendon repair. After applying synthetic mesh for repair quadriceps tendon ruptures showed no complications during operation, no postoperative ruptures with range of motionMorrey, *et al*., (2016), In spite of Interlocking horizontal mattress tendon repairs were significantly higher tensile strength and more resistant to gapping than conventional repairs (Henderson *et al*., 2013).

On the other hands polypropylene mesh is a successful substitutional to autogenous graft in the treatment of Achilles tendon rupture (Fridman *et al*., 2008). Rawson et al., 2013 explain the pathophysiology of many cases of rupture and adhesion formation after repair of tendonby suturing show the relevance of cell death inflammation at the areas of highest stress in repairs around the grasping throws**,** Also Wong*et al.,* 2006 hasbeen shown that the process of suturing tendon causes cell death directlybut placement of an untied suture in tendon did not produce this effect; that give good explanation for dissemination of large number of inflammatory cellsparticularly around the thread passage areas in present study. The clinical results by Morrey *et al*., (2016), were durable, no re-ruptures and good motion range after applying of Synthetic mesh to repair tendon injury, these study compatible with our result of no re-rapture in mesh group.Polypropylene meshes very closely to the physical properties of a normal tendon and

provided a framework for ingrowth collagen bundles (Spinella *et al*., 2010), that may explain outweighs mesh group collagen maturity on kessler group. According to results of recent study and results of other studiesin the field of tendon surgery we conclude that polypropylene mesh is an effective than suturing methods and also alternative to autogenous grafts or tendon transfers in the treatment of tendon rupture.

REFERENCES

1. Bu rgisser, M. G., Calcagni M., Bachmann E., Fessel G., Snedeker, G J., Giovanoli, P. and Buschmann, J. (2016). Rabbit Achilles tendon full transection model – wound healing, adhesion formation and biomechanics at 3, 6 and 12 weeks post-surgery. Company of Biologists Ltd | Biology. 5, 1324-1333.
2. Carriel, V.,Campos, A., Alaminos, M., Raimondo, S. and Geuna, S. (2017). Staining Methods for Normal and Regenerative Myelin in the Nervous System. Histochemistry of Single Molecules, 1560 of the series Methods in Molecular Biology pp. 207-218.
3. Dal-Bó, Í. S., Auada Ferrigno, C. R. and, Galeazzi, V. S. (2016). Tenorrhaphy of the Common Calcaneal Tendon in Dogs and Cats. Acta Scientiae Veterinariae, 44(1): 144.
4. Fridman, R., Rahimi, F., Lucas, P., Daugherty, R, and Hoffmann, H, (2008). Repair of Nelgected Achilles Tendon Rupture with Monofilament Polypropylene Mesh: A Case Study of 12 Patients.The Foot & Ankle Journal 1 (5): 2.
5. Goshima, K., Nakase, J., Xu, Q., Matsumoto, K., Tsuchiya, H. (2012). Repair of segmental bone defects in rabbit tibia promoted by a complex of β- tricalcium phosphate and hepatocyte growth factor. J Orthop Sci., 17 (5): 639–648.
6. Harasen, G. (2006).Ruptures of the common calcaneal tendon. Can Vet J., 47(12):1219-20.
7. Henderson, J., Sutcliffe, M. and Gillespie, Patrick. (2013). Epitendinous Suture Techniques in Extensor Tendon Repairs—An Experimental Evaluation. Journal of the hand surgery, 36 (12):1968–1973.
8. Hope, M. and Saxby, T.S. Tendon healing. Foot Ankle Clin 2007;12(4):553–67.
9. Karjalainen, T., He, M., Chong, A., Lim, A. and Ryhanen, J. (2010). Nickel-Titanium Wire in Circumferential Suture of a Flexor Tendon Repair: A Comparison to Polypropylene. 35 (7):1160–1164.
10. Montgomery, R., Fitch, R. (2003): Muscle and tendon disorders. In: Slatter: Textbook of Small Animal Surgery. 3rd ed. 2266–2267.
11. Morrey, M. C., Barlow, J. D., Abd, M. P., & Hanssen, A. D. (2016). Synthetic mesh augmentation of acute and subacute quadriceps tendon repair. *Orthopedics*, *39*(1), e9-e13.
12. Narayan, R. (2009). Biomedical materials. P p.138.
13. Nielsen, C., & Pluhar, G. E. (2006). Outcome following surgical repair of achilles tendon rupture and comparison between post-operative tibiotarsal immobilization methods in dogs: 28 cases (1997-2004). *Veterinary and Comparative Orthopaedics and Traumatology*, *19*(4), 246-249.
14. Rawson, S., Cartmell, S.,and Wong, J. (2013).Suture techniques for tendon repair; a comparative review. Ligaments and Tendons Journal CIC Edizioni Internazionali, 3(3): 220–228.
15. Sharma, P. and Maffulli, N. (2005).Tendon injury and Tendino pathy : healing repair " The journal of Bone .joint surgery",(87) : 187-202.
16. Shearer, J. K., Van Amstel, S. R. and Brodersen, B. W. (2012). Clinical Diagnosis of Foot and Leg Lameness in Cattle. Veterinary Clinics of North America: Food Animal Practice, 28 (3):535-556.
17. Silver,F. H., Freeman, J.W. and Bradica G.(2006). Structure and Function of Ligaments, Tendons, and Joint Capsule. Repair and Regeneration of Ligaments, Tendons, and Joint Capsule Part of the series Orthopedic Biology and Medicine pp 15-47.
18. Spinella, G., Tamburro, R., Loprete, G., Vilar, J. M., and Valentini, S. (2010). Surgical repair of Achilles tendon rupture in dogs: a review of the literature, a case report and new perspectives. Veterinarni Medicina., 55 (7): 303–310.
19. Stavrou, M. (2013). Treatment for Achilles tendon ruptures in athletes. Ortho. Journal of Bone and joint surgery, (21) :232.

20. Szaro, P., Witkowski, G., Bartyzel, B., Ciszek, B. (2011). Anatomy of the Common Calcaneal Tendon in Horse (*equus caballus*). Ejpau., 14(4).
21. Truntzer, J.N., Triana. B., Harris A.H. S., Baker, L., Chou, L and Kamal R. N. (2017). Cost-minimization Analysis of the Management of Acute Achilles Tendon Rupture. J Am Acad Orthop Surg., 25:449-457.
22. Voleti, P.B., Buckley, M. R. and Soslowsky, L, J. Tendon healing: repair and regeneration. Annual review of biomedical engineering. 2012;14:47–71.
23. Wong, J. K ., Cerovac, S., Ferguson, M. W., McGrouther, D. A. (2006) The cellular effect of a single interrupted suture on tendon. Journal of hand surgery (Edinburgh, Scotland).;31(4):358-67.

Indian Journal of Natural Sciences www.tnsroindia.org.in ©IJONS

Vol.9 /Issue 51 / December / 2018 *International Bimonthly* *ISSN: 0976 – 0997*

RESEARCH ARTICLE

Impact of Silicon Induced Physiological Factors on Rice Stem Borer, *Scirphophaga incertulas* Hubner

P.Chandramani

Professor (Entomology), Agricultural College and Research Institute, Kudumiyanmalai – 622 104, Pudukkottai, TamilNadu, India.

Received: 15 Aug 2018 Revised: 18 Sep 2018 Accepted: 20 Oct 2018

***Address for Correspondence**
P.Chandramani
Professor (Entomology),
Agricultural College and Research Institute,
Kudumiyanmalai – 622 104,
Pudukkottai, TamilNadu, India.
Email : pcento12@ gmail.com

ABSTRACT

Certain physiological factors were analyzed in rice plants treated with silica nutrients. Basal application of calcium silicate 200kg/ha with foliar spray of 0.25% SMS recorded more silica content (12.16%), polyphenol oxidase (55.38 Δ_{495nm} /mg^{-1} g^{-1}) and phenylalanine ammonia lyase (70.38 Δ_{290nm} /µmol m^{-1} ml^{-1} gm^{-1}). This treatment significantly reduced the incidence of rice stem borer to a tune of 73.98%. The occurrence of stem borer was negatively correlated with Si, PPO and PAL activity.

Key words : Rice stem borer, silica ,calcium silicate, sodium meta silicate, PPO, PALase.

INTRODUCTION

Rice (*Oryza sativa* L.) is one among the most important crops all over the world since it is consumed as a staple as well as primary source of energy (Zhang *et al.,* 2008). Rice production is affected by various biotic and abiotic stresses. The projected yield loss due to insect stress ranged from 20 to 30% (Widawsky, 1998). The rice stem borer is one of the major insect pests in rice and yied loss due to stem borer accounting for about 9.17 per cent. Rice is a typical silicon-accumulating plant and it benefits from silicon supplementation. Silicon may act directly on insect herbivores leading to reduction in insect performance and plant damage. Various indirect effects may also be caused, for example, by delaying herbivore establishment and thus an increased chance of exposure to natural enemies, adverse weather events that target exposed insects. Silicon is widely considered as an activator by stimulating the expression of natural defense reaction through the production of phenolic compounds. In India, yellow stem borer caused 1 to19% yield loss in early planted rice and 38 to 80% yield loss in late-planted rice (Catindig and Heong, 2003). The application of Si in crops provides a viable component of integrated management of insect pests because it leaves no

insecticide residues in food or the environment, and it can be easily integrated with other pest management practices, including biological control.

MATERIALS AND METHODS

Experiments were conducted to find out the effect of silica nutrition on rice stem borer in rice ecosystem. The treatments of field experiments conducted at AC & RI, Madurai included were T_1 - Rice straw 5 t / ha + Silicate Solubilizing Bacteria (SSB) 2kg / ha, T_2 - Rice straw 2.5 t/ ha + SSB 2kg / ha, T_3 - Basal application of calcium silicate – 50 kg/ha, T_4 - Basal application of calcium silicate – 100 kg/ha, T_5 - Basal application of calcium silicate – 150 kg/ha, T_6 - Basal application of calcium silicate – 200 kg/ha, T_7 – Foliar spray of 0.25% Sodium meta silicate, T_8 - T_3 + T_7, T_9 – T_4 + T_7, T_{10} – T_5 + T_7, T_{11} – T_6 + T_7, T_{12} – Untreated check. Pest population count was taken at 15 days after transplanting in each plot.

Assessment of pest population

Stem borer

The incidence of stem borer was measured as percentage of dead heart and white ear in randomly selected 10 plants after flowering.

$$\text{Stem borer damage as dead heart or white ear (\%)} = \frac{\text{No. of affected tillers}}{\text{Total no. of tillers}} \times 100$$

Laboratory experiments

The leaf and leaf sheath samples were collected from the field during critical phases of the crop *viz.,* 25 DAT, 50 DAT and 75 DAT in all treatments and utilized for analyzing certain biochemical factors as per the standard procedures.

Physiological factor	**Reference**
Polyphenol oxidase (PPO) activity	Sadasivam and Manickam 1992
Phenyl alanine ammonia lyase (PAL)	Singh and Prithiviraj, 1997
Silica content	Ram Prasad, 2010

Statistical analysis

Data collected in field experiments and laboratory experiments were statistically analyzed. The percentage values were subjected to angular transformation. The treatment mean were compared by least significant difference (LSD) for their significance (Gomez and Gomez, 1985).

RESULTS AND DISCUSSION

The results of field experiment revealed that the dead heart and white ear damage due to stem borer differed significantly among various treatments at all the plant stages observed. The mean stem borer incidence ranged from 2.48 to 9.54 percent respectively throughout the period of experimentation. The dead heart per cent was significantly less in the treatment with basal application of calcium silicate 200kg/ha and foliar spray of 0.25% SMS (2.48 %) sprayed during critical phases of the crop followed by basal application of calcium silicate 150kg/ha with foliar spray of 0.25% SMS (2.87 %).

During the period of observation from 45 DAT to 90 DAT, the white ear damage ranged from 1.42 to 1.79 per cent in basal application of calcium silicate 200kg/ha and foliar spray of 0.25% SMS and it varied from 1.84 to 1.96 to per cent in the next best treatment *viz*., basal application of calcium silicate 150kg/ha with foliar spray of 0.25% SMS. The per cent reduction observed in calcium silicate 200kg/ha with foliar spray of SMS 0.25% was 73.98 per cent and 69.97 per cent in calcium silicate 150kg/ha with foliar spray of SMS 0.25% over untreated check. This is in agreement with findings of Maxwell *et al*. (1972) and Panda *et al*. (1977) who found that the infestations of rice stem borer were markedly reduced by adding silicon to soil. This is again in endorsement with the findings of Subbarao and Perraju (1976) who stated that the higher Si content resulted in lower stem borer incidence and higher insect mortality. Similarly Tayabi and Azizi (1984) concluded that the application of silica at 1t / ha reduced the density of stem borer, *S. incertulas*.Regarding silica content in treated plants, the plants treated with calcium silicate 200kg/ha with 0.25% foliar spray of SMS recorded maximum silica content (11.74%) followed by calcium silicate 150kg/ha with foliar spray of 0.25% SMS (10.93%) and calcium silicate 200kg/ha (10.73%). While comparing the basal application and foliar spray, foliar spray of 0.25% SMS was found to be on par with rice straw 2.5t/ha along with SSB 2kg/ha. The silica content recorded in the untreated check was 4.57 per cent. The presence of high silicon content was negatively correlated with the incidence of stem borer (r =-0.93424).

This is in consonance with findings of Ukwungwu and Odebiyi (1985) who recorded a negative correlation between percentage of silicon content in rice varieties and the percentage of stems bored by African striped borer, *Chilo zacconius* (Bleszynski) and the number of living larvae per plant. When the effect of Si fertilization on Si content of plants and penetration time of yellow stem borer larvae in rice plants grown in nutrient solution was studied, the penetration time of first instar increased (IRRI, 1990). Silica concentration was increased in rice stems as Si content of soil was increased which resulted in roughening of the stems and consequently inhibiting the feeding of rice stem borer larvae (Liang, 1998). Similarly Chandramani (2003) reported a reduction in stem borer damage due to increased silicon content by application of lignite fly ash and various soil amendments. The application of FYM, biofertilizers either with or without lignite fly ash and neem cake applied in splits was highly effective in reducing yellow stem borer damage in all growth stages of MDU5 in Tamil Nadu. The results of the current study are in agreement with those of Saeb and Oskou (2004).

The present study is supported by Ranganathan *et al*. (2006) in Hyderabad who reported that the addition of silicon led to reduction of damage due to yellow stem borer and this could be due to a lower preference as well as digestibility of the leaves and straw by the insect owing to the presence of higher silicon content. This is in confirmation with the finding of Voleti *et al*. (2008) who suggested that due to the application of silica nutritions on rice, stem borer damage was significantly reduced and this enhances the solubilization of silica by 3-5-fold as indicated by the augmented silicic acid present in stem of the rice plant and that of silica in rice leaves. Similarly Arivuselvi (2014) confirmed that rice infestation with rice stem borer (*Scirpophaga incertulas*) can be reduced by the basal application of sodium meta silicate 2t/ha and rice straw 5t/ha.This is again in consonance with finding of Djamin and Pathak (1967) who reported that the larvae of the stem borer *Chilo supressalis* fed on plants with high silicon content had their mandibles damaged. This is in agreement with finding of Savant *et al.* (1997) who stated that rice nurseries fertilized with silicon using ashes of rice husk as source of this element showed lower number of plants with "dead heart" caused by the stem-borer on the cultivar Jaya after transplantation.

The analysis of Polyphenol oxidase (PPO) in the treated plants revealed that the plants applied with calcium silicate 200kg/ha with foliar spray of 0.25% of SMS recorded maximum PPO content (55.38 Δ_{495nm} /mg^{-1} g^{-1}) followed by calcium silicate 150 kg/ha with foliar spray of 0.25% SMS where PPO content recorded was 55.98 Δ_{495nm} /mg^{-1} g^{-1}. The next effective treatment was basal application of calcium silicate 200kg/ha where the PPO content recorded was 42.95Δ_{495nm} /mg^{-1} g^{-1}. While comparing the basal application, basal application of calcium silicate 100 kg/ha (39.43Δ_{495nm} /mg^{-1} g^{-1}) was found to be on par with rice straw 5t/ha along with SSB 2kg/ha (38.84Δ_{495nm} /mg^{-1} g^{-1}). The presence of high polyphenol oxidase activity (r = -0.62504) was negatively correlated with the incidence of stem borer.

The analysis of Phenylalanine ammonia lyase (PALase) in the treated plants revealed that the plants treated with calcium silicate 200kg/ha with foliar spray of 0.25 % of SMS recorded maximum PALase content of 70.38 Δ_{290nm} /µmol m^{-1} ml^{-1} gm^{-1} followed by calcium silicate 150kg/ha with foliar spray of 0.25% SMS where PALase content recorded was 70.98 Δ_{290nm} /µmol m^{-1} ml^{-1} gm^{-1}. The next effective treatment was basal application of calcium silicate 200kg/ha where the PALase content recorded was 57.95Δ_{290nm} /µmol m^{-1} ml^{-1} gm^{-1}. When comparing basal application of organic and inorganic sources of silica, basal application of calcium silicate 100kg/ha (54.43 Δ_{290nm} / µmol m^{-1} ml^{-1} gm^{-1}) was found to be on par with rice straw 5t/ha along with SSB 2kg/ha (53.84 Δ_{290nm} /µmol m^{-1} ml^{-1} gm^{-1}). The presence of high phenylalanine ammonia lyase activity was negatively correlated with stem borer incidence (r = -0.73367).The PPO and PALase activities were negatively correlated with insect incidence. This is in line with findings of Ma (2004) who demonstrated that silicon application changed the activities of antioxidant enzymes such as POD and SOD and Si nutrition increased lignin content and enhanced activities of peroxidase, polyphenol oxidase and phenylalanine ammonia lyase (PAL) in rice leaves exposed to rice pests. The silica content was significantly high in calcium silicate 200kg/ha with foliar spray of 0.25% SMS treated plants followed by calcium silicate 150kg/ha with foliar spray of 0.25% SMS treated plants.

To conclude, this study clearly indicated that enhanced silica, PPO and PALase activity in rice plants due to the basal application of calcium silicate 200kg/ha with foliar spray of 0.25% SMS led to the reduction of dead heart and white ear damage thus imparting induced resistance particularly systemic acquired resistance.

REFERENCES

1. Anderson, D.L and O. Sosa. 2001. Effect of silicon on expression of resistance to sugarcane borer (*Diatraea saccharalis*). J. American Soc. Sugar Cane Technol., 21: 43 -50.
2. Arivuselvi, A. 2014. Silicon induced resistance against major insect pests of rice. M.Sc. (Ag.) Thesis, TNAU, Madurai
3. Catindig, J.L. A and H.L. Heong. 2003. Rice doctor. Manila (Philippines): International Rice Research Institute.
4. Chandramani, P. 2003. Studies on the induced resistance through organic sources of nutrition to major insect pests of rice. Ph.D.Thesis,Tamil Nadu Agricultural University, Coimbatore.
5. Djamin, A and M.D. Pathak. 1967. Role of silica in resistance to Asiatic rice borer, *Chilo suppressalis* (Walker) in rice varieties. J. Econ. Entomol., 60: 347-351.
6. Gomez, K.A and A.A.Gomez. 1985. *Statistical Procedures for Agricultural Research* John wiley and sons. New York. 650p.
7. International Rice Research Institute (IRRI). 1990. Programme report for 1989. Los Banos,Laguna, Philippines.
8. Liang, Y.C. 1998. Effects of silicon on leaf ultrastructure, chlorophyll content and photo synthetic activity in barley under salt stress. Pedosphere 8 (4) : 289 - 296.
9. Maxwell, F. G., J. N. Jenkins and W. L. Parroot. 1972. Resistance of plants to insects. Advan. Agron., 24: 187 - 265.
10. Panda, N., B Pradhan, A. P. Samalo and P. S. P. Rao. 1977. Note on the relationship of some biochemical factors with resistance in rice varieties to yellow borer. Indian J. Agric. Sci., 45: 499-500.
11. Ram Prasad, B., Vidya Sagar Singh and Subhash Chander. 2010. Role of silica in varietal resistance against rice leaf folder, *Cnaphalocrocis medinalis* (Guenee). Indian J. Entomol., 72(3): 196 - 197.
12. Ranganathan, S., V. Suvarchala, Y.B.R.D. Rajesh, M. Srinivasa Prasad, A. Padmakumari and S.R. Voleti. 2006. Effects of silicon sources on its deposition, chlorophyll content and disease and pest resistance in rice. Biologia Plantarum, 50 (4): 713 - 716.
13. Sadasivam, S and A. Manickam. 1992. *Biochemical Methods for Agricultural Sciences*. Wiley Eastern Limited New Delhi and TNAU Coimbatore, pp106-107.
14. Saeb, H and T. Oskou. 2004. Study of effective factors on resistance of rice cultivars to rice stem borer. Iranian Rice Research Institute Press, 40p.
15. Savant N.K., G.H. Snyder, L.E. Datnoff. 1997. Silicon management and sustainable rice production. Adv. Agron., 5 : 99.

16. Singh UP, Prithviraj B. 1997. Neemazal, a product of neem (*Azadirachta indica*) inducers resistance in pea (*Pisum sativum*) against *Erysiphae pisi*. Phys. Mol. Plant Pathol., 51: 181-194.
17. Subbarao and Perraju. 1976. Resistance in some rice strains to first instar larvae of *Tryporyza incertilas* (Walk.) in relation to plant nutrients and anatomical structure of the plants. IRRN., 1(1):14-15.
18. Tayabi, K and P. Azizi. 1984. Influence of silica on rice yield and stem-borer in Rash Iran. Pesticides, 18: 20-22.
19. Ukwungwu, M.N and J.A. Odebiyi. 1985. Resistance of some rice varieties to the African striped borer, *Chilo agamemnon* Bleszynski. Insect Sci. App., 6 (59) :873-907.
20. Ukwungwu, M.N and J.A. Odebiyi. 1985. Resistance of some rice varieties to the African striped borer, *Chilo agamemnon* Bleszynski. Insect Sci. App., 6 (59) :873-907.
21. Voleti, S.R., A.P. Padmakumari, V.S. Raju, Setty Mallikarjuna Babu, Subramania Ranganathan. 2008. Effect of silicon solubilizers on silica transportation, induced pest and disease resistance in rice (Oryza sativa L.). Crop protection, 27 : 1398– 1402
22. Widawsky, D., S. Rozella, S. Jin and J.K. Huang. 1998. Pesticide productivity, host plant resistance and productivity in China. Agric. Econ., 19: 203-217.
23. Zhang, c., wang, L., Nie, Q., Zhang, W. and Zhang, F. 2008. Long term effect of exogenous silicon on cadmium translocation and toxicity in rice (*Oryza sativa* L.). Environ. Exp. Bot. 62:300-307.

Table 1 : Effect of silicon on rice stem borer and physiological factors in rice plants

S.No	Treatments	Stem borer incidence (% damage)		Physiological factors		
		Mean	% reduction over control	Silicon content (%)	PPO (Δ_{495nm} / mg^{-1} g^{-1})	PALase (Δ_{290nm} /µmol m^{-1} ml^{-1} gm^{-1})
1.	Rice straw 2.5 t/ ha + SSB 2kg / ha	5.93 $(14.09)^{h}$	37.87	6.74 $(15.04)^{gh}$	27.98 $(5.29)^{f}$	44.93 $(6.70)^{f}$
2.	Rice straw 5t/ha + SSB 2kg/ha	5.96 $(14.13)^{h}$	37.58	6.40 $(14.65)^{h}$	38.84 $(6.23)^{c}$	53.84 $(7.34)^{c}$
3.	Basal - calcium silicate 50 kg/ha	4.65 $(12.45)^{f}$	51.28	7.65 $(16.05)^{f}$	34.64 $(5.89)^{e}$	49.64 $(7.05)^{d}$
4.	Basal - calcium silicate 100 kg/ha	4.8 $(12.65)^{f}$	49.71	8.66 $(17.11)^{e}$	39.43 $(6.28)^{c}$	54.43 $(7.38)^{c}$
5.	Basal - calcium silicate 150 kg/ha	4.02 $(11.56)^{e}$	57.89	9.64 $(18.08)^{c}$	28.13 $(5.30)^{f}$	43.13 $(6.57)^{f}$
6.	Basal - calcium silicate 200 kg/ha	3.19 $(10.28)^{c}$	66.59	10.73 $(19.11)^{b}$	42.95 $(6.55)^{b}$	57.95 $(7.61)^{b}$
7.	Foliar spray of 0.25 % sodium meta silicate	5.04 $(12.97)^{g}$	47.22	6.86 $(15.18)^{g}$	33.95 $(5.83)^{e}$	48.95 $(7.00)^{e}$
8.	$T_3 + T_7$	3.65 $(11.01)^{d}$	61.71	9.28 $(17.72)^{d}$	35.08 $(5.92)^{e}$	50.08 $(7.08)^{d}$
9.	$T_4 + T_7$	3.69 $(11.07)^{d}$	61.29	9.9 $(18.33)^{c}$	37.13 $(6.09)^{d}$	52.13 $(7.22)^{d}$
10.	$T_5 + T_7$	2.87 $(9.75)^{b}$	69.97	10.93 $(19.29)^{b}$	55.98 $(7.48)^{a}$	70.98 $(8.42)^{a}$
11.	$T_6 + T_7$	2.48 $(9.06)^{a}$	73.98	11.74 $(20.03)^{a}$	55.38 $(7.44)^{a}$	70.38 $(8.39)^{a}$
12.	Untreated check	9.54 $(17.99)^{i}$	-	4.57 $(12.34)^{i}$	22.67 $(4.76)^{g}$	37.67 $(6.14)^{g}$
	SEd	0.15		0.18	0.05	0.09
	CD (0.05)	0.32		0.39	0.10	0.18

*Mean of three replications and four observations: DAT- Days after transplanting. Values in parenthesis are arc sine transformation In a column, mean followed by same letters are not significantly different at P = 0.05 as per LSD

Table: 2- Effect of silica nutrition against stem borer, Scirpophaga incertulas in rice – Field Experiment

Treatments details		Stem borer incidence (% damage)*				Mean	% reduction over control
		45 DAT	60 DAT	75 DAT	90 DAT		
T_1	Rice straw 2.5 t/ ha + SSB 2kg / ha	5.82 (13.96)^{f}	7.76 (16.17)^{g}	5.17 (13.14)^{g}	4.96 (12.86)^{h}	5.93 (14.09)^{h}	37.87
T_2	Rice straw 5t/ha + SSB 2kg/ha	5.98 (14.15)^{f}	6.81 (15.12)^{f}	5.88 (14.03)^{h}	5.15 (13.11)^{i}	5.96 (14.13)^{h}	37.58
T_3	Basal - calcium silicate 50 kg/ha	4.75 (12.58)^{e}	5.36 (13.38)^{d}	4.36 (12.05)^{e}	4.12 (11.71)^{f}	4.65 (12.45)^{f}	51.28
T_4	Basal - calcium silicate 100 kg/ha	4.93 (12.82)^{e}	5.48 (13.53)^{d}	4.54 (12.30)^{e}	4.24 (11.88)^{f}	4.8 (12.65)^{f}	49.71
T_5	Basal - calcium silicate 150 kg/ha	3.87 (11.34)^{d}	4.82 (12.68)^{c}	3.92 (11.41)^{c}	3.46 (10.72)^{e}	4.02 (11.56)^{e}	57.89
T_6	Basal - calcium silicate 200 kg/ha	3.26 (10.40)^{c}	4.24 (11.88)^{b}	3.07 (10.09)^{a}	2.18 (8.49)^{c}	3.19 (10.28)^{c}	66.59
T_7	Foliar spray of 0.25 % sodium meta silicate	4.87 (12.74)^{e}	5.84 (13.98)^{e}	4.86 (12.73)^{f}	4.57 (12.34)^{g}	5.04 (12.97)^{g}	47.22
T_8	$T_3 + T_7$	3.26 (10.40)^{c}	5.01 (12.93)^{c}	4.12 (11.71)^{d}	2.22 (8.56)^{c}	3.65 (11.01)^{d}	61.71
T_9	$T_4 + T_7$	3.19 (10.28)^{c}	4.88 (12.76)^{c}	3.76 (11.18)^{c}	2.94 (9.87)^{d}	3.69 (11.07)^{d}	61.29
T_{10}	$T_5 + T_7$	1.84 (7.79)^{b}	4.38 (12.08)^{b}	3.28 (10.43)^{a}	1.96 (8.04)^{b}	2.87 (9.75)^{b}	69.97
T_{11}	$T_6 + T_7$	1.42 (6.84)^{a}	3.74 (11.15)^{a}	2.98 (9.94)^{a}	1.79 (7.68)^{a}	2.48 (9.06)^{a}	73.98
T_{12}	Untreated check	8.36 (16.80)^{g}	10.57 (18.97)^{h}	9.87 (18.31)^{i}	9.36 (17.81)^{j}	9.54 (17.99)^{i}	-
	SEd	0.14	0.12	0.16	0.10	0.15	
	CD (0.05)	0.30	0.26	0.33	0.21	0.32	

Indian Journal of Natural Sciences www.tnsroindia.org.in ©IJONS

Vol.9 /Issue 51 / December / 2018 *International Bimonthly* *ISSN: 0976 – 0997*

RESEARCH ARTICLE

Rainwater Harvesting (RWH) in Maidan Sub-Catchment NE Dayala by RS Techniques

Saad Hashim Saeed[1]* and Mustafa Ali Hassan[2]

[1]Department of Geology, College of Science, University of Baghdad, Baghdad, Iraq.
[2]Unit of Remote Sensing, College of Science, University of Baghdad, Baghdad, Iraq.

Received: 10 Aug 2018 Revised: 13 Sep 2018 Accepted: 16 Oct 2018

***Address for Correspondence**
Saad Hashim Saeed
Department of Geology,
College of Science,
University of Baghdad,
Baghdad, Iraq.

ABSTRACT

Remote sensing techniques can be used to calculation runoff and monitor the pleases to harvesting water by many steps using in this study. It starts by compiling the climate data from NOAA satellites to calculate the annual and daily rainfall rate. make a supervised classification to study area by using landsat-8 images and extract them LULC & HSG to calculate runoff by SCS method. Determining the area for the construction of the check dam according to the conditions and scientific foundations placed to rainwater harvesting. The results show that the average annual rainfall is equal 406.3 mm with annual runoff 2457911.5 m3, According to calculations in this study the amount of annual rainfall will cover about 3473775 m2 with 17 m water depth if this check dam was established.

Key words : Remote, techniques, study, calculations, annual, rainfall.

INTRODUCTION

Ancient evidence of the use of rainwater harvesting (RWH) techniques has been found in many countries around the world, including Jordan, Palestine, Syria, Tunisia, and Iraq (Al-Adamat, 2008). Critchley, Siegert, and Chapman (1991) defined RWH as the collection of runoff for productive use. (Mekdaschi & Liniger, 2013) Said " the collection and management of flood water or rain water runoff to increase water availability for domestic and agricultural use as well as ecosystem sustenance ". The main role of RWH is to increase the amount of available water by capturing rain water in one area for local use or for transfer to another area. All water harvesting systems consist of the following components (Oweis et al., 2012): A catchment : the part of an area from which some of the rainfall is harvested. It is also known as a runoff area .This area can be a few square meters to several square kilometers in size and may be agricultural, rocky, a paved road, or a rooftop.

Storage facility :the area that holds the harvested runoff water until used for crops, animals, or people. Water can be stored above ground (e.g. reservoirs or ponds), in the soil profile, and in under ground storage containers (e.g. cisterns). Target : the end point of a water harvesting system, where the harvested water is used for crop production or domestic use.The Soil Conservation Service (SCS) method is the most widely used approach for estimating surface runoff from small catchments after a rainfall event (Gupta etal.,1997). It considers the relationship between land cover and hydrologic soil group, which together make up the curve number (Kadam et al., 2012). With this approach, the suitable locations for RWH structures were located in areas with the highest capacity for runoff generation and nearby to existing drainage lines. The WH structure suggested in this study is Check dams that are small barriers built across the direction of water flow on shallow rivers and streams for the purpose of water harvesting (Vashist, 2016). The following criteria have been followed for making decision on selecting suitable site for water harvesting structures (Check dams)

1. The slope should be less than 15 per cent.
2. The land use may be barren, shrub land and riverbed.
3. The infiltration rate of the soil should be less.
4. The type of soil should be sandy clay loam (Bamne, 2014).

Study Area

The study area is located in the north east Dayala governorate (fig. 1), north east Iraq between latitude 34°42'0" – 35°4'0" and longitude 45°26'0" – 45°44'0" . It covers an area of 651.5 km2 which was calculated from GIS with elevation ranges from 250 to 954 m the elevation of the study area decreases from northeast to southwest (fig. 2), The area is bounded by Bammu mountain in east part, Hawasan valley in central, Sirwan river in west part and Qara Dagh anticline in the north..

METHODOLOGY AND RESULTS

Provided a detail of the spatially explicit method and presented suitability map for RWH site in study area. Using DEM (Digital elevation model) with spatial resolution 12.5 m and WMS v. 10.1 software to delineation sub-catchment within study area and calculation depth of water, area of sub-catchment and volume of sub-catchment if constriction check dams in selection point showed in (Table 1) (Fig. 3&4), and using climatic data from NOAA satellites to calculation average of rainfall and runoff by SCS method in area study for the period (1997-2014).

Image classification

For got SCS and LULC maps must be make supervised classification for image by using MLC method or other method, Image classification is the process of assigning land cover classes to pixels. In supervised classification, select representative samples for each land cover class. The software then uses these “training sites” and applies them to the entire image. Supervised classification uses the spectral signature defined in the training set. For example, it determines each class on what it resembles most in the training set. The common supervised classification algorithms are maximum likelihood classification (MLC). Use False color in this classification (landsat 8 RGB 5,7,1) because this band combination is good for discerning variations in a landscape that does not contain an abundance of vegetation. It is good for geologic applications. This band combination makes use of the NIR, SWIR2, and Coastal Aerosol bands, respectively. The Coastal Aerosol band is unique to Landsat 8 and is used primarily to track one particles like dust and smoke, and also to peer into shallow water. With this color combination, vegetation appears orange (peters, 2015).

This classification was done using satellite images in addition to the geological map of the study area, According to this classification the area of water in the region is about 10 km2, while the area of Vegetation is about 173 km2 , urban 6 km2 and other classes cover 472 km2 (fig. 5).

Hydrological soil group (HSG)

From MLC and according to (tables 2&3) can selection type of hydrological soil (fig.6).

Land Use/ Land Cover (LULC)

The world "Land" has more than one meaning the most agreeable one is: an area of the earth surface, the characteristics of which embrace all reasonably stable or predictably cyclic attributes of the biosphere vertically above and below this area including those of the atmosphere, the soil and underlying geology, the hydrology, the plant and animal populations, and the results of past and present human activity to the extent that these attributes exert a significant influence on present and future uses of the land by man (FAO (1976)). Land use/land cover change is a key driver of global change (Vitousek, 1992), from MLC we can classification done of LULC map (fig. 7).

The SCS Runoff Curve Number

The Soil Conservation Service (SCS) model developed by United States Department of Agriculture (USDA) computes direct runoff through an empirical equation that requires the rainfall and a watershed coefficient as inputs. The watershed coefficient is called as the curve number (CN), which represents the runoff potential of the land cover soil complex. This model involves relationship between land cover, hydrologic soil class and curve number.

The method is based on an assumption of proportionality between retention and runoff in the form. Normally the SCS model computes direct runoff with the help of following relationship.

$S = (24500/CN) - 254$ ..... (1)
$Q = ((P - 0.2S)^2)/(P + 0.8S)$ ..... (2)
Where, **$CN = (\Sigma (CNi * Ai))/A$ .....(3)**
CN = weighted curve number.
CNi = curve number from 1 to any no. N.
Ai = area with curve number CNi
where CN is the runoff curve number of hydrologic soil cover complex, which is a function of soil type, land cover and antecedent moisture condition (AMC), Q: actual direct runoff, mm; P: total storm rainfall, mm; and S: the potential maximum retention of water by the soil, mm or reservoir capacity (Hand book of Hydrology, 1972).

By using intersect tool in ArcGIS v. 10.5 software between HSG & LULC we got to (Table 3) to calculation CN and runoff by AMC methd. Three basic requirements if we want application of Soil Conservation Service Curve Number method (NRCS – CN) model are land use and land cover, hydrologic soil group and Antecedent moisture conditions (AMC) which It is an indicator of watershed wetness and availability of soil moisture storage prior to a storm and can have a significant effect on runoff volume (Al-Jabari, 2007). The Soil Conservation Service Curve Number (SCS-CN) method is widely used to compute direct surface runoff (or rainfall-excess) from rainfall events using curve number derived from watershed characteristics and 5-day antecedent rainfall (Jain and et al, 2006) . Antecedent moisture condition (AMC) is an indicator of wetness and soil moisture availability prior to the storm which has a significant effect on runoff volume. Three types of AMC conditions were present in SCS based on rainfall magnitude of previous five days and season. Different types of AMC are given in Table **(**Joy, 2016) Table shows seasonal rainfall limits for three AMC conditions in the (NRCS – CN) method, the values of CN is estimated for AMC-II. The following equations are used to adjust the CN for other two AMC (Chow et al., 2002):

$$CNI = \frac{4.2 * \text{CNII}}{10 - (0.058 * \text{CNII})}$$

$$CNIII = \frac{23 * \text{CNII}}{10 + (0.13 * \text{CNII})}$$

By applying equations above and Runoff occurs only when P > 0.2 S we got on :

P>0.2S	S	CN	CN TYPE	AMC
17.20	85.98	74.71	CNI	AMC I
7.22	36.11	87.55	CNII	AMC II
3.14	15.70	94.18	CNIII	AMC III

Estimating runoff volume

The rainfall data and the result of surface runoff for the water years (1997- 2014) in the study area are tabulated in (table 6) . As a result of the calculation, it is found that the average annual surface runoff depth is equal to 43.5 mm multiplied by the area of the study (651.5 km2) giving the total average volume of runoff, Average of runoff of sub-catchment equal about 2457911 m3 which mean the annual rainfall will cover 16 m depth and the area of water about 2977406 m2 with 294 m elevation above sea level if constriction check dam in selection point.

CONCLUSION AND DISCUSSION

The classification was done using satellite images in addition to the geological map of the study area, According to this classification the area of water in the region is about 10 km2, while the area of Vegetation is about 173 km2 , urban 6 km2 and other classes cover 472 km2. According to the USDA soil classification system, four hydrological soil groups are recognized: A, B, C, and D with 20%, 4%, 45%, and 31 %, respectively, the high percentage extension of moderately infiltration group (A,B and C). Four land use/ land cover classes are recognized: The first part of LULC is Water (10.2km2), the second part is Agriculture and forest (190.5 km2), the third part is urban (6.5 km2) and the fourth part is Barren land (443 km2). The application of the soil conservation service curve number method (SCS-NC) method showed that the average annual surface runoff depth was 43.5mm. Multiply this figure with surface area of the study area gives 2457911.5m3 as runoff volume.Average of runoff of sub-catchment equal about 2457911 m3 which mean the annual rainfall will cover 16 m water depth and the area of water about 2977406 m3 with 294 m elevation above sea level if constriction check dam in selection point but if we need dam with 305 m elevation we need 11333129 m3 with 28 for (H) sa showed in (table1).

REFERENCES

1. Al-Adamat, R. (2008). GIS as a decision support system for siting water harvesting ponds in the Basalt Aquifer/NE Jordan. Journal of Environmental Assessment Policy and Management, 10(02), 189–206.
2. Al-Jabari, S. J., 2007. Estimation of runoff for agricultural watershed using SCS curve number and GIS, Master thesis, Birzeit University, Palestine, 91p.
3. Bamne Y., Patil K. A., Vikhe S. D.: Selection of Appropriate Sites for Structures of Water Harvesting in a Watershed using Remote Sensing andGeographical Information System: International Journal of Emerging Technology and Advanced Engineering, Volume 4, Issue 11, 270-275(2014).
4. Chow, V. T., Maidment, D. K., and Mays, L. W., 2002. Applied Hydrology, McGrow-Hill Book Company, New York, USA. 588p.

5. FAO. 1976. A framework for land evaluation. FAO Soils Bulletin 32 . FAO, Rome.
6. Gupta, K.K., Deelstra, J., & Sharma, K.D. (1997). Estimation of water harvesting potential for a semiarid area using GIS and remote sensing. IAHS Publications- Series of Proceedings and Reports-Intern Assoc Hydrological Sciences, (pp.63), 242.
7. Joy Rajbanshi, Estimation of Runoff Depth and Volume Using NRCS-CN Method in Konar Catchment (Jharkhand, India), Journal of Civil & Environmental Engineering, May 14, 2016; Accepted date: May 30, 2016; Published date: May 31, 2016.
8. Kadam, A.K., Kale, S.S., Pawar, N.J., Sankhua, R.N., & Pawar, N.J. (2012). Identifying potential rain water harvesting sites of a semiarid, basalticregion of Western India, using SCS-CN method. Water Resource Management, 26(9), 2537–2554.
9. Mekdaschi, S., R., &Liniger, H.(2013). Water harvesting : guide line stogood practice. Centre for Development and Environment(CDE), Bern; Rain water Harvesting Implementation Network(RAIN), Amsterdam; MetaMeta, Wageningen (p. 210) Rome: The International Fundfor Agricultural Development(IFAD).
10. Oweis, T.Y., Prinz, D., & Hachum, A.Y.(2012). Rain water harvesting for agriculture in the dry areas (p. 262) London, UK: CRC Press.
11. Petters joe, The Many Band Combinations of Landsat-8, Harris geospatial solution, 29, 2015. 36694.
12. Vashist, 2016 ; CHECK DAM ; A TOOL FOR SUSTAINABLE DEVELOPMENT, THE MONTHLY NEWS LETTER ON ISSUES OF SUSTAINABLE DEVELOPMENT

Table 1 : showed change of information sub-catchment with deferent depths

A (m2)	ΔA (m2)	ΔV (m3)	H (m)	H (m)	V (m3)	Z (m)
8741	15557	13379	0.86	1	10171	**278.3**
24298	21208	18239	0.86	2	23550	**279.1**
45506	26503	23057	0.87	3	41789	**280.0**
72009	35184	30258	0.86	3	64846	**280.9**
107192	46623	40095	0.86	4	95104	**281.7**
153815	63528	54634	0.86	5	135200	**282.6**
217343	82898	71293	0.86	6	189834	**283.4**
300242	98082	84350	0.86	7	261127	**284.3**
398324	115768	100718	0.87	8	345477	**285.2**
514091	140132	120514	0.86	9	446195	**286.0**
654223	162348	139620	0.86	9	566709	**286.9**
816572	190656	163964	0.86	10	706328	**287.7**
1007227	221961	190886	0.86	11	870292	**288.6**
1229188	262785	225995	0.86	12	1061178	**289.5**
1491973	307122	264125	0.86	13	1287173	**290.3**
1799096	342450	297932	0.87	14	1551299	**291.2**
2141546	391721	336880	0.86	15	1849230	**292.1**
2533267	444139	381960	0.86	16	2186110	**292.9**
2977406	496369	426877	0.86	16	2568070	**293.8**

3473775	545595	469212	0.86	17	2994947	**294.6**
4019370	595116	511799	0.86	18	3464159	**295.5**
4614485	637486	554612	0.87	19	3975958	**296.4**
5251971	690875	594152	0.86	20	4530571	**297.2**
5942846	733873	631131	0.86	21	5124723	**298.1**
6676718	775787	667177	0.86	22	5755854	**298.9**
7452506	818430	703850	0.86	22	6423031	**299.8**
8270936	865842	744624	0.86	23	7126881	**300.7**
9136778	921665	792632	0.86	24	7871505	**301.5**
10058443	969965	843870	0.87	25	8664137	**302.4**
11028408	1033877	889134	0.86	26	9508007	**303.3**
12062285	1088359	935989	0.86	27	10397141	**304.1**
13150644	1150478	989411	0.86	28	11333129	**305.0**
14301122	1213637	1043728	0.86	28	12322540	**305.8**
15514759	1284115	1104339	0.86	29	13366268	**306.7**
16798874	1343510	1168853	0.87	30	14470607	**307.6**
18142383	1437055	1235867	0.86	31	15639460	**308.4**
19579438	1515458	1303294	0.86	32	16875327	**309.3**
21094896	1590804	1368091	0.86	33	18178621	**310.1**

Table 2 : SCS Hydrologic soil group (USDA,1986)

Soil group	Description	Final infiltration rate (mm)
A	Lowest runoff potential. Includes deep sands with very little silt and clay, also deep, rapidly permeable loess.	8-1
B	Moderately low runoff potential. Mostly sandy soils less deep than A, and less deep or less aggregated than A, but the group as a whole has above-average infiltration after thorough wetting.	4-8
C	Moderately high runoff potential. Comprises shallow soils and soils containing considerable clay and colloids, though less than those of group D. The group has below – average infiltration after pre saturation.	1-4
D	Highest runoff potential: Includes mostly clays of high selling percent, but the group also includes some shallow soils with nearly impermeable sub horizons near the surface.	0-1

Table 3 : Caculation of CN For study area

CN*AREA	AREA	CN	SOIL GROUP	LULC
506.70	6.58057	77	A	BARREN LAND
0.47	0.00550	86	B	
3434.61	37.74298	91	C	
12.69	0.13498	94	D	
0.33	0.00675	49	A	AGRICULTURE & FOREST
40.41	0.58565	69	B	
8.16	0.10334	79	C	
937.61	11.16202	84	D	
7.81	0.20020	39	A	URBAN
0.01	0.00023	61	B	
0.01	0.00018	74	C	
1.57	0.01967	80	D	
0.18	0.00179	100	C	WATER
4950.58	56.54			

Table 4 : showed CN values for each HSG with Land cover (USDA)

Land Cover	Hydrologic Soil Group			
	A	B	C	D
11 – Open Water	100	100	100	100
12 – Perennial Ice and Snow	100	100	100	100
21 – Developed, Open Space	39	61	74	80
22 – Developed, Low Intensity	57	72	81	86
23 - Developed, Medium Intensity	59	82	87	90
24 - Developed, High Intensity	61	92	94	95
31 - Barren Land	77	86	91	94
41 - Deciduous Forest	36	60	73	79
42 - Evergreen Forest	36	60	73	79
43 - Mixed Forest	36	60	73	79
52 - Scrub/Shrub	35	56	70	77
71 - Grassland/Herbaceous	49	69	79	84
81 - Pasture/Hay	49	69	79	84
82 - Cultivated Crops	70	80	86	90
90 - Woody Wetlands	36	60	73	79
95 - Emergent Herbaceous Wetland	49	69	79	84

Table 5: Different antecedent moisture condition.

AMC	**Total Rain in Previous 5 days**
I	Less than 12.7mm
II	12.7 to 27.9 mm
III	More than 27.9 mm

Table 6 : showed averages of runoff and rainfall of sub-catchment for (1997-2014) period

YEARS	Total rainfall (mm)	Total runoff (mm)	Runoff volume (m3)
1997	465.8	31.3	1769648.0
1998	477.5	67.6	3816268.8
1999	323.0	14.3	807296.0
2000	394.7	41.0	2314942.6
2001	324.4	37.6	2131454.5
2002	543.7	99.4	5613663.2
2003	512.5	79.3	4474703.0
2004	449.5	92.5	5224390.3
2005	435.1	61.8	3489028.8
2006	541.4	95.1	5365936.1
2007	360.3	29.0	1634455.7
2008	307.5	8.3	470626.7
2009	386.5	29.8	1683674.1
2010	316.7	16.0	900564.7
2011	353.5	23.8	1342217.9
2012	396.8	22.5	1271189.1
2013	377.9	26.7	1507655.8
2014	346.3	7.5	424692.2
Average	406.3	43.5	2457911.5

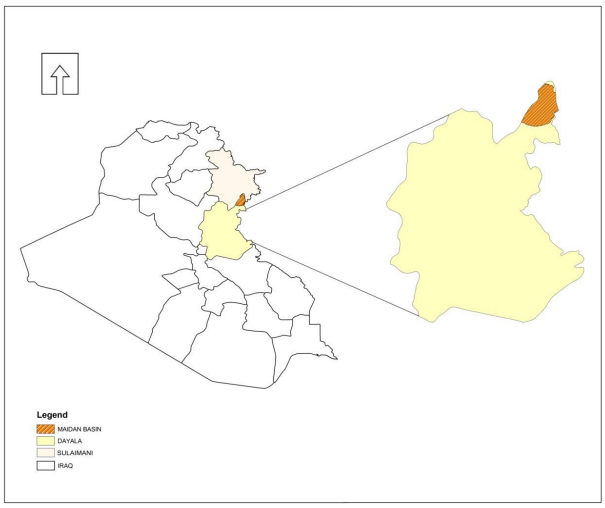

Fig. 1 : Location of study area

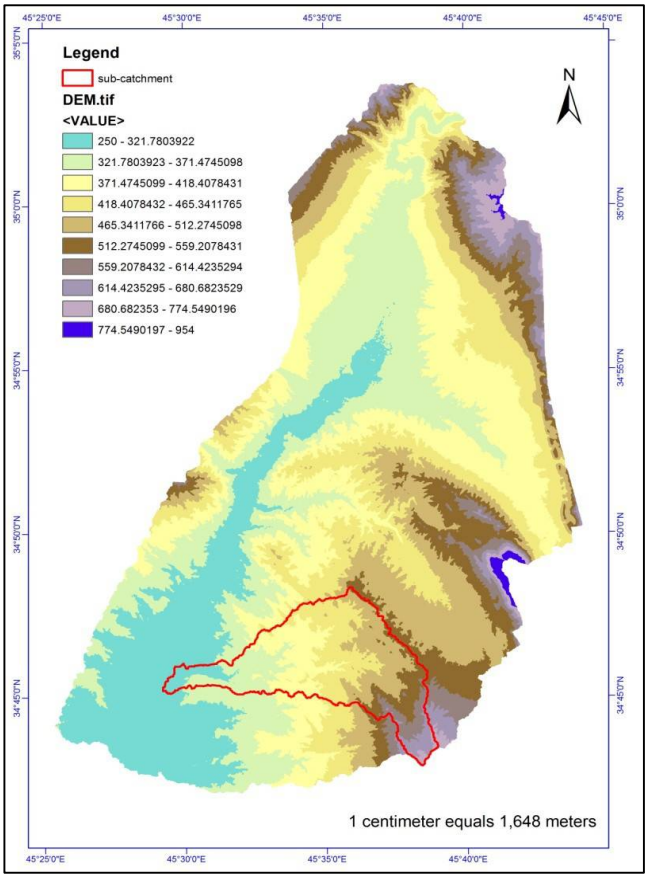

Fig. 2 : Elevations of area study area (DEM) with sub-catchment within study

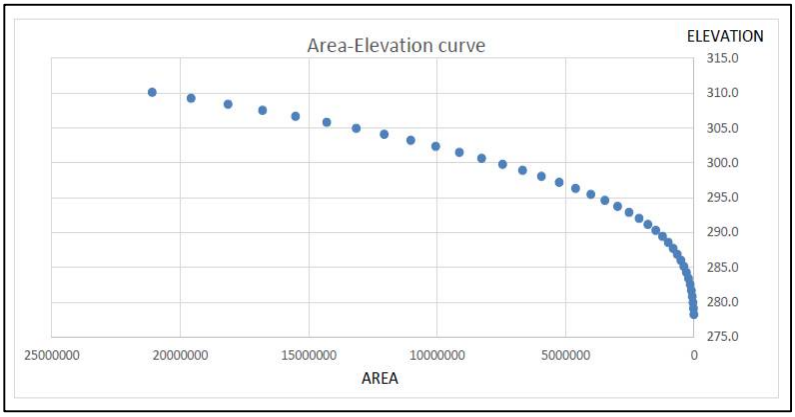

Fig.3 : curve showed the relationship between area and elevation

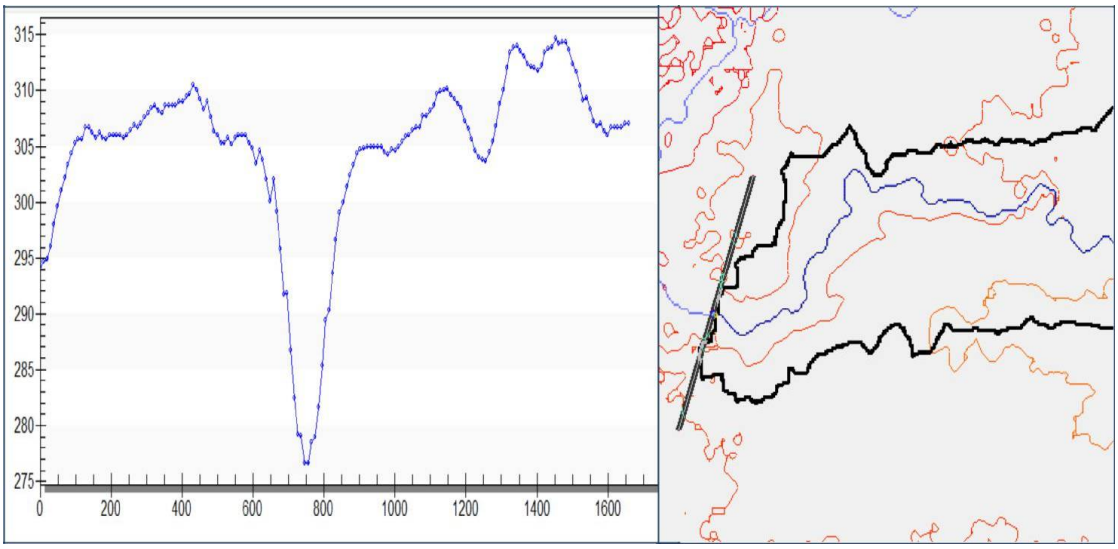

Fig. 4 : Cross section for head of sub-catchment (check dam place)

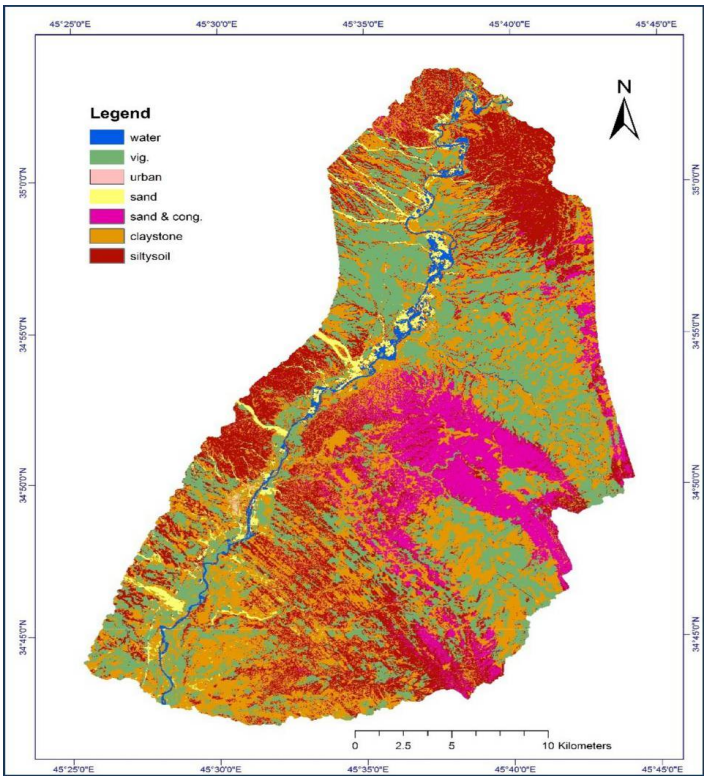

Fig. 5 : MLC of study area

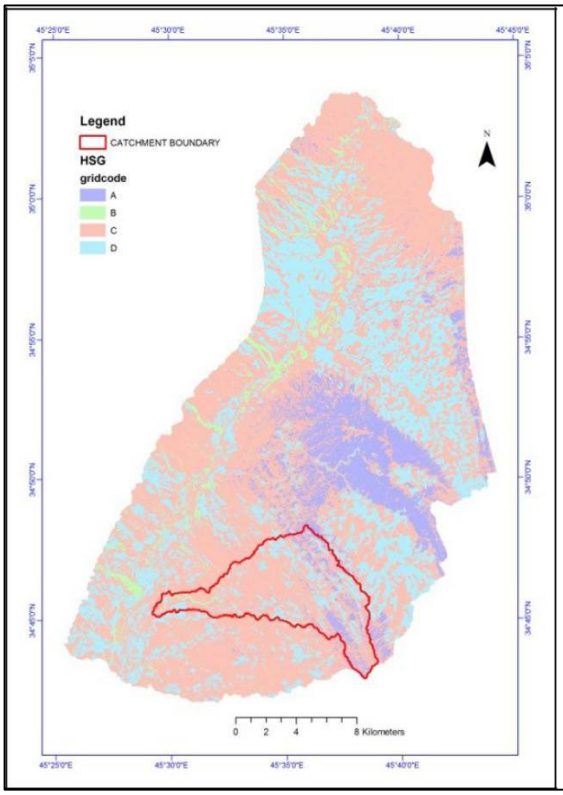

Fig. 6 : HSG for sub-catchment

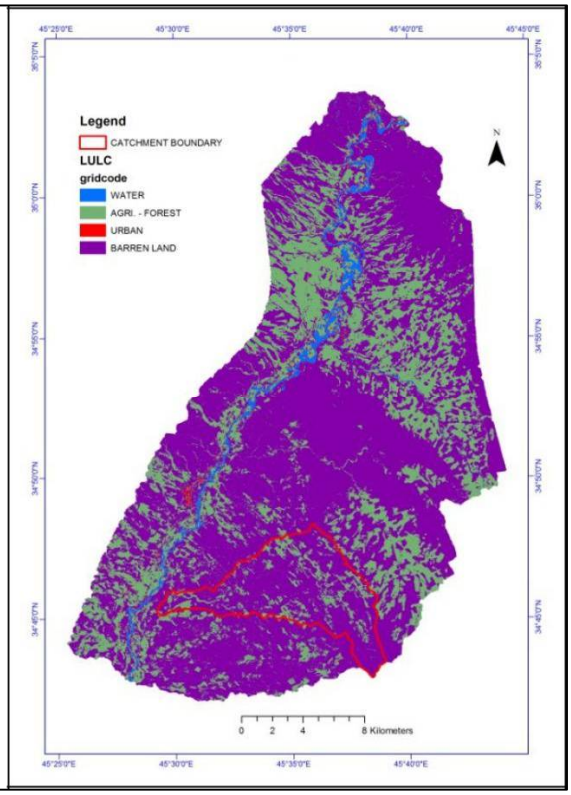

Fig. 7 : LULC for sub-catchment

Indian Journal of Natural Sciences www.tnsroindia.org.in ©IJONS

Vol.9 /Issue 51 / December / 2018 *International Bimonthly* *ISSN: 0976 – 0997*

RESEARCH ARTICLE

Rearing Practices of Cattle Adopted by Landless Dairy Farmers of Peerumedu, Kerala

S.K. George[1, 2]*, A. Prasad[2], M.T. Dipu[2] and Muhammad Aslam M K[2]

[1]Assistant Professor, Base Farm, Kolahalamedu, Kerala, India.
[2] Kerala Veterinary & Animal Sciences University, Pookode, Wayanad, Kerala, India.

Received: 18 Sep 2018 Revised: 20 Oct 2018 Accepted: 22 Nov 2018

***Address for Correspondence**
S.K. George
Assistant Professor,
Base Farm, Kolahalamedu,
Kerala, India.
Email: skgeorge31@gmail.com

ABSTRACT

The present study was conducted to document the rearing practice of cattle by landless farmers of Peerumedu Taluk in Idukki District. There are reports of a dwarf cattle variety which used to freely graze in large numbers in the grass lands of Peerumade taluk. After the implementation of cross breeding, these cows were reared along with cross bred animals by many farmers of Peerumedu. At present the cattle possessed by landless farmers of the locality are medium sized and the common herd size of a dairy farmer is 6-8. The cattle rearing practice of landless farmers are also unique in its character. The farmers let their cattle for grazing in the grass lands and meadows during day time, after they are milked once in the early morning. The cattle return back to the farmer's yard during late evening in specific herds. This rearing practice often results in inbreeding and thus the maintenance of a greater degree of zebu characteristics. Since these cattle are predominantly maintained by grazing, the rearing practice provides a subsidiary income to the people of the locality and has a major role in the improvement of economic status of landless dairy farmers of the region. However, the presence of feral cattle in the locality poses threat to domesticated animals as they could be carriers of infectious diseases, besides they also compete for the limited forage resources.

Key words: cattle, breeding, farmers, during, animals,

INTRODUCTION

The western region of ancient Tamilnadu (Thamilagam), which includes the present state of Kerala, was once part of Chera kingdom, one of the three Tamil kingdoms. After the fall of Chera empire, several small rulers reigned over this area. Towards the end of 12th century AD, Poonjar Kingdom took control over the area that includes the present day Peerumedu, Devikulam and Udumbanchola taluks of Idduki district and the areas adjoining Gudalur, Cumbam, Uthamapalayam and Bodi taluks of Tamilnadu until the end of 19th Century. A considerable portion of the catchment area of the Mullaiperiyar, where the water is being accumulated and the dam is situated, falls in the Peerumedu taluk. Peerumedu is a hill station which lies 915 metres (3,002 ft) above sea level in the Western Ghats about 85 kilometres east of Kottayam on the way to Thekkady. Peerumedu Taluk includes 10 villages viz Elappara, Kokkayar, Kumily, Manjumala, Mlappara, Peerumedu, Periyar, Peruvanthanam, Upputhara and Vagamon. Cattle rearing provides subsidiary income to landless agricultural labourers residing in the locality. Therefore, a preliminary investigation was conducted in all the villages of Peerumedu Taluk to document the adoption of indigenous rearing practice of cattle by landless farmers.

METHODOLOGY

The investigation was undertaken in ten villages of Peerumedu Taluk of Idukki District. These areas are located at a latitude of 9.5760° N and longitude of 77.0255° E, the altitude range is from 27 to 1200 m above sea level, with an annual rainfall of 2295 mm. All the villages were accessed through main roads and 42 farmers were available for questioning at their homesteads. Observations of the daily management practices of the livestock and the grazing areas were also recorded. The collected data were grouped as follows:

- Number and type of livestock owned
- Management practices (grazing pattern, feeding strategies and general husbandry)
- Breeding practices
- Problems

RESULTS AND DISCUSSION

There are reports of the existence of a native dwarf variety of cattle in Peerumedu Taluk which is termed Highrange dwarf (Raman, 2010). These cows, as the name suggests, are reported to be small in size, provide milk below two litres, and has a greater tolerenace to adverse environmental conditions than that of other varieties. It has a small hump on its back, and the horns are straight and lengthy (Raman, 2010). However, the population of this dwarf variety with specific breed characterestics is found to be meagre during the present investigation. These dwarf variety might have interbred with cross bred animals produced during the implementation of cross breeding programme. At present, majority of the animals reared by landless farmers of the locality have medium body size, very small hump and they provide milk up to four litres a day. The rearing practices of these cattle are also unique in its character. The common herd size of a landless dairy farmer is 6-8 as against the 1-2 cows in other parts of Kerala. The farmers let their cattle for grazing in the grass lands, hills and meadows during day time, after they are milked once in the early morning. The cattle return back to the farmer's yard during late evening in specific herds. This rearing practice often results in inbreeding and thus the maintenance of a higher level of zebu characteristics. However, the increase in inbreeding coefficient can cause losses in productive and reproductive traits in the future (Filho *et al*., 2015). With the growing acceptance of the concept of zero-budget farming, this rearing practice is presently adopted by lot many landless farmers of the taluk.

Extent of adoption of indigenous feeding practices by keepers of these cattle was also investigated. It can be inferred that the most extensively adopted practice was that of feeding animals with thin rice gruel along with house hold vegetarian food waste in the morning prior to milking. The least adopted indigenous feeding practice was that of feeding fodder since the animals were left outside through out the day for grazing. A few of the farmers practiced feeding rice porridge to pregnant animals along with cultivated fodder when they assume that the animal may calve within a week. In most of the cases calving takes place when the animal is outside for grazing and in such cases the animal may not return to the farmers premises in the evening. In such a situation the farmer will go along with other cows in the very next morning to find out the cow which had calved and will bring back the cow and calf to his premises. During the first week after calving the cow is not left out for grazing and is housed in *katcha* sheds attached to farmers house. Farmers agreed that this rearing practice is profitable since the day to day expenses required for the feeding of animals was minimum.

The survey also identified the presence of feral cattle in various locations of Peerumedu Taluk especially in Vagamon and Kumily villages agreeing the earlier reports (Raman, 2016). Feral cattle consist of bulls, cows and calves in the various hilly terrains un occupied by human beings. Though the animals appear wild in nature, they are not listed as wild animals. The increased number of feral cattle poses threat to domesticated animals as they could be carriers of infectious diseases, besides they also compete for the limited forage resources. The feral cattle move in groups of 10-30 and run away from human presence. They are wild in nature and attack human beings, if they suspect danger. The largest number of feral cattle was found in the Valakode and Vagamon areas, during the preliminary investigation

CONCLUSION

The small and medium sized cattle of Peerumedu taluk domesticated by landless farmers are mostly maintained by grazing in hilly terrains. This rearing practice provides a subsidiary income to the people of the locality and has a major role in the improvement of economic status of landless dairy farmers of the region. However, the presence of feral cattle poses threat to domesticated animals as they could be carriers of infectious diseases, besides they also compete for the limited forage resources.

REFERENCES

1. Filho, J.C.R., Verneque, R.S., Torres, R.A., Lopes, P.S., Raidan, F.S.S., Toral, F.L.B. (2015). Inbreeding on productive and reproductive traits of dairy Gyr cattle. R. Bras. Zootec., 44(5):174-179.
2. Raman, G.K., (2010, October 31). Rare species of cow in Peerumade faces extinction. *The Hindu*.
3. Raman, G.K., (2016, August 3). Feral cattle pose a threat to wildlife in Idukki sanctuary. *The Hindu.*

Indian Journal of Natural Sciences www.tnsroindia.org.in ©IJONS

Vol.9 /Issue 51 / December / 2018 *International Bimonthly* *ISSN: 0976 – 0997*

RESEARCH ARTICLE

Change Detection for Some Land Cover Types of Wasit Province (Eastern Iraq) Using Remote Sensing and GIS Techniques for Years 1989 - 2017

THAIR MUDHER FAHMY AL-AZZAWI[1]* and AWAD ALI SAHAR AL-ZIRGANY[2]

[1]Assist. Prof., Department of Geography, Education College for women, University of Baghdad, Baghdad, Iraq.

[2]Assist. Prof., Department of Surveying Techniques, Kut Technical Institute, Middle Technical University, Iraq.

Received: 13 Aug 2018 Revised: 15 Sep 2018 Accepted: 17 Oct 2018

***Address for Correspondence**

THAIR MUDHER FAHMY AL-AZZAWI

Assist. Prof.,
Department of Geography,
Education College for women,
University of Baghdad,
Baghdad, Iraq.
Email: 6thair.alazawi@gmail.com

ABSTRACT

In recent years, the study of land cover and their changes by remote sensing and GIS techniques has become a key subject in planning, management and local / global environmental change studies.In this paper, remote sensing and geographic information systems (GIS) are integrated to monitor, map, and quantify the main land cover types (vegetation, water and salinity covers) in the eastern part of Iraq (Wasit Province was taken as a case study), covering about 17753 km^2 between longitude 43°18'E - 44°33'E, and latitude 31°39'N - 33°10'N.The research aimed to use remote sensing techniques and digital image processing of Landsat images (TM) depending on the Normalized Difference Vegetation Index (NDVI), Normalized Difference Water Index (NDWI), and Salinity Index (SI) to calculate the areas of vegetation, water and salinity relative to the total area of Wasit province. Moreover, to detect the changes of these three types of land cover for preceding three years 1989, 2002, 2017. The cartographic representation of all data was performed by ArcGIS10.5 software.The study concluded the importance of water cover in the changes of vegetation and the salinity covers area. As it showed that the drying of most important marshes such as Al-Damlaj, Al- Saadiya, Al-Showeja, Al- Shobicha and other small swamps between the period 1989-2002 played an important role in reducing the area of water and vegetation cover and increasing the salinity, especially in the South-Western part of the study area. The process of rehabilitating and refilling these marshes for the period 2003-2017 has effectively contributed

to increase water and vegetation cover areas in the study area. Additionally, the results of the comparison showed that the declination of vegetation cover and increment of salinity cover in 2017 compared with 1989 is due to urbanization expansion, especially in the Eastern and North-Eastern parts of the study area.

Keywords: Remote Sensing, Land cover, Landsat , GIS.

INTRODUCTION

Land cover, defined as the assemblage of biotic and abiotic components on the Earth's surface, is one of the most crucial properties of the Earth system. There are three fundamental ways in which it is important [1]. The first lies in the interaction of land cover with the atmosphere, which leads to regulation of the hydrologic cycle and energy budget, and as such is needed both for weather and climate prediction [2]. Second, land cover plays a major role in the carbon cycle acting as both sources and sinks of carbon. In particular, the rates of deforestation [3]. Finally, land cover also reflects the availability of food, fuel, timber, fiber, and shelter resources for human populations, and serves as a critical indicator of other ecosystem services such as biodiversity. Information on land cover is fundamental to many national/global applications including planning, management activities and is considered an essential element for modeling and understanding the earth as a system. [4]. Thus, need to monitor land cover is derived from multiple intersecting drivers, including the climate, ecosystem health, agricultural productivity and social needs.In simple words, land cover is the physical material at the surface of the earth. Land cover includes grass, trees,water, asphalt, bare ground, salinity, etc. There are two primary methods for capturing information on any land cover, Field survey and analysis of remotely sensed imagery integration with GIS techniques [5].

This study utilizes remote sensing and GIS techniques to monitor some land cover types of Wasit Province (vegetation, water and salinity covers). All used Landsat TM images were obtained during the spring season for years 1989, 2002 and 2017, from which the area of each land cover was calculated to detect the changes for these three years. Then the reasons for these changes were explained relatively.

Aims of the study

This study has three objectives

1. Study some land cover types (vegetation, water and salinity) of Wasit Province and calculate their areas, in order to detect their changesusing Landsat TM images for three years 1989, 2002 and 2017; then to explain the reasons of these changes along studied them.
2. Stating the importance of remote sensing and GIS techniques to monitor some types of land cover, and especially their characteristics.
3. Study the possibility of developing a plan to monitor the land cover, whether quarterly or monthly using remote sensing and GIS techniques.

Study Area

Location

The studied area is located in Wasit Governorate, East of Iraq, 180 Km South-East of Baghdad. It situates between Longitude 43°18'E - 44°33'E and Latitude 31°39'N - 33°10'N, covering an area of about 17753 km² (Figure 1).

Geological setting

The area of study is part of the foothill zone and the Mesopotamian zone within twisted and unstable region of Iraq (unstable shelf), Which is characterized by a broad, concave and convex folds affected by the movements builds mountains[6]. Geological formations which exposed in some parts of the study area, ranging in age from (Lower Miocene) to (Holocene). There are geological formations belonging to (Lower Miocene) exposed along the North-Eastern border of the study area series of Southern Hamrin mountain, While covering the Quaternary deposits(Pleistocene and Holocene) central and south of the study area[7]. The Stratigraphic Succession of the study area consists of the following formations: Euphrates Formation (L.Miocene), Fatha Formation (M.Miocene), Injana Formation (U. Miocene), Muqdadiyah Formation (U.Miocene-Pliocene), Bai Hassan Formation (Pliocene), in addition to Quaternary sediments. Some of these formations deposited in shallow marine environments and some are deposited in a continental environment (Figure 2).

Climate

The study area is located in the East-Central parts of Iraq. The study area is characterized by a dry climate with limited and seasonal rain, where the rainy season starts from October to April. Therefore, the study area is characterized by a long dry period due to the interruption of rainfall from May to October accompanied by high evaporation due to high temperatures, and this contributes to the drought and the disintegration of the soil in the area.

MATERIALS AND METHODS

The data and Software used in the study:

- **Landsat images**

The study area is covered by four scenes of the Landsat TM witha spatial resolution of 15-30 m. Landsat images were obtained from the USGS (United States Geological Survey)website [8] for paths and rows as follow: (167-37), (167-38), (168-37) and (168,38), taken in March 2017 ,2002 , 1989. (Figure-3).

- **Software used in this study**

- ERDAS IMAGINE (Version 15, 2015).
- ArcGIS (Version 10.5).

- **Digital Image processing**

- **Pre-processing**

- Georeferencing, Transform, and Resampling maps.
- Layer Stack, Mosaic and Extracting (sub setting) of the study area.

- **Image Enhancement and Transformation**

- Normalized Difference Vegetation Index (NDVI).
- Normalized Difference Water index (NDWI).
- Salinity Index (SI)

Normalized Difference Vegetation Index (NDVI)

The NDVI is a commonly used vegetation index derived from remotely sensed measurements of electromagnetic energy in the red and near-infrared spectral regions. To determine the density of green on a patch of land it is a must to observe the distinct colors (wavelengths) of visible and near-infrared sunlight reflected by the plants. As can be seen through a prism, many different wavelengths make up the spectrum of sunlight. When sunlight strikes objects, certain wavelengths of this spectrum are absorbed and other wavelengths are reflected [9]. The pigment in plant leaves, Chlorophyll, strongly absorbs visible light (from 0.4 to 0.7 μm) for use in Photosynthesis. The cell structure of the leaves, on the other hand, strongly reflects near-infrared light (from 0.7 to 1.1 μm). The more leaves a plant has, the more these wavelengths of light are affected, respectively. (Figure-4). Lyon et al. [10] concluded that the NDVI method is best performed when comparing several vegetation diseases for change detection. The most common methods, the NDVI is expressed as the difference between the near Infra-Red (NIR) and Red (R) bands normalized by the sum of those bands (equation 1) [11]

$$NDVI = \frac{NIR - R}{NIR + R} \text{.....(1)}$$

By using the NDVI algebra to explore and estimating green vegetation cover and monitored for years 198 , 2002 , 2017(Figure 5). It has an interval a gray scale from -1 to 1 and all vegetation pixels has pixel value more than 0.2. The raster map was divided into two classes depending on its histogram using the 0.2 as a threshold number, then separation and calculation of the area of vegetation (figure 5).

Normalized Difference Water Index (NDWI)

Remote sensing techniques provide important capabilities to map surface water features and monitor the dynamics of surface water [12].The Normalized DifferenceWater Index is one of the most important indicators used in the field of monitoring of water resources, which provided by measurements of remote sensing of the electromagnetic spectrum in the Visible and Near-Infrared Bands. Water index (WI) associated directly with process of interacting between the electromagnetic spectrum and the surface of the water where water surfaces absorb most of the Infrared and Near-Infrared bands evenly, while those surfaces reflect a small amount of the Visible spectrum (Visible Band) especially the Blue and Green bands depending on the purity of water, contaminated, contain impurities, as well as the effect of water depths (Figure 6). Depending on the behavior of water toward the electromagnetic spectrum; the water reflects part of the visible spectrum while absorbed most of the remaining electromagnetic spectrum, especially the Infrared and Near-infraredspectrum, thus the Normalized Difference Water Index (NDWI)can be calculated directly from the following equation:

NDWI = Green-NIR / Green+NIR.....[13]

Where Green is the Green band such as Landsat 8 band 3, and NIR is the Near Infrared band such as Landsat 8 band 5. This index is designed to: (1) Maximize reflectance of water by using Green wavelengths; (2) Minimize the low reflectance of NIR by water features; and (3) Take advantage of the high reflectance of NIR by vegetation and soil features. As a result, water features have positive values and thus are enhanced, while vegetation and soil usually have zero or negative values and therefore are suppressed [13]. In this study, the NDWI is calculated for study area using satellite images of Landsat 8 for the years 1989 , 2002 , 2017, then the area of water is calculated (Figure 7).

Salinity Index (SI)

Salinization is the concentration of salts on the surface or near-surface zones of the soil and it is a major process of land degradation [14].It is a natural process resulting from high levels of salt in the soil, originating from landscape features that allow salts to become mobile (movement of the ground water table) and from climatic trends in favor of salt accumulation. Alternatively, it may occur resulting from management practices [15]. The latter, human-induced, salinization is often referred to as 'secondary salinization' to distinguish it from naturally affected soils [14]. Salinization occurs when the following conditions occur together [15]:

- Presence of soluble salts in the soil.
- High ground water table.
- High rate of evaporation.
- Low annual rainfall

Remote Sensing has the ability to predict soil salinity accurately. It saves labor, time and effort when compared to field data collection of lands at risk of white death (salinization). Satellite data has a great potential for monitoring salinization in both spatial and temporal extents (Abbas, 1999). Green and Red bands have been used repeatedly to detect salinity soil:

$$(SI) = \frac{Green\ x\ \mathrm{Re}\ d}{2} \text{.....} \text{(Abbas, 2010).}$$

In this study, the salinity is calculated for study area using satellite images of Landsat 8 for the years 1989, 2002, 2017, thenthe area of Salinity is calculated as shown in the (Figure 8).

RESULTS AND DISCUSSION

In general, the maximum density of vegetation zones is located in the Western part of the study area and along the Tigris River, while the salinity zones are located in the North-East of the study area. The various methods of digital change detection using Landsat TM images, such as NDVI, NDWI and SI for the years (1989, 2002 & 2017) have supported the thematic map production for the three land cover classes of vegetation, water & salinity covers (figures5, 7, 8).The detected changed areas of Wasit province in the year 2002 compared with years 1989 and 2017 (table -1) revealed declination of vegetation and water intensity. While the increment of the salinity cover area is clearly related to drying some of the most important and the biggest swamps of the study area such as Al-Damlaj, Al-Saadiya, Al-Showeja, Al- Shobicha and other small swamps as showed in (Figure -1). Moreover, the areas which are subject to immersion, because of political and security governmental decisions for the period from (1991-2003), have had negative effects on agricultural lands and environmental balance.The thematic comparison between the years 2002 and 2017 showed that in the year 2017 there were incremental vegetation and water intensity, while presented declination of salinity, and that occurred because of refilling and restoration of most swamps. Most zones which are subject to immersion in the study area, have had a positive effect on agricultural activities and effectively limited the land degradation as well as partially remedied the environmental changes.

The thematic comparison between the years 1989 and 2017 showed declination in vegetation and water areas, and an increment in the salinity in 2017. This is revealed clearly as a result of accelerated processes of urbanization expansion, which has negative effects on agriculture and caused land degradation in the study area. Remote sensing techniques and satellite image processing provide advanced pathways to detect and monitor land covers and their changes; therefore we can implement these geo-information technologies to make sequential monitoring, whether

monthly or quarterly for any part of the country. Study the changes of vegetation, water and salinity covers is useful and important for planning, management, thematic mapping and environmental change purposes.

REFERENCES

1. Turner CA, Mack DH, Davis MM.A novel zinc finger containing protein that can drive the maturation of Blymphocytes into immunoglobulin-secreting, 1994, cells. Cell 77:297–306.
2. DeFries et al. Human modification of the landscape and surface climate in the next fifty years. Global Change Biology. 2002, 8: 438-458.
3. IPCC , land use change and forestry. A Special Report of the Intergovernmental Panel on Climate Change. Cambridge University Press, Cambridge. UK. 2000, 377p.
4. Lillesand T., Kiefer R. ,Chipman J. Remote sensing and image interpretation. 5thED, New York, John Wiley and sons, 2004.
5. Mohsin N.,Venkatesh J.,Ali H. Land Use and Land Cover Changes of Al-Kut City in Iraq using Remote Sensing and GIS Techniques, International Journal of Scientific Engineering and Technology Research, 2014, Vol.03. Issue.17 P.3555-3560.
6. Buday T. &Jassim Z. The regional geology of Iraq Tectonism,Magmatism and Metamorphism, 1987, V. 2, GEOSURV, Baghdad.
7. Hassan A.; EloubaidyZ.;Griolet P.;Ayob S.; Abbas L.; Jamal N.; Smoor B. GalalBabra project area, part1: Geological and hydrological Investigations. 1977, Bull. No. 106.Scientific Research Foundation .Ministry of Higher Education and Scientific Research. Baghdad .Iraq. 35P.
8. United States Geological Survey https://earthexplorer.usgs.gov.
9. Jasim, A. Monitoring Desertification in Badra Area Eastern Iraq by Using Landsat Image Data, 2012, M.Sc. thesis, Baghdad University.
10. Lyon G., Yuan D., LunettaS., and Elvidge D. A change detection experiment using vegetation indices, IEEE photogrammetric Engineering and remote sensing,1998, 64, 143-150.
11. Main S. A remote sensing change detection study in the arid Richtersveld Region of South Africa, M.Sc. thesis, Univ. of the Western Cape, 2007.
12. Alsdorf E., Rodríguez E.,Lettenmaier P. Measuring surface water from space, Reviews of Geophysics, 2007.
13. McfeetersK. The use of normalized difference water index (NDWI) in the delineation of open water features. International Journal of Remote Sensing, 1996, 17, pp. 1425–1432.
14. Thomas S., Middleton J. Salinization: new perspectives on a major desertification issue. Journal of Arid Environments, 1993, 24, 95–105.
15. USDA, 1998. Soil Quality Information Sheet, Soil Quality Resource Concerns : Salinization. National Soil Survey Center, available at: http://soils.usda.gov/sqi/publications/files/Salinzation.pdf
16. Abbas A. Analysis of Environmental land degradation in the semiarid region of Faisalabad, Pakistan using remote sensing and GIS. Research Report, JIRCAS, Japan, 1999.
17. Abbas A. Desertification Study of Dalmaj Lake Area in Mesopotamian Plain by Using Remote Sensing Techniques, PhD thesis, Collegeof Science , Baghdad University, 2010.

Table 1: Land cover change in the studied area as extracted from the digital images

Land cover Class Name	Landsat TM5 1989		Landsat TM7 2002		Landsat TM8 2017	
	Area(km²)	(%)	Area(km²)	(%)	Area(km²)	(%)
Vegetation	5285	29.76	2874	16.18	3975	22.39
Water	721	4.06	394	2.21	450	2.53
Salinity	810	4.56	2219	12.49	1900	10.70

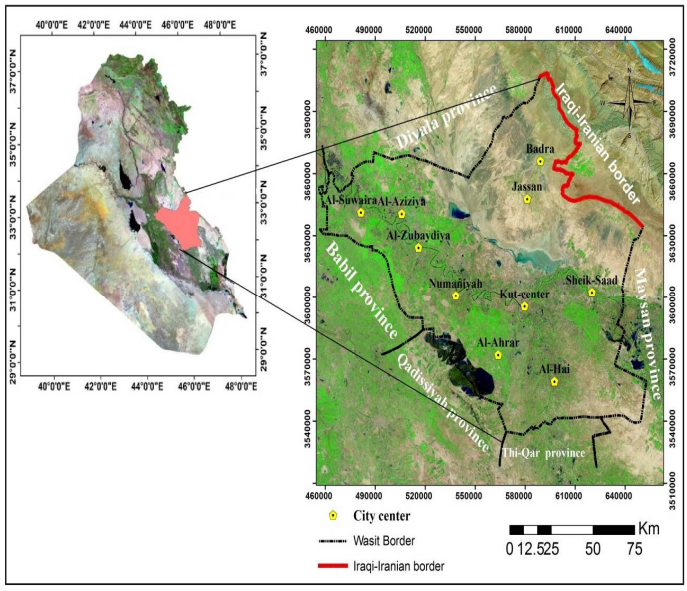

Figure 1: Digital map of Iraq showing the study area

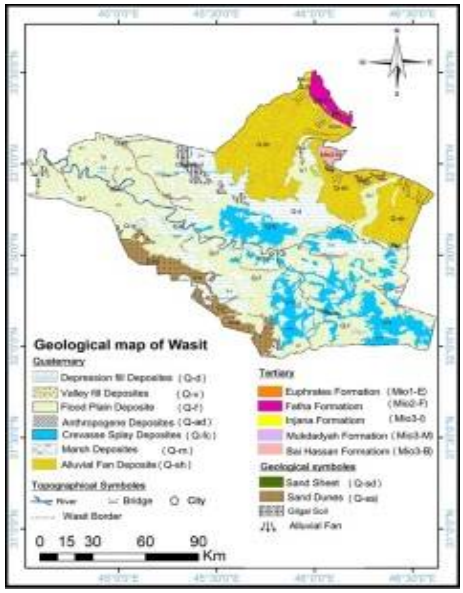

Figure 2: Geological map of the study area (Drawn by the authors according to geological maps of State Company for Geological Survey and Mining).

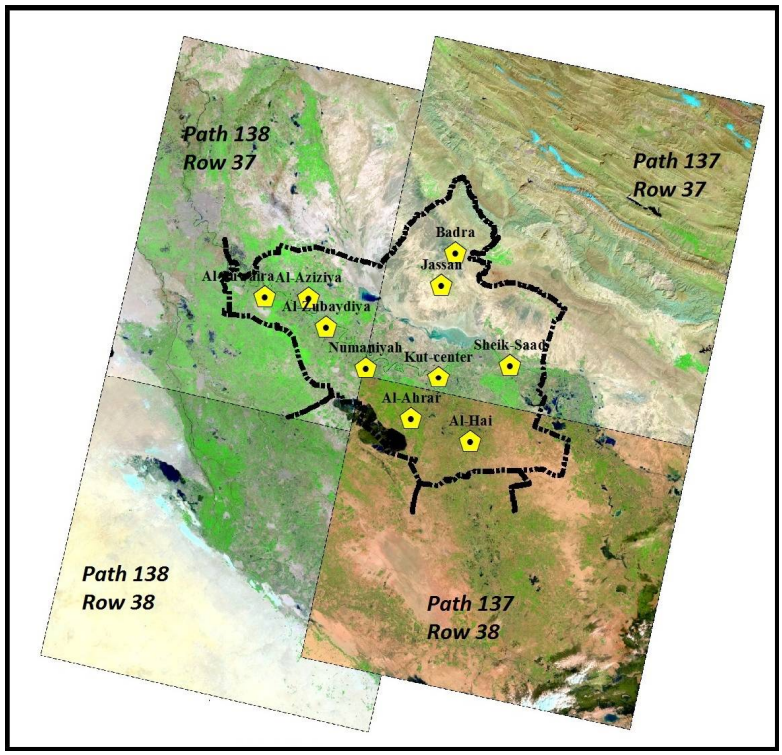

Figure 3: Landsat images covering the study area

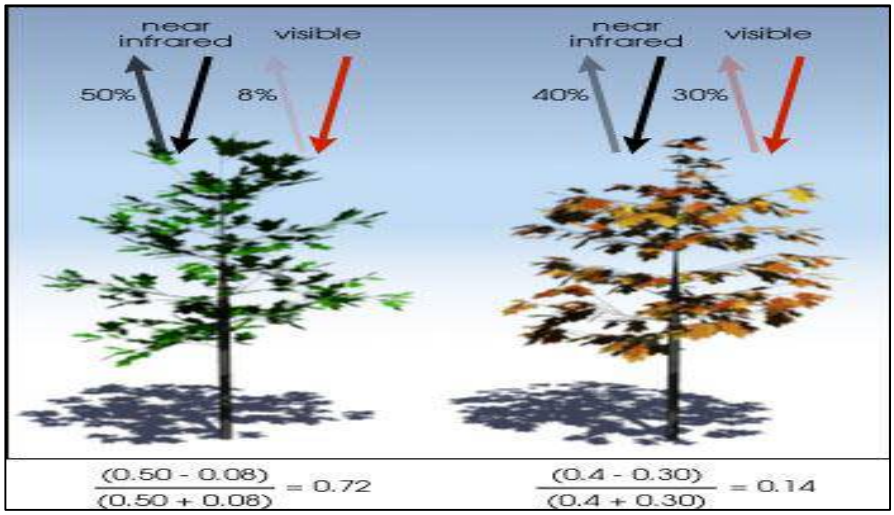

Figure 4: NDVI is calculated from the visible and near-infrared light reflected by vegetation. Healthy vegetation (left) absorbs most of the visible light that hits it, and reflects a large portion of the near-infrared light. Unhealthy or sparse vegetation (right) reflects more visible light and less near-infrared light. The numbers on the figure above are representative of actual values, but real vegetation is much more varied.
https://earthobservatory.nasa.gov/Features/MeasuringVegetation/measuring_vegetation_2.php

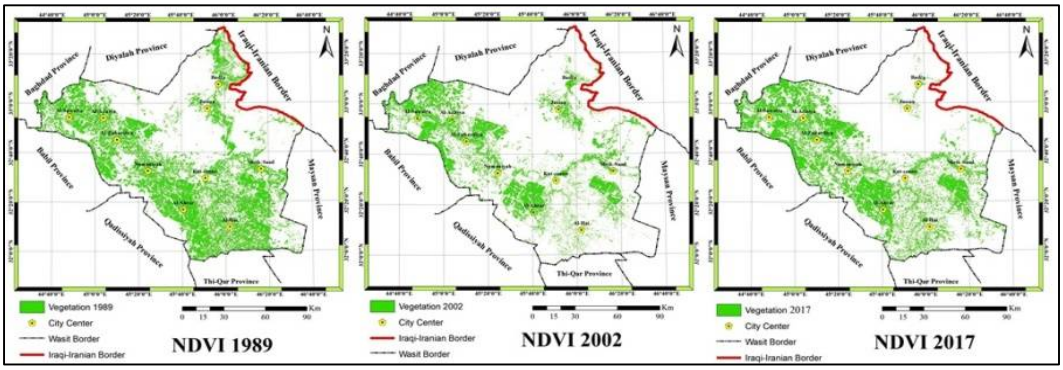

Figure-5: Normalized Difference Vegetation Index (NDVI) of study area for three years 1989, 2002 and 2017.

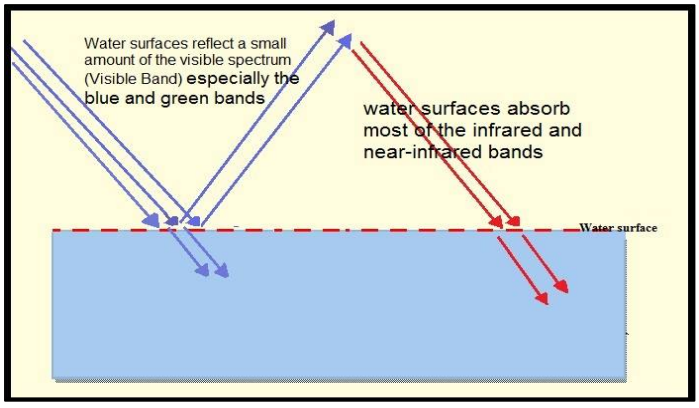

Figure 6 : Spectral behavior of water in Visible and Infrared bands

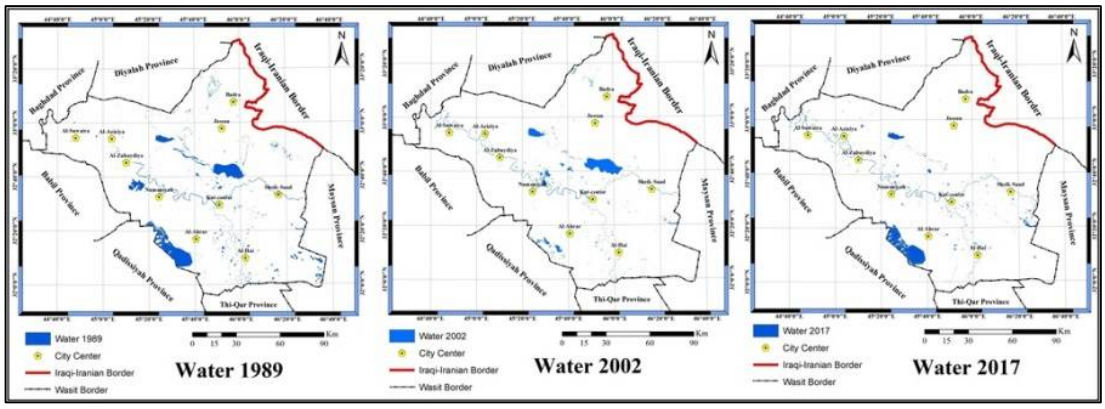

Figure 7: Normalized Difference Water Index (NDWI) of study area for three years 1989, 2002 and 2017

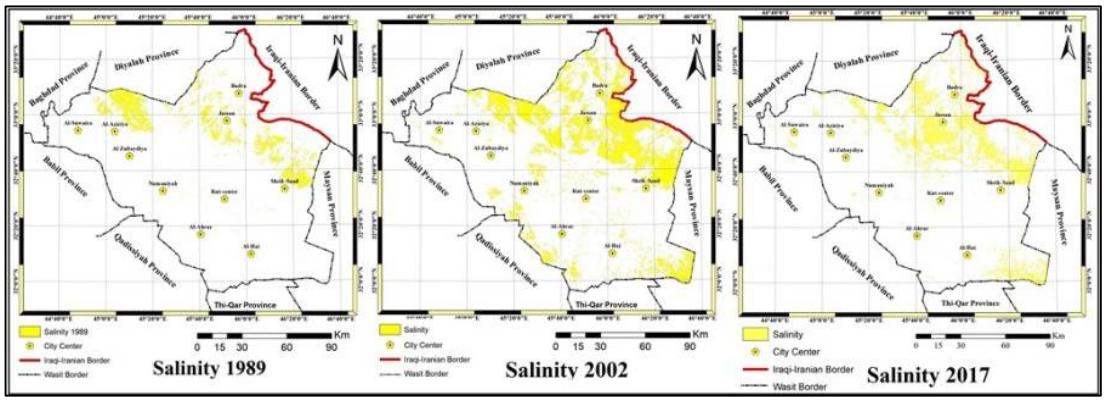

Figure-8 : Salinity Index (SI) of study area for three years 1989 , 2002 and 2017 .

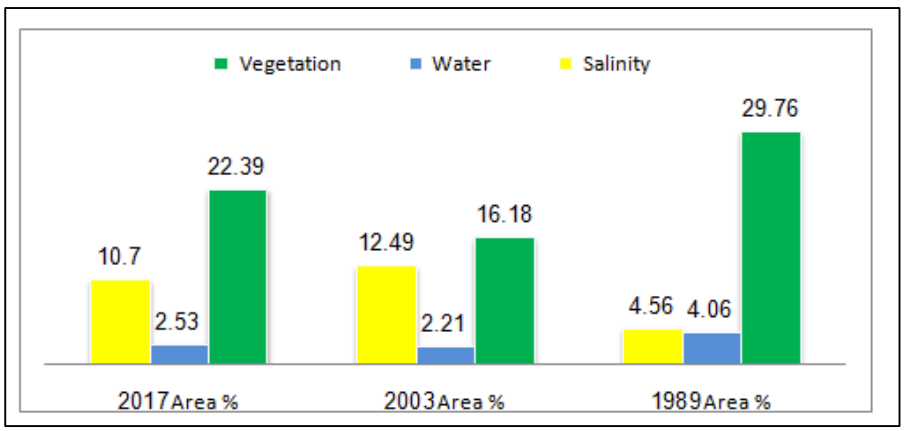

Figure-9: Study area Land Cover Classification

Indian Journal of Natural Sciences www.tnsroindia.org.in ©IJONS

Vol.9 /Issue 51 / December / 2018 *International Bimonthly* *ISSN: 0976 – 0997*

RESEARCH ARTICLE

Histomorphology and Histochemical Study of Duodenum and Pancreas in Gray Mongoose (*Herpestes edwardsii*) In Iraq

Hussein.B.Mahmood[1] and Khalid.K.Kadhim[2]*

[1]Department of Anatomy and Histology, College of Veterinary Medicine, University of Kerbala, Iraq.
[2]Department of Anatomy and Histology, College of Veterinary Medicine, University of Baghdad, Iraq.

Received: 26 Aug 2018 Revised: 29 Sep 2018 Accepted: 31 Oct 2018

***Address for Correspondence**
Khalid.K.Kadhim
Department of Anatomy and Histology,
College of Veterinary Medicine,
University of Baghdad, Iraq.

ABSTRACT

The duodenum and pancreas of wild adult gray Iraqi mongoose were studied. Fourteen samples were collected from orchards near the Tigris River. Morphological and histochemical studies were done. Anatomically, G shape, ascending and descending duodenum, length of duodenum (6.4) cm and occupied by compact pancreas that tightly attached. The organ connected pyloric of stomach with jejunum, located dorsally; bounded by muscles of lumber region and vertebral column, ventrally by abdominal muscles and omentum, laterally in left side bounded by spleen and lateral abdominal muscles and bounded in right side by the cranial flexure of duodenum. Cranially was bounded by liver. Caudally bounded by the small intestine and cecum. Both the pancreatic duct and common bile duct drain in duodenum by common pancreatic duct through major duodenalpapilla one at one cm from pyloric region.The pancreas was compact and consists of three parts; large dorsal, ventral thinner and longer splenic lobe, Histologically, the duodenum was consisted from four basic layers; tunica mucosa, submucosa, muscularis and serosa. The mucosa of duodenum was featured by simple columnar epithelia with goblet cells covered thin elongated villi. The lamina propria contained intestine mucous glands; these glands were simple tubular gland which increased in caudal part of ascending duodenum. The goblet cells had mixed neutral and acid mucin. While the crypt of Lieberkühn and Burners glands showed neutral mucin. Pancreas showed islets of Langerhans were appeared in splenic lobe more than others. The exocrine alveolar acini were consisted of two types of cells with spherical nuclei located peripherally. The main pancreatic and interlobular duct lined by simple cuboidal epithelia, beneath epithelia was located of serous gland lined by cuboidal epithelia.

Keywords: Histomorphology, histochemical, duodenum, pancreas, gray mongoose.

INTRODUCTION

Mongooses (Herpestidae) are small, wide spread carnivores occupying various habitats from Africa to Southeast Asia[1]. The Indian gray mongoose or common grey mongoose (*Herpestes edwardsii*) is a species of mongoose mainly found in southern Asia mainly India, Pakistan, Nepal, Sri Lanka and some other parts of Asia [2].Researchers reported that the small intestine in canine is the longest structures of the gastrointestinal tract[3,4]. It is a rounded hollow tube that is approximately three to four times the length of the animal's body. The duodenum is the first and most important part of the small intestine. Within the duodenum, the digestive juices enter from the pancreas and gallbladder. The small intestine in African Giant Rat was made up of the duodenum, the jejunum and the ileum. The duodenum is the first part of the small intestine and occupied the right dorso-lateral part of the abdominal cavity with largest diameter and longest part. The duodenum receives secretions of Bile, Pancreatic and Intestinal juice [6].The duodenum in ferret have major duodenal papilla contains the common opening for the bile and pancreatic ducts. This is located about 3 cm from the pylorus, whilethe minor papilla may be absent [7,8].In most animals the pancreas is an oblong, pinkish organ that lies in the first bend of the small intestine. In rodents and rabbits, it is spread thinly through the mesentery and is sometimes difficult to see [9].]. In most of domestic animals the tunica mucosa of duodenum is composed of three layers: lamina mucosa, lamina propria and lamina muscularis. The cells are enterocytes having striated border (absorptive cells), goblet cells, Paneth cells, enteroendocrine, intestinal glands, [10,11] and the Brunner's glands that occupy the entire submucosa layer in rat [12].

The canine pancreas consists of a right and a left lobe united by the pancreatic body. The right lobe is positioned in the peritoneal fold of the descending duodenum. The left lobe is located in the peritoneal fold of the dorsal mesogastrum [13]. While in rats, the pancreas is divided into four parts, the gastric, splenic, parabiliary, and duodenal segments [14]. Most of the pancreatic tissueis an exocrine gland, the Islets of Langerhans are small clusters of cells [9].There is dearth of information about the anatomy of the grey mongoose in Iraq. Sothis study dealt with some anatomical and histological aspects of certain digestive organs of this animal.

MATERIALS AND METHODS

Fourteen healthy gray mongooses of both sexes were used in this study (Fig, 1). The average weight of the animals was (350±23.3) gm. The average body length was (54±5.7) cm. The animals were caught from orchards near Tigris Rivers. The animals euthanized by intra muscular administration of diazepam (1mg/1kg) combined with ketamine HCL (30Mg, 1Kg) [15].Anatomical and histochemical studies of duodenum and pancreas were done. The morphological parameters of the target organs included shape, length and relation with other organs. Length were recorded in centimeter (cm) using a calibrated scale. The weight was recorded in gram (gm) using the sensitive electronic balance. Samples for histological and histochemical purposes were fixed in 10% neutral buffered formaldehyde and sectioned serially at 5µm. Sections were stained with H&E, combined PAS + Alcian blue (PH 2.5) for Neutral and acid mucin [16].

RESULTS

Duodenum

Morphology

The duodenum was not only an important part of the digestive system, but also acts as endocrine function by secreting some hormones that play roles on the regulation of other organs.The small intestine covered by network of peritoneal membrane rich in adipose tissue (Fig, 2). The duodenum started at the pylorus region with a cranial portion, which dilated forming a duodenal ampulla.The duodenum was a tubular structure within the abdominal

cavity connection with the stomach cranially and with jejunum caudally. The duodenum appeared as (G) shaped. Total Length was (6.4±0.4) cm. between its ascending and descending limb. The average length of duodenum for length of body was(11.8) cmrelatively.The duodenum started at the pylorus with a cranial, dilated portion, directed to the right and forming a duodenal ampulla. The following portions of the duodenum were the cranial flexure which located against to medial lobe of liver and the descending duodenum that ended at the caudal flexure that located caudally to the right kidney. From the caudal flexure the duodenum passed cranially as the ascending portion. The ascending duodenum was directed caudally to form doudno-jejunal flexure (Fig, 3).The pancreas was Located between the duodenal limbs. The pancreas was characteristic by compact mass, white to pink in color, which consists of relatively ventral part, dorsal part and splenic part, which united both of dorsal and ventral in two regions, at descending part of duodenum and cranial flexure to form pancreatic body. The splenic part was longer and thinner, passes between left kidney and visceral surface of spleen which extended caudally exceeds the spleen with about (1) cm (Fig,5). Generally the pancreas had two surfaces; dorsal and ventral occupied G shape duodenum. The pancreatic duct was emerge from the ventral surface of pancreas and passed dorsally to enter the duodenum. There was only one pancreatic duct, this duct union with common bile duct to form common pancreatic duct which opened at about 1 cm from the pyloric orifice (Fig,6).

Histologically the duodenum was consisted from four basic layers; tunica mucosa, submucosa, muscularis and serosa. The duodenal villi were elongated projection in lumen. The mucosa was featured by simple columnar epithelia was contain elongated dark nuclei,the goblet cells distributed between the main mucous cells. The lamina propria was occupied by simple tubular glands (crypts of Lieberkühn) (Fig,7,8). The Lieberkühn occupied on the thick layers of lamina muscularis, these Lieberkühn were separated from each other by connective tissue of the lamina propria. The lamina muscularis was consisted of two layers of smooth muscle fibers. Submucosa in duodenum consists of loose connective tissue with blood vessels. The Burner's glands wereaggregated as groupsin submucosa, separated from each other by connective tissue. The Burner's glands were simpletubular mucous glands that appeared mostly in middle and ascending duodenum. The cross section of each gland composed of eight to ten cells around a narrow lumen and the cells had a shortened pyramidal shape, the nucleus in these cells was rounded, located near the basement membrane (Fig,10). Tunica muscularis of duodenum was composed of two layers of smooth muscle fibers; inner circular and outer longitudinal. Tunica serosa was a thin layer of loose connective tissue which covered by mesothelium (Fig, 11).

The duodenal papillae had wide lumen, which composed of tunica mucosa, tunica submucosa and muscularis, the mucosa had very short simple mucosal folds which lined with simple columnar epithelium that not invaded with goblet cells, and contained light cells with rounded nuclei. There are numerous of simple tubularseromucous glands surrounded by lumen of duodenal papillae, These glandsoccupied by circular smooth muscle fibers around the duodenal papillae. The serosa of duodenal papillae was interfering with serosa of duodenum (Fig, 12,13). Histochemically, the duodenal sections that stained with combined AB-PAS (pH 2.5) showed negative reaction of the main mucous cells while the goblet cellsgave strong positive reactionand found in to two color (red-violate to dark-blue) (Fig,14). The crypt of Lieberkühn and Burners glands in submucosa stained positively that appears red-pink (Fig, 15). The pancreas sectionscomposed of many lobes each lobe separated from others by connective tissue septa. The ductal system is started with centro-acinar cells, followed by the intralobular, interlobular, and main ducts (Fig, 16). The main duct and interlobular ducts was lined by simple cuboidal epithelia, surrounded by few amount of connective tissue and smooth muscle fibers (Fig,17).

Beneath epithelia there were serous gland lined by cuboidal epithelia. (Fig, 18). The parenchyma of pancreas was composed of two types of epithelial cell, ductal epithelial cells and closely packed pancreatic acini, these cells found into two shapes; once of cells were irregular in shape and more acidophilic and others regular and rounded in shape with pale cytoplasm with rounded nuclei located peripherally. The acinar cells comprised the major portion of the pancreas. These cells were arranged inrandomly and anastomosing cords separated by blood vessels (Fig,19). The dorsal and ventral part of pancreas don't have islets of Langerhans (Fig,20), while the splenic part was containing a

few numbers of islets of Langerhans which appeared as non-capsulated pale stained oval or irregular clumped cells(Fig,21). There are two types of cell can be distinguished in Langerhans islets, once was rounded, pale-bright stain this featured corresponding for beta- cells, while the Alfa- cells were irregular shape, acidophilic stain which spread with more in number than beta cells (Fig, 22).

DISCUSSION

The present study was explained the small intestine in gray mongoose. As a wild animal, the intestine was covered by network of peritoneal membrane rich in adipose tissue. Spiral shaped small intestine by their centripetal coiled portion this finding unlike with unlike other carnivore,example in dog [3,4] and in rodent[5]. The duodenum in gray mongoose was (G) shape, had three flexure; cranial, caudal and dodeno-jejunal flexure which unlike with [17]who stated that theduodenum was appeared U in shape in mice, rats, dogs.In mongoose, the opening of the major duodenal orifice showed no different than cat. Alsono minor papilla was detected as in ferrets [7,8]. The mongoose pancreas composed of three parts; ventral, dorsal and splenic lobe, compact, white-pink in color this is seems similar to canine pancreas [10]. The duodenum of gray mongoos was consisted from four tunica as in other animals [14,17,18]. However, In this study showing the lamina propria of duodenum was rich with simple tubular mucous glandsandCrypts of Lieberkühn,similar observation mentionedin Persian squirrel[19] that these glands was simple tubular glands and comparable with most domestic animals[20].

Burner's glands were find mostly in transvers and ascending segment of duodenum were aggregated as groups unakin with previous research[21] that stated the distribution of duodenal submucosal glands extend along the duodenum to jejunum in rabbits. Furthermore,in this study, the intestinal mucous gland were reported to be present along the duodenum and extent into jejunum, this result comparable with [22] who describe that the intestinal glands located along of duodenum in bison, deer, voles, and cotton-tailed and domestic rabbits, and Japanese macaques, cats, raccoons, rats and opossums. The present study explained the duodenal goblet cells had both neutral and acidic mucin while the crypt of Lieberkühn and Burners glands showed neutral mucin which it's similar with [23,24] who reported secretions with acid and neutral mucopolysaccharides. In the current study, the exocrine part of pancreas composed of pancreatic acini, spread as accord and there are two types of cells rounded and irregular cells had spherical nuclei located peripherally, this results similar with [25] who stated that the pancreas had two types of exocrine cells, acinar and ductal cells.In mongoose, the islets of Langerhans were very rear in duodenal parts and restricted mostly in splenic lobewhich incountraswith that reported in rats, Monkey,Minipigs which it is numerous, however, it was in right lobe of pancreas in dog [26], also this result may be to the natural diet of carnivores differs substantially from that of non-carnivores. In addition, in carnivores consuming a natural diet, the When the diet contains low amounts of carbohydras and glucose, hepatic gluconeogenesis is predicted to be the major pathway to maintain blood glucose[27].

In this study, the cross section of pancreatic main duct showed simple cuboidal epithelia that line duct. Beneath epithelia were located (2-3) glands lined by cuboidal epithelia which opened into wide lumen,however this duct is lined by a simple cuboidal to columnar epithelium in dog and sheep [28,29,30]. These glands found to secrete some of enzymes and substance assistant to metabolic processes from glands to the duodenum, this finding akin with [31] who describe that the exocrine cells produce exocrine enzymes and at least part of the secretin-stimulated bicarbonate rich pancreatic fluid secretion.The current study finding the interlobular ducts smaller size rounded lined by simple cuboidal epithelia with rounded pale nuclei, this result unakin with [31] who describe that the small interlobular ducts were not easily identified with the dissecting microscope, except when they remained attached to larger ducts. Also, these results disagree with [32] who stated in human and mice that the pancreatic epithelium is heterogeneous, and the contribution of the pancreatic ductal gland to regeneration of the terminal ducts remains unknown. Although pancreatic duct glands (PDG) have been found throughout the pancreas, PDG-like cells have not been identified in the terminal duct system.

REFERENCES

1. Thulin, C.G., Simberloff, D., Barun, A., Pascal, M., & Islam, M.A. (2006). Genetic divergence in the small Indian mongoose (Herpestes auropunctatus), a widely distributed invasive species. Molecular Ecology. 15: 3947–3956.
2. Choudhury, A., Wozencraft, C., Muddapa, D., Yonzon, P., Jennings, A. and Geraldine, V. (2011). Herpestes edwardsii. In: IUCN 2012. IUCN Red List of Threatened Species. Version.1. www.iucnredlist.org.
3. 3-Budras, K.D., Fricke, W., Richter, R., Mcarty, P.H. (2002).Anatomy of the Dog. 4th ed., Schl.terscheVerlag und Druckerei, Hannover.
4. SeyinY, Kadri A, Ühsaniye C, Bahri Y. (2004). A Geometric Modeling of Dog Intestine. Department of Anatomy, Faculty of Veterinary Medicine, UludaÛ University, 16059 G.r.kle, Bursa - Turk. J. Vet. Anim. Sci.
5. Nowak, E., Kuchinka, J., Szczurkowski, A. and Kuder, T. (2015).Extrahepatic Biliary Tract in Chinchilla (Chinchilla laniger, Molina). Anat. Histol. Embryol., 44: 236–240.
6. Ruth.L,(2013). Anatomy and Physiology of Animals. PDF generated using the open source mwlib toolkit. See http://code.pediapress.com/ for more information.19:02:32 UTC.
7. Evans HE, An NQ. (1998). Anatomy of the ferret. In Fox JG, ed. *Biology and Diseases of the Ferret*. 2nd ed.Baltimore, MD: Williams & Wilkins;:19–69.
8. OdekunleA,Chinnah TI. (2003). Brainstem origin of duodenal vagal preganglionic parasympathetic neurons. A WGAHRP study in the ferret (*Mustela putoriusfuro*) human model. *West Indian Med J.*;52:267–272.
9. Jubb, K,(1993). The Pancreas. In: Pathology of Domestic Animals, 4th edn. Jubb KVF, Kennedy PC, Palmer N (eds). San Diego: Academic Press pp 407–418.
10. Takehana, K., H. Ueda Eerdunchaoluo, A. Kobayashi, K. Iwasa and K. Sou, (2000). A histochemical study of the camel (*Camelusbactrianus*) duodenal glands. J. Vet. Med. Sci., 62: 449-452.
11. Linden, S.K., T.H.J. Florin and M.A. McGuckin, (2008). Mucin dynamics in intestinal bacterial infection. PLoS ONE, Vol. 3. 10.1371/journal.pone.0003952.
12. Olayemi, K., Omamuyovwi M. and Stephen O. (2014). Histological and Histomorphometric studies of ethanol-injured pylorus and duodenum of Wistar rats pre-treated with Moringaoliefera extract. Al Ameen J Med Sci; 7(2) :104-111 _ US National Library of Medicine enlisted journal _ ISSN 0974-1143.
13. Alexey E, Gashkova,V, Alexander P. , Saveljev& Alexei .V. (2015). Histologic features of the gastrointestinal tract of Laonastesaenigmamus (Rodentia: Diatomyidae). Russian Research Institute of Game Management and Fur Farming, 79 Preobrazhenskaya St., Kirov, 610000, Russia — 2 Zoological Institute of the Russian Academy of Sciences, UniversitetskayaEmb. 1, Saint Petersburg, 199034, Russia — Corresponding author: Alexey Scopin; scopin (at)bk.ru. 65 (1): 151–163 4.5.
14. Haschek WM, Rousseaux CG, and Wallig MA. (2010). Pancreas. Section I Exocrine Pancreas. Normal Structure of Exocrine Pancreas. In: Fundamentals of Toxicologic Pathology, 2nd ed. WM Haschek, CG Rousseaux, and MA Wallig (eds). Academic Press, Inc., Amsterdam. 238–240.
15. Thurmon, J.C., Tranquilli, W.J., Benson, G.J. (1996).Lumb& Jones Veterinary Anesthesia. 3rd ed. Lea & Fibiger, London.
16. Bancroft, J.D., and Stevens, A. (2012). Theory and Practice of Histological Techniques. 7th Edition. Churchill Livingstone. Pp: 127-129.
17. Lin, J.H., M. Chiba and T.A. Baillie, (1999). Is the role of the small intestine in first-pass metabolism overemphasized?. Am. Soc. Pharmacol. Exp. Therapeutics, 51: 135-158.
18. Powell, D.W., R.C. Mifflin, J.D. Valentich, S.E. Crowe, J.I. Saada and A.B. West, (1999). Myofibroblasts. II. Intestinal subepithlialmyofibroblasts. Am. J. Physiol., 277: 183-201.
19. Cunningham, J. G. & B. G. Klein, (2007). Textbook of Veterinary Physiology, 4th edn, Elsevier Health Sciences.
20. Krause, W.J., (2000). Brunner's glands: A structural, histochemical and pathological profile. Progr. Histochem. Cytochem., 35: 259-367.
21. Schumacher, U., M. Duku, M. Katoh, J. Jorns& W. Krause, (2004). Histochemical similaritiesofmucins produced by Brunner's glands and pyloric glands: A comparative study. *The Anatomical Record*, **278**,540–550.

22. Linden, S.K., T.H.J. Florin and M.A. McGuckin, (2008). Mucin dynamics in intestinal bacterial infection. PLoS ONE, Vol. 3. 10.1371/journal.pone.0003952.
23. Shibata, T., Imai, M., Moriguchi, k. and Takada, Y. (1990). Do the cardiac glands Excist, The Cat. Okajimas Folia Anatomica. 67 (1):31-36.
24. Wali N.O and Kadhim K K . (2014). Histomorphological Comparison of Proventriculus and Small Intestine of Heavy and Light Line Pre- and at Hatching. international Journal of Animal and Veterinary Advances 6(1): 40-47.
25. Cattley RC, Popp JA, and Vonderfecht SL. (2013). Liver, Gallbladder, and Exocrine Pancreas. Exocrine Pancreas. In: Toxicologic Pathology: Nonclinical Safety Assessment. PS Sahota, JA Popp, JF Hardisty, and C Gopinath (eds). CRC Press, Boca Raton. 345–356.
26. Minoru T, Junko, S and Hiroko, K. (2016).A comparison of the anatomical structure of the pancreas in experimental animals. 1Pathology Department, Nonclinical Research Center, LSI Medience Corporation, 14-1 Sunayama, Kamisu, Ibaraki 314-0255, Japan. J ToxicolPathol; 29: 147–154.
27. Schermerhorn.T, (2013).Normal glucose metabolism in carnivores overlaps with diabetes pathology in non-carnivores.Department of Clinical Sciences, College of Veterinary Medicine, Kansas State University, Manhattan, KS, USA.Volume 4.188-1
28. Ekholm, R., T. Zelander, and Edlund. Y. (1962). The ultrastructural organization of the rat exocrine panderncreas .11 .Centroacinar cells, intercalary and intralobular ducts. J. Ultrasiruet. Res. 7:73-83 .
29. Gemmell, R. T., and Heath. T. (1973). Structure and function of the biliary and pancreatic tracts of the sheep. J. Anal . 115:221-236.
30. Ichikawa,A. (1965). Fine structural changes in response to hormonalstimulation of the perfused canine pancreas . J. Cell Biol. 24:369-385.
31. Githen.S, Holmquist,GandRuby.R. (1980). Characterization of ductus isolated from the pancreas of the rat. From the Department of Biological Sciences, University of New Orleans, Lakefront, New Orleans, Louisiana 70122, and the Department of Anatomy, Louisiana State University Medical Center, New Orleans, Louisiana 70122. V- 85. 122-135.
32. Yamaguchi, J., Liss, A. S., Sontheimer, A., Mino-Kenudson, M., Castillo, C. F., Warshaw, A. L., & Thayer, S. P. (2015). Pancreatic duct glands (PDGs) are a progenitor compartment responsible for pancreatic ductal epithelial repair. Stem Cell Research, 15(1), 190–202. doi:10.1016/j.scr.05.006.

Fig.1.Gray mongoose in Iraq

Fig.2.Abdominal cavity of gray mongoose show the intestine surrounded by layer of peritoneal highly lipid (yellow arrows).

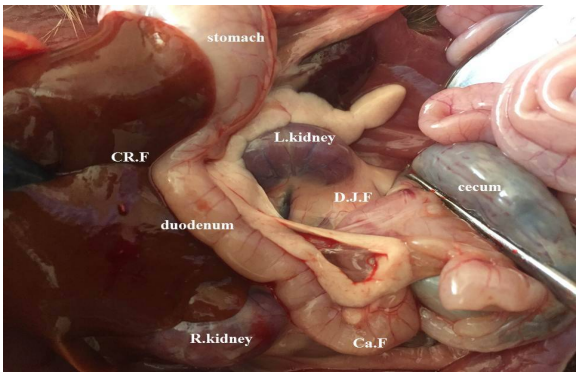

Fig.3.Duodenum in gray mongoose showing G shape, CR.F-(creanial flexure),Ca.f-(caudal flexure),D.J.F-(Duodeno-Jejunal flexure).

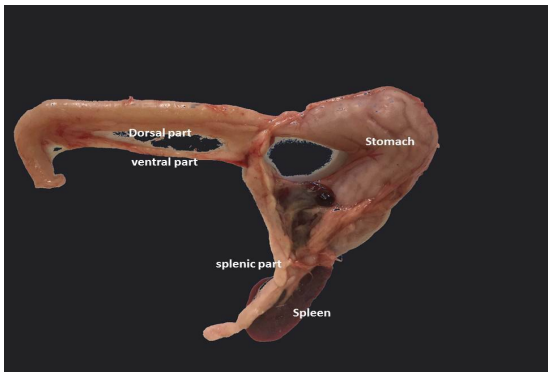

Fig4. Pancreas of gray mongoose showing compact mass occupied induodenum,consist of three part,cranial, caudal and splenic part.

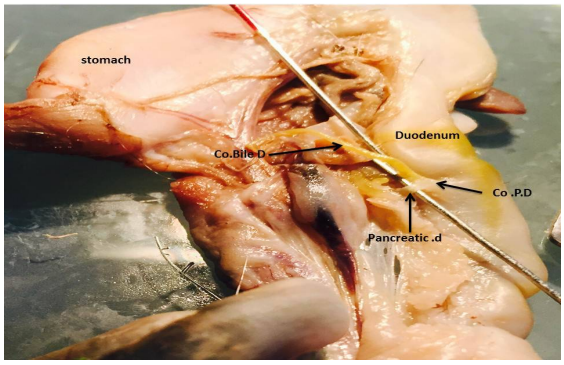

Fig.5. Common pancreatic duct in gray mongoose united with common bile duct before entering to duodenum

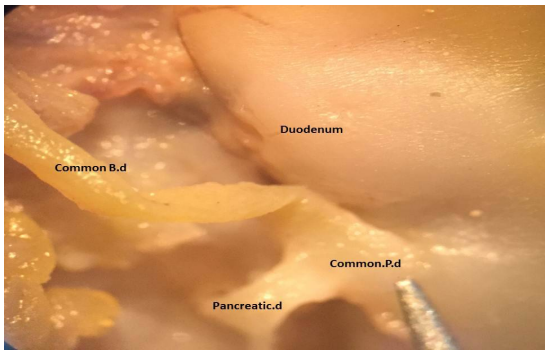

Fig.6. Common pancreatic duct consist from union by common bile duct and pancreatic duct before entering to duodenum.

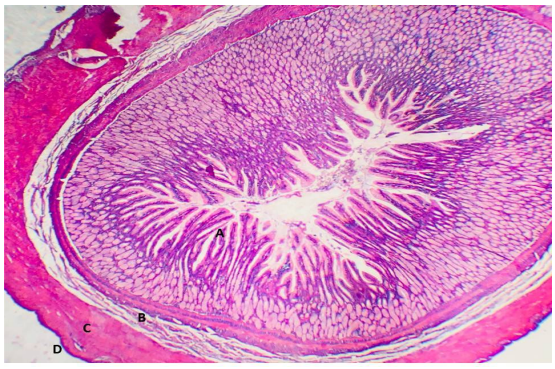

Fig.7. Descending part of duodenum showing four basic layers, A-Tunica mucosa,B-Tunica submucosa ,C-Tunica muscularis and D-Tunica serosa. H&E staining.100X.

Fig.8.duodenum in gray mongoose showing the simple columnar epithelia with goblet cells(yellow arrow).H&E stain, 400X

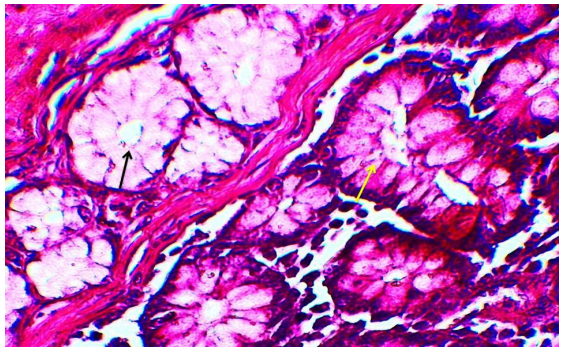

Fig.9. Duodenum in gray mongoose showing the Lieberkühn in duodenum (yellow arrow) and mucous Brunner's glands (black arrow). H&E stain,400X.

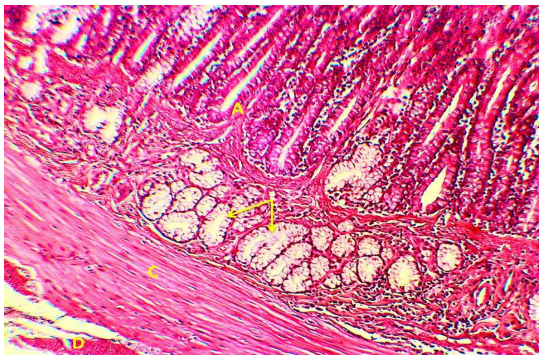

Fig.10. Ascending part of duodenum showing the submucosa contains Brunner's glands (yellow arrows). H&E stain.100X.

Fig.11. Duodenum of gray mongoose showing Tunica muscularis and tunica serosa.H&E stain.400X.

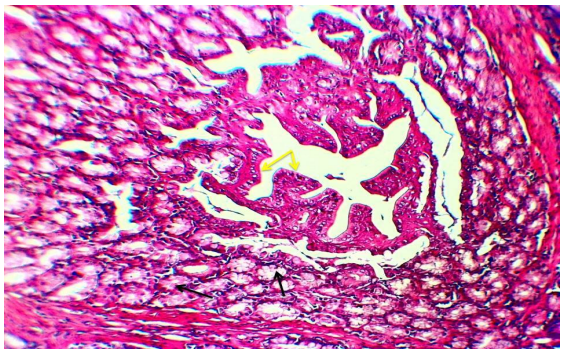

Fig.12. Duodenal papilla lined by short simple columnar epithelia (yellow arrow) surrounded by serous and mucous gland (black arrow).H&E stain, 100X.

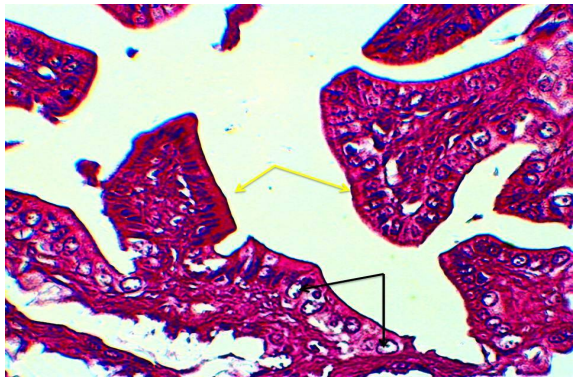

Fig.13. Duodenalpapilla lined by short principle simple columnar epithelia and absent of goblet cells(yellow arrows) andlight cells (black arrows). H&E stain.400X.

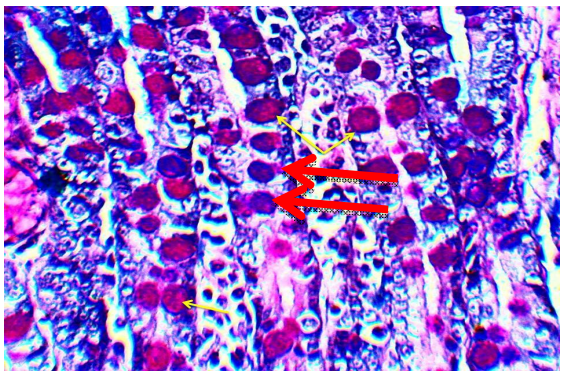

Fig,14) Tunica mucosa of duodenum showing the epithelia,the goblet cells had red in color(yellow arrows) and magenta color (red arrows).AB-PAS stain.400X.

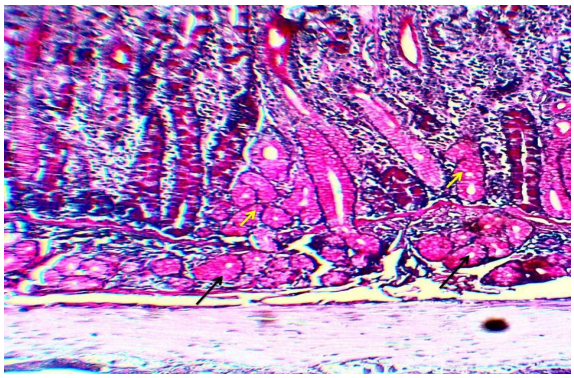

Fig.15.Duodenum in gray mongoose showing the intestinal gland (yellow arrow) and burner's glands (black arrows) .Alician blue-PAS stain.100X.

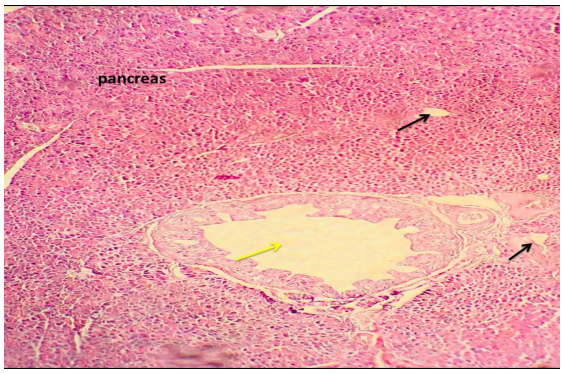

Fig.16. Pancreas of gray mongoose showing main pancreatic duct (yellow arrows) and interlobular pancreatic duct (black arrows). H&E stain.40X.

Fig.17.Main pancreatic duct lined by simple cuboidal epithelia (yellow arrows).H&E stain.n400X

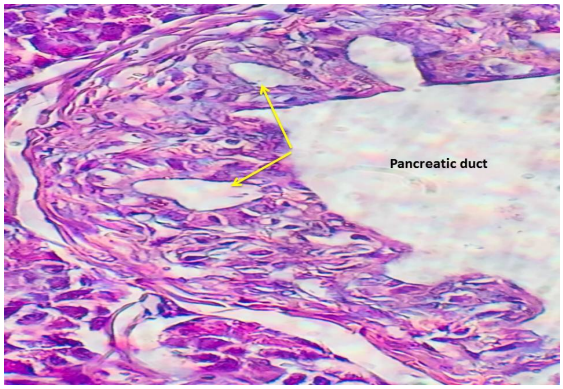

Fig.18. Main pancreatic duct contain serous glands which lined by cuboidal cells (yellow arrows).H&E stain.400X

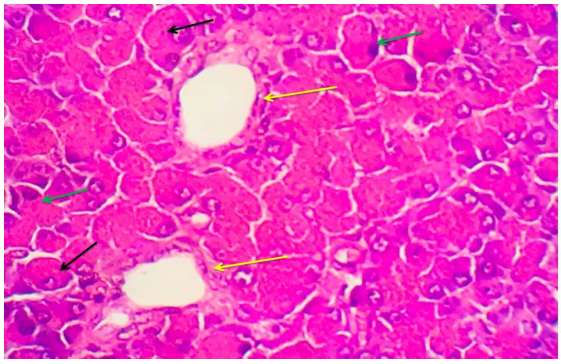

Fig.19. Pancreas of gray mongoose showing inter lobular duct lined by simple cuboidal epithelia(yellow arrows) and two types of acinar cells;regular (green arrows) and irregular (black arrows).H&E stain.400X.

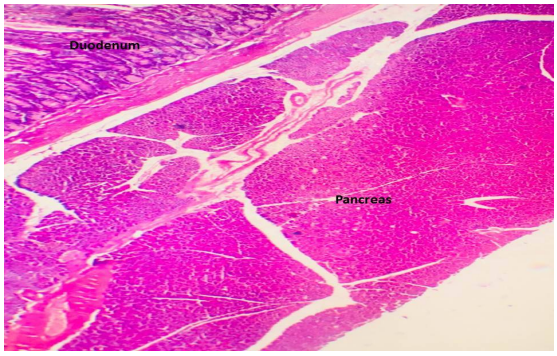

Fig.20. Duodenal part of pancreas showing the pancreas absenceof islet of Langerhans.H&E stain.40X.

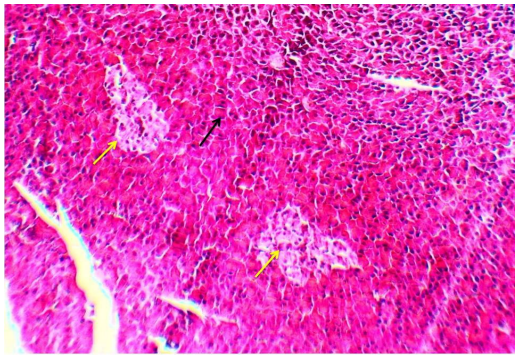

Fig.21 Splenic part of pancreas in gray mongoose showing the islet of Langerhans (yellow arrow) and pancreas acini (black arrow).H&E stain, 100X.

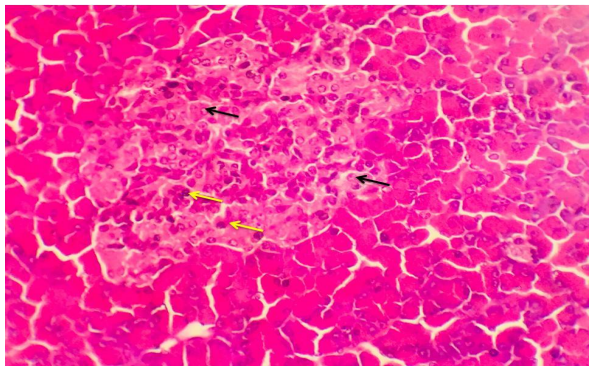

(Fig,22) Pancreas of gray mongoose showing islet of Langerhans had two types of cells rounded-palecells (black arrows) and irregular-dark cells (yellow arrows). H&E stain.400X

Indian Journal of Natural Sciences www.tnsroindia.org.in ©IJONS

Vol.9 /Issue 51 / December / 2018 *International Bimonthly* *ISSN: 0976 – 0997*

RESEARCH ARTICLE

The Effect of the Nd: YAG Laser Irradiation on the Bactericidal Action of the Sodium Hypochlorite: an *in vitro* Study.

Hareth A. Alrikaby[1]* and Balsam S. Abdulhameed[2]

[1]Laser Institute for Postgraduate Studies, Department of Biomedical Application, University of Baghdad, Baghdad, Iraq.

[2]Ministry of Health, Al-Kadhimyia Teaching Hospital, Department of Maxillofacial Surgery, Baghdad, Iraq.

Received: 12 Aug 2018 Revised: 16 Sep 2018 Accepted: 18 Oct 2018

***Address for Correspondence**
Hareth A. Alrikaby
Laser Institute for Postgraduate Studies,
Department of Biomedical Application,
University of Baghdad,
Baghdad, Iraq.

ABSTRACT

Objective: to explore the effect of Nd:YAG laser 1064 nm on the ability of sodium hypochlorite 5.25% in killing bacterial cells (in vitro). Background: the bactericidal action of sodium hypochlorite could be enhanced remarkably through agitation and activation of the solution. Materials and methods: bacterial samples were taken from infected root canals immediately after tooth extraction. The samples were divided into three groups each group contained ten individuals. In the first group, the samples were irradiated by laser for 2 minutes immediately after treatment by sodium hypochlorite. In the second group, the samples were treated with sodium hypochlorite for 2 minutes then irradiated by laser for 2 minutes. In the third group, the samples were treated with sodium hypochlorite solution for 5 minutes then irradiated by laser for 2 minutes. Bacterial swabs were taken from these samples before and after treatment.These swabs were streaked on blood agar and incubated, and the number of the colony forming units was recorded. Results: All the groups showed a bactericidal activity with different levels, according to the time of NaOCl exposure. The bactericidal activity in group one (immediate irradiation after NaOCl exposure) was about 49%, while in group two (irradiation after 2 min of NaOCl exposure) was about 73%. The most effective antibacterial activity was in group 3 (irradiation after 5 min of NaOCl treatment) where the percent reached about 96%. Discussion and conclusion: the 1064 nm Nd:YAG laser has a good impact on the bactericidal action of the sodium hypochlorite solution. The Nd:YAG laser was able to agitate the fluid and raising its temperature, which positively reflected on the role of the solution. The Nd:YAG could be used as a co-adjunctive agent in combination with sodium hypochlorite.

Key words: Nd:YAG Laser, Sodium hypochlorite, Bactericidal, Colony forming units.

INTRODUCTION

The term "Endodontic treatment" refers to the group of sequenced steps performed to treat an infected or inflamed pulp. These steps are done by a qualified dentist. The procedure includes creating an access cavity to reach the soft tissues of the pulp, then removing these tissues by using different metal instruments and solutions. Then the root canals will be filled and a final filling will be placed to close the cavity. There are many types of liquids used to facilitate this procedure, either for lubrication purposes (i.e.to make the movement of the metal instrument easier) or for sterilization of the canals and eradication of the bacteria. One of the most important solutions used in endodontic treatment is the sodium hypochlorite (NaOCl). This fluid came in many concentrations (1%, 2.5%, 5%, 7%,…etc). This fluid has very unique bactericidal effects since it can dissolve the organic components (protein-based components) and converting them to fatty acids[1]. With the progression of the science and technology, new materials and methods were introduced in endodontic treatments, and the laser is one of these new technologies. The laser systems played an important role in the easiness of the endodontic treatment.

They can be used in cavity preparation, stop bleeding and oozing, shaping of the root canals, activation of the irrigation solutions, cleaning, sterilization and killing of the microorganisms inside the root canals. There are many laser systems used for these purposes, Diode, Er:YAG, ErCr:YSGG, Nd:YAG. The activation of the sodium hypochlorite solution (NaOCl) during the irrigation process is very important since it can enhance the virulence of the solution and speeding its action[2]. The laser light has the ability to kill the bacterial cells by its thermal effects[3], and also through raising the temperature of the NaOCl which speeds the reaction between the NaOCl fluid and the organic components presents inside the root canal[4]. The Nd:YAG laser system 1064 nm categorized as a solid state laser that emits radiation at the near-infrared region. The Nd:YAG laser could be used in the eradication of bacteria that lived in the root canal walls. This laser could be delivered inside the root canal through optical fibers, and the laser beam can penetrate deeply through dentin of the root canals, reaches about 800 µm[5].

MATERIALS AND METHODS

30 extracted teeth, single rooted and primarily infected root canal, divided into three groups, each group contained ten samples. Bacterial swabs were taken from these canals immediately after extraction. These swabs immersed in a broth liquid nutritive media and incubated for 24 hours. Then the samples undergone a serial dilution and streaked on agar plates and incubated for 24 hours to determine the number of colony forming units (CFU) before the treatment. A pilot study was achieved to choose the most appropriate parameters. The desired parameter should be able to elevate the sample temperature to (25-40 C°) which is the temperature required for activation of NaOCl. Also, the desired parameter should reduce as much as possible the numbers of bacterial cells (which means less number of CFU on growth media). The desired laser parameters were 110-joule energy, 2 Hertz frequency, 40 ms pulse duration, 6 mm spot size (the same diameter of the Eppendorf tube opening), energy density $3.8924*10^4$ j/ cm^2.

In the first group in this study, one milliliter of sodium hypochlorite 5.25% (NaOCl) was added to one milliliter of the bacterial sample and irradiated by Nd:YAG laser for 2 minutes immediately after exposure to NaOCl (an Eppendorf tube 2 ml capacity was used as a container). In the second group, 1ml of the bacterial sample was treated by NaOCl 5.25% for 2 minutes, then exposed to Nd:YAG laser beam for 2 minutes. In the third group, 1 ml of bacterial sample was treated with NaOCl 5.25% for 5 minutes then exposed to the laser beam for 2 minutes. After treatment, swabs were taken from each treated sample and streaked on blood agar in order to count the number of CFU. The difference between the number of CFU before and after treatment was calculated to determine the best result from these groups. **.** Descriptive data analysis methods were used such as Mean value, Standard Deviation, Standard Error, 95% confidence interval of studied parameters in studied population as well as two extreme values (minimum, and maximum) of the measured readings. Graphical presentation also used by using Stem-Leaf (Explorer) Plot charts.

RESULTS

All the three groups showed different levels of antibacterial activity according to the diminishing in number of CFU after treatment. The first group (immediate Nd:YAG laser irradiation after NaOCl treatment) showed the least antibacterial activity, where the number of CFU was reduced to about 49% from the original number before the treatment. In the second group (Nd:YAG laser irradiation after 2 minutes of NaOCl treatment) the number of CFU was reduced to about 73%. The last group showed the best antibacterial activity where the number of the CFUs was reduced to about 96% from the original number before the treatment.

DISCUSSION

The eradication of bacteria and other infected tissue is one of the most important goals during root canal treatment. Here came the necessity of using an efficient bactericidal agent and seeking methods to enhance its action. There are many bactericidal agents used in the treatment of infected root canal, such as sodium hypochlorite (NaOCl), Chlorhexidine (CHX), ethylene–diamine–tetra-acetic acid (EDTA) in different concentrations[6,7,8]. NaOCl is the most used by many dentists because of its low cost and powerful effect. There are many techniques for activation and exaggerating the effect of the NaOCl solution, for example (manual activation by metal instrument, by an ultrasonic tip, preheating the liquid, or by using laser light)[9,10]. **José F. Siqueira *et al*[11]** tested many concentrations of NaOCl (1 %, 2.5%, 5.25%) to figure out which concentration has the more powerful bactericidal effect (in vitro). He used the NaOCl on root canals intentionally infected by *E.faecalis*, and count the bacteria(as CFU) before and after application of the solution. He concluded that "All the concentrations were effective in reducing bacterial count, and there were no significant differences between them."

Laser-assisted irrigation is a method starts to spread widely in the endodontic treatment with increasing usage of lasers in the dental field. Many laser systems used for this purpose, including (Er:YAG, ErCr:YSGG, Nd:YAG, and diode). Lasers have been recently proposed to activate irrigation solutions by the transfer of pulsed energy (mainly Diode, Nd: YAG, Er: YAG). Laser-activated irrigation has also been proposed to enhance the antimicrobial action of sodium hypochlorite[12]. Asnaashari M *et al*[13]. found that "Maximum effect is obtained when laser light is used in canals in combination with sodium hypochlorite irrigating substance in appropriate concentration" which coincides with this study. He compares between different laser wavelengths including Diode (810nm), Er:YAG (2940nm), Er,Cr:YSGG (2780nm) and Nd:YAG (1064nm) in killing bacterial cells and conclude that all " all lasers were efficacious in reducing bacterial population without damaging thermal effects. The Nd:YAG laser system categorized as a solid state laser system used mainly for soft tissue treatment, It contains a solid-state lasing medium, Neodymium-doped yttrium aluminum garnet). The Nd:YAG laser system operates in the near infrared area and emit radiation at 1064 nm and also operate invisible area and emit radiation at 532 nm (as a second harmonic generation). The 1064 nm wavelength has strong absorption by the pigments, such as melanin, hemoglobin, and pigmented bacteria[14]. Many studies were achieved on the role of Nd:YAG on the irrigation**.**

Sucheta *et al*.[15] tested the Nd:YAG laser effect on the NaOCl solution (in vitro). He used 1.5W at very short pulse mode of 15 Hz, three cycles of 5 seconds. Flexible laser fiber of 200 µm was used with a constant circular motion from apical to the coronal direction and kept 1 mm short of the apex, then observe the results under SEM. The results showed improved cleaning; The root canal surfaces exhibited open tubules, scattered residual debris, and a very thin smear layer. Rahimi *et al*[16]. Worked on roots of extracted teeth and he used Nd:YAG laser, NaOCl, and the combination of both to sterilize the canals. He proved that the effect of Nd:YAG laser beam on the bacterial cells is weaker than the effect of NaOCl 5.25%, and the combination of both agents gave the best results. Teruo ikarugi *et al.*[17] used Nd:YAG laser in combination with NaOCl (in vitro) and examine the results under SEM. He used pulsed Nd:YAG laser applied at an output of 1-3 Watt and a frequency of 15 Hz for 5 seconds, and a 320 µm fiber was inserted into the root canal that filled with NaOCl. The optical fiber has been moved up and down within a range of 5

mm from the apical end. He concluded that "By combining Nd:YAG laser and NaOCl, statistically significant cleaning effects have been obtained and elimination of the smear layer without damaging effects to the inside of the canal.Retamozo B *et al*[18] figured out that the best time for NaOCl application is 40 min to achieve very good bacterial eradication. In this study, the perfect bacterial elimination has been achieved by activation of NaOCl by utilizing Nd:YAG laser and the time required was reduced to 5 min only.

The Er:YAG family appeared more effect on the NaOCl liquid through many studies achieved and published. The Erbium family has more bactericidal action because of 2940, 2780 nm wavelengths have very strong absorption in water (which forms the most component of any living cell). The erbium laser has an ablative action which damages the walls of the root canals during the treatment. This is considered the main disadvantage of such type of laser[19]. Zhu X *et al*[20]. Used combination of NaOCl and Er:YAG to eradicate bacterial cells from experimentally contaminated root canals. He concluded that the laser-assisted irrigation has more ability than the conventional method to remove the smear layer and opening of dentinal tubules, which in turn will permit more penetration depth for NaOCl and sealer material for the dentinal tubules That explains the excellent bactericidal effect of this regime. Cheng *et al*.[21] tested (in vitro) the antibacterial effect of many laser systems (Nd:YAG, Er:YAG, ErCr:YSGG) on experimentally contaminated root canals, and found that the combination of Er:YAG laser with NaOCl has a very excellent bactericidal effect. At the end it could be concluded that the Nd:YAG has the ability to agitate and activate NaOCl solution and enhance its action. It can reduce the time of NaOCl usage to about 5 minutes.

ACKNOWLEDGMENTS

- Dr. Layla M. Hassan, The Head of the biomedical department, Institute of laser for postgraduate studies/ Baghdad University, Iraq.
- Dr. Hanadee A. Jasim, Assistant professor, college of medicine- Department of Microbiology/University of Basra, Iraq.
- Zainab A. Al-khafaji (Bacteriologist), MSc Microbiology, Ibn-Al Nafees medical laboratory, Basra, Iraq.
- Dr. Abdulkhaleq A. Al-Naqeeb (Biostatistician), College of Health and Medical Technology, Baghdad – Iraq.
- Al-Borooj company for medical supplies, Basra, Iraq.

REFERENCES

1. HAAPASALO et al. Persistent, recurrent, and acquired infection of the root canal system post-treatment (2004), *Endodontic Topics journal*.
2. Asnaashari M, Safavi N (2013). Disinfection of Contaminated Canals by Different Laser Wavelengths while Performing Root Canal Therapy. *Journal of Lasers in Medical Science*,Vol.4.
3. Adam Stabholz, Sharonit Sahar-Helft, Joshua Moshonov, Lasers in endodontics (2004). *Dental clinics of North America* web journal.
4. Giovanni Olivi, MD, DDS, Laser Use in Endodontics: Evolution from Direct Laser Irradiation to Laser-Activated Irrigation (scientific review) (2013). *Journal of Laser Dentistry*
5. Berkiten et al. Comparative evaluation of antibacterial effects of Nd: YAG laser irradiation in root canals and dentinal tubules. Journal of Endodontics (2000). Vol 26 issue 5. *Elsevier Inc*.
6. Bettina Ruth Basrani, endodontic irrigation: chemical disinfection of root canal system (2015), pages 65-115. *Springer*.
7. Nisha Garg, Amish Garg, Textbook of endodontics (2013) 2nd edition. Pages 210-230. *Jaypee Brothers Medical Publishers*.
8. Z. Mohammadi & P. V. Abbott. REVIEW The properties and applications of chlorhexidine in endodontics (2009). *International Endodontic Journal*.

9. De Gregorio C, Estevez R, Cisneros R, Heilborn C, Cohenca N. Effect of EDTA, sonic, and ultrasonic activation on the penetration of sodium hypochlorite into simulated lateral canals: an in vitro study(2009). Journal of Endodontics.Vol.35 issue 6.
10. Deleu E, Meire MA, De Moor RJ. Efficacy of laser-based irrigant activation methods in removing debris from simulated root canal irregularities(2015). Lasers in medical science. Vol.30 issue 2.
11. José F. Siqueira et al. Chemomechanical Reduction of the Bacterial Population in the Root Canal after Instrumentation and Irrigation with 1%, 2.5%, and 5.25% Sodium Hypochlorite (2005). Journal of Endodontics, Vol 26, issue 6. *Elsevier Inc*.
12. Giovanni Olivi, MD, DDS, Laser Use in Endodontics: Evolution from Direct Laser Irradiation to Laser-Activated Irrigation (scientific review) (2013). *Journal of Laser Dentistry.*
13. Asnaashari M, Safavi N (2013). Disinfection of Contaminated Canals by Different Laser Wavelengths while Performing Root Canal Therapy. *Journal of Lasers in Medical Science*,Vol.4.
14. Adam Stabholz, Sharonit Sahar-Helft, Joshua Moshonov, Lasers in endodontics (2004). *Dental clinics of North America* web journal.
15. Sucheta Sathe, Vivek Hegde, Paresh Arvind Jain, Dhananjay Ghunawat. Effectiveness of Er: YAG (PIPS) and Nd: YAG activation on final irrigants for smear layer removal - SEM observation (2014). Journal of dental lasers, Vol.8 issue 1.
16. Rahimi *et al*. (2012). Bactericidal effects of Nd:YAG laser irradiation and sodium hypochlorite solution on Enterococcus faecalis biofilms. *Journal of Photomedicine and laser surgery*, Vol.30.
17. Teruo ikarugi et al. Root canal irrigation using Nd:YAG laser in combination with various solution: a morphological study (2008). Journal of oral laser application, Vol.8 issue 3.
18. Retamozo et al. (2010). Minimum contact time and concentration of NaOCl required to eliminate E.faecalis. *Journal of endodontics*, Vol.36.
19. Mozammal Hossain et al. (2009). Ablation Depths and Morphological Changes in Human Enamel and Dentin after Er:YAG Laser Irradiation with or without Water Mist. Journal of Photomedicine and laser surgery, Vol 17 issue 3. *Mary Ann Liebert Inc.*
20. Zhu X, Yin X, Chang JW, Wang Y, Cheung GS, Zhang C (2013). Comparison of the antibacterial effect and smear layer removal using photon-initiated photoacoustic streaming aided irrigation versus a conventional irrigation in single-rooted canals: an in vitro study. *Journal of Photomedicine and Laser Surgery*, Vol.8
21. Cheng et al. Evaluation of the bactericidal effect of Nd:YAG, Er:YAG, Er,Cr:YSGG laser radiation, and antimicrobial photodynamic therapy (PDT) in experimentally infected root canals(2012). Lasers in surgery and medicine. Vol.44 issue 10.

Table (1): Summary statistics of groups treated with (NaOCl+Laser) techniques.

Groups	Periods	No.	Mean	Std. D.	Std. E.
Immediate	**Before**	**10.0**	**1107**	**222.0**	**70.19**
	After		**588**	**116.6**	**36.87**
2 Minute	**Before**	**10.0**	**990**	**188.9**	**59.72**
	After		**262**	**47.8**	**15.11**
5 Minute	**Before**	**10.0**	**1230**	**293.2**	**92.71**
	After		**47**	**32.0**	**10.12**

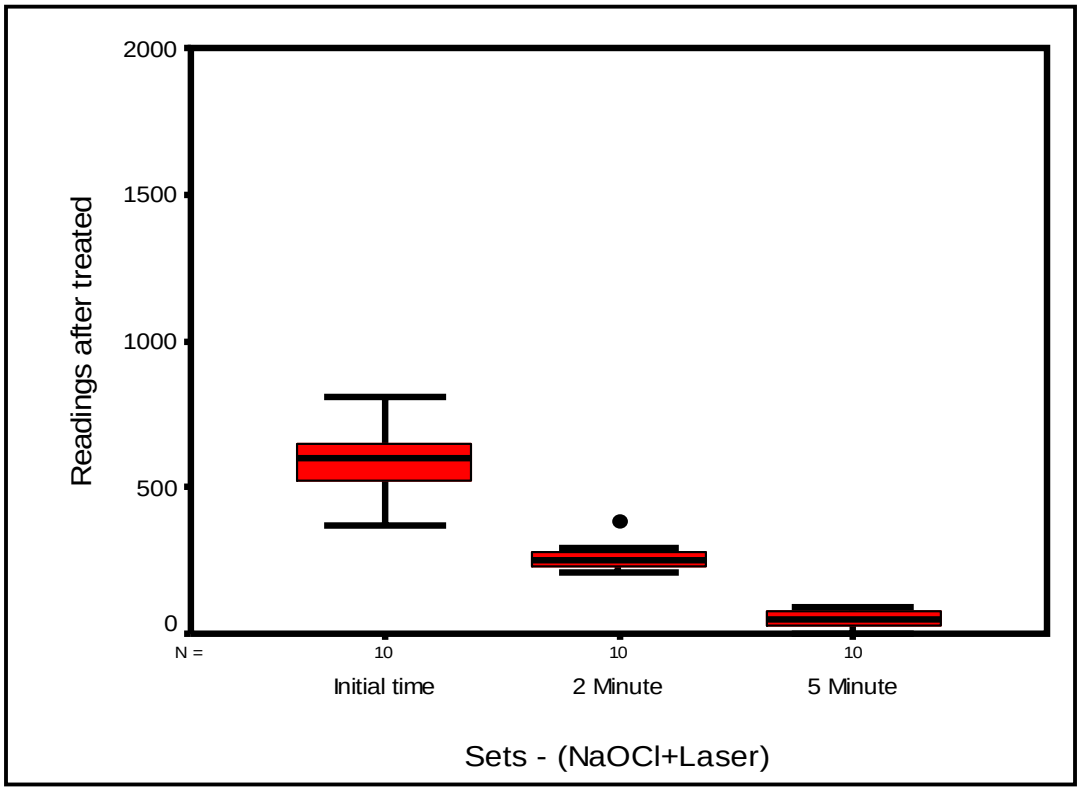

Fig. (1) shows the numbers of CFU after treatment with NaOCl and laser irradiation for all three groups.

Indian Journal of Natural Sciences www.tnsroindia.org.in ©IJONS

Vol.9 /Issue 51 / December / 2018 *International Bimonthly* *ISSN: 0976 – 0997*

RESEARCH ARTICLE

Comparison between the Structural, Morphological and Optical Characteristic of Nanocrystalline CdO Thin Films Deposited by Spray Pyrolysis Processes and Pulsed Laser Deposition (PLD) Technique

Maysar A. Salim[1]*, Isam M. Ibrahim[2] and Iftikhar M.Ali[2]

[1]Department of Energy Engineering, College of Engineering, University of Baghdad, Baghdad, Iraq.
[2]Physics Department, Science College, University of Baghdad, Baghdad, Iraq.

Received: 15 Aug 2018 Revised: 18 Sep 2018 Accepted: 20 Oct 2018

***Address for Correspondence**
Maysar A. Salim
Department of Energy Engineering,
College of Engineering,
University of Baghdad,
Baghdad, Iraq.
E mail: Maysar88888@gmail.com

ABSTRACT

Cadmium Oxide (CdO) thin films, of nanocrystalline structure, 100nm thickness were prepared on corning glass substrate, ultrasonically cleaned. by both spray pyrolysis method at 250°C. and pulsed laser deposition(PLD) technique at R.T. the structural , morphological and optical properties of the deposited CdO thin films were studied using X- ray diffraction (XRD) , Atomic Force Microscopy (AFM) analysis , and UV-VIS-NIR spectroscopy. a comparison between the optical , morphological and structural characteristics of the prepared thin films ,show that all the prepared thin films are polycrystalline with the preferred direction of (111), cubic Lattice constant(a) of (4.694 °A), while a higher values for all other calculated structural , morphological, and optical parameters for spray pyrolysis prepared thin films ,such as grain size(D) , peak to valley roughness, root mean square(RMS) roughness ,grain diameters , optical transmittance (T), a direct and indirect optical energy gap (E_g^{opt}) ,which confirm their affected by method of preparation and the different deposition parameter used. Ananocrystalline ofwide band gap semiconducting CdOthin films are widely used in optoelectronic applications such as solar cells.

Key words: CdO thin film, nanocrystalline, spray pyrolysis, PLD, XRD, AFM, optical characteristics.

A (II-IV) semiconductor compound which include the transparent conducting oxides materials (TCOs), such asCadmium Oxide (CdO), Zinc Oxide (ZnO), Tin Oxide (SnO_2), Indium Oxide ($In_2 O_3$), In particular Cadmium Oxide (CdO) is a promising material because of their high transmission in the VIS- region of solar spectrum, that make them be used in many applications especially in the optoelectronic devices such as solar cells, transparent electrodes , gas Sensor , optical communication, phototransistor , photodiode and the most important properties make them to be used in smart windows are their high reflectance in IR region of solar spectrum . [1-3] undoped CdO is an n - type semiconductor with a rock-saltcrystal structure (FCC)[4,5],CdO is widely studied as n-type nonstoichiometric semiconducting oxide with lower electric resistivity 10^{-2} - 10^{-4} (Ω .cm) which may be due to the Oxygen vacancies and Cadmium interstitials[6,7], with direct optical band gap of 2.5 ev and an Indirect one of 1.98 ev [8], CdO rhombus and Cauliflower nanocrystalline thin film are used as a water purifier for the absorption of Cango red dye from water [9,10] , the physical properties of CdO thin films have remarkable dependence on the crystallite size which depend on the synthesis method, and the various deposition parameter such as , substrate temperature [11] , post annealing [12], film thickness[13] , etc … . the various nanostructure of CdO such as Nano wires , Nano rods , quantum dot were synthesis to improve the properties of a bulk CdO and their application [14,15]. Various methods are used to deposited Undoped and doped CdO thin films such as spray pyrolysis method [3,15] , sol-gel method [4,5],physical vapor deposition (PVD)[6],pulsed laser deposition(PLD) technique [16], Ion beam sputtering, etc.…

In this work a comparison between the structural ,morphological and optical properties of CdO thin films , 100nm thickness , deposited by spray pyrolysis method at 250°C and pulse laser deposition(PLD) technique at R.T. ,each method has several advantages compared with others ,for spray pyrolysis method , Recently spray pyrolysis method are widely used for preparation metal oxide material of nanostructure properties which are used in microelectronic applications [6],because of low cost due to the simplicity of the equipment required ,easy and fast in preparing thin films, the possibility of getting flexible panel display ,In addition it is relatively inexpensive[18,19]. large area thin films with the required thickness , in addition the prepared thin films have high stability with time in their physical properties [17], while the advantages of PLD , technique are: the composition of the target used and the prepared thin films are quite close ,because of high kinetic energies of the ejected atoms and the ionized species in the plasma produced by the laserso PLD films were crystalline at lower temperature with respect to other physical vapor deposition (PVD) , this method was used to grow CdO films.

EXPERIMENTAL METHODS

Cadmium Oxide thin films ,100nm thickness ,were deposited by two method : (1) Spray pyrolysis method , In this method Cadmium Oxide (CdO) thin films of 100nm thickness were deposited on ultrasonically cleaned corning glass substrate , by dissolving Cadmium acetate in distilled water of (0.1M) an aqueous solution of Cadmium acetate were prepared , spraying of the solution on the substrate heated to 250° C, Cadmium Oxide (CdO) thin films were deposited as a result of pyrolytic decomposition of the sprayed droplet reaching the hot substrate , while other compounds were in the gas phase escape out [1].

$$Cd(CH_3COO)_2\,2H_2O \rightarrow CdO(s) + CH_3COOCH_3(g) + CO_2(g) + 2H_2O(g) \quad \ldots(1)$$

The mass of the material(CdO) (g) = volume (mL)* molecular concentration (moL/L) * gram molecular weight(g/mole).The flows of the solution and gas carrier were kept constant at 5mL/min and 61ml/min respectively, the distance between the nozzle and the substrate was 35 cm ,the time of spraying is 20 min while the air pressure inside the glass room were kept constant at 3 bar, it is necessary to leave the prepared thin film on the electric heater for 1h at least to complete oxidation and crystalline growth process .

(2)-pulsed laser deposition technique (PLD), first the glass substrates were cleaned ultrasonically, target were prepared from cadmium Oxide powder (99.99%) using cold pressing (5 Ton on 12mm diameter pellet) , the substrate was placed on a rotating holder at a distance of 1.5 cm above the target, the target (CdO pellet) were ablated using a-ND-YAG laser source (λ =1064nm) and an energy of 600mJ, No. of shoot 500 ,the ablation were carried when the substrate at R.T. and an ambient Oxygen pressure of 0.02mbar ,laser beam were focus toward the rotating target at an angle of incident of 45°, the laser were operated at a pulse rate of 6Hz for a period for two min .because of a combination of low ambient pressure in the chamber and the high energy of laser beam ablating the target ,an ejected flux of atoms, ions and electrons are normal to the target surface , condensed on the substrate opposite to the target . weighting method were used to estimate the amount of CdO needed to prepare the required thickness (t) according to the following formula [20]:

$$t = \frac{m}{2\pi R^2 p} \quad \ldots\ldots\ldots (2)$$

m : is the mass of the used material (g) , R: is the source (target) to substrate distance (cm) , P : is the density of the material to be evaporated (g/cm^3) , the error percentage of this method~30%. The precious film thickness (t) was measured according to the following formula:

$$t = \frac{\lambda}{2}\frac{\Delta X}{X} \quad \ldots\ldots\ldots\ldots\ldots\ldots (3)$$

where λ : is the wavelength of He – Ne laser (632.8 nm) , Δx; fringe shift , x : is the fringe width The structure of CdO thin film were examined Using (Philips 3710pw) XRD system with Cuk$\propto$radiation (λ = 0.15466 nm) .The surface morphology for CdO thin film were examined Using Atomic Force Microscopy (AFM) (SPM, Model A A3000 Using (shimodzuUV1650 PC) spectrophotometer to measure the transmittance of CdO thin films in the wavelength range (300-1100)nm

RESULTS AND DISCUSSION

Structural Studies

Fig. 1 and Fig. 2 show XRD spectra of as - deposited CdO thin films , 100 nm thickness, prepared by Spray pyrolysis method and pulsed laser deposition (PLD) technique respectively, a polycrystalline films of space group Fm3m , the detail of the crystalline structure (the interplanar spacing ,grain size and lattice constant) are shown in table .1 ,the two prepared films (by spray pyrolysis and PLD) show the diffraction peaks (111), (200) and (220) with the preferred direction of (111), this is in agreement with Ref.[4,7] .the interplanar spacing (d_{hkl}) were calculated according to the following equation [21]:

$$d = \frac{n\lambda}{\sin\theta} \quad \ldots\ldots\ldots (4)$$

n = is reflection order, the values of the interplanar spacing are nearly similar to the standards values in ICDD Card No. (96-900-8610), the lattice constant (a) with face Center Cubic (FCC) crystal were calculated according to the following equation [25]:

$$a = d_{hkl}(h^2 + k^2 + l^2)^{1/2} \quad \ldots\ldots\ldots\ldots\ldots\ldots (5)$$

Where h,k,l are the Miller indices of a given orientation , the average value of the lattice Constant (a) of CdO thin film prepared by spray pyrolysis method and PLD technique, are 4.696 ˚A and 4.693 ˚A respectively, which are in agreement with Ref [5,23],the grain Size (D) of CdO thin film were examined Using Debye Scherrer relation [24]:

$D = 0.9\lambda/\beta\cos\vartheta$ ……..(6)

Where β is the full width at half maximum (FWHM) of the diffraction peak ,the grain Size (D) of CdO thin film were calculated according to equation (6) , the narrower FWHM for CdO thin films prepared by PLD technique Compared to that prepared by Spray pyrolysis method which inturn give higher values for the grain Size of 23.66 nm while it is 15.93 nm for spray pyrolysis prepared thin film which prove the nanocrystallite structure [26], this mean that PLD CdO thin films have better crystalline.

Morphological Studies

Fig. 3 and Fig. 4 show Atomic Force Microscopy(AFM) Images of CdO thin films , 100nm thickness , deposited by spray pyrolysis method and PID respectively ,the films were seen to be very Smooth , void - free and yellowish in color which are the property of Cadmium Compounds , the surface analysis showed that the peak to valley roughness for prepared by spray pyrolysis and PID are 3.87 nm and 2.32 nm respectively , this parameter is very important in preparing good optoelectronic devices since the leakage current increase as the peak to valley roughness increase [25], the root mean square(RMS) roughness of CdO thin films prepared by spray pyrolysis and PLD are 4.47nm and 2.71nm respectively ,which are superior for Indium doped Tin Oxide films (~4nm), commercially available [30].the average grain diameter (grain height) for CdO thin film prepared by spray pyrolysis and PLD were 96.82 and 94.20 nm respectively . which are in agreement with Ref. [26].Fig. 5 and Fig. 6 show the percentage distribution of the grain diameters of CdO thin films, 100nm thickness, that are prepared by spray pyrolysis method and PLD respectively, which show a more homogenous, for the Latter thin film than for the former.

Optical properties

Fig. 7 show the transmittance of CdO thin film 100nm thickness , prepared by spray pyrolysis method and PLD technique in spectrum range (300-1100nm), the higher transmittance for spray pyrolysis prepared film (~ 50%) than that of PLD film (~35%) I.e. higher transmitance (T) for the lower gram size (D) thin films,which subsequently show a decrease in the absorption coefficient (α) at the related wavelength since it related to it according to equation(7),it can be also shown that the increase in the transmittance in UV – region are not sharp (non-sharp decrease in absorption coefficient), this indicate that the absorption band gap transition are due to direct and indirect transition [4] ,the absorption coefficients(α) are calculated according to the following equation[17] :

$$\alpha = \frac{\ln 1/T}{t} \quad \text{..... (7)}$$

Where t:is the film thickness.

Fig.8 show the absorption coefficient (α) of CdO spray pyrolysis and PLD thin films prepared, in the wavelength range (300-1100nm).The extinction coefficient (k) which related to the exponential decay of the electromagnetic radiation in the medium was calculated according to the following equation [27]:

$K = \alpha\lambda/2\pi$…….(8)

Fig.9 show the relation between the extinction coefficient (k) and the wavelength in (300-1100nm) for spray pyrolysis and PLD thin films prepared, in general the extinction coefficients (k) decrease as the energy of the

incident increase (λ decrease), the higher value for the extinction coefficient(α) of spray pyrolysis for the lower transmittance since it related to it and derive from it. The fundamental absorption which related to the transition of the electron from the valence band to Conduction band , which can be used to determine the nature of the electronic transition and the value of the optical energy gap (E_g^{opt}) using Taue equation [28].

$$\alpha h\upsilon = B\,(h\upsilon - E_g^{opt})^n \qquad \text{.....(9)}$$

Where B : is the Taue constant, hυ: is the photon energy (ev), n : assume the values 1/2, 2, 3/2 and 3 for allowed direct, allowed indirect, forbidden direct , and forbidden indirect transition respectively . the type of optical transition can be understood by plotting each of $(\alpha h\upsilon)^{1/2}$, $(\alpha h\upsilon)^2$,$(\alpha h\upsilon)^{1/3}$ and $(\alpha h\upsilon)^3$ vs photon energy (hυ) , it was observed that the relation show linear dependence for n = ½ and n= 2 which confirm that the deposited CdO thin films have direct and indirect optical energy gap (E_g^{opt}) which were determined by extrapolating the linear portion at the photon energy axis (hυ) (i.e. $\alpha h\upsilon = 0$) Fig. 10 and Fig.11show the variation of $(\alpha h\upsilon)^2$ and $(\alpha h\upsilon)^{½}$ as a function of photon energy (hυ) for CdO thin films prepared by spray pyrolysis and PLD, the direct (Indirect) energy gap for spray pyrolysis and PLD are 3.8ev (3.15ev) and 3.7ev (3.00ev) respectively .the lower value for the CdO thin film PLD prepared may be due to the higher grain size [26], the high value for the optical energy gaps confirm the nanocrystalline nature because of the quantum size effect [25].

CONCLUSIONS

Nancrystalline transparent conducting Oxide (TCO) CdO, 100nm thickness thin film were deposited or ultrasonically cleaned Corning glass substrate by two method , spray pyrolysis at 250 ˚C and pulsed laser deposition (PLD) technique at R.T. , the structural studies showed the CdO thin film prepared by spray pyrolysis and PLD were confirms CdO phase polycrystalline grain size (D) with the preferred orientation along (111) plane , with cubic Crystal lattice, of (4,693˚A) while a higher grain size (D) for PLD film prepared ,but a higher values for all other measured morphological properties such as peak to valley roughness , root mean square (RMS) roughness ,the grain diameter and the optical properties, such transmittance(T) , direct and indirect optical energy gap, these results Confirm the dependence of the structural , morphological and optical properties on the method of preparation also the experimental analysis show that spray pyrolysis method is best method to prepare CdO nanocrystalline thin films which can be used widely in optoelectronic devices and gas sensors.

ACKNOWLEDGENMENTS

Authors are grateful to the department of Physics, College of Science, Baghdad University, Iraq.The authors would like to thank friends for generous supports and valuable discussions and comments.

REFERENCES

1. B. G. Jeyaprakash, K.Kesavan, R.AshokKumar,S.Mohan and A.Amalarani,"Temperature dependent grain-size and microstrainnn of CdO thin films prepared by spray pyrolysis method ", *Bull. Mater. Sci.*,34(4):601-605(2011)
2. Z.Zhau,D.L.MorelandC.S.Ferekides, "Electrical and optical properties of tin-doped CdO films deposited by atmospheric metalorganic chemical vapor deposition ",Thin Solid Film,412: 203-211(2002).
3. M.Yan,M.Lan,C.R.Kannewurf,andR.P.H.Chang," Highly conductive epitaxial CdO thin films prepared by pulsed laser deposition, "*Appl.phys. Lett.*,78:2342-2344(2001)
4. D.M.Carballeda-Galicia,R.Castanedo-Perez,O.Jimenez-Sandoval, S. .Jimenez-Sandoval, G.Torres-Delgado, C.1. Zuniga-Romero," High transmittance CdO thin films obtained by the sol-gel method",*Thin solid films*,,371:105-108 (2000).

5. A. AbdolahzadehZiabari and F.E Ghodsi," *Optical and Structural Studies of Sol-Gel Deposited Nanostructured CdO Thin Films Annealing Effect* " ,*ActaphysicaPolonica A* , 120(3): 536-540(2011) .
6. R.S.Rusu, G.I.Rusu," On the electrical Optical characteristics of CdO thin films", the *Journal of Optoelectronics and Advanced Materials*,7(2):823-828(2005)
7. Z. Zhao, D . L. Morel , C.S. Ferekides," Electrical and optical properties of Tin-doped CdO films deposited by atmospheric metalorganic chemical vapor deposition",*Thin Solid Films, 413: 203-211 (2002)*
8. D. R .Lide (Ed), CRC Handbook of Chemistry and Physics, 77thed, CRC Press, Boca Raton, 1996/ 1997.
9. AzadehTadjarodi, Mina Imani and Hamedkerdari," adsorption Kinetics thermodynamic studies, and high performance of CdO Cauliflower –Like nanostructic structure on the removal of Congo red from aqueous Solution" *J. Nanostructure in Chemistry*, 3 (51): 1-8 ,(2013).
10. AzadehTadjarodi, Mina Imani, Hamedkerdari, Keyvanbijanzad, Dorsankhaledi and Maryam Rad, "Preparation of CdO Rhombus - like nanostructure and its photocatalytic degradation of Azo dyes from aqueous solution ", *Nanomater. nanotechnoL*.,4(16): 1-6(2014).
11. A .U.Ubale, Y.S. Sakhare ," Effect of substrate temperature on optical ,structural,, and electrical properties of FeSe thin films deposited by Spray pyrolysis Technique", *J .Physics and Chemistry of Solid* ,74(10):1459-1464(2013).
12. Ashok U. Ubale , Naina R. Welekar, Amruta V. Mitkari," Effect of annealing on physical properties of CBO synthesized nanocrystallineFeSe thin films", *Mater. Sci. Semi. Processing*, 27:280-287(2014).
13. Maysar A. salim,"Effect of thickness on the optical properties of ZnO thin films prepared by pulsed laser deposition technique ", *Iraqi journal of physics*15 (32): 114 – 121 (2017).
14. H. S. Virk ," Effect of 90 MeV Carbon ion irradiation on Cadmium Oxide quantum dots ". *Current Science* ,100(10): 1540 -1542 (2011).
15. B.J. Lokhande ,P.S. Patil, M.D. Uplane , "Studies on cadmium oxide sprayed thin films deposited through non-aqueous medium" J ,*Mater. Chem. Phys.*, 84: 238- 248(2004).
16. R.K. Gupta , K. Ghosh , R. Patel , S,R. Mishra , P.K. Kahol, " preparation and characterization of highly condueting and transparent Al doped CdO thin films by pulsed laser deposition", *Current Applied Physics*, 9 (3): 673-677 (2009) .
17. Raoof Ali Ahmed , "A .C. mechanism of doped ZnS thin films", *M.Sc. thesis* , university of Baghdad, Iraq, (2014).
18. N. F .Sanice, " structural , Electrical and optical properties of transparent Conducting Si-doped ZnO thin film grown by pulsed laser Deposition ", *M.Sc . thesisuniversity of Birmingham , Great Britain*, (2009).
19. B.D.Chrisey ,G.k. Hubler, *Pulsed laser Deposition of Thin Films, Wiley. New, York,* 1994.
20. L.K.Chopra, *Thin Film phenomena, Mc. Graw. Hill Book Company,*(1969).
21. C.Kittle,"*Introduction to Solid State Physics*", Thomsen press, New Delhi, 8th Edition (2005).
22. A.U.Ubale , S.S. Wadnerkar, P.N.SononeandG,D,Tayade," Study of structural optical and electrical properties of CdO thin film deposited by sol –gel spin coating teachnique", *Archives Physics Research*,5(6): 43-48(2014).
23. O.Vigil, F.Cruz, A. Morales-Acevedo , G, Conteras-Puente, L.Vaillant, G.Santana," Structural and optical properties of annealed CdO thin films prepared spray pyrolysis", *Materials Chemistry and physics* ,68: 249-252 (2001).
24. B. Ray, *II-VI Compounds* , Pergamum press, Ist edition printed in Great Britain by Neil and Co. L.t.d. of Edinburgh (1969).
25. Y.-H.Tak, K.-B. Kim, H.-G.park, K.-H. Lee J.- R. Lee,"Criteria for ITO (Indium-Tin-Oxide thin film as the bottom electrode of an organic light emitting diode ", *Thin Solid Films*, 411(1):12-16(2002).
26. R.R.Salunkhe, D.S. Dha wale, C.D. Lokhande ,"Sprayed CdO thin films for liquefied petroleum gas (LPG) detection", *Sensors and Actuators B:Chemical* ,140: 86-91 (2009)
27. J. Taue, "*Amorphous and liquid Semiconductor*, plenums press, New york and London(1974) .
28. A.Jain, P.S.agar, R.Mchra, J. Materials Science 25 (1), 233-242,(2007).

Table 1. The crystallographic parameter : FWHM (Deg.) , the interplanar spacing (d_{hkl}) (˚A) experimental and standard values , grain Size (D) (nm) and lattice (a) (˚A), of as-deposited CdO thin films (100 nm) thickness prepared by spray pyrolysis method at 250 ˚C . and PLD technique at R.T.

Spray pyrolysis method								
2θ (Deg.)	FWHM (Deg.)	Int (a.u)	d_{hkl} Exp. (˚A)	G.S (nm)	hKL	a (˚A)	Phase	d_{hkl} Std. (˚A)
33.020	0.353	465	2.710	23.5	(111)	4.693	CdO	2.7108
38.320	0.356	343	2.347	23.6	(200)	4.694	CdO	2.3477
55.320	0.376	140	1.6593	23.9	(202)	4.693	Cd0	1.6600
PLD technique								
2θ (Deg.)	FWHM (Deg.)	Int. (a.u)	d_{hkl} Exp.(˚A)	G.S (nm)	hkl	a (˚A)	Phase	d_{hkl} Std.(˚A)
32.98 3	0.553	180	2.7135	15.0	(111)	4.694	CdO	2.7108
38.25 6	0.556	90	2.3508	15.1	(200)	4.7016	CdO	2.3477
55.317	0.576	60	1.6594	15.6	220	4.693	CdO	1.6600

Table 2: The values of average peak to valley roughness (nm) , RMS roughness (nm) and average grain diameter (nm) of CdO thin film ,100 nm thickness, prepared by spray pyrolysis method at 250˚C and PLD technique at R.T.

Spray pyrolysis method.			
CdO	Ave. roughness (nm)	RMS roughness(nm)	Ave. grain diam. (nm)
Pure	3.87	3.87	96.82
PLD Technique.			
CdO	Ave. roughness (nm)	RMS roughness (nm)	Ave. grain dram. (nm)
pure	2.32	2.71	94.2

Table 3: The values of direct and indirect energy gap for CdO thin films ,100nm thickness, prepared by spray pyrolysis at 250˚C and PLD technique at R.T.

Method of preparation	**Direct energy gap(eV)**	**Indirect energy gap(eV)**
Spray pyrolysis	3.85	3.15
PLD technique	3.7	3.00

Table 4 Comparison of the structural, AFM and optical properties : Reflection planes, preferred orientation Av.Grain size (D), Av. Lattice constant (a),peak to valley roughness, RMS roughness, grain diameter, transmittance(T),direct and indirect energy gap for CdO thin films prepared by spray pyrolysis at 250°C and PLD technique. at R.T.

	Spray pyrolysis method	PLD technique
Refraction planes	(111),(200),(220)	(111),(200),(220)
preferred orientation	(111)	(111)
Av. Grain size(nm)	15.23	23.66
Av. Lattice constant(°A)	4.696	4.693
Peak to valley roughness(nm)	3.87	2.32
RMS roughness(nm)	4.47	2.77
Grain diameter(nm)	96.82	94.20
Transmittance(T)	~ 50 %	~ 35 %
Direct energy gap(eV)	3.85	3.7
Indirect energy gap (eV)	3.15	3.00

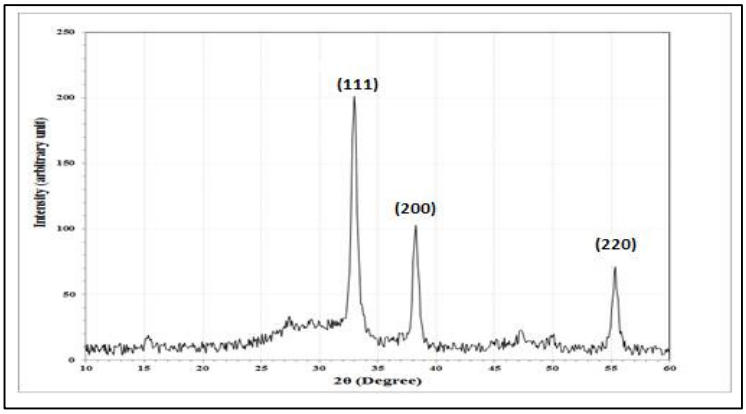

Fig. 1 : The XRD spectrum of as – deposited CdO thin films , 100 nm thickness, prepared by spray pyrolysis method at 250 ° C

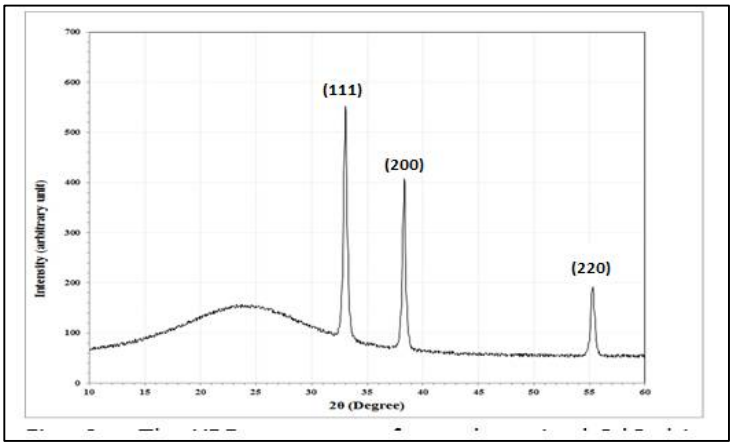

Fig 2: The XRD spectrum of as – deposited CdO thin films, 100 nm thickness, prepared by PLD technique at R.T.

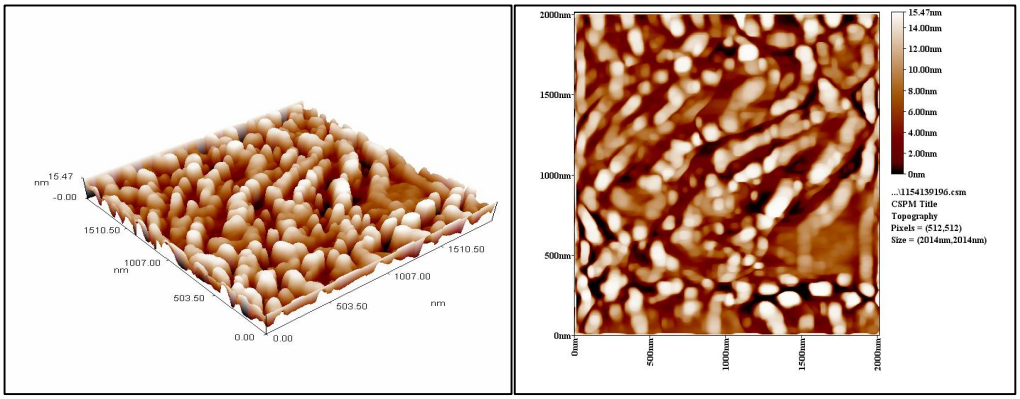

Fig. 3: AFM left, front and the right , 3 – dimensional images of CdO thin films , 100nm thickness, prepared by spray pyrolysis method at 250˚ C.

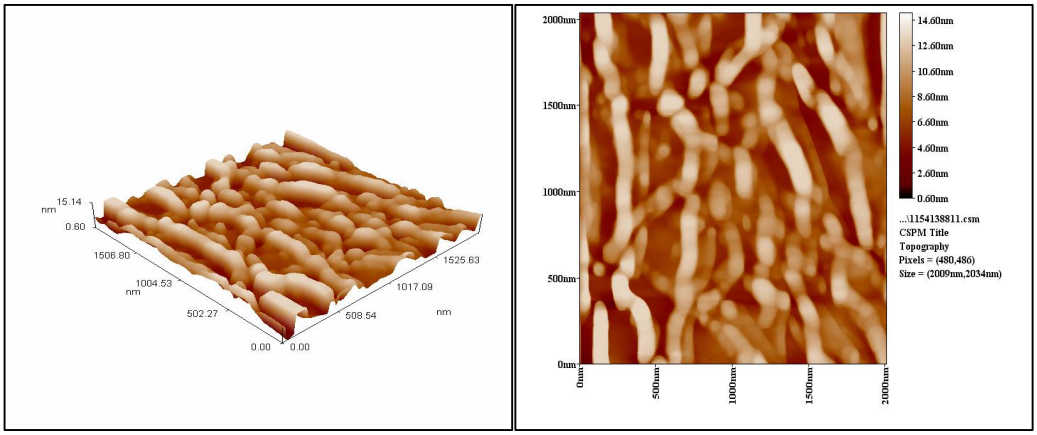

Fig. 4: AFM left ,front and the right, 3 – dimensional images of CdO thin films , 100nm thickness, prepared by PLD technique at R.M.

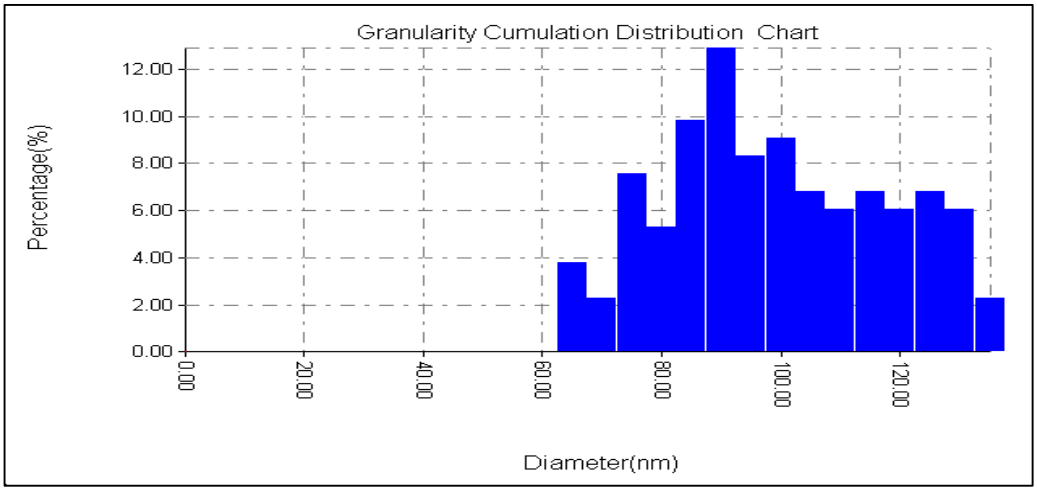

Fig. 5: Granularity accumulation Distribution chart for of CdO thin film of 100 nm thickness , prepared by spray pyrolysis method at 250˚C .

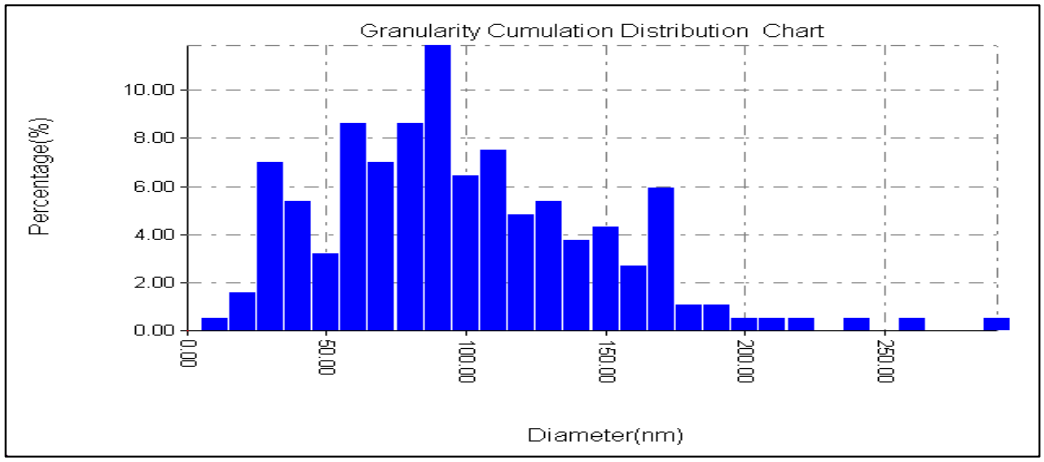

Fig. 6: Granularity accumulation Distribution chart for of CdO thin film , 100 nm thickness , prepared by PLD technique .

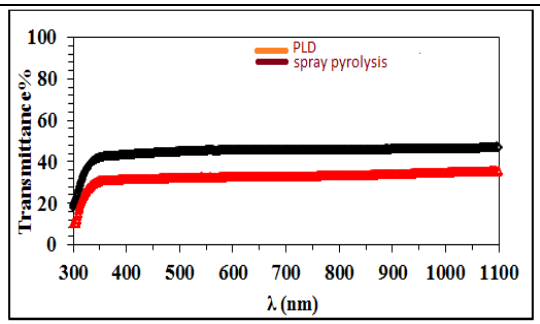

Fig.7 : Transmittance Vs wavelength of CdO thin films,100 nm thickness, prepared by spray pyrolysis method at 250˚C and PLD technique at R.T.

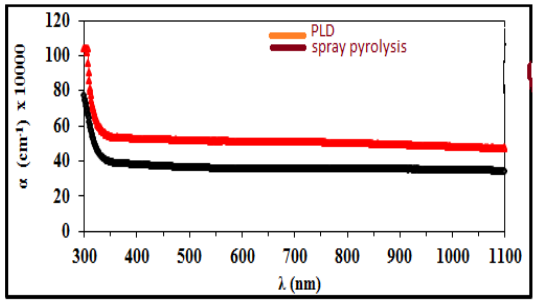

Fig. 8:Absorption coefficient(α) Vs wavelength of CdO thin films ,100 nm thickness ,prepared by spray pyrolysis Method at 250˚C and PLD technique at R.T.

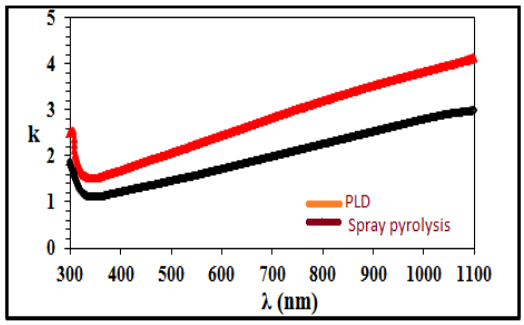

Fig.9: Extinction Coefficient (k) Vs wavelength of CdO thin films, 100 nm thickness , prepared by spray pyrolysis method at 250˚C and PLD technique at R.T.

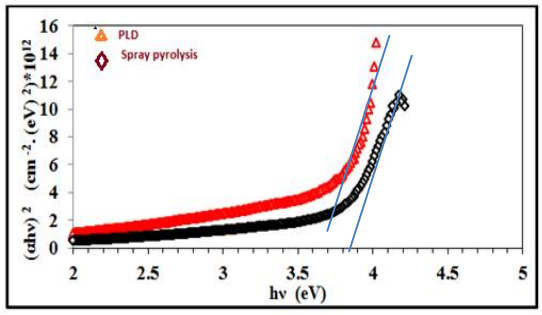

Fig. 10: plots of (αhυ)² Vs the photon energy (hυ) for CdO thin films ,100 nm thickness , prepared spray pyrolysis method at 250˚C and PLD technique at R.T.

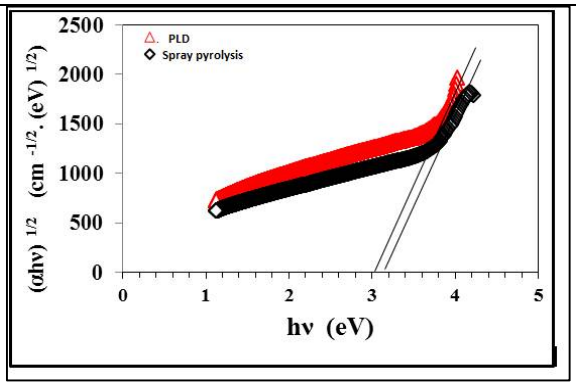

Fig. 11: plots of $(\alpha h\upsilon)^{1/2}$ Vs the photon energy (hυ) for CdO thin films, ,100 nm thickness ,prepared by spray pyrolysis method at 250˚C and PLD technique at R.T.

Indian Journal of Natural Sciences www.tnsroindia.org.in ©IJONS

Vol.9 /Issue 51 / December / 2018 *International Bimonthly* *ISSN: 0976 – 0997*

RESEARCH ARTICLE

Evaluation of the Feasibility of OmpF Proteins against *Salmonella typhimurium* when used for Vaccination Trail in Poultry Model

Annie Navomi Philip[1]*, Prejit[1,2], Asha K[1] Pratheesh P.T[1] and Jess Vergis[1,2]

[1]Department of Veterinary Public Health, College of Veterinary and Animal Sciences, Pookode, KVASU, Wayanad, Kerala, India.
[2]Centre for One Health, Education, Advocacy, Research and Training, KVASU, Pookode, Kerala, India.

Received: 20 Sep 2018 Revised: 22 Oct 2018 Accepted: 24 Nov 2018

***Address for Correspondence**
Annie Navomi Philip
Department of Veterinary Public Health,
College of Veterinary and Animal Sciences,
Pookode, KVASU,
Wayanad, Kerala, India.
Email: navomiannie@gmail.com

ABSTRACT

Salmonella typhimurium is a major global threat affecting the health of both humans and animals including poultry. Majority of the *Salmonella* outbreaks are due to the consumption of poultry meat and eggs. Control of Salmonellosis in poultry would provide significant benefit in improving public health, ensuring food safety, enhancing consumer confidence in consumption of poultry products. In the present study the recombinant OmpF protein was constructed and administered as a vaccine candidate against *Salmonella typhimurium* infection in poultry. *Salmonella* free layer birds were divided into groups of 20 each. Group I and group II were given with rOmpF and rOmpC proteins mixed with adjvuants and group III and group IV were given with commercial vaccine and PBS. The first dose of vaccination was given to the birds at around 4 weeks of age. Three weeks later booster dose was given. Humoral Immune response elicited by vaccinated and control birds were determined by ELISA at weekly intervals each after primary immunization and after booster dose. The humoral immune response in birds induced against r OmpF and rOmpC proteins of *Salmonella typhimurium* was assessed by single dilution ELISA of Briggs and Skeeles (1984) with slight modifications. There was a significant ($P<0.001$) increase in the mean OD of all the vaccinated groups in the first three weeks following primary vaccination. Response showed by commercial vaccine group reached at peak and highly significant ($P<0.001$) level at third week post vaccination with mean OD of 0.628± 0.009. Highest humoral response at third week was observed in commercial vaccine group with mean OD value of 1.190± 0.162. There was a significant ($P<0.001$) increase in the response showed by vaccinated groups at 1st, 2nd and 3rd week after booster dose ($P<0.001$).

This study concluded that rOmpF protein proved to show significant immune response against *S.typhimurium* in poultry and generation of protective antibody.

Key words: *Salmonella typhimurium,* rOmpF protein, vaccine, Immune, significant.

INTRODUCTION

In poultry, *Salmonella typhimurium* has been isolated from broilers, breeders and commercial egg-laying flocks (Chima *et al*., 1998). Birds shed the organism through their faeces without showing any symptoms (Adzitey *et al*., 2012). Among non-typhoidal serovars, *S.* Enteritidis and *Salmonella typhimurium* are most frequently associated with human food poisoning (Oliveira *et al.,* 2002). *Salmonella typhimurium* is associated with an invasive disease and causes bacteraemia in adults and children (Gal-Mor *et al.,* 2014). The prevalence of *Salmonella* in the global food chain, ubiquitous distribution, virulence, and its potential to cause serious economic impact in the food industry necessitates the need for strict vigilance and control measures at all levels. Attenuated vaccines are used against Salmonellosis in poultry industry. However, insufficient attenuation can make such vaccines more hazardous. In such a scenario development of a vaccine based on non toxic components has gained the attraction of researchers, and studies were done to determine the complex antigens of *Salmonella* (Secundino *et al*., 2005; El-Fakar and Rabie (2009). In this regard attention is now being focused towards the possible use of outer membrane proteins (OMPs) from *Salmonella* spp.

The major porins in *Salmonella* are OmpC, OmpF, OmpD, out of which OmpC and OmpF are found to be major surface antigen with unique exposed epitopes. The recombinant OmpC and OmpF of *S.* Typhi porins were cloned, expressed in *E. coli* and were proved to be useful in vaccination against *S.* Typhi (Verma *et al*., 2009). Tatavarthy and Cannons (2010) stated that *omp*F gene was present in various tested *Salmonella* strains. Toobak *et al*. (2013) mentioned the efficacy of porin antigens as OmpF>OmpC>OmpA.Thus, the study is envisaged to elucidate Thus, the study is envisaged to elucidate the protective propensity of *Salmonella* porins in poultry model.

MATERIALS AND METHODS

Expression of Omp*F* and Omp*C* gene of *S.typhimurium*

The glycerol stock of OmpF and OmpC clones were expressed in pRham N-His SUMO Kan Vector, these clones were then revived in the lab and used. LB broth containing 30 µg/ ml kanamycin was inoculated with a single colony of *E.*coli cells containing pRham expression construct and incubated at 37ºC with vigorous shaking at 220 rpm. To induce expression, L- rhamnose was added to the remainder of the culture at a final concentration of 0.2 per cent. The overnight shaking was continued at 37°C for an optimum induction period of 16 h based on previous studies done by Nimisha (2018).

Preparation of rOmpFand rOmpC for immunization

The total protein extracted was purified under denaturing condition using His-Pur Ni- NTA purification Column (Thermo Fisher Scientific, USA) at room temperature. The cell lysate containing recombinant protein was mixed with equal amount of equilibration buffer and it was passed three to four times through the column. The resin was washed using two resin bed volume of equilibration buffer. His- tagged proteins bound to the Ni-NTA column were eluted by elution buffer (pH-5) in an aliquot of 1 ml fractions as they are eluted from the column.

Purified proteins were confirmed by SDS-PAGE analysis. The eluted rOmpF and rOmpC proteins were dialyzed overnight at 4ºC using a pre-treated dialysis tubing (50KDa molecular weight cut off size). The urea was removed gradually during dialysis by sequential changes of dialysis buffer that contained 6, 4, 2 and then 0 M urea in PBS (pH 7.4), to provide gradual re-folding of rOmpF protein. Following dialysis, concentration of recombinant protein was assessed by BCA protein estimation kit. Standard curve was prepared by plotting the average blank corrected OD values for each BSA standard versus its concentration in µg /ml. Concentration of the recombinant protein was determined from the standard curve by placing its OD value and calculation was done using the formula, Sample concentration = X/V mg/ ml, where X= Value from graph (µg) and V is the volume in µl.

Confirmation of recombinant OmpF and OmpC proteins by Western blotting

The expressed recombinant OmpC and OmpF proteins, positive (BFP protein) and negative (total protein from untransformed cells) control proteins were run on a 10 per cent SDS PAGE along with a prestained protein molecular weight marker. Then the gel was soaked in transfer buffer for 10 min. Buffer wet sheet of nitrocellulose membrane was placed over the gel carefully without any air bubbles. Then it was sandwiched between additional cover of wet filter paper and a pair of sponge. Blotting was carried out at 80 V for 30 min in mini protean tetra system gel electrophoresis apparatus. After the transfer, the nitrocellulose paper was blocked for one hour in five per cent skimmed milk prepared in 1X TBST at 4ºC. After washing in TBST, the membrane was incubated overnight with 6X-His Tag antibody HRP conjugate (1:1000) at 4ºC. After three times washing, the membrane was dipped for development of colour in developing solution containing 250 µl of one per cent diaminobenzidine (DAB) and a fresh 250 µl of 0.3 per cent H_2O_2 in 5 ml of 1X PBS (DAB-peroxidase substrate solution). The reaction was stopped by rinsing the membrane with distilled water.

Procurement of commercial *Salmonella* vaccine

Commercial *Salmonella* polyvalent inactivated vaccine was kindly provided by Ventri biologicals, Vaccine Division and was used for comparing the protective efficacy of recombinant OmpF and OmpC based vaccine.

Procurement of Montanide ISA 71 VG

In the present study, Montanide ISA 71 VG was used as an adjuvant, which was kindly provided by IVRI, Izatnagar. It is a ready to use oily vaccine adjuvant consisting of an enriched light mineral oil with an extremely refined emulsifier obtained from mannitol and purified oleic acid of vegetable origin. Immunising emulsion containing ISA VG 71 adjuvant was prepared by mixing adjuvant and recombinant protein (in PBS) in the ratio of 50:50 (w/w) and passing the suspension 20 times through the injection needle G20.

Vaccination trail

Eighty layer birds were procured from ILFC, COVAS, Pookode. One week before vaccination, the birds were screened for *Salmonella* by cloacal swab culture, followed by PCR confirmation for *invA* gene. Only *Salmonella* free birds were used for the immunization trial. Birds were randomly divided into rOmpF, rOmpC *Salmonella* inactivated commercial vaccine and control groups as shown in Table. The first dose of vaccination was given to the birds at around 4 weeks of age. Three weeks later booster dose was given.

Vaccination group	No. of Birds	Dose	Route
rOmpF+ montanide	20	0.6 ml (100µg per bird)	IM
rOmpC+ montanide	20	0.5ml (100µg per bird)	IM
Commercial Vaccine	20	0.5ml	IM
PBS	20	0.5ml	IM

Immune response to vaccination

The humoral immune response in birds induced against r OmpF and rOmpC proteins of *Salmonella typhimurium* was assessed by single dilution ELISA of Briggs and Skeeles (1984) with slight modifications. Antigen (OmpF, OmpC antigens) and antibody dilutions were standardized by checkerboard analysis. Antigen in concentration of 100 ng/well and antibody at 1:400 dilutions were used for indirect ELISA. Antigen preparation in 100 µl quantity was used for coating of the wells of flat bottomed polystyrene ELISA plates and the plates were kept overnight at 4ºC. After adding all the reagents as per the protocol the plates were kept for 20 min to visualize colour development. The reaction was stopped by adding 100 µl of 1.8 N H_2SO_4 to all the wells. The reading was taken at 450 nm in an ELISA reader (BIORAD).The results of ELISA were statistically analyzed using software package SPSS (IBM SPSS Statistics-22.0). One way ANOVA was performed to compare the titres of various groups.

RESULTS AND DISCUSSION

The study was carried out to evaluate the protective antibody response elicited after administration of rOmpF protein along with montanide adjuvant.

Expression of OmpF and OmpC gene

The clone of OmpC and OmpF was succesfully revived and expressed in SUMO vector. The molecular size of the expressed rOmpFand rOmpC proteins was 57 Kda and 58 KDa respectively. Induced cells were harvested and lysed with 8 M urea to facilitate the lysis of the recombinant protein which had formed as inclusion bodies.

Protein purification and characterisation

Supernatant of the cell lysate was allowed to react with Ni-NTA agarose for affinity purification. Only recombinant protein was bound to nickel resin due to the presence of 6x histidine tag. The property of 6X histidine tag present in the expressed protein to bind with the Nickel chelating agent present in the resin column is utilised in the purification of protein (Bornhorst and Falke, 2000). The bound recombinant protein was eluted (Fig.1) and analysed on SDS-PAGE. Single protein was obtained after purification invarious elutes as shown in figure 2. Denaturating agent like urea can solubilize the aggregated protein and its concentration determines the extent of solubilization (Verma *et al*., 2009) by binding to protein. Here the protein was solubilized in 8M urea to get maximum yield. Dialysis of the purified proteins was carried out by sequential changes in the concentartion of urea. After dialysis the concentration of protein was determined by Lowry's method and it was found to be 375 µg/ml and 500 µg/ml for OmpF and OmpC proteins, respectively. In this study, the expressed OmpF protein with 6x histidine tag was bound with NI-HRP and the band size of the expressed purified protein OmpF protein (57KDa) (Figure 3).

Western blotting

This protein bands which on Western blot analysis reacted specifically with corresponding anti recombinant OmpF and OmpC hyper immune sera raised in birds (Fig.4). Western blot analysis confirmed the presence of rOmpF and rOmpC proteins. This result was consistent with previous reports confirming the Omp of *Salmonella* such as OmpC and OmpA (Avinash, 2017) and rOmpF (Nimisha, 2018). Antigenic epitope present in the rOmpF protein could recognize the *Salmonella* antibodies, this confirmed the role of protein in vaccine studies. These results are in accordance with the findings of previous workers who have proved the immunogenic potential of OmpC fraction (Kannan, 2004; Sung *et al*., 2005; Porteen *et al*., 2007).

Immune response in birds

All the 80 birds screened for the presence of *Salmonella* spp, one week before vaccination were found negative for the organism. Immune response was assessed by indirect ELISA from serum samples collected post primary immunization for three weeks, post booster dose for three weeks. The standard concentrations of antigen, antibody and conjugate used in ELISA were determined by checkerboard titration. ELISA test results of the three porins revealed IgG titer against the OMPs in the following order: anti-OmpF > anti-OmpC > anti-OmpA (Toobak *et al*., 2013). These results suggest that OmpF could be considered as a vaccine candidate against *Salmonella typhimurium* in poultry.

In all the treatment groups, antibody levels were maximum at 3rd week after booster dose. The ELISA OD_{450} antibody level differed highly significantly (P<0.001) among treatment groups, when compared to control group across weeks (table 1). From the 5th to 10th week the ELISA titres of all the vaccinated groups were found to increase significantly (P<0.001). In all the six weeks, commercial vaccine group gave higher response compared to rOmpF and rOmpC groups. This might be due to presence of multiple immunodominant epitopes in the commercial vaccine. The rOmpF was showing higher titres than rOmpC in the 5th and 10th weeks (figure 5). All these results were in accordance with the studies previously conducted which proved the immunogenic potential of rOmpC, rOmpA, rOmpD (Prejit, 2009; Avinash, 2017).

REFERENCES

1. Adzitey, F., Rusul, G. and Huda, N. 2012. Prevalence and antibiotic resistance of *Salmonella* serovars in ducks, duck rearing and processing environments in Penang, Malaysia. *Food Res. Int.* 45: 947-952.
2. Avinash Reddy. 2017. Evaluation of rBapB, rOmpC and rOmpF proteins of *Salmonella Typhimurium*(ST)as vaccine candidates against Poultry Salmonellosis. PhD thesis, Indian Veterinary Research Institute, Izatnagar, 131p.
3. Bornhorst, J. A. and Falke, J. J. 2000. Purification of proteins using polyhistidine affinity tags. *Methods Enzymol*. 326: 245-254.
4. Chima, J. C and Ogbogu, D. A. 1998. Chronic fowl typhoid infection in a commercial poultry farm. *Niger. Vet. J.* 19: 1-4.
5. El-Fakar, S. A. Z. and Rabie, N. S. 2009. Immunogenic properties of outer membrane proteins of *Salmonella* in chicken. *Global Veterinaria*. 3: 75-79.
6. Gal-Mor, O., Boyle, E.C., and Grassl, G.A. 2014. Same species, different diseases: how andwhy typhoidal and non-typhoidal*Salmonella* entericaserovars differ. *Frontiers Microbiol*. 5: 391-396.
7. Kannan, P. 2004. Cloning and expression of outer membrane protein C (Omp C) gene of*Salmonella Gallinarum.* Ph.D. Thesis submitted to Deemed University, IVRI, Izatnagar, U.P. India.
8. Nimisha, M. 2018. Development of recombiantompF based Indirect ELISA for the detection of *Salmonella* antibodies in poultry. M.V.Sc thesis, Kerala Veterinary and Animal Sciences University, Pookode, 136p.
9. Oliveira, S.D., Santos, L.R., Schuch, D.M.T., Silva, A.B., Salle, C.T.P. and Canal, C.W.2002. Detection and identification of *Salmonella* from poultry related samples byPCR. *Vet. Microbiol*.,87: 25-35.
10. Porteen, K. 2007. Evaluation of recombinant ompC for immunogenicity and protection. Ph. Dthesis submitted to Indian veterinary Research Institute, Izatnagar.
11. Prejit, 2009. Immune response and protective propensity of recombiantompC developed from poultry isolate of *Salmonella Typhimurium.* PhD thesis, Indian Veterinary Research Institute, Izatnagar, 136p.
12. Secundino, I., López-Macías, C., Cervantes-Barragán, L., Gil-Cruz, C., Ríos-Sarabia, N., Pastelin-Palacios, R., Villasis-Keever, M.A., Becker, I., Puente, J.L., Calva, E. and Isibasi, A. 2006. *Salmonella* porins induce a sustained, lifelong specific bactericidal antibody memory response. *Immunology*. 117: 59-70.

13. Sung, Y. L., Kyoung-Seong, C., Myeong-Chul, K., Jae-Cheol, H., Jin-Ho, P., Devendra,H.S. and Joon-Seok, C. 2005. Purification of outer membrane protein C (ompC)from S. Gallinarum for characterization of its immunogenicity. *Indian J. Anim*. Sci. 75: 164-167.
14. Tatavarthy, A. and Cannons, A. 2010. Real-time PCR detection of *Salmonella* species using a novel target: the outer membrane porin F gene (*omp*F). *J. Appl. Microbiol*. 50: 645-652.
15. Toobak, H., Rasooli, I., Talei, D., Jahangiri, A., Owlia, P. and Astaneh, S. D. A. 2013. Immune response variations to *Salmonella entericas*erovarTyphi recombinant porin proteins in mice. *Biologicals*. 41: 224-230.
16. Verma, S. K., Gautam, V., Balakrishna, K. and Kumar, S. 2009. Over expression, purification, and immunogenicity of recombinant porin proteins of *Salmonellaenterica*SerovarTyphi (S. Typhi). *J. Microbiol. Biotechnol*. 19: 1034-1040.

Table 1: Kinetics of humoral immune response at different weeks after vaccination trail

Group	Week 5	Week 6	Week 7	Week 8 Post Booster	Week 9	Week 10	
I. rOmpC+ montanide	0.292 ± 0.010 ^{bF}	0.574 ± 0.012 ^{aE}	0.570 ± 0.009 ^{bD}	0.825± 0.008 ^{bC}	1.077 ± 0.014 ^{bB}	1.151 ± 0.003 ^{bA}	P Value ** <0.001
II. rOmpF+montanide	0.314 ± 0.013 ^{bF}	0.457 ± 0.015 ^{bE}	0.630 ± 0.014 ^{cD}	0.760 ± 0.009 ^{cC}	1.025 ± 0.015 ^{cB}	1.143 ± 0.005 ^{bA}	
III. Commercial vaccine	0.506± 0.009 ^{aF}	0.587± 0.008 ^{aE}	0.628± 0.009 ^{aD}	0.987± 0.008 ^{aC}	1.130± 0.007 ^{aB}	1.190± 0.162 ^{aA}	
IV. Control	0.109 ± 0.001 ^{cC}	0.119 ± 0.002 ^{cA}	0.110± 0.002 ^{dC}	0.111 ± 0.002 ^{dBC}	0.114 ± 0.001 ^{dAB}	0.120 ± 0.003 ^{cA}	
P Value ** <0.001							

**** Significant at 0.001 level**
Values are mean± standard error of ELISA OD450 from sera of 20 birds per group put in duplicate wells each
Means bearing different small letter as superscript are significantly different within a column (P<0.001)
Means bearing different capital letter as superscript are significantly different within a row (P<0.001)

Figure.1 Elution of the purified proteins through the Ni purification column

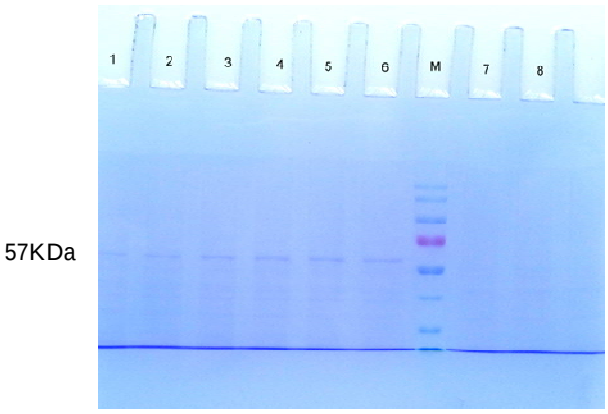

Figure. 2 Different elutes of OmpF protein after purification

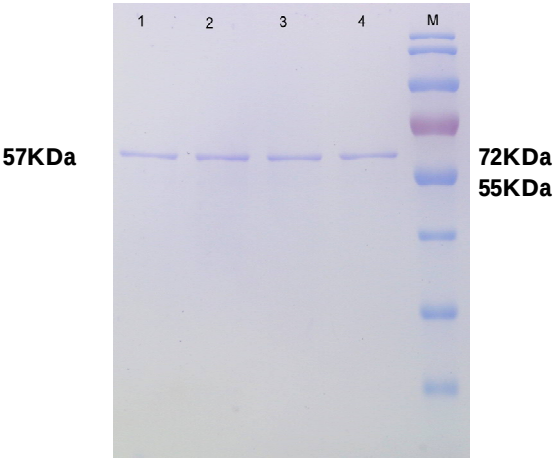

Figure 3. SDS-PAGE analysis of the purified and dialysed OmpF protein
Lane 1-4: rOmpF protein (57KDa)
Lane M : protein marker

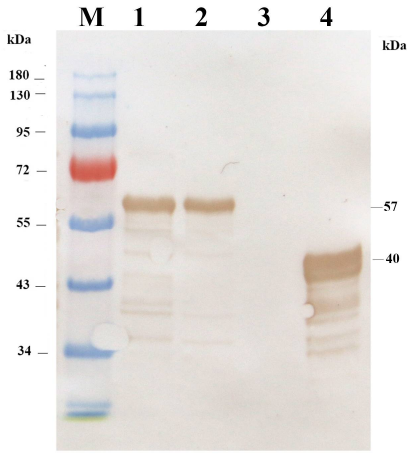

Figure 4. Western blot analysis of OmpF and OmpC proteins
Lane M– Protein Marker
Lane 1– OmpC Protein (58kDa)
Lane 2– OmpF Protein (57kDa)
Lane 4– Positive control

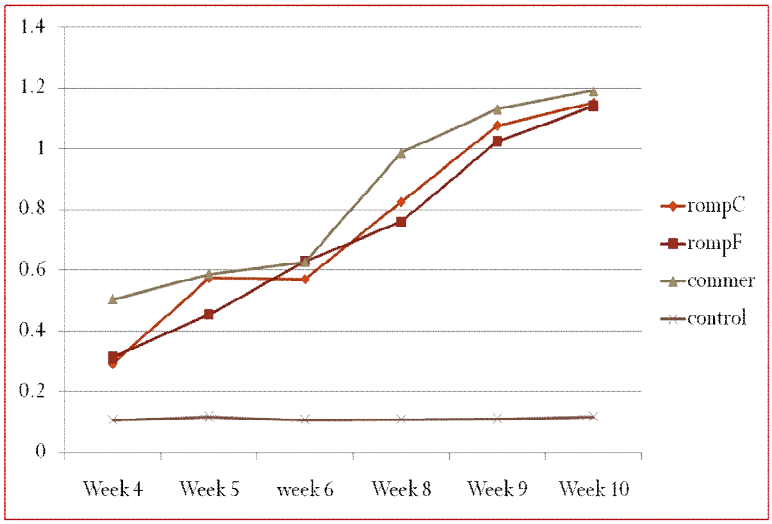

Figure 5. Kinetics of Humoral Immune response at different weeks after vaccination trail

Indian Journal of Natural Sciences www.tnsroindia.org.in ©IJONS

Vol.9 /Issue 51 / December / 2018 *International Bimonthly* *ISSN: 0976 – 0997*

RESEARCH ARTICLE

Effect of Ozone Depletion on the Climate Change and Human Health above Baghdad

Doaa Jamal M. Ali and Najat M. R. Al-Ubaidi*

Department of Astronomy and Space, College of Science, University of Baghdad, Baghdad, Iraq.

Received: 15 Aug 2018 Revised: 17 Sep 2018 Accepted: 19 Oct 2018

***Address for Correspondence**
Najat M. R. Al-Ubaidi
Department of Astronomy and Space,
College of Science,
University of Baghdad,
Baghdad, Iraq.

ABSTRACT

Ozone is one out of many gases in the stratosphere it plays an important role for life on Earth due to its ability to absorb ultraviolet radiation (UV) from the Sun which heats the stratosphere. The ozone depletion was very important in global environmental and climate change, therefore the aim of this research is to find the effect of atmospheric ozone depletion on the climate change and the human health above Baghdad the Capital of Iraq. In this study the data for the daily average of Total Column Ozone (TCO), UV-index, UV Dose, Vitamin D and DNA Damage parameters are selected on the basis of the available from the TEMIS satellite for Baghdad (latitude 33.3^{o} N; longitude 44.43^{o} E). The data are taken from the years (2005-2016), for the time period from the sunrise to sunset. The data for the temperature above two meters from the Earth surface are taken from the satellite (ERA), for the year 2014 at hour 12:00pm in UT. From results it is found that the minimum values of the daily average ozone in October and the maximum values in spring. There are a reversible relation between the daily average ozone and temperature at hour 12:00pm in the year 2014 for Baghdad. Also there are reversible relations between daily averages UV-index, UV Dose, Vitamin D, and DNA Damage parameters with the daily average atmospheric ozone for all years selected (2005-2016).

Keywords: Ozone depletion; UV-index; UV dose; DNA damage; Vitamin D; Climate change**.**

INTRODUCTION

The most important global environmental issues which emerged in the last century is ozone depletion on the globe, especially after the discovery of the ozone hole for the first time over Antarctica in 1984, as a result of this became the ozone issue as the global focus of scientists in different countries of the world to the risks involved [1]. Ozone is one out of many gases in the stratosphere; although the concentration of ozone is relatively small it plays an

important role for life on Earth due to its ability to absorb ultraviolet radiation (UV) from the Sun. In the course of the last 40 years they have often heard about "the depletion of the ozone layer" which has been considered as a threat to our health and environment. Every day they release a number of gases that pollute the atmosphere and some of these gases may also have a negative influence on the ozone layer [2]. The majority of the ozone (about 97%) is concentrated in the stratosphere at an altitude of 15 to 55 km. This stratospheric ozone provides an important service to life on the Earth as it absorbs harmful ultraviolet radiation [3]. At different temperatures and pressures or different altitudes within the stratosphere, also at different solar activities or during geomagnetic storms there are different formations and destruction rates of ozone which is leads to the variation of ozone amount within the stratosphere with the variation of altitude, ozone concentrations are highest between 19 and 23 km [4]. The amount of harmful ultraviolet (UV) radiation that will reach the Earth's surface is directly related to the thickness of the UV absorbing ozone layer (between 10-40 km altitudes). The atmospheric changes are manifesting themselves through aspects of climate change (heating of the Earth) and ozone depletion [5].

Previous Studies

There are many studies illustrating the relationship between ozone, UV radiation, temperature and human health, the two scientists, Krishna and Sarma, (2016) made a comprehensive on this topic and literature survey for many research started from (1966-2015), most of studies are about the UV-B irradiance and stratosphere ozone others about the impact of UV-B irradiance on plants growth and human health for different latitudes. They found that the UV-B irradiance levels increased which implies a decrease in Ozone [6]. Atkinson's, (1997) study the ozone changes daily for several stations in Australia for the period from July 1995 to June 1996, he found that there is a change in total ozone amount from day to day which are smaller at the beginning of summer until the middle of winter and have significant ozone change in the spring [7]. David and Susan, (2002), they found that the largest and most significant troposphere trends can be traced to recent trends in the lower stratospheric polar vortex, which are due largely to photochemical ozone losses. During the summer-fall season, the trend toward stronger circumpolar flow has contributed substantially to the observed warming over the Antarctic Peninsula and Patagonia and to the cooling over eastern Antarctica and the Antarctic plateau [8].

Ann and Ola, (2006), they are defined a standard vitamin D dose on the basis of recently recommended requirements for vitamin D that take account of its risk reduction role in a variety of diseases. When solar UV is sufficient, a risk-benefit analysis of sunburn vs. vitamin D synthesis shows that the best time for brief sun exposure is in the middle of the day. For low solar elevation angles common at high latitudes, a fine line exists between adequate UV exposure for vitamin D synthesis and a risk of sunburn [9]. Sivasakthivel and Siva, (2011), objective of their paper is to review the origin, causes, mechanisms and bio effects of ozone layer depletion as well as the protective measures of this vanishing Layer, However, the future behavior of ozone will also be affected by the changing atmospheric abundances of methane, nitrous oxide, water vapor, sulphate aerosol, and changing climate [2]. Kais et al., (2014), they are investigated the relative influence of clouds on UV irradiance on Baghdad city in Iraq. They found that the ratio of UV irradiance to the total solar irradiance increases with cloud cover and approximately constant it's ranged between (3.6% – 4.3%) [10].

Ali and Siaf, (2016), they studied the global solar radiation and ultraviolet (UVA and UVB). They analyzed their measurements under different sky conditions for Baghdad city. During studied period the highest value in the summer and the highest daily average solar radiation measured was (897 W/m^2) on 8 June, whereas the daily minimum global radiation (120 W/m^2) was recorded on 30 December. The maximum daily variation values of UVA in spring and summer, its maximum value reach in 13 June (50.1 W/m^2), while the minimum values in autumn and winter [11]. Krishna et al., (2016), they studied the incoming solar ultraviolet radiation for the period (2006-2015). They found that the UV Index at Bangalore has a minimum value of 9.15 and a maximum value of 13.4 for period selected. This indicates that the city is receiving maximum ultraviolet radiation with high to very high risk. Keeping this in view, measures need to be taken for safeguarding the people of Bangalore from ultraviolet radiation [12].

Gonzalo et al., (2017), they described and analysis the erythemal ultraviolet radiation (UVER) received by a driver and passenger inside a vehicle in Valencia, Spain. They found that the UVER exposure, in some of the driver's positions, exceeds the exposure limits given by the (ICNIRP) [13]. In this research the variation of the ozone amount and its effect on the climate change through the temperature variation at two meters above Earth surface and also the ozone variation effect on the human health through the parameters UV Index, UV Dose, vitamin-D and the DNA damage were studied above Baghdad Capital of Iraq.

Absorption of UV-radiation

The solar radiation will partly be absorbed in the atmosphere. The absorption is determined by the composition of atoms and molecules. UV-radiation with the shortest wavelengths is absorbed by oxygen far out in the atmosphere (70 - 80 km above sea level). Next, a significant fraction of the radiation in the UVC and UVB regions is absorbed by the ozone layer. The absorption of radiation can be described by Lambert-Beers law: When a parallel monochromatic beam penetrates a medium (a gas, liquid or a solid compound), the intensity decreases according to an exponential law ($I_x=I_0e^{-\alpha x}$), where I_0 is the intensity when the depth (x=0), I_x is the intensity at depth x, and α is a constant called the "absorption coefficient". The absorption depends on the wavelength of radiation and the constant α, which is given as the absorption per unit length. The absorption spectrum varies from one compound to another. The absorption is much larger in UVB and UVC than in UVA [2].

UV Index

Is basically forecasted with a resolution in time of one hour and is a physically defined quantity for the erythemal effective irradiation on a horizontal plane. The hourly UV Index divided by the constant 40 W^{-1} m^2 and multiplied by 3600 s is the hourly erythemal effective UV dose in Jm^{-2}. The level of the erythemal effective UV dose is influenced by all factors valid for the UV Index too, namely Sun elevation, cloud optical depth, total ozone column, altitude, ground reflectivity, aerosol load and properties. The susceptibility of skin to damages by a given erythemal effective UV dose depends from the individual skin type and the varying status of skin protection acquired in the course of the year, e.g. by tanning. One minimal erythemal dose (MED) is defined as the effective UV dose that causes a perceptible reddening of previously unexposed human skin [14].

Erythemal Effective UV Dose

The erythemal effective UV dose is the amount of energy received by a horizontal plane within a time interval; dimension is Jm^{-2}. For the forecasts products the integration time comprises one day [5].

Vitamin D

Vitamin D comprises a group of fat found naturally only in a few foods, such as fish-liver oils, fatty fish, mushrooms, egg yolks, and liver. Under conditions of regular Sun exposure, dietary vitamin D intake is of minor importance. Most of the dietary intake of vitamin D comes from fortified milk products and other fortified foods such as breakfast cereals and orange juice [15].

DNA Damage

Damage to DNA is nothing but effect on primary structure of double helix. It occurs due to environmental factors and normal metabolic processes inside the cell. UV source have higher proportion of radiation bordering between UV-B and UV-A. Such solar UV radiation should produce a higher proportion of Dewar isomers. The ability of UV radiation to damage a given base is determined by flexibility of DNA. Whereas damage due to exogenous agents is by UV radiations such as UV-B light which cause direct DNA damage, ionizing radiations damage DNA by

radioactive decay or cosmic ray causing strand breaks. Depuration and single strand breaks caused by thermal disruption at elevated temperature can affect the DNA helix structure [16].

Data Selection

In this research the data are selected on the basis of the available from TEMIS used to be part of the Data User Programmer (DUP) of the European Space Agency (ESA) sited (http://www.temis.nl), for the daily average of Total Column ozone (TCO), UV-index radiation, DNA Damage, Vitamin D and UV Dose parameter for Baghdad (latitude 33.3^{o} N; longitude 44.43^{o} E). The data are taken for the time period from the sunrise to sunset in intervals of 10 minutes from the years (2005-2016). To study the climate change, the data taken from the European Centre for Medium-Range Weather Forecasts (ECMWF) sited in (http://apps.ecmwf.int) and from the satellite (ERA), the year 2014 at hour 12:00pm in Universal Time (UT) chosen for the temperature variation in Kelvin above two meters from the Earth surface for Baghdad.

RESULTS AND DISCUSSION

Figure (1) shows the monthly daily average of Ozone and temperature at 12:00pm in UT for year 2014, the linear trend lines for each curve shows the linear fitting of these two parameters along the months of the year selected, in which revealed that there are a difference in the relationship between ozone and temperature along the months or there is no specific relationship between these two parameters. For more illustration, Figure (2) shows the daily change during the same year 2014 and time 12:00 pm between the temperature and ozone, the trend line reveals that there is an inverse relationship between ozone and temperature over Baghdad for year 2014. It seen that there is non-linear relation between ozone and temperature, so to find the variation of ozone with respect to temperature the ratio (ΔTCO/ΔT2m) are taken and drawn in Figure (3) for the same year and time selected, linear trend line revealed the reversible relation between them. Figure (4) represents the annual average variation for the TCO and UV-index for the period selected in this research (2005-2016).Figure (5) indicate the variation of TCO (in the stratosphere), UV-index, UV Dose, Vitamin-D and DNA Damage for Baghdad from years 2005-2016, it is clear from figure that there are a fluctuations in ozone values between the years selected the maximum value (463.6 DU in 6/2/2010) and the minimum value (237 DU in 9/12/2005). About the UV-index values it is increase from (1.698 to 12.363), according to World Health Organization (WHO) UV-index risk shown in table (1), it is in the risk side in noon time.

It means that the UV-index levels received by Baghdad are indicating high risk which should be addressed immediately. Also it is found that the minimum value for UV Dose is (0.756 kJ/m^2) in (11/1/2015) and maximum value is (6.686 kJ/m^2) in (16/6/2007), while the minimum value for Vitamin-D is (0.916 kJ/m^2) in (11/1/2015) and maximum value is (13.106 kJ/m^2) in (16/6/2007), minimum value for DNA Damage is (0.162 kJ/m^2) in (11/1/2015) and maximum value is (4.211 kJ/m^2) in (6/7/2007). Figure (6) represents the variation of ozone with human health parameters UV-index, UV Dose, Vitamin-D and DNA Damage for Baghdad from years (2005-2016), it is found that there are a reversible relation between ozone and the all parameters.Figures from (7-10) indicates the yearly selected ozone with UV-index, UV Dose, Vitamin-D and DNA Damage respectively, in which the reversible relation revealed. Because there are non-linear relation between the values of TCO and all human health parameters, so to find their relation accurately we take the ratio between TCO and the parameters, only two parameters selected in this study for their important and related to the human health directly. Figures (11 and 12) represents the ratio of yearly variation of TCO to the UV-index and TCO to the Vitamin-D respectively for the same years selected. The polynomial curve fitting equation given by ($y=a_0+a_1x+a_2x^2$) shown in figures, where (y) is the (ΔTCO/Δparameter), and (a_0, a_1, a_2) are the coefficients of polynomial equations shown in tables (2 and 3) for TCO to the UV-index and TCO to the Vitamin-D respectively, in which the reversible relation revealed.

CONCLUSION

From results we can concluded that the minimum values of the daily average ozone in October and the maximum values in spring. There are a reversible relation between the daily average ozone and temperature at hour 12:00pm in the year 2014 for Baghdad. Also there are reversible relations for all parameters between daily average UV-index, DNA Damage, Vitamin D and UV Dose parameters with the daily average atmospheric ozone for all years selected (2005-2016).

ACKNOWLEDGMENTS

This work relates to University of Baghdad/ College of Science/ Department of Astronomy and Space. The data are provided from the European Centre for Medium-Range Weather Forecasts (ECMWF) and European Space Agency (ESA), for whom I would like to introduce my utmost appreciation and thanks.

REFERENCES

1. Staehelin J., Harris N., Appenzeler C., and Eberhard J., (2001), "Ozone trend: A review", Review of Geophysics, Vol. 39 No. 2, pp. 231-290.
2. Sivasakthivel T. and K.K.Siva Kumar Reddy, (2011), "Ozone Layer Depletion and Its Effects: A Review", International Journal of Environmental Science and Development, Vol.2, No.1, pp. 30-37. ISSN: 2010-0264.
3. Chandrasekar A., (2013), "Basic of Atmospheric Science", Estern Economy Edition, pp.416-418, ISBN-978-81-203-4022-0.
4. Najat M. R. Al-Ubaidi, Zahraa T. I., (2018), "Investigate the Ozone Thickness and Temperature above Iraq during Severe and Strong Geomagnetic Storms", Journal of Geoscience and Environment Protection, 6, pp. 50-61. http://www.scirp.org/journal/gep
5. Kok C. T., Hwee S. L., Mohd. Z. M. J., (2017), "Study on solar ultraviolet erythemal dose distribution over Peninsular Malaysia using Ozone Monitoring Instrument", The Egyptian Journal of Remote Sensing and Space Sciences.in press http://dx.doi.org/10.1016/j.ejrs.2017.01.001.
6. Krishna P. N., Sarma M. S., (2016), "Literature survey of UV-B and ozone over a period of 1966-2015", International Journal of Advanced Research, Vol. 4, Issue 2, pp. 1032-1034.
7. Atkinson R. J., (1997), "Ozone variability over the southern hemisphere", Australian Meteorological Magazine, Vol. 46, pp. 195-201.
8. David W. J., Susan S., (2002), "Interpretation of Recent Southern Hemisphere Climate Change", Science, Vol. 296, Issue 5569, pp.895-899, DOI: 10.1126/science.1069270.
9. Ann R. Webb, Ola Engelsen, (2006), "Calculated Ultraviolet Exposure Levels for a Healthy Vitamin D Status", Photochemistry and Photobiology, Vol. 82, No. 6, pp. 1697-1703.
10. Kais J. AL-Jumaily, Natiq A. Zaki, Ali M. AL-Salihi, (2014), "Impact of Cloud Cover on Global UV Irradiance over Baghdad, Iraq", IOSR Journal of Applied Physics, (IOSR-JAP), Vol. 6, Issue 1 Ver. I (Jan.), pp. 63-69, e-ISSN: 2278-4861.
11. Ali M. Alsalihi and Siaf H. Abdulatif, (2016), "Analysis Global and Ultraviolet Radiation in Baghdad City, Iraq", Journal of Natural Sciences Research, Vol. 6, No. 22, pp. 117-124.
12. Krishna P. N., Sarma M. S., Murthy K. S. R., Prasad K. S. D. L. K., Madhavi N., (2016), "Variation in Total Ozone Content And Solar UV Index over a High Altitude Station Bangalore For A Decade 2006-2015", International Journal of Innovative Research & Development, Vol. 5 Issue 5, pp. 37-40. ISSN: 2278 – 0211.
13. Gonzalo Gurrea Ysasi, Vicente Blanca, Juan Carlos Moreno, M. Antonia Serrano, (2017), "Analysis of Erythemal UVB Dose Received Inside a Car in Valencia, Spain", DOI:10.1111/php.12865. http://dx.doi.org/10.4236/acs.2016.61011

14. Vanicek, K., Frei T., Litynska Z., Schmalwieser, A., (2000), "UV-Index for the Public", A guide for publication and interpretation of solar UV Index forecasts for the public prepared by the Working Group 4 of the COST-713 Action "UVB Forecasting". COST-713 Action, European Commission, Luxembourg: Office for Official Publications of the European Communities, pp. 27.
15. Fakhra Anwar, Fahad Nazir Chaudhry, Saiqa Nazeer, Noshila Zaman, Saba Azam, (2016), "Causes of Ozone Layer Depletion and Its Effects on Human: Review", Atmospheric and Climate Sciences, 6, pp. 129-134. http://www.scirp.org/journal/acs
16. Shrinivas S. A., Shanta S. H. and Prajakta B. B., (2017), "DNA: Damage and Repair Mechanisms in Humans", Global Journal of Pharmaceutical Science, Vol. 3, Issue 3-July, pp. 1-8.

Table 1: showing Risk vs. UV Index as per WHO [12].

No.	UV- Index	Risk
1	1-2	Minimum
2	3-4	Low
3	5-6	Moderate
4	7-9	High
5	10 and above	Very High

Table 2.Trend line equations coefficients for daily variation of Ozone with UV during years 2005-2016.

Year	2005	2006	2007	2008	2009	2010	2011	2012	2013	2014	2015	2016
a0	134.62	131.2	140.98	125.33	133.08	132.28	135.77	125.12	116.01	133.7	137.8	130.55
a1	-1.2114	-1.2754	-1.2996	-1.1938	-1.2491	-1.1638	-1.2602	-1.1488	-1.1155	-1.2203	-1.286	-1.1685
a2	0.0032	0.0036	0.0035	0.0033	0.0035	0.0031	0.0034	0.0032	0.0032	0.0033	0.0035	0.0031

Table 3.Trend line equations coefficients for daily variation of Ozone with Vitamin-D during years 2005-2016.

Year	2005	2006	2007	2008	2009	2010	2011	2012	2013	2014	2015	2016
a0	203.97	200.21	214.91	189.66	201.89	199.75	205.32	187.37	174.39	202.15	211.51	196.41
a1	-2.04	-2.1687	-2.1908	-2.0052	-2.116	-1.9616	-2.1076	-1.9216	-1.9002	-2.0556	-2.1974	-1.9639
a2	0.0055	0.0061	0.0059	0.0056	0.0059	0.0052	0.0058	0.0053	0.0056	0.0056	0.0061	0.0053

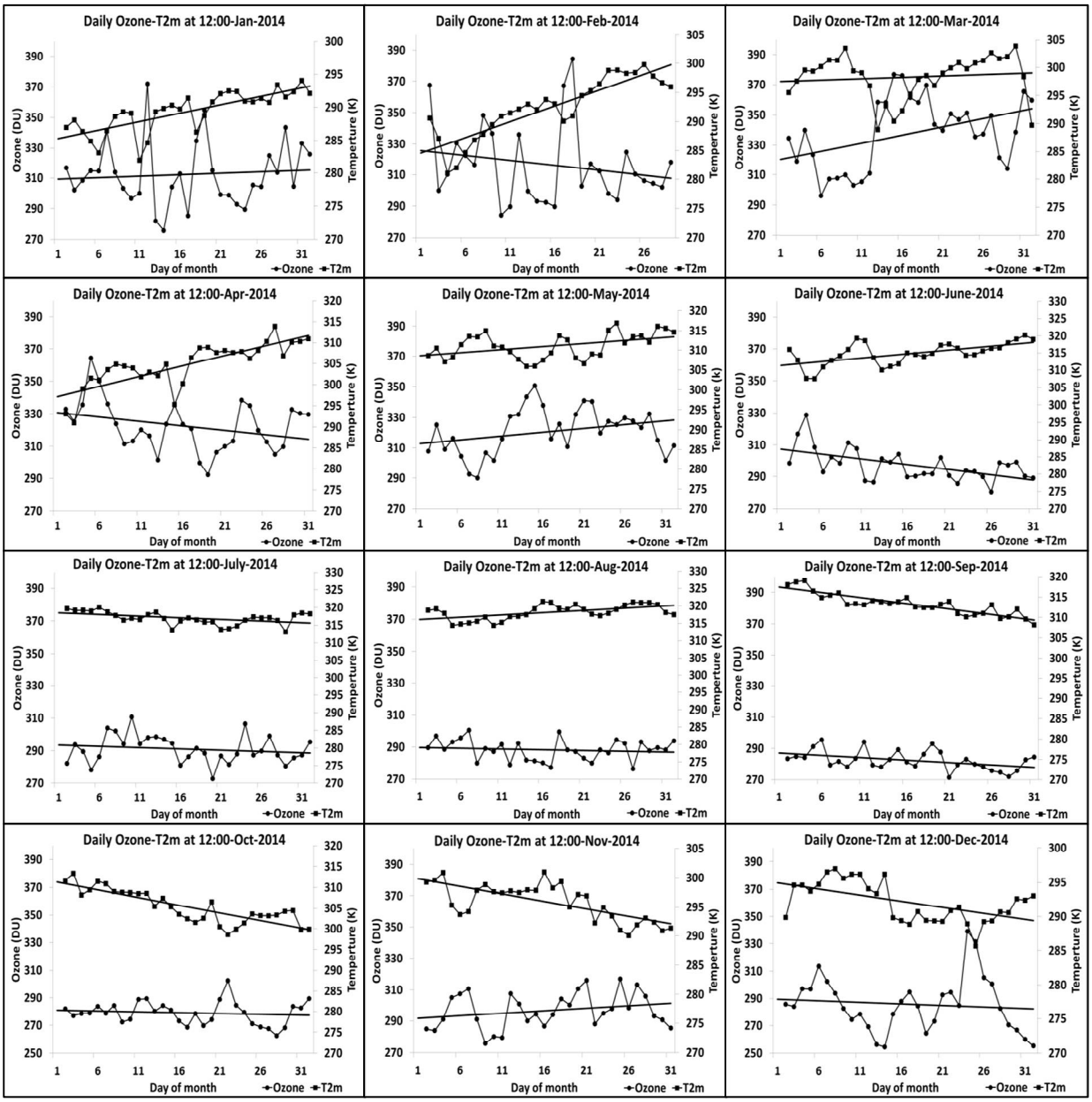

Figure (1): Daily average ozone with daily average Temperature above (2m) at hour 12:00UT for year 2014, where the black line represents the linear curve fitting.

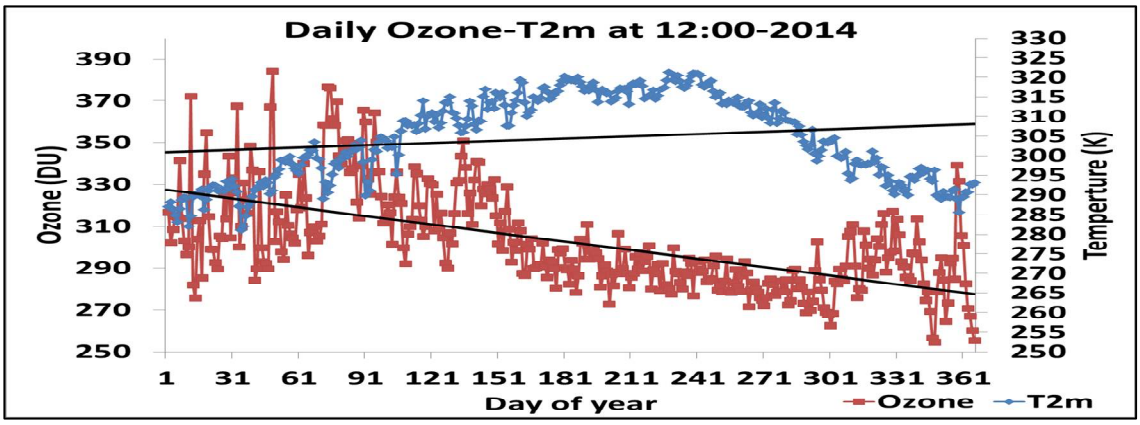

Figure (2): Daily average ozone and daily temperature at hour 12:00UT of year 2014for Baghdad city, the black line represents the linear curve fitting.

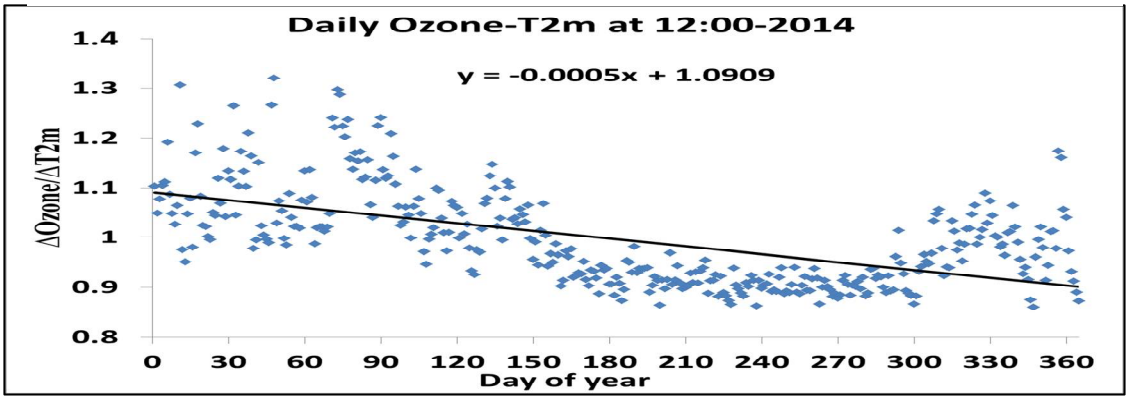

Figure (3): The ratio of the Daily ozone variation to the variation of Temperature at hour 12:00UT of year 2014, black line represents the linear curve fitting.

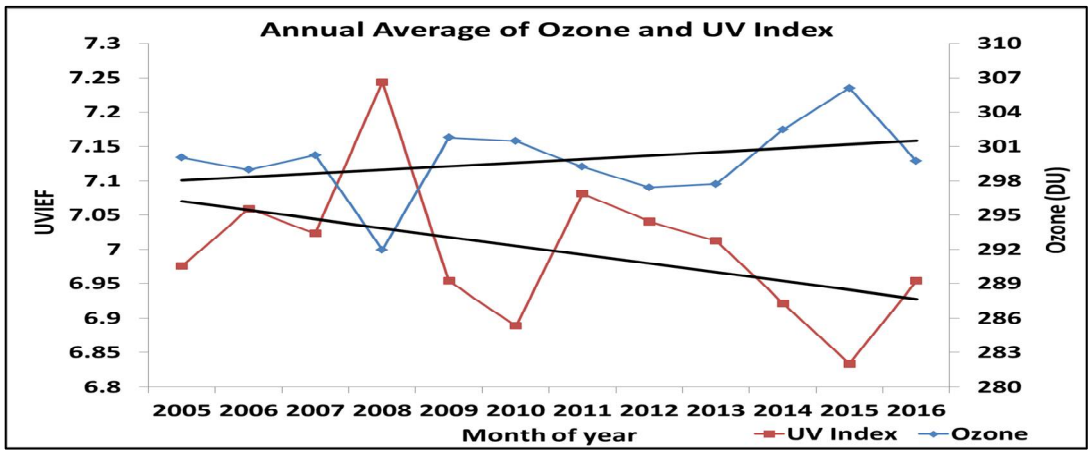

Figure (4): Annual average of ozone and UV-index from years 2005-2016 for Baghdad, where the black line represents the linear curve fitting.

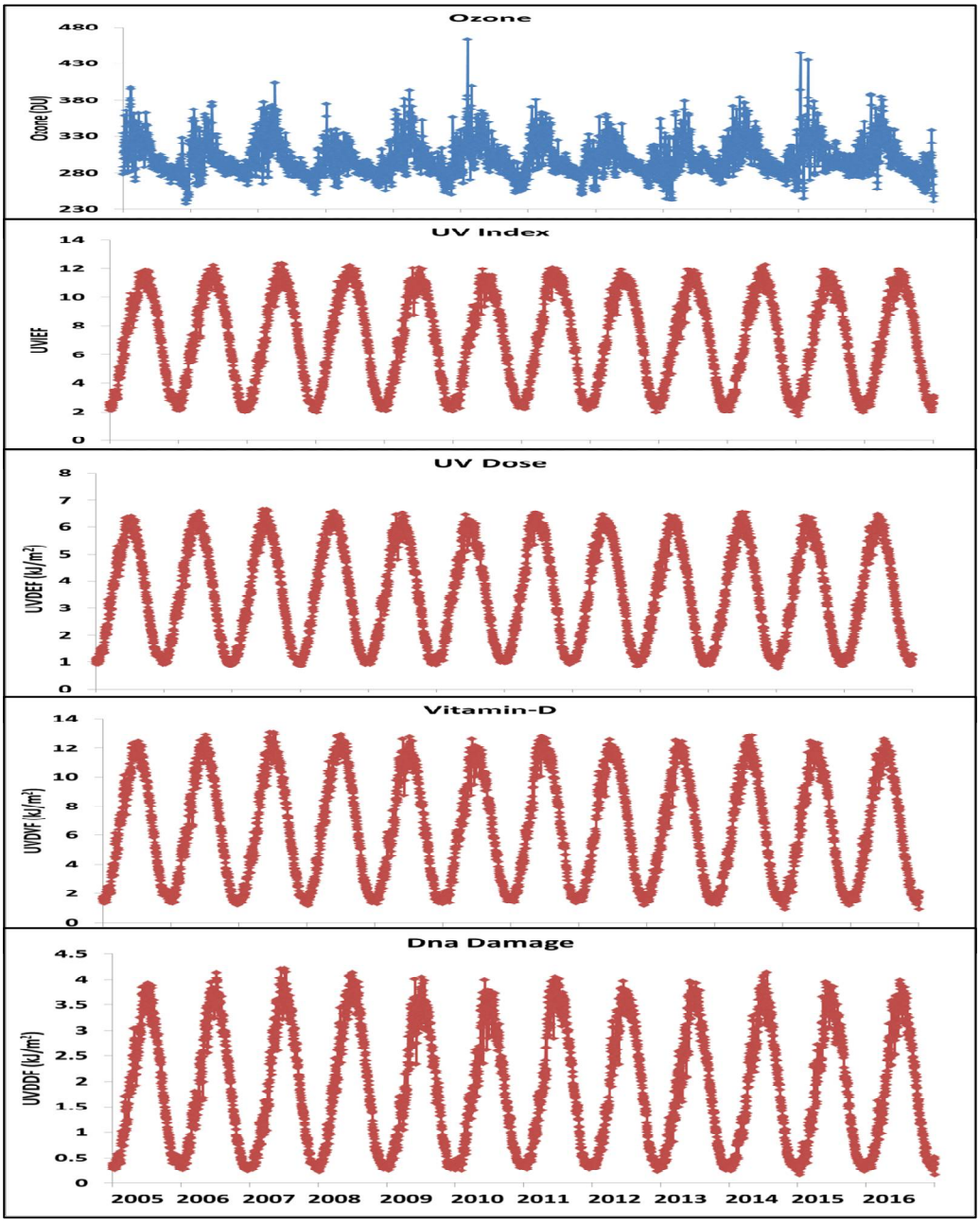

Figure (5): Annual variation of ozone, UV-index, UV Dose, Vitamin-D and DNA Damage for years 2005-2016.

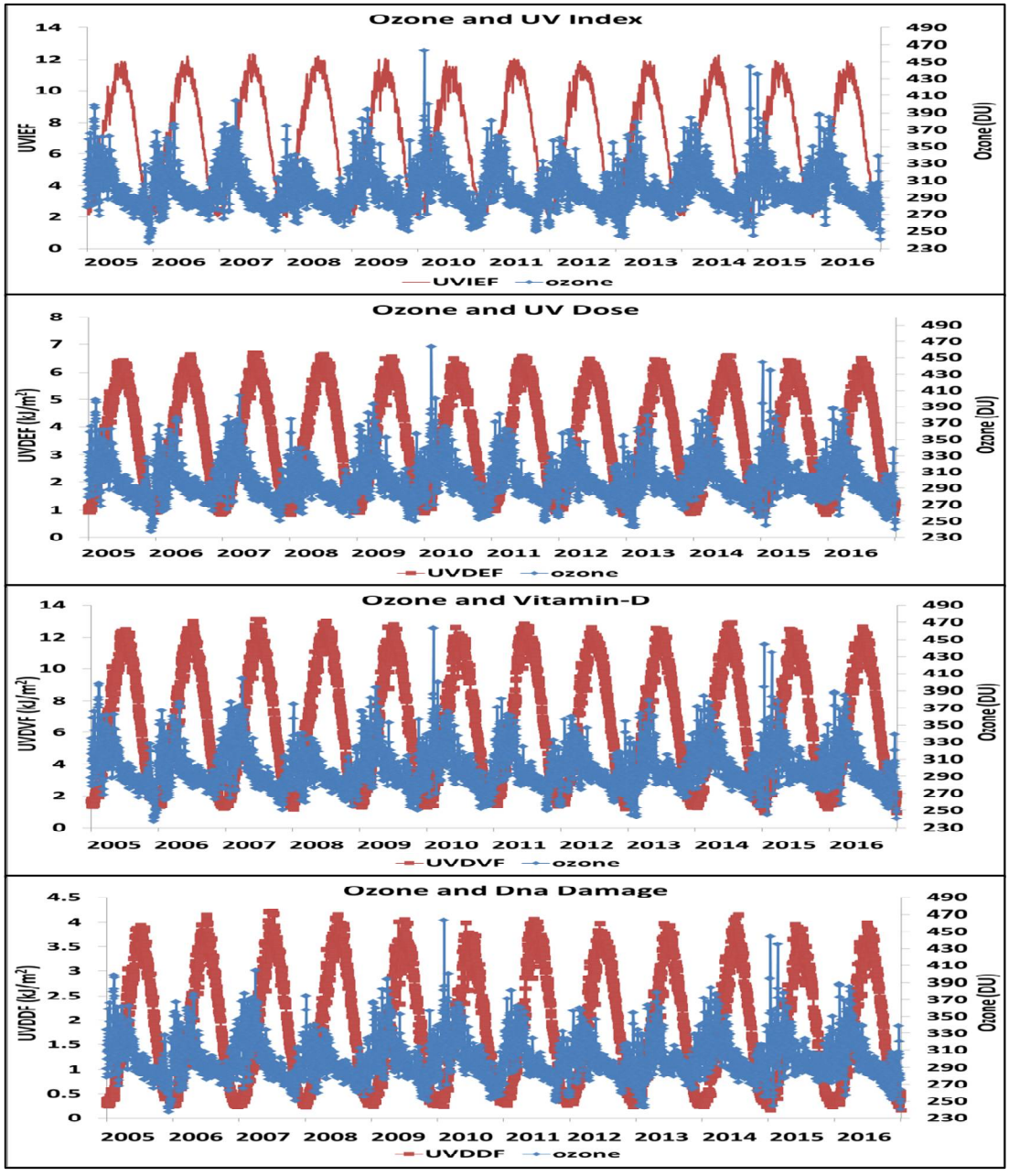

Figure (6): Annual variation of UV-index, UV Dose, Vitamin-D and DNA Damage with the annual ozone variation for years 2005-2016.

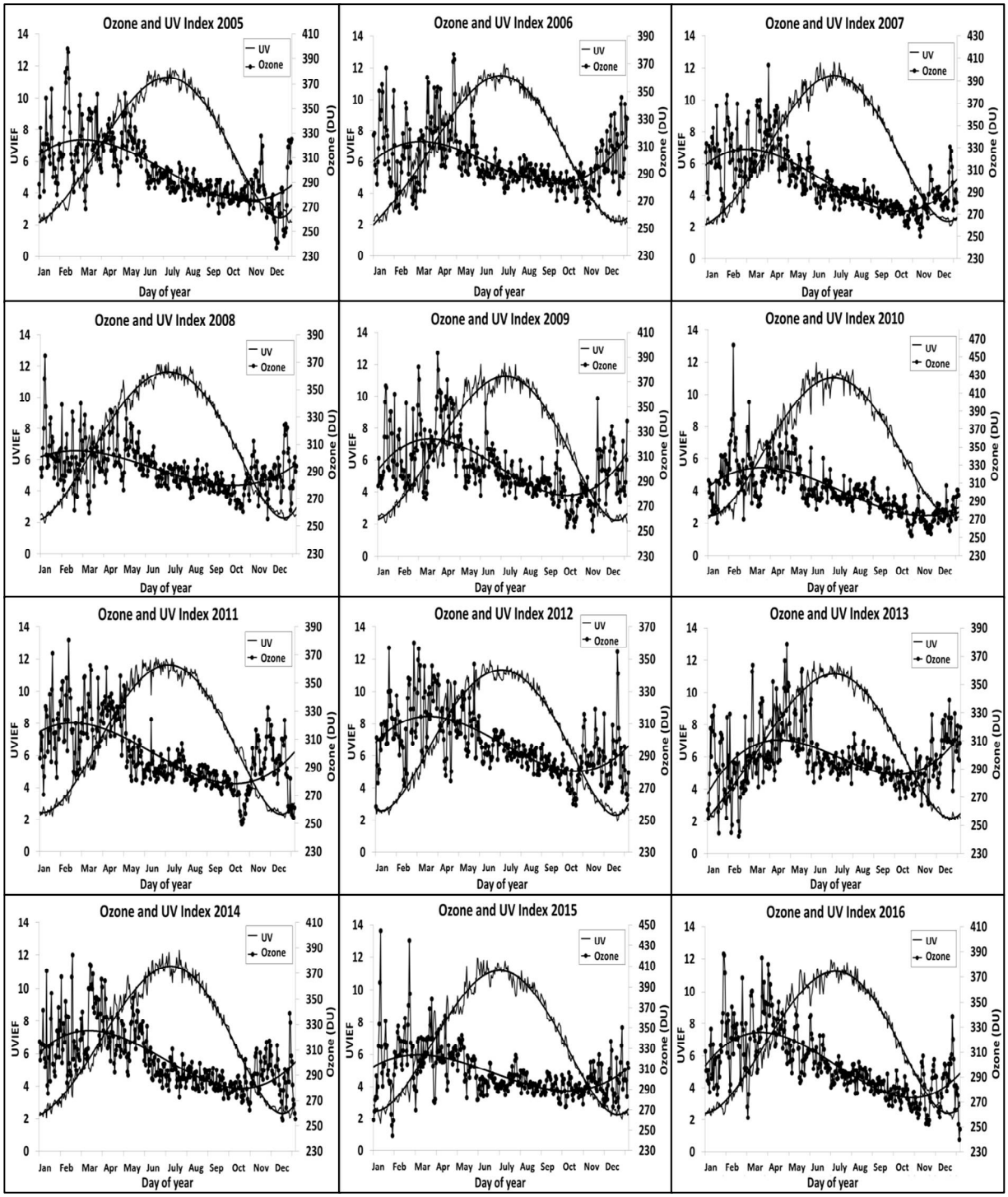

Figure (7): Daily average of ozone and UV-index for 12 months from years 2005-2016, black line represents the polynomial curve fitting.

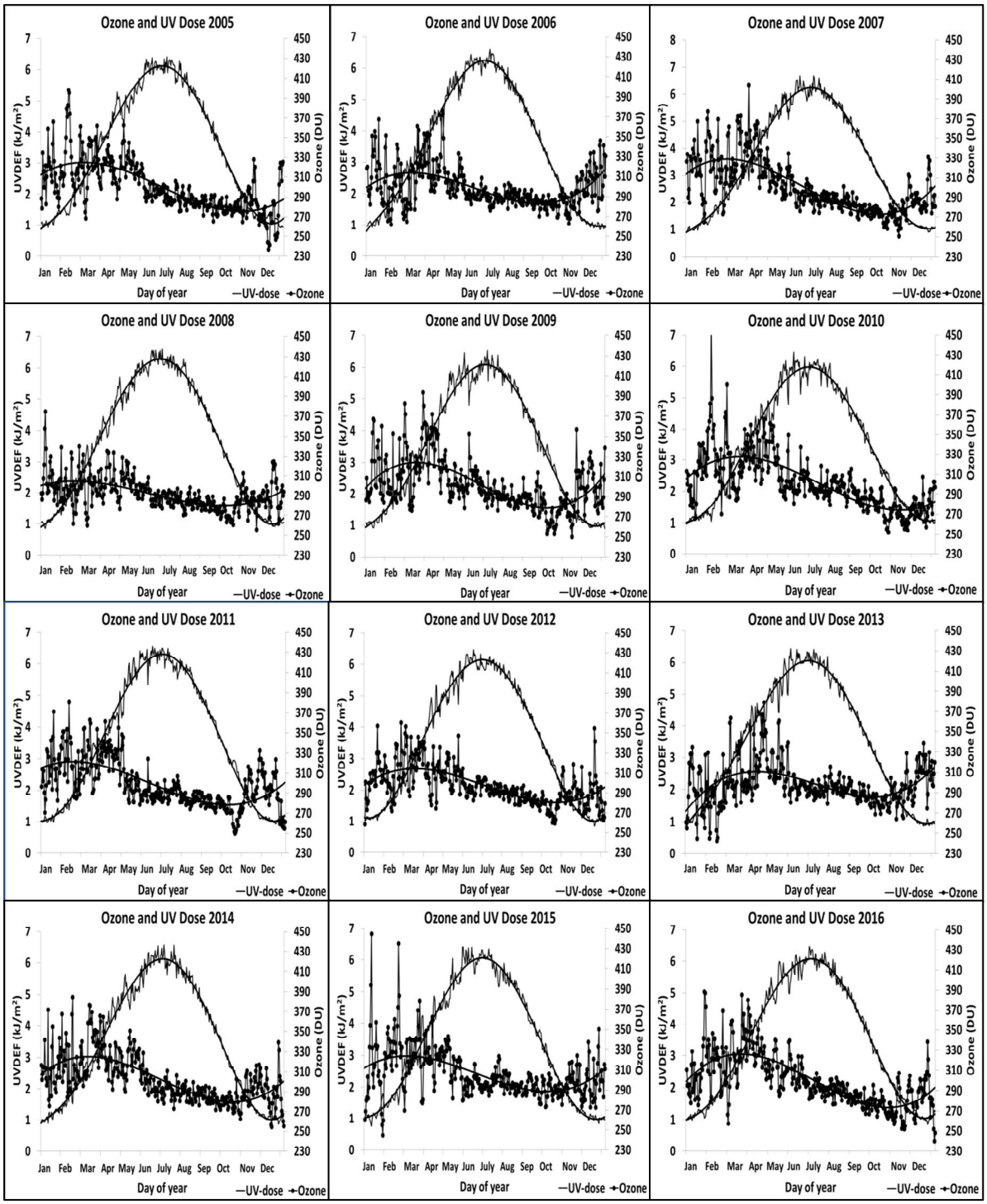

Figure (8): Daily average of ozone and UV-Dose for 12 months from years 2005-2016, black line represents the polynomial curve fitting.

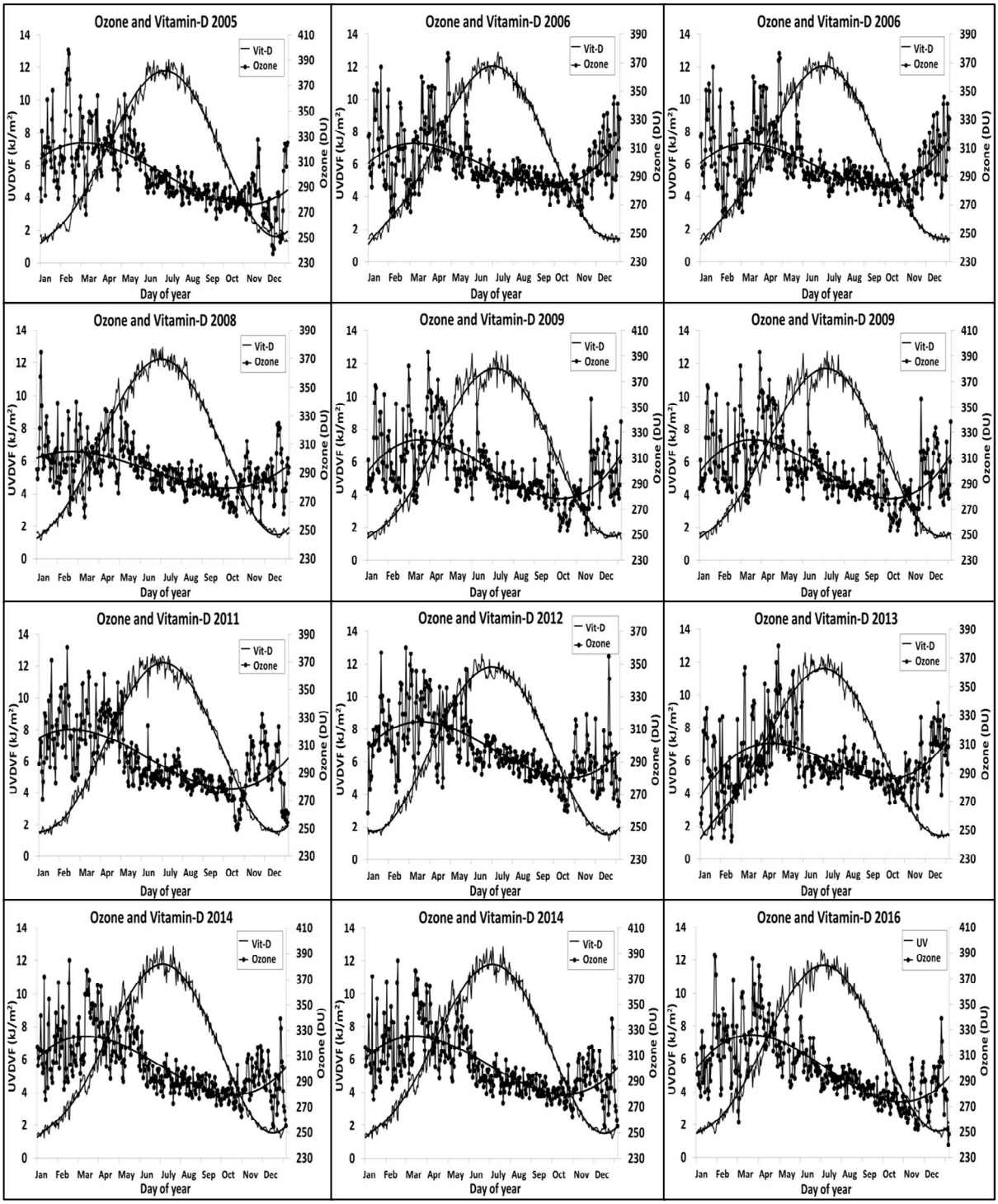

Figure (9): Daily average of ozone and Vitamin-D for 12 months from years 2005-2016, black line represents the polynomial curve fitting.

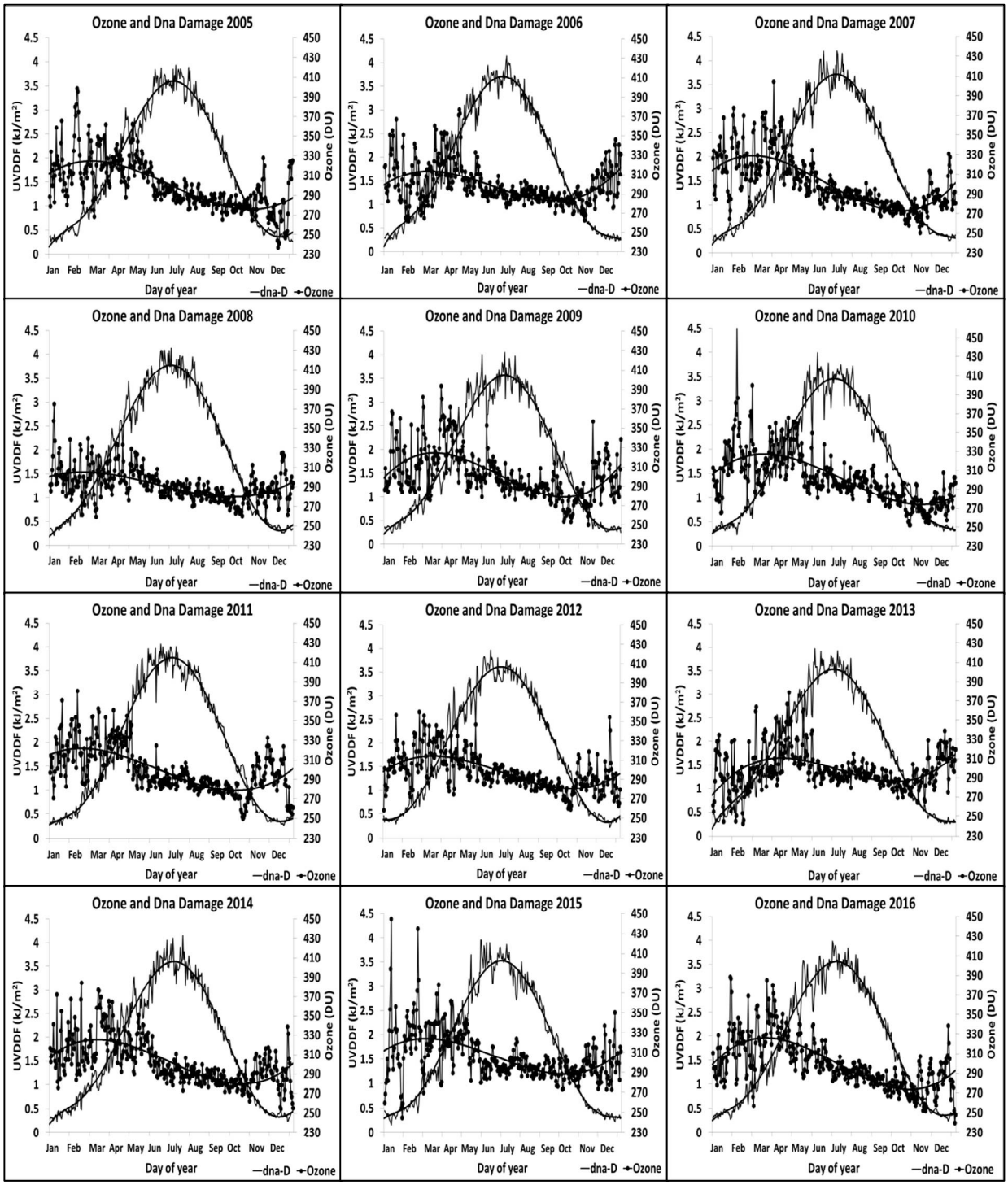

Figure (10): Daily average of ozone and DNA Damage for 12 months from years 2005-2016, black line represents the polynomial curve fitting.

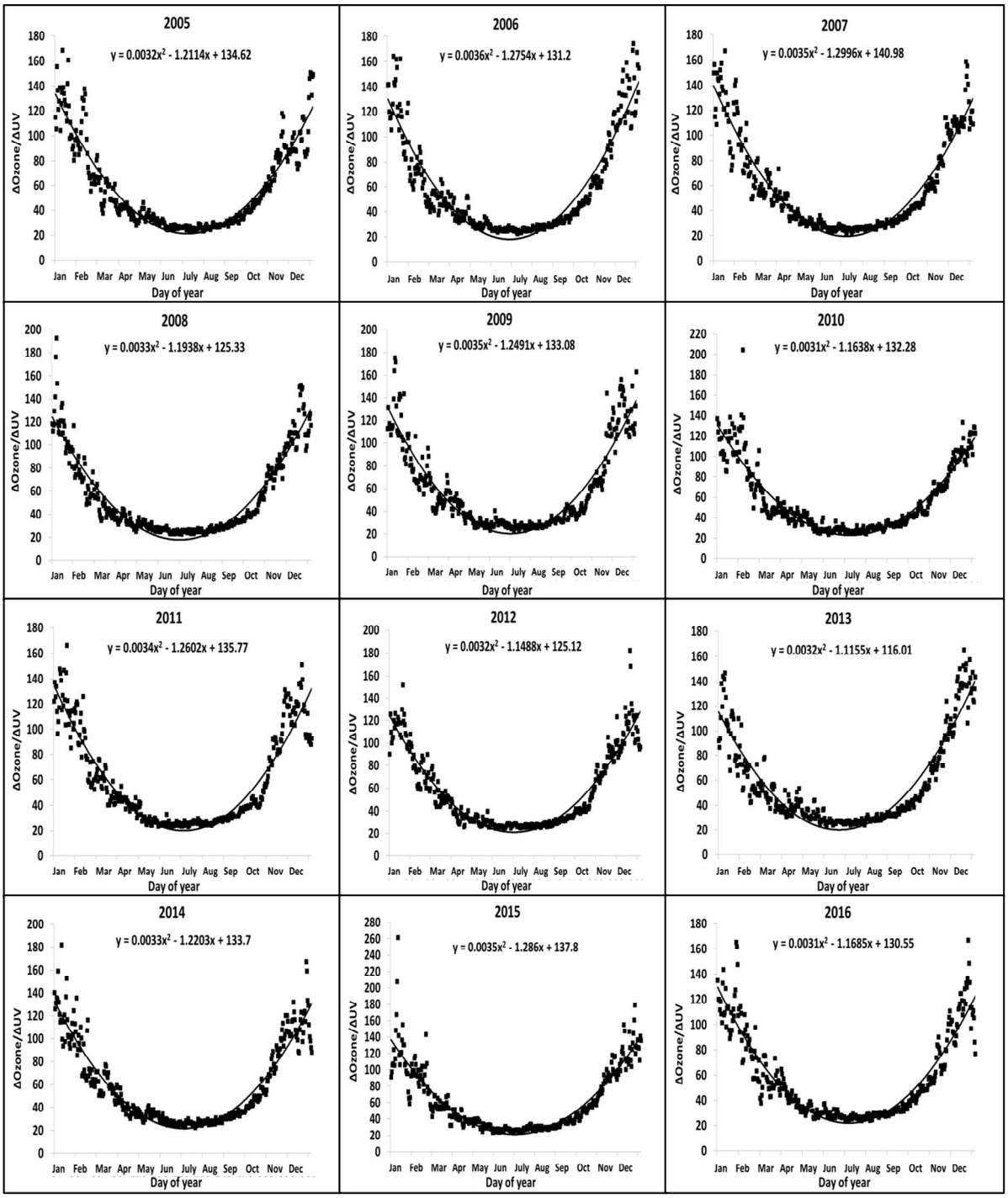

Figure (11): Ratio of daily average variation of (Δozone/ΔUV-index) for 12 months from years 2005-2016, black line represents the polynomial curve fitting.

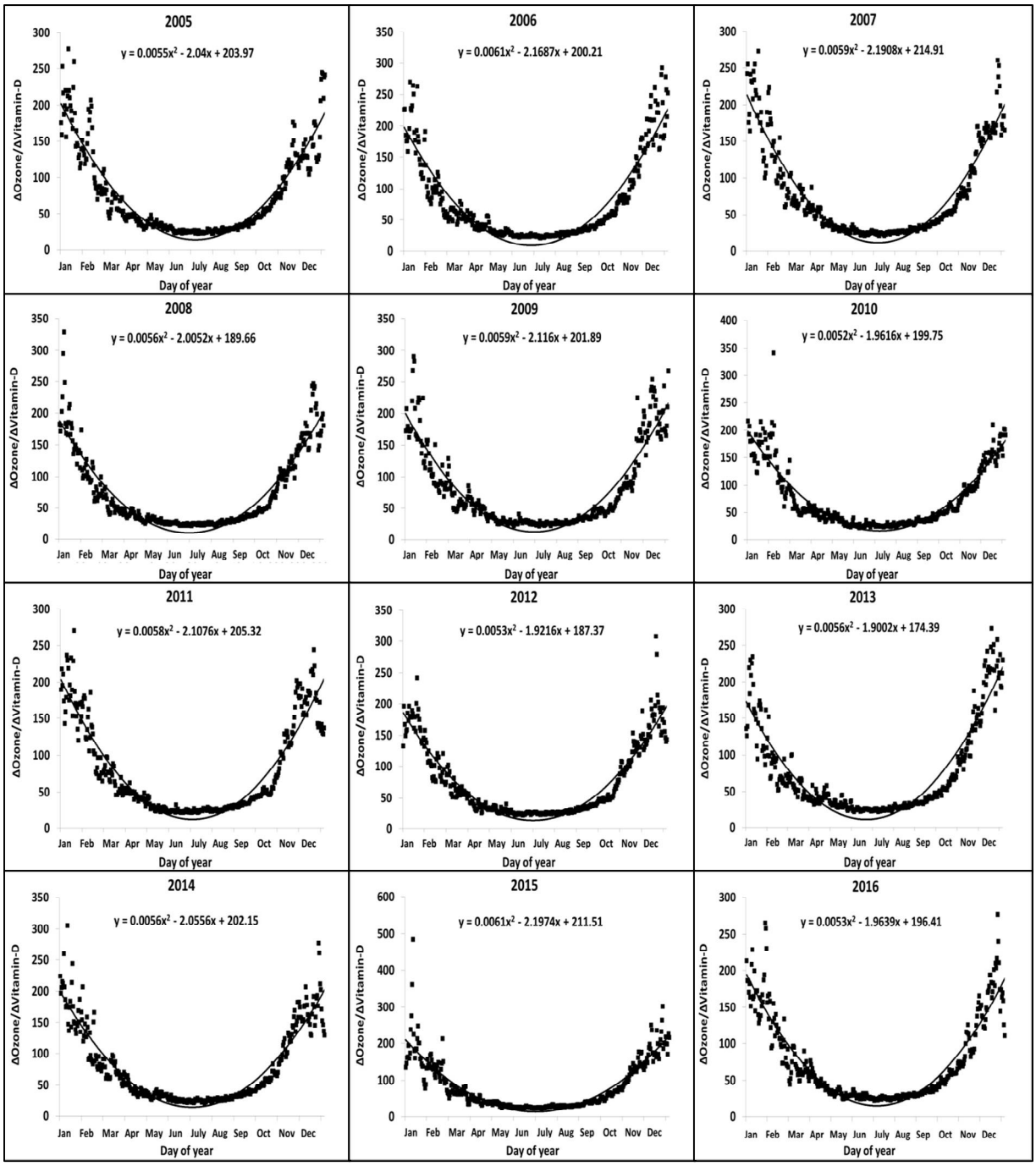

Figure (12): Ratio of daily average variation of (Δozone/Δ Vitamin-D) for 12 months from years 2005-2016, black line represents the polynomial curve fitting.

Indian Journal of Natural Sciences www.tnsroindia.org.in ©IJONS

Vol.9 /Issue 51 / December / 2018 *International Bimonthly* *ISSN: 0976 – 0997*

RESEARCH ARTICLE

CCAF- A Model to Increase Security for the Data in Cloud using Attribution Based Scheme

P.Priyadharshini, R.Athilakshmi, R.Bhaskaran*,G.Muthupandi and P.Senthilkumar

Department of Information Technology, PSNA College Of Engineering & Technology, Dindigul, Tamilnadu,India.

Received: 17 Sep 2018 Revised: 20 Oct 2018 Accepted: 23 Nov 2018

***Address for Correspondence**
R.Bhaskaran
Associate Professor
Department of Information Technology,
PSNA College Of Engineering & Technology,
Dindigul, Tamilnadu, India.
Email:

ABSTRACT

For the large grow in data storage in cloud, a change in model is required.A continuous audit on cloud security communicates that the security of customers' data has the most lifted need and furthermore concern. We believe this must have the ability to achieve with a philosophy that is proficient, adoptable and all around composed. Therefore, this paper has developed a framework known as Cloud Computing Adoption Framework (CCAF) which has been changed for securing cloud data. This paper clears up the diagram, technique for thinking and sections in the CCAF to guarantee data security. CCAF is illustrated by the system arrangement reliant on the essentials and the execution appeared by the CCAF multi-layered security. Since our Data Center has 10 petabytes of data, there is huge task to give continuous security and seclude. We use Business Process Modeling Notation (BPMN) to mirror how data is being utilized. The use of BPMN diversion empowers us to evaluate the picked security presentations before certified execution. Results exhibit that a chance to take control of security break can take some place in the scope of 50 and 125 hours. The server ranches have encountered challenges of quick addition in the data. For example, in a server cultivate that the lead maker used to work with, step by step addition of 100 terabytes of data was standard this suggests additional security is required to ensure all data is particularly guaranteed in the pressing 125 hours. This paper has similarly shown that CCAF multi-layered security can guarantee data logically and it has three layers of security: 1) firewall and access control; 2) identity organization and interference balancing activity and 3) joined encryption. To affirm CCAF, this paper has grasped two courses of action of good hacking tests required with invasion testing with 10,000 Trojans and contaminations. The CCAF multi-layered security can square 9,919 diseases and Trojans which can be smashed like a blaze and the remaining ones can be disconnected

or isolated. The tests show up regardless of the way that the level of blocking can lessen for diligent mixture of diseases and Trojans, 97.43 percent of them can be detached. Our CCAF multi-layered security has a typical of 20 percent ideal execution over the single-layered philosophy which could just block7, 438 contaminations and Trojans.

Keywords: CCAF Cloud Computing Adoption Framework, BPMN Business Process Modeling Notation, ABE Attribute Based Encryption**.**

INTRODUCTION

In traditional networking schemes, if a network entity wants to access some information content, it has to locate and connect to the server that provides such service following network routing protocols. As a result, the information is tightly associated with the location of the server. The entire network is centered on the connections between content consumers and content providers, making connection status an important factor to the network. In ICN architecture, the focus is shifted from consumer-server connections to consumer-content connections. Thus, in-stead of identifying the content owner's address, the network changes to identify authentic content copies. In this way, the consumers do not need to know where the content locates,i.e. the IP address of the content owner. The content name is sufficient to direct the consumer to a content copy. Content owners publish the content, which can be copied and stored in the network using network caches. This design enables contents being efficiently delivered to consumers.The proposed scheme can be divided into two levels. At the upper-level, to address the attribute management problem, we present an ontology-based attribute management solution to manage the distributed attributes in ICN network. In this scheme, attributes defined by different authorities can be synchronized more efficiently than traditional approaches. Content consumers do not need to negotiate their attribute keys when they request contents from other authorities. At the lower-level, we propose an ABE-based naming scheme.

Attribute Based Encryption (ABE) Schemes

In our approach, each network entity is assigned with a set of attributes with the help of a Trusted Third Party (TTP) accord-in to their real identities. The access control policy is enforced according to the content names instead of the contents. Moreover, privacy-preservation is provided for the content access policies. This feature can greatly improve the privacy protection on ICN data when they are distributed in the public domain. In this way, a user is able to identify its eligibility of the accessed contents through the encrypted names before actually accessing the data content. To further support the use of ontology in attribute management, the proposed scheme enables. Comparison between attributes, which gives the capability to rank attributes and associate different privileges accordingly. In summary, the contributions of our work can be listed as follows: It provides ontology-based attribute management, which greatly reduces the cost for attribute management in distributed deployment. The proposed management scheme supports flexible attribute combination operations in access control policies; it enables attribute rankings and access privilege management, making it flexible to construct a data access policy in real-world scenario. The content access policy is confidentially preserved. Ineligible consumers cannot derive the data access policies even if they collude together. It proposes a naming scheme for ICN network which combines the flexible attribute management solution with the privacy preserving access policy. It significantly reduces the computation and communication overhead for a potential consumer to determine his eligibility to access the content. All these ICN solutions focus on the efficiency and security aspects of the network while access control to the content and content privacy is not well addressed. In an through a component called the Relaying Party (RP). An additional component called Access Control Provider (ACP) is in charge of creating access policies and enforcing the policies to consumers' credentials.

This system incorporates access control into ICN systems but requires much more network inter-actions. For content privacy purposes, proposes a design in which each file is divided into blocks.

RELATED WORK

Distributed computing and its reception has been a theme of dialog in the previous couple of years. It has been a motivation for hierarchical reception because of advantages in cost-funds, enhancement in work efficiencies, business deftness and nature of administrations .With the quick ascent in distributed computing, programming as an administration (SaaS) is especially popular, since it offers benefits that suit clients' need. For instance, Health informatics can enable restorative analysts to analyze testing illnesses and tumors. Monetary investigation can guarantee exact and quick reproductions to be accessible for financial specialists. Instruction as an administration enhances the nature of training and conveyance. Portable applications enable clients to play web based amusements and simple to-utilize applications to between act with their companions. While more individuals and associations utilize the cloud administrations, security and protection wind up essential to guarantee that every one of the information they utilize and share are all around ensured. A few specialists state that security ought to be actualized before the utilization of any cloud benefits in place.This makes a testing appropriation situation for associations since security ought to be authorized and executed in parallel with any administrations. In spite of the fact that associations that receive distributed computing recognize benefits offered by cloud administrations, difficulties, for example, security and protection remain an investigation for authoritative appropriation. While directing the significance of security, the product building and improvement process ought to dependably configuration, execute and test security highlights. The server farms have experienced difficulties of quick increment in the information. For instance, in a server farm that the lead creator used to work with, every day increment of 100 terabytes of information was common. If the association has experienced a fast ascent of information development and can't react rapidly and proficiently, issues, for example, information movement, information security and administration level assertion issues can occur. In this paper, we center on the information security while encountering a substantial increment of information, regardless of whether they are from the outer sources, for example, assault of infections or Trojans; or they from the inner sources if clients or customers gather many terabytes of information every day. This is inquiring about test for information security which is fundamental for the better administration of the server farm to deal with a fast increment in the data. The future extension to work with the accompanying:

I. To handle with hacking of information
II. Non-Existence
III. Data Management as per stockpiling
IV. Scalability

METHODOLOGY

CCAF SELECTION

Application Layer

Application layer security alludes to strategies for ensuring Web applications at the application (layer 7 of the seven-layer OSI display) from noxious assaults that may uncover private data. Security is connected to the application layer particularly to ensure against unapproved access and assaults. Application level security alludes to those security benefits that are conjured at the interface between an application and a line director to which it is associated. Application level security is otherwise called end-to-end security or message level security

Virtual Machine

A virtual machine (VM) is an operating system (OS) or application environment that is installed on software, which imitates dedicated hardware. The end user has the same experience on a virtual machine as they would have on dedicated hardware. Most virtual machines are hosted on, or work inside of, a physical machine. For virtual machine to work, the hosted physical machine provides software called hypervisor. The virtual machine function is a function for the realization of virtual machine environment. This function enables you to create multiple independent virtual machines on one physical machine by virtualizing resources such as the CPU, memory, network and disk that are installed on a physical machine (Fig.1).

Computation Layer

Planning is a noteworthy issue in distributed computing. To run remote PCs, booking is an imperative errand. Many number of complex applications are arriving worry towards distributed computing. Distributed computing is a critical worldview to go through remote focuses. Booking issues are on a fundamental level of cloud planning. This investigates the different booking issues in cloud planning and different existing models to fathom them. In this, different computational model of distributed computing, planning issue (Fig.1).

Initial Phase

In the underlying stage, the login procedures are performed. In the event that the client is new client implies, the enrollment procedure perfumed and the client will enlist their data into the database. Again the client login processes are performed. After that the document will be put away appropriately (Fig.2).

Content Owner's Data

Content proprietor need to choose the information and the information might be at any configuration. On the off chance that the information is in pdf or ppt doc implies that information are changed over into content arrangement. At that point it will be encoded by a similar way.

Content Owner Encryption

Information proprietor creates the message validation code for the data.This MAC is utilized as the key for the encryption of the data.For encryption Data Encryption Standard calculation (DES) is used.It utilizes 56 bits as key size and furthermore the information proprietor send the approval rules. It contains the name of the beneficiaries. Just those approved clients can get the information from CSP.

CSP RE-ENCRYPTION

CSP (Cloud Service Provider) gets the accompanying substance from information proprietor. They are

- Encrypted information.
- Authorization Rules.
- Re-Encryption keys.

utilizing the re encryption key the scrambled information have be encoded again.Then the cloud specialist co-op is prepared to give administration to the information user.Cloud benefit supplier gets the demand from information user.This re encryption system builds the security of the information.

User Retrieval

Data user have to login into the system.And send the request to the cloud service provider.Cloud service provider validates the request from the data user. For this validation process the authorization rules are used. If the data user name is present in the authorization rules means the CSP will provide the data. Otherwise CSP will not provide the data. Then the data user decrypts the data received from the cloud service provider.

CONCLUSION

This paper demonstrated the CCAF multi-layered security for the data security in the Data Center under the pro-postal and recommendation of CCAF guidelines. We explained the rationale, overview, components in the CCAF, where the design was based on the requirements and the implementation was illustrated by its multi-layered security. We explained how multi-layered security was a suitable method and recommendation, since it offered multiple pro-section and improvement of security for 10 PB of data in the Data Center based at the University of London Computing Center. We explained the technical details in each layer of security and propose an integrated solution to check all the data when data is intensively used. We used the Business Process Modeling Notation to simulate the cases of how the data can be used, either at rest, in use, or in motion. All simulations could be completed within 2 seconds. Our BPMN simulation results showed that it could take up to 50 hours to protect all the 2 PB data and up to125 hours to raise an alarm to take control of the situation in the ULCC Data Center. This means that an integrated approach was required to ensure data protection, in case that the data center is under the attack or potential threat from the rapid rise of data growth in the data center, which Comparison between CCAF and Other Single-Layered Services Precision Recall F-Measure can be due to the external intrusion or the internal rapid consumption. We then used FGSM for the penetration test-in. 10,000 viruses and Trojans were injected into Data Cen-term with two experiments performed. The first experiment showed that firewall, identity management and encryption could block 5,423, 3,742 and 842 viruses and Trojans respectively. The remaining 81 could be either quarantined or isolated. The second experiment showed that continuous injection of 10,000 viruses and Trojans could make the block-in rate decreased from the 99.19 to 76.00 percent in 125 despite of this result, the CCAF multi-layered security could quarantine and isolate 97.53 percent of viruses and Trojans. Our work can demonstrate that the use of CCAF multi-layered security can protect the data center from the rapid data growth due to the security breach, and the use of BPMN can calculate how much time required for rescue action if the data security is compromised. In this way, we can work out the better tactics and plans for data recovery and security

REFERENCES

[1] S. Marston, Z. Li, S. Bandyopadhyay, J. Zhang, and A. Thalassic,"Cloud computing – The business perspective," Decision Support Syst., vol. 51, no. 1, pp. 176–189, 2011.

[2] M. A. Vouch, "Cloud computing—issues, research and implementations," J. Compute. Inf. Technol. —CIT, v o l. 4, p p. 2 3 5– 24 6, 2 0 08.

[3] A. K. Johan, C. M. DesRoches, E. G. Campbell, K. Don élan, S. R. Rao, T. G. Ferris, and D. Blumenthal, "Use of electronic health records In US hospitals," New England J. Med., vol. 360, no. 16, pp. 1628–1638, 2009.

[4] H. T. Peng, W. W. Hsu, C. H. Chen, F. Lai, and J. M. Ho, "Financial Cloud: open cloud framework of derivative pricing," in Proc. Int.Conf. Social Compute. Sep. 2013, pp. 782–789.

[5] M. Marcia and A. I. Andreessen, "Using cloud computing in higher Education: A strategy to improve agility in the current financial Crisis, "common. IBIMA, vol. 2011, pp. 1–15, 2011.

[6] M. Armrest, A. Fox, R. Griffith, A. D. Joseph, R. H. Katz, Kaminski, G. Lee, D. Patterson, A. Rabin, I. Stoical, and M. Zaharias, "Above the clouds: A Berkeley view of cloud Computing," common. ACM, vol. 53, no. 4, pp. 50– 58, 2010.

[7] L. Liu, E. Yu, and J. Mylopoulos, "Security and privacy require-mints analysis within a social setting," in Proc. 11th IEEE Int. Requirements Eng. Conf., Sep. 2003, pp. 151–161.
[8] T. Mather, S. Kumaraswamy, and S. Latin, Cloud Security and Privacy: An Enterprise Perspective on Risks and Compliance. Sebastopol, CA, USA: O'Reilly Media, 2009.
[9] M. Pop and S. L. Salzburg, "Bioinformatics challenges of new Sequencing technology, "TrendsGenetics, vol. 24, no. 3, pp.
[11]Q. Zhang, L. Cheng, and R. Boothbay, "Cloud computing: state-of-the-art and research challenges," J. Internet Services Appl. , vol. 1,No. 1, pp. 7–18, 2010.
[12]J. J. Cibola and L. R. Young, "A taxonomy of operational cyber Security," Soft. Eng. Inst., Tech. Note: CMU/SEI-2010-TN-028, Pittsburgh, PA, USA, Dec. 2010.
[13]S. Yu, C. Wang, K. Ren, and W. Lou, "Achieving secure, scalable, And fine-grained data access control in cloud computing," in Proc. IEEE INFOCOM, Mar. 14–19, 2010, pp. 1–9.
[14]G. Wang, Q. Liu, and J. Wu, "Hierarchical attribute-based encryption for fine-grained access control in cloud storage services," in Proc. 17th ACM Conf. Compute. Common. Security, Oct. 2010, pp. 735–737.
[16]G. McGraw, Software Security: Building Security. Reading, MA, USA: Addison-Wesley, 2006.
[17]P. Brooks and J. Chittenden, Metrics for Service Management: Designing for ITIL. Zaltbommel, Netherlands: Van Harem Publish-in, 2012.
[18]V. Chang, R. J. Walters, and G. Wills, Cloud Storage and Bioinformatics in a Private Cloud Deployment: Lessons for Data Intensive Research. New York, NY, USA: Springer CLOSER 2012, CCIS 367, pp. 245–264, 2013.
[19]V. Chang, "Business intelligence as service in the cloud," Future Genre. Compute. Syst., vol. 37, pp. 512–534, 2014.
[20]I. A. Toned et al., "Security requirements for rest of us: A survey," IEEE Soft., Special Issue Security Agile Requirement Eng. Methods, vol. 25, no. 1, pp. 20–27, Jan. /Feb. 2008.
[21]N. R. Mead, T. Stoney, "Security quality requirements engineering (SQUARE) methodology," AC M, vol. 30, no 4, pp. 1–7, 2005.
[22]Oracle. (2012). Data Security Challenges. Oracle9i security over-view release number 2(9.2), accessed on 4th November nline].Available:
[23]V. Kumar, M. S. Swathe, M. S. Muneshwara, and S. Prakash "Cloud computing: Towards case study of data security mechanism," Int. J. Adv. Technol. Eng. Res., vol. 2, no. 4, pp. 1–8, Jul. 2012.
[24]F. Wen, and L. Xiang, "The study on data security in cloud com-putting based on virtualization," in Proc. IEEE Int. Sump. IT Med. Edu. , 2011, vol. 2, no. 1, pp. 257–261.
[25]B. Schneider, Beyond Fear. New York, NY, USA: Copernicus Books,2003.
[26]IBM, "Eleven habits for highly successful BPMprograms," IBM-Thought Leadership White Paper, 2010.
[27]G. M. Camino and G. Tagline, "An interval-valued approach to Business process simulation based on genetic algorithms and the BPMN," Information, vol. 5, pp. 319– 356, 2014.
[28]A. Buhl and K. Buhl, "An analysis of cloud computing security Issues," in Proc. World Conger. Inf. common. Technol., Trivandrum, India, Nov. 2012, pp. 109–114.
[29]V. Vardharajan and U. Tupakula, "Security as a service model for cloud environment," IEEE Trans. Newt. Service Manage. , vol. 11,No. 1, pp. 60–75, Mar. 2014.
[30]M. Bishop, "About penetration testing," IEEE Security Privacy ,vol. 5, no. 6, pp. 84–87, Nov. /Dec. 2007.

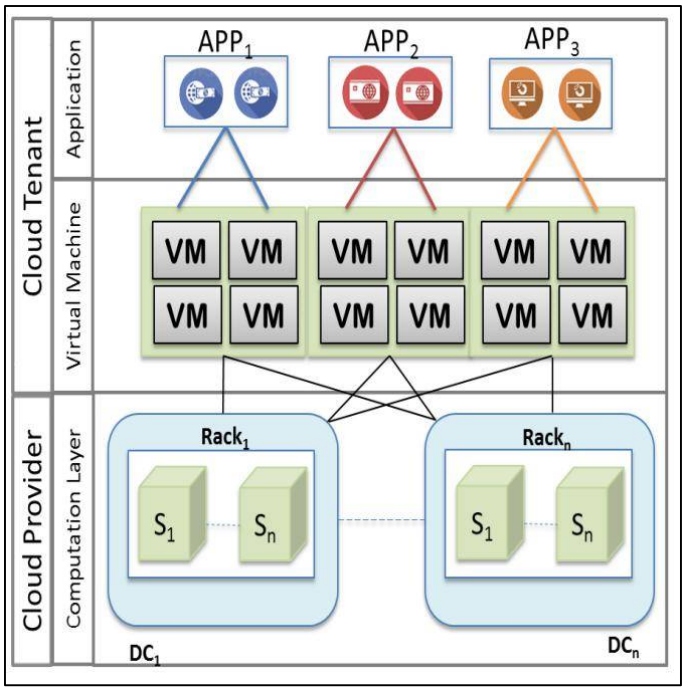

Figure 1. CCAF Selection

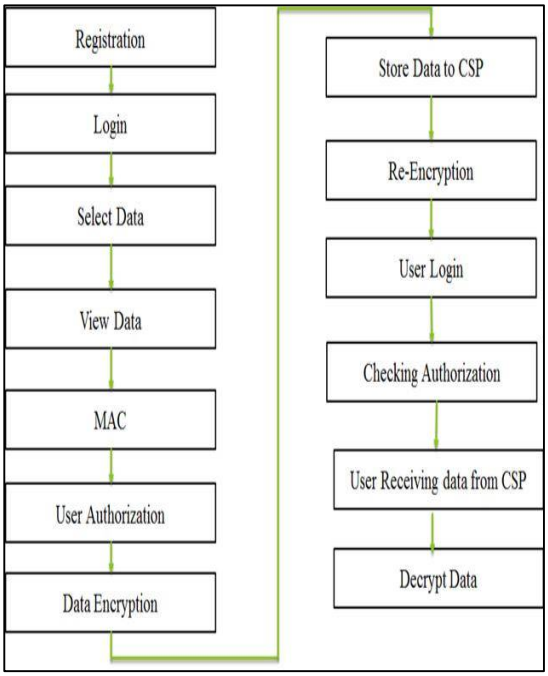

Figure 2.Module Description